



July 2010

PARTICLE PHYSICS BOOKLET

Extracted from the *Review of Particle Physics*
K. Nakamura, *et al.* (Particle Data Group),
Journal of Physics G **37**, 075021 (2010)

See <http://pdg.lbl.gov/> for Particle Listings, complete
reviews, and pdgLive (our interactive database)

Available from PDG at LBNL and CERN

For copies of this Booklet and of the full *Review* to be sent to addresses in the Americas, Australasia, or the Far East, visit

<http://pdg.lbl.gov/pdgmail>

or write to

Particle Data Group
MS 50R6008
Lawrence Berkeley National Laboratory
Berkeley, CA 94720-8166, USA

From all other areas, visit

<http://www.cern.ch/library>

or write to

CERN Scientific Information Service
CH-1211 Geneva 23
Switzerland

To make comments or corrections, send e-mail to PDG@LBL.GOV. We acknowledge all e-mail via e-mail. No reply indicates nonreceipt. Please try again.

Visit our WWW site: <http://pdg.lbl.gov/>

The publication of the *Review of Particle Physics* is supported by the Director, Office of Science, Office of High Energy and Nuclear Physics, the Division of High Energy Physics of the U.S. Department of Energy under Contract No. DE-AC02-05CH11231; by the U.S. National Science Foundation under Agreement No. PHY-0652989; by the European Laboratory for Particle Physics (CERN); by an implementing arrangement between the governments of Japan (MEXT: Ministry of Education, Culture, Sports, Science and Technology) and the United States (DOE) on cooperative research and development; and by the Italian National Institute of Nuclear Physics (INFN).

PARTICLE PHYSICS BOOKLET

Extracted from the *Review of Particle Physics**

K. Nakamura *et al.* (Particle Data Group), JP G **37**, 075021 (2010)

(next edition: July 2012)

PARTICLE DATA GROUP

K. Nakamura, K. Hagiwara, K. Hikasa, H. Murayama, M. Tanabashi, T. Watari, C. Amsler, M. Antonelli, D.M. Asner, H. Baer, H.R. Band, R.M. Barnett, T. Basaglia, E. Bergren, J. Beringer, G. Bernardi, W. Bertl, H. Bichsel, O. Biebel, E. Blucher, S. Blusk, R.N. Cahn, M. Carena, A. Ceccucci, D. Chakraborty, M.-C. Chen, R.S. Chivukula, G. Cowan, O. Dahl, G. D'Ambrosio, T. Damour, D. de Florian, A. de Gouvêa, T. DeGrand, G. Dissertori, B. Dobrescu, M. Doser, M. Drees, D.A. Edwards, S. Eidelman, J. Erler, V.V. Ezhela, W. Fetscher, B.D. Fields, B. Foster, T.K. Gaiser, L. Garren, H.-J. Gerber, G. Gerbier, T. Gherghetta, G.F. Giudice, S. Golwala, M. Goodman, C. Grab, A.V. Griksan, J.-F. Grivaz, D.E. Groom, M. Grünewald, A. Gurtu, T. Gutsche, H.E. Haber, C. Hagmann, K.G. Hayes, M. Heffner, B. Heltsley, J.J. Hernández-Rey, A. Höcker, J. Holder, J. Huston, J.D. Jackson, K.F. Johnson, T. Junk, A. Karle, D. Karlen, B. Kayser, D. Kirkby, S.R. Klein, C. Kolda, R.V. Kowalewski, B. Krusche, Yu.V. Kuyanov, Y. Kwon, O. Lahav, P. Langacker, A. Liddle, Z. Ligeti, C.-J. Lin, T.M. Liss, L. Littenberg, K.S. Lugovsky, S.B. Lugovsky, J. Lys, H. Mahlke, T. Mannel, A.V. Manohar, W.J. Marciano, A.D. Martin, A. Masoni, D. Milstead, R. Miquel, K. Mönig, M. Narain, P. Nason, S. Navas, P. Nevski, Y. Nir, K.A. Olive, L. Pape, C. Patrignani, J.A. Peacock, S.T. Petcov, A. Piepke, G. Punzi, A. Quadt, S. Raby, G. Raffelt, B.N. Ratcliff, P. Richardson, S. Roesler, S. Rolli, A. Romaniouk, L.J. Rosenberg, J.L. Rosner, C.T. Sachrajda, Y. Sakai, G.P. Salam, S. Sarkar, F. Sauli, O. Schneider, K. Scholberg, D. Scott, W.G. Seligman, M.H. Shaevitz, M. Silari, T. Sjöstrand, J.G. Smith, G.F. Smoot, S. Spanier, H. Spieler, A. Stahl, T. Stanev, S.L. Stone, T. Sumiyoshi, M.J. Syphers, J. Terning, M. Titov, N.P. Tkachenko, N.A. Törnqvist, D. Tovey, T.G. Trippe, G. Valencia, K. van Bibber, G. Venanzoni, M.G. Vincter, P. Vogel, A. Vogt, W. Walkowiak, C.W. Walter, D.R. Ward, B.R. Webber, G. Weiglein, E.J. Weinberg, J.D. Wells, A. Wheeler, L.R. Wiencke, C.G. Wohl, L. Wolfenstein, J. Womersley, C.L. Woody, R.L. Workman, A. Yamamoto, W.-M. Yao, O.V. Zenin, J. Zhang, R.-Y. Zhu, P.A. Zyla

Technical Associates:

G. Harper, V.S. Lugovsky, P. Schaffner

*The full *Review* lists all the data, with references, used in obtaining the values given in the Particle Summary Tables. It also contains much additional information. Some of the material that does appear in this Booklet is only an abbreviated version of what appears in the full *Review*.

PARTICLE PHYSICS BOOKLET TABLE OF CONTENTS

1. Physical constants (rev.)	4
2. Astrophysical constants (rev.)	6
<i>Summary Tables of Particle Physics</i>	
Gauge and Higgs bosons	8
Leptons	13
Quarks	21
Mesons	23
Baryons*	135
Searches	161
Tests of conservation laws*	165
<i>Reviews, Tables, and Plots</i>	
9. Quantum chromodynamics (new)*	169
10. Electroweak model and constraints on new physics (rev.)*	172
11. Cabibbo-Kobayashi-Maskawa quark mixing matrix (rev.)*	181
12. <i>CP</i> violation (rev.)*	188
13. Neutrino Mass, Mixing and Oscillations (new)*	193
14. Quark model (rev.)*	200
16. Structure functions (rev.)*	203
19. Big-bang cosmology (rev.)*	208
21. The Cosmological Parameters (rev.)*	214
22. Dark matter (rev.)*	218
23. Cosmic Microwave Background (rev.)*	221
24. Cosmic rays (new)*	224
25. Accelerator physics of colliders (rev.)*	225
26. High-energy collider parameters (rev.)*	226
27. Passage of particles through matter (rev.)*	229
28. Particle detectors at accelerators (rev.)*	244
29. Particle detectors for non-accelerator physics (new)*	256
30. Radioactivity and radiation protection (rev.)*	263
31. Commonly used radioactive sources	265
32. Probability (rev.)*	267
33. Statistics (rev.)*	271
36. Clebsch-Gordan coefficients, spherical harmonics, and <i>d</i> functions	285
39. Kinematics (rev.)*	287
40. Cross-section formulae for specific processes (rev.)*	296
41. Plots of cross sections and related quantities (rev.)*	301
6. Atomic and nuclear properties of materials *	302
4. Periodic table of the elements (rev.)	inside back cover

*Abridged from the full *Review of Particle Physics*.

The following are found only in the full *Review* and on the Web:

<http://pdg.lbl.gov>

3. International System of Units (SI)
5. Electronic structure of the elements
7. Electromagnetic relations
8. Naming scheme for hadrons
15. Grand Unified Theories
17. Fragmentation functions in e^+e^- annihilation
and lepton-nucleon DIS (rev.)
18. Experimental tests of gravitational theory (rev.)
20. Big-bang nucleosynthesis (rev.)
34. Monte Carlo techniques (rev.)
35. Monte Carlo particle numbering scheme (rev.)
37. SU(3) isoscalar factors and representation matrices
38. SU(n) multiplets and Young diagrams

Table 1.1. Reviewed 2010 by P.J. Mohr (NIST). The set of constants excluding the last group (which come from the Particle Data Group) is recommended by CODATA for international use. The 1- σ uncertainties in the last digits are given in parentheses after the values. See the full edition of this *Review* for references and further explanation.

Quantity	Symbol, equation	Value	Uncertainty (ppb)
speed of light in vacuum	c	299 792 458 m s ⁻¹	exact*
Planck constant	h	6.626 068 96(33) × 10 ⁻³⁴ J s	50
Planck constant, reduced	$\hbar \equiv h/2\pi$	1.054 571 628(53) × 10 ⁻³⁴ J s = 6.582 118 99(16) × 10 ⁻²² MeV s	50
electron charge magnitude	e	1.602 176 487(40) × 10 ⁻¹⁹ C = 4.803 204 27(12) × 10 ⁻¹⁰ esu	25, 25
conversion constant	$\hbar c$	197.326 9631(49) MeV fm	25
conversion constant	$(\hbar c)^2$	0.389 379 304(19) GeV ² mbarn	50
electron mass	m_e	0.510 998 910(13) MeV/c ² = 9.109 382 15(45) × 10 ⁻³¹ kg	25, 50
proton mass	m_p	938.272 013(23) MeV/c ² = 1.672 621 637(83) × 10 ⁻²⁷ kg = 1.007 276 466 77(10) u = 1836.152 672 47(80) m_e	25, 50 0.10, 0.43
deuteron mass	m_d	1875.612 793(47) MeV/c ²	25
unified atomic mass unit (u)	(mass ¹² C atom)/12 = (1 g)/(N _A mol)	931.494 028(23) MeV/c ² = 1.660 538 782(83) × 10 ⁻²⁷ kg	25, 50
permittivity of free space	$\epsilon_0 = 1/\mu_0 c^2$	8.854 187 817 ... × 10 ⁻¹² F m ⁻¹	exact
permeability of free space	μ_0	4 π × 10 ⁻⁷ N A ⁻² = 12.566 370 614 ... × 10 ⁻⁷ N A ⁻²	exact
fine-structure constant	$\alpha = e^2/4\pi\epsilon_0\hbar c$	7.297 352 5376(50) × 10 ⁻³ = 1/137.035 999 679(94) [†]	0.68, 0.68
classical electron radius	$r_e = e^2/4\pi\epsilon_0 m_e c^2$	2.817 940 2894(58) × 10 ⁻¹⁵ m	2.1
(e ⁻ Compton wavelength)/2 π	$\lambda_e = \hbar/m_e c = r_e \alpha^{-1}$	3.861 592 6459(53) × 10 ⁻¹³ m	1.4
Bohr radius ($m_{\text{nucleus}} = \infty$)	$a_\infty = 4\pi\epsilon_0 \hbar^2 / m_e e^2 = r_e \alpha^{-2}$	0.529 177 208 59(36) × 10 ⁻¹⁰ m	0.68
wavelength of 1 eV/c particle	$\hbar c/(1 \text{ eV})$	1.239 841 875(31) × 10 ⁻⁶ m	25
Rydberg energy	$\hbar c R_\infty = m_e e^4 / 2(4\pi\epsilon_0)^2 \hbar^2 = m_e c^2 \alpha^2 / 2$	13.605 691 93(34) eV	25
Thomson cross section	$\sigma_T = 8\pi r_e^2 / 3$	0.665 245 8558(27) barn	4.1

Bohr magneton	$\mu_B = eh/2m_e$	5.788 381 7555(79) $\times 10^{-11}$ MeV T ⁻¹	1.4
nuclear magneton	$\mu_N = eh/2m_p$	3.152 451 2326(45) $\times 10^{-14}$ MeV T ⁻¹	1.4
electron cyclotron freq./field	$\omega_{\text{cycl}}^e/B = e/m_e$	1.758 820 150(44) $\times 10^{11}$ rad s ⁻¹ T ⁻¹	25
proton cyclotron freq./field	$\omega_{\text{cycl}}^p/B = e/m_p$	9.578 833 92(24) $\times 10^7$ rad s ⁻¹ T ⁻¹	25
gravitational constant [‡]	G_N	6.674 28(67) $\times 10^{-11}$ m ³ kg ⁻¹ s ⁻² = 6.708 81(67) $\times 10^{-39}$ hc (GeV/c ²) ⁻²	1.0 $\times 10^5$ 1.0 $\times 10^5$
standard gravitational accel.	g_N	9.806 65 m s ⁻²	exact
Avogadro constant	N_A	6.022 141 79(30) $\times 10^{23}$ mol ⁻¹	50
Boltzmann constant	k	1.380 6504(24) $\times 10^{-23}$ J K ⁻¹ = 8.617 343(15) $\times 10^{-5}$ eV K ⁻¹	1700 1700
molar volume, ideal gas at STP	$N_A k(273.15 \text{ K}) / (101\,325 \text{ Pa})$	22.413 996(39) $\times 10^{-3}$ m ³ mol ⁻¹	1700
Wien displacement law constant	$b = \lambda_{\text{max}} T$	2.897 7685(51) $\times 10^{-3}$ m K	1700
Stefan-Boltzmann constant	$\sigma = \pi^2 k^4 / 60h^3 c^2$	5.670 400(40) $\times 10^{-8}$ W m ⁻² K ⁻⁴	7000
Fermi coupling constant**	$G_F / (hc)^3$	1.166 37(1) $\times 10^{-5}$ GeV ⁻²	9000
weak-mixing angle	$\sin^2 \theta(M_Z)$ ($\overline{\text{MS}}$)	0.231 16(13) ^{††}	5.6 $\times 10^5$
W^\pm boson mass	m_W	80.399(23) GeV/c ²	2.9 $\times 10^5$
Z^0 boson mass	m_Z	91.1876(21) GeV/c ²	2.3 $\times 10^4$
strong coupling constant	$\alpha_s(m_Z)$	0.1184(7)	5.9 $\times 10^6$
π		e = 2.718 281 828 459 045 235 1 eV = 1.602 176 487(40) $\times 10^{-19}$ J 1 eV/c ² = 1.782 661 758(44) $\times 10^{-36}$ kg	$\gamma = 0.577\,215\,664\,901\,532\,861$ kT at 300 K = [38.681 685(68)] ⁻¹ eV 0 °C \equiv 273.15 K
1 in \equiv 0.0254 m	1 G \equiv 10 ⁻⁴ T		
1 Å \equiv 0.1 nm	1 dyne \equiv 10 ⁻⁵ N		
1 barn \equiv 10 ⁻²⁸ m ²	1 erg \equiv 10 ⁻⁷ J	2.997 924 58 $\times 10^9$ esu = 1 C	1 atmosphere \equiv 760 Torr \equiv 101 325 Pa

* The meter is the length of the path traveled by light in vacuum during a time interval of 1/299 792 458 of a second.

† At $Q^2 = 0$. At $Q^2 \approx m_W^2$, the value is $\sim 1/128$. • † Absolute lab measurements of G_N have been made only on scales of about 1 cm to 1 m.

** See the discussion in Sec. 10, "Electroweak model and constraints on new physics."

†† The corresponding $\sin^2 \theta$ for the effective angle is 0.23146(12).

2. ASTROPHYSICAL CONSTANTS AND PARAMETERS

Table 2.1. Revised May 2010 by E. Bergren and D.E. Groom (IBNL). Figures in parentheses give $1-\sigma$ uncertainties in last place(s). This table represents neither a critical review nor an adjustment of the constants, and is not intended as a primary reference. See the full edition of this *Review* for references and detailed explanations.

Quantity	Symbol, equation	Value	Reference, footnote
speed of light	c	299 792 458 m s ⁻¹	exact[4]
Newtonian gravitational constant	G_N	$6.6743(7) \times 10^{-11}$ m ³ kg ⁻¹ s ⁻²	[1]
Planck mass	$\sqrt{\hbar c/G_N}$	$1.22089(6) \times 10^{19}$ GeV/ c^2 $= 2.17644(11) \times 10^{-8}$ kg	[1]
Planck length	$\sqrt{\hbar G_N/c^3}$	$1.61625(8) \times 10^{-35}$ m	[1]
standard gravitational acceleration	g_N	9.80665 ms ⁻² $\approx \pi^2$	exact[1]
jansky (flux density)	Jy	10^{-26} W m ⁻² Hz ⁻¹	definition
tropical year (equinox to equinox) (2011)	yr	$31\,556\,925.2$ s $\approx \pi \times 10^7$ s	[5]
sidereal year (fixed star to fixed star) (2011)	yr	$31\,558\,149.8$ s $\approx \pi \times 10^7$ s	[5]
mean sidereal day (2011) (time between vernal equinox transits)		$23^{\text{h}}\,56^{\text{m}}\,04^{\text{s}}.090\,53$	[5]
astronomical unit	au, A	$149\,597\,870\,700(3)$ m	[6]
parsec (1 au/1 arc sec)	pc	3.0856776×10^{16} m = $3.262 \dots$ ly	[7]
light year (deprecated unit)	ly	$0.3066 \dots$ pc = $0.946053 \dots \times 10^{16}$ m	
Schwarzschild radius of the Sun	$2G_N M_\odot/c^2$	$2.9532500770(2)$ km	[8]
Solar mass	M_\odot	$1.9884(2) \times 10^{30}$ kg	[9]
Solar equatorial radius	R_\odot	$6.9551(4) \times 10^8$ m	[10]
Solar luminosity	L_\odot	$3.8427(14) \times 10^{26}$ W	[11]
Schwarzschild radius of the Earth	$2G_N M_\oplus/c^2$	$8.87005594(2)$ mm	[12]
Earth mass	M_\oplus	$5.9722(6) \times 10^{24}$ kg	[13]
Earth mean equatorial radius	R_\oplus	6.378137×10^6 m	[5]
luminosity conversion (deprecated)	L	$3.02 \times 10^{28} \times 10^{-0.4 M_{\text{bol}}}$ W	[14]
flux conversion (deprecated)	\mathcal{F}	(M_{bol} = absolute bolometric magnitude = bolometric magnitude at 10 pc) $2.52 \times 10^{-8} \times 10^{-0.4 m_{\text{bol}}}$ W m ⁻²	from above
ABsolute monochromatic magnitude	AB	(m_{bol} = apparent bolometric magnitude) $-2.5 \log_{10} f_\nu - 56.10$ (for f_ν in W m ⁻² Hz ⁻¹) $= -2.5 \log_{10} f_\nu + 8.90$ (for f_ν in Jy)	[15]
Solar distance from Galactic center	R_0	$8.4(4)$ kpc	[16]
Solar circular velocity at R_0/R_0	v_\odot/R_0	30.2 ± 0.2 km s ⁻¹ kpc ⁻¹	[17]
circular velocity at R_0	Θ_0	$240(10)$ km s ⁻¹	[18]
local disk density	ρ_{disk}	$3\text{--}12 \times 10^{-24}$ g cm ⁻³ $\approx 2\text{--}7$ GeV/ c^2 cm ⁻³	[19]
local dark matter density	ρ_χ	canonical value 0.3 GeV/ c^2 cm ⁻³ within factor 2-3	[20]
escape velocity from Galaxy	v_{esc}	498 km/s $< v_{\text{esc}} < 608$ km/s	[21]

present day CMB temperature	T_0	2.725(1) K	[22]
present day CMB dipole amplitude		3.355(8) mK	[2]
Solar velocity with respect to CMB	v_{LG}	369(11) km/s towards $(l, b) = (263.99(14)^\circ, 48.26(3)^\circ)$	[2]
Local Group velocity with respect to CMB	s/h	627(22) km/s towards $(l, b) = (276(3)^\circ, 30(3)^\circ)$	[23]
entropy density/Boltzmann constant	n_γ	2.889.2 $(T/2.725)^3 \text{ cm}^{-3}$	[14]
number density of CMB photons	$\eta = n_b/n_\gamma$	410.5 $(T/2.725)^3 \text{ cm}^{-3}$	[24]
baryon-to-photon ratio [†]		6.23(17) $\times 10^{-10}$	[2]
number density of baryons [‡]	n_b	$5.1 \times 10^{-10} \leq \eta \leq 6.5 \times 10^{-10}$ (95% CL)	[25]
present day Hubble expansion rate	H_0	$(2.56 \pm 0.07) \times 10^{-7} \text{ cm}^{-3}$	from η in [2]
Hubble length	h	$(2.1 \times 10^{-7} < n_b < 2.7 \times 10^{-7}) \text{ cm}^{-3}$ (95% CL)	from η in [25]
scale factor for cosmological constant	c/H_0	$100 h \text{ km s}^{-1} \text{ Mpc}^{-1} = h \times (9.777752 \text{ Gyr})^{-1}$	[26]
critical density of the Universe	$\rho_c = 3H_0^2/8\pi G_N$	0.72(3)	[2,3]
		$0.925\,063 \times 10^{26} h^{-1} \text{ m} = 1.28(5) \times 10^{26} \text{ m}$	
		$2.852 \times 10^{51} h^{-2} \text{ m}^2 = 5.5(5) \times 10^{51} \text{ m}^2$	
		$2.775\,366\,27 \times 10^{11} h^2 M_\odot \text{ Mpc}^{-3}$	
		$= 1.878\,35(19) \times 10^{-29} h^2 \text{ g cm}^{-3}$	
		$= 1.053\,68(11) \times 10^{-5} h^2 (\text{GeV}/c^2) \text{ cm}^{-3}$	
pressureless matter density of the Universe [†]	$\Omega_m = \rho_m/\rho_c$	0.133(6) $h^{-2} = 0.26(2)$	[2,3]
baryon density of the Universe [†]	$\Omega_b = \rho_b/\rho_c$	0.0227(6) $h^{-2} = 0.044(4)$	[2,3]
dark matter density of the universe [†]	$\Omega_{\text{cdm}} = \Omega_m - \Omega_b - \Omega_\nu$	0.110(6) $h^{-2} = 0.21(2)$	[2,3]
dark energy density of the Λ CDM Universe [†]	Ω_Λ	0.74(3)	[2,3]
dark energy equation of state parameter	w	$-1.04^{+0.00}_{-0.10}$	[27]
CMB radiation density of the Universe	$\Omega_\gamma = \rho_\gamma/\rho_c$	$2.471 \times 10^{-5} (T/2.725)^4 h^{-2} = 4.8(4) \times 10^{-5}$	[24]
neutrino density of the Universe [†]	$\Omega_{\text{tot}} = \Omega_m + \dots + \Omega_\Lambda$	0.0005 $< \Omega_\nu h^2 < 0.025 \Rightarrow 0.0009 < \Omega_\nu < 0.048$	[28]
total energy density of the Universe [†]	σ_8	1.006(6)	[2,3]
fluctuation amplitude at $8h^{-1}$ Mpc scale [†]	$\Delta_{\mathcal{R}}$	0.80(4)	[2,3]
curvature fluctuation amplitude, $k_0 = 0.002 \text{ Mpc}^{-1 \ddagger}$	n_s	$2.41(11) \times 10^{-9}$	[2,3]
scalar spectral index [†]	$dn_s/d \ln k$	0.96(1)	[2,3]
running spectral index slope, $k_0 = 0.002 \text{ Mpc}^{-1 \ddagger}$	$r = T/S$	$-0.04(3)$	[2]
tensor-to-scalar field perturbations ratio,	z_*	< 0.43 at 95% C.L.	[2,3]
redshift at decoupling [†]	z_*	1090(1)	[2]
age at decoupling [†]	t_*	$3.80(6) \times 10^5 \text{ yr}$	[2]
sound horizon at decoupling [†]	$r_s(z_*)$	147(2) Mpc	[2]
redshift of matter-radiation equality [†]	z_{eq}	3180 ± 150	[2]
redshift of reionization [†]	z_{reion}	11.0 ± 1.4	[2]
age at reionization [†]	t_{reion}	$430^{+90}_{-70} \text{ Myr}$	[2,26]
reionization optical depth [†]	τ	0.09(2)	[2,3]
age of the Universe [†]	t_0	$13.69 \pm 0.13 \text{ Gyr}$	[2]

SUMMARY TABLES OF PARTICLE PROPERTIES

Extracted from the Particle Listings of the
Review of Particle Physics

K. Nakamura *et al.* (Particle Data Group), JP G **37**, 075021 (2010)
Available at <http://pdg.lbl.gov>

©Regents of the University of California
(Approximate closing date for data: January 15, 2010)

GAUGE AND HIGGS BOSONS

γ

$$I(J^{PC}) = 0,1(1^{--})$$

Mass $m < 1 \times 10^{-18}$ eV
Charge $q < 1 \times 10^{-35}$ e
Mean life $\tau = \text{Stable}$

g
or gluon

$$I(J^P) = 0(1^-)$$

Mass $m = 0$ [a]
SU(3) color octet

W

$$J = 1$$

Charge = ± 1 e
Mass $m = 80.399 \pm 0.023$ GeV
 $m_Z - m_W = 10.4 \pm 1.6$ GeV
 $m_{W^+} - m_{W^-} = -0.2 \pm 0.6$ GeV
Full width $\Gamma = 2.085 \pm 0.042$ GeV
 $\langle N_{\pi^\pm} \rangle = 15.70 \pm 0.35$
 $\langle N_{K^\pm} \rangle = 2.20 \pm 0.19$
 $\langle N_p \rangle = 0.92 \pm 0.14$
 $\langle N_{\text{charged}} \rangle = 19.39 \pm 0.08$

W^- modes are charge conjugates of the modes below.

W^+ DECAY MODES	Fraction (Γ_i/Γ)	Confidence level	p (MeV/c)
$\ell^+ \nu$	[b] $(10.80 \pm 0.09) \%$		—
$e^+ \nu$	$(10.75 \pm 0.13) \%$		40199
$\mu^+ \nu$	$(10.57 \pm 0.15) \%$		40199
$\tau^+ \nu$	$(11.25 \pm 0.20) \%$		40180
hadrons	$(67.60 \pm 0.27) \%$		—
$\pi^+ \gamma$	< 8	$\times 10^{-5}$	95% 40199
$D_s^+ \gamma$	< 1.3	$\times 10^{-3}$	95% 40175
cX	$(33.4 \pm 2.6) \%$		—
$c\bar{s}$	$(31^{+13}_{-11}) \%$		—
invisible	[c] $(1.4 \pm 2.9) \%$		—

Z

$$J = 1$$

$$\text{Charge} = 0$$

$$\text{Mass } m = 91.1876 \pm 0.0021 \text{ GeV } [d]$$

$$\text{Full width } \Gamma = 2.4952 \pm 0.0023 \text{ GeV}$$

$$\Gamma(\ell^+ \ell^-) = 83.984 \pm 0.086 \text{ MeV } [b]$$

$$\Gamma(\text{invisible}) = 499.0 \pm 1.5 \text{ MeV } [e]$$

$$\Gamma(\text{hadrons}) = 1744.4 \pm 2.0 \text{ MeV}$$

$$\Gamma(\mu^+ \mu^-) / \Gamma(e^+ e^-) = 1.0009 \pm 0.0028$$

$$\Gamma(\tau^+ \tau^-) / \Gamma(e^+ e^-) = 1.0019 \pm 0.0032 [f]$$

Average charged multiplicity

$$\langle N_{\text{charged}} \rangle = 20.76 \pm 0.16 \quad (S = 2.1)$$

Couplings to leptons

$$g_V^\ell = -0.03783 \pm 0.00041$$

$$g_V^u = 0.29^{+0.10}_{-0.08}$$

$$g_V^d = -0.33^{+0.05}_{-0.07}$$

$$g_A^\ell = -0.50123 \pm 0.00026$$

$$g_A^u = 0.50^{+0.04}_{-0.07}$$

$$g_A^d = -0.524^{+0.050}_{-0.030}$$

$$g^{\nu\ell} = 0.5008 \pm 0.0008$$

$$g^{\nu e} = 0.53 \pm 0.09$$

$$g^{\nu\mu} = 0.502 \pm 0.017$$

Asymmetry parameters [g]

$$A_e = 0.1515 \pm 0.0019$$

$$A_\mu = 0.142 \pm 0.015$$

$$A_\tau = 0.143 \pm 0.004$$

$$A_S = 0.90 \pm 0.09$$

$$A_C = 0.670 \pm 0.027$$

$$A_b = 0.923 \pm 0.020$$

Charge asymmetry (%) at Z pole

$$A_{FB}^{(0\ell)} = 1.71 \pm 0.10$$

$$A_{FB}^{(0u)} = 4 \pm 7$$

$$A_{FB}^{(0s)} = 9.8 \pm 1.1$$

$$A_{FB}^{(0c)} = 7.07 \pm 0.35$$

$$A_{FB}^{(0b)} = 9.92 \pm 0.16$$

Z DECAY MODES	Fraction (Γ_i/Γ)	Scale factor/ Confidence level	p (MeV/c)
$e^+ e^-$	(3.363 \pm 0.004) %		45594
$\mu^+ \mu^-$	(3.366 \pm 0.007) %		45594
$\tau^+ \tau^-$	(3.367 \pm 0.008) %		45559
$\ell^+ \ell^-$	[b] (3.3658 \pm 0.0023) %		—
invisible	(20.00 \pm 0.06) %		—
hadrons	(69.91 \pm 0.06) %		—
$(u\bar{u} + c\bar{c})/2$	(11.6 \pm 0.6) %		—
$(d\bar{d} + s\bar{s} + b\bar{b})/3$	(15.6 \pm 0.4) %		—
$c\bar{c}$	(12.03 \pm 0.21) %		—
$b\bar{b}$	(15.12 \pm 0.05) %		—
$b\bar{b}b\bar{b}$	(3.6 \pm 1.3) $\times 10^{-4}$		—

$g g g$		< 1.1	%	CL=95%	—
$\pi^0 \gamma$		< 5.2	$\times 10^{-5}$	CL=95%	45594
$\eta \gamma$		< 5.1	$\times 10^{-5}$	CL=95%	45592
$\omega \gamma$		< 6.5	$\times 10^{-4}$	CL=95%	45590
$\eta'(958) \gamma$		< 4.2	$\times 10^{-5}$	CL=95%	45589
$\gamma \gamma$		< 5.2	$\times 10^{-5}$	CL=95%	45594
$\gamma \gamma \gamma$		< 1.0	$\times 10^{-5}$	CL=95%	45594
$\pi^\pm W^\mp$	[h]	< 7	$\times 10^{-5}$	CL=95%	10150
$\rho^\pm W^\mp$	[h]	< 8.3	$\times 10^{-5}$	CL=95%	10124
$J/\psi(1S)X$		(3.51 $\pm^{+0.23}_{-0.25}$)	$\times 10^{-3}$	S=1.1	—
$\psi(2S)X$		(1.60 ± 0.29)	$\times 10^{-3}$		—
$\chi_{c1}(1P)X$		(2.9 ± 0.7)	$\times 10^{-3}$		—
$\chi_{c2}(1P)X$		< 3.2	$\times 10^{-3}$	CL=90%	—
$\Upsilon(1S)X + \Upsilon(2S)X + \Upsilon(3S)X$		(1.0 ± 0.5)	$\times 10^{-4}$		—
$\Upsilon(1S)X$		< 4.4	$\times 10^{-5}$	CL=95%	—
$\Upsilon(2S)X$		< 1.39	$\times 10^{-4}$	CL=95%	—
$\Upsilon(3S)X$		< 9.4	$\times 10^{-5}$	CL=95%	—
$(D^0/\bar{D}^0)X$		(20.7 ± 2.0)	%		—
$D^\pm X$		(12.2 ± 1.7)	%		—
$D^*(2010)^\pm X$	[h]	(11.4 ± 1.3)	%		—
$D_{s1}(2536)^\pm X$		(3.6 ± 0.8)	$\times 10^{-3}$		—
$D_{sJ}(2573)^\pm X$		(5.8 ± 2.2)	$\times 10^{-3}$		—
$D^{*'}(2629)^\pm X$		searched for			—
$B^+ X$	[l]	(6.08 ± 0.13)	%		—
$B_S^0 X$	[l]	(1.59 ± 0.13)	%		—
$B_c^+ X$		searched for			—
$\Lambda_c^+ X$		(1.54 ± 0.33)	%		—
$\Xi_c^0 X$		seen			—
$\Xi_b X$		seen			—
b -baryon X	[l]	(1.38 ± 0.22)	%		—
anomalous γ + hadrons	[j]	< 3.2	$\times 10^{-3}$	CL=95%	—
$e^+ e^- \gamma$	[j]	< 5.2	$\times 10^{-4}$	CL=95%	45594
$\mu^+ \mu^- \gamma$	[j]	< 5.6	$\times 10^{-4}$	CL=95%	45594
$\tau^+ \tau^- \gamma$	[j]	< 7.3	$\times 10^{-4}$	CL=95%	45559
$\ell^+ \ell^- \gamma \gamma$	[k]	< 6.8	$\times 10^{-6}$	CL=95%	—
$q \bar{q} \gamma \gamma$	[k]	< 5.5	$\times 10^{-6}$	CL=95%	—
$\nu \bar{\nu} \gamma \gamma$	[k]	< 3.1	$\times 10^{-6}$	CL=95%	45594
$e^\pm \mu^\mp$	LF	[h] < 1.7	$\times 10^{-6}$	CL=95%	45594
$e^\pm \tau^\mp$	LF	[h] < 9.8	$\times 10^{-6}$	CL=95%	45576
$\mu^\pm \tau^\mp$	LF	[h] < 1.2	$\times 10^{-5}$	CL=95%	45576
$p e$	L,B	< 1.8	$\times 10^{-6}$	CL=95%	45589
$p \mu$	L,B	< 1.8	$\times 10^{-6}$	CL=95%	45589

Higgs Bosons — H^0 and H^\pm , Searches for

The limits for H_1^0 and A_0 refer to the m_h^{max} benchmark scenario for the supersymmetric parameters.

H^0 Mass $m > 114.4$ GeV, CL = 95%

H_1^0 in Supersymmetric Models ($m_{H_1^0} < m_{H_2^0}$)

Mass $m > 92.8$ GeV, CL = 95%

A^0 Pseudoscalar Higgs Boson in Supersymmetric Models [1]

Mass $m > 93.4$ GeV, CL = 95% $\tan\beta > 0.4$

H^\pm Mass $m > 79.3$ GeV, CL = 95%

See the Particle Listings in the Full *Review of Particle Physics* for a Note giving details of Higgs Bosons.

Heavy Bosons Other Than Higgs Bosons, Searches for
Additional W Bosons

W' with standard couplings decaying to $e\nu$

Mass $m > 1.000 \times 10^3$ GeV, CL = 95%

Additional Z Bosons

Z'_{SM} with standard couplings

Mass $m > 1.030 \times 10^3$ GeV, CL = 95% ($p\bar{p}$ direct search)

Mass $m > 1500$ GeV, CL = 95% (electroweak fit)

Z_{LR} of $SU(2)_L \times SU(2)_R \times U(1)$ (with $g_L = g_R$)

Mass $m > 630$ GeV, CL = 95% ($p\bar{p}$ direct search)

Mass $m > 998$ GeV, CL = 95% (electroweak fit)

Z_χ of $SO(10) \rightarrow SU(5) \times U(1)_\chi$ (with $g_\chi = e/\cos\theta_W$)

Mass $m > 892$ GeV, CL = 95% ($p\bar{p}$ direct search)

Mass $m > 781$ GeV, CL = 95% (electroweak fit)

Z_ψ of $E_6 \rightarrow SO(10) \times U(1)_\psi$ (with $g_\psi = e/\cos\theta_W$)

Mass $m > 878$ GeV, CL = 95% ($p\bar{p}$ direct search)

Mass $m > 475$ GeV, CL = 95% (electroweak fit)

Z_η of $E_6 \rightarrow SU(3) \times SU(2) \times U(1) \times U(1)_\eta$ (with $g_\eta = e/\cos\theta_W$)

Mass $m > 904$ GeV, CL = 95% ($p\bar{p}$ direct search)

Mass $m > 619$ GeV, CL = 95% (electroweak fit)

Scalar Leptoquarks

Mass $m > 299$ GeV, CL = 95% (1st generation, pair prod.)

Mass $m > 298$ GeV, CL = 95% (1st gener., single prod.)

Mass $m > 316$ GeV, CL = 95% (2nd gener., pair prod.)

Mass $m > 73$ GeV, CL = 95% (2nd gener., single prod.)

Mass $m > 229$ GeV, CL = 95% (3rd gener., pair prod.)

(See the Particle Listings in the Full *Review of Particle Physics* for assumptions on leptoquark quantum numbers and branching fractions.)

Axions (A^0) and Other Very Light Bosons, Searches for

The standard Peccei-Quinn axion is ruled out. Variants with reduced couplings or much smaller masses are constrained by various data. The Particle Listings in the full *Review* contain a Note discussing axion searches.

The best limit for the half-life of neutrinoless double beta decay with Majoron emission is $> 7.2 \times 10^{24}$ years (CL = 90%).

NOTES

In this Summary Table:

When a quantity has “(S = ...)” to its right, the error on the quantity has been enlarged by the “scale factor” S, defined as $S = \sqrt{\chi^2/(N-1)}$, where N is the number of measurements used in calculating the quantity. We do this when $S > 1$, which often indicates that the measurements are inconsistent. When $S > 1.25$, we also show in the Particle Listings an ideogram of the measurements. For more about S, see the Introduction.

A decay momentum p is given for each decay mode. For a 2-body decay, p is the momentum of each decay product in the rest frame of the decaying particle. For a 3-or-more-body decay, p is the largest momentum any of the products can have in this frame.

[a] Theoretical value. A mass as large as a few MeV may not be precluded.

[b] ℓ indicates each type of lepton (e , μ , and τ), not sum over them.

[c] This represents the width for the decay of the W boson into a charged particle with momentum below detectability, $p < 200$ MeV.

[d] The Z -boson mass listed here corresponds to a Breit-Wigner resonance parameter. It lies approximately 34 MeV above the real part of the position of the pole (in the energy-squared plane) in the Z -boson propagator.

[e] This partial width takes into account Z decays into $\nu\bar{\nu}$ and any other possible undetected modes.

[f] This ratio has not been corrected for the τ mass.

[g] Here $A \equiv 2g_V g_A / (g_V^2 + g_A^2)$.

[h] The value is for the sum of the charge states or particle/antiparticle states indicated.

[i] This value is updated using the product of (i) the $Z \rightarrow b\bar{b}$ fraction from this listing and (ii) the b -hadron fraction in an unbiased sample of weakly decaying b -hadrons produced in Z -decays provided by the Heavy Flavor Averaging Group (HFAG, http://www.slac.stanford.edu/xorg/hfag/osc/PDG_2009/#FRACZ).

[j] See the Z Particle Listings in the Full *Review of Particle Physics* for the γ energy range used in this measurement.

[k] For $m_{\gamma\gamma} = (60 \pm 5)$ GeV.

[l] The limits assume no invisible decays.

LEPTONS

e

$$J = \frac{1}{2}$$

$$\text{Mass } m = (548.57990943 \pm 0.00000023) \times 10^{-6} \text{ u}$$

$$\text{Mass } m = 0.510998910 \pm 0.000000013 \text{ MeV}$$

$$|m_{e^+} - m_{e^-}|/m < 8 \times 10^{-9}, \text{ CL} = 90\%$$

$$|q_{e^+} + q_{e^-}|/e < 4 \times 10^{-8}$$

Magnetic moment anomaly

$$(g-2)/2 = (1159.65218073 \pm 0.00000028) \times 10^{-6}$$

$$(g_{e^+} - g_{e^-}) / g_{\text{average}} = (-0.5 \pm 2.1) \times 10^{-12}$$

$$\text{Electric dipole moment } d = (0.07 \pm 0.07) \times 10^{-26} \text{ e cm}$$

$$\text{Mean life } \tau > 4.6 \times 10^{26} \text{ yr, CL} = 90\% \text{ [a]}$$

 μ

$$J = \frac{1}{2}$$

$$\text{Mass } m = 0.1134289256 \pm 0.0000000029 \text{ u}$$

$$\text{Mass } m = 105.658367 \pm 0.0000004 \text{ MeV}$$

$$\text{Mean life } \tau = (2.197034 \pm 0.000021) \times 10^{-6} \text{ s } (S = 1.2)$$

$$\tau_{\mu^+}/\tau_{\mu^-} = 1.00002 \pm 0.00008$$

$$c\tau = 658.654 \text{ m}$$

$$\text{Magnetic moment anomaly } (g-2)/2 = (11659209 \pm 6) \times 10^{-10}$$

$$(g_{\mu^+} - g_{\mu^-}) / g_{\text{average}} = (-0.11 \pm 0.12) \times 10^{-8}$$

$$\text{Electric dipole moment } d = (-0.1 \pm 0.9) \times 10^{-19} \text{ e cm}$$

Decay parameters [b]

$$\rho = 0.7503 \pm 0.0004$$

$$\eta = 0.057 \pm 0.034$$

$$\delta = 0.7504 \pm 0.0006$$

$$\xi P_{\mu} = 1.0007 \pm 0.0035 \text{ [c]}$$

$$\xi P_{\mu} \delta / \rho > 0.99682, \text{ CL} = 90\% \text{ [c]}$$

$$\xi' = 1.00 \pm 0.04$$

$$\xi'' = 0.7 \pm 0.4$$

$$\alpha/A = (0 \pm 4) \times 10^{-3}$$

$$\alpha'/A = (-10 \pm 20) \times 10^{-3}$$

$$\beta/A = (4 \pm 6) \times 10^{-3}$$

$$\beta'/A = (2 \pm 7) \times 10^{-3}$$

$$\bar{\eta} = 0.02 \pm 0.08$$

μ^+ modes are charge conjugates of the modes below.

μ^- DECAY MODES	Fraction (Γ_i/Γ)	Confidence level	P (MeV/c)
$e^- \bar{\nu}_e \nu_{\mu}$	$\approx 100\%$		53
$e^- \bar{\nu}_e \nu_{\mu} \gamma$	[d] $(1.4 \pm 0.4) \%$		53
$e^- \bar{\nu}_e \nu_{\mu} e^+ e^-$	[e] $(3.4 \pm 0.4) \times 10^{-5}$		53
Lepton Family number (LF) violating modes			
$e^- \nu_e \bar{\nu}_{\mu}$	LF [f] < 1.2	%	90%
$e^- \gamma$	LF < 1.2	$\times 10^{-11}$	90%
$e^- e^+ e^-$	LF < 1.0	$\times 10^{-12}$	90%
$e^- 2\gamma$	LF < 7.2	$\times 10^{-11}$	90%

τ

$$J = \frac{1}{2}$$

Mass $m = 1776.82 \pm 0.16$ MeV

$(m_{\tau^+} - m_{\tau^-})/m_{\text{average}} < 2.8 \times 10^{-4}$, CL = 90%

Mean life $\tau = (290.6 \pm 1.0) \times 10^{-15}$ s

$$c\tau = 87.11 \mu\text{m}$$

Magnetic moment anomaly > -0.052 and < 0.013 , CL = 95%

$\text{Re}(d_\tau) = -0.22$ to 0.45×10^{-16} e cm, CL = 95%

$\text{Im}(d_\tau) = -0.25$ to 0.008×10^{-16} e cm, CL = 95%

Weak dipole moment

$\text{Re}(d_\tau^W) < 0.50 \times 10^{-17}$ e cm, CL = 95%

$\text{Im}(d_\tau^W) < 1.1 \times 10^{-17}$ e cm, CL = 95%

Weak anomalous magnetic dipole moment

$\text{Re}(\alpha_\tau^W) < 1.1 \times 10^{-3}$, CL = 95%

$\text{Im}(\alpha_\tau^W) < 2.7 \times 10^{-3}$, CL = 95%

Decay parameters

See the τ Particle Listings in the Full *Review of Particle Physics* for a note concerning τ -decay parameters.

$$\rho(e \text{ or } \mu) = 0.745 \pm 0.008$$

$$\rho(e) = 0.747 \pm 0.010$$

$$\rho(\mu) = 0.763 \pm 0.020$$

$$\xi(e \text{ or } \mu) = 0.985 \pm 0.030$$

$$\xi(e) = 0.994 \pm 0.040$$

$$\xi(\mu) = 1.030 \pm 0.059$$

$$\eta(e \text{ or } \mu) = 0.013 \pm 0.020$$

$$\eta(\mu) = 0.094 \pm 0.073$$

$$(\delta\xi)(e \text{ or } \mu) = 0.746 \pm 0.021$$

$$(\delta\xi)(e) = 0.734 \pm 0.028$$

$$(\delta\xi)(\mu) = 0.778 \pm 0.037$$

$$\xi(\pi) = 0.993 \pm 0.022$$

$$\xi(\rho) = 0.994 \pm 0.008$$

$$\xi(a_1) = 1.001 \pm 0.027$$

$$\xi(\text{all hadronic modes}) = 0.995 \pm 0.007$$

τ^+ modes are charge conjugates of the modes below. “ h^\pm ” stands for π^\pm or K^\pm . “ ℓ ” stands for e or μ . “Neutrals” stands for γ 's and/or π^0 's.

τ^- DECAY MODES	Fraction (Γ_i/Γ)	Scale factor/ Confidence level	p (MeV/c)
Modes with one charged particle			
particle $^- \geq 0$ neutrals $\geq 0K^0\nu_\tau$ (“1-prong”)	(85.36 \pm 0.08) %	S=1.3	–
particle $^- \geq 0$ neutrals $\geq 0K_L^0\nu_\tau$	(84.72 \pm 0.08) %	S=1.4	–
$\mu^- \bar{\nu}_\mu \nu_\tau$	[g] (17.36 \pm 0.05) %		885
$\mu^- \bar{\nu}_\mu \nu_\tau \gamma$	[e] (3.6 \pm 0.4) $\times 10^{-3}$		885
$e^- \bar{\nu}_e \nu_\tau$	[g] (17.85 \pm 0.05) %		888
$e^- \bar{\nu}_e \nu_\tau \gamma$	[e] (1.75 \pm 0.18) %		888
$h^- \geq 0K_L^0 \nu_\tau$	(12.13 \pm 0.07) %	S=1.1	883
$h^- \nu_\tau$	(11.61 \pm 0.06) %	S=1.1	883
$\pi^- \nu_\tau$	[g] (10.91 \pm 0.07) %	S=1.1	883
$K^- \nu_\tau$	[g] (6.96 \pm 0.23) $\times 10^{-3}$	S=1.1	820

$h^- \geq 1$ neutrals ν_τ	(37.06 ± 0.10) %	S=1.2	—
$h^- \geq 1\pi^0 \nu_\tau$ (ex. K^0)	(36.54 ± 0.11) %	S=1.2	—
$h^- \pi^0 \nu_\tau$	(25.94 ± 0.09) %	S=1.1	878
$\pi^- \pi^0 \nu_\tau$ [g]	(25.51 ± 0.09) %	S=1.1	878
$\pi^- \pi^0$ non- $\rho(770) \nu_\tau$	(3.0 ± 3.2) × 10 ⁻³		878
$K^- \pi^0 \nu_\tau$ [g]	(4.29 ± 0.15) × 10 ⁻³		814
$h^- \geq 2\pi^0 \nu_\tau$	(10.85 ± 0.12) %	S=1.3	—
$h^- 2\pi^0 \nu_\tau$	(9.51 ± 0.11) %	S=1.2	862
$h^- 2\pi^0 \nu_\tau$ (ex. K^0)	(9.35 ± 0.11) %	S=1.2	862
$\pi^- 2\pi^0 \nu_\tau$ (ex. K^0) [g]	(9.29 ± 0.11) %	S=1.2	862
$\pi^- 2\pi^0 \nu_\tau$ (ex. K^0),	< 9 × 10 ⁻³	CL=95%	862
scalar			
$\pi^- 2\pi^0 \nu_\tau$ (ex. K^0),	< 7 × 10 ⁻³	CL=95%	862
vector			
$K^- 2\pi^0 \nu_\tau$ (ex. K^0) [g]	(6.5 ± 2.3) × 10 ⁻⁴		796
$h^- \geq 3\pi^0 \nu_\tau$	(1.34 ± 0.07) %	S=1.1	—
$h^- \geq 3\pi^0 \nu_\tau$ (ex. K^0)	(1.25 ± 0.07) %	S=1.1	—
$h^- 3\pi^0 \nu_\tau$	(1.18 ± 0.08) %		836
$\pi^- 3\pi^0 \nu_\tau$ (ex. K^0) [g]	(1.04 ± 0.07) %		836
$K^- 3\pi^0 \nu_\tau$ (ex. K^0, η) [g]	(4.9 ± 2.3) × 10 ⁻⁴	S=1.1	765
$h^- 4\pi^0 \nu_\tau$ (ex. K^0)	(1.5 ± 0.4) × 10 ⁻³		800
$h^- 4\pi^0 \nu_\tau$ (ex. K^0, η) [g]	(1.1 ± 0.4) × 10 ⁻³		800
$K^- \geq 0\pi^0 \geq 0K^0 \geq 0\gamma \nu_\tau$	(1.57 ± 0.04) %	S=1.1	820
$K^- \geq 1 (\pi^0 \text{ or } K^0 \text{ or } \gamma) \nu_\tau$	(8.72 ± 0.32) × 10 ⁻³	S=1.1	—

Modes with K^0 's

K_S^0 (particles) $^- \nu_\tau$	(9.2 ± 0.4) × 10 ⁻³	S=1.5	—
$h^- \overline{K}^0 \nu_\tau$	(1.00 ± 0.05) %	S=1.8	812
$\pi^- \overline{K}^0 \nu_\tau$ [g]	(8.4 ± 0.4) × 10 ⁻³	S=2.1	812
$\pi^- \overline{K}^0$ (non- $K^*(892)^-$) ν_τ	(5.4 ± 2.1) × 10 ⁻⁴		812
$K^- K^0 \nu_\tau$ [g]	(1.59 ± 0.16) × 10 ⁻³		737
$K^- K^0 \geq 0\pi^0 \nu_\tau$	(3.18 ± 0.24) × 10 ⁻³		737
$h^- \overline{K}^0 \pi^0 \nu_\tau$	(5.5 ± 0.4) × 10 ⁻³		794
$\pi^- \overline{K}^0 \pi^0 \nu_\tau$ [g]	(4.0 ± 0.4) × 10 ⁻³		794
$\overline{K}^0 \rho^- \nu_\tau$	(2.2 ± 0.5) × 10 ⁻³		612
$K^- K^0 \pi^0 \nu_\tau$ [g]	(1.59 ± 0.20) × 10 ⁻³		685
$\pi^- \overline{K}^0 \geq 1\pi^0 \nu_\tau$	(3.2 ± 1.0) × 10 ⁻³		—
$\pi^- \overline{K}^0 \pi^0 \pi^0 \nu_\tau$	(2.6 ± 2.4) × 10 ⁻⁴		763
$K^- K^0 \pi^0 \pi^0 \nu_\tau$	< 1.6 × 10 ⁻⁴	CL=95%	619
$\pi^- K^0 \overline{K}^0 \nu_\tau$	(1.7 ± 0.4) × 10 ⁻³	S=1.6	682
$\pi^- K_S^0 K_S^0 \nu_\tau$ [g]	(2.4 ± 0.5) × 10 ⁻⁴		682
$\pi^- K_S^0 K_L^0 \nu_\tau$ [g]	(1.2 ± 0.4) × 10 ⁻³	S=1.7	682
$\pi^- K^0 \overline{K}^0 \pi^0 \nu_\tau$	(3.1 ± 2.3) × 10 ⁻⁴		614
$\pi^- K_S^0 K_S^0 \pi^0 \nu_\tau$	< 2.0 × 10 ⁻⁴	CL=95%	614
$\pi^- K_S^0 K_L^0 \pi^0 \nu_\tau$	(3.1 ± 1.2) × 10 ⁻⁴		614
$K^0 h^+ h^- h^- \geq 0$ neutrals ν_τ	< 1.7 × 10 ⁻³	CL=95%	760
$K^0 h^+ h^- h^- \nu_\tau$	(2.3 ± 2.0) × 10 ⁻⁴		760

Modes with three charged particles

$h^- h^- h^+ \geq 0$ neutrals $\geq 0K_L^0 \nu_\tau$	(15.19 ± 0.08) %	S=1.4	861
$h^- h^- h^+ \geq 0$ neutrals ν_τ	(14.56 ± 0.08) %	S=1.3	861
(ex. $K_S^0 \rightarrow \pi^+ \pi^-$) ("3-prong")			
$h^- h^- h^+ \nu_\tau$	(9.80 ± 0.08) %	S=1.4	861
$h^- h^- h^+ \nu_\tau$ (ex. K^0)	(9.46 ± 0.07) %	S=1.3	861
$h^- h^- h^+ \nu_\tau$ (ex. K^0, ω)	(9.42 ± 0.07) %	S=1.3	861

$\pi^- \pi^+ \pi^- \nu_\tau$	(9.32±0.07) %	S=1.2	861
$\pi^- \pi^+ \pi^- \nu_\tau$ (ex. K^0)	(9.03±0.06) %	S=1.2	861
$\pi^- \pi^+ \pi^- \nu_\tau$ (ex. K^0), non-axial vector	< 2.4 %	CL=95%	861
$\pi^- \pi^+ \pi^- \nu_\tau$ (ex. K^0, ω)	[g] (9.00±0.06) %	S=1.2	861
$h^- h^- h^+ \geq 1$ neutrals ν_τ	(5.38±0.07) %	S=1.2	—
$h^- h^- h^+ \geq 1 \pi^0 \nu_\tau$ (ex. K^0)	(5.08±0.06) %	S=1.1	—
$h^- h^- h^+ \pi^0 \nu_\tau$	(4.75±0.06) %	S=1.2	834
$h^- h^- h^+ \pi^0 \nu_\tau$ (ex. K^0)	(4.56±0.06) %	S=1.2	834
$h^- h^- h^+ \pi^0 \nu_\tau$ (ex. K^0, ω)	(2.79±0.08) %	S=1.2	834
$\pi^- \pi^+ \pi^- \pi^0 \nu_\tau$	(4.61±0.06) %	S=1.1	834
$\pi^- \pi^+ \pi^- \pi^0 \nu_\tau$ (ex. K^0)	(4.48±0.06) %	S=1.2	834
$\pi^- \pi^+ \pi^- \pi^0 \nu_\tau$ (ex. K^0, ω)	[g] (2.70±0.08) %	S=1.2	834
$h^- h^- h^+ \geq 2 \pi^0 \nu_\tau$ (ex. K^0)	(5.18±0.33) × 10 ⁻³	—	—
$h^- h^- h^+ 2 \pi^0 \nu_\tau$	(5.06±0.32) × 10 ⁻³	—	797
$h^- h^- h^+ 2 \pi^0 \nu_\tau$ (ex. K^0)	(4.95±0.32) × 10 ⁻³	—	797
$h^- h^- h^+ 2 \pi^0 \nu_\tau$ (ex. K^0, ω, η)	[g] (10 ± 4) × 10 ⁻⁴	—	797
$h^- h^- h^+ 3 \pi^0 \nu_\tau$	[g] (2.3 ± 0.7) × 10 ⁻⁴	S=1.3	749
$K^- h^+ h^- \geq 0$ neutrals ν_τ	(6.24±0.24) × 10 ⁻³	S=1.5	794
$K^- h^+ \pi^- \nu_\tau$ (ex. K^0)	(4.27±0.20) × 10 ⁻³	S=2.4	794
$K^- h^+ \pi^- \pi^0 \nu_\tau$ (ex. K^0)	(8.7 ± 1.2) × 10 ⁻⁴	S=1.1	763
$K^- \pi^+ \pi^- \geq 0$ neutrals ν_τ	(4.78±0.21) × 10 ⁻³	S=1.3	794
$K^- \pi^+ \pi^- \geq 0 \pi^0 \nu_\tau$ (ex. K^0)	(3.68±0.20) × 10 ⁻³	S=1.4	794
$K^- \pi^+ \pi^- \nu_\tau$	(3.42±0.17) × 10 ⁻³	S=1.8	794
$K^- \pi^+ \pi^- \nu_\tau$ (ex. K^0)	[g] (2.87±0.16) × 10 ⁻³	S=2.1	794
$K^- \rho^0 \nu_\tau \rightarrow K^- \pi^+ \pi^- \nu_\tau$	(1.4 ± 0.5) × 10 ⁻³	—	—
$K^- \pi^+ \pi^- \pi^0 \nu_\tau$	(1.36±0.14) × 10 ⁻³	—	763
$K^- \pi^+ \pi^- \pi^0 \nu_\tau$ (ex. K^0)	(8.1 ± 1.2) × 10 ⁻⁴	—	763
$K^- \pi^+ \pi^- \pi^0 \nu_\tau$ (ex. K^0, η)	[g] (7.7 ± 1.2) × 10 ⁻⁴	—	763
$K^- \pi^+ \pi^- \pi^0 \nu_\tau$ (ex. K^0, ω)	(3.7 ± 0.9) × 10 ⁻⁴	—	763
$K^- \pi^+ K^- \geq 0$ neut. ν_τ	< 9 × 10 ⁻⁴	CL=95%	685
$K^- K^+ \pi^- \geq 0$ neut. ν_τ	(1.46±0.06) × 10 ⁻³	S=1.6	685
$K^- K^+ \pi^- \nu_\tau$	[g] (1.40±0.05) × 10 ⁻³	S=1.7	685
$K^- K^+ \pi^- \pi^0 \nu_\tau$	[g] (6.1 ± 2.5) × 10 ⁻⁵	S=1.4	618
$K^- K^+ K^- \geq 0$ neut. ν_τ	< 2.1 × 10 ⁻³	CL=95%	471
$K^- K^+ K^- \nu_\tau$	(1.58±0.18) × 10 ⁻⁵	—	471
$K^- K^+ K^- \nu_\tau$ (ex. ϕ)	< 2.5 × 10 ⁻⁶	CL=90%	—
$K^- K^+ K^- \pi^0 \nu_\tau$	< 4.8 × 10 ⁻⁶	CL=90%	345
$\pi^- K^+ \pi^- \geq 0$ neut. ν_τ	< 2.5 × 10 ⁻³	CL=95%	794
$e^- e^- e^+ \bar{\nu}_e \nu_\tau$	(2.8 ± 1.5) × 10 ⁻⁵	—	888
$\mu^- e^- e^+ \bar{\nu}_\mu \nu_\tau$	< 3.6 × 10 ⁻⁵	CL=90%	885

Modes with five charged particles

$3h^- 2h^+ \geq 0$ neutrals ν_τ (ex. $K_S^0 \rightarrow \pi^- \pi^+$) ("5-prong")	(1.02±0.04) × 10 ⁻³	S=1.1	794
$3h^- 2h^+ \nu_\tau$ (ex. K^0)	[g] (8.39±0.35) × 10 ⁻⁴	S=1.1	794
$3h^- 2h^+ \pi^0 \nu_\tau$ (ex. K^0)	[g] (1.78±0.27) × 10 ⁻⁴	—	746
$3h^- 2h^+ 2 \pi^0 \nu_\tau$	< 3.4 × 10 ⁻⁶	CL=90%	687

Miscellaneous other allowed modes

$(5\pi)^- \nu_\tau$	(7.6 ± 0.5) × 10 ⁻³	—	800
$4h^- 3h^+ \geq 0$ neutrals ν_τ ("7-prong")	< 3.0 × 10 ⁻⁷	CL=90%	682
$4h^- 3h^+ \nu_\tau$	< 4.3 × 10 ⁻⁷	CL=90%	682
$4h^- 3h^+ \pi^0 \nu_\tau$	< 2.5 × 10 ⁻⁷	CL=90%	612

$X^-(S=-1)\nu_\tau$	(2.86±0.07) %	S=1.3	—
$K^*(892)^- \geq 0 \text{ neutrals} \geq$	(1.42±0.18) %	S=1.4	665
$0K_L^0\nu_\tau$			
$K^*(892)^-\nu_\tau$	(1.20±0.07) %	S=1.8	665
$K^*(892)^-\nu_\tau \rightarrow \pi^-\bar{K}^0\nu_\tau$	(7.8 ± 0.5) × 10 ⁻³		—
$K^*(892)^0K^-\nu_\tau$	(3.2 ± 1.4) × 10 ⁻³		542
$K^*(892)^0K^-\nu_\tau$	(2.1 ± 0.4) × 10 ⁻³		542
$\bar{K}^*(892)^0\pi^-\nu_\tau$	(3.8 ± 1.7) × 10 ⁻³		655
$\bar{K}^*(892)^0\pi^-\nu_\tau$	(2.2 ± 0.5) × 10 ⁻³		655
$(\bar{K}^*(892)\pi)^-\nu_\tau \rightarrow \pi^-\bar{K}^0\pi^0\nu_\tau$	(1.0 ± 0.4) × 10 ⁻³		—
$K_1(1270)^-\nu_\tau$	(4.7 ± 1.1) × 10 ⁻³		433
$K_1(1400)^-\nu_\tau$	(1.7 ± 2.6) × 10 ⁻³	S=1.7	335
$K^*(1410)^-\nu_\tau$	(1.5 ^{+1.4} _{-1.0}) × 10 ⁻³		326
$K_0^*(1430)^-\nu_\tau$	< 5 × 10 ⁻⁴	CL=95%	317
$K_2^*(1430)^-\nu_\tau$	< 3 × 10 ⁻³	CL=95%	316
$\eta\pi^-\nu_\tau$	< 1.4 × 10 ⁻⁴	CL=95%	797
$\eta\pi^-\pi^0\nu_\tau$	[g] (1.39±0.10) × 10 ⁻³	S=1.4	778
$\eta\pi^-\pi^0\pi^0\nu_\tau$	(1.5 ± 0.5) × 10 ⁻⁴		746
$\eta K^-\nu_\tau$	[g] (1.61±0.11) × 10 ⁻⁴	S=1.1	719
$\eta K^*(892)^-\nu_\tau$	(1.38±0.15) × 10 ⁻⁴		511
$\eta K^-\pi^0\nu_\tau$	(4.8 ± 1.2) × 10 ⁻⁵		665
$\eta K^-\pi^0(\text{non-}K^*(892))\nu_\tau$	< 3.5 × 10 ⁻⁵	CL=90%	—
$\eta\bar{K}^0\pi^-\nu_\tau$	(9.3 ± 1.5) × 10 ⁻⁵		661
$\eta\bar{K}^0\pi^-\pi^0\nu_\tau$	< 5.0 × 10 ⁻⁵	CL=90%	590
$\eta K^-K^0\nu_\tau$	< 9.0 × 10 ⁻⁶	CL=90%	430
$\eta\pi^+\pi^-\pi^-\nu_\tau$	< 3 × 10 ⁻³	CL=90%	743
$\eta\pi^-\pi^+\pi^-\nu_\tau(\text{ex.}K^0)$	(1.64±0.12) × 10 ⁻⁴		743
$\eta a_1(1260)^-\nu_\tau \rightarrow \eta\pi^-\rho^0\nu_\tau$	< 3.9 × 10 ⁻⁴	CL=90%	—
$\eta\eta\pi^-\nu_\tau$	< 7.4 × 10 ⁻⁶	CL=90%	637
$\eta\eta\pi^-\pi^0\nu_\tau$	< 2.0 × 10 ⁻⁴	CL=95%	559
$\eta\eta K^-\nu_\tau$	< 3.0 × 10 ⁻⁶	CL=90%	382
$\eta'(958)\pi^-\nu_\tau$	< 7.2 × 10 ⁻⁶	CL=90%	620
$\eta'(958)\pi^-\pi^0\nu_\tau$	< 8.0 × 10 ⁻⁵	CL=90%	591
$\phi\pi^-\nu_\tau$	(3.4 ± 0.6) × 10 ⁻⁵		585
$\phi K^-\nu_\tau$	(3.70±0.33) × 10 ⁻⁵	S=1.3	445
$f_1(1285)\pi^-\nu_\tau$	(3.6 ± 0.7) × 10 ⁻⁴		408
$f_1(1285)\pi^-\nu_\tau \rightarrow$	(1.11±0.08) × 10 ⁻⁴		—
$\eta\pi^-\pi^+\pi^-\nu_\tau$			
$\pi(1300)^-\nu_\tau \rightarrow (\rho\pi)^-\nu_\tau \rightarrow$	< 1.0 × 10 ⁻⁴	CL=90%	—
$(3\pi)^-\nu_\tau$			
$\pi(1300)^-\nu_\tau \rightarrow$	< 1.9 × 10 ⁻⁴	CL=90%	—
$((\pi\pi)_{S\text{-wave}}\pi)^-\nu_\tau \rightarrow$			
$(3\pi)^-\nu_\tau$			
$h^-\omega \geq 0 \text{ neutrals} \nu_\tau$	(2.41±0.09) %	S=1.2	708
$h^-\omega\nu_\tau$	[g] (1.99±0.08) %	S=1.3	708
$K^-\omega\nu_\tau$	(4.1 ± 0.9) × 10 ⁻⁴		610
$h^-\omega\pi^0\nu_\tau$	[g] (4.1 ± 0.4) × 10 ⁻³		684
$h^-\omega 2\pi^0\nu_\tau$	(1.4 ± 0.5) × 10 ⁻⁴		644
$h^-2\omega\nu_\tau$	< 5.4 × 10 ⁻⁷	CL=90%	249
$2h^-h^+\omega\nu_\tau$	(1.20±0.22) × 10 ⁻⁴		641

**Lepton Family number (*LF*), Lepton number (*L*),
or Baryon number (*B*) violating modes**

L means lepton number violation (e.g. $\tau^- \rightarrow e^+ \pi^- \pi^-$). Following common usage, *LF* means lepton family violation *and not* lepton number violation (e.g. $\tau^- \rightarrow e^- \pi^+ \pi^-$). *B* means baryon number violation.

$e^- \gamma$	<i>LF</i>	< 3.3	$\times 10^{-8}$	CL=90%	888
$\mu^- \gamma$	<i>LF</i>	< 4.4	$\times 10^{-8}$	CL=90%	885
$e^- \pi^0$	<i>LF</i>	< 8.0	$\times 10^{-8}$	CL=90%	883
$\mu^- \pi^0$	<i>LF</i>	< 1.1	$\times 10^{-7}$	CL=90%	880
$e^- K_S^0$	<i>LF</i>	< 3.3	$\times 10^{-8}$	CL=90%	819
$\mu^- K_S^0$	<i>LF</i>	< 4.0	$\times 10^{-8}$	CL=90%	815
$e^- \eta$	<i>LF</i>	< 9.2	$\times 10^{-8}$	CL=90%	804
$\mu^- \eta$	<i>LF</i>	< 6.5	$\times 10^{-8}$	CL=90%	800
$e^- \rho^0$	<i>LF</i>	< 4.6	$\times 10^{-8}$	CL=90%	719
$\mu^- \rho^0$	<i>LF</i>	< 2.6	$\times 10^{-8}$	CL=90%	715
$e^- \omega$	<i>LF</i>	< 1.1	$\times 10^{-7}$	CL=90%	716
$\mu^- \omega$	<i>LF</i>	< 8.9	$\times 10^{-8}$	CL=90%	711
$e^- K^*(892)^0$	<i>LF</i>	< 5.9	$\times 10^{-8}$	CL=90%	665
$\mu^- K^*(892)^0$	<i>LF</i>	< 5.9	$\times 10^{-8}$	CL=90%	659
$e^- \bar{K}^*(892)^0$	<i>LF</i>	< 4.6	$\times 10^{-8}$	CL=90%	665
$\mu^- \bar{K}^*(892)^0$	<i>LF</i>	< 7.3	$\times 10^{-8}$	CL=90%	659
$e^- \eta'(958)$	<i>LF</i>	< 1.6	$\times 10^{-7}$	CL=90%	630
$\mu^- \eta'(958)$	<i>LF</i>	< 1.3	$\times 10^{-7}$	CL=90%	625
$e^- f_0(980) \rightarrow e^- \pi^+ \pi^-$	<i>LF</i>	< 3.2	$\times 10^{-8}$	CL=90%	—
$\mu^- f_0(980) \rightarrow \mu^- \pi^+ \pi^-$	<i>LF</i>	< 3.4	$\times 10^{-8}$	CL=90%	—
$e^- \phi$	<i>LF</i>	< 3.1	$\times 10^{-8}$	CL=90%	596
$\mu^- \phi$	<i>LF</i>	< 1.3	$\times 10^{-7}$	CL=90%	590
$e^- e^+ e^-$	<i>LF</i>	< 3.6	$\times 10^{-8}$	CL=90%	888
$e^- \mu^+ \mu^-$	<i>LF</i>	< 3.7	$\times 10^{-8}$	CL=90%	882
$e^+ \mu^- \mu^-$	<i>LF</i>	< 2.3	$\times 10^{-8}$	CL=90%	882
$\mu^- e^+ e^-$	<i>LF</i>	< 2.7	$\times 10^{-8}$	CL=90%	885
$\mu^+ e^- e^-$	<i>LF</i>	< 2.0	$\times 10^{-8}$	CL=90%	885
$\mu^- \mu^+ \mu^-$	<i>LF</i>	< 3.2	$\times 10^{-8}$	CL=90%	873
$e^- \pi^+ \pi^-$	<i>LF</i>	< 4.4	$\times 10^{-8}$	CL=90%	877
$e^+ \pi^- \pi^-$	<i>L</i>	< 8.8	$\times 10^{-8}$	CL=90%	877
$\mu^- \pi^+ \pi^-$	<i>LF</i>	< 3.3	$\times 10^{-8}$	CL=90%	866
$\mu^+ \pi^- \pi^-$	<i>L</i>	< 3.7	$\times 10^{-8}$	CL=90%	866
$e^- \pi^+ K^-$	<i>LF</i>	< 5.8	$\times 10^{-8}$	CL=90%	813
$e^- \pi^- K^+$	<i>LF</i>	< 5.2	$\times 10^{-8}$	CL=90%	813
$e^+ \pi^- K^-$	<i>L</i>	< 6.7	$\times 10^{-8}$	CL=90%	813
$e^- K_S^0 K_S^0$	<i>LF</i>	< 2.2	$\times 10^{-6}$	CL=90%	736
$e^- K^+ K^-$	<i>LF</i>	< 5.4	$\times 10^{-8}$	CL=90%	738
$e^+ K^- K^-$	<i>L</i>	< 6.0	$\times 10^{-8}$	CL=90%	738
$\mu^- \pi^+ K^-$	<i>LF</i>	< 1.6	$\times 10^{-7}$	CL=90%	800
$\mu^- \pi^- K^+$	<i>LF</i>	< 1.0	$\times 10^{-7}$	CL=90%	800
$\mu^+ \pi^- K^-$	<i>L</i>	< 9.4	$\times 10^{-8}$	CL=90%	800
$\mu^- K_S^0 K_S^0$	<i>LF</i>	< 3.4	$\times 10^{-6}$	CL=90%	696
$\mu^- K^+ K^-$	<i>LF</i>	< 6.8	$\times 10^{-8}$	CL=90%	699
$\mu^+ K^- K^-$	<i>L</i>	< 9.6	$\times 10^{-8}$	CL=90%	699
$e^- \pi^0 \pi^0$	<i>LF</i>	< 6.5	$\times 10^{-6}$	CL=90%	878
$\mu^- \pi^0 \pi^0$	<i>LF</i>	< 1.4	$\times 10^{-5}$	CL=90%	867
$e^- \eta \eta$	<i>LF</i>	< 3.5	$\times 10^{-5}$	CL=90%	699
$\mu^- \eta \eta$	<i>LF</i>	< 6.0	$\times 10^{-5}$	CL=90%	653
$e^- \pi^0 \eta$	<i>LF</i>	< 2.4	$\times 10^{-5}$	CL=90%	798

$\mu^- \pi^0 \eta$	LF	< 2.2	$\times 10^{-5}$	CL=90%	784
$\bar{p} \gamma$	L, B	< 3.5	$\times 10^{-6}$	CL=90%	641
$\bar{p} \pi^0$	L, B	< 1.5	$\times 10^{-5}$	CL=90%	632
$\bar{p} 2\pi^0$	L, B	< 3.3	$\times 10^{-5}$	CL=90%	604
$\bar{p} \eta$	L, B	< 8.9	$\times 10^{-6}$	CL=90%	475
$\bar{p} \pi^0 \eta$	L, B	< 2.7	$\times 10^{-5}$	CL=90%	360
$\Lambda \pi^-$	L, B	< 7.2	$\times 10^{-8}$	CL=90%	525
$\bar{\Lambda} \pi^-$	L, B	< 1.4	$\times 10^{-7}$	CL=90%	525
e^- light boson	LF	< 2.7	$\times 10^{-3}$	CL=95%	–
μ^- light boson	LF	< 5	$\times 10^{-3}$	CL=95%	–

Heavy Charged Lepton Searches

L^\pm – charged lepton

Mass $m > 100.8$ GeV, CL = 95% ^[h] Decay to νW .

L^\pm – stable charged heavy lepton

Mass $m > 102.6$ GeV, CL = 95%

Neutrino Properties

See the note on “Neutrino properties listings” in the Particle Listings.

Mass $m < 2$ eV (tritium decay)

Mean life/mass, $\tau/m > 300$ s/eV, CL = 90% (reactor)

Mean life/mass, $\tau/m > 7 \times 10^9$ s/eV (solar)

Mean life/mass, $\tau/m > 15.4$ s/eV, CL = 90% (accelerator)

Magnetic moment $\mu < 0.54 \times 10^{-10} \mu_B$, CL = 90% (solar)

Number of Neutrino Types

Number $N = 2.984 \pm 0.008$ (Standard Model fits to LEP data)

Number $N = 2.92 \pm 0.05$ ($S = 1.2$) (Direct measurement of invisible Z width)

Neutrino Mixing

The following values are obtained through data analyses based on the 3-neutrino mixing scheme described in the review “Neutrino Mass, Mixing, and Oscillations” by K. Nakamura and S.T. Petcov in this *Review*.

$$\sin^2(2\theta_{12}) = 0.87 \pm 0.03$$

$$\Delta m_{21}^2 = (7.59 \pm 0.20) \times 10^{-5} \text{ eV}^2$$

$$\sin^2(2\theta_{23}) > 0.92 \text{ [i]}$$

$$\Delta m_{32}^2 = (2.43 \pm 0.13) \times 10^{-3} \text{ eV}^2 \text{ [j]}$$

$$\sin^2(2\theta_{13}) < 0.15, \text{ CL} = 90\%$$

Heavy Neutral Leptons, Searches for

For excited leptons, see Compositeness Limits below.

Stable Neutral Heavy Lepton Mass Limits

Mass $m > 45.0$ GeV, CL = 95% (Dirac)

Mass $m > 39.5$ GeV, CL = 95% (Majorana)

Neutral Heavy Lepton Mass Limits

Mass $m > 90.3$ GeV, CL = 95%

(Dirac ν_L coupling to e, μ, τ ; conservative case(τ))

Mass $m > 80.5$ GeV, CL = 95%

(Majorana ν_L coupling to e, μ, τ ; conservative case(τ))

NOTES

In this Summary Table:

When a quantity has “(S = ...)” to its right, the error on the quantity has been enlarged by the “scale factor” S, defined as $S = \sqrt{\chi^2/(N-1)}$, where N is the number of measurements used in calculating the quantity. We do this when $S > 1$, which often indicates that the measurements are inconsistent. When $S > 1.25$, we also show in the Particle Listings an ideogram of the measurements. For more about S, see the Introduction.

A decay momentum p is given for each decay mode. For a 2-body decay, p is the momentum of each decay product in the rest frame of the decaying particle. For a 3-or-more-body decay, p is the largest momentum any of the products can have in this frame.

- [a] This is the best limit for the mode $e^- \rightarrow \nu\gamma$. The best limit for “electron disappearance” is 6.4×10^{24} yr.
- [b] See the “Note on Muon Decay Parameters” in the μ Particle Listings in the Full *Review of Particle Physics* for definitions and details.
- [c] P_μ is the longitudinal polarization of the muon from pion decay. In standard $V-A$ theory, $P_\mu = 1$ and $\rho = \delta = 3/4$.
- [d] This only includes events with the γ energy > 10 MeV. Since the $e^- \bar{\nu}_e \nu_\mu$ and $e^- \bar{\nu}_e \nu_\mu \gamma$ modes cannot be clearly separated, we regard the latter mode as a subset of the former.
- [e] See the relevant Particle Listings in the Full *Review of Particle Physics* for the energy limits used in this measurement.
- [f] A test of additive vs. multiplicative lepton family number conservation.
- [g] Basis mode for the τ .
- [h] L^\pm mass limit depends on decay assumptions; see the Full Listings.
- [i] The limit quoted corresponds to the projection onto the $\sin^2(2\theta_{23})$ axis of the 90% CL contour in the $\sin^2(2\theta_{23})-\Delta m_{32}^2$ plane.
- [j] The sign of Δm_{32}^2 is not known at this time. The range quoted is for the absolute value.

QUARKS

The u -, d -, and s -quark masses are estimates of so-called “current-quark masses,” in a mass-independent subtraction scheme such as $\overline{\text{MS}}$ at a scale $\mu \approx 2$ GeV. The c - and b -quark masses are the “running” masses in the $\overline{\text{MS}}$ scheme. For the b -quark we also quote the 1S mass. These can be different from the heavy quark masses obtained in potential models.

u

$$I(J^P) = \frac{1}{2}(\frac{1}{2}^+)$$

$$m_u = 1.7\text{--}3.3 \text{ MeV} \quad \text{Charge} = \frac{2}{3} e \quad I_z = +\frac{1}{2}$$

$$m_u/m_d = 0.35\text{--}0.60$$

d

$$I(J^P) = \frac{1}{2}(\frac{1}{2}^+)$$

$$m_d = 4.1\text{--}5.8 \text{ MeV} \quad \text{Charge} = -\frac{1}{3} e \quad I_z = -\frac{1}{2}$$

$$m_s/m_d = 17 \text{ to } 22$$

$$\overline{m} = (m_u + m_d)/2 = 3.0\text{--}4.8 \text{ MeV}$$

s

$$I(J^P) = 0(\frac{1}{2}^+)$$

$$m_s = 101_{-21}^{+29} \text{ MeV} \quad \text{Charge} = -\frac{1}{3} e \quad \text{Strangeness} = -1$$

$$m_s / ((m_u + m_d)/2) = 22 \text{ to } 30$$

c

$$I(J^P) = 0(\frac{1}{2}^+)$$

$$m_c = 1.27_{-0.09}^{+0.07} \text{ GeV} \quad \text{Charge} = \frac{2}{3} e \quad \text{Charm} = +1$$

b

$$I(J^P) = 0(\frac{1}{2}^+)$$

$$\text{Charge} = -\frac{1}{3} e \quad \text{Bottom} = -1$$

$$m_b(\overline{\text{MS}}) = 4.19_{-0.06}^{+0.18} \text{ GeV}$$

$$m_b(1S) = 4.67_{-0.06}^{+0.18} \text{ GeV}$$

t

$$I(J^P) = 0(\frac{1}{2}^+)$$

$$\text{Charge} = \frac{2}{3} e \quad \text{Top} = +1$$

Mass $m = 172.0 \pm 0.9 \pm 1.3 \text{ GeV}$ [a] (direct observation of top events)

Full width $\Gamma < 13.1 \text{ GeV}$, CL = 95%

$$\Gamma(Wb)/\Gamma(Wq(q = b, s, d)) = 0.99^{+0.09}_{-0.08}$$

t DECAY MODES	Fraction (Γ_i/Γ)	Confidence level	ρ (MeV/c)
$Wq(q = b, s, d)$			—
Wb			—
$\ell\nu_\ell$ anything	[b,c] $(9.4 \pm 2.4) \%$		—
$\gamma q(q = u, c)$	[d] $< 5.9 \times 10^{-3}$	95%	—
$\Delta T = 1$ weak neutral current (T1) modes			
$Zq(q = u, c)$	T1 [e] $< 3.7 \%$	95%	—

b' (4th Generation) Quark, Searches for

- Mass $m > 190 \text{ GeV}$, CL = 95% ($p\bar{p}$, quasi-stable b')
- Mass $m > 199 \text{ GeV}$, CL = 95% ($p\bar{p}$, neutral-current decays)
- Mass $m > 128 \text{ GeV}$, CL = 95% ($p\bar{p}$, charged-current decays)
- Mass $m > 46.0 \text{ GeV}$, CL = 95% (e^+e^- , all decays)

t' (4th Generation) Quark, Searches for

Mass $m > 256 \text{ GeV}$, CL = 95% ($p\bar{p}$, $t'\bar{t}'$ prod., $t' \rightarrow Wq$)

Free Quark Searches

All searches since 1977 have had negative results.

NOTES

[a] Based on published top mass measurements using data from Tevatron Run-I and Run-II. Including also the most recent unpublished results from Run-II, the Tevatron Electroweak Working Group reports a top mass of $173.1 \pm 0.6 \pm 1.1 \text{ GeV}$. See the note "The Top Quark" in the Quark Particle Listings of this Review.

[b] ℓ means e or μ decay mode, not the sum over them.

[c] Assumes lepton universality and W -decay acceptance.

[d] This limit is for $\Gamma(t \rightarrow \gamma q)/\Gamma(t \rightarrow Wb)$.

[e] This limit is for $\Gamma(t \rightarrow Zq)/\Gamma(t \rightarrow Wb)$.

LIGHT UNFLAVORED MESONS ($S = C = B = 0$)

For $I = 1$ (π , b , ρ , a): $u\bar{d}$, $(u\bar{u} - d\bar{d})/\sqrt{2}$, $d\bar{u}$;
for $I = 0$ (η , η' , h , h' , ω , ϕ , f , f'): $c_1(u\bar{u} + d\bar{d}) + c_2(s\bar{s})$

π^\pm

$$I^G(J^P) = 1^-(0^-)$$

Mass $m = 139.57018 \pm 0.00035$ MeV ($S = 1.2$)

Mean life $\tau = (2.6033 \pm 0.0005) \times 10^{-8}$ s ($S = 1.2$)

$$c\tau = 7.8045$$
 m

$\pi^\pm \rightarrow \ell^\pm \nu \gamma$ form factors [a]

$$F_V = 0.0254 \pm 0.0017$$

$$F_A = 0.0119 \pm 0.0001$$

$$F_V \text{ slope parameter } a = 0.10 \pm 0.06$$

$$R = 0.059^{+0.009}_{-0.008}$$

π^- modes are charge conjugates of the modes below.

For decay limits to particles which are not established, see the section on Searches for Axions and Other Very Light Bosons.

π^+ DECAY MODES	Fraction (Γ_i/Γ)	Confidence level	ρ (MeV/c)
$\mu^+ \nu_\mu$	[b] (99.98770 \pm 0.00004) %		30
$\mu^+ \nu_\mu \gamma$	[c] (2.00 \pm 0.25) $\times 10^{-4}$		30
$e^+ \nu_e$	[b] (1.230 \pm 0.004) $\times 10^{-4}$		70
$e^+ \nu_e \gamma$	[c] (7.39 \pm 0.05) $\times 10^{-7}$		70
$e^+ \nu_e \pi^0$	(1.036 \pm 0.006) $\times 10^{-8}$		4
$e^+ \nu_e e^+ e^-$	(3.2 \pm 0.5) $\times 10^{-9}$		70
$e^+ \nu_e \nu \bar{\nu}$	< 5 $\times 10^{-6}$	90%	70
Lepton Family number (LF) or Lepton number (L) violating modes			
$\mu^+ \bar{\nu}_e$	L [d] < 1.5 $\times 10^{-3}$	90%	30
$\mu^+ \nu_e$	LF [d] < 8.0 $\times 10^{-3}$	90%	30
$\mu^- e^+ e^+ \nu$	LF < 1.6 $\times 10^{-6}$	90%	30

π^0

$$I^G(J^{PC}) = 1^-(0^{-+})$$

Mass $m = 134.9766 \pm 0.0006$ MeV ($S = 1.1$)

$$m_{\pi^\pm} - m_{\pi^0} = 4.5936 \pm 0.0005$$
 MeV

Mean life $\tau = (8.4 \pm 0.5) \times 10^{-17}$ s ($S = 2.6$)

$$c\tau = 25.1$$
 nm

For decay limits to particles which are not established, see the appropriate Search sections (A^0 (axion) and Other Light Boson (X^0) Searches, etc.).

π^0 DECAY MODES	Fraction (Γ_i/Γ)	Scale factor/ Confidence level	ρ (MeV/c)
2γ	(98.823 \pm 0.034) %	S=1.5	67
$e^+ e^- \gamma$	(1.174 \pm 0.035) %	S=1.5	67
γ positronium	(1.82 \pm 0.29) $\times 10^{-9}$		67
$e^+ e^+ e^- e^-$	(3.34 \pm 0.16) $\times 10^{-5}$		67

$e^+ e^-$		$(6.46 \pm 0.33) \times 10^{-8}$		67
4γ		$< 2 \times 10^{-8}$	CL=90%	67
$\nu\bar{\nu}$	$[e]$	$< 2.7 \times 10^{-7}$	CL=90%	67
$\nu_e\bar{\nu}_e$		$< 1.7 \times 10^{-6}$	CL=90%	67
$\nu_\mu\bar{\nu}_\mu$		$< 1.6 \times 10^{-6}$	CL=90%	67
$\nu_\tau\bar{\nu}_\tau$		$< 2.1 \times 10^{-6}$	CL=90%	67
$\gamma\nu\bar{\nu}$		$< 6 \times 10^{-4}$	CL=90%	67

Charge conjugation (C) or Lepton Family number (LF) violating modes

3γ	C	$< 3.1 \times 10^{-8}$	CL=90%	67
$\mu^+ e^-$	LF	$< 3.8 \times 10^{-10}$	CL=90%	26
$\mu^- e^+$	LF	$< 3.4 \times 10^{-9}$	CL=90%	26
$\mu^+ e^- + \mu^- e^+$	LF	$< 3.6 \times 10^{-10}$	CL=90%	26

η

$$I^G(J^{PC}) = 0^+(0^-+)$$

Mass $m = 547.853 \pm 0.024$ MeV

Full width $\Gamma = 1.30 \pm 0.07$ keV

C-nonconserving decay parameters

$\pi^+ \pi^- \pi^0$	left-right asymmetry	$= (0.09^{+0.11}_{-0.12}) \times 10^{-2}$
$\pi^+ \pi^- \pi^0$	sextant asymmetry	$= (0.12^{+0.10}_{-0.11}) \times 10^{-2}$
$\pi^+ \pi^- \pi^0$	quadrant asymmetry	$= (-0.09 \pm 0.09) \times 10^{-2}$
$\pi^+ \pi^- \gamma$	left-right asymmetry	$= (0.9 \pm 0.4) \times 10^{-2}$
$\pi^+ \pi^- \gamma$	β (D-wave)	$= -0.02 \pm 0.07$ (S = 1.3)

CP-nonconserving decay parameters

$\pi^+ \pi^- e^+ e^-$ decay-plane asymmetry $A_\phi = (-0.6 \pm 3.1) \times 10^{-2}$

Dalitz plot parameter

$\pi^0 \pi^0 \pi^0$ $\alpha = -0.0317 \pm 0.0016$

η DECAY MODES	Fraction (Γ_i/Γ)	Scale factor/ Confidence level	ρ (MeV/c)
Neutral modes			
neutral modes	$(71.90 \pm 0.34) \%$	S=1.2	—
2γ	$(39.31 \pm 0.20) \%$	S=1.1	274
$3\pi^0$	$(32.57 \pm 0.23) \%$	S=1.1	179
$\pi^0 2\gamma$	$(2.7 \pm 0.5) \times 10^{-4}$	S=1.1	257
$2\pi^0 2\gamma$	$< 1.2 \times 10^{-3}$	CL=90%	238
4γ	$< 2.8 \times 10^{-4}$	CL=90%	274
invisible	$< 6 \times 10^{-4}$	CL=90%	—
Charged modes			
charged modes	$(28.10 \pm 0.34) \%$	S=1.2	—
$\pi^+ \pi^- \pi^0$	$(22.74 \pm 0.28) \%$	S=1.2	174
$\pi^+ \pi^- \gamma$	$(4.60 \pm 0.16) \%$	S=2.1	236
$e^+ e^- \gamma$	$(7.0 \pm 0.7) \times 10^{-3}$	S=1.5	274
$\mu^+ \mu^- \gamma$	$(3.1 \pm 0.4) \times 10^{-4}$		253
$e^+ e^-$	$< 2.7 \times 10^{-5}$	CL=90%	274
$\mu^+ \mu^-$	$(5.8 \pm 0.8) \times 10^{-6}$		253
$2e^+ 2e^-$	$< 6.9 \times 10^{-5}$	CL=90%	274
$\pi^+ \pi^- e^+ e^- (\gamma)$	$(2.68 \pm 0.11) \times 10^{-4}$		235
$e^+ e^- \mu^+ \mu^-$	$< 1.6 \times 10^{-4}$	CL=90%	253

$2\mu^+ 2\mu^-$	< 3.6	$\times 10^{-4}$	CL=90%	161
$\mu^+ \mu^- \pi^+ \pi^-$	< 3.6	$\times 10^{-4}$	CL=90%	113
$\pi^+ \pi^- 2\gamma$	< 2.0	$\times 10^{-3}$		236
$\pi^+ \pi^- \pi^0 \gamma$	< 5	$\times 10^{-4}$	CL=90%	174
$\pi^0 \mu^+ \mu^- \gamma$	< 3	$\times 10^{-6}$	CL=90%	210

**Charge conjugation (C), Parity (P),
Charge conjugation \times Parity (CP), or
Lepton Family number (LF) violating modes**

$\pi^0 \gamma$	C	< 9	$\times 10^{-5}$	CL=90%	257
$\pi^+ \pi^-$	P, CP	< 1.3	$\times 10^{-5}$	CL=90%	236
$2\pi^0$	P, CP	< 3.5	$\times 10^{-4}$	CL=90%	238
$2\pi^0 \gamma$	C	< 5	$\times 10^{-4}$	CL=90%	238
$3\pi^0 \gamma$	C	< 6	$\times 10^{-5}$	CL=90%	179
3γ	C	< 1.6	$\times 10^{-5}$	CL=90%	274
$4\pi^0$	P, CP	< 6.9	$\times 10^{-7}$	CL=90%	40
$\pi^0 e^+ e^-$	C	[f] < 4	$\times 10^{-5}$	CL=90%	257
$\pi^0 \mu^+ \mu^-$	C	[f] < 5	$\times 10^{-6}$	CL=90%	210
$\mu^+ e^- + \mu^- e^+$	LF	< 6	$\times 10^{-6}$	CL=90%	264

$f_0(600)$ ^[g]
or σ

$$J^{PC} = 0^+(0^{++})$$

Mass $m = (400-1200)$ MeV

Full width $\Gamma = (600-1000)$ MeV

$f_0(600)$ DECAY MODES	Fraction (Γ_i/Γ)	ρ (MeV/c)
$\pi\pi$	dominant	—
$\gamma\gamma$	seen	—

$\rho(770)$ ^[h]

$$J^{PC} = 1^+(1^{--})$$

Mass $m = 775.49 \pm 0.34$ MeV

Full width $\Gamma = 149.1 \pm 0.8$ MeV

$\Gamma_{ee} = 7.04 \pm 0.06$ keV

$\rho(770)$ DECAY MODES	Fraction (Γ_i/Γ)	Scale factor/ Confidence level	ρ (MeV/c)
$\pi\pi$	~ 100	%	363
$\rho(770)^\pm$ decays			
$\pi^\pm \gamma$	(4.5 ± 0.5) $\times 10^{-4}$	S=2.2	375
$\pi^\pm \eta$	< 6	CL=84%	153
$\pi^\pm \pi^+ \pi^- \pi^0$	< 2.0	CL=84%	254
$\rho(770)^0$ decays			
$\pi^+ \pi^- \gamma$	(9.9 ± 1.6) $\times 10^{-3}$		362
$\pi^0 \gamma$	(6.0 ± 0.8) $\times 10^{-4}$		376
$\eta \gamma$	(3.00 ± 0.20) $\times 10^{-4}$		194
$\pi^0 \pi^0 \gamma$	(4.5 ± 0.8) $\times 10^{-5}$		363
$\mu^+ \mu^-$	[f] (4.55 ± 0.28) $\times 10^{-5}$		373
$e^+ e^-$	[f] (4.72 ± 0.05) $\times 10^{-5}$		388

$\pi^+ \pi^- \pi^0$	$(1.01^{+0.54}_{-0.36} \pm 0.34) \times 10^{-4}$	323
$\pi^+ \pi^- \pi^+ \pi^-$	$(1.8 \pm 0.9) \times 10^{-5}$	251
$\pi^+ \pi^- \pi^0 \pi^0$	$(1.6 \pm 0.8) \times 10^{-5}$	257
$\pi^0 e^+ e^-$	$< 1.2 \times 10^{-5}$	CL=90% 376

 $\omega(782)$

$$I^G(J^{PC}) = 0^-(1^{--})$$

 Mass $m = 782.65 \pm 0.12$ MeV ($S = 1.9$)

 Full width $\Gamma = 8.49 \pm 0.08$ MeV

 $\Gamma_{ee} = 0.60 \pm 0.02$ keV

$\omega(782)$ DECAY MODES	Fraction (Γ_i/Γ)	Scale factor/ Confidence level	ρ (MeV/c)
$\pi^+ \pi^- \pi^0$	$(89.2 \pm 0.7) \%$		327
$\pi^0 \gamma$	$(8.28 \pm 0.28) \%$	S=2.1	380
$\pi^+ \pi^-$	$(1.53^{+0.11}_{-0.13}) \%$	S=1.2	366
neutrals (excluding $\pi^0 \gamma$)	$(8^{+8}_{-5}) \times 10^{-3}$	S=1.1	—
$\eta \gamma$	$(4.6 \pm 0.4) \times 10^{-4}$	S=1.1	200
$\pi^0 e^+ e^-$	$(7.7 \pm 0.6) \times 10^{-4}$		380
$\pi^0 \mu^+ \mu^-$	$(1.3 \pm 0.4) \times 10^{-4}$	S=2.1	349
$e^+ e^-$	$(7.28 \pm 0.14) \times 10^{-5}$	S=1.3	391
$\pi^+ \pi^- \pi^0 \pi^0$	$< 2 \times 10^{-4}$	CL=90%	262
$\pi^+ \pi^- \gamma$	$< 3.6 \times 10^{-3}$	CL=95%	366
$\pi^+ \pi^- \pi^+ \pi^-$	$< 1 \times 10^{-3}$	CL=90%	256
$\pi^0 \pi^0 \gamma$	$(6.6 \pm 1.1) \times 10^{-5}$		367
$\eta \pi^0 \gamma$	$< 3.3 \times 10^{-5}$	CL=90%	162
$\mu^+ \mu^-$	$(9.0 \pm 3.1) \times 10^{-5}$		377
3γ	$< 1.9 \times 10^{-4}$	CL=95%	391

Charge conjugation (C) violating modes

$\eta \pi^0$	C	$< 2.1 \times 10^{-4}$	CL=90%	162
$2\pi^0$	C	$< 2.1 \times 10^{-4}$	CL=90%	367
$3\pi^0$	C	$< 2.3 \times 10^{-4}$	CL=90%	330

 $\eta'(958)$

$$I^G(J^{PC}) = 0^+(0^{-+})$$

 Mass $m = 957.78 \pm 0.06$ MeV

 Full width $\Gamma = 0.194 \pm 0.009$ MeV

$\eta'(958)$ DECAY MODES	Fraction (Γ_i/Γ)	Confidence level	ρ (MeV/c)
$\pi^+ \pi^- \eta$	$(43.2 \pm 0.7) \%$		232
$\rho^0 \gamma$ (including non-resonant $\pi^+ \pi^- \gamma$)	$(29.3 \pm 0.5) \%$		165
$\pi^0 \pi^0 \eta$	$(21.7 \pm 0.8) \%$		239
$\omega \gamma$	$(2.75 \pm 0.22) \%$		159
$\gamma \gamma$	$(2.22 \pm 0.08) \%$		479
$3\pi^0$	$(1.68 \pm 0.22) \times 10^{-3}$		430
$\mu^+ \mu^- \gamma$	$(1.09 \pm 0.27) \times 10^{-4}$		467
$\pi^+ \pi^- \mu^+ \mu^-$	$< 2.2 \times 10^{-4}$	90%	401
$\pi^+ \pi^- \pi^0$	$(3.6^{+1.1}_{-0.9}) \times 10^{-3}$		428
$\pi^0 \rho^0$	$< 4 \%$	90%	111
$2(\pi^+ \pi^-)$	$< 2.4 \times 10^{-4}$	90%	372

$\pi^+ \pi^- 2\pi^0$	< 2.5	$\times 10^{-3}$	90%	376
$2(\pi^+ \pi^-)$ neutrals	< 1	%	95%	—
$2(\pi^+ \pi^-)\pi^0$	< 1.9	$\times 10^{-3}$	90%	298
$2(\pi^+ \pi^-)2\pi^0$	< 1	%	95%	197
$3(\pi^+ \pi^-)$	< 5	$\times 10^{-4}$	90%	189
$\pi^+ \pi^- e^+ e^-$	(2.4 $\begin{smallmatrix} +1.3 \\ -1.0 \end{smallmatrix}$)	$\times 10^{-3}$		458
$\gamma e^+ e^-$	< 9	$\times 10^{-4}$	90%	479
$\pi^0 \gamma \gamma$	< 8	$\times 10^{-4}$	90%	469
$4\pi^0$	< 5	$\times 10^{-4}$	90%	380
$e^+ e^-$	< 2.1	$\times 10^{-7}$	90%	479
invisible	< 9	$\times 10^{-4}$	90%	—

**Charge conjugation (C), Parity (P),
Lepton family number (LF) violating modes**

$\pi^+ \pi^-$	P, CP	< 2.9	$\times 10^{-3}$	90%	458
$\pi^0 \pi^0$	P, CP	< 1.0	$\times 10^{-3}$	90%	459
$\pi^0 e^+ e^-$	C	[f] < 1.4	$\times 10^{-3}$	90%	469
$\eta e^+ e^-$	C	[f] < 2.4	$\times 10^{-3}$	90%	322
3γ	C	< 1.0	$\times 10^{-4}$	90%	479
$\mu^+ \mu^- \pi^0$	C	[f] < 6.0	$\times 10^{-5}$	90%	445
$\mu^+ \mu^- \eta$	C	[f] < 1.5	$\times 10^{-5}$	90%	273
$e \mu$	LF	< 4.7	$\times 10^{-4}$	90%	473

$f_0(980)$ [J]

$$J^{PC} = 0^+(0^{++})$$

Mass $m = 980 \pm 10$ MeV

Full width $\Gamma = 40$ to 100 MeV

$f_0(980)$ DECAY MODES	Fraction (Γ_i/Γ)	ρ (MeV/c)
$\pi \pi$	dominant	471
$K \bar{K}$	seen	†
$\gamma \gamma$	seen	490

$a_0(980)$ [J]

$$J^{PC} = 1^-(0^{++})$$

Mass $m = 980 \pm 20$ MeV

Full width $\Gamma = 50$ to 100 MeV

$a_0(980)$ DECAY MODES	Fraction (Γ_i/Γ)	ρ (MeV/c)
$\eta \pi$	dominant	319
$K \bar{K}$	seen	†
$\gamma \gamma$	seen	490

$\phi(1020)$

$$J^{PC} = 0^-(1^{--})$$

Mass $m = 1019.455 \pm 0.020$ MeV ($S = 1.1$)

Full width $\Gamma = 4.26 \pm 0.04$ MeV ($S = 1.4$)

$\phi(1020)$ DECAY MODES	Fraction (Γ_i/Γ)	Scale factor/ Confidence level	ρ (MeV/c)
$K^+ K^-$	(48.9 ± 0.5) %	$S=1.1$	127
$K_L^0 K_S^0$	(34.2 ± 0.4) %	$S=1.1$	110
$\rho \pi + \pi^+ \pi^- \pi^0$	(15.32 ± 0.32) %	$S=1.1$	—

$\eta\gamma$	(1.309 ± 0.024) %	S=1.2	363
$\pi^0\gamma$	(1.27 ± 0.06) × 10 ⁻³		501
$\ell^+\ell^-$	—		510
e^+e^-	(2.954 ± 0.030) × 10 ⁻⁴	S=1.1	510
$\mu^+\mu^-$	(2.87 ± 0.19) × 10 ⁻⁴		499
ηe^+e^-	(1.15 ± 0.10) × 10 ⁻⁴		363
$\pi^+\pi^-$	(7.4 ± 1.3) × 10 ⁻⁵		490
$\omega\pi^0$	(4.7 ± 0.5) × 10 ⁻⁵		171
$\omega\gamma$	< 5 %	CL=84%	209
$\rho\gamma$	< 1.2 × 10 ⁻⁵	CL=90%	215
$\pi^+\pi^-\gamma$	(4.1 ± 1.3) × 10 ⁻⁵		490
$f_0(980)\gamma$	(3.22 ± 0.19) × 10 ⁻⁴	S=1.1	39
$\pi^0\pi^0\gamma$	(1.13 ± 0.06) × 10 ⁻⁴		492
$\pi^+\pi^-\pi^+\pi^-$	(4.0 $^{+2.8}_{-2.2}$) × 10 ⁻⁶		410
$\pi^+\pi^+\pi^-\pi^-\pi^0$	< 4.6 × 10 ⁻⁶	CL=90%	342
$\pi^0e^+e^-$	(1.12 ± 0.28) × 10 ⁻⁵		501
$\pi^0\eta\gamma$	(7.27 ± 0.30) × 10 ⁻⁵	S=1.5	346
$a_0(980)\gamma$	(7.6 ± 0.6) × 10 ⁻⁵		39
$K^0\bar{K}^0\gamma$	< 1.9 × 10 ⁻⁸	CL=90%	110
$\eta'(958)\gamma$	(6.25 ± 0.21) × 10 ⁻⁵		60
$\eta\pi^0\pi^0\gamma$	< 2 × 10 ⁻⁵	CL=90%	293
$\mu^+\mu^-\gamma$	(1.4 ± 0.5) × 10 ⁻⁵		499
$\rho\gamma\gamma$	< 1.2 × 10 ⁻⁴	CL=90%	215
$\eta\pi^+\pi^-$	< 1.8 × 10 ⁻⁵	CL=90%	288
$\eta\mu^+\mu^-$	< 9.4 × 10 ⁻⁶	CL=90%	321

$h_1(1170)$

$$J^G(J^{PC}) = 0^-(1^{+-})$$

Mass $m = 1170 \pm 20$ MeV

Full width $\Gamma = 360 \pm 40$ MeV

$h_1(1170)$ DECAY MODES	Fraction (Γ_i/Γ)	ρ (MeV/c)
$\rho\pi$	seen	307

$b_1(1235)$

$$J^G(J^{PC}) = 1^+(1^{+-})$$

Mass $m = 1229.5 \pm 3.2$ MeV (S = 1.6)

Full width $\Gamma = 142 \pm 9$ MeV (S = 1.2)

$b_1(1235)$ DECAY MODES	Fraction (Γ_i/Γ)	Confidence level	ρ (MeV/c)
$\omega\pi$	dominant		348
[D/S amplitude ratio = 0.277 ± 0.027]			
$\pi^\pm\gamma$	(1.6 ± 0.4) × 10 ⁻³		607
$\eta\rho$	seen		†
$\pi^+\pi^+\pi^-\pi^0$	< 50 %	84%	535
$(K\bar{K})^\pm\pi^0$	< 8 %	90%	248
$K_S^0 K_L^0 \pi^\pm$	< 6 %	90%	235
$K_S^0 K_S^0 \pi^\pm$	< 2 %	90%	235
$\phi\pi$	< 1.5 %	84%	147

$a_1(1260)$ [k]

$$J^G(J^{PC}) = 1^-(1^{++})$$

Mass $m = 1230 \pm 40$ MeV [l]Full width $\Gamma = 250$ to 600 MeV

$a_1(1260)$ DECAY MODES	Fraction (Γ_i/Γ)	ρ (MeV/c)
$(\rho\pi)_{S\text{-wave}}$	seen	353
$(\rho\pi)_{D\text{-wave}}$	seen	353
$(\rho(1450)\pi)_{S\text{-wave}}$	seen	†
$(\rho(1450)\pi)_{D\text{-wave}}$	seen	†
$\sigma\pi$	seen	—
$f_0(980)\pi$	not seen	189
$f_0(1370)\pi$	seen	†
$f_2(1270)\pi$	seen	†
$K\bar{K}^*(892) + \text{c.c.}$	seen	†
$\pi\gamma$	seen	608

 $f_2(1270)$

$$J^G(J^{PC}) = 0^+(2^{++})$$

Mass $m = 1275.1 \pm 1.2$ MeV (S = 1.1)Full width $\Gamma = 185.1^{+2.9}_{-2.4}$ MeV (S = 1.5)

$f_2(1270)$ DECAY MODES	Fraction (Γ_i/Γ)	Scale factor/ Confidence level	ρ (MeV/c)
$\pi\pi$	$(84.8^{+2.4}_{-1.2})\%$	S=1.2	623
$\pi^+\pi^-2\pi^0$	$(7.1^{+1.4}_{-2.7})\%$	S=1.3	562
$K\bar{K}$	$(4.6 \pm 0.4)\%$	S=2.8	403
$2\pi^+2\pi^-$	$(2.8 \pm 0.4)\%$	S=1.2	559
$\eta\eta$	$(4.0 \pm 0.8) \times 10^{-3}$	S=2.1	326
$4\pi^0$	$(3.0 \pm 1.0) \times 10^{-3}$		564
$\gamma\gamma$	$(1.64 \pm 0.19) \times 10^{-5}$	S=1.9	638
$\eta\pi\pi$	$< 8 \times 10^{-3}$	CL=95%	477
$K^0K^-\pi^+ + \text{c.c.}$	$< 3.4 \times 10^{-3}$	CL=95%	293
e^+e^-	$< 6 \times 10^{-10}$	CL=90%	638

 $f_1(1285)$

$$J^G(J^{PC}) = 0^+(1^{++})$$

Mass $m = 1281.8 \pm 0.6$ MeV (S = 1.6)Full width $\Gamma = 24.3 \pm 1.1$ MeV (S = 1.4)

$f_1(1285)$ DECAY MODES	Fraction (Γ_i/Γ)	Scale factor/ Confidence level	ρ (MeV/c)
4π	$(33.1^{+2.1}_{-1.8})\%$	S=1.3	568
$\pi^0\pi^0\pi^+\pi^-$	$(22.0^{+1.4}_{-1.2})\%$	S=1.3	566
$2\pi^+2\pi^-$	$(11.0^{+0.7}_{-0.6})\%$	S=1.3	563
$\rho^0\pi^+\pi^-$	$(11.0^{+0.7}_{-0.6})\%$	S=1.3	336
$\rho^0\rho^0$	seen		†
$4\pi^0$	$< 7 \times 10^{-4}$	CL=90%	568

$\eta\pi\pi$	(52 ± 5) %	482
$a_0(980)\pi$ [ignoring $a_0(980) \rightarrow K\bar{K}$]	(36 ± 7) %	238
$\eta\pi\pi$ [excluding $a_0(980)\pi$]	(16 ± 7) %	482
$K\bar{K}\pi$	(9.0±0.4) %	S=1.1 308
$K\bar{K}^*(892)$	not seen	†
$\gamma\rho^0$	(5.5±1.3) %	S=2.8 406
$\phi\gamma$	(7.4±2.6) × 10 ⁻⁴	236

$\eta(1295)$

$$J^G(J^{PC}) = 0^+(0^{-+})$$

Mass $m = 1294 \pm 4$ MeV (S = 1.6)

Full width $\Gamma = 55 \pm 5$ MeV

$\eta(1295)$ DECAY MODES	Fraction (Γ_i/Γ)	ρ (MeV/c)
$\eta\pi^+\pi^-$	seen	487
$a_0(980)\pi$	seen	248
$\eta\pi^0\pi^0$	seen	490
$\eta(\pi\pi)$ s-wave	seen	-

$\pi(1300)$

$$J^G(J^{PC}) = 1^-(0^{-+})$$

Mass $m = 1300 \pm 100$ MeV [1]

Full width $\Gamma = 200$ to 600 MeV

$\pi(1300)$ DECAY MODES	Fraction (Γ_i/Γ)	ρ (MeV/c)
$\rho\pi$	seen	404
$\pi(\pi\pi)$ s-wave	seen	-

$a_2(1320)$

$$J^G(J^{PC}) = 1^-(2^{++})$$

Mass $m = 1318.3 \pm 0.6$ MeV (S = 1.2)

Full width $\Gamma = 107 \pm 5$ MeV [1]

$a_2(1320)$ DECAY MODES	Fraction (Γ_i/Γ)	Scale factor/ Confidence level	ρ (MeV/c)
3π	(70.1 ± 2.7) %	S=1.2	624
$\eta\pi$	(14.5 ± 1.2) %		535
$\omega\pi\pi$	(10.6 ± 3.2) %	S=1.3	366
$K\bar{K}$	(4.9 ± 0.8) %		437
$\eta'(958)\pi$	(5.3 ± 0.9) × 10 ⁻³		288
$\pi^\pm\gamma$	(2.68±0.31) × 10 ⁻³		652
$\gamma\gamma$	(9.4 ± 0.7) × 10 ⁻⁶		659
e^+e^-	< 5 × 10 ⁻⁹	CL=90%	659

$f_0(1370)$ [1]

$$J^G(J^{PC}) = 0^+(0^{++})$$

Mass $m = 1200$ to 1500 MeV

Full width $\Gamma = 200$ to 500 MeV

$f_0(1370)$ DECAY MODES	Fraction (Γ_i/Γ)	ρ (MeV/c)
$\pi\pi$	seen	672
4π	seen	617

$4\pi^0$	seen	617
$2\pi^+ 2\pi^-$	seen	612
$\pi^+ \pi^- 2\pi^0$	seen	615
$\rho\rho$	dominant	†
$2(\pi\pi)$ s-wave	seen	–
$\pi(1300)\pi$	seen	†
$a_1(1260)\pi$	seen	35
$\eta\eta$	seen	411
$K\bar{K}$	seen	475
$K\bar{K}n\pi$	not seen	†
6π	not seen	508
$\omega\omega$	not seen	†
$\gamma\gamma$	seen	685
$e^+ e^-$	not seen	685

 $\pi_1(1400)$ ^[m]

$$J^G(J^{PC}) = 1^-(1^-+)$$

Mass $m = 1354 \pm 25$ MeV (S = 1.8)Full width $\Gamma = 330 \pm 35$ MeV

$\pi_1(1400)$ DECAY MODES	Fraction (Γ_i/Γ)	ρ (MeV/c)
$\eta\pi^0$	seen	557
$\eta\pi^-$	seen	556

 $\eta(1405)$ ^[n]

$$J^G(J^{PC}) = 0^+(0^-+)$$

Mass $m = 1409.8 \pm 2.5$ MeV ^[l] (S = 2.2)Full width $\Gamma = 51.1 \pm 3.4$ MeV ^[l] (S = 2.0)

$\eta(1405)$ DECAY MODES	Fraction (Γ_i/Γ)	Confidence level	ρ (MeV/c)
$K\bar{K}\pi$	seen		425
$\eta\pi\pi$	seen		563
$a_0(980)\pi$	seen		345
$\eta(\pi\pi)$ s-wave	seen		–
$f_0(980)\eta$	seen		†
4π	seen		639
$\rho\rho$	<58 %	99.85%	†
$\rho^0\gamma$	seen		492
$K^*(892)K$	seen		125

 $f_1(1420)$ ^[o]

$$J^G(J^{PC}) = 0^+(1^++)$$

Mass $m = 1426.4 \pm 0.9$ MeV (S = 1.1)Full width $\Gamma = 54.9 \pm 2.6$ MeV

$f_1(1420)$ DECAY MODES	Fraction (Γ_i/Γ)	ρ (MeV/c)
$K\bar{K}\pi$	dominant	438
$K\bar{K}^*(892) + \text{c.c.}$	dominant	163
$\eta\pi\pi$	possibly seen	573
$\phi\gamma$	seen	349

$\omega(1420)$ [ρ]

$$I^G(J^{PC}) = 0^-(1^{--})$$

Mass m (1400–1450) MeV
 Full width Γ (180–250) MeV

$\omega(1420)$ DECAY MODES	Fraction (Γ_i/Γ)	ρ (MeV/c)
$\rho\pi$	dominant	486
$\omega\pi\pi$	seen	444
$b_1(1235)\pi$	seen	125
e^+e^-	seen	710

$a_0(1450)$ [η]

$$I^G(J^{PC}) = 1^-(0^{++})$$

Mass $m = 1474 \pm 19$ MeV
 Full width $\Gamma = 265 \pm 13$ MeV

$a_0(1450)$ DECAY MODES	Fraction (Γ_i/Γ)	ρ (MeV/c)
$\pi\eta$	seen	627
$\pi\eta'(958)$	seen	410
$K\bar{K}$	seen	547
$\omega\pi\pi$	seen	484
$a_0(980)\pi\pi$	seen	342
$\gamma\gamma$	seen	737

$\rho(1450)$ [η]

$$I^G(J^{PC}) = 1^+(1^{--})$$

Mass $m = 1465 \pm 25$ MeV [η]
 Full width $\Gamma = 400 \pm 60$ MeV [η]

$\rho(1450)$ DECAY MODES	Fraction (Γ_i/Γ)	ρ (MeV/c)
$\pi\pi$	seen	720
4π	seen	669
e^+e^-	seen	732
$\eta\rho$	possibly seen	310
$a_2(1320)\pi$	not seen	55
$K\bar{K}$	not seen	541
$K\bar{K}^*(892) + \text{c.c.}$	possibly seen	229
$\eta\gamma$	possibly seen	630

$\eta(1475)$ [η]

$$I^G(J^{PC}) = 0^+(0^{-+})$$

Mass $m = 1476 \pm 4$ MeV ($S = 1.3$)
 Full width $\Gamma = 85 \pm 9$ MeV ($S = 1.5$)

$\eta(1475)$ DECAY MODES	Fraction (Γ_i/Γ)	ρ (MeV/c)
$K\bar{K}\pi$	dominant	477
$K\bar{K}^*(892) + \text{c.c.}$	seen	245
$a_0(980)\pi$	seen	396
$\gamma\gamma$	seen	738

$f_0(1500)$ ^[m]

$$J^G(J^{PC}) = 0^+(0^{++})$$

Mass $m = 1505 \pm 6$ MeV (S = 1.3)

Full width $\Gamma = 109 \pm 7$ MeV

$f_0(1500)$ DECAY MODES	Fraction (Γ_i/Γ)	Scale factor	ρ (MeV/c)
$\pi\pi$	(34.9 ± 2.3) %	1.2	741
$\pi^+\pi^-$	seen		740
$2\pi^0$	seen		741
4π	(49.5 ± 3.3) %	1.2	691
$4\pi^0$	seen		691
$2\pi^+2\pi^-$	seen		687
$2(\pi\pi)_{S\text{-wave}}$	seen		—
$\rho\rho$	seen		†
$\pi(1300)\pi$	seen		144
$a_1(1260)\pi$	seen		218
$\eta\eta$	(5.1 ± 0.9) %	1.4	516
$\eta\eta'(958)$	(1.9 ± 0.8) %	1.7	†
$K\bar{K}$	(8.6 ± 1.0) %	1.1	568
$\gamma\gamma$	not seen		753

 $f'_2(1525)$

$$J^G(J^{PC}) = 0^+(2^{++})$$

Mass $m = 1525 \pm 5$ MeV [l]

Full width $\Gamma = 73^{+6}_{-5}$ MeV [l]

$f'_2(1525)$ DECAY MODES	Fraction (Γ_i/Γ)	ρ (MeV/c)
$K\bar{K}$	(88.7 ± 2.2) %	581
$\eta\eta$	(10.4 ± 2.2) %	530
$\pi\pi$	(8.2 ± 1.5) × 10 ⁻³	750
$\gamma\gamma$	(1.11 ± 0.14) × 10 ⁻⁶	763

 $\pi_1(1600)$ ^[m]

$$J^G(J^{PC}) = 1^-(1^{-+})$$

Mass $m = 1662^{+15}_{-11}$ MeV (S = 1.2)

Full width $\Gamma = 234 \pm 50$ MeV (S = 1.7)

$\pi_1(1600)$ DECAY MODES	Fraction (Γ_i/Γ)	ρ (MeV/c)
$\pi\pi\pi$	not seen	803
$\rho^0\pi^-$	not seen	641
$f_2(1270)\pi^-$	not seen	319
$b_1(1235)\pi$	seen	357
$\eta'(958)\pi^-$	seen	543
$f_1(1285)\pi$	seen	315

$\eta_2(1645)$

$$I^G(J^{PC}) = 0^+(2^{-+})$$

Mass $m = 1617 \pm 5$ MeV
 Full width $\Gamma = 181 \pm 11$ MeV

$\eta_2(1645)$ DECAY MODES	Fraction (Γ_i/Γ)	p (MeV/c)
$a_2(1320)\pi$	seen	242
$K\bar{K}\pi$	seen	580
$K^*\bar{K}$	seen	404
$\eta\pi^+\pi^-$	seen	685
$a_0(980)\pi$	seen	499
$f_2(1270)\eta$	not seen	†

$\omega(1650)$ [r]

$$I^G(J^{PC}) = 0^-(1^{--})$$

Mass $m = 1670 \pm 30$ MeV
 Full width $\Gamma = 315 \pm 35$ MeV

$\omega(1650)$ DECAY MODES	Fraction (Γ_i/Γ)	p (MeV/c)
$\rho\pi$	seen	646
$\omega\pi\pi$	seen	617
$\omega\eta$	seen	500
e^+e^-	seen	835

$\omega_3(1670)$

$$I^G(J^{PC}) = 0^-(3^{--})$$

Mass $m = 1667 \pm 4$ MeV
 Full width $\Gamma = 168 \pm 10$ MeV [l]

$\omega_3(1670)$ DECAY MODES	Fraction (Γ_i/Γ)	p (MeV/c)
$\rho\pi$	seen	645
$\omega\pi\pi$	seen	615
$b_1(1235)\pi$	possibly seen	361

$\pi_2(1670)$

$$I^G(J^{PC}) = 1^-(2^{-+})$$

Mass $m = 1672.4 \pm 3.2$ MeV [l] ($S = 1.4$)
 Full width $\Gamma = 259 \pm 9$ MeV [l] ($S = 1.3$)

$\pi_2(1670)$ DECAY MODES	Fraction (Γ_i/Γ)	Confidence level	p (MeV/c)
3π	$(95.8 \pm 1.4)\%$		809
$f_2(1270)\pi$	$(56.3 \pm 3.2)\%$		329
$\rho\pi$	$(31 \pm 4)\%$		648
$\sigma\pi$	$(10.9 \pm 3.4)\%$		—
$(\pi\pi)$ s-wave	$(8.7 \pm 3.4)\%$		—
$K\bar{K}^*(892) + \text{c.c.}$	$(4.2 \pm 1.4)\%$		455
$\omega\rho$	$(2.7 \pm 1.1)\%$		304
$\gamma\gamma$	$< 2.8 \times 10^{-7}$	90%	836
$\rho(1450)\pi$	$< 3.6 \times 10^{-3}$	97.7%	148

$b_1(1235)\pi$	$< 1.9 \times 10^{-3}$	97.7%	366
$f_1(1285)\pi$	possibly seen		323
$a_2(1320)\pi$	not seen		292

 $\phi(1680)$

$$J^G(J^{PC}) = 0^-(1^{--})$$

Mass $m = 1680 \pm 20$ MeV [I]

Full width $\Gamma = 150 \pm 50$ MeV [I]

$\phi(1680)$ DECAY MODES	Fraction (Γ_i/Γ)	ρ (MeV/c)
$K\bar{K}^*(892) + \text{c.c.}$	dominant	462
$K_S^0 K\pi$	seen	621
$K\bar{K}$	seen	680
e^+e^-	seen	840
$\omega\pi\pi$	not seen	623
$K^+K^-\pi^+\pi^-$	seen	544

 $\rho_3(1690)$

$$J^G(J^{PC}) = 1^+(3^{--})$$

Mass $m = 1688.8 \pm 2.1$ MeV [I]

Full width $\Gamma = 161 \pm 10$ MeV [I] (S = 1.5)

$\rho_3(1690)$ DECAY MODES	Fraction (Γ_i/Γ)	Scale factor	ρ (MeV/c)
4π	(71.1 \pm 1.9) %		790
$\pi^\pm\pi^+\pi^-\pi^0$	(67 \pm 22) %		787
$\omega\pi$	(16 \pm 6) %		655
$\pi\pi$	(23.6 \pm 1.3) %		834
$K\bar{K}\pi$	(3.8 \pm 1.2) %		629
$K\bar{K}$	(1.58 \pm 0.26) %	1.2	685
$\eta\pi^+\pi^-$	seen		727
$\rho(770)\eta$	seen		520
$\pi\pi\rho$	seen		633
Excluding 2ρ and $a_2(1320)\pi$.			
$a_2(1320)\pi$	seen		307
$\rho\rho$	seen		334

 $\rho(1700)$ [q]

$$J^G(J^{PC}) = 1^+(1^{--})$$

Mass $m = 1720 \pm 20$ MeV [I] ($\eta\rho^0$ and $\pi^+\pi^-\pi^0$ modes)

Full width $\Gamma = 250 \pm 100$ MeV [I] ($\eta\rho^0$ and $\pi^+\pi^-\pi^0$ modes)

$\rho(1700)$ DECAY MODES	Fraction (Γ_i/Γ)	ρ (MeV/c)
$2(\pi^+\pi^-)$	large	803
$\rho\pi\pi$	dominant	653
$\rho^0\pi^+\pi^-$	large	650
$\rho^\pm\pi^\mp\pi^0$	large	652
$a_1(1260)\pi$	seen	404
$h_1(1170)\pi$	seen	447
$\pi(1300)\pi$	seen	349
$\rho\rho$	seen	372

$\pi^+ \pi^-$	seen	849
$\pi \bar{\pi}$	seen	849
$K \bar{K}^*(892) + \text{c.c.}$	seen	496
$\eta \rho$	seen	545
$a_2(1320) \pi$	not seen	334
$K \bar{K}$	seen	704
$e^+ e^-$	seen	860
$\pi^0 \omega$	seen	674

$f_0(1710)$ [S]

$$I^G(J^{PC}) = 0^+(0^{++})$$

Mass $m = 1720 \pm 6$ MeV (S = 1.6)

Full width $\Gamma = 135 \pm 8$ MeV (S = 1.1)

$f_0(1710)$ DECAY MODES	Fraction (Γ_i/Γ)	ρ (MeV/c)
$K \bar{K}$	seen	704
$\eta \eta$	seen	663
$\pi \pi$	seen	849
$\omega \omega$	seen	357

$\pi(1800)$

$$I^G(J^{PC}) = 1^-(0^{-+})$$

Mass $m = 1816 \pm 14$ MeV (S = 2.3)

Full width $\Gamma = 208 \pm 12$ MeV

$\pi(1800)$ DECAY MODES	Fraction (Γ_i/Γ)	ρ (MeV/c)
$\pi^+ \pi^- \pi^-$	seen	881
$f_0(600) \pi^-$	seen	—
$f_0(980) \pi^-$	seen	634
$f_0(1370) \pi^-$	seen	371
$f_0(1500) \pi^-$	not seen	254
$\rho \pi^-$	not seen	735
$\eta \eta \pi^-$	seen	664
$a_0(980) \eta$	seen	477
$a_2(1320) \eta$	not seen	†
$f_2(1270) \pi$	not seen	445
$f_0(1370) \pi^-$	not seen	371
$f_0(1500) \pi^-$	seen	254
$\eta \eta' (958) \pi^-$	seen	380
$K_0^*(1430) K^-$	seen	†
$K^*(892) K^-$	not seen	573

$\phi_3(1850)$

$$I^G(J^{PC}) = 0^-(3^{--})$$

Mass $m = 1854 \pm 7$ MeV

Full width $\Gamma = 87^{+28}_{-23}$ MeV (S = 1.2)

$\phi_3(1850)$ DECAY MODES	Fraction (Γ_i/Γ)	ρ (MeV/c)
$K \bar{K}$	seen	785
$K \bar{K}^*(892) + \text{c.c.}$	seen	602

$\pi_2(1880)$

$$J^G(J^{PC}) = 1^-(2^-+)$$

Mass $m = 1895 \pm 16$ MeVFull width $\Gamma = 235 \pm 34$ MeV **$f_2(1950)$**

$$J^G(J^{PC}) = 0^+(2^{++})$$

Mass $m = 1944 \pm 12$ MeV ($S = 1.5$)Full width $\Gamma = 472 \pm 18$ MeV **$f_2(1950)$ DECAY MODES**

	Fraction (Γ_i/Γ)	ρ (MeV/c)
$K^*(892)\bar{K}^*(892)$	seen	387
$\pi^+\pi^-\pi^0$	seen	962
$\pi^0\pi^0$	seen	963
4π	seen	925
$\eta\eta$	seen	803
$K\bar{K}$	seen	837
$\gamma\gamma$	seen	972

 $f_2(2010)$

$$J^G(J^{PC}) = 0^+(2^{++})$$

Mass $m = 2011_{-80}^{+60}$ MeVFull width $\Gamma = 202 \pm 60$ MeV **$f_2(2010)$ DECAY MODES**

	Fraction (Γ_i/Γ)	ρ (MeV/c)
$\phi\phi$	seen	†
$K\bar{K}$	seen	876

 $a_4(2040)$

$$J^G(J^{PC}) = 1^-(4^{++})$$

Mass $m = 2001 \pm 10$ MeVFull width $\Gamma = 235 \pm 29$ MeV ($S = 1.3$) **$a_4(2040)$ DECAY MODES**

	Fraction (Γ_i/Γ)	ρ (MeV/c)
$K\bar{K}$	seen	870
$\pi^+\pi^-\pi^0$	seen	976
$\rho\pi$	seen	844
$f_2(1270)\pi$	seen	583
$\omega\pi^-\pi^0$	seen	821
$\omega\rho$	seen	627
$\eta\pi^0$	seen	920
$\eta'(958)\pi$	seen	764

 $f_4(2050)$

$$J^G(J^{PC}) = 0^+(4^{++})$$

Mass $m = 2018 \pm 11$ MeV ($S = 2.1$)Full width $\Gamma = 237 \pm 18$ MeV ($S = 1.9$) **$f_4(2050)$ DECAY MODES**

	Fraction (Γ_i/Γ)	ρ (MeV/c)
$\omega\omega$	seen	637
$\pi\pi$	(17.0±1.5) %	1000

$K\bar{K}$	$(6.8^{+3.4}_{-1.8}) \times 10^{-3}$	880
$\eta\eta$	$(2.1 \pm 0.8) \times 10^{-3}$	848
$4\pi^0$	< 1.2 %	964
$a_2(1320)\pi$	seen	567

$\phi(2170)$ $I^G(J^{PC}) = 0^-(1^{--})$

Mass $m = 2175 \pm 15$ MeV (S = 1.6)
 Full width $\Gamma = 61 \pm 18$ MeV

$\phi(2170)$ DECAY MODES	Fraction (Γ_i/Γ)	p (MeV/c)
e^+e^-	seen	1087
$\phi f_0(980)$	seen	427
$K^+K^- f_0(980) \rightarrow K^+K^-\pi^+\pi^-$	seen	—
$K^+K^- f_0(980) \rightarrow K^+K^-\pi^0\pi^0$	seen	—
$K^{*0}K^\pm\pi^\mp$	not seen	770

$f_2(2300)$ $I^G(J^{PC}) = 0^+(2^{++})$

Mass $m = 2297 \pm 28$ MeV
 Full width $\Gamma = 149 \pm 40$ MeV

$f_2(2300)$ DECAY MODES	Fraction (Γ_i/Γ)	p (MeV/c)
$\phi\phi$	seen	529
$K\bar{K}$	seen	1037
$\gamma\gamma$	seen	1149

$f_2(2340)$ $I^G(J^{PC}) = 0^+(2^{++})$

Mass $m = 2339 \pm 60$ MeV
 Full width $\Gamma = 319^{+80}_{-70}$ MeV

$f_2(2340)$ DECAY MODES	Fraction (Γ_i/Γ)	p (MeV/c)
$\phi\phi$	seen	573
$\eta\eta$	seen	1033

STRANGE MESONS

($S = \pm 1, C = B = 0$)

$$K^+ = u\bar{s}, K^0 = d\bar{s}, \bar{K}^0 = \bar{d}s, K^- = \bar{u}s, \text{ similarly for } K^{*s}$$

 K^\pm

$$I(J^P) = \frac{1}{2}(0^-)$$

$$\text{Mass } m = 493.677 \pm 0.016 \text{ MeV } [^t] \quad (S = 2.8)$$

$$\text{Mean life } \tau = (1.2380 \pm 0.0021) \times 10^{-8} \text{ s} \quad (S = 1.9)$$

$$c\tau = 3.712 \text{ m}$$

Slope parameter g [u]

(See Particle Listings for quadratic coefficients and alternative parametrization related to $\pi\pi$ scattering)

$$K^\pm \rightarrow \pi^\pm \pi^+ \pi^- \quad g = -0.21134 \pm 0.00017$$

$$(g_+ - g_-) / (g_+ + g_-) = (-1.5 \pm 2.2) \times 10^{-4}$$

$$K^\pm \rightarrow \pi^\pm \pi^0 \pi^0 \quad g = 0.626 \pm 0.007$$

$$(g_+ - g_-) / (g_+ + g_-) = (1.8 \pm 1.8) \times 10^{-4}$$

 K^\pm decay form factors [$^a, ^v$]

Assuming μ -e universality

$$\lambda_+(K_{\mu 3}^+) = \lambda_+(K_{e 3}^+) = (2.97 \pm 0.05) \times 10^{-2}$$

$$\lambda_0(K_{\mu 3}^+) = (1.95 \pm 0.12) \times 10^{-2}$$

Not assuming μ -e universality

$$\lambda_+(K_{e 3}^+) = (2.98 \pm 0.05) \times 10^{-2}$$

$$\lambda_+(K_{\mu 3}^+) = (2.96 \pm 0.17) \times 10^{-2}$$

$$\lambda_0(K_{\mu 3}^+) = (1.96 \pm 0.13) \times 10^{-2}$$

$K_{e 3}$ form factor quadratic fit

$$\lambda'_+(K_{e 3}^\pm) \text{ linear coeff.} = (2.48 \pm 0.17) \times 10^{-2}$$

$$\lambda''_+(K_{e 3}^\pm) \text{ quadratic coeff.} = (0.19 \pm 0.09) \times 10^{-2}$$

$$K_{e 3}^+ \quad |f_S/f_+| = (-0.3^{+0.8}_{-0.7}) \times 10^{-2}$$

$$K_{e 3}^+ \quad |f_T/f_+| = (-1.2 \pm 2.3) \times 10^{-2}$$

$$K_{\mu 3}^+ \quad |f_S/f_+| = (0.2 \pm 0.6) \times 10^{-2}$$

$$K_{\mu 3}^+ \quad |f_T/f_+| = (-0.1 \pm 0.7) \times 10^{-2}$$

$$K^+ \rightarrow e^+ \nu_e \gamma \quad |F_A + F_V| = 0.133 \pm 0.008 \quad (S = 1.3)$$

$$K^+ \rightarrow \mu^+ \nu_\mu \gamma \quad |F_A + F_V| = 0.165 \pm 0.013$$

$$K^+ \rightarrow e^+ \nu_e \gamma \quad |F_A - F_V| < 0.49$$

$$K^+ \rightarrow \mu^+ \nu_\mu \gamma \quad |F_A - F_V| = -0.24 \text{ to } 0.04, \text{ CL} = 90\%$$

Charge Radius

$$\langle r \rangle = 0.560 \pm 0.031 \text{ fm}$$

CP violation parameters

$$\Delta(K_{\pi e e}^\pm) = (-2.2 \pm 1.6) \times 10^{-2}$$

$$\Delta(K_{\pi \mu \mu}^\pm) = -0.02 \pm 0.12$$

T violation parameters

$$K^+ \rightarrow \pi^0 \mu^+ \nu_\mu \quad P_T = (-1.7 \pm 2.5) \times 10^{-3}$$

$$K^+ \rightarrow \mu^+ \nu_\mu \gamma \quad P_T = (-0.6 \pm 1.9) \times 10^{-2}$$

$$K^+ \rightarrow \pi^0 \mu^+ \nu_\mu \quad \text{Im}(\xi) = -0.006 \pm 0.008$$

K^- modes are charge conjugates of the modes below.

K⁺ DECAY MODES	Fraction (Γ_i/Γ)	Scale factor/ Confidence level	ρ (MeV/c)
Leptonic and semileptonic modes			
$K^+ \rightarrow e^+ \nu_e$	$(1.584 \pm 0.020) \times 10^{-5}$		247
$K^+ \rightarrow \mu^+ \nu_\mu$	$(63.55 \pm 0.11) \%$	S=1.2	236
$K^+ \rightarrow \pi^0 e^+ \nu_e$	$(5.07 \pm 0.04) \%$	S=2.1	228
Called K_{e3}^+ .			
$K^+ \rightarrow \pi^0 \mu^+ \nu_\mu$	$(3.353 \pm 0.034) \%$	S=1.8	215
Called $K_{\mu3}^+$.			
$K^+ \rightarrow \pi^0 \pi^0 e^+ \nu_e$	$(2.2 \pm 0.4) \times 10^{-5}$		206
$K^+ \rightarrow \pi^+ \pi^- e^+ \nu_e$	$(4.09 \pm 0.10) \times 10^{-5}$		203
$K^+ \rightarrow \pi^+ \pi^- \mu^+ \nu_\mu$	$(1.4 \pm 0.9) \times 10^{-5}$		151
$K^+ \rightarrow \pi^0 \pi^0 \pi^0 e^+ \nu_e$	$< 3.5 \times 10^{-6}$	CL=90%	135
Hadronic modes			
$K^+ \rightarrow \pi^+ \pi^0$	$(20.66 \pm 0.08) \%$	S=1.2	205
$K^+ \rightarrow \pi^+ \pi^0 \pi^0$	$(1.761 \pm 0.022) \%$	S=1.1	133
$K^+ \rightarrow \pi^+ \pi^+ \pi^-$	$(5.59 \pm 0.04) \%$	S=1.3	125
Leptonic and semileptonic modes with photons			
$K^+ \rightarrow \mu^+ \nu_\mu \gamma$	[w,x] $(6.2 \pm 0.8) \times 10^{-3}$		236
$K^+ \rightarrow \mu^+ \nu_\mu \gamma (\text{SD}^+)$	[a,y] $(1.33 \pm 0.22) \times 10^{-5}$		-
$K^+ \rightarrow \mu^+ \nu_\mu \gamma (\text{SD}^+ \text{INT})$	[a,y] $< 2.7 \times 10^{-5}$	CL=90%	-
$K^+ \rightarrow \mu^+ \nu_\mu \gamma (\text{SD}^- + \text{SD}^- \text{INT})$	[a,y] $< 2.6 \times 10^{-4}$	CL=90%	-
$K^+ \rightarrow e^+ \nu_e \gamma$	$(9.4 \pm 0.4) \times 10^{-6}$		247
$K^+ \rightarrow \pi^0 e^+ \nu_e \gamma$	[w,x] $(2.56 \pm 0.16) \times 10^{-4}$		228
$K^+ \rightarrow \pi^0 e^+ \nu_e \gamma (\text{SD})$	[a,y] $< 5.3 \times 10^{-5}$	CL=90%	228
$K^+ \rightarrow \pi^0 \mu^+ \nu_\mu \gamma$	[w,x] $(1.5 \pm 0.4) \times 10^{-5}$		215
$K^+ \rightarrow \pi^0 \pi^0 e^+ \nu_e \gamma$	$< 5 \times 10^{-6}$	CL=90%	206
Hadronic modes with photons or $\ell\bar{\ell}$ pairs			
$K^+ \rightarrow \pi^+ \pi^0 \gamma$	[w,x] $(2.75 \pm 0.15) \times 10^{-4}$		205
$K^+ \rightarrow \pi^+ \pi^0 \gamma (\text{DE})$	[w,z] $(4.3 \pm 0.7) \times 10^{-6}$		205
$K^+ \rightarrow \pi^+ \pi^0 \pi^0 \gamma$	[w,x] $(7.6 \pm_{-3.0}^{+6.0}) \times 10^{-6}$		133
$K^+ \rightarrow \pi^+ \pi^+ \pi^- \gamma$	[w,x] $(1.04 \pm 0.31) \times 10^{-4}$		125
$K^+ \rightarrow \pi^+ \gamma \gamma$	[w] $(1.10 \pm 0.32) \times 10^{-6}$		227
$K^+ \rightarrow \pi^+ 3\gamma$	[w] $< 1.0 \times 10^{-4}$	CL=90%	227
$K^\pm \rightarrow \pi^+ e^+ e^- \gamma$	$(1.19 \pm 0.13) \times 10^{-8}$		227
Leptonic modes with $\ell\bar{\ell}$ pairs			
$K^+ \rightarrow e^+ \nu_e \nu \bar{\nu}$	$< 6 \times 10^{-5}$	CL=90%	247
$K^+ \rightarrow \mu^+ \nu_\mu \nu \bar{\nu}$	$< 6.0 \times 10^{-6}$	CL=90%	236
$K^+ \rightarrow e^+ \nu_e e^+ e^-$	$(2.48 \pm 0.20) \times 10^{-8}$		247
$K^+ \rightarrow \mu^+ \nu_\mu e^+ e^-$	$(7.06 \pm 0.31) \times 10^{-8}$		236
$K^+ \rightarrow e^+ \nu_e \mu^+ \mu^-$	$(1.7 \pm 0.5) \times 10^{-8}$		223
$K^+ \rightarrow \mu^+ \nu_\mu \mu^+ \mu^-$	$< 4.1 \times 10^{-7}$	CL=90%	185

**Lepton Family number (LF), Lepton number (L), $\Delta S = \Delta Q$ (SQ)
violating modes, or $\Delta S = 1$ weak neutral current (SI) modes**

$K^+ \rightarrow \pi^+ \pi^+ e^- \bar{\nu}_e$	SQ	< 1.2	$\times 10^{-8}$	CL=90%	203
$K^+ \rightarrow \pi^+ \pi^+ \mu^- \bar{\nu}_\mu$	SQ	< 3.0	$\times 10^{-6}$	CL=95%	151
$K^+ \rightarrow \pi^+ e^+ e^-$	SI	(3.00 \pm 0.09)	$\times 10^{-7}$		227
$K^+ \rightarrow \pi^+ \mu^+ \mu^-$	SI	(8.1 \pm 1.4)	$\times 10^{-8}$	S=2.7	172
$K^+ \rightarrow \pi^+ \nu \bar{\nu}$	SI	(1.7 \pm 1.1)	$\times 10^{-10}$		227
$K^+ \rightarrow \pi^+ \pi^0 \nu \bar{\nu}$	SI	< 4.3	$\times 10^{-5}$	CL=90%	205
$K^+ \rightarrow \mu^- \nu e^+ e^+$	LF	< 2.0	$\times 10^{-8}$	CL=90%	236
$K^+ \rightarrow \mu^+ \nu_e$	LF	[d] < 4	$\times 10^{-3}$	CL=90%	236
$K^+ \rightarrow \pi^+ \mu^+ e^-$	LF	< 1.3	$\times 10^{-11}$	CL=90%	214
$K^+ \rightarrow \pi^+ \mu^- e^+$	LF	< 5.2	$\times 10^{-10}$	CL=90%	214
$K^+ \rightarrow \pi^- \mu^+ e^+$	L	< 5.0	$\times 10^{-10}$	CL=90%	214
$K^+ \rightarrow \pi^- e^+ e^+$	L	< 6.4	$\times 10^{-10}$	CL=90%	227
$K^+ \rightarrow \pi^- \mu^+ \mu^+$	L	[d] < 3.0	$\times 10^{-9}$	CL=90%	172
$K^+ \rightarrow \mu^+ \bar{\nu}_e$	L	[d] < 3.3	$\times 10^{-3}$	CL=90%	236
$K^+ \rightarrow \pi^0 e^+ \bar{\nu}_e$	L	< 3	$\times 10^{-3}$	CL=90%	228
$K^+ \rightarrow \pi^+ \gamma$	[aa]	< 2.3	$\times 10^{-9}$	CL=90%	227

 K^0

$$I(J^P) = \frac{1}{2}(0^-)$$

50% K_S , 50% K_L

$$\text{Mass } m = 497.614 \pm 0.024 \text{ MeV} \quad (S = 1.6)$$

$$m_{K^0} - m_{K^\pm} = 3.937 \pm 0.028 \text{ MeV} \quad (S = 1.8)$$

Mean Square Charge Radius

$$\langle r^2 \rangle = -0.077 \pm 0.010 \text{ fm}^2$$

T-violation parameters in K^0 - \bar{K}^0 mixing [v]

$$\text{Asymmetry } A_T \text{ in } K^0\text{-}\bar{K}^0 \text{ mixing} = (6.6 \pm 1.6) \times 10^{-3}$$

CPT-violation parameters [v]

$$\text{Re } \delta = (2.3 \pm 2.7) \times 10^{-4}$$

$$\text{Im } \delta = (0.4 \pm 2.1) \times 10^{-5}$$

$$\text{Re}(y), K_{e3} \text{ parameter} = (0.4 \pm 2.5) \times 10^{-3}$$

$$\text{Re}(x_-), K_{e3} \text{ parameter} = (-2.9 \pm 2.0) \times 10^{-3}$$

$$|m_{K^0} - m_{\bar{K}^0}| / m_{\text{average}} < 8 \times 10^{-19}, \text{ CL} = 90\% [bb]$$

$$(\Gamma_{K^0} - \Gamma_{\bar{K}^0}) / m_{\text{average}} = (8 \pm 8) \times 10^{-18}$$

Tests of $\Delta S = \Delta Q$

$$\text{Re}(x_+), K_{e3} \text{ parameter} = (-0.9 \pm 3.0) \times 10^{-3}$$

 K_S^0

$$I(J^P) = \frac{1}{2}(0^-)$$

Mean life $\tau = (0.8953 \pm 0.0005) \times 10^{-10}$ s (S = 1.1) Assuming CPT

Mean life $\tau = (0.8958 \pm 0.0005) \times 10^{-10}$ s Not assuming CPT

$$c\tau = 2.6842 \text{ cm} \quad \text{Assuming CPT}$$

CP-violation parameters ^[cc]

$$\text{Im}(\eta_{+-0}) = -0.002 \pm 0.009$$

$$\text{Im}(\eta_{000}) = (-0.1 \pm 1.6) \times 10^{-2}$$

$$|\eta_{000}| = |A(K_S^0 \rightarrow 3\pi^0)/A(K_L^0 \rightarrow 3\pi^0)| < 0.018, \text{ CL} = 90\%$$

$$\text{CP asymmetry } A \text{ in } \pi^+ \pi^- e^+ e^- = (-1 \pm 4)\%$$

K_S^0 DECAY MODES	Fraction (Γ_i/Γ)	Scale factor/ Confidence level	ρ (MeV/c)
Hadronic modes			
$\pi^0 \pi^0$	$(30.69 \pm 0.05)\%$		209
$\pi^+ \pi^-$	$(69.20 \pm 0.05)\%$		206
$\pi^+ \pi^- \pi^0$	$(3.5 \pm_{-0.9}^{+1.1}) \times 10^{-7}$		133
Modes with photons or $\ell\bar{\ell}$ pairs			
$\pi^+ \pi^- \gamma$	[x, dd] $(1.79 \pm 0.05) \times 10^{-3}$		206
$\pi^+ \pi^- e^+ e^-$	$(4.69 \pm 0.30) \times 10^{-5}$		206
$\pi^0 \gamma \gamma$	[dd] $(4.9 \pm 1.8) \times 10^{-8}$		231
$\gamma \gamma$	$(2.63 \pm 0.17) \times 10^{-6}$	S=3.0	249
Semileptonic modes			
$\pi^\pm e^\mp \nu_e$	[ee] $(7.04 \pm 0.08) \times 10^{-4}$		229
CP violating (CP) and $\Delta S = 1$ weak neutral current (S1) modes			
$3\pi^0$	CP $< 1.2 \times 10^{-7}$	CL=90%	139
$\mu^+ \mu^-$	S1 $< 3.2 \times 10^{-7}$	CL=90%	225
$e^+ e^-$	S1 $< 9 \times 10^{-9}$	CL=90%	249
$\pi^0 e^+ e^-$	S1 [dd] $(3.0 \pm_{-1.2}^{+1.5}) \times 10^{-9}$		230
$\pi^0 \mu^+ \mu^-$	S1 $(2.9 \pm_{-1.2}^{+1.5}) \times 10^{-9}$		177

 K_L^0

$$I(J^P) = \frac{1}{2}(0^-)$$

$$m_{K_L} - m_{K_S}$$

$$= (0.5292 \pm 0.0009) \times 10^{10} \hbar \text{ s}^{-1} \quad (S = 1.2) \quad \text{Assuming } CPT$$

$$= (3.483 \pm 0.006) \times 10^{-12} \text{ MeV} \quad \text{Assuming } CPT$$

$$= (0.5290 \pm 0.0015) \times 10^{10} \hbar \text{ s}^{-1} \quad (S = 1.1) \quad \text{Not assuming } CPT$$

$$\text{Mean life } \tau = (5.116 \pm 0.020) \times 10^{-8} \text{ s}$$

$$c\tau = 15.34 \text{ m}$$

Slope parameter g ^[u]

(See Particle Listings for quadratic coefficients)

$$K_L^0 \rightarrow \pi^+ \pi^- \pi^0: g = 0.678 \pm 0.008 \quad (S = 1.5)$$

 K_L decay form factors ^[v]Linear parametrization assuming μ - e universality

$$\lambda_+(K_{\mu 3}^0) = \lambda_+(K_{e 3}^0) = (2.82 \pm 0.04) \times 10^{-2} \quad (S = 1.1)$$

$$\lambda_0(K_{\mu 3}^0) = (1.38 \pm 0.18) \times 10^{-2} \quad (S = 2.2)$$

Quadratic parametrization assuming μ - e universality

$$\lambda'_+(K_{\mu 3}^0) = \lambda'_+(K_{e 3}^0) = (2.40 \pm 0.12) \times 10^{-2} \quad (S = 1.2)$$

$$\lambda''_+(K_{\mu 3}^0) = \lambda''_+(K_{e 3}^0) = (0.20 \pm 0.05) \times 10^{-2} \quad (S = 1.2)$$

$$\lambda_0(K_{\mu 3}^0) = (1.16 \pm 0.09) \times 10^{-2} \quad (S = 1.2)$$

Pole parametrization assuming μ - e universality

$$M_V^\mu(K_{\mu 3}^0) = M_V^e(K_{e 3}^0) = 878 \pm 6 \text{ MeV} \quad (S = 1.1)$$

$$M_S^\mu(K_{\mu 3}^0) = 1252 \pm 90 \text{ MeV} \quad (S = 2.6)$$

$$K_{e 3}^0 \quad |f_S/f_+| = (1.5_{-1.6}^{+1.4}) \times 10^{-2}$$

$$K_{e 3}^0 \quad |f_T/f_+| = (5_{-5}^{+4}) \times 10^{-2}$$

$$K_{\mu 3}^0 \quad |f_T/f_+| = (12 \pm 12) \times 10^{-2}$$

$$K_L \rightarrow \ell^+ \ell^- \gamma, K_L \rightarrow \ell^+ \ell^- \ell'^+ \ell'^-: \alpha_{K^*} = -0.205 \pm 0.022 \quad (S = 1.8)$$

$$K_L^0 \rightarrow \ell^+ \ell^- \gamma, K_L^0 \rightarrow \ell^+ \ell^- \ell'^+ \ell'^-: \alpha_{DIP} = -1.69 \pm 0.08 \quad (S = 1.7)$$

$$K_L \rightarrow \pi^+ \pi^- e^+ e^-: a_1/a_2 = -0.737 \pm 0.014 \text{ GeV}^2$$

$$K_L \rightarrow \pi^0 2\gamma: a_V = -0.43 \pm 0.06 \quad (S = 1.5)$$

CP-violation parameters [cc]

$$A_L = (0.332 \pm 0.006)\%$$

$$|\eta_{00}| = (2.221 \pm 0.011) \times 10^{-3} \quad (S = 1.8)$$

$$|\eta_{+-}| = (2.232 \pm 0.011) \times 10^{-3} \quad (S = 1.8)$$

$$|\epsilon| = (2.228 \pm 0.011) \times 10^{-3} \quad (S = 1.8)$$

$$|\eta_{00}/\eta_{+-}| = 0.9951 \pm 0.0008 \text{ [ff]} \quad (S = 1.6)$$

$$\text{Re}(\epsilon'/\epsilon) = (1.65 \pm 0.26) \times 10^{-3} \text{ [ff]} \quad (S = 1.6)$$

Assuming CPT

$$\phi_{+-} = (43.51 \pm 0.05)^\circ \quad (S = 1.1)$$

$$\phi_{00} = (43.52 \pm 0.05)^\circ \quad (S = 1.1)$$

$$\phi_\epsilon = \phi_{\text{SW}} = (43.51 \pm 0.05)^\circ \quad (S = 1.1)$$

Not assuming CPT

$$\phi_{+-} = (43.4 \pm 0.7)^\circ \quad (S = 1.3)$$

$$\phi_{00} = (43.7 \pm 0.8)^\circ \quad (S = 1.2)$$

$$\phi_\epsilon = (43.5 \pm 0.7)^\circ \quad (S = 1.3)$$

$$CP \text{ asymmetry } A \text{ in } K_L^0 \rightarrow \pi^+ \pi^- e^+ e^- = (13.7 \pm 1.5)\%$$

$$\beta_{CP} \text{ from } K_L^0 \rightarrow e^+ e^- e^+ e^- = -0.19 \pm 0.07$$

$$\gamma_{CP} \text{ from } K_L^0 \rightarrow e^+ e^- e^+ e^- = 0.01 \pm 0.11 \quad (S = 1.6)$$

$$j \text{ for } K_L^0 \rightarrow \pi^+ \pi^- \pi^0 = 0.0012 \pm 0.0008$$

$$f \text{ for } K_L^0 \rightarrow \pi^+ \pi^- \pi^0 = 0.004 \pm 0.006$$

$$|\eta_{+-\gamma}| = (2.35 \pm 0.07) \times 10^{-3}$$

$$\phi_{+-\gamma} = (44 \pm 4)^\circ$$

$$|\epsilon'_{+-\gamma}|/\epsilon < 0.3, \text{ CL} = 90\%$$

$$|g_{E1}| \text{ for } K_L^0 \rightarrow \pi^+ \pi^- \gamma < 0.21, \text{ CL} = 90\%$$

T-violation parameters

$$\text{Im}(\xi) \text{ in } K_{\mu 3}^0 = -0.007 \pm 0.026$$

CPT invariance tests

$$\phi_{00} - \phi_{+-} = (0.2 \pm 0.4)^\circ$$

$$\text{Re}(\frac{2}{3}\eta_{+-} + \frac{1}{3}\eta_{00}) - \frac{A_L}{2} = (-3 \pm 35) \times 10^{-6}$$

$\Delta S = -\Delta Q$ in K_{L3}^0 decay

$$\text{Re } x = -0.002 \pm 0.006$$

$$\text{Im } x = 0.0012 \pm 0.0021$$

K_L^0 DECAY MODES	Fraction (Γ_i/Γ)	Scale factor/ Confidence level	ρ (MeV/c)
Semileptonic modes			
$\pi^\pm e^\mp \nu_e$ Called K_{e3}^0 .	[ee] (40.55 \pm 0.12) %	S=1.9	229
$\pi^\pm \mu^\mp \nu_\mu$ Called $K_{\mu3}^0$.	[ee] (27.04 \pm 0.07) %	S=1.1	216
$(\pi\mu\text{atom})\nu$	(1.05 \pm 0.11) $\times 10^{-7}$		188
$\pi^0 \pi^\pm e^\mp \nu$	[ee] (5.20 \pm 0.11) $\times 10^{-5}$		207
$\pi^\pm e^\mp \nu e^+ e^-$	[ee] (1.26 \pm 0.04) $\times 10^{-5}$		229
Hadronic modes, including Charge conjugation \times Parity Violating (CPV) modes			
$3\pi^0$	(19.52 \pm 0.12) %	S=1.7	139
$\pi^+ \pi^- \pi^0$	(12.54 \pm 0.05) %		133
$\pi^+ \pi^-$	CPV [gg] (1.966 \pm 0.010) $\times 10^{-3}$	S=1.6	206
$\pi^0 \pi^0$	CPV (8.65 \pm 0.06) $\times 10^{-4}$	S=1.8	209
Semileptonic modes with photons			
$\pi^\pm e^\mp \nu_e \gamma$	[x,ee,hh] (3.79 \pm 0.06) $\times 10^{-3}$		229
$\pi^\pm \mu^\mp \nu_\mu \gamma$	(5.65 \pm 0.23) $\times 10^{-4}$		216
Hadronic modes with photons or $\ell\bar{\ell}$ pairs			
$\pi^0 \pi^0 \gamma$	< 2.43 $\times 10^{-7}$	CL=90%	209
$\pi^+ \pi^- \gamma$	[x,hh] (4.15 \pm 0.15) $\times 10^{-5}$	S=2.8	206
$\pi^+ \pi^- \gamma$ (DE)	(2.84 \pm 0.11) $\times 10^{-5}$	S=2.0	206
$\pi^0 2\gamma$	[hh] (1.273 \pm 0.034) $\times 10^{-6}$		231
$\pi^0 \gamma e^+ e^-$	(1.62 \pm 0.17) $\times 10^{-8}$		230
Other modes with photons or $\ell\bar{\ell}$ pairs			
2γ	(5.47 \pm 0.04) $\times 10^{-4}$	S=1.2	249
3γ	< 2.4 $\times 10^{-7}$	CL=90%	249
$e^+ e^- \gamma$	(9.4 \pm 0.4) $\times 10^{-6}$	S=2.0	249
$\mu^+ \mu^- \gamma$	(3.59 \pm 0.11) $\times 10^{-7}$	S=1.3	225
$e^+ e^- \gamma \gamma$	[hh] (5.95 \pm 0.33) $\times 10^{-7}$		249
$\mu^+ \mu^- \gamma \gamma$	[hh] (1.0 $^{+0.8}_{-0.6}$) $\times 10^{-8}$		225
Charge conjugation \times Parity (CP) or Lepton Family number (LF) violating modes, or $\Delta S = 1$ weak neutral current (S1) modes			
$\mu^+ \mu^-$	S1 (6.84 \pm 0.11) $\times 10^{-9}$		225
$e^+ e^-$	S1 (9 $^{+6}_{-4}$) $\times 10^{-12}$		249
$\pi^+ \pi^- e^+ e^-$	S1 [hh] (3.11 \pm 0.19) $\times 10^{-7}$		206
$\pi^0 \pi^0 e^+ e^-$	S1 < 6.6 $\times 10^{-9}$	CL=90%	209
$\mu^+ \mu^- e^+ e^-$	S1 (2.69 \pm 0.27) $\times 10^{-9}$		225
$e^+ e^- e^+ e^-$	S1 (3.56 \pm 0.21) $\times 10^{-8}$		249
$\pi^0 \mu^+ \mu^-$	CP,S1 [ii] < 3.8 $\times 10^{-10}$	CL=90%	177
$\pi^0 e^+ e^-$	CP,S1 [ii] < 2.8 $\times 10^{-10}$	CL=90%	230
$\pi^0 \nu \bar{\nu}$	CP,S1 [jj] < 6.7 $\times 10^{-8}$	CL=90%	231
$\pi^0 \pi^0 \nu \bar{\nu}$	S1 < 4.7 $\times 10^{-5}$	CL=90%	209

$e^\pm \mu^\mp$	LF	[ee] < 4.7	$\times 10^{-12}$	CL=90%	238
$e^\pm e^\pm \mu^\mp \mu^\mp$	LF	[ee] < 4.12	$\times 10^{-11}$	CL=90%	225
$\pi^0 \mu^\pm e^\mp$	LF	[ee] < 7.6	$\times 10^{-11}$	CL=90%	217
$\pi^0 \pi^0 \mu^\pm e^\mp$	LF	< 1.7	$\times 10^{-10}$	CL=90%	159

 $K^*(892)$

$$I(J^P) = \frac{1}{2}(1^-)$$

$K^*(892)^\pm$ mass $m = 891.66 \pm 0.26$ MeV

Mass $m = 895.5 \pm 0.8$ MeV

$K^*(892)^0$ mass $m = 895.94 \pm 0.22$ MeV (S = 1.4)

$K^*(892)^\pm$ full width $\Gamma = 50.8 \pm 0.9$ MeV

Full width $\Gamma = 46.2 \pm 1.3$ MeV

$K^*(892)^0$ full width $\Gamma = 48.7 \pm 0.8$ MeV (S = 1.7)

$K^*(892)$ DECAY MODES	Fraction (Γ_i/Γ)	Confidence level	ρ (MeV/c)
$K\pi$	~ 100	%	289
$K^0\gamma$	(2.39±0.21) $\times 10^{-3}$		307
$K^\pm\gamma$	(9.9 ±0.9) $\times 10^{-4}$		309
$K\pi\pi$	< 7	$\times 10^{-4}$	95% 223

 $K_1(1270)$

$$I(J^P) = \frac{1}{2}(1^+)$$

Mass $m = 1272 \pm 7$ MeV [1]

Full width $\Gamma = 90 \pm 20$ MeV [1]

$K_1(1270)$ DECAY MODES	Fraction (Γ_i/Γ)	ρ (MeV/c)
$K\rho$	(42 ±6) %	45
$K_0^*(1430)\pi$	(28 ±4) %	†
$K^*(892)\pi$	(16 ±5) %	302
$K\omega$	(11.0±2.0) %	†
$K f_0(1370)$	(3.0±2.0) %	†
γK^0	seen	539

 $K_1(1400)$

$$I(J^P) = \frac{1}{2}(1^+)$$

Mass $m = 1403 \pm 7$ MeV

Full width $\Gamma = 174 \pm 13$ MeV (S = 1.6)

$K_1(1400)$ DECAY MODES	Fraction (Γ_i/Γ)	ρ (MeV/c)
$K^*(892)\pi$	(94 ±6) %	402
$K\rho$	(1.2±0.6) %	292
$K f_0(1370)$	(2.0±2.0) %	†
$K\omega$	(1.0±1.0) %	284
$K_0^*(1430)\pi$	not seen	†
γK^0	seen	613

$K^*(1410)$

$$I(J^P) = \frac{1}{2}(1^-)$$

Mass $m = 1414 \pm 15$ MeV (S = 1.3)

Full width $\Gamma = 232 \pm 21$ MeV (S = 1.1)

$K^*(1410)$ DECAY MODES	Fraction (Γ_i/Γ)	Confidence level	ρ (MeV/c)
$K^*(892)\pi$	> 40 %	95%	410
$K\pi$	(6.6±1.3) %		612
$K\rho$	< 7 %	95%	305
γK^0	seen		619

$K_0^*(1430)$ ^[kk]

$$I(J^P) = \frac{1}{2}(0^+)$$

Mass $m = 1425 \pm 50$ MeV

Full width $\Gamma = 270 \pm 80$ MeV

$K_0^*(1430)$ DECAY MODES	Fraction (Γ_i/Γ)	ρ (MeV/c)
$K\pi$	(93±10) %	619

$K_2^*(1430)$

$$I(J^P) = \frac{1}{2}(2^+)$$

$K_2^*(1430)^\pm$ mass $m = 1425.6 \pm 1.5$ MeV (S = 1.1)

$K_2^*(1430)^0$ mass $m = 1432.4 \pm 1.3$ MeV

$K_2^*(1430)^\pm$ full width $\Gamma = 98.5 \pm 2.7$ MeV (S = 1.1)

$K_2^*(1430)^0$ full width $\Gamma = 109 \pm 5$ MeV (S = 1.9)

$K_2^*(1430)$ DECAY MODES	Fraction (Γ_i/Γ)	Scale factor/ Confidence level	ρ (MeV/c)
$K\pi$	(49.9±1.2) %		619
$K^*(892)\pi$	(24.7±1.5) %		419
$K^*(892)\pi\pi$	(13.4±2.2) %		372
$K\rho$	(8.7±0.8) %	S=1.2	318
$K\omega$	(2.9±0.8) %		311
$K^+\gamma$	(2.4±0.5) × 10 ⁻³	S=1.1	627
$K\eta$	(1.5 ^{+3.4} _{-1.0}) × 10 ⁻³	S=1.3	486
$K\omega\pi$	< 7.2 × 10 ⁻⁴	CL=95%	100
$K^0\gamma$	< 9 × 10 ⁻⁴	CL=90%	626

$K^*(1680)$

$$I(J^P) = \frac{1}{2}(1^-)$$

Mass $m = 1717 \pm 27$ MeV (S = 1.4)

Full width $\Gamma = 322 \pm 110$ MeV (S = 4.2)

$K^*(1680)$ DECAY MODES	Fraction (Γ_i/Γ)	ρ (MeV/c)
$K\pi$	(38.7±2.5) %	781
$K\rho$	(31.4 ^{+5.0} _{-2.1}) %	570
$K^*(892)\pi$	(29.9 ^{+2.2} _{-5.0}) %	618

$K_2(1770)$ ^[M]

$$I(J^P) = \frac{1}{2}(2^-)$$

Mass $m = 1773 \pm 8$ MeVFull width $\Gamma = 186 \pm 14$ MeV

$K_2(1770)$ DECAY MODES	Fraction (Γ_i/Γ)	ρ (MeV/c)
$K\pi\pi$		794
$K_2^*(1430)\pi$	dominant	288
$K^*(892)\pi$	seen	654
$Kf_2(1270)$	seen	55
$K\phi$	seen	441
$K\omega$	seen	607

 $K_3^*(1780)$

$$I(J^P) = \frac{1}{2}(3^-)$$

Mass $m = 1776 \pm 7$ MeV ($S = 1.1$)Full width $\Gamma = 159 \pm 21$ MeV ($S = 1.3$)

$K_3^*(1780)$ DECAY MODES	Fraction (Γ_i/Γ)	Confidence level	ρ (MeV/c)
$K\rho$	(31 \pm 9) %		613
$K^*(892)\pi$	(20 \pm 5) %		656
$K\pi$	(18.8 \pm 1.0) %		813
$K\eta$	(30 \pm 13) %		719
$K_2^*(1430)\pi$	< 16 %	95%	291

 $K_2(1820)$ ^[mm]

$$I(J^P) = \frac{1}{2}(2^-)$$

Mass $m = 1816 \pm 13$ MeVFull width $\Gamma = 276 \pm 35$ MeV

$K_2(1820)$ DECAY MODES	Fraction (Γ_i/Γ)	ρ (MeV/c)
$K_2^*(1430)\pi$	seen	327
$K^*(892)\pi$	seen	681
$Kf_2(1270)$	seen	186
$K\omega$	seen	638

 $K_4^*(2045)$

$$I(J^P) = \frac{1}{2}(4^+)$$

Mass $m = 2045 \pm 9$ MeV ($S = 1.1$)Full width $\Gamma = 198 \pm 30$ MeV

$K_4^*(2045)$ DECAY MODES	Fraction (Γ_i/Γ)	ρ (MeV/c)
$K\pi$	(9.9 \pm 1.2) %	958
$K^*(892)\pi\pi$	(9 \pm 5) %	802
$K^*(892)\pi\pi\pi$	(7 \pm 5) %	768
$\rho K\pi$	(5.7 \pm 3.2) %	741
$\omega K\pi$	(5.0 \pm 3.0) %	738
$\phi K\pi$	(2.8 \pm 1.4) %	594
$\phi K^*(892)$	(1.4 \pm 0.7) %	363

CHARMED MESONS

($C = \pm 1$)

$$D^+ = c\bar{d}, D^0 = c\bar{u}, \bar{D}^0 = \bar{c}u, D^- = \bar{c}d, \text{ similarly for } D^{*s}$$

 D^\pm

$$I(J^P) = \frac{1}{2}(0^-)$$

$$\text{Mass } m = 1869.60 \pm 0.16 \text{ MeV} \quad (S = 1.1)$$

$$\text{Mean life } \tau = (1040 \pm 7) \times 10^{-15} \text{ s}$$

$$c\tau = 311.8 \text{ } \mu\text{m}$$

c-quark decays

$$\Gamma(c \rightarrow \ell^+ \text{ anything}) / \Gamma(c \rightarrow \text{ anything}) = 0.096 \pm 0.004 \text{ }^{[nn]}$$

$$\Gamma(c \rightarrow D^*(2010)^+ \text{ anything}) / \Gamma(c \rightarrow \text{ anything}) = 0.255 \pm 0.017$$

CP-violation decay-rate asymmetries

$$A_{CP}(\mu^\pm \nu) = 0.08 \pm 0.08$$

$$A_{CP}(K_S^0 \pi^\pm) = -0.009 \pm 0.009$$

$$A_{CP}(K^\mp 2\pi^\pm) = -0.005 \pm 0.010$$

$$A_{CP}(K^\mp \pi^\pm \pi^\pm \pi^0) = 0.010 \pm 0.013$$

$$A_{CP}(K_S^0 \pi^\pm \pi^0) = 0.003 \pm 0.009$$

$$A_{CP}(K_S^0 \pi^\pm \pi^+ \pi^-) = 0.001 \pm 0.013$$

$$A_{CP}(K_S^0 K^\pm) = 0.07 \pm 0.06$$

$$A_{CP}(K^+ K^- \pi^\pm) = (0.3 \pm 0.6)\%$$

$$A_{CP}(K^\pm K^{*0}) = (0.1 \pm 1.3)\%$$

$$A_{CP}(\phi \pi^\pm) = (-0.9 \pm 1.1)\%$$

$$A_{CP}(K^\pm K_0^*(1430)^0) = (8_{-6}^{+7})\%$$

$$A_{CP}(K^\pm K_2^*(1430)^0) = (43_{-26}^{+20})\%$$

$$A_{CP}(K^\pm K_0^*(800)) = (-12_{-13}^{+18})\%$$

$$A_{CP}(a_0(1450)^0 \pi^\pm) = (-19_{-16}^{+14})\%$$

$$A_{CP}(\phi(1680) \pi^\pm) = (-9 \pm 26)\%$$

$$A_{CP}(\pi^+ \pi^- \pi^\pm) = -0.02 \pm 0.04$$

$$A_{CP}(K_S^0 K^\pm \pi^+ \pi^-) = -0.04 \pm 0.07$$

T-violation decay-rate asymmetry

$$A_T(K_S^0 K^\pm \pi^+ \pi^-) = 0.02 \pm 0.07$$

 D^+ form factors

$$f_+(0) |V_{cs}| \text{ in } \bar{K}^0 \ell^+ \nu_\ell = 0.707 \pm 0.013$$

$$r_1 \equiv a_1/a_0 \text{ in } \bar{K}^0 \ell^+ \nu_\ell = -1.7 \pm 0.5$$

$$r_2 \equiv a_2/a_0 \text{ in } \bar{K}^0 \ell^+ \nu_\ell = -14 \pm 11$$

$$f_+(0) |V_{cd}| \text{ in } \pi^0 \ell^+ \nu_\ell = 0.146 \pm 0.007$$

$$r_1 \equiv a_1/a_0 \text{ in } \pi^0 \ell^+ \nu_\ell = -1.4 \pm 0.9$$

$$r_2 \equiv a_2/a_0 \text{ in } \pi^0 \ell^+ \nu_\ell = -4 \pm 5$$

$$r_\nu \equiv V(0)/A_1(0) \text{ in } \bar{K}^*(892)^0 \ell^+ \nu_\ell = 1.62 \pm 0.08 \quad (S = 1.5)$$

$$r_2 \equiv A_2(0)/A_1(0) \text{ in } \bar{K}^*(892)^0 \ell^+ \nu_\ell = 0.83 \pm 0.05$$

$$r_3 \equiv A_3(0)/A_1(0) \text{ in } \bar{K}^*(892)^0 \ell^+ \nu_\ell = 0.0 \pm 0.4$$

$$\Gamma_L/\Gamma_T \text{ in } \bar{K}^*(892)^0 \ell^+ \nu_\ell = 1.13 \pm 0.08$$

$$\Gamma_+/\Gamma_- \text{ in } \bar{K}^*(892)^0 \ell^+ \nu_\ell = 0.22 \pm 0.06 \quad (S = 1.6)$$

Most decay modes (other than the semileptonic modes) that involve a neutral K meson are now given as K_S^0 modes, not as \bar{K}^0 modes. Nearly always it is

a K_S^0 that is measured, and interference between Cabibbo-allowed and doubly Cabibbo-suppressed modes can invalidate the assumption that $2\Gamma(K_S^0) = \Gamma(\bar{K}^0)$.

D⁺ DECAY MODES	Fraction (Γ_i/Γ)	Scale factor/ Confidence level	p (MeV/c)
Inclusive modes			
e^+ semileptonic	(16.07 ± 0.30) %		—
μ^+ anything	(17.6 ± 3.2) %		—
K^- anything	(25.7 ± 1.4) %		—
\bar{K}^0 anything + K^0 anything	(61 ± 5) %		—
K^+ anything	(5.9 ± 0.8) %		—
$K^*(892)^-$ anything	(6 ± 5) %		—
$\bar{K}^*(892)^0$ anything	(23 ± 5) %		—
$K^*(892)^0$ anything	< 6.6 %	CL=90%	—
η anything	(6.3 ± 0.7) %		—
η' anything	(1.04 ± 0.18) %		—
ϕ anything	(1.03 ± 0.12) %		—
Leptonic and semileptonic modes			
$e^+ \nu_e$	< 8.8 × 10 ⁻⁶	CL=90%	935
$\mu^+ \nu_\mu$	(3.82 ± 0.33) × 10 ⁻⁴		932
$\tau^+ \nu_\tau$	< 1.2 × 10 ⁻³	CL=90%	90
$\bar{K}^0 e^+ \nu_e$	(8.83 ± 0.22) %		869
$\bar{K}^0 \mu^+ \nu_\mu$	(9.4 ± 0.8) %	S=1.2	865
$K^- \pi^+ e^+ \nu_e$	(4.1 ± 0.6) %	S=1.1	864
$\bar{K}^*(892)^0 e^+ \nu_e$,	(3.68 ± 0.21) %		722
$\bar{K}^*(892)^0 \rightarrow K^- \pi^+$			
$K^- \pi^+ e^+ \nu_e$ nonresonant	< 7 × 10 ⁻³	CL=90%	864
$K^- \pi^+ \mu^+ \nu_\mu$	(3.9 ± 0.5) %		851
$\bar{K}^*(892)^0 \mu^+ \nu_\mu$,	(3.7 ± 0.3) %		717
$\bar{K}^*(892)^0 \rightarrow K^- \pi^+$			
$K^- \pi^+ \mu^+ \nu_\mu$ nonresonant	(2.1 ± 0.6) × 10 ⁻³		851
$K^- \pi^+ \pi^0 \mu^+ \nu_\mu$	< 1.7 × 10 ⁻³	CL=90%	825
$\pi^0 e^+ \nu_e$	(4.05 ± 0.18) × 10 ⁻³		930
$\eta e^+ \nu_e$	(1.33 ± 0.21) × 10 ⁻³		855
$\rho^0 e^+ \nu_e$	(2.2 ± 0.4) × 10 ⁻³		774
$\rho^0 \mu^+ \nu_\mu$	(2.5 ± 0.5) × 10 ⁻³		770
$\omega e^+ \nu_e$	(1.6 $\begin{smallmatrix} +0.7 \\ -0.6 \end{smallmatrix}$) × 10 ⁻³		771
$\eta'(958) e^+ \nu_e$	< 3.5 × 10 ⁻⁴	CL=90%	689
$\phi e^+ \nu_e$	< 1.6 × 10 ⁻⁴	CL=90%	657
Fractions of some of the following modes with resonances have already appeared above as submodes of particular charged-particle modes.			
$\bar{K}^*(892)^0 e^+ \nu_e$	(5.53 ± 0.32) %	S=1.2	722
$\bar{K}^*(892)^0 \mu^+ \nu_\mu$	(5.5 ± 0.5) %	S=1.2	717
$\bar{K}_0^*(1430)^0 \mu^+ \nu_\mu$	< 2.5 × 10 ⁻⁴		380
$\bar{K}^*(1680)^0 \mu^+ \nu_\mu$	< 1.6 × 10 ⁻³		105

Hadronic modes with a \bar{K} or $\bar{K}K\bar{K}$			
$K_S^0 \pi^+$	(1.49±0.04) %	S=1.4	863
$K_L^0 \pi^+$	(1.46±0.05) %		863
$K^- 2\pi^+$	[oo] (9.4 ± 0.4) %	S=2.2	846
$(K^- \pi^+)_{S\text{-wave}} \pi^+$	(7.52±0.33) %		846
$\bar{K}_0^*(1430)^0 \pi^+$,	[pp] (1.25±0.08) %		382
$\bar{K}_0^*(1430)^0 \rightarrow K^- \pi^+$			
$\bar{K}^*(892)^0 \pi^+$,	(1.04±0.12) %		714
$\bar{K}^*(892)^0 \rightarrow K^- \pi^+$			
$\bar{K}^*(1410)^0 \pi^+$, $\bar{K}^{*0} \rightarrow K^- \pi^+$	not seen		381
$\bar{K}_2^*(1430)^0 \pi^+$,	[pp] (2.3 ± 0.7) × 10 ⁻⁴		371
$\bar{K}_2^*(1430)^0 \rightarrow K^- \pi^+$			
$\bar{K}^*(1680)^0 \pi^+$,	[pp] (2.2 ± 1.1) × 10 ⁻⁴		58
$\bar{K}^*(1680)^0 \rightarrow K^- \pi^+$			
$K^- (2\pi^+)_{I=2}$	(1.45±0.27) %		—
$K_S^0 \pi^+ \pi^0$	[oo] (6.90±0.32) %	S=1.3	845
$K_S^0 \rho^+$	(4.7 ± 1.0) %		677
$\bar{K}^*(892)^0 \pi^+$,	(1.3 ± 0.6) %		714
$\bar{K}^*(892)^0 \rightarrow K_S^0 \pi^0$			
$K_S^0 \pi^+ \pi^0$ nonresonant	(9 ± 7) × 10 ⁻³		845
$K^- 2\pi^+ \pi^0$	[qq] (6.08±0.29) %	S=1.6	816
$K_S^0 2\pi^+ \pi^-$	[qq] (3.10±0.11) %	S=1.1	814
$K^- 3\pi^+ \pi^-$	[oo] (5.7 ± 0.6) × 10 ⁻³	S=1.2	772
$\bar{K}^*(892)^0 2\pi^+ \pi^-$,	(1.2 ± 0.4) × 10 ⁻³		645
$\bar{K}^*(892)^0 \rightarrow K^- \pi^+$			
$\bar{K}^*(892)^0 \rho^0 \pi^+$,	(2.3 ± 0.4) × 10 ⁻³		239
$\bar{K}^*(892)^0 \rightarrow K^- \pi^+$			
$\bar{K}^*(892)^0 a_1(1260)^+$	[rr] (9.3 ± 1.9) × 10 ⁻³		†
$K^- \rho^0 2\pi^+$	(1.72±0.29) × 10 ⁻³		524
$K^- 3\pi^+ \pi^-$ nonresonant	(4.0 ± 3.0) × 10 ⁻⁴		772
$K^+ 2K_S^0$	(4.6 ± 2.1) × 10 ⁻³		545
$K^+ K^- K_S^0 \pi^+$	(2.4 ± 0.5) × 10 ⁻⁴		436

Pionic modes

$\pi^+ \pi^0$	(1.26±0.09) × 10 ⁻³		925
$2\pi^+ \pi^-$	(3.27±0.22) × 10 ⁻³		909
$\rho^0 \pi^+$	(8.3 ± 1.5) × 10 ⁻⁴		767
$\pi^+ (\pi^+ \pi^-)_{S\text{-wave}}$	(1.83±0.18) × 10 ⁻³		909
$\sigma \pi^+$, $\sigma \rightarrow \pi^+ \pi^-$	(1.38±0.13) × 10 ⁻³		—
$f_0(980) \pi^+$,	(1.57±0.34) × 10 ⁻⁴		669
$f_0(980) \rightarrow \pi^+ \pi^-$			
$f_0(1370) \pi^+$,	(8 ± 4) × 10 ⁻⁵		—
$f_0(1370) \rightarrow \pi^+ \pi^-$			
$f_2(1270) \pi^+$,	(5.0 ± 0.9) × 10 ⁻⁴		485
$f_2(1270) \rightarrow \pi^+ \pi^-$			
$\rho(1450)^0 \pi^+$,	< 8 × 10 ⁻⁵	CL=95%	338
$\rho(1450)^0 \rightarrow \pi^+ \pi^-$			
$f_0(1500) \pi^+$,	(1.1 ± 0.4) × 10 ⁻⁴		—
$f_0(1500) \rightarrow \pi^+ \pi^-$			
$f_0(1710) \pi^+$,	< 5 × 10 ⁻⁵	CL=95%	—
$f_0(1710) \rightarrow \pi^+ \pi^-$			
$f_0(1790) \pi^+$,	< 7 × 10 ⁻⁵	CL=95%	—
$f_0(1790) \rightarrow \pi^+ \pi^-$			
$(\pi^+ \pi^+)_{S\text{-wave}} \pi^-$	< 1.2 × 10 ⁻⁴	CL=95%	909

$2\pi^+\pi^-$ nonresonant	$< 1.1 \times 10^{-4}$	CL=95%	909
$\pi^+2\pi^0$	$(4.7 \pm 0.4) \times 10^{-3}$		910
$2\pi^+\pi^-\pi^0$	$(1.16 \pm 0.09) \%$		883
$\eta\pi^+, \eta \rightarrow \pi^+\pi^-\pi^0$	$(7.8 \pm 0.5) \times 10^{-4}$		848
$\omega\pi^+, \omega \rightarrow \pi^+\pi^-\pi^0$	$< 3 \times 10^{-4}$	CL=90%	763
$3\pi^+2\pi^-$	$(1.66 \pm 0.17) \times 10^{-3}$	S=1.1	845

Fractions of some of the following modes with resonances have already appeared above as submodes of particular charged-particle modes.

$\eta\pi^+$	$(3.43 \pm 0.22) \times 10^{-3}$		848
$\eta\pi^+\pi^0$	$(1.38 \pm 0.35) \times 10^{-3}$		830
$\omega\pi^+$	$< 3.4 \times 10^{-4}$	CL=90%	764
$\eta'(958)\pi^+$	$(4.4 \pm 0.4) \times 10^{-3}$		681
$\eta'(958)\pi^+\pi^0$	$(1.6 \pm 0.5) \times 10^{-3}$		654

Hadronic modes with a $K\bar{K}$ pair

$K^+K_S^0$	$(2.86 \pm 0.12) \times 10^{-3}$	S=1.9	793
$K^+K^-\pi^+$	[$o\phi$] $(9.8 \pm 0.4) \times 10^{-3}$	S=1.9	744
$\phi\pi^+, \phi \rightarrow K^+K^-$	$(2.72 \pm 0.13) \times 10^{-3}$		647
$K^+\bar{K}^*(892)^0$, $\bar{K}^*(892)^0 \rightarrow K^-\pi^+$	$(2.51^{+0.13}_{-0.17}) \times 10^{-3}$		613
$K^+\bar{K}_0^*(1430)^0, \bar{K}_0^*(1430)^0 \rightarrow$ $K^-\pi^+$	$(1.8 \pm 0.4) \times 10^{-3}$		—
$K^+\bar{K}_2^*(1430)^0, \bar{K}_2^* \rightarrow K^-\pi^+$	$(1.7^{+1.2}_{-0.8}) \times 10^{-4}$		—
$K^+\bar{K}_0^*(800), \bar{K}_0^* \rightarrow K^-\pi^+$	$(6.8^{+3.5}_{-2.1}) \times 10^{-4}$		—
$a_0(1450)^0\pi^+, a_0^0 \rightarrow K^+K^-$	$(4.5^{+7.0}_{-1.9}) \times 10^{-4}$		—
$\phi(1680)\pi^+, \phi \rightarrow K^+K^-$	$(5.0^{+4.0}_{-1.9}) \times 10^{-5}$		—
$K^+K^-\pi^+$ nonresonant	not seen		744
$K^+K_S^0\pi^+\pi^-$	$(1.74 \pm 0.18) \times 10^{-3}$		678
$K_S^0K^-\pi^+$	$(2.38 \pm 0.18) \times 10^{-3}$		678
$K^+K^-\pi^+\pi^-$	$(2.3 \pm 1.2) \times 10^{-4}$		600

A few poorly measured branching fractions:

$\phi\pi^+\pi^0$	$(2.3 \pm 1.0) \%$		619
$\phi\rho^+$	$< 1.5 \%$	CL=90%	259
$K^+K^-\pi^+\pi^0$ non- ϕ	$(1.5^{+0.7}_{-0.6}) \%$		682
$K^*(892)^+K_S^0$	$(1.6 \pm 0.7) \%$		612

Doubly Cabibbo-suppressed modes

$K^+\pi^0$	$(2.37 \pm 0.32) \times 10^{-4}$		864
$K^+\pi^+\pi^-$	$(5.42 \pm 0.30) \times 10^{-4}$		846
$K^+\rho^0$	$(2.1 \pm 0.5) \times 10^{-4}$		679
$K^*(892)^0\pi^+, K^*(892)^0 \rightarrow$ $K^+\pi^-$	$(2.5 \pm 0.5) \times 10^{-4}$		714
$K^+f_0(980), f_0(980) \rightarrow \pi^+\pi^-$	$(4.8 \pm 2.9) \times 10^{-5}$		—
$K_2^*(1430)^0\pi^+, K_2^*(1430)^0 \rightarrow$ $K^+\pi^-$	$(4.4 \pm 2.9) \times 10^{-5}$		—
$K^+\pi^+\pi^-$ nonresonant	not seen		846
$2K^+K^-$	$(8.9 \pm 2.1) \times 10^{-5}$		550

$\Delta C = 1$ weak neutral current (CI) modes, or Lepton Family number (LF) or Lepton number (L) violating modes					
$\pi^+ e^+ e^-$	CI	< 7.4	$\times 10^{-6}$	$CL=90\%$	930
$\pi^+ \phi, \phi \rightarrow e^+ e^-$	[ss]	$(2.7 \begin{smallmatrix} +4.0 \\ -1.8 \end{smallmatrix})$	$\times 10^{-6}$		—
$\pi^+ \mu^+ \mu^-$	CI	< 3.9	$\times 10^{-6}$	$CL=90\%$	918
$\pi^+ \phi, \phi \rightarrow \mu^+ \mu^-$	[ss]	(1.8 ± 0.8)	$\times 10^{-6}$		—
$\rho^+ \mu^+ \mu^-$	CI	< 5.6	$\times 10^{-4}$	$CL=90\%$	757
$K^+ e^+ e^-$	[tt]	< 6.2	$\times 10^{-6}$	$CL=90\%$	870
$K^+ \mu^+ \mu^-$	[tt]	< 9.2	$\times 10^{-6}$	$CL=90\%$	856
$\pi^+ e^\pm \mu^\mp$	LF	$[ee] < 3.4$	$\times 10^{-5}$	$CL=90\%$	927
$K^+ e^\pm \mu^\mp$	LF	$[ee] < 6.8$	$\times 10^{-5}$	$CL=90\%$	866
$\pi^- 2e^+$	L	< 3.6	$\times 10^{-6}$	$CL=90\%$	930
$\pi^- 2\mu^+$	L	< 4.8	$\times 10^{-6}$	$CL=90\%$	918
$\pi^- e^+ \mu^+$	L	< 5.0	$\times 10^{-5}$	$CL=90\%$	927
$\rho^- 2\mu^+$	L	< 5.6	$\times 10^{-4}$	$CL=90\%$	757
$K^- 2e^+$	L	< 4.5	$\times 10^{-6}$	$CL=90\%$	870
$K^- 2\mu^+$	L	< 1.3	$\times 10^{-5}$	$CL=90\%$	856
$K^- e^+ \mu^+$	L	< 1.3	$\times 10^{-4}$	$CL=90\%$	866
$K^*(892)^- 2\mu^+$	L	< 8.5	$\times 10^{-4}$	$CL=90\%$	703

 D^0

$$I(J^P) = \frac{1}{2}(0^-)$$

Mass $m = 1864.83 \pm 0.14$ MeV $m_{D^\pm} - m_{D^0} = 4.77 \pm 0.10$ MeV ($S = 1.1$)Mean life $\tau = (410.1 \pm 1.5) \times 10^{-15}$ s $c\tau = 122.9$ μm

$$|m_{D_1^0} - m_{D_2^0}| = (2.39 \begin{smallmatrix} +0.59 \\ -0.63 \end{smallmatrix}) \times 10^{10} \hbar \text{ s}^{-1}$$

$$(\Gamma_{D_1^0} - \Gamma_{D_2^0})/\Gamma = 2y = (1.66 \pm 0.32) \times 10^{-2}$$

$$|q/p| = 0.86 \begin{smallmatrix} +0.18 \\ -0.15 \end{smallmatrix}$$

$$A_F = (1.4 \pm 2.7) \times 10^{-3}$$

$$K^+ \pi^- \text{ relative strong phase: } \cos \delta = 1.03 \begin{smallmatrix} +0.32 \\ -0.18 \end{smallmatrix}$$

$$K^- \pi^+ \pi^0 \text{ coherence factor } R_{K \pi \pi^0} = 0.78 \begin{smallmatrix} +0.11 \\ -0.25 \end{smallmatrix}$$

$$K^- \pi^+ \pi^0 \text{ average relative strong phase } \delta^{K \pi \pi^0} = (239 \begin{smallmatrix} +32 \\ -28 \end{smallmatrix})^\circ$$

$$K^- \pi^- 2\pi^+ \text{ coherence factor } R_{K 3\pi} = 0.36 \begin{smallmatrix} +0.24 \\ -0.30 \end{smallmatrix}$$

$$K^- \pi^- 2\pi^+ \text{ average relative strong phase } \delta^{K 3\pi} = (118 \begin{smallmatrix} +60 \\ -50 \end{smallmatrix})^\circ$$

CP-violation decay-rate asymmetries (labeled by the D^0 decay)

$$\begin{aligned}
A_{CP}(K^+ K^-) &= (-0.17 \pm 0.31) \times 10^{-2} \quad (S = 1.3) \\
A_{CP}(2K_S^0) &= -0.23 \pm 0.19 \\
A_{CP}(\pi^+ \pi^-) &= (0.2 \pm 0.4) \times 10^{-2} \\
A_{CP}(2\pi^0) &= 0.00 \pm 0.05 \\
A_{CP}(\pi^+ \pi^- \pi^0) &= (0.3 \pm 0.4)\% \\
A_{CP}(\rho(770)^+ \pi^- \rightarrow \pi^+ \pi^- \pi^0) &= (1.6 \pm 1.2)\% \\
A_{CP}(\rho(770)^0 \pi^0 \rightarrow \pi^+ \pi^- \pi^0) &= (-1.6 \pm 1.5)\% \\
A_{CP}(\rho(770)^- \pi^+ \rightarrow \pi^+ \pi^- \pi^0) &= (-0.7 \pm 1.2)\% \\
A_{CP}(\rho(1450)^+ \pi^- \rightarrow \pi^+ \pi^- \pi^0) &= (0.0 \pm 0.14)\% \\
A_{CP}(\rho(1450)^0 \pi^0 \rightarrow \pi^+ \pi^- \pi^0) &= (-0.1 \pm 0.22)\% \\
A_{CP}(\rho(1450)^- \pi^+ \rightarrow \pi^+ \pi^- \pi^0) &= (0.2 \pm 0.32)\% \\
A_{CP}(\rho(1700)^+ \pi^- \rightarrow \pi^+ \pi^- \pi^0) &= (-0.4 \pm 1.1)\% \\
A_{CP}(\rho(1700)^0 \pi^0 \rightarrow \pi^+ \pi^- \pi^0) &= (1.3 \pm 0.9)\% \\
A_{CP}(\rho(1700)^- \pi^+ \rightarrow \pi^+ \pi^- \pi^0) &= (0.5 \pm 0.7)\% \\
A_{CP}(f_0(980) \pi^0 \rightarrow \pi^+ \pi^- \pi^0) &= (0.0 \pm 0.14)\% \\
A_{CP}(f_0(1370) \pi^0 \rightarrow \pi^+ \pi^- \pi^0) &= (0.2 \pm 0.14)\% \\
A_{CP}(f_0(1500) \pi^0 \rightarrow \pi^+ \pi^- \pi^0) &= (0.0 \pm 0.14)\% \\
A_{CP}(f_0(1710) \pi^0 \rightarrow \pi^+ \pi^- \pi^0) &= (0.0 \pm 0.14)\% \\
A_{CP}(f_2(1270) \pi^0 \rightarrow \pi^+ \pi^- \pi^0) &= (-0.1 \pm 0.14)\% \\
A_{CP}(\sigma(400) \pi^0 \rightarrow \pi^+ \pi^- \pi^0) &= (0.1 \pm 0.14)\% \\
A_{CP}(\text{nonresonant } \pi^+ \pi^- \pi^0) &= (-0.2 \pm 0.4)\% \\
A_{CP}(K^+ K^- \pi^0) &= (-1.0 \pm 1.7)\% \\
A_{CP}(K^*(892)^+ K^- \rightarrow K^+ K^- \pi^0) &= (-0.8 \pm 1.2)\% \\
A_{CP}(K^*(1410)^+ K^- \rightarrow K^+ K^- \pi^0) &= (-1.7 \pm 1.9)\% \\
A_{CP}((K^+ \pi^0)_{S\text{-wave}} K^- \rightarrow K^+ K^- \pi^0) &= (2 \pm 5)\% \\
A_{CP}(\phi(1020) \pi^0 \rightarrow K^+ K^- \pi^0) &= (0.4 \pm 0.8)\% \\
A_{CP}(f_0(980) \pi^0 \rightarrow K^+ K^- \pi^0) &= (-0.4 \pm 2.6)\% \\
A_{CP}(a_0(980)^0 \pi^0 \rightarrow K^+ K^- \pi^0) &= (-0.6 \pm 1.9)\% \\
A_{CP}(f'_2(1525) \pi^0 \rightarrow K^+ K^- \pi^0) &= (0.0 \pm 0.32)\% \\
A_{CP}(K^*(892)^- K^+ \rightarrow K^+ K^- \pi^0) &= (-1.7 \pm 1.4)\% \\
A_{CP}(K^*(1410)^- K^+ \rightarrow K^+ K^- \pi^0) &= (-1.7 \pm 2.9)\% \\
A_{CP}((K^- \pi^0)_{S\text{-wave}} K^+ \rightarrow K^+ K^- \pi^0) &= (-0.4 \pm 2.5)\% \\
A_{CP}(K_S^0 \phi) &= -0.03 \pm 0.09 \\
A_{CP}(K_S^0 \pi^0) &= 0.001 \pm 0.013 \\
A_{CP}(K^- \pi^+) &= -0.004 \pm 0.010 \\
A_{CP}(K^+ \pi^-) &= 0.022 \pm 0.032 \\
A_{CP}(K^- \pi^+ \pi^0) &= 0.002 \pm 0.009 \\
A_{CP}(K^+ \pi^- \pi^0) &= 0.00 \pm 0.05 \\
A_{CP}(K_S^0 \pi^+ \pi^-) &= -0.009 \pm_{-0.060}^{+0.026} \\
A_{CP}(K^*(892)^- \pi^+ \rightarrow K_S^0 \pi^+ \pi^-) &< 3.5 \times 10^{-4}, \text{ CL} = 95\% \\
A_{CP}(K^*(892)^+ \pi^- \rightarrow K_S^0 \pi^+ \pi^-) &< 7.8 \times 10^{-4}, \text{ CL} = 95\% \\
A_{CP}(\bar{K}^0 \rho^0 \rightarrow K_S^0 \pi^+ \pi^-) &< 4.8 \times 10^{-4}, \text{ CL} = 95\% \\
A_{CP}(\bar{K}^0 \omega \rightarrow K_S^0 \pi^+ \pi^-) &< 9.2 \times 10^{-4}, \text{ CL} = 95\% \\
A_{CP}(\bar{K}^0 f_0(980) \rightarrow K_S^0 \pi^+ \pi^-) &< 6.8 \times 10^{-4}, \text{ CL} = 95\% \\
A_{CP}(\bar{K}^0 f_2(1270) \rightarrow K_S^0 \pi^+ \pi^-) &< 13.5 \times 10^{-4}, \text{ CL} = 95\% \\
A_{CP}(\bar{K}^0 f_0(1370) \rightarrow K_S^0 \pi^+ \pi^-) &< 25.5 \times 10^{-4}, \text{ CL} = 95\% \\
A_{CP}(K_0^*(1430)^- \pi^+ \rightarrow K_S^0 \pi^+ \pi^-) &< 9.0 \times 10^{-4}, \text{ CL} = 95\% \\
A_{CP}(K_2^*(1430)^- \pi^+ \rightarrow K_S^0 \pi^+ \pi^-) &< 6.5 \times 10^{-4}, \text{ CL} = 95\% \\
A_{CP}(K^*(1680)^- \pi^+ \rightarrow K_S^0 \pi^+ \pi^-) &< 28.4 \times 10^{-4}, \text{ CL} = 95\% \\
A_{CP}(K^- \pi^+ \pi^+ \pi^-) &= 0.007 \pm 0.010
\end{aligned}$$

$$A_{CP}(K^+ \pi^- \pi^+ \pi^-) = -0.02 \pm 0.04$$

$$A_{CP}(K^+ K^- \pi^+ \pi^-) = -0.08 \pm 0.07$$

T-violation decay-rate asymmetry

$$A_T(K^+ K^- \pi^+ \pi^-) = 0.01 \pm 0.07$$

CPT-violation decay-rate asymmetry

$$A_{CPT}(K^\mp \pi^\pm) = 0.008 \pm 0.008$$

Form factors

$$r_V \equiv V(0)/A_1(0) \text{ in } D^0 \rightarrow K^*(892)^- \ell^+ \nu_\ell = 1.7 \pm 0.8$$

$$r_2 \equiv A_2(0)/A_1(0) \text{ in } D^0 \rightarrow K^*(892)^- \ell^+ \nu_\ell = 0.9 \pm 0.4$$

$$f_+(0) |V_{cs}| \text{ in } D^0 \rightarrow K^- \ell^+ \nu_\ell = 0.726 \pm 0.009$$

$$r_1 \equiv a_1/a_0 \text{ in } D^0 \rightarrow K^- \ell^+ \nu_\ell = -2.65 \pm 0.35$$

$$r_2 \equiv \bar{a}_1/a_0 \text{ in } D^0 \rightarrow K^- \ell^+ \nu_\ell = 13 \pm 9$$

$$f_+(0) |V_{cd}| \text{ in } D^0 \rightarrow \pi^- \ell^+ \nu_\ell = 0.152 \pm 0.005$$

$$r_1 \equiv a_1/a_0 \text{ in } D^0 \rightarrow \pi^- \ell^+ \nu_\ell = -2.8 \pm 0.5$$

$$r_2 \equiv \bar{a}_1/a_0 \text{ in } D^0 \rightarrow \pi^- \ell^+ \nu_\ell = 6 \pm 3.0$$

Most decay modes (other than the semileptonic modes) that involve a neutral K meson are now given as K_S^0 modes, not as \bar{K}^0 modes. Nearly always it is a K_S^0 that is measured, and interference between Cabibbo-allowed and doubly Cabibbo-suppressed modes can invalidate the assumption that $2 \Gamma(K_S^0) = \Gamma(\bar{K}^0)$.

D⁰ DECAY MODES	Fraction (Γ_i/Γ)	Scale factor/ Confidence level	p (MeV/c)
Topological modes			
0-prongs	[uu] (17 ± 6) %		—
2-prongs	(69 ± 6) %		—
4-prongs	[vv] (14.3 ± 0.5) %		—
6-prongs	[ww] (6.4 ± 1.3) × 10 ⁻⁴		—
Inclusive modes			
e^+ anything	[xx] (6.49 ± 0.11) %		—
μ^+ anything	(6.7 ± 0.6) %		—
K^- anything	(54.7 ± 2.8) %	S=1.3	—
\bar{K}^0 anything + K^0 anything	(47 ± 4) %		—
K^+ anything	(3.4 ± 0.4) %		—
$K^*(892)^-$ anything	(15 ± 9) %		—
$\bar{K}^*(892)^0$ anything	(9 ± 4) %		—
$K^*(892)^+$ anything	< 3.6 %	CL=90%	—
$K^*(892)^0$ anything	(2.8 ± 1.3) %		—
η anything	(9.5 ± 0.9) %		—
η' anything	(2.48 ± 0.27) %		—
ϕ anything	(1.05 ± 0.11) %		—
Semileptonic modes			
$K^- e^+ \nu_e$	(3.55 ± 0.05) %	S=1.2	867
$K^- \mu^+ \nu_\mu$	(3.31 ± 0.13) %		864
$K^*(892)^- e^+ \nu_e$	(2.17 ± 0.16) %		719
$K^*(892)^- \mu^+ \nu_\mu$	(1.98 ± 0.24) %		714
$K^- \pi^0 e^+ \nu_e$	(1.6 ± $\frac{1.3}{0.5}$) %		861
$\bar{K}^0 \pi^- e^+ \nu_e$	(2.7 ± $\frac{0.9}{0.7}$) %		860

$K^- \pi^+ \pi^- e^+ \nu_e$	$(2.8 \begin{smallmatrix} + 1.4 \\ - 1.1 \end{smallmatrix}) \times 10^{-4}$		843
$K_1(1270)^- e^+ \nu_e$	$(7.6 \begin{smallmatrix} + 4.0 \\ - 3.1 \end{smallmatrix}) \times 10^{-4}$		498
$K^- \pi^+ \pi^- \mu^+ \nu_\mu$	$< 1.2 \times 10^{-3}$	CL=90%	821
$(\bar{K}^*(892)\pi)^- \mu^+ \nu_\mu$	$< 1.4 \times 10^{-3}$	CL=90%	692
$\pi^- e^+ \nu_e$	$(2.89 \pm 0.08) \times 10^{-3}$	S=1.1	927
$\pi^- \mu^+ \nu_\mu$	$(2.37 \pm 0.24) \times 10^{-3}$		924
$\rho^- e^+ \nu_e$	$(1.9 \pm 0.4) \times 10^{-3}$		771
Hadronic modes with one \bar{K}			
$K^- \pi^+$	$(3.89 \pm 0.05) \%$	S=1.2	861
$K_S^0 \pi^0$	$(1.22 \pm 0.05) \%$		860
$K_S^0 \pi^0$	$(10.0 \pm 0.7) \times 10^{-3}$		860
$K_S^0 \pi^+ \pi^-$	[<i>oo</i>] $(2.94 \pm 0.16) \%$	S=1.1	842
$K_S^0 \rho^0$	$(6.6 \begin{smallmatrix} + 0.6 \\ - 0.8 \end{smallmatrix}) \times 10^{-3}$		674
$K_S^0 \omega, \omega \rightarrow \pi^+ \pi^-$	$(2.1 \pm 0.6) \times 10^{-4}$		670
$K_S^0 (\pi^+ \pi^-)_{S\text{-wave}}$	$(3.5 \pm 0.8) \times 10^{-3}$		842
$K_S^0 f_0(980),$ $f_0(980) \rightarrow \pi^+ \pi^-$	$(1.27 \begin{smallmatrix} + 0.40 \\ - 0.24 \end{smallmatrix}) \times 10^{-3}$		549
$K_S^0 f_0(1370),$ $f_0(1370) \rightarrow \pi^+ \pi^-$	$(2.9 \begin{smallmatrix} + 0.9 \\ - 1.3 \end{smallmatrix}) \times 10^{-3}$		†
$K_S^0 f_2(1270),$ $f_2(1270) \rightarrow \pi^+ \pi^-$	$(9 \begin{smallmatrix} + 10 \\ - 6 \end{smallmatrix}) \times 10^{-5}$		262
$K^*(892)^- \pi^+,$ $K^*(892)^- \rightarrow K_S^0 \pi^-$	$(1.73 \begin{smallmatrix} + 0.14 \\ - 0.17 \end{smallmatrix}) \%$		711
$K_0^*(1430)^- \pi^+,$ $K_0^*(1430)^- \rightarrow K_S^0 \pi^-$	$(2.81 \begin{smallmatrix} + 0.40 \\ - 0.33 \end{smallmatrix}) \times 10^{-3}$		378
$K_2^*(1430)^- \pi^+,$ $K_2^*(1430)^- \rightarrow K_S^0 \pi^-$	$(3.5 \begin{smallmatrix} + 2.0 \\ - 1.1 \end{smallmatrix}) \times 10^{-4}$		367
$K^*(1680)^- \pi^+,$ $K^*(1680)^- \rightarrow K_S^0 \pi^-$	$(5 \pm 4) \times 10^{-4}$		46
$K^*(892)^+ \pi^-,$ $K^*(892)^+ \rightarrow K_S^0 \pi^+$	[<i>yy</i>] $(1.18 \begin{smallmatrix} + 0.60 \\ - 0.35 \end{smallmatrix}) \times 10^{-4}$		711
$K_0^*(1430)^+ \pi^-, K_0^*(1430)^+ \rightarrow$ $K_S^0 \pi^+$	[<i>yy</i>] $< 1.5 \times 10^{-5}$	CL=95%	-
$K_2^*(1430)^+ \pi^-, K_2^*(1430)^+ \rightarrow$ $K_S^0 \pi^+$	[<i>yy</i>] $< 3.5 \times 10^{-5}$	CL=95%	-
$K_S^0 \pi^+ \pi^-$ nonresonant	$(2.7 \begin{smallmatrix} + 6.0 \\ - 1.7 \end{smallmatrix}) \times 10^{-4}$		842
$K^- \pi^+ \pi^0$	[<i>oo</i>] $(13.9 \pm 0.5) \%$	S=1.7	844
$K^- \rho^+$	$(10.8 \pm 0.7) \%$		675
$K^- \rho(1700)^+,$ $\rho(1700)^+ \rightarrow \pi^+ \pi^0$	$(7.9 \pm 1.7) \times 10^{-3}$		†
$K^*(892)^- \pi^+,$ $K^*(892)^- \rightarrow K^- \pi^0$	$(2.22 \begin{smallmatrix} + 0.40 \\ - 0.19 \end{smallmatrix}) \%$		711
$\bar{K}^*(892)^0 \pi^0,$ $\bar{K}^*(892)^0 \rightarrow K^- \pi^+$	$(1.88 \pm 0.23) \%$		711
$K_0^*(1430)^- \pi^+,$ $K_0^*(1430)^- \rightarrow K^- \pi^0$	$(4.6 \pm 2.1) \times 10^{-3}$		378

$\overline{K}_0^*(1430)^0 \pi^0$,		$(5.7 \begin{smallmatrix} + 5.0 \\ - 1.5 \end{smallmatrix}) \times 10^{-3}$	379
$\overline{K}_0^*(1430)^0 \rightarrow K^- \pi^+$			
$K^*(1680)^- \pi^+$,		$(1.8 \pm 0.7) \times 10^{-3}$	46
$K^*(1680)^- \rightarrow K^- \pi^0$			
$K^- \pi^+ \pi^0$ nonresonant		$(1.11 \begin{smallmatrix} + 0.50 \\ - 0.19 \end{smallmatrix}) \%$	844
$K_S^0 2\pi^0$		$(8.3 \pm 0.6) \times 10^{-3}$	843
$\overline{K}^*(892)^0 \pi^0$,		$(6.7 \begin{smallmatrix} + 1.8 \\ - 1.5 \end{smallmatrix}) \times 10^{-3}$	711
$\overline{K}^*(892)^0 \rightarrow K_S^0 \pi^0$			
$K_S^0 2\pi^0$ nonresonant		$(4.5 \pm 1.1) \times 10^{-3}$	843
$K^- 2\pi^+ \pi^-$	[00]	$(8.09 \begin{smallmatrix} + 0.21 \\ - 0.18 \end{smallmatrix}) \%$	S=1.3 813
$K^- \pi^+ \rho^0$ total		$(6.76 \pm 0.33) \%$	609
$K^- \pi^+ \rho^0$ 3-body		$(5.1 \pm 2.3) \times 10^{-3}$	609
$\overline{K}^*(892)^0 \rho^0$,		$(1.06 \pm 0.23) \%$	416
$\overline{K}^*(892)^0 \rightarrow K^- \pi^+$			
$K^- a_1(1260)^+$,		$(3.6 \pm 0.6) \%$	327
$a_1(1260)^+ \rightarrow 2\pi^+ \pi^-$			
$\overline{K}^*(892)^0 \pi^+ \pi^-$ total,		$(1.6 \pm 0.4) \%$	685
$\overline{K}^*(892)^0 \rightarrow K^- \pi^+$			
$\overline{K}^*(892)^0 \pi^+ \pi^-$ 3-body,		$(9.9 \pm 2.3) \times 10^{-3}$	685
$\overline{K}^*(892)^0 \rightarrow K^- \pi^+$			
$K_1(1270)^- \pi^+$,	[zz]	$(2.9 \pm 0.3) \times 10^{-3}$	484
$K_1(1270)^- \rightarrow K^- \pi^+ \pi^-$			
$K^- 2\pi^+ \pi^-$ nonresonant		$(1.88 \pm 0.26) \%$	813
$K_S^0 \pi^+ \pi^- \pi^0$	[aaa]	$(5.4 \pm 0.6) \%$	813
$K_S^0 \eta, \eta \rightarrow \pi^+ \pi^- \pi^0$		$(9.8 \pm 0.6) \times 10^{-4}$	772
$K_S^0 \omega, \omega \rightarrow \pi^+ \pi^- \pi^0$		$(9.9 \pm 0.5) \times 10^{-3}$	670
$K^- 2\pi^+ \pi^- \pi^0$		$(4.2 \pm 0.4) \%$	771
$\overline{K}^*(892)^0 \pi^+ \pi^- \pi^0$,		$(1.3 \pm 0.6) \%$	643
$\overline{K}^*(892)^0 \rightarrow K^- \pi^+$			
$K^- \pi^+ \omega, \omega \rightarrow \pi^+ \pi^- \pi^0$		$(2.7 \pm 0.5) \%$	605
$\overline{K}^*(892)^0 \omega$,		$(6.5 \pm 3.0) \times 10^{-3}$	410
$\overline{K}^*(892)^0 \rightarrow K^- \pi^+$,			
$\omega \rightarrow \pi^+ \pi^- \pi^0$			
$K_S^0 \eta \pi^0$		$(5.6 \pm 1.2) \times 10^{-3}$	721
$K_S^0 a_0(980), a_0(980) \rightarrow \eta \pi^0$		$(6.7 \pm 2.1) \times 10^{-3}$	-
$\overline{K}^*(892)^0 \eta$,		$(1.6 \pm 0.5) \times 10^{-3}$	-
$\overline{K}^*(892)^0 \rightarrow K_S^0 \pi^0$			
$K_S^0 2\pi^+ 2\pi^-$		$(2.80 \pm 0.30) \times 10^{-3}$	768
$K_S^0 \rho^0 \pi^+ \pi^-$, no $K^*(892)^-$		$(1.1 \pm 0.7) \times 10^{-3}$	-
$K^*(892)^- 2\pi^+ \pi^-$,		$(5 \pm 8) \times 10^{-4}$	642
$K^*(892)^- \rightarrow K_S^0 \pi^-$, no ρ^0			
$K^*(892)^- \rho^0 \pi^+, K^*(892)^- \rightarrow$		$(1.7 \pm 0.7) \times 10^{-3}$	230
$K_S^0 \pi^-$			
$K_S^0 2\pi^+ 2\pi^-$ nonresonant	< 1.3	$\times 10^{-3}$	CL=90% 768
$K^- 3\pi^+ 2\pi^-$		$(2.2 \pm 0.6) \times 10^{-4}$	713

Fractions of many of the following modes with resonances have already appeared above as submodes of particular charged-particle modes. (Modes

for which there are only upper limits and $\overline{K}^*(892)\rho$ submodes only appear below.)

$K_S^0 \eta$	$(4.29 \pm 0.27) \times 10^{-3}$	772
$K_S^0 \omega$	$(1.11 \pm 0.06) \%$	670
$K_S^0 \eta'(958)$	$(9.3 \pm 1.4) \times 10^{-3}$	565
$K^- a_1(1260)^+$	$(7.8 \pm 1.1) \%$	327
$K^- a_2(1320)^+$	$< 2 \times 10^{-3}$	CL=90% 198
$\overline{K}^*(892)^0 \pi^+ \pi^-$ total	$(2.4 \pm 0.5) \%$	685
$\overline{K}^*(892)^0 \pi^+ \pi^-$ 3-body	$(1.48 \pm 0.34) \%$	685
$\overline{K}^*(892)^0 \rho^0$	$(1.58 \pm 0.35) \%$	417
$\overline{K}^*(892)^0 \rho^0$ transverse	$(1.7 \pm 0.6) \%$	417
$\overline{K}^*(892)^0 \rho^0$ S-wave	$(3.0 \pm 0.6) \%$	417
$\overline{K}^*(892)^0 \rho^0$ S-wave long.	$< 3 \times 10^{-3}$	CL=90% 417
$\overline{K}^*(892)^0 \rho^0$ P-wave	$< 3 \times 10^{-3}$	CL=90% 417
$\overline{K}^*(892)^0 \rho^0$ D-wave	$(2.1 \pm 0.6) \%$	417
$K_1(1270)^- \pi^+$	[zz] $(1.6 \pm 0.8) \%$	484
$K_1(1400)^- \pi^+$	$< 1.2 \%$	CL=90% 386
$\overline{K}^*(892)^0 \pi^+ \pi^- \pi^0$	$(1.9 \pm 0.9) \%$	643
$K^- \pi^+ \omega$	$(3.0 \pm 0.6) \%$	605
$\overline{K}^*(892)^0 \omega$	$(1.1 \pm 0.5) \%$	410
$K^- \pi^+ \eta'(958)$	$(7.5 \pm 1.9) \times 10^{-3}$	479
$\overline{K}^*(892)^0 \eta'(958)$	$< 1.1 \times 10^{-3}$	CL=90% 119

Hadronic modes with three K's

$K_S^0 K^+ K^-$	$(4.65 \pm 0.30) \times 10^{-3}$	544
$K_S^0 a_0(980)^0, a_0^0 \rightarrow K^+ K^-$	$(3.1 \pm 0.4) \times 10^{-3}$	-
$K^- a_0(980)^+, a_0^+ \rightarrow K^+ K_S^0$	$(6.2 \pm 1.8) \times 10^{-4}$	-
$K^+ a_0(980)^-, a_0^- \rightarrow K^- K_S^0$	$< 1.2 \times 10^{-4}$	CL=95% -
$K_S^0 f_0(980), f_0 \rightarrow K^+ K^-$	$< 1.0 \times 10^{-4}$	CL=95% -
$K_S^0 \phi, \phi \rightarrow K^+ K^-$	$(2.14 \pm 0.15) \times 10^{-3}$	520
$K_S^0 f_0(1370), f_0 \rightarrow K^+ K^-$	$(1.8 \pm 1.1) \times 10^{-4}$	-
$3K_S^0$	$(9.5 \pm 1.3) \times 10^{-4}$	539
$K^+ 2K^- \pi^+$	$(2.21 \pm 0.32) \times 10^{-4}$	434
$K^+ K^- \overline{K}^*(892)^0,$ $\overline{K}^*(892)^0 \rightarrow K^- \pi^+$	$(4.4 \pm 1.7) \times 10^{-5}$	†
$K^- \pi^+ \phi, \phi \rightarrow K^+ K^-$	$(4.0 \pm 1.7) \times 10^{-5}$	422
$\phi \overline{K}^*(892)^0,$ $\phi \rightarrow K^+ K^-,$ $\overline{K}^*(892)^0 \rightarrow K^- \pi^+$	$(1.06 \pm 0.20) \times 10^{-4}$	†
$K^+ 2K^- \pi^+$ nonresonant	$(3.3 \pm 1.5) \times 10^{-5}$	434
$2K_S^0 K^\pm \pi^\mp$	$(6.2 \pm 1.3) \times 10^{-4}$	427

Pionic modes

$\pi^+ \pi^-$	$(1.397 \pm 0.026) \times 10^{-3}$	922
$2\pi^0$	$(8.0 \pm 0.8) \times 10^{-4}$	923
$\pi^+ \pi^- \pi^0$	$(1.44 \pm 0.06) \%$	S=1.8 907
$\rho^+ \pi^-$	$(9.8 \pm 0.4) \times 10^{-3}$	764
$\rho^0 \pi^0$	$(3.73 \pm 0.22) \times 10^{-3}$	764
$\rho^- \pi^+$	$(4.97 \pm 0.23) \times 10^{-3}$	764
$\rho(1450)^+ \pi^-, \rho(1450)^+ \rightarrow$ $\pi^+ \pi^0$	$(1.6 \pm 2.0) \times 10^{-5}$	-
$\rho(1450)^0 \pi^0, \rho(1450)^0 \rightarrow$ $\pi^+ \pi^-$	$(4.3 \pm 1.9) \times 10^{-5}$	-
$\rho(1450)^- \pi^+, \rho(1450)^- \rightarrow$ $\pi^- \pi^0$	$(2.6 \pm 0.4) \times 10^{-4}$	-

$\rho(1700)^+ \pi^-$, $\rho(1700)^+ \rightarrow \pi^+ \pi^0$	$(5.9 \pm 1.4) \times 10^{-4}$	-
$\rho(1700)^0 \pi^0$, $\rho(1700)^0 \rightarrow \pi^+ \pi^-$	$(7.2 \pm 1.7) \times 10^{-4}$	-
$\rho(1700)^- \pi^+$, $\rho(1700)^- \rightarrow \pi^- \pi^0$	$(4.6 \pm 1.1) \times 10^{-4}$	-
$f_0(980) \pi^0$, $f_0(980) \rightarrow \pi^+ \pi^-$	$(3.6 \pm 0.8) \times 10^{-5}$	-
$f_0(600) \pi^0$, $f_0(600) \rightarrow \pi^+ \pi^-$	$(1.18 \pm 0.21) \times 10^{-4}$	-
$f_0(1370) \pi^0$, $f_0(1370) \rightarrow \pi^+ \pi^-$	$(5.3 \pm 2.1) \times 10^{-5}$	-
$f_0(1500) \pi^0$, $f_0(1500) \rightarrow \pi^+ \pi^-$	$(5.6 \pm 1.5) \times 10^{-5}$	-
$f_0(1710) \pi^0$, $f_0(1710) \rightarrow \pi^+ \pi^-$	$(4.5 \pm 1.5) \times 10^{-5}$	-
$f_2(1270) \pi^0$, $f_2(1270) \rightarrow \pi^+ \pi^-$	$(1.90 \pm 0.20) \times 10^{-4}$	-
$\pi^+ \pi^- \pi^0$ nonresonant	$(1.21 \pm 0.35) \times 10^{-4}$	907
$3\pi^0$	$< 3.5 \times 10^{-4}$	CL=90% 908
$2\pi^+ 2\pi^-$	$(7.44 \pm 0.21) \times 10^{-3}$	S=1.1 880
$a_1(1260)^+ \pi^-$, $a_1^+ \rightarrow 2\pi^+ \pi^-$ total	$(4.46 \pm 0.31) \times 10^{-3}$	-
$a_1(1260)^+ \pi^-$, $a_1^+ \rightarrow \rho^0 \pi^+$ S-wave	$(3.22 \pm 0.25) \times 10^{-3}$	-
$a_1(1260)^+ \pi^-$, $a_1^+ \rightarrow \rho^0 \pi^+$ D-wave	$(1.9 \pm 0.5) \times 10^{-4}$	-
$a_1(1260)^+ \pi^-$, $a_1^+ \rightarrow \sigma \pi^+$	$(6.2 \pm 0.7) \times 10^{-4}$	-
$2\rho^0$ total	$(1.82 \pm 0.13) \times 10^{-3}$	518
$2\rho^0$, parallel helicities	$(8.2 \pm 3.2) \times 10^{-5}$	-
$2\rho^0$, perpendicular helicities	$(4.8 \pm 0.6) \times 10^{-4}$	-
$2\rho^0$, longitudinal helicities	$(1.25 \pm 0.10) \times 10^{-3}$	-
Resonant $(\pi^+ \pi^-) \pi^+ \pi^-$	$(1.49 \pm 0.12) \times 10^{-3}$	-
3-body total		
$\sigma \pi^+ \pi^-$	$(6.1 \pm 0.9) \times 10^{-4}$	-
$f_0(980) \pi^+ \pi^-$, $f_0 \rightarrow \pi^+ \pi^-$	$(1.8 \pm 0.5) \times 10^{-4}$	-
$f_2(1270) \pi^+ \pi^-$, $f_2 \rightarrow \pi^+ \pi^-$	$(3.6 \pm 0.6) \times 10^{-4}$	-
$\pi^+ \pi^- 2\pi^0$	$(1.00 \pm 0.09) \%$	882
$\eta \pi^0$	[bbb] $(6.4 \pm 1.1) \times 10^{-4}$	846
$\omega \pi^0$	[bbb] $< 2.6 \times 10^{-4}$	CL=90% 761
$2\pi^+ 2\pi^- \pi^0$	$(4.2 \pm 0.5) \times 10^{-3}$	844
$\eta \pi^+ \pi^-$	[bbb] $(1.09 \pm 0.16) \times 10^{-3}$	827
$\omega \pi^+ \pi^-$	[bbb] $(1.6 \pm 0.5) \times 10^{-3}$	738
$3\pi^+ 3\pi^-$	$(4.2 \pm 1.2) \times 10^{-4}$	795
$\eta'(958) \pi^0$	$(8.1 \pm 1.6) \times 10^{-4}$	678
$\eta'(958) \pi^+ \pi^-$	$(4.5 \pm 1.7) \times 10^{-4}$	650
2η	$(1.67 \pm 0.19) \times 10^{-3}$	754
$\eta \eta'(958)$	$(1.26 \pm 0.27) \times 10^{-3}$	537
Hadronic modes with a $K\bar{K}$ pair		
$K^+ K^-$	$(3.94 \pm 0.07) \times 10^{-3}$	S=1.3 791
$2K_S^0$	$(1.9 \pm 0.7) \times 10^{-4}$	S=2.5 789
$K_S^0 K^- \pi^+$	$(3.5 \pm 0.5) \times 10^{-3}$	S=1.1 739
$\bar{K}^*(892)^0 K_S^0$	$< 6 \times 10^{-4}$	CL=90% 608
$\bar{K}^*(892)^0 \rightarrow K^- \pi^+$		
$K_S^0 K^+ \pi^-$	$(2.6 \pm 0.5) \times 10^{-3}$	739
$K^*(892)^0 K_S^0$	$< 2.9 \times 10^{-4}$	CL=90% 608
$K^*(892)^0 \rightarrow K^+ \pi^-$		

$K^+ K^- \pi^0$		$(3.29 \pm 0.13) \times 10^{-3}$		743
$K^*(892)^+ K^-$,		$(1.46 \pm 0.07) \times 10^{-3}$		—
$K^*(892)^+ \rightarrow K^+ \pi^0$				
$K^*(892)^- K^+$,		$(5.2 \pm 0.4) \times 10^{-4}$		—
$K^*(892)^- \rightarrow K^- \pi^0$				
$(K^+ \pi^0)_{S\text{-wave}} K^-$		$(2.34 \pm 0.17) \times 10^{-3}$		743
$(K^- \pi^0)_{S\text{-wave}} K^+$		$(1.3 \pm 0.4) \times 10^{-4}$		743
$f_0(980) \pi^0, f_0 \rightarrow K^+ K^-$		$(3.5 \pm 0.6) \times 10^{-4}$		—
$\phi \pi^0, \phi \rightarrow K^+ K^-$		$(6.4 \pm 0.4) \times 10^{-4}$		—
$2K_S^0 \pi^0$		$< 5.9 \times 10^{-4}$		740
$K^+ K^- \pi^+ \pi^-$	[ccc]	$(2.43 \pm 0.12) \times 10^{-3}$		677
$\phi \pi^+ \pi^-$ 3-body, $\phi \rightarrow K^+ K^-$		$(2.4 \pm 2.4) \times 10^{-5}$		614
$\phi \rho^0, \phi \rightarrow K^+ K^-$		$(7.1 \pm 0.6) \times 10^{-4}$		250
$K^+ K^- \rho^0$ 3-body		$(5 \pm 7) \times 10^{-5}$		302
$f_0(980) \pi^+ \pi^-$, $f_0 \rightarrow K^+ K^-$		$(3.6 \pm 0.9) \times 10^{-4}$		—
$K^*(892)^0 K^\mp \pi^\pm$ 3-body,	[ddd]	$(2.7 \pm 0.6) \times 10^{-4}$		531
$K^{*0} \rightarrow K^\pm \pi^\mp$				
$K^*(892)^0 K^*(892)^0, K^{*0} \rightarrow$		$(7 \pm 5) \times 10^{-5}$		272
$K^\pm \pi^\mp$				
$K_1(1270)^\pm K^\mp, K_1(1270)^\pm \rightarrow$		$(8.0 \pm 1.8) \times 10^{-4}$		—
$K^\pm \pi^+ \pi^-$				
$K_1(1400)^\pm K^\mp, K_1(1400)^\pm \rightarrow$		$(5.3 \pm 1.2) \times 10^{-4}$		—
$K^\pm \pi^+ \pi^-$				
$2K_S^0 \pi^+ \pi^-$		$(1.28 \pm 0.24) \times 10^{-3}$		673
$K_S^0 K^- 2\pi^+ \pi^-$		$< 1.5 \times 10^{-4}$	CL=90%	595
$K^+ K^- \pi^+ \pi^- \pi^0$		$(3.1 \pm 2.0) \times 10^{-3}$		600

Other $K\bar{K}X$ modes. They include all decay modes of the ϕ, η , and ω .

$\phi \eta$		$(1.4 \pm 0.5) \times 10^{-4}$		489
$\phi \omega$		$< 2.1 \times 10^{-3}$	CL=90%	238

Radiative modes

$\rho^0 \gamma$		$< 2.4 \times 10^{-4}$	CL=90%	771
$\omega \gamma$		$< 2.4 \times 10^{-4}$	CL=90%	768
$\phi \gamma$		$(2.70 \pm 0.35) \times 10^{-5}$		654
$\bar{K}^*(892)^0 \gamma$		$(3.28 \pm 0.34) \times 10^{-4}$		719

Doubly Cabibbo suppressed (DC) modes or $\Delta C = 2$ forbidden via mixing (C2M) modes

$K^+ \ell^- \bar{\nu}_\ell$ via \bar{D}^0		$< 2.2 \times 10^{-5}$	CL=90%	—
K^+ or $K^*(892)^+ e^- \bar{\nu}_e$ via \bar{D}^0		$< 6 \times 10^{-5}$	CL=90%	—
$K^+ \pi^-$	DC	$(1.48 \pm 0.07) \times 10^{-4}$		861
$K^+ \pi^-$ via DCS		$(1.31 \pm 0.08) \times 10^{-4}$		—
$K^+ \pi^-$ via \bar{D}^0		$< 1.6 \times 10^{-5}$	CL=95%	861
$K_S^0 \pi^+ \pi^-$ in $D^0 \rightarrow \bar{D}^0$		$< 1.9 \times 10^{-4}$	CL=95%	—
$K^*(892)^+ \pi^-$,	DC	$(1.18 \pm_{-0.35}^{+0.60}) \times 10^{-4}$		711
$K^*(892)^+ \rightarrow K_S^0 \pi^+$				
$K_0^*(1430)^+ \pi^-$,	DC	$< 1.5 \times 10^{-5}$		—
$K_0^*(1430)^+ \rightarrow K_S^0 \pi^+$				
$K_2^*(1430)^+ \pi^-$,	DC	$< 3.5 \times 10^{-5}$		—
$K_2^*(1430)^+ \rightarrow K_S^0 \pi^+$				
$K^+ \pi^- \pi^0$	DC	$(3.05 \pm 0.17) \times 10^{-4}$		844
$K^+ \pi^- \pi^0$ via \bar{D}^0		$(7.3 \pm 0.5) \times 10^{-4}$		—

$K^+ \pi^+ 2\pi^-$	DC	$(2.62 \pm_{-0.19}^{+0.21}) \times 10^{-4}$	813
$K^+ \pi^+ 2\pi^-$ via \overline{D}^0		$< 4 \times 10^{-4}$	CL=90% 812
μ^- anything via \overline{D}^0		$< 4 \times 10^{-4}$	CL=90% -

**$\Delta C = 1$ weak neutral current (CI) modes,
Lepton Family number (LF) violating modes,
Lepton (L) or Baryon (B) number violating modes**

$\gamma\gamma$	CI	< 2.7	$\times 10^{-5}$	CL=90%	932
$e^+ e^-$	CI	< 1.2	$\times 10^{-6}$	CL=90%	932
$\mu^+ \mu^-$	CI	< 1.3	$\times 10^{-6}$	CL=90%	926
$\pi^0 e^+ e^-$	CI	< 4.5	$\times 10^{-5}$	CL=90%	928
$\pi^0 \mu^+ \mu^-$	CI	< 1.8	$\times 10^{-4}$	CL=90%	915
$\eta e^+ e^-$	CI	< 1.1	$\times 10^{-4}$	CL=90%	852
$\eta \mu^+ \mu^-$	CI	< 5.3	$\times 10^{-4}$	CL=90%	838
$\pi^+ \pi^- e^+ e^-$	CI	< 3.73	$\times 10^{-4}$	CL=90%	922
$\rho^0 e^+ e^-$	CI	< 1.0	$\times 10^{-4}$	CL=90%	771
$\pi^+ \pi^- \mu^+ \mu^-$	CI	< 3.0	$\times 10^{-5}$	CL=90%	894
$\rho^0 \mu^+ \mu^-$	CI	< 2.2	$\times 10^{-5}$	CL=90%	754
$\omega e^+ e^-$	CI	< 1.8	$\times 10^{-4}$	CL=90%	768
$\omega \mu^+ \mu^-$	CI	< 8.3	$\times 10^{-4}$	CL=90%	751
$K^- K^+ e^+ e^-$	CI	< 3.15	$\times 10^{-4}$	CL=90%	791
$\phi e^+ e^-$	CI	< 5.2	$\times 10^{-5}$	CL=90%	654
$K^- K^+ \mu^+ \mu^-$	CI	< 3.3	$\times 10^{-5}$	CL=90%	710
$\phi \mu^+ \mu^-$	CI	< 3.1	$\times 10^{-5}$	CL=90%	631
$\overline{K}^0 e^+ e^-$		$[tt] < 1.1$	$\times 10^{-4}$	CL=90%	866
$\overline{K}^0 \mu^+ \mu^-$		$[tt] < 2.6$	$\times 10^{-4}$	CL=90%	852
$K^- \pi^+ e^+ e^-$	CI	< 3.85	$\times 10^{-4}$	CL=90%	861
$\overline{K}^*(892)^0 e^+ e^-$		$[tt] < 4.7$	$\times 10^{-5}$	CL=90%	719
$K^- \pi^+ \mu^+ \mu^-$	CI	< 3.59	$\times 10^{-4}$	CL=90%	829
$\overline{K}^*(892)^0 \mu^+ \mu^-$		$[tt] < 2.4$	$\times 10^{-5}$	CL=90%	700
$\pi^+ \pi^- \pi^0 \mu^+ \mu^-$	CI	< 8.1	$\times 10^{-4}$	CL=90%	863
$\mu^\pm e^\mp$	LF	$[ee] < 8.1$	$\times 10^{-7}$	CL=90%	929
$\pi^0 e^\pm \mu^\mp$	LF	$[ee] < 8.6$	$\times 10^{-5}$	CL=90%	924
$\eta e^\pm \mu^\mp$	LF	$[ee] < 1.0$	$\times 10^{-4}$	CL=90%	848
$\pi^+ \pi^- e^\pm \mu^\mp$	LF	$[ee] < 1.5$	$\times 10^{-5}$	CL=90%	911
$\rho^0 e^\pm \mu^\mp$	LF	$[ee] < 4.9$	$\times 10^{-5}$	CL=90%	767
$\omega e^\pm \mu^\mp$	LF	$[ee] < 1.2$	$\times 10^{-4}$	CL=90%	764
$K^- K^+ e^\pm \mu^\mp$	LF	$[ee] < 1.8$	$\times 10^{-4}$	CL=90%	754
$\phi e^\pm \mu^\mp$	LF	$[ee] < 3.4$	$\times 10^{-5}$	CL=90%	648
$\overline{K}^0 e^\pm \mu^\mp$	LF	$[ee] < 1.0$	$\times 10^{-4}$	CL=90%	863
$K^- \pi^+ e^\pm \mu^\mp$	LF	$[ee] < 5.53$	$\times 10^{-4}$	CL=90%	848
$\overline{K}^*(892)^0 e^\pm \mu^\mp$	LF	$[ee] < 8.3$	$\times 10^{-5}$	CL=90%	714
$2\pi^- 2e^+ + c.c.$	L	< 1.12	$\times 10^{-4}$	CL=90%	922
$2\pi^- 2\mu^+ + c.c.$	L	< 2.9	$\times 10^{-5}$	CL=90%	894
$K^- \pi^- 2e^+ + c.c.$	L	< 2.06	$\times 10^{-4}$	CL=90%	861
$K^- \pi^- 2\mu^+ + c.c.$	L	< 3.9	$\times 10^{-4}$	CL=90%	829
$2K^- 2e^+ + c.c.$	L	< 1.52	$\times 10^{-4}$	CL=90%	791
$2K^- 2\mu^+ + c.c.$	L	< 9.4	$\times 10^{-5}$	CL=90%	710
$\pi^- \pi^- e^+ \mu^+ + c.c.$	L	< 7.9	$\times 10^{-5}$	CL=90%	911
$K^- \pi^- e^+ \mu^+ + c.c.$	L	< 2.18	$\times 10^{-4}$	CL=90%	848
$2K^- e^+ \mu^+ + c.c.$	L	< 5.7	$\times 10^{-5}$	CL=90%	754
pe^-	L, B	$[eee] < 1.0$	$\times 10^{-5}$	CL=90%	696
$\overline{p}e^+$	L, B	$[fff] < 1.1$	$\times 10^{-5}$	CL=90%	696

$D^*(2007)^0$

$I(J^P) = \frac{1}{2}(1^-)$
 I, J, P need confirmation.

Mass $m = 2006.96 \pm 0.16$ MeV
 $m_{D^{*0}} - m_{D^0} = 142.12 \pm 0.07$ MeV
 Full width $\Gamma < 2.1$ MeV, CL = 90%

$\bar{D}^*(2007)^0$ modes are charge conjugates of modes below.

$D^*(2007)^0$ DECAY MODES	Fraction (Γ_i/Γ)	ρ (MeV/c)
$D^0\pi^0$	(61.9±2.9) %	43
$D^0\gamma$	(38.1±2.9) %	137

$D^*(2010)^\pm$

$I(J^P) = \frac{1}{2}(1^-)$
 I, J, P need confirmation.

Mass $m = 2010.25 \pm 0.14$ MeV
 $m_{D^{*(2010)+}} - m_{D^+} = 140.65 \pm 0.10$ MeV ($S = 1.1$)
 $m_{D^{*(2010)+}} - m_{D^0} = 145.421 \pm 0.010$ MeV ($S = 1.1$)
 Full width $\Gamma = 96 \pm 22$ keV

$D^*(2010)^-$ modes are charge conjugates of the modes below.

$D^*(2010)^\pm$ DECAY MODES	Fraction (Γ_i/Γ)	ρ (MeV/c)
$D^0\pi^+$	(67.7±0.5) %	39
$D^+\pi^0$	(30.7±0.5) %	38
$D^+\gamma$	(1.6±0.4) %	136

$D_0^*(2400)^0$

$I(J^P) = \frac{1}{2}(0^+)$

Mass $m = 2318 \pm 29$ MeV ($S = 1.7$)
 Full width $\Gamma = 267 \pm 40$ MeV

$D_0^*(2400)^0$ DECAY MODES	Fraction (Γ_i/Γ)	ρ (MeV/c)
$D^+\pi^-$	seen	385

$D_1(2420)^0$

$I(J^P) = \frac{1}{2}(1^+)$
 I, J, P need confirmation.

Mass $m = 2422.0 \pm 0.6$ MeV
 $m_{D_1^0} - m_{D^{*+}} = 411.7 \pm 0.6$
 Full width $\Gamma = 20.4 \pm 1.7$ MeV

$\bar{D}_1(2420)^0$ modes are charge conjugates of modes below.

$D_1(2420)^0$ DECAY MODES	Fraction (Γ_i/Γ)	ρ (MeV/c)
$D^*(2010)^+\pi^-$	seen	354
$D^0\pi^+\pi^-$	seen	426
$D^+\pi^-$	not seen	473
$D^{*0}\pi^+\pi^-$	not seen	280

$D_2^*(2460)^0$

$$I(J^P) = \frac{1}{2}(2^+)$$

 $J^P = 2^+$ assignment strongly favored.

Mass $m = 2462.8 \pm 1.0$ MeV ($S = 1.5$)

$m_{D_2^{*0}} - m_{D^+} = 593.2 \pm 1.0$ MeV ($S = 1.5$)

$m_{D_2^{*0}} - m_{D^{*+}} = 452.6 \pm 1.0$ MeV ($S = 1.5$)

Full width $\Gamma = 42.9 \pm 3.1$ MeV ($S = 1.7$)

 $\bar{D}_2^*(2460)^0$ modes are charge conjugates of modes below. **$D_2^*(2460)^0$ DECAY MODES**Fraction (Γ_i/Γ) ρ (MeV/c)

$D^+ \pi^-$	seen	507
$D^*(2010)^+ \pi^-$	seen	391
$D^0 \pi^+ \pi^-$	not seen	464
$D^{*0} \pi^+ \pi^-$	not seen	326

 $D_2^*(2460)^\pm$

$$I(J^P) = \frac{1}{2}(2^+)$$

 $J^P = 2^+$ assignment strongly favored.

Mass $m = 2460.1_{-3.5}^{+2.6}$ MeV ($S = 1.5$)

$m_{D_2^*(2460)^\pm} - m_{D_2^*(2460)^0} = 2.4 \pm 1.7$ MeV

Full width $\Gamma = 37 \pm 6$ MeV ($S = 1.4$)

 $D_2^*(2460)^\pm$ modes are charge conjugates of modes below. **$D_2^*(2460)^\pm$ DECAY MODES**Fraction (Γ_i/Γ) ρ (MeV/c)

$D^0 \pi^+$	seen	508
$D^{*0} \pi^+$	seen	391
$D^+ \pi^+ \pi^-$	not seen	457
$D^{*+} \pi^+ \pi^-$	not seen	320

CHARMED, STRANGE MESONS ($C = S = \pm 1$)

$$D_s^+ = c\bar{s}, D_s^- = \bar{c}s, \quad \text{similarly for } D_s^{* \pm}$$

 D_s^\pm

$$I(J^P) = 0(0^-)$$

Mass $m = 1968.47 \pm 0.33$ MeV ($S = 1.3$)

$m_{D_s^\pm} - m_{D^\pm} = 98.88 \pm 0.30$ MeV ($S = 1.4$)

Mean life $\tau = (500 \pm 7) \times 10^{-15}$ s ($S = 1.3$)

$c\tau = 149.9 \mu\text{m}$

CP-violating decay-rate asymmetries

$$\begin{aligned}
A_{CP}(\mu^\pm \nu) &= 0.05 \pm 0.06 \\
A_{CP}(K^\pm K_S^0) &= 0.049 \pm 0.023 \\
A_{CP}(K^+ K^- \pi^\pm) &= 0.003 \pm 0.014 \\
A_{CP}(K^+ K^- \pi^\pm \pi^0) &= -0.06 \pm 0.04 \\
A_{CP}(K_S^0 K^\mp 2\pi^\pm) &= -0.01 \pm 0.04 \\
A_{CP}(\pi^+ \pi^- \pi^\pm) &= 0.02 \pm 0.05 \\
A_{CP}(\pi^\pm \eta) &= -0.08 \pm 0.05 \\
A_{CP}(\pi^\pm \eta') &= -0.06 \pm 0.04 \\
A_{CP}(K^\pm \pi^0) &= 0.02 \pm 0.29 \\
A_{CP}(K_S^0 \pi^\pm) &= 0.27 \pm 0.11 \\
A_{CP}(K^\pm \pi^+ \pi^-) &= 0.11 \pm 0.07 \\
A_{CP}(K^\pm \eta) &= -0.20 \pm 0.18 \\
A_{CP}(K^\pm \eta'(958)) &= -0.2 \pm 0.4
\end{aligned}$$

T-violating decay-rate asymmetry

$$A_T(K_S^0 K^\pm \pi^+ \pi^-) = -0.04 \pm 0.07 \text{ [ggg]}$$

 $D_S^+ \rightarrow \phi \ell^+ \nu_\ell$ form factors

$$\begin{aligned}
r_2 &= 0.84 \pm 0.11 \quad (S = 2.4) \\
r_V &= 1.80 \pm 0.08 \\
\Gamma_L/\Gamma_T &= 0.72 \pm 0.18
\end{aligned}$$

Unless otherwise noted, the branching fractions for modes with a resonance in the final state include all the decay modes of the resonance. D_S^- modes are charge conjugates of the modes below.

D_S^+ DECAY MODES	Fraction (Γ_i/Γ)	Scale factor/ Confidence level	ρ (MeV/c)
Inclusive modes			
e^+ semileptonic	[hhh] (6.5 \pm 0.4) %		—
π^+ anything	(119.3 \pm 1.4) %		—
π^- anything	(43.2 \pm 0.9) %		—
π^0 anything	(123 \pm 7) %		—
K^- anything	(18.7 \pm 0.5) %		—
K^+ anything	(28.9 \pm 0.7) %		—
K_S^0 anything	(19.0 \pm 1.1) %		—
η anything	[iii] (29.9 \pm 2.8) %		—
ω anything	(6.1 \pm 1.4) %		—
η' anything	[jjj] (11.7 \pm 1.8) %		—
$f_0(980)$ anything, $f_0 \rightarrow \pi^+ \pi^-$	< 1.3 %	CL=90%	—
ϕ anything	(15.7 \pm 1.0) %		—
$K^+ K^-$ anything	(15.8 \pm 0.7) %		—
$K_S^0 K^+$ anything	(5.8 \pm 0.5) %		—
$K_S^0 K^-$ anything	(1.9 \pm 0.4) %		—
$2K_S^0$ anything	(1.70 \pm 0.32) %		—
$2K^+$ anything	< 2.6 $\times 10^{-3}$	CL=90%	—
$2K^-$ anything	< 6 $\times 10^{-4}$	CL=90%	—
Leptonic and semileptonic modes			
$e^+ \nu_e$	< 1.2 $\times 10^{-4}$	CL=90%	984
$\mu^+ \nu_\mu$	(5.8 \pm 0.4) $\times 10^{-3}$		981
$\tau^+ \nu_\tau$	(5.6 \pm 0.4) %		182
$K^+ K^- e^+ \nu_e$	—		851
$\phi e^+ \nu_e$	[kkk] (2.49 \pm 0.14) %		720

$\eta e^+ \nu_e + \eta'(958) e^+ \nu_e$	[kkk]	(3.66 ± 0.37) %		—
$\eta e^+ \nu_e$	[kkk]	(2.67 ± 0.29) %	S=1.1	908
$\eta'(958) e^+ \nu_e$	[kkk]	(9.9 ± 2.3) × 10 ⁻³		751
$K^0 e^+ \nu_e$		(3.7 ± 1.0) × 10 ⁻³		921
$K^*(892)^0 e^+ \nu_e$	[kkk]	(1.8 ± 0.7) × 10 ⁻³		782
$f_0(980) e^+ \nu_e, f_0 \rightarrow \pi^+ \pi^-$		(2.00 ± 0.32) × 10 ⁻³		—
Hadronic modes with a $K\bar{K}$ pair				
$K^+ K_S^0$		(1.49 ± 0.08) %		850
$K^+ K^- \pi^+$	[oo]	(5.50 ± 0.27) %		805
$\phi \pi^+$	[kkk, III]	(4.5 ± 0.4) %		712
$\phi \pi^+, \phi \rightarrow K^+ K^-$	[III]	(2.32 ± 0.14) %		712
$K^+ \bar{K}^*(892)^0, \bar{K}^{*0} \rightarrow K^- \pi^+$		(2.60 ± 0.15) %		416
$f_0(980) \pi^+, f_0 \rightarrow K^+ K^-$		(1.55 ± 0.16) %		732
$f_0(1370) \pi^+, f_0 \rightarrow K^+ K^-$		(2.4 ± 0.4) × 10 ⁻³		—
$f_0(1710) \pi^+, f_0 \rightarrow K^+ K^-$		(1.87 ± 0.33) × 10 ⁻³		198
$K^+ \bar{K}_0^*(1430)^0, \bar{K}_0^* \rightarrow K^- \pi^+$		(2.1 ± 0.4) × 10 ⁻³		218
$K^0 \bar{K}^0 \pi^+$		—		802
$K^*(892) + \bar{K}^0$	[kkk]	(5.4 ± 1.2) %		683
$K^+ K^- \pi^+ \pi^0$		(5.6 ± 0.5) %		748
$\phi \rho^+$	[kkk]	(8.4 $^{+1.9}_{-2.3}$) %		401
$K_S^0 K^- 2\pi^+$		(1.64 ± 0.12) %		744
$K^*(892) + \bar{K}^*(892)^0$	[kkk]	(7.2 ± 2.6) %		417
$K^+ K_S^0 \pi^+ \pi^-$		(9.6 ± 1.3) × 10 ⁻³		744
$K^+ K^- 2\pi^+ \pi^-$		(8.8 ± 1.6) × 10 ⁻³		673
$\phi 2\pi^+ \pi^-$	[kkk]	(1.21 ± 0.16) %		640
$K^+ K^- \rho^0 \pi^+$ non- ϕ		< 2.6 × 10 ⁻⁴	CL=90%	249
$\phi \rho^0 \pi^+, \phi \rightarrow K^+ K^-$		(6.6 ± 1.3) × 10 ⁻³		181
$\phi a_1(1260)^+, \phi \rightarrow K^+ K^-,$ $a_1^+ \rightarrow \rho^0 \pi^+$		(7.5 ± 1.3) × 10 ⁻³		†
$K^+ K^- 2\pi^+ \pi^-$ nonresonant		(9 ± 7) × 10 ⁻⁴		673
$2K_S^0 2\pi^+ \pi^-$		(8.4 ± 3.5) × 10 ⁻⁴		669
Hadronic modes without K's				
$\pi^+ \pi^0$		< 6 × 10 ⁻⁴	CL=90%	975
$2\pi^+ \pi^-$		(1.10 ± 0.06) %		959
$\rho^0 \pi^+$		(2.0 ± 1.2) × 10 ⁻⁴		825
$\pi^+ (\pi^+ \pi^-)_{S\text{-wave}}$	[mmm]	(9.2 ± 0.6) × 10 ⁻³		959
$f_2(1270) \pi^+, f_2 \rightarrow \pi^+ \pi^-$		(1.11 ± 0.20) × 10 ⁻³		559
$\rho(1450)^0 \pi^+, \rho^0 \rightarrow \pi^+ \pi^-$		(3.0 ± 2.0) × 10 ⁻⁴		421
$\pi^+ 2\pi^0$		(6.5 ± 1.3) × 10 ⁻³		961
$2\pi^+ \pi^- \pi^0$		—		935
$\eta \pi^+$	[kkk]	(1.56 ± 0.20) %		902
$\omega \pi^+$	[kkk]	(2.3 ± 0.6) × 10 ⁻³		822
$3\pi^+ 2\pi^-$		(8.0 ± 0.9) × 10 ⁻³		899
$2\pi^+ \pi^- 2\pi^0$		—		902
$\eta \rho^+$	[kkk]	(8.9 ± 0.8) %		724
$\eta \pi^+ \pi^0$ 3-body	[kkk]	< 5 %	CL=90%	886
$\omega \pi^+ \pi^0$	[kkk]	(2.8 ± 0.7) %		802
$3\pi^+ 2\pi^- \pi^0$		(4.9 ± 3.2) %		856
$\omega 2\pi^+ \pi^-$	[kkk]	(1.6 ± 0.5) %		766
$\eta'(958) \pi^+$	[ljj, kkk]	(3.8 ± 0.4) %		743
$3\pi^+ 2\pi^- 2\pi^0$		—		803

$\omega\eta\pi^+$	$[kkk] < 2.13$	%	CL=90%	654
$\eta'(958)\rho^+$	$[jjj, kkk] (12.5 \pm 2.2)$	%		465
$\eta'(958)\pi^+\pi^0$ 3-body	$[kkk] < 1.8$	%	CL=90%	720
Modes with one or three K's				
$K^+\pi^0$	$(8.2 \pm 2.2) \times 10^{-4}$			917
$K_S^0\pi^+$	$(1.20 \pm 0.08) \times 10^{-3}$			916
$K^+\eta$	$[kkk] (1.39 \pm 0.30) \times 10^{-3}$			835
$K^+\omega$	$[kkk] < 2.4$	$\times 10^{-3}$	CL=90%	741
$K^+\eta'(958)$	$[kkk] (1.6 \pm 0.5) \times 10^{-3}$			646
$K^+\pi^+\pi^-$	$(6.9 \pm 0.5) \times 10^{-3}$			900
$K^+\rho^0$	$(2.7 \pm 0.5) \times 10^{-3}$			745
$K^+\rho(1450)^0, \rho^0 \rightarrow \pi^+\pi^-$	$(7.3 \pm 2.6) \times 10^{-4}$			—
$K^*(892)^0\pi^+, K^{*0} \rightarrow K^+\pi^-$	$(1.50 \pm 0.26) \times 10^{-3}$			775
$K^*(1410)^0\pi^+, K^{*0} \rightarrow K^+\pi^-$	$(1.30 \pm 0.31) \times 10^{-3}$			—
$K^*(1430)^0\pi^+, K^{*0} \rightarrow K^+\pi^-$	$(5 \pm 4) \times 10^{-4}$			—
$K^+\pi^+\pi^-$ nonresonant	$(1.1 \pm 0.4) \times 10^{-3}$			900
$K_S^0\pi^+\pi^0$	$(1.00 \pm 0.18) \%$			900
$K_S^0 2\pi^+\pi^-$	$(2.9 \pm 1.1) \times 10^{-3}$			870
$K^+\omega\pi^0$	$[kkk] < 8.2$	$\times 10^{-3}$	CL=90%	684
$K^+\omega\pi^+\pi^-$	$[kkk] < 5.4$	$\times 10^{-3}$	CL=90%	603
$K^+\omega\eta$	$[kkk] < 7.9$	$\times 10^{-3}$	CL=90%	367
$2K^+K^-$	$(4.9 \pm 1.7) \times 10^{-4}$			628
ϕK^+	$[kkk] < 6$	$\times 10^{-4}$	CL=90%	607
Doubly Cabibbo-suppressed modes				
$2K^+\pi^-$	$(1.29 \pm 0.18) \times 10^{-4}$			805
Baryon-antibaryon mode				
$\rho\bar{\pi}$	$(1.3 \pm 0.4) \times 10^{-3}$			295
$\Delta C = 1$ weak neutral current (CI) modes, Lepton family number (LF), or Lepton number (L) violating modes				
$\pi^+e^+e^-$	$[tt] < 2.7$	$\times 10^{-4}$	CL=90%	979
$\pi^+\mu^+\mu^-$	$[tt] < 2.6$	$\times 10^{-5}$	CL=90%	968
$K^+e^+e^-$	$CI < 1.6$	$\times 10^{-3}$	CL=90%	922
$K^+\mu^+\mu^-$	$CI < 3.6$	$\times 10^{-5}$	CL=90%	909
$K^*(892)^+\mu^+\mu^-$	$CI < 1.4$	$\times 10^{-3}$	CL=90%	765
$\pi^+e^\pm\mu^\mp$	$LF [ee] < 6.1$	$\times 10^{-4}$	CL=90%	976
$K^+e^\pm\mu^\mp$	$LF [ee] < 6.3$	$\times 10^{-4}$	CL=90%	919
π^-2e^+	$L < 6.9$	$\times 10^{-4}$	CL=90%	979
$\pi^-2\mu^+$	$L < 2.9$	$\times 10^{-5}$	CL=90%	968
$\pi^-e^+\mu^+$	$L < 7.3$	$\times 10^{-4}$	CL=90%	976
K^-2e^+	$L < 6.3$	$\times 10^{-4}$	CL=90%	922
$K^-2\mu^+$	$L < 1.3$	$\times 10^{-5}$	CL=90%	909
$K^-e^+\mu^+$	$L < 6.8$	$\times 10^{-4}$	CL=90%	919
$K^*(892)^-2\mu^+$	$L < 1.4$	$\times 10^{-3}$	CL=90%	765

$D_s^{*\pm}$

$$I(J^P) = 0(?^?)$$

J^P is natural, width and decay modes consistent with 1^- .

$$\text{Mass } m = 2112.3 \pm 0.5 \text{ MeV} \quad (S = 1.1)$$

$$m_{D_s^{*\pm}} - m_{D_s^\pm} = 143.8 \pm 0.4 \text{ MeV}$$

$$\text{Full width } \Gamma < 1.9 \text{ MeV, CL} = 90\%$$

D_s^{*-} modes are charge conjugates of the modes below.

D_s^{*+} DECAY MODES	Fraction (Γ_i/Γ)	ρ (MeV/c)
$D_s^+ \gamma$	(94.2±0.7) %	139
$D_s^+ \pi^0$	(5.8±0.7) %	48

$D_{s0}^*(2317)^\pm$

$$I(J^P) = 0(0^+)$$

J, P need confirmation.

J^P is natural, low mass consistent with 0^+ .

$$\text{Mass } m = 2317.8 \pm 0.6 \text{ MeV} \quad (S = 1.1)$$

$$m_{D_{s0}^*(2317)^\pm} - m_{D_s^\pm} = 349.3 \pm 0.6 \text{ MeV} \quad (S = 1.1)$$

$$\text{Full width } \Gamma < 3.8 \text{ MeV, CL} = 95\%$$

$D_{s0}^*(2317)^-$ modes are charge conjugates of modes below.

$D_{s0}^*(2317)^\pm$ DECAY MODES	Fraction (Γ_i/Γ)	ρ (MeV/c)
$D_s^+ \pi^0$	seen	298
$D_s^+ \pi^0 \pi^0$	not seen	205

$D_{s1}(2460)^\pm$

$$I(J^P) = 0(1^+)$$

$$\text{Mass } m = 2459.5 \pm 0.6 \text{ MeV} \quad (S = 1.1)$$

$$m_{D_{s1}(2460)^\pm} - m_{D_s^{*\pm}} = 347.2 \pm 0.8 \text{ MeV} \quad (S = 1.2)$$

$$m_{D_{s1}(2460)^\pm} - m_{D_s^\pm} = 491.1 \pm 0.7 \text{ MeV} \quad (S = 1.1)$$

$$\text{Full width } \Gamma < 3.5 \text{ MeV, CL} = 95\%$$

$D_{s1}(2460)^-$ modes are charge conjugates of the modes below.

$D_{s1}(2460)^+$ DECAY MODES	Fraction (Γ_i/Γ)	Scale factor/ Confidence level	ρ (MeV/c)
$D_s^{*+} \pi^0$	(48 ±11) %		297
$D_s^+ \gamma$	(18 ± 4) %		442
$D_s^+ \pi^+ \pi^-$	(4.3 ± 1.3) %	S=1.1	363
$D_s^{*+} \gamma$	< 8 %	CL=90%	323
$D_{s0}^*(2317)^+ \gamma$	(3.7 ⁺ _{-2.4}) %		138

$D_{s1}(2536)^\pm$

$$I(J^P) = 0(1^+)$$

J, P need confirmation.

$$\text{Mass } m = 2535.29 \pm 0.20 \text{ MeV}$$

$$\text{Full width } \Gamma < 2.3 \text{ MeV, CL} = 90\%$$

$D_{s1}(2536)^-$ modes are charge conjugates of the modes below.

$D_{s1}(2536)^+$ DECAY MODES	Fraction (Γ_i/Γ)	ρ (MeV/c)
$D^*(2010)^+ K^0$	seen	149
$D^*(2007)^0 K^+$	seen	168
$D^+ K^0$	not seen	382

$D^0 K^+$	not seen	391
$D_S^{*+} \gamma$	possibly seen	388
$D_S^+ \pi^+ \pi^-$	seen	437

 $D_{S2}^*(2573)$

$$I(J^P) = 0(?^?)$$

J^P is natural, width and decay modes consistent with 2^+ .

Mass $m = 2572.6 \pm 0.9$ MeV

Full width $\Gamma = 20 \pm 5$ MeV ($S = 1.3$)

$D_{S2}^*(2573)^-$ modes are charge conjugates of the modes below.

$D_{S2}^*(2573)^+$ DECAY MODES	Fraction (Γ_i/Γ)	ρ (MeV/c)
$D^0 K^+$	seen	435
$D^*(2007)^0 K^+$	not seen	244

BOTTOM MESONS

($B = \pm 1$)

$$B^+ = u\bar{b}, B^0 = d\bar{b}, \bar{B}^0 = \bar{d}b, B^- = \bar{u}b, \text{ similarly for } B^{*'}\text{'s}$$

B-particle organization

Many measurements of B decays involve admixtures of B hadrons. Previously we arbitrarily included such admixtures in the B^\pm section, but because of their importance we have created two new sections: “ B^\pm/B^0 Admixture” for $\Upsilon(4S)$ results and “ $B^\pm/B^0/B_S^0/b$ -baryon Admixture” for results at higher energies. Most inclusive decay branching fractions and χ_b at high energy are found in the Admixture sections. B^0 - \bar{B}^0 mixing data are found in the B^0 section, while B_S^0 - \bar{B}_S^0 mixing data and B - \bar{B} mixing data for a B^0/B_S^0 admixture are found in the B_S^0 section. CP -violation data are found in the B^\pm , B^0 , and B^\pm/B^0 Admixture sections. b -baryons are found near the end of the Baryon section.

The organization of the B sections is now as follows, where bullets indicate particle sections and brackets indicate reviews.

- B^\pm
mass, mean life, CP violation, branching fractions
- B^0
mass, mean life, $B^0-\bar{B}^0$ mixing, CP violation, branching fractions
- $B^\pm B^0$ Admixtures
 CP violation, branching fractions
- $B^\pm/B^0/B_S^0/b$ -baryon Admixtures
mean life, production fractions, branching fractions
- B^*
mass
- $B_1(5721)^0$
mass
- $B_2^*(5747)^0$
mass
- B_S^0
mass, mean life, $B_S^0-\bar{B}_S^0$ mixing, CP violation, branching fractions
- B_S^*
mass
- $B_{S1}(5830)^0$
mass
- $B_{S2}^8(5840)^0$
mass
- B_c^\pm
mass, mean life, branching fractions

At the end of Baryon Listings:

- Λ_b
mass, mean life, branching fractions
- Σ_b
mass
- Σ_b^*
mass
- Ξ_b^0, Ξ_b^-
mass, mean life, branching fractions
- Ω_b^-
mass, branching fractions
- b -baryon Admixture
mean life, branching fractions

B[±]

$$I(J^P) = \frac{1}{2}(0^-)$$

I, J, P need confirmation. Quantum numbers shown are quark-model predictions.

$$\text{Mass } m_{B^\pm} = 5279.17 \pm 0.29 \text{ MeV}$$

$$\text{Mean life } \tau_{B^\pm} = (1.638 \pm 0.011) \times 10^{-12} \text{ s}$$

$$c\tau = 491.1 \text{ } \mu\text{m}$$

CP violation

$$A_{CP}(B^+ \rightarrow J/\psi(1S)K^+) = 0.009 \pm 0.008 \quad (S = 1.3)$$

$$A_{CP}(B^+ \rightarrow J/\psi(1S)\pi^+) = 0.01 \pm 0.07 \quad (S = 1.3)$$

$$A_{CP}(B^+ \rightarrow J/\psi\rho^+) = -0.11 \pm 0.14$$

$$A_{CP}(B^+ \rightarrow J/\psi K^*(892)^+) = -0.048 \pm 0.033$$

$$A_{CP}(B^+ \rightarrow \eta_c K^+) = -0.16 \pm 0.08$$

$$A_{CP}(B^+ \rightarrow \psi(2S)\pi^+) = 0.02 \pm 0.09$$

$$A_{CP}(B^+ \rightarrow \psi(2S)K^+) = -0.025 \pm 0.024$$

$$A_{CP}(B^+ \rightarrow \psi(2S)K^*(892)^+) = 0.08 \pm 0.21$$

$$A_{CP}(B^+ \rightarrow \chi_{c1}(1P)\pi^+) = 0.07 \pm 0.18$$

$$A_{CP}(B^+ \rightarrow \chi_{c0}K^+) = -0.11 \pm 0.12$$

$$A_{CP}(B^+ \rightarrow \chi_{c1}K^+) = -0.009 \pm 0.033$$

$$A_{CP}(B^+ \rightarrow \chi_{c1}K^*(892)^+) = 0.5 \pm 0.5$$

$$A_{CP}(B^+ \rightarrow \bar{D}^0\pi^+) = -0.008 \pm 0.008$$

$$A_{CP}(B^+ \rightarrow D_{CP(+1)}\pi^+) = 0.035 \pm 0.024$$

$$A_{CP}(B^+ \rightarrow D_{CP(-1)}\pi^+) = 0.017 \pm 0.026$$

$$A_{CP}(B^+ \rightarrow \bar{D}^0K^+) = 0.07 \pm 0.04$$

$$r_B(B^+ \rightarrow D^0K^+) = 0.101 \pm 0.032$$

$$\delta_B(B^+ \rightarrow D^0K^+) = 126 \pm 21 \text{ degrees}$$

$$r_B(B^+ \rightarrow DK^{*+}) = 0.34 \pm 0.09 \quad (S = 1.3)$$

$$\delta_B(B^+ \rightarrow DK^{*+}) = 157 \pm 70 \text{ degrees} \quad (S = 2.0)$$

$$A_{CP}(B^+ \rightarrow [K^-\pi^+]_D K^+) = -0.1_{-1.1}^{+0.9}$$

$$A_{CP}(B^+ \rightarrow [K^-\pi^+]_{\bar{D}} K^*(892)^+) = -0.3 \pm 0.5$$

$$A_{CP}(B^+ \rightarrow [K^-\pi^+]_D \pi^+) = -0.02 \pm 0.16$$

$$A_{CP}(B^+ \rightarrow [\pi^+\pi^-\pi^0]_D K^+) = -0.02 \pm 0.15$$

$$A_{CP}(B^+ \rightarrow D_{CP(+1)}K^+) = 0.24 \pm 0.08 \quad (S = 1.1)$$

$$A_{CP}(B^+ \rightarrow D_{CP(-1)}K^+) = -0.10 \pm 0.08$$

$$A_{CP}(B^+ \rightarrow \bar{D}^{*0}\pi^+) = -0.014 \pm 0.015$$

$$A_{CP}(B^+ \rightarrow (D_{CP(+1)}^*)^0\pi^+) = -0.02 \pm 0.05$$

$$A_{CP}(B^+ \rightarrow (D_{CP(-1)}^*)^0\pi^+) = -0.09 \pm 0.05$$

$$A_{CP}(B^+ \rightarrow D^{*0}K^+) = -0.07 \pm 0.04$$

$$r_B^*(B^+ \rightarrow D^{*0}K^+) = 0.14 \pm 0.05$$

$$\delta_B^*(B^+ \rightarrow D^{*0}K^+) = 299 \pm 24 \text{ degrees}$$

$$A_{CP}(B^+ \rightarrow D_{CP(+1)}^{*0}K^+) = -0.12 \pm 0.08$$

$$A_{CP}(B^+ \rightarrow D_{CP(-1)}^*K^+) = 0.07 \pm 0.10$$

$$A_{CP}(B^+ \rightarrow D_{CP(+1)}K^*(892)^+) = 0.09 \pm 0.14$$

$$A_{CP}(B^+ \rightarrow D_{CP(-1)}K^*(892)^+) = -0.23 \pm 0.22$$

$$A_{CP}(B^+ \rightarrow D^{*+}\bar{D}^{*0}) = -0.15 \pm 0.11$$

$$A_{CP}(B^+ \rightarrow D^{*+}\bar{D}^0) = -0.06 \pm 0.13$$

$$A_{CP}(B^+ \rightarrow D^+\bar{D}^{*0}) = 0.13 \pm 0.18$$

$$A_{CP}(B^+ \rightarrow D^+\bar{D}^0) = -0.03 \pm 0.07$$

$A_{CP}(B^+ \rightarrow K_S^0 \pi^+) = 0.009 \pm 0.029$ (S = 1.2)
$A_{CP}(B^+ \rightarrow K^+ \pi^0) = 0.051 \pm 0.025$
$A_{CP}(B^+ \rightarrow \eta' K^+) = 0.013 \pm 0.017$
$A_{CP}(B^+ \rightarrow \eta' K^*(892)^+) = -0.30^{+0.33}_{-0.40}$
$A_{CP}(B^+ \rightarrow \eta K^+) = -0.37 \pm 0.09$
$A_{CP}(B^+ \rightarrow \eta K^*(892)^+) = 0.02 \pm 0.06$
$A_{CP}(B^+ \rightarrow \eta K_0^*(1430)^+) = 0.05 \pm 0.13$
$A_{CP}(B^+ \rightarrow \eta K_2^*(1430)^+) = -0.45 \pm 0.30$
$A_{CP}(B^+ \rightarrow \omega K^+) = 0.02 \pm 0.05$
$A_{CP}(B^+ \rightarrow \omega K^{*+}) = 0.29 \pm 0.35$
$A_{CP}(B^+ \rightarrow \omega(K\pi)_0^{*+}) = -0.10 \pm 0.09$
$A_{CP}(B^+ \rightarrow \omega K_2^*(1430)^+) = 0.14 \pm 0.15$
$A_{CP}(B^+ \rightarrow K^*(892)^+ \pi^0) = 0.04 \pm 0.29$
$A_{CP}(B^+ \rightarrow K^{*0} \pi^+) = -0.04 \pm 0.09$ (S = 2.1)
$A_{CP}(B^+ \rightarrow K^+ \pi^- \pi^+) = 0.038 \pm 0.022$
$A_{CP}(B^+ \rightarrow f_0(980) K^+) = -0.10^{+0.05}_{-0.04}$
$A_{CP}(B^+ \rightarrow f_2(1270) K^+) = -0.68^{+0.19}_{-0.17}$
$A_{CP}(B^+ \rightarrow f_X(1300) K^+) = 0.28 \pm 0.30$
$A_{CP}(B^+ \rightarrow \rho^0 K^+) = 0.37 \pm 0.10$
$A_{CP}(B^+ \rightarrow K_0^*(1430)^0 \pi^+) = 0.055 \pm 0.033$
$A_{CP}(B^+ \rightarrow K_2^*(1430)^0 \pi^+) = 0.05^{+0.29}_{-0.24}$
$A_{CP}(B^+ \rightarrow K^0 \rho^+) = (-0.12 \pm 0.17) \times 10^{-6}$
$A_{CP}(B^+ \rightarrow K^{*+} \pi^+ \pi^-) = 0.07 \pm 0.08$
$A_{CP}(B^+ \rightarrow \rho \bar{\Lambda} \gamma) = 0.17 \pm 0.17$
$A_{CP}(B^+ \rightarrow \rho \bar{\Lambda} \pi^0) = 0.01 \pm 0.17$
$A_{CP}(B^+ \rightarrow \rho^0 K^*(892)^+)$
$A_{CP}(B^+ \rightarrow K^*(892)^+ f_0(980)) = -0.34 \pm 0.21$
$A_{CP}(B^+ \rightarrow a_1^+ K^0) = 0.12 \pm 0.11$
$A_{CP}(B^+ \rightarrow b_1^+ K^0) = -0.03 \pm 0.15$
$A_{CP}(B^+ \rightarrow K^*(892)^0 \rho^+) = -0.01 \pm 0.16$
$A_{CP}(B^+ \rightarrow b_1^0 K^+) = -0.46 \pm 0.20$
$A_{CP}(B^+ \rightarrow K^0 K^+) = 0.12 \pm 0.18$
$A_{CP}(B^+ \rightarrow K^+ K_S^0 K_S^0) = -0.04 \pm 0.11$
$A_{CP}(B^+ \rightarrow K^+ K^- \pi^+) = 0.00 \pm 0.10$
$A_{CP}(B^+ \rightarrow K^+ K^- K^+) = -0.017 \pm 0.030$
$A_{CP}(B^+ \rightarrow \phi K^+) = -0.01 \pm 0.06$
$A_{CP}(B^+ \rightarrow X_0(1550) K^+) = -0.04 \pm 0.07$
$A_{CP}(B^+ \rightarrow K^{*+} K^+ K^-) = 0.11 \pm 0.09$
$A_{CP}(B^+ \rightarrow \phi K^*(892)^+) = -0.01 \pm 0.08$
$A_{CP}(B^+ \rightarrow \phi(K\pi)_0^{*+}) = 0.04 \pm 0.16$
$A_{CP}(B^+ \rightarrow \phi K_1(1270)^+) = 0.15 \pm 0.20$
$A_{CP}(B^+ \rightarrow \phi K_2^*(1430)^+) = -0.23 \pm 0.20$
$A_{CP}(B^+ \rightarrow K^*(892)^+ \gamma) = 0.018 \pm 0.029$
$A_{CP}(B^+ \rightarrow \eta K^+ \gamma) = -0.12 \pm 0.07$
$A_{CP}(B^+ \rightarrow \phi K^+ \gamma) = -0.26 \pm 0.15$
$A_{CP}(B^+ \rightarrow \rho^+ \gamma) = -0.11 \pm 0.33$
$A_{CP}(B^+ \rightarrow \pi^+ \pi^0) = 0.06 \pm 0.05$
$A_{CP}(B^+ \rightarrow \pi^+ \pi^- \pi^+) = 0.03 \pm 0.06$
$A_{CP}(B^+ \rightarrow \rho^0 \pi^+) = 0.18^{+0.09}_{-0.17}$
$A_{CP}(B^+ \rightarrow f_2(1270) \pi^+) = 0.41 \pm 0.30$

$$\begin{aligned}
A_{CP}(B^+ \rightarrow \rho^0(1450)\pi^+) &= -0.1^{+0.4}_{-0.5} \\
A_{CP}(B^+ \rightarrow f_0(1370)\pi^+) &= 0.72 \pm 0.22 \\
A_{CP}(B^+ \rightarrow \pi^+\pi^-\pi^+ \text{ nonresonant}) &= -0.14^{+0.23}_{-0.16} \\
A_{CP}(B^+ \rightarrow \rho^+\pi^0) &= 0.02 \pm 0.11 \\
A_{CP}(B^+ \rightarrow \rho^+\rho^0) &= -0.05 \pm 0.05 \\
A_{CP}(B^+ \rightarrow b_1^0\pi^+) &= 0.05 \pm 0.16 \\
A_{CP}(B^+ \rightarrow \omega\pi^+) &= -0.04 \pm 0.06 \\
A_{CP}(B^+ \rightarrow \omega\rho^+) &= -0.20 \pm 0.09 \\
A_{CP}(B^+ \rightarrow \eta\pi^+) &= -0.13 \pm 0.10 \quad (S = 1.5) \\
A_{CP}(B^+ \rightarrow \eta'\pi^+) &= 0.06 \pm 0.16 \\
A_{CP}(B^+ \rightarrow \eta\rho^+) &= 0.11 \pm 0.11 \\
A_{CP}(B^+ \rightarrow \eta'\rho^+) &= 0.04 \pm 0.28 \\
A_{CP}(B^+ \rightarrow \rho\bar{\rho}\pi^+) &= 0.00 \pm 0.04 \\
A_{CP}(B^+ \rightarrow \rho\bar{\rho}K^+) &= -0.16 \pm 0.07 \\
A_{CP}(B^+ \rightarrow \rho\bar{\rho}K^*(892)^+) &= 0.21 \pm 0.16 \quad (S = 1.4) \\
A_{CP}(B^+ \rightarrow K^+\ell^+\ell^-) &= -0.01 \pm 0.09 \quad (S = 1.1) \\
A_{CP}(B^+ \rightarrow K^+e^+e^-) &= 0.14 \pm 0.14 \\
A_{CP}(B^+ \rightarrow K^+\mu^+\mu^-) &= -0.05 \pm 0.13 \\
A_{CP}(B^+ \rightarrow K^{*+}\ell^+\ell^-) &= -0.09 \pm 0.14 \\
A_{CP}(B^+ \rightarrow K^{*+}e^+e^-) &= -0.14 \pm 0.23 \\
A_{CP}(B^+ \rightarrow K^{*+}\mu^+\mu^-) &= -0.12 \pm 0.24 \\
\gamma(B^+ \rightarrow D^{(*)}K^{(*)+}) &= (62 \pm 15)^\circ
\end{aligned}$$

B^- modes are charge conjugates of the modes below. Modes which do not identify the charge state of the B are listed in the B^\pm/B^0 ADMIXTURE section.

The branching fractions listed below assume 50% $B^0\bar{B}^0$ and 50% B^+B^- production at the $\Upsilon(4S)$. We have attempted to bring older measurements up to date by rescaling their assumed $\Upsilon(4S)$ production ratio to 50:50 and their assumed D , D_S , D^* , and ψ branching ratios to current values whenever this would affect our averages and best limits significantly.

Indentation is used to indicate a subchannel of a previous reaction. All resonant subchannels have been corrected for resonance branching fractions to the final state so the sum of the subchannel branching fractions can exceed that of the final state.

For inclusive branching fractions, e.g., $B \rightarrow D^\pm$ anything, the values usually are multiplicities, not branching fractions. They can be greater than one.

B^\pm DECAY MODES	Fraction (Γ_i/Γ)	Scale factor/ Confidence level (MeV/c)	p
Semileptonic and leptonic modes			
$\ell^+ \nu_\ell$ anything	[nnn] (10.99 \pm 0.28) %		—
$e^+ \nu_e X_c$	(10.8 \pm 0.4) %		—
$D \ell^+ \nu_\ell$ anything	(9.8 \pm 0.7) %		—
$\bar{D}^0 \ell^+ \nu_\ell$	[nnn] (2.23 \pm 0.11) %		2310
$\bar{D}^0 \tau^+ \nu_\tau$	(7 \pm 4) $\times 10^{-3}$		1911
$\bar{D}^*(2007)^0 \ell^+ \nu_\ell$	[nnn] (5.68 \pm 0.19) %		2258
$\bar{D}^*(2007)^0 \tau^+ \nu_\tau$	(2.0 \pm 0.5) %		1839
$D^- \pi^+ \ell^+ \nu_\ell$	(4.2 \pm 0.5) $\times 10^{-3}$		2306
$\bar{D}_0^*(2420)^0 \ell^+ \nu_\ell \times B(\bar{D}_0^{*0} \rightarrow D^+ \pi^-)$	(2.5 \pm 0.5) $\times 10^{-3}$		—
$\bar{D}_2^*(2460)^0 \ell^+ \nu_\ell \times B(\bar{D}_2^{*0} \rightarrow D^+ \pi^-)$	(1.67 \pm 0.30) $\times 10^{-3}$	S=1.2	2065

$D^{(*)} n \pi \ell^+ \nu_\ell (n \geq 1)$	(1.86 ± 0.26) %	—
$D^{*-} \pi^+ \ell^+ \nu_\ell$	(6.1 ± 0.6) × 10 ⁻³	2254
$\overline{D}_1(2420)^0 \ell^+ \nu_\ell \times B(\overline{D}_1^0 \rightarrow D^{*+} \pi^-)$	(3.03 ± 0.20) × 10 ⁻³	2084
$\overline{D}'_1(2430)^0 \ell^+ \nu_\ell \times B(\overline{D}_1^0 \rightarrow D^{*+} \pi^-)$	(2.7 ± 0.6) × 10 ⁻³	—
$\overline{D}_2^*(2460)^0 \ell^+ \nu_\ell \times B(\overline{D}_2^{*0} \rightarrow D^{*+} \pi^-)$	(1.85 ± 0.27) × 10 ⁻³	S=1.3 2065
$\pi^0 \ell^+ \nu_\ell$	(7.7 ± 1.2) × 10 ⁻⁵	2638
$\eta \ell^+ \nu_\ell$	(3.7 ± 1.3) × 10 ⁻⁵	S=1.5 2611
$\eta' \ell^+ \nu_\ell$	(1.7 ± 2.2) × 10 ⁻⁵	2553
$\omega \ell^+ \nu_\ell$	[<i>nnn</i>] (1.15 ± 0.17) × 10 ⁻⁴	2582
$\rho^0 \ell^+ \nu_\ell$	[<i>nnn</i>] (1.28 ± 0.18) × 10 ⁻⁴	2583
$\rho \overline{p} e^+ \nu_e$	< 5.2 × 10 ⁻³	CL=90% 2467
$e^+ \nu_e$	< 1.9 × 10 ⁻⁶	CL=90% 2640
$\mu^+ \nu_\mu$	< 1.0 × 10 ⁻⁶	CL=90% 2639
$\tau^+ \nu_\tau$	(1.8 ± 0.5) × 10 ⁻⁴	2341
$\ell^+ \nu_\ell \gamma$	< 1.56 × 10 ⁻⁵	CL=90% 2640
$e^+ \nu_e \gamma$	< 1.7 × 10 ⁻⁵	CL=90% 2640
$\mu^+ \nu_\mu \gamma$	< 2.4 × 10 ⁻⁵	CL=90% 2639

Inclusive modes

$D^0 X$	(8.6 ± 0.7) %	—
$\overline{D}^0 X$	(79 ± 4) %	—
$D^+ X$	(2.5 ± 0.5) %	—
$D^- X$	(9.9 ± 1.2) %	—
$D_s^+ X$	(7.9 $\begin{smallmatrix} +1.4 \\ -1.3 \end{smallmatrix}$) %	—
$D_s^- X$	(1.10 $\begin{smallmatrix} +0.40 \\ -0.32 \end{smallmatrix}$) %	—
$\Lambda_c^+ X$	(2.1 $\begin{smallmatrix} +0.9 \\ -0.6 \end{smallmatrix}$) %	—
$\overline{\Lambda}_c^- X$	(2.8 $\begin{smallmatrix} +1.1 \\ -0.9 \end{smallmatrix}$) %	—
$\overline{c} X$	(97 ± 4) %	—
$c X$	(23.4 $\begin{smallmatrix} +2.2 \\ -1.8 \end{smallmatrix}$) %	—
$\overline{c} c X$	(120 ± 6) %	—

D, D^* , or D_s modes

$\overline{D}^0 \pi^+$	(4.84 ± 0.15) × 10 ⁻³	2308
$D_{CP(+1)} \pi^+$	[<i>ooo</i>] (2.3 ± 0.4) × 10 ⁻³	—
$D_{CP(-1)} \pi^+$	[<i>ooo</i>] (2.0 ± 0.4) × 10 ⁻³	—
$\overline{D}^0 \rho^+$	(1.34 ± 0.18) %	2237
$\overline{D}^0 K^+$	(3.68 ± 0.33) × 10 ⁻⁴	2280
$D_{CP(+1)} K^+$	[<i>ooo</i>] (2.01 ± 0.26) × 10 ⁻⁴	—
$D_{CP(-1)} K^+$	[<i>ooo</i>] (1.89 ± 0.27) × 10 ⁻⁴	—
$[K^- \pi^+]_D K^+$	[<i>ppp</i>] < 2.8 × 10 ⁻⁷	CL=90% —
$[K^+ \pi^-]_D K^+$	[<i>ppp</i>] < 4 × 10 ⁻⁵	CL=90% —
$[K^- \pi^+]_D \pi^+$	[<i>ppp</i>] (6.3 ± 1.1) × 10 ⁻⁷	—
$[K^+ \pi^-]_D \pi^+$	(1.9 ± 0.4) × 10 ⁻⁴	—
$[\pi^+ \pi^- \pi^0]_D K^-$	(4.6 ± 0.9) × 10 ⁻⁶	—
$\overline{D}^0 K^*(892)^+$	(5.3 ± 0.4) × 10 ⁻⁴	2213
$D_{CP(-1)} K^*(892)^+$	[<i>ooo</i>] (2.7 ± 0.8) × 10 ⁻⁴	—
$D_{CP(+1)} K^*(892)^+$	[<i>ooo</i>] (5.8 ± 1.1) × 10 ⁻⁴	—
$\overline{D}^0 K^+ \overline{K}^0$	(5.5 ± 1.6) × 10 ⁻⁴	2189

$\overline{D}^0 K^+ \overline{K}^*(892)^0$	(7.5 ±1.7) × 10 ⁻⁴		2071
$\overline{D}^0 \pi^+ \pi^+ \pi^-$	(1.1 ±0.4) %		2289
$\overline{D}^0 \pi^+ \pi^+ \pi^-$ nonresonant	(5 ±4) × 10 ⁻³		2289
$\overline{D}^0 \pi^+ \rho^0$	(4.2 ±3.0) × 10 ⁻³		2207
$\overline{D}^0 a_1(1260)^+$	(4 ±4) × 10 ⁻³		2123
$\overline{D}^0 \omega \pi^+$	(4.1 ±0.9) × 10 ⁻³		2206
$D^*(2010)^- \pi^+ \pi^+$	(1.35 ±0.22) × 10 ⁻³		2247
$D^- \pi^+ \pi^+$	(1.07 ±0.05) × 10 ⁻³		2299
$D^+ K^0$	< 5.0 × 10 ⁻⁶	CL=90%	2278
$\overline{D}^*(2007)^0 \pi^+$	(5.19 ±0.26) × 10 ⁻³		2256
$\overline{D}_{CP(+)}^{*0} \pi^+$	[<i>qqq</i>] (2.9 ±0.7) × 10 ⁻³		-
$D_{CP(-)}^{*0} \pi^+$	[<i>qqq</i>] (2.6 ±1.0) × 10 ⁻³		-
$\overline{D}^*(2007)^0 \omega \pi^+$	(4.5 ±1.2) × 10 ⁻³		2149
$\overline{D}^*(2007)^0 \rho^+$	(9.8 ±1.7) × 10 ⁻³		2181
$\overline{D}^*(2007)^0 K^+$	(4.21 ±0.35) × 10 ⁻⁴		2227
$\overline{D}_{CP(+)}^{*0} K^+$	[<i>qqq</i>] (2.8 ±0.4) × 10 ⁻⁴		-
$\overline{D}_{CP(-)}^{*0} K^+$	[<i>qqq</i>] (2.32 ±0.33) × 10 ⁻⁴		-
$\overline{D}^*(2007)^0 K^*(892)^+$	(8.1 ±1.4) × 10 ⁻⁴		2156
$\overline{D}^*(2007)^0 K^+ \overline{K}^0$	< 1.06 × 10 ⁻³	CL=90%	2132
$\overline{D}^*(2007)^0 K^+ K^*(892)^0$	(1.5 ±0.4) × 10 ⁻³		2008
$\overline{D}^*(2007)^0 \pi^+ \pi^+ \pi^-$	(1.03 ±0.12) %		2236
$\overline{D}^*(2007)^0 a_1(1260)^+$	(1.9 ±0.5) %		2062
$\overline{D}^*(2007)^0 \pi^- \pi^+ \pi^+ \pi^0$	(1.8 ±0.4) %		2219
$\overline{D}^{*0} 3\pi^+ 2\pi^-$	(5.7 ±1.2) × 10 ⁻³		2196
$D^*(2010)^+ \pi^0$	< 3.6 × 10 ⁻⁶		2255
$D^*(2010)^+ K^0$	< 9.0 × 10 ⁻⁶	CL=90%	2225
$D^*(2010)^- \pi^+ \pi^+ \pi^0$	(1.5 ±0.7) %		2235
$D^*(2010)^- \pi^+ \pi^+ \pi^+ \pi^-$	(2.6 ±0.4) × 10 ⁻³		2217
$\overline{D}^{*0} \pi^+$	[<i>rrr</i>] (5.9 ±1.3) × 10 ⁻³		-
$\overline{D}_1^*(2420)^0 \pi^+$	(1.5 ±0.6) × 10 ⁻³	S=1.3	2081
$\overline{D}_1(2420)^0 \pi^+ \times B(\overline{D}_1^0 \rightarrow \overline{D}^0 \pi^+ \pi^-)$	(1.9 ^{+0.5} _{-0.6}) × 10 ⁻⁴		2081
$\overline{D}_2^*(2462)^0 \pi^+$	(3.5 ±0.4) × 10 ⁻⁴		-
$\times B(\overline{D}_2^*(2462)^0 \rightarrow D^- \pi^+)$			
$\overline{D}_0^*(2400)^0 \pi^+$	(6.4 ±1.4) × 10 ⁻⁴		2128
$\times B(\overline{D}_0^*(2400)^0 \rightarrow D^- \pi^+)$			
$\overline{D}_1(2421)^0 \pi^+$	(6.8 ±1.5) × 10 ⁻⁴		-
$\times B(\overline{D}_1(2421)^0 \rightarrow D^{*-} \pi^+)$			
$\overline{D}_2^*(2462)^0 \pi^+$	(1.8 ±0.5) × 10 ⁻⁴		-
$\times B(\overline{D}_2^*(2462)^0 \rightarrow D^{*-} \pi^+)$			
$\overline{D}'_1(2427)^0 \pi^+$	(5.0 ±1.2) × 10 ⁻⁴		-
$\times B(\overline{D}'_1(2427)^0 \rightarrow D^{*-} \pi^+)$			
$\overline{D}_1(2420)^0 \pi^+ \times B(\overline{D}_1^0 \rightarrow \overline{D}^{*0} \pi^+ \pi^-)$	< 6 × 10 ⁻⁶	CL=90%	2081
$\overline{D}_1^*(2420)^0 \rho^+$	< 1.4 × 10 ⁻³	CL=90%	1996
$\overline{D}_2^*(2460)^0 \pi^+$	< 1.3 × 10 ⁻³	CL=90%	2062
$\overline{D}_2^*(2460)^0 \pi^+ \times B(\overline{D}_2^{*0} \rightarrow \overline{D}^{*0} \pi^+ \pi^-)$	< 2.2 × 10 ⁻⁵	CL=90%	2062
$\overline{D}_2^*(2460)^0 \rho^+$	< 4.7 × 10 ⁻³	CL=90%	1975
$\overline{D}_S^0 D_S^+$	(10.0 ±1.7) × 10 ⁻³		1815

$D_{S0}(2317)^+ \bar{D}^0 \times$ $B(D_{S0}(2317)^+ \rightarrow D_S^+ \pi^0)$	(7.3 $\begin{smallmatrix} +2.2 \\ -1.7 \end{smallmatrix}$) $\times 10^{-4}$		1605
$D_{S0}(2317)^+ \bar{D}^0 \times$ $B(D_{S0}(2317)^+ \rightarrow D_S^{*+} \gamma)$	< 7.6 $\times 10^{-4}$	CL=90%	1605
$D_{S0}(2317)^+ \bar{D}^* (2007)^0 \times$ $B(D_{S0}(2317)^+ \rightarrow D_S^+ \pi^0)$	(9 ± 7) $\times 10^{-4}$		1511
$D_{sJ}(2457)^+ \bar{D}^0$	(3.1 $\begin{smallmatrix} +1.0 \\ -0.9 \end{smallmatrix}$) $\times 10^{-3}$		-
$D_{sJ}(2457)^+ \bar{D}^0 \times$ $B(D_{sJ}(2457)^+ \rightarrow D_S^+ \gamma)$	(4.6 $\begin{smallmatrix} +1.3 \\ -1.1 \end{smallmatrix}$) $\times 10^{-4}$		-
$D_{sJ}(2457)^+ \bar{D}^0 \times$ $B(D_{sJ}(2457)^+ \rightarrow$ $D_S^+ \pi^+ \pi^-)$	< 2.2 $\times 10^{-4}$	CL=90%	-
$D_{sJ}(2457)^+ \bar{D}^0 \times$ $B(D_{sJ}(2457)^+ \rightarrow D_S^+ \pi^0)$	< 2.7 $\times 10^{-4}$	CL=90%	-
$D_{sJ}(2457)^+ \bar{D}^0 \times$ $B(D_{sJ}(2457)^+ \rightarrow D_S^{*+} \gamma)$	< 9.8 $\times 10^{-4}$	CL=90%	-
$D_{sJ}(2457)^+ \bar{D}^* (2007)^0$	(1.20 ± 0.30) %		-
$D_{sJ}(2457)^+ \bar{D}^* (2007)^0 \times$ $B(D_{sJ}(2457)^+ \rightarrow D_S^+ \gamma)$	(1.4 $\begin{smallmatrix} +0.7 \\ -0.6 \end{smallmatrix}$) $\times 10^{-3}$		-
$\bar{D}^0 D_{S1}(2536)^+ \times$ $B(D_{S1}(2536)^+ \rightarrow$ $D^* (2007)^0 K^+)$	(2.2 ± 0.7) $\times 10^{-4}$		1447
$\bar{D}^* (2007)^0 D_{S1}(2536)^+ \times$ $B(D_{S1}(2536)^+ \rightarrow$ $D^* (2007)^0 K^+)$	(5.5 ± 1.6) $\times 10^{-4}$		1338
$\bar{D}^0 D_{S1}(2536)^+ \times$ $B(D_{S1}(2536)^+ \rightarrow D^{*+} K^0)$	(2.3 ± 1.1) $\times 10^{-4}$		1447
$\bar{D}^0 D_{sJ}(2700)^+ \times$ $B(D_{sJ}(2700)^+ \rightarrow D^0 K^+)$	(1.13 $\begin{smallmatrix} +0.26 \\ -0.40 \end{smallmatrix}$) $\times 10^{-3}$		-
$\bar{D}^{*0} D_{S1}(2536)^+ \times$ $B(D_{S1}(2536)^+ \rightarrow D^{*+} K^0)$	(3.9 ± 2.6) $\times 10^{-4}$		1338
$\bar{D}^{*0} D_{sJ}(2573)^+ \times$ $B(D_{sJ}(2573)^+ \rightarrow D^0 K^+)$	< 2 $\times 10^{-4}$	CL=90%	1306
$\bar{D}^* (2007)^0 D_{sJ}(2573)^+ \times$ $B(D_{sJ}(2573)^+ \rightarrow D^0 K^+)$	< 5 $\times 10^{-4}$	CL=90%	1306
$\bar{D}^0 D_S^{*+}$	(7.6 ± 1.6) $\times 10^{-3}$		1734
$\bar{D}^* (2007)^0 D_S^+$	(8.2 ± 1.7) $\times 10^{-3}$		1737
$\bar{D}^* (2007)^0 D_S^{*+}$	(1.71 ± 0.24) %		1651
$D_S^{(*)+} \bar{D}^{**0}$	(2.7 ± 1.2) %		-
$\bar{D}^* (2007)^0 D^* (2010)^+$	(8.1 ± 1.7) $\times 10^{-4}$		1713
$\bar{D}^0 D^* (2010)^+ + \bar{D}^* (2007)^0 D^+$	< 1.30 %	CL=90%	1792
$\bar{D}^0 D^* (2010)^+$	(3.9 ± 0.5) $\times 10^{-4}$		1792
$\bar{D}^0 D^+$	(3.8 ± 0.4) $\times 10^{-4}$		1866
$\bar{D}^0 D^+ K^0$	< 2.8 $\times 10^{-3}$	CL=90%	1571
$D^+ \bar{D}^* (2007)^0$	(6.3 ± 1.7) $\times 10^{-4}$		1791
$\bar{D}^* (2007)^0 D^+ K^0$	< 6.1 $\times 10^{-3}$	CL=90%	1474
$\bar{D}^0 \bar{D}^* (2010)^+ K^0$	(5.2 ± 1.2) $\times 10^{-3}$		1476
$\bar{D}^* (2007)^0 D^* (2010)^+ K^0$	(7.8 ± 2.6) $\times 10^{-3}$		1362
$\bar{D}^0 D^0 K^+$	(2.10 ± 0.26) $\times 10^{-3}$		1577
$\bar{D}^* (2007)^0 D^0 K^+$	< 3.8 $\times 10^{-3}$	CL=90%	1481
$\bar{D}^0 D^* (2007)^0 K^+$	(4.7 ± 1.0) $\times 10^{-3}$		1481

$\bar{D}^*(2007)^0 D^*(2007)^0 K^+$	(5.3 \pm 1.6) \times 10 ⁻³		1368
$D^- D^+ K^+$	< 4 \times 10 ⁻⁴	CL=90%	1570
$D^- D^*(2010)^+ K^+$	< 7 \times 10 ⁻⁴	CL=90%	1475
$D^*(2010)^- D^+ K^+$	(1.5 \pm 0.4) \times 10 ⁻³		1475
$D^*(2010)^- D^*(2010)^+ K^+$	< 1.8 \times 10 ⁻³	CL=90%	1363
$(\bar{D} + \bar{D}^*)(D + D^*) K$	(3.5 \pm 0.6) %		-
$D_S^+ \pi^0$	(1.6 \pm 0.5) \times 10 ⁻⁵		2270
$D_S^{*+} \pi^0$	< 2.6 \times 10 ⁻⁴	CL=90%	2215
$D_S^+ \eta$	< 4 \times 10 ⁻⁴	CL=90%	2235
$D_S^{*+} \eta$	< 6 \times 10 ⁻⁴	CL=90%	2178
$D_S^+ \rho^0$	< 3.0 \times 10 ⁻⁴	CL=90%	2197
$D_S^{*+} \rho^0$	< 4 \times 10 ⁻⁴	CL=90%	2138
$D_S^+ \omega$	< 4 \times 10 ⁻⁴	CL=90%	2195
$D_S^{*+} \omega$	< 6 \times 10 ⁻⁴	CL=90%	2136
$D_S^+ a_1(1260)^0$	< 1.8 \times 10 ⁻³	CL=90%	2079
$D_S^{*+} a_1(1260)^0$	< 1.3 \times 10 ⁻³	CL=90%	2014
$D_S^+ \phi$	< 1.9 \times 10 ⁻⁶	CL=90%	2141
$D_S^{*+} \phi$	< 1.2 \times 10 ⁻⁵	CL=90%	2079
$D_S^+ \bar{K}^0$	< 8 \times 10 ⁻⁴	CL=90%	2241
$D_S^{*+} \bar{K}^0$	< 9 \times 10 ⁻⁴	CL=90%	2184
$D_S^+ \bar{K}^*(892)^0$	< 4 \times 10 ⁻⁴	CL=90%	2172
$D_S^{*+} \bar{K}^*(892)^0$	< 3.5 \times 10 ⁻⁴	CL=90%	2112
$D_S^- \pi^+ K^+$	(1.80 \pm 0.22) \times 10 ⁻⁴		2222
$D_S^{*-} \pi^+ K^+$	(1.45 \pm 0.24) \times 10 ⁻⁴		2164
$D_S^- \pi^+ K^*(892)^+$	< 5 \times 10 ⁻³	CL=90%	2138
$D_S^{*-} \pi^+ K^*(892)^+$	< 7 \times 10 ⁻³	CL=90%	2076
$D_S^- K^+ K^+$	(1.1 \pm 0.4) \times 10 ⁻⁵		2149
$D_S^{*-} K^+ K^+$	< 1.5 \times 10 ⁻⁵	CL=90%	2088
Charmonium modes			
$\eta_c K^+$	(9.1 \pm 1.3) \times 10 ⁻⁴		1753
$\eta_c K^*(892)^+$	(1.2 \pm 0.7 / -0.6) \times 10 ⁻³		1648
$\eta_c(2S) K^+$	(3.4 \pm 1.8) \times 10 ⁻⁴		1320
$J/\psi(1S) K^+$	(1.014 \pm 0.034) \times 10 ⁻³		1683
$J/\psi(1S) K^+ \pi^+ \pi^-$	(1.07 \pm 0.19) \times 10 ⁻³	S=1.9	1612
$h_c(1P) K^+ \times B(h_c(1P) \rightarrow J/\psi \pi^+ \pi^-)$	< 3.4 \times 10 ⁻⁶	CL=90%	1401
$X(3872) K^+$	< 3.2 \times 10 ⁻⁴	CL=90%	1141
$X(3872) K^+ \times B(X \rightarrow J/\psi \pi^+ \pi^-)$	(9.5 \pm 1.9) \times 10 ⁻⁶	S=1.3	1141
$X(3872) K^+ \times B(X \rightarrow J/\psi \gamma)$	(2.8 \pm 0.8) \times 10 ⁻⁶		1141
$X(3872) K^*(892)^+ \times B(X \rightarrow J/\psi \gamma)$	< 4.8 \times 10 ⁻⁶	CL=90%	939
$X(3872) K^+ \times B(X \rightarrow \psi(2S) \gamma)$	(9.5 \pm 2.8) \times 10 ⁻⁶		1141
$X(3872) K^*(892)^+ \times B(X \rightarrow \psi(2S) \gamma)$	< 2.8 \times 10 ⁻⁵	CL=90%	939
$X(3872) K^+ \times B(X \rightarrow D^0 \bar{D}^0)$	< 6.0 \times 10 ⁻⁵	CL=90%	1141
$X(3872) K^+ \times B(X \rightarrow D^+ D^-)$	< 4.0 \times 10 ⁻⁵	CL=90%	1141
$X(3872) K^+ \times B(X \rightarrow D^0 \bar{D}^0 \pi^0)$	(1.0 \pm 0.4) \times 10 ⁻⁴		1141
$X(3872) K^+ \times B(X \rightarrow \bar{D}^{*0} D^0)$	(8.5 \pm 2.6) \times 10 ⁻⁵	S=1.4	1141

$X(3872)K^+$ $\times B(X(3872) \rightarrow J/\psi(1S)\eta)$	< 7.7	$\times 10^{-6}$	CL=90%	1141
$X(3872)^+K^0 \times B(X(3872)^+ \rightarrow$ $J/\psi(1S)\pi^+\pi^0)$ [sss]	< 2.2	$\times 10^{-5}$	CL=90%	—
$X(4430)^+K^0 \times B(X^+ \rightarrow$ $J/\psi\pi^+)$	< 1.5	$\times 10^{-5}$	CL=95%	—
$X(4430)^+K^0 \times B(X^+ \rightarrow$ $\psi(2S)\pi^+)$	< 4.7	$\times 10^{-5}$	CL=95%	—
$X(4260)^0K^+ \times B(X^0 \rightarrow$ $J/\psi\pi^+\pi^-)$	< 2.9	$\times 10^{-5}$	CL=95%	—
$X(3945)^0K^+ \times B(X^0 \rightarrow J/\psi\gamma)$	< 1.4	$\times 10^{-5}$	CL=90%	—
$Z(3930)^0K^+ \times B(Z^0 \rightarrow J/\psi\gamma)$	< 2.5	$\times 10^{-6}$	CL=90%	—
$J/\psi(1S)K^*(892)^+$	(1.43 \pm 0.08)	$\times 10^{-3}$		1571
$J/\psi(1S)K(1270)^+$	(1.8 \pm 0.5)	$\times 10^{-3}$		1390
$J/\psi(1S)K(1400)^+$	< 5	$\times 10^{-4}$	CL=90%	1308
$J/\psi(1S)\eta K^+$	(1.08 \pm 0.33)	$\times 10^{-4}$		1510
$J/\psi(1S)\eta' K^+$	< 8.8	$\times 10^{-5}$	CL=90%	1273
$J/\psi(1S)\phi K^+$	(5.2 \pm 1.7)	$\times 10^{-5}$	S=1.2	1227
$J/\psi(1S)\omega K^+$ nonresonant	(3.5 \pm 0.4)	$\times 10^{-4}$		1388
$J/\psi(1S)\pi^+$	(4.9 \pm 0.4)	$\times 10^{-5}$	S=1.2	1727
$J/\psi(1S)\rho^+$	(5.0 \pm 0.8)	$\times 10^{-5}$		1611
$J/\psi(1S)\pi^+\pi^0$ nonresonant	< 7.3	$\times 10^{-6}$	CL=90%	1717
$J/\psi(1S)a_1(1260)^+$	< 1.2	$\times 10^{-3}$	CL=90%	1415
$J/\psi(1S)\rho\bar{1}$	(1.18 \pm 0.31)	$\times 10^{-5}$		567
$J/\psi(1S)\bar{\Sigma}^0 p$	< 1.1	$\times 10^{-5}$	CL=90%	—
$J/\psi(1S)D^+$	< 1.2	$\times 10^{-4}$	CL=90%	870
$J/\psi(1S)\bar{D}^0\pi^+$	< 2.5	$\times 10^{-5}$	CL=90%	665
$\psi(2S)\pi^+$	(2.58 \pm 0.29)	$\times 10^{-5}$		1347
$\psi(2S)K^+$	(6.46 \pm 0.33)	$\times 10^{-4}$		1284
$\psi(2S)K^*(892)^+$	(6.2 \pm 1.2)	$\times 10^{-4}$		1115
$\psi(2S)K^+\pi^+\pi^-$	(1.9 \pm 1.2)	$\times 10^{-3}$		1178
$\psi(3770)K^+$	(4.9 \pm 1.3)	$\times 10^{-4}$		1218
$\psi(3770)K^+ \times B(\psi \rightarrow D^0\bar{D}^0)$	(1.6 \pm 0.4)	$\times 10^{-4}$	S=1.1	1218
$\psi(3770)K^+ \times B(\psi \rightarrow D^+D^-)$	(9.4 \pm 3.5)	$\times 10^{-5}$		1218
$\chi_{c0}\pi^+ \times B(\chi_{c0} \rightarrow \pi^+\pi^-)$	< 1	$\times 10^{-7}$	CL=90%	1531
$\chi_{c0}(1P)K^+$	(1.33 $^{+0.19}_{-0.16}$)	$\times 10^{-4}$		1478
$\chi_{c0}K^*(892)^+$	< 2.1	$\times 10^{-4}$	CL=90%	1341
$\chi_{c2}\pi^+ \times B(\chi_{c2} \rightarrow \pi^+\pi^-)$	< 1	$\times 10^{-7}$	CL=90%	1437
$\chi_{c2}K^+$	< 1.8	$\times 10^{-5}$	CL=90%	1379
$\chi_{c2}K^*(892)^+$	< 1.2	$\times 10^{-4}$	CL=90%	1227
$\chi_{c1}(1P)\pi^+$	(2.0 \pm 0.4)	$\times 10^{-5}$		1468
$\chi_{c1}(1P)K^+$	(4.6 \pm 0.4)	$\times 10^{-4}$	S=1.6	1412
$\chi_{c1}(1P)K^*(892)^+$	(3.0 \pm 0.6)	$\times 10^{-4}$	S=1.1	1265
$h_c(1P)K^+$	< 3.8	$\times 10^{-5}$		1401

K or K* modes

$K^0\pi^+$	(2.31 \pm 0.10)	$\times 10^{-5}$		2614
$K^+\pi^0$	(1.29 \pm 0.06)	$\times 10^{-5}$		2615
$\eta'K^+$	(7.06 \pm 0.25)	$\times 10^{-5}$		2528
$\eta'K^*(892)^+$	(4.9 \pm 2.0)	$\times 10^{-6}$		2472
ηK^+	(2.33 $^{+0.33}_{-0.29}$)	$\times 10^{-6}$	S=1.4	2588
$\eta K^*(892)^+$	(1.93 \pm 0.16)	$\times 10^{-5}$		2534
$\eta K_0^*(1430)^+$	(1.8 \pm 0.4)	$\times 10^{-5}$		—
$\eta K_2^*(1430)^+$	(9.1 \pm 3.0)	$\times 10^{-6}$		2414

$\eta(1295)K^+ \times B(\eta(1295) \rightarrow \eta\pi\pi)$	$(2.9^{+0.8}_{-0.7}) \times 10^{-6}$		2455
$\eta(1405)K^+ \times B(\eta(1405) \rightarrow \eta\pi\pi)$	$< 1.3 \times 10^{-6}$	CL=90%	2425
$\eta(1405)K^+ \times B(\eta(1405) \rightarrow K^*K)$	$< 1.2 \times 10^{-6}$	CL=90%	2425
$\eta(1475)K^+ \times B(\eta(1475) \rightarrow K^*K)$	$(1.38^{+0.21}_{-0.18}) \times 10^{-5}$		2406
$f_1(1285)K^+$	$< 2.0 \times 10^{-6}$	CL=90%	2458
$f_1(1420)K^+ \times B(f_1(1420) \rightarrow \eta\pi\pi)$	$< 2.9 \times 10^{-6}$	CL=90%	2420
$f_1(1420)K^+ \times B(f_1(1420) \rightarrow K^*K)$	$< 4.1 \times 10^{-6}$	CL=90%	2420
$\phi(1680)K^+ \times B(\phi(1680) \rightarrow K^*K)$	$< 3.4 \times 10^{-6}$	CL=90%	2344
ωK^+	$(6.7 \pm 0.8) \times 10^{-6}$	S=1.8	2557
$\omega K^*(892)^+$	$< 7.4 \times 10^{-6}$	CL=90%	2503
$\omega(K\pi)_0^{*+}$	$(2.7 \pm 0.4) \times 10^{-5}$		-
$\omega K_0^*(1430)^+$	$(2.4 \pm 0.5) \times 10^{-5}$		-
$\omega K_2^*(1430)^+$	$(2.1 \pm 0.4) \times 10^{-5}$		2380
$a_0(980)^+ K^0 \times B(a_0(980)^+ \rightarrow \eta\pi^+)$	$< 3.9 \times 10^{-6}$	CL=90%	-
$a_0(980)^0 K^+ \times B(a_0(980)^0 \rightarrow \eta\pi^0)$	$< 2.5 \times 10^{-6}$	CL=90%	-
$K^*(892)^0 \pi^+$	$(1.01 \pm 0.09) \times 10^{-5}$		2562
$K^*(892)^+ \pi^0$	$(6.9 \pm 2.4) \times 10^{-6}$		2562
$K^+ \pi^- \pi^+$	$(5.10 \pm 0.29) \times 10^{-5}$		2609
$K^+ \pi^- \pi^+$ nonresonant	$(1.63^{+0.21}_{-0.15}) \times 10^{-5}$		2609
$\omega(782)K^+$	$(6 \pm 9) \times 10^{-6}$		2557
$K^+ f_0(980) \times B(f_0(980) \rightarrow \pi^+ \pi^-)$	$(9.4^{+1.0}_{-1.2}) \times 10^{-6}$		2524
$f_2(1270)^0 K^+$	$(1.07 \pm 0.27) \times 10^{-6}$		-
$f_0(1370)^0 K^+ \times B(f_0(1370)^0 \rightarrow \pi^+ \pi^-)$	$< 1.07 \times 10^{-5}$	CL=90%	-
$\rho^0(1450)K^+ \times B(\rho^0(1450) \rightarrow \pi^+ \pi^-)$	$< 1.17 \times 10^{-5}$	CL=90%	-
$K^+ f_X(1300) \times B(f_X \rightarrow \pi^+ \pi^-)$	$(7 \pm 5) \times 10^{-7}$		-
$f_0(1500)K^+ \times B(f_0(1500) \rightarrow \pi^+ \pi^-)$	$< 4.4 \times 10^{-6}$	CL=90%	2398
$f_2'(1525)K^+ \times B(f_2'(1525) \rightarrow \pi^+ \pi^-)$	$< 3.4 \times 10^{-6}$	CL=90%	2392
$K^+ \rho^0$	$(3.7 \pm 0.5) \times 10^{-6}$		2559
$K_0^*(1430)^0 \pi^+$	$(4.5^{+0.9}_{-0.7}) \times 10^{-5}$	S=1.5	2445
$K_2^*(1430)^0 \pi^+$	$(5.6^{+2.2}_{-1.5}) \times 10^{-6}$		2445
$K^*(1410)^0 \pi^+$	$< 4.5 \times 10^{-5}$	CL=90%	2448
$K^*(1680)^0 \pi^+$	$< 1.2 \times 10^{-5}$	CL=90%	2358
$K^- \pi^+ \pi^+$	$< 9.5 \times 10^{-7}$	CL=90%	2609
$K^- \pi^+ \pi^+$ nonresonant	$< 5.6 \times 10^{-5}$	CL=90%	2609
$K_1(1270)^0 \pi^+$	$< 4.0 \times 10^{-5}$	CL=90%	2484
$K_1(1400)^0 \pi^+$	$< 3.9 \times 10^{-5}$	CL=90%	2451
$K^0 \pi^+ \pi^0$	$< 6.6 \times 10^{-5}$	CL=90%	2609

$K^0 \rho^+$	(8.0 ±1.5) × 10 ⁻⁶		2558
$K^*(892)^+ \pi^+ \pi^-$	(7.5 ±1.0) × 10 ⁻⁵		2556
$K^*(892)^+ \rho^0$	< 6.1 × 10 ⁻⁶	CL=90%	2504
$K^*(892)^+ f_0(980)$	(5.2 ±1.3) × 10 ⁻⁶		2468
$a_1^+ K^0$	(3.5 ±0.7) × 10 ⁻⁵		—
$b_1^+ K^0 \times B(b_1^+ \rightarrow \omega \pi^+)$	(9.6 ±1.9) × 10 ⁻⁶		—
$K^*(892)^0 \rho^+$	(9.2 ±1.5) × 10 ⁻⁶		2504
$K_1(1400)^+ \rho^0$	< 7.8 × 10 ⁻⁴	CL=90%	2387
$K_2^*(1430)^+ \rho^0$	< 1.5 × 10 ⁻³	CL=90%	2381
$b_1^0 K^+ \times B(b_1^0 \rightarrow \omega \pi^0)$	(9.1 ±2.0) × 10 ⁻⁶		—
$b_1^+ K^{*0} \times B(b_1^+ \rightarrow \omega \pi^+)$	< 5.9 × 10 ⁻⁶	CL=90%	—
$b_1^0 K^{*+} \times B(b_1^0 \rightarrow \omega \pi^0)$	< 6.7 × 10 ⁻⁶	CL=90%	—
$K^+ \bar{K}^0$	(1.36 ±0.27) × 10 ⁻⁶		2593
$\bar{K}^0 K^+ \pi^0$	< 2.4 × 10 ⁻⁵	CL=90%	2578
$K^+ K_S^0 K_S^0$	(1.15 ±0.13) × 10 ⁻⁵		2521
$K_S^0 K_S^0 \pi^+$	< 5.1 × 10 ⁻⁷	CL=90%	2577
$K^+ K^- \pi^+$	(5.0 ±0.7) × 10 ⁻⁶		2578
$K^+ K^- \pi^+$ nonresonant	< 7.5 × 10 ⁻⁵	CL=90%	2578
$K^+ \bar{K}^*(892)^0$	< 1.1 × 10 ⁻⁶	CL=90%	2540
$K^+ \bar{K}_0^*(1430)^0$	< 2.2 × 10 ⁻⁶	CL=90%	2421
$K^+ K^+ \pi^-$	< 1.6 × 10 ⁻⁷	CL=90%	2578
$K^+ K^+ \pi^-$ nonresonant	< 8.79 × 10 ⁻⁵	CL=90%	2578
$K^{*+} \pi^+ K^-$	< 1.18 × 10 ⁻⁵	CL=90%	2524
$K^*(892)^+ K^*(892)^0$	(1.2 ±0.5) × 10 ⁻⁶		2484
$K^{*+} K^+ \pi^-$	< 6.1 × 10 ⁻⁶	CL=90%	2524
$K^+ K^- K^+$	(3.37 ±0.22) × 10 ⁻⁵	S=1.4	2522
$K^+ \phi$	(8.3 ±0.7) × 10 ⁻⁶		2516
$f_0(980) K^+ \times B(f_0(980) \rightarrow K^+ K^-)$	< 2.9 × 10 ⁻⁶	CL=90%	2524
$a_2(1320) K^+ \times B(a_2(1320) \rightarrow K^+ K^-)$	< 1.1 × 10 ⁻⁶	CL=90%	2449
$f_2'(1525) K^+ \times B(f_2'(1525) \rightarrow K^+ K^-)$	< 4.9 × 10 ⁻⁶	CL=90%	2392
$X_0(1550) K^+ \times B(X_0(1550) \rightarrow K^+ K^-)$	(4.3 ±0.7) × 10 ⁻⁶		—
$\phi(1680) K^+ \times B(\phi(1680) \rightarrow K^+ K^-)$	< 8 × 10 ⁻⁷	CL=90%	2344
$f_0(1710) K^+ \times B(f_0(1710) \rightarrow K^+ K^-)$	(1.7 ±1.0) × 10 ⁻⁶		2331
$K^+ K^- K^+$ nonresonant	(2.8 $\begin{smallmatrix} +0.9 \\ -1.6 \end{smallmatrix}$) × 10 ⁻⁵	S=3.3	2522
$K^*(892)^+ K^+ K^-$	(3.6 ±0.5) × 10 ⁻⁵		2466
$K^*(892)^+ \phi$	(10.0 ±2.0) × 10 ⁻⁶	S=1.7	2460
$\phi(K\pi)_0^{*+}$	(8.3 ±1.6) × 10 ⁻⁶		—
$\phi K_1(1270)^+$	(6.1 ±1.9) × 10 ⁻⁶		2375
$\phi K_1(1400)^+$	< 3.2 × 10 ⁻⁶	CL=90%	2339
$\phi K^*(1410)^+$	< 4.3 × 10 ⁻⁶	CL=90%	—
$\phi K_0^*(1430)^+$	(7.0 ±1.6) × 10 ⁻⁶		—
$\phi K_2^*(1430)^+$	(8.4 ±2.1) × 10 ⁻⁶		2332
$\phi K_2^*(1770)^+$	< 1.50 × 10 ⁻⁵	CL=90%	—
$\phi K_2^*(1820)^+$	< 1.63 × 10 ⁻⁵	CL=90%	—
$K^+ \phi \phi$	(4.9 $\begin{smallmatrix} +2.4 \\ -2.2 \end{smallmatrix}$) × 10 ⁻⁶	S=2.9	2306
$\eta' \eta' K^+$	< 2.5 × 10 ⁻⁵	CL=90%	2338

$\omega\phi K^+$	< 1.9	$\times 10^{-6}$	CL=90%	2374
$X(1812)K^+ \times B(X \rightarrow \omega\phi)$	< 3.2	$\times 10^{-7}$	CL=90%	-
$K^*(892)^+\gamma$	(4.21 \pm 0.18)	$\times 10^{-5}$		2564
$K_1(1270)^+\gamma$	(4.3 \pm 1.3)	$\times 10^{-5}$		2486
$\eta K^+\gamma$	(7.9 \pm 0.9)	$\times 10^{-6}$		2588
$\eta' K^+\gamma$	< 4.2	$\times 10^{-6}$	CL=90%	2528
$\phi K^+\gamma$	(3.5 \pm 0.6)	$\times 10^{-6}$		2516
$K^+\pi^-\pi^+\gamma$	(2.76 \pm 0.22)	$\times 10^{-5}$	S=1.2	2609
$K^*(892)^0\pi^+\gamma$	(2.0 $^{+0.7}_{-0.6}$)	$\times 10^{-5}$		2562
$K^+\rho^0\gamma$	< 2.0	$\times 10^{-5}$	CL=90%	2559
$K^+\pi^-\pi^+\gamma$ nonresonant	< 9.2	$\times 10^{-6}$	CL=90%	2609
$K^0\pi^+\pi^0\gamma$	(4.6 \pm 0.5)	$\times 10^{-5}$		2609
$K_1(1400)^+\gamma$	< 1.5	$\times 10^{-5}$	CL=90%	2453
$K_2^*(1430)^+\gamma$	(1.4 \pm 0.4)	$\times 10^{-5}$		2447
$K^*(1680)^+\gamma$	< 1.9	$\times 10^{-3}$	CL=90%	2360
$K_3^*(1780)^+\gamma$	< 3.9	$\times 10^{-5}$	CL=90%	2341
$K_4^*(2045)^+\gamma$	< 9.9	$\times 10^{-3}$	CL=90%	2244

Light unflavored meson modes

$\rho^+\gamma$	(9.8 \pm 2.5)	$\times 10^{-7}$		2583
$\pi^+\pi^0$	(5.7 \pm 0.5)	$\times 10^{-6}$	S=1.4	2636
$\pi^+\pi^+\pi^-$	(1.52 \pm 0.14)	$\times 10^{-5}$		2630
$\rho^0\pi^+$	(8.3 \pm 1.2)	$\times 10^{-6}$		2581
$\pi^+ f_0(980) \times B(f_0(980) \rightarrow \pi^+\pi^-)$	< 1.5	$\times 10^{-6}$	CL=90%	2547
$\pi^+ f_2(1270)$	(1.6 $^{+0.7}_{-0.4}$)	$\times 10^{-6}$		2484
$\rho(1450)^0\pi^+ \times B(\rho^0 \rightarrow \pi^+\pi^-)$	(1.4 $^{+0.6}_{-0.9}$)	$\times 10^{-6}$		2434
$f_0(1370)\pi^+ \times B(f_0(1370) \rightarrow \pi^+\pi^-)$	< 4.0	$\times 10^{-6}$	CL=90%	2460
$f_0(600)\pi^+ \times B(f_0(600) \rightarrow \pi^+\pi^-)$	< 4.1	$\times 10^{-6}$	CL=90%	-
$\pi^+\pi^-\pi^+$ nonresonant	(5.3 $^{+1.5}_{-1.1}$)	$\times 10^{-6}$		2630
$\pi^+\pi^0\pi^0$	< 8.9	$\times 10^{-4}$	CL=90%	2631
$\rho^+\pi^0$	(1.09 \pm 0.14)	$\times 10^{-5}$		2581
$\pi^+\pi^-\pi^+\pi^0$	< 4.0	$\times 10^{-3}$	CL=90%	2621
$\rho^+\rho^0$	(2.40 \pm 0.19)	$\times 10^{-5}$		2523
$\rho^+ f_0(980) \times B(f_0(980) \rightarrow \pi^+\pi^-)$	< 2.0	$\times 10^{-6}$	CL=90%	2488
$a_1(1260)^+\pi^0$	(2.6 \pm 0.7)	$\times 10^{-5}$		2494
$a_1(1260)^0\pi^+$	(2.0 \pm 0.6)	$\times 10^{-5}$		2494
$\omega\pi^+$	(6.9 \pm 0.5)	$\times 10^{-6}$		2580
$\omega\rho^+$	(1.59 \pm 0.21)	$\times 10^{-5}$		2522
$\eta\pi^+$	(4.07 \pm 0.32)	$\times 10^{-6}$		2609
$\eta\rho^+$	(7.0 \pm 2.9)	$\times 10^{-6}$	S=2.8	2553
$\eta'\pi^+$	(2.7 \pm 0.9)	$\times 10^{-6}$	S=1.9	2551
$\eta'\rho^+$	(8.7 $^{+4.0}_{-3.1}$)	$\times 10^{-6}$		2492
$\phi\pi^+$	< 2.4	$\times 10^{-7}$	CL=90%	2539
$\phi\rho^+$	< 3.0	$\times 10^{-6}$	CL=90%	2480
$a_0(980)^0\pi^+ \times B(a_0(980)^0 \rightarrow \eta\pi^0)$	< 5.8	$\times 10^{-6}$	CL=90%	-
$a_0(980)^+\pi^0 \times B(a_0^+ \rightarrow \eta\pi^+)$	< 1.4	$\times 10^{-6}$	CL=90%	-

$\pi^+ \pi^+ \pi^+ \pi^- \pi^-$	< 8.6	$\times 10^{-4}$	CL=90%	2608
$\rho^0 a_1(1260)^+$	< 6.2	$\times 10^{-4}$	CL=90%	2433
$\rho^0 a_2(1320)^+$	< 7.2	$\times 10^{-4}$	CL=90%	2410
$b_1^0 \pi^+ \times B(b_1^0 \rightarrow \omega \pi^0)$	(6.7 \pm 2.0)	$\times 10^{-6}$		—
$b_1^+ \pi^0 \times B(b_1^+ \rightarrow \omega \pi^+)$	< 3.3	$\times 10^{-6}$	CL=90%	—
$\pi^+ \pi^+ \pi^+ \pi^- \pi^- \pi^0$	< 6.3	$\times 10^{-3}$	CL=90%	2592
$b_1^+ \rho^0 \times B(b_1^+ \rightarrow \omega \pi^+)$	< 5.2	$\times 10^{-6}$	CL=90%	—
$a_1(1260)^+ a_1(1260)^0$	< 1.3	%	CL=90%	2335
$b_1^0 \rho^+ \times B(b_1^0 \rightarrow \omega \pi^0)$	< 3.3	$\times 10^{-6}$	CL=90%	—

Charged particle (h^\pm) modes

$$h^\pm = K^\pm \text{ or } \pi^\pm$$

$h^+ \pi^0$	(1.6 $\begin{smallmatrix} +0.7 \\ -0.6 \end{smallmatrix}$)	$\times 10^{-5}$		2636
ωh^+	(1.38 $\begin{smallmatrix} +0.27 \\ -0.24 \end{smallmatrix}$)	$\times 10^{-5}$		2580
$h^+ X^0$ (Familon)	< 4.9	$\times 10^{-5}$	CL=90%	—

Baryon modes

$p \bar{p} \pi^+$	(1.62 \pm 0.20)	$\times 10^{-6}$		2439
$p \bar{p} \pi^+$ nonresonant	< 5.3	$\times 10^{-5}$	CL=90%	2439
$p \bar{p} K^+$	(5.9 \pm 0.5)	$\times 10^{-6}$	S=1.5	2348
$\Theta(1710)^{++} \bar{p} \times B(\Theta(1710)^{++} \rightarrow p K^+)$	[<i>ttt</i>] < 9.1	$\times 10^{-8}$	CL=90%	—
$f_J(2220) K^+ \times B(f_J(2220) \rightarrow p \bar{p})$	[<i>ttt</i>] < 4.1	$\times 10^{-7}$	CL=90%	2135
$p \bar{\Lambda}(1520)$	< 1.5	$\times 10^{-6}$	CL=90%	2322
$p \bar{p} K^+$ nonresonant	< 8.9	$\times 10^{-5}$	CL=90%	2348
$p \bar{p} K^*(892)^+$	(3.6 $\begin{smallmatrix} +0.8 \\ -0.7 \end{smallmatrix}$)	$\times 10^{-6}$		2215
$f_J(2220) K^{*+} \times B(f_J(2220) \rightarrow p \bar{p})$	< 7.7	$\times 10^{-7}$	CL=90%	2059
$p \bar{\Lambda}$	< 3.2	$\times 10^{-7}$	CL=90%	2430
$p \bar{\Lambda} \gamma$	(2.5 $\begin{smallmatrix} +0.5 \\ -0.4 \end{smallmatrix}$)	$\times 10^{-6}$		2430
$p \bar{\Lambda} \pi^0$	(3.0 $\begin{smallmatrix} +0.7 \\ -0.6 \end{smallmatrix}$)	$\times 10^{-6}$		2402
$p \bar{\Sigma}(1385)^0$	< 4.7	$\times 10^{-7}$	CL=90%	2362
$\Delta^+ \bar{\Lambda}$	< 8.2	$\times 10^{-7}$	CL=90%	—
$p \bar{\Sigma} \gamma$	< 4.6	$\times 10^{-6}$	CL=90%	2413
$p \bar{\Lambda} \pi^+ \pi^-$	(5.9 \pm 1.1)	$\times 10^{-6}$		2367
$p \bar{\Lambda} \rho^0$	(4.8 \pm 0.9)	$\times 10^{-6}$		2214
$p \bar{\Lambda} f_2(1270)$	(2.0 \pm 0.8)	$\times 10^{-6}$		2026
$\Lambda \bar{\Lambda} \pi^+$	< 9.4	$\times 10^{-7}$	CL=90%	2358
$\Lambda \bar{\Lambda} K^+$	(3.4 \pm 0.6)	$\times 10^{-6}$		2251
$\Lambda \bar{\Lambda} K^{*+}$	(2.2 $\begin{smallmatrix} +1.2 \\ -0.9 \end{smallmatrix}$)	$\times 10^{-6}$		2098
$\bar{\Delta}^0 p$	< 1.38	$\times 10^{-6}$	CL=90%	2402
$\Delta^{++} \bar{p}$	< 1.4	$\times 10^{-7}$	CL=90%	2402
$D^+ p \bar{p}$	< 1.5	$\times 10^{-5}$	CL=90%	1860
$D^*(2010)^+ p \bar{p}$	< 1.5	$\times 10^{-5}$	CL=90%	1786
$\bar{\Lambda}_c^- p \pi^+$	(2.8 \pm 0.8)	$\times 10^{-4}$		1980
$\bar{\Lambda}_c^- \Delta(1232)^{++}$	< 1.9	$\times 10^{-5}$	CL=90%	1928
$\bar{\Lambda}_c^- \Delta_X(1600)^{++}$	(5.9 \pm 1.9)	$\times 10^{-5}$		—
$\bar{\Lambda}_c^- \Delta_X(2420)^{++}$	(4.7 \pm 1.6)	$\times 10^{-5}$		—
$(\bar{\Lambda}_c^- p)_s \pi^+$	[<i>uuu</i>] (3.9 \pm 1.3)	$\times 10^{-5}$		—

$\overline{\Sigma}_c(2520)^0 p$	<	2.6	$\times 10^{-6}$	CL=90%	1904
$\overline{\Sigma}_c(2800)^0 p$	(3.3	± 1.3)	$\times 10^{-5}$	-
$\overline{\Lambda}_c^- p \pi^+ \pi^0$	(1.8	± 0.6)	$\times 10^{-3}$	1935
$\overline{\Lambda}_c^- p \pi^+ \pi^+ \pi^-$	(2.3	± 0.7)	$\times 10^{-3}$	1880
$\overline{\Lambda}_c^- p \pi^+ \pi^+ \pi^- \pi^0$	<	1.34	%	CL=90%	1822
$\Lambda_c^+ \Lambda_c^- K^+$	(8.7	± 3.5)	$\times 10^{-4}$	-
$\overline{\Sigma}_c(2455)^0 p$	(3.5	± 1.0)	$\times 10^{-5}$	1938
$\overline{\Sigma}_c(2455)^0 p \pi^0$	(4.4	± 1.8)	$\times 10^{-4}$	1896
$\overline{\Sigma}_c(2455)^0 p \pi^- \pi^+$	(4.4	± 1.7)	$\times 10^{-4}$	1845
$\overline{\Sigma}_c(2455)^- p \pi^+ \pi^+$	(2.8	± 1.2)	$\times 10^{-4}$	1845
$\Lambda_c(2593)^- / \overline{\Lambda}_c(2625)^- p \pi^+$	<	1.9	$\times 10^{-4}$	CL=90%	-
$\Xi_c^0 \Lambda_c^+ \times B(\Xi_c^0 \rightarrow \Xi^+ \pi^-)$	(3.0	± 1.1)	$\times 10^{-5}$	1144
$\Xi_c^0 \Lambda_c^+ \times B(\Xi_c^0 \rightarrow \Lambda K^+ \pi^-)$	(2.6	± 1.1)	$\times 10^{-5}$	S=1.1 1144

**Lepton Family number (LF) or Lepton number (L) violating modes, or
 $\Delta B = 1$ weak neutral current (BI) modes**

$\pi^+ \ell^+ \ell^-$	B1	<	4.9	$\times 10^{-8}$	CL=90%	2638
$\pi^+ e^+ e^-$	B1	<	8.0	$\times 10^{-8}$	CL=90%	2638
$\pi^+ \mu^+ \mu^-$	B1	<	6.9	$\times 10^{-8}$	CL=90%	2634
$\pi^+ \nu \overline{\nu}$	B1	<	1.0	$\times 10^{-4}$	CL=90%	2638
$K^+ \ell^+ \ell^-$	B1 [nnn]	(5.1	± 0.5)	$\times 10^{-7}$	2617
$K^+ e^+ e^-$	B1	(5.5	± 0.7)	$\times 10^{-7}$	2617
$K^+ \mu^+ \mu^-$	B1	(5.2	± 0.7)	$\times 10^{-7}$	2612
$K^+ \overline{\nu} \nu$	B1	<	1.4	$\times 10^{-5}$	CL=90%	2617
$\rho^+ \nu \overline{\nu}$	B1	<	1.5	$\times 10^{-4}$	CL=90%	2583
$K^*(892)^+ \ell^+ \ell^-$	B1 [nnn]	(1.29	± 0.21)	$\times 10^{-6}$	2564
$K^*(892)^+ e^+ e^-$	B1	(1.55	$\begin{smallmatrix} +0.40 \\ -0.31 \end{smallmatrix}$)	$\times 10^{-6}$	2564
$K^*(892)^+ \mu^+ \mu^-$	B1	(1.16	$\begin{smallmatrix} +0.31 \\ -0.27 \end{smallmatrix}$)	$\times 10^{-6}$	2560
$K^*(892)^+ \nu \overline{\nu}$	B1	<	8	$\times 10^{-5}$	CL=90%	2564
$\pi^+ e^+ \mu^-$	LF	<	6.4	$\times 10^{-3}$	CL=90%	2637
$\pi^+ e^- \mu^+$	LF	<	6.4	$\times 10^{-3}$	CL=90%	2637
$\pi^+ e^\pm \mu^\mp$	LF	<	1.7	$\times 10^{-7}$	CL=90%	2637
$K^+ e^+ \mu^-$	LF	<	9.1	$\times 10^{-8}$	CL=90%	2615
$K^+ e^- \mu^+$	LF	<	1.3	$\times 10^{-7}$	CL=90%	2615
$K^+ e^\pm \mu^\mp$	LF	<	9.1	$\times 10^{-8}$	CL=90%	2615
$K^+ \mu^\pm \tau^\mp$	LF	<	7.7	$\times 10^{-5}$	CL=90%	2298
$K^*(892)^+ e^+ \mu^-$	LF	<	1.3	$\times 10^{-6}$	CL=90%	2563
$K^*(892)^+ e^- \mu^+$	LF	<	9.9	$\times 10^{-7}$	CL=90%	2563
$K^*(892)^+ e^\pm \mu^\mp$	LF	<	1.4	$\times 10^{-7}$	CL=90%	2563
$\pi^- e^+ e^+$	L	<	1.6	$\times 10^{-6}$	CL=90%	2638
$\pi^- \mu^+ \mu^+$	L	<	1.4	$\times 10^{-6}$	CL=90%	2634
$\pi^- e^+ \mu^+$	L	<	1.3	$\times 10^{-6}$	CL=90%	2637
$\rho^- e^+ e^+$	L	<	2.6	$\times 10^{-6}$	CL=90%	2583
$\rho^- \mu^+ \mu^+$	L	<	5.0	$\times 10^{-6}$	CL=90%	2578
$\rho^- e^+ \mu^+$	L	<	3.3	$\times 10^{-6}$	CL=90%	2582
$K^- e^+ e^+$	L	<	1.0	$\times 10^{-6}$	CL=90%	2617
$K^- \mu^+ \mu^+$	L	<	1.8	$\times 10^{-6}$	CL=90%	2612
$K^- e^+ \mu^+$	L	<	2.0	$\times 10^{-6}$	CL=90%	2615
$K^*(892)^- e^+ e^+$	L	<	2.8	$\times 10^{-6}$	CL=90%	2564
$K^*(892)^- \mu^+ \mu^+$	L	<	8.3	$\times 10^{-6}$	CL=90%	2560
$K^*(892)^- e^+ \mu^+$	L	<	4.4	$\times 10^{-6}$	CL=90%	2563

B⁰

$$I(J^P) = \frac{1}{2}(0^-)$$

I, J, P need confirmation. Quantum numbers shown are quark-model predictions.

$$\text{Mass } m_{B^0} = 5279.50 \pm 0.30 \text{ MeV}$$

$$m_{B^0} - m_{B^\pm} = 0.33 \pm 0.06 \text{ MeV}$$

$$\text{Mean life } \tau_{B^0} = (1.525 \pm 0.009) \times 10^{-12} \text{ s}$$

$$c\tau = 457.2 \mu\text{m}$$

$$\tau_{B^+}/\tau_{B^0} = 1.071 \pm 0.009 \quad (\text{direct measurements})$$

B⁰- \bar{B}^0 mixing parameters

$$\chi_d = 0.1872 \pm 0.0024$$

$$\Delta m_{B^0} = m_{B_H^0} - m_{B_L^0} = (0.507 \pm 0.005) \times 10^{12} \hbar \text{ s}^{-1}$$

$$= (3.337 \pm 0.033) \times 10^{-10} \text{ MeV}$$

$$x_d = \Delta m_{B^0}/\Gamma_{B^0} = 0.774 \pm 0.008$$

$$\text{Re}(\lambda_{CP} / |\lambda_{CP}|) \text{Re}(z) = 0.01 \pm 0.05$$

$$\Delta\Gamma \text{Re}(z) = -0.007 \pm 0.004$$

$$\text{Re}(z) = 0.00 \pm 0.12$$

$$\text{Im}(z) = -0.015 \pm 0.008$$

CP violation parameters

$$\text{Re}(\epsilon_{B^0})/(1+|\epsilon_{B^0}|^2) = (-0.1 \pm 1.4) \times 10^{-3}$$

$$A_{T/CP} = 0.005 \pm 0.018$$

$$A_{CP}(B^0 \rightarrow D^*(2010)^+ D^-) = 0.02 \pm 0.04$$

$$\mathbf{ACP}(B^0 \rightarrow K^+ \pi^-) = -0.098 \pm 0.013$$

$$A_{CP}(B^0 \rightarrow \eta' K^*(892)^0) = 0.08 \pm 0.25$$

$$\mathbf{ACP}(B^0 \rightarrow \eta K^*(892)^0) = 0.19 \pm 0.05$$

$$A_{CP}(B^0 \rightarrow \omega K^{*0}) = 0.45 \pm 0.25$$

$$A_{CP}(B^0 \rightarrow \omega(K\pi)_0^{*0}) = -0.07 \pm 0.09$$

$$A_{CP}(B^0 \rightarrow \omega K_2^*(1430)^0) = -0.37 \pm 0.17$$

$$A_{CP}(B^0 \rightarrow K^0 K^0) = (-0.6 \pm 0.7) \times 10^{-6}$$

$$A_{CP}(B^0 \rightarrow \eta K_0^*(1430)^0) = 0.06 \pm 0.13$$

$$A_{CP}(B^0 \rightarrow \eta K_2^*(1430)^0) = -0.07 \pm 0.19$$

$$A_{CP}(B^0 \rightarrow K^+ \pi^- \pi^0) = (0 \pm 6) \times 10^{-2}$$

$$A_{CP}(B^0 \rightarrow \rho^- K^+) = 0.15 \pm 0.13$$

$$A_{CP}(B^0 \rightarrow K^+ \pi^- \pi^0 \text{ nonresonant}) = 0.23_{-0.29}^{+0.22}$$

$$A_{CP}(B^0 \rightarrow (K\pi)_0^{*+} \pi^-) = 0.10 \pm 0.07$$

$$A_{CP}(B^0 \rightarrow (K\pi)_0^{*0} \pi^0) = -0.22 \pm 0.32$$

$$A_{CP}(B^0 \rightarrow K^*(892)^+ \pi^-) = -0.19 \pm 0.07$$

$$A_{CP}(B^0 \rightarrow K^{*0} \pi^0) = -0.09_{-0.26}^{+0.23}$$

$$A_{CP}(B^0 \rightarrow K^0 \pi^+ \pi^-) = -0.01 \pm 0.05$$

$$A_{CP}(B^0 \rightarrow K^*(892)^0 \pi^+ \pi^-) = 0.07 \pm 0.05$$

$$A_{CP}(B^0 \rightarrow K^*(892)^0 \rho^0) = 0.09 \pm 0.19$$

$$A_{CP}(B^0 \rightarrow a_1^- K^+) = -0.16 \pm 0.12$$

$$A_{CP}(B^0 \rightarrow b_1 K^+) = -0.07 \pm 0.12$$

$$A_{CP}(B^0 \rightarrow K^*(892)^0 K^+ K^-) = 0.01 \pm 0.05$$

$$A_{CP}(B^0 \rightarrow K^*(892)^0 \phi) = 0.01 \pm 0.05$$

$$A_{CP}(B^0 \rightarrow K^*(892)^0 K^- \pi^+) = 0.2 \pm 0.4$$

$$A_{CP}(B^0 \rightarrow \phi(K\pi)_0^{*0}) = 0.20 \pm 0.15$$

$$A_{CP}(B^0 \rightarrow \phi K_2^*(1430)^0) = -0.08 \pm 0.13$$

$$\begin{aligned}
A_{CP}(B^0 \rightarrow \rho^+ \pi^-) &= 0.08 \pm 0.12 \quad (S = 2.0) \\
A_{CP}(B^0 \rightarrow \rho^- \pi^+) &= -0.16 \pm 0.23 \quad (S = 1.7) \\
A_{CP}(B^0 \rightarrow a_1(1260)^\pm \pi^\mp) &= -0.07 \pm 0.07 \\
A_{CP}(B^0 \rightarrow b_1 \pi^+) &= -0.05 \pm 0.10 \\
A_{CP}(B^0 \rightarrow K^*(892)^0 \gamma) &= -0.016 \pm 0.023 \\
A_{CP}(B^0 \rightarrow K^*(1430) \gamma) &= -0.08 \pm 0.15 \\
A_{CP}(B^0 \rightarrow p \bar{p} K^*(892)^0) &= 0.05 \pm 0.12 \\
A_{CP}(B^0 \rightarrow p \bar{\Lambda} \pi^-) &= 0.04 \pm 0.07 \\
A_{CP}(B^0 \rightarrow K^{*0} \ell^+ \ell^-) &= -0.05 \pm 0.10 \\
A_{CP}(B^0 \rightarrow K^{*0} e^+ e^-) &= -0.21 \pm 0.19 \\
A_{CP}(B^0 \rightarrow K^{*0} \mu^+ \mu^-) &= 0.00 \pm 0.15 \\
C_{D^*-D^+}(B^0 \rightarrow D^*(2010)^- D^+) &= 0.07 \pm 0.14 \\
\mathbf{S_{D^*-D^+}(B^0 \rightarrow D^*(2010)^- D^+)} &= -0.78 \pm 0.21 \\
C_{D^{*+}D^-}(B^0 \rightarrow D^*(2010)^+ D^-) &= -0.09 \pm 0.22 \quad (S = 1.6) \\
\mathbf{S_{D^{*+}D^-}(B^0 \rightarrow D^*(2010)^+ D^-)} &= -0.61 \pm 0.19 \\
C_{D^{*+}D^{*-}}(B^0 \rightarrow D^{*+} D^{*-}) &= -0.01 \pm 0.09 \quad (S = 1.2) \\
\mathbf{S_{D^{*+}D^{*-}}(B^0 \rightarrow D^{*+} D^{*-})} &= -0.76 \pm 0.14 \\
C_+(B^0 \rightarrow D^{*+} D^{*-}) &= 0.00 \pm 0.12 \\
\mathbf{S_+(B^0 \rightarrow D^{*+} D^{*-})} &= -0.76 \pm 0.16 \\
C_-(B^0 \rightarrow D^{*+} D^{*-}) &= 0.4 \pm 0.5 \\
S_-(B^0 \rightarrow D^{*+} D^{*-}) &= -1.8 \pm 0.7 \\
C(B^0 \rightarrow D^*(2010)^+ D^*(2010)^- K_S^0) &= 0.01 \pm 0.29 \\
S(B^0 \rightarrow D^*(2010)^+ D^*(2010)^- K_S^0) &= 0.1 \pm 0.4 \\
C_{D^+D^-}(B^0 \rightarrow D^+ D^-) &= -0.5 \pm 0.4 \quad (S = 2.5) \\
\mathbf{S_{D^+D^-}(B^0 \rightarrow D^+ D^-)} &= -0.87 \pm 0.26 \\
C_{J/\psi(1S)\pi^0}(B^0 \rightarrow J/\psi(1S)\pi^0) &= -0.13 \pm 0.13 \\
\mathbf{S_{J/\psi(1S)\pi^0}(B^0 \rightarrow J/\psi(1S)\pi^0)} &= -0.94 \pm 0.29 \quad (S = 1.9) \\
C_{D_{CP}^{(*)}h^0}(B^0 \rightarrow D_{CP}^{(*)}h^0) &= -0.23 \pm 0.16 \\
S_{D_{CP}^{(*)}h^0}(B^0 \rightarrow D_{CP}^{(*)}h^0) &= -0.56 \pm 0.24 \\
C_{K_S^0\pi^0}(B^0 \rightarrow K^0\pi^0) &= 0.00 \pm 0.13 \quad (S = 1.4) \\
\mathbf{S_{K_S^0\pi^0}(B^0 \rightarrow K^0\pi^0)} &= 0.58 \pm 0.17 \\
C_{\eta'(958)K}(B^0 \rightarrow \eta'(958)K_S^0) &= -0.04 \pm 0.20 \quad (S = 2.5) \\
S_{\eta'(958)K}(B^0 \rightarrow \eta'(958)K_S^0) &= 0.43 \pm 0.17 \quad (S = 1.5) \\
C_{\eta'K^0}(B^0 \rightarrow \eta'K^0) &= -0.05 \pm 0.05 \\
\mathbf{S_{\eta'K^0}(B^0 \rightarrow \eta'K^0)} &= 0.60 \pm 0.07 \\
C_{\omega K_S^0}(B^0 \rightarrow \omega K_S^0) &= -0.30 \pm 0.28 \quad (S = 1.6) \\
S_{\omega K_S^0}(B^0 \rightarrow \omega K_S^0) &= 0.43 \pm 0.24 \\
C(B^0 \rightarrow K_S^0\pi^0\pi^0) &= 0.2 \pm 0.5 \\
S(B^0 \rightarrow K_S^0\pi^0\pi^0) &= 0.7 \pm 0.7 \\
C_{\rho^0 K_S^0}(B^0 \rightarrow \rho^0 K_S^0) &= -0.04 \pm 0.20 \\
S_{\rho^0 K_S^0}(B^0 \rightarrow \rho^0 K_S^0) &= 0.50^{+0.17}_{-0.21} \\
C_{f_0 K_S^0}(B^0 \rightarrow f_0(980)K_S^0) &= 0.07 \pm 0.14 \\
S_{f_0 K_S^0}(B^0 \rightarrow f_0(980)K_S^0) &= -0.73^{+0.27}_{-0.09} \quad (S = 1.6) \\
S_{f_2 K_S^0}(B^0 \rightarrow f_2(1270)K_S^0) &= -0.5 \pm 0.5 \\
C_{f_2 K_S^0}(B^0 \rightarrow f_2(1270)K_S^0) &= 0.3 \pm 0.4
\end{aligned}$$

$$S_{f_x K_S^0} (B^0 \rightarrow f_x(1300) K_S^0) = -0.2 \pm 0.5$$

$$C_{f_x K_S^0} (B^0 \rightarrow f_x(1300) K_S^0) = 0.13 \pm 0.35$$

$$S_{K^0 \pi^+ \pi^-} (B^0 \rightarrow K^0 \pi^+ \pi^- \text{ nonresonant}) = -0.01 \pm 0.33$$

$$C_{K^0 \pi^+ \pi^-} (B^0 \rightarrow K^0 \pi^+ \pi^- \text{ nonresonant}) = 0.01 \pm 0.26$$

$$C_{K_S^0 K_S^0} (B^0 \rightarrow K_S^0 K_S^0) = 0.0 \pm 0.4 \quad (S = 1.4)$$

$$S_{K_S^0 K_S^0} (B^0 \rightarrow K_S^0 K_S^0) = -0.8 \pm 0.5$$

$$C_{K^+ K^- K_S^0} (B^0 \rightarrow K^+ K^- K_S^0) = 0.07 \pm 0.08$$

$$\mathbf{S_{K^+ K^- K_S^0} (B^0 \rightarrow K^+ K^- K_S^0)} = -0.74_{-0.10}^{+0.12}$$

$$C_{K^+ K^- K_S^0} (B^0 \rightarrow K^+ K^- K_S^0 \text{ inclusive}) = 0.01 \pm 0.09$$

$$\mathbf{S_{K^+ K^- K_S^0} (B^0 \rightarrow K^+ K^- K_S^0 \text{ inclusive})} = -0.65 \pm 0.12$$

$$C_{\phi K_S^0} (B^0 \rightarrow \phi K_S^0) = -0.01 \pm 0.12$$

$$S_{\phi K_S^0} (B^0 \rightarrow \phi K_S^0) = 0.39 \pm 0.17$$

$$C_{K_S K_S K_S} (B^0 \rightarrow K_S K_S K_S) = -0.15 \pm 0.16 \quad (S = 1.1)$$

$$S_{K_S K_S K_S} (B^0 \rightarrow K_S K_S K_S) = -0.4 \pm 0.5 \quad (S = 2.5)$$

$$C_{K_S^0 \pi^0 \gamma} (B^0 \rightarrow K_S^0 \pi^0 \gamma) = 0.36 \pm 0.33$$

$$S_{K_S^0 \pi^0 \gamma} (B^0 \rightarrow K_S^0 \pi^0 \gamma) = -0.8 \pm 0.6$$

$$C_{K^{*0} \gamma} (B^0 \rightarrow K^*(892)^0 \gamma) = -0.04 \pm 0.16 \quad (S = 1.2)$$

$$S_{K^{*0} \gamma} (B^0 \rightarrow K^*(892)^0 \gamma) = -0.15 \pm 0.22$$

$$C_{\eta K^0 \gamma} (B^0 \rightarrow \eta K^0 \gamma) = -0.3 \pm 0.4$$

$$S_{\eta K^0 \gamma} (B^0 \rightarrow \eta K^0 \gamma) = -0.2 \pm 0.5$$

$$C(B^0 \rightarrow K_S^0 \rho^0 \gamma) = -0.05 \pm 0.19$$

$$S(B^0 \rightarrow K_S^0 \rho^0 \gamma) = 0.11 \pm 0.34$$

$$C(B^0 \rightarrow \rho^0 \gamma) = 0.4 \pm 0.5$$

$$S(B^0 \rightarrow \rho^0 \gamma) = -0.8 \pm 0.7$$

$$C_{\pi \pi} (B^0 \rightarrow \pi^+ \pi^-) = -0.38 \pm 0.17 \quad (S = 2.6)$$

$$\mathbf{S_{\pi \pi} (B^0 \rightarrow \pi^+ \pi^-)} = -0.61 \pm 0.08$$

$$C_{\pi^0 \pi^0} (B^0 \rightarrow \pi^0 \pi^0) = -0.48 \pm 0.30$$

$$C_{\rho \pi} (B^0 \rightarrow \rho^+ \pi^-) = 0.01 \pm 0.14 \quad (S = 1.9)$$

$$S_{\rho \pi} (B^0 \rightarrow \rho^+ \pi^-) = 0.01 \pm 0.09$$

$$\mathbf{\Delta C_{\rho \pi} (B^0 \rightarrow \rho^+ \pi^-)} = 0.37 \pm 0.08$$

$$\Delta S_{\rho \pi} (B^0 \rightarrow \rho^+ \pi^-) = -0.05 \pm 0.10$$

$$C_{\rho^0 \pi^0} (B^0 \rightarrow \rho^0 \pi^0) = 0.3 \pm 0.4$$

$$S_{\rho^0 \pi^0} (B^0 \rightarrow \rho^0 \pi^0) = 0.1 \pm 0.4$$

$$C_{a_1 \pi} (B^0 \rightarrow a_1(1260)^+ \pi^-) = -0.10 \pm 0.17$$

$$S_{a_1 \pi} (B^0 \rightarrow a_1(1260)^+ \pi^-) = 0.37 \pm 0.22$$

$$\Delta C_{a_1 \pi} (B^0 \rightarrow a_1(1260)^+ \pi^-) = 0.26 \pm 0.17$$

$$\Delta S_{a_1 \pi} (B^0 \rightarrow a_1(1260)^+ \pi^-) = -0.14 \pm 0.22$$

$$C(B^0 \rightarrow b_1^- K^+) = -0.22 \pm 0.24$$

$$\Delta C(B^0 \rightarrow b_1^- \pi^+) = -1.04 \pm 0.24$$

$$C_{\rho^0 \rho^0} (B^0 \rightarrow \rho^0 \rho^0) = 0.2 \pm 0.9$$

$$S_{\rho^0 \rho^0} (B^0 \rightarrow \rho^0 \rho^0) = 0.3 \pm 0.7$$

$$C_{\rho \rho} (B^0 \rightarrow \rho^+ \rho^-) = -0.05 \pm 0.13$$

$$S_{\rho \rho} (B^0 \rightarrow \rho^+ \rho^-) = -0.06 \pm 0.17$$

$$|\lambda| (B^0 \rightarrow J/\psi K^*(892)^0) < 0.25, \text{ CL} = 95\%$$

$$\begin{aligned}
\cos 2\beta (B^0 \rightarrow J/\psi K^*(892)^0) &= 1.7^{+0.7}_{-0.9} \quad (S = 1.6) \\
\cos 2\beta (B^0 \rightarrow [K_S^0 \pi^+ \pi^-]_{D^{(*)}} h^0) &= 1.0^{+0.6}_{-0.7} \quad (S = 1.8) \\
(S_+ + S_-)/2 (B^0 \rightarrow D^{*-} \pi^+) &= -0.037 \pm 0.012 \\
(S_- - S_+)/2 (B^0 \rightarrow D^{*-} \pi^+) &= -0.006 \pm 0.016 \\
(S_+ + S_-)/2 (B^0 \rightarrow D^- \pi^+) &= -0.046 \pm 0.023 \\
(S_- - S_+)/2 (B^0 \rightarrow D^- \pi^+) &= -0.022 \pm 0.021 \\
(S_+ + S_-)/2 (B^0 \rightarrow D^- \rho^+) &= -0.024 \pm 0.032 \\
(S_- - S_+)/2 (B^0 \rightarrow D^- \rho^+) &= -0.10 \pm 0.06 \\
C_{\eta_c K_S^0} (B^0 \rightarrow \eta_c K_S^0) &= 0.08 \pm 0.13 \\
\mathbf{S}_{\eta_c K_S^0} (B^0 \rightarrow \eta_c K_S^0) &= 0.93 \pm 0.17 \\
C_{c\bar{c}K^{(*)0}} (B^0 \rightarrow c\bar{c}K^{(*)0}) &= 0.004 \pm 0.019 \\
\mathbf{\sin(2\beta)} &= 0.671 \pm 0.023 \\
C_{J/\psi(nS)K^0} (B^0 \rightarrow J/\psi(nS)K^0) &= (-0.2 \pm 2.0) \times 10^{-2} \\
\mathbf{S}_{J/\psi(nS)K^0} (B^0 \rightarrow J/\psi(nS)K^0) &= 0.658 \pm 0.024 \\
C_{J/\psi K^{*0}} (B^0 \rightarrow J/\psi K^{*0}) &= 0.03 \pm 0.10 \\
S_{J/\psi K^{*0}} (B^0 \rightarrow J/\psi K^{*0}) &= 0.60 \pm 0.25 \\
C_{\chi_{c0} K_S^0} (B^0 \rightarrow \chi_{c0} K_S^0) &= -0.3^{+0.5}_{-0.4} \\
S_{\chi_{c0} K_S^0} (B^0 \rightarrow \chi_{c0} K_S^0) &= -0.7 \pm 0.5 \\
C_{\chi_{c1} K_S^0} (B^0 \rightarrow \chi_{c1} K_S^0) &= 0.13 \pm 0.11 \\
\mathbf{S}_{\chi_{c1} K_S^0} (B^0 \rightarrow \chi_{c1} K_S^0) &= 0.61 \pm 0.16 \\
\sin(2\beta_{\text{eff}})(B^0 \rightarrow \phi K^0) &= 0.22 \pm 0.30 \\
\sin(2\beta_{\text{eff}})(B^0 \rightarrow \phi K_0^*(1430)^0) &= 0.97^{+0.03}_{-0.52} \\
\mathbf{\sin(2\beta_{\text{eff}})(B^0 \rightarrow K^+ K^- K_S^0)} &= 0.77^{+0.13}_{-0.12} \\
\sin(2\beta_{\text{eff}})(B^0 \rightarrow [K_S^0 \pi^+ \pi^-]_{D^{(*)}} h^0) &= 0.45 \pm 0.28 \\
|\lambda| (B^0 \rightarrow [K_S^0 \pi^+ \pi^-]_{D^{(*)}} h^0) &= 1.01 \pm 0.08 \\
|\sin(2\beta + \gamma)| &> 0.40, \text{ CL} = 90\% \\
2\beta + \gamma &= (83 \pm 60)^\circ \\
\gamma(B^0 \rightarrow D^0 K^{*0}) &= (162 \pm 60)^\circ \\
\alpha &= (90 \pm 5)^\circ
\end{aligned}$$

\bar{B}^0 modes are charge conjugates of the modes below. Reactions indicate the weak decay vertex and do not include mixing. Modes which do not identify the charge state of the B are listed in the B^\pm/B^0 ADMIXTURE section.

The branching fractions listed below assume 50% $B^0 \bar{B}^0$ and 50% $B^+ B^-$ production at the $\Upsilon(4S)$. We have attempted to bring older measurements up to date by rescaling their assumed $\Upsilon(4S)$ production ratio to 50:50 and their assumed D , D_S , D^* , and ψ branching ratios to current values whenever this would affect our averages and best limits significantly.

Indentation is used to indicate a subchannel of a previous reaction. All resonant subchannels have been corrected for resonance branching fractions to the final state so the sum of the subchannel branching fractions can exceed that of the final state.

For inclusive branching fractions, e.g., $B \rightarrow D^\pm$ anything, the values usually are multiplicities, not branching fractions. They can be greater than one.

B^0 DECAY MODES	Fraction (Γ_i/Γ)	Scale factor/ Confidence level	p (MeV/c)
$\ell^+ \nu_\ell$ anything	[nnn] (10.33 ± 0.28) %		—
$e^+ \nu_e X_C$	(10.1 ± 0.4) %		—

$D\ell^+\nu_\ell$ anything	(9.3 ± 0.9) %	—
$D^-\ell^+\nu_\ell$	[<i>nnn</i>] (2.17 ± 0.12) %	2309
$D^-\tau^+\nu_\tau$	(1.1 ± 0.4) %	1909
$D^*(2010)^-\ell^+\nu_\ell$	[<i>nnn</i>] (5.01 ± 0.12) %	2257
$D^*(2010)^-\tau^+\nu_\tau$	(1.5 ± 0.5) %	S=1.3 1837
$\overline{D}^0\pi^-\ell^+\nu_\ell$	(4.3 ± 0.6) × 10 ⁻³	2308
$D_0^*(2400)^-\ell^+\nu_\ell \times$ $B(D_0^{*-} \rightarrow \overline{D}^0\pi^-)$	(3.0 ± 1.2) × 10 ⁻³	S=1.8 —
$D_2^*(2460)^-\ell^+\nu_\ell \times$ $B(D_2^{*-} \rightarrow \overline{D}^0\pi^-)$	(2.2 ± 0.6) × 10 ⁻³	2067
$\overline{D}^{(*)}n\pi\ell^+\nu_\ell$ ($n \geq 1$)	(2.3 ± 0.5) %	—
$\overline{D}^{*0}\pi^-\ell^+\nu_\ell$	(4.9 ± 0.8) × 10 ⁻³	2256
$D_1(2420)^-\ell^+\nu_\ell \times B(D_1^- \rightarrow$ $\overline{D}^{*0}\pi^-)$	(2.80 ± 0.28) × 10 ⁻³	—
$D_1'(2430)^-\ell^+\nu_\ell \times B(D_1'^- \rightarrow$ $\overline{D}^{*0}\pi^-)$	(3.1 ± 0.9) × 10 ⁻³	—
$D_2^*(2460)^-\ell^+\nu_\ell \times$ $B(D_2^{*-} \rightarrow \overline{D}^{*0}\pi^-)$	(1.2 ± 0.5) × 10 ⁻³	S=2.7 2067
$\rho^-\ell^+\nu_\ell$	[<i>nnn</i>] (2.47 ± 0.33) × 10 ⁻⁴	2583
$\pi^-\ell^+\nu_\ell$	[<i>nnn</i>] (1.34 ± 0.08) × 10 ⁻⁴	2638

Inclusive modes

K^\pm anything	(78 ± 8) %	—
D^0X	(8.1 ± 1.5) %	—
\overline{D}^0X	(47.4 ± 2.8) %	—
D^+X	< 3.9 %	CL=90% —
D^-X	(36.9 ± 3.3) %	—
D_s^+X	(10.3 $\begin{smallmatrix} + \\ - \end{smallmatrix}$ $\begin{smallmatrix} 2.1 \\ 1.8 \end{smallmatrix}$) %	—
D_s^-X	< 2.6 %	CL=90% —
Λ_c^+X	< 3.1 %	CL=90% —
$\overline{\Lambda}_c^-X$	(5.0 $\begin{smallmatrix} + \\ - \end{smallmatrix}$ $\begin{smallmatrix} 2.1 \\ 1.5 \end{smallmatrix}$) %	—
$\overline{c}X$	(95 ± 5) %	—
cX	(24.6 ± 3.1) %	—
$\overline{c}cX$	(119 ± 6) %	—

D, D^* , or D_s modes

$D^-\pi^+$	(2.68 ± 0.13) × 10 ⁻³	2306
$D^-\rho^+$	(7.6 ± 1.3) × 10 ⁻³	2235
$D^-K^0\pi^+$	(4.9 ± 0.9) × 10 ⁻⁴	2259
$D^-K^*(892)^+$	(4.5 ± 0.7) × 10 ⁻⁴	2211
$D^-\omega\pi^+$	(2.8 ± 0.6) × 10 ⁻³	2204
D^-K^+	(2.0 ± 0.6) × 10 ⁻⁴	2279
$D^-K^+\overline{K}^0$	< 3.1 × 10 ⁻⁴	CL=90% 2188
$D^-K^+\overline{K}^*(892)^0$	(8.8 ± 1.9) × 10 ⁻⁴	2070
$\overline{D}^0\pi^+\pi^-$	(8.4 ± 0.9) × 10 ⁻⁴	2301
$D^*(2010)^-\pi^+$	(2.76 ± 0.13) × 10 ⁻³	2255
$D^-\pi^+\pi^+\pi^-$	(8.0 ± 2.5) × 10 ⁻³	2287
$(D^-\pi^+\pi^+\pi^-)$ nonresonant	(3.9 ± 1.9) × 10 ⁻³	2287
$D^-\pi^+\rho^0$	(1.1 ± 1.0) × 10 ⁻³	2206
$D^-a_1(1260)^+$	(6.0 ± 3.3) × 10 ⁻³	2121
$D^*(2010)^-\pi^+\pi^0$	(1.5 ± 0.5) %	2247
$D^*(2010)^-\rho^+$	(6.8 ± 0.9) × 10 ⁻³	2180
$D^*(2010)^-K^+$	(2.14 ± 0.16) × 10 ⁻⁴	2226

$D^*(2010)^- K^0 \pi^+$	(3.0 ± 0.8) × 10 ⁻⁴		2205
$D^*(2010)^- K^*(892)^+$	(3.3 ± 0.6) × 10 ⁻⁴		2155
$D^*(2010)^- K^+ \bar{K}^0$	< 4.7 × 10 ⁻⁴	CL=90%	2131
$D^*(2010)^- K^+ \bar{K}^*(892)^0$	(1.29 ± 0.33) × 10 ⁻³		2007
$D^*(2010)^- \pi^+ \pi^+ \pi^-$	(7.0 ± 0.8) × 10 ⁻³	S=1.3	2235
$(D^*(2010)^- \pi^+ \pi^+ \pi^-)$ nonresonant	(0.0 ± 2.5) × 10 ⁻³		2235
$D^*(2010)^- \pi^+ \rho^0$	(5.7 ± 3.2) × 10 ⁻³		2150
$D^*(2010)^- a_1(1260)^+$	(1.30 ± 0.27) %		2061
$D^*(2010)^- \pi^+ \pi^+ \pi^- \pi^0$	(1.76 ± 0.27) %		2218
$D^{*-} 3\pi^+ 2\pi^-$	(4.7 ± 0.9) × 10 ⁻³		2195
$\bar{D}^*(2010)^- \omega \pi^+$	(2.89 ± 0.30) × 10 ⁻³		2148
$D_1(2430)^0 \omega \times B(D_1(2430)^0 \rightarrow D^{*-} \pi^+)$	(4.1 ± 1.6) × 10 ⁻⁴		1992
$\bar{D}^{*-} \pi^+$	[rrr] (2.1 ± 1.0) × 10 ⁻³		-
$D_1(2420)^- \pi^+ \times B(D_1^- \rightarrow D^- \pi^+ \pi^-)$	(8.9 \pm $\frac{2.3}{3.5}$) × 10 ⁻⁵		-
$D_1(2420)^- \pi^+ \times B(D_1^- \rightarrow D^{*-} \pi^+ \pi^-)$	< 3.3 × 10 ⁻⁵	CL=90%	-
$\bar{D}_2^*(2460)^- \pi^+ \times B(D_2^*(2460)^- \rightarrow D^0 \pi^-)$	(2.15 ± 0.35) × 10 ⁻⁴		2064
$\bar{D}_0^*(2400)^- \pi^+ \times B(D_0^*(2400)^- \rightarrow D^0 \pi^-)$	(6.0 ± 3.0) × 10 ⁻⁵		2090
$D_2^*(2460)^- \pi^+ \times B((D_2^*)^- \rightarrow D^{*-} \pi^+ \pi^-)$	< 2.4 × 10 ⁻⁵	CL=90%	-
$\bar{D}_2^*(2460)^- \rho^+$	< 4.9 × 10 ⁻³	CL=90%	1977
$D^0 \bar{D}^0$	< 4.3 × 10 ⁻⁵	CL=90%	1868
$D^{*0} \bar{D}^0$	< 2.9 × 10 ⁻⁴	CL=90%	1794
$D^- D^+$	(2.11 ± 0.31) × 10 ⁻⁴	S=1.2	1864
$D^- D_s^+$	(7.2 ± 0.8) × 10 ⁻³		1812
$D^*(2010)^- D_s^+$	(8.0 ± 1.1) × 10 ⁻³		1735
$D^- D_s^{*+}$	(7.4 ± 1.6) × 10 ⁻³		1731
$D^*(2010)^- D_s^{*+}$	(1.77 ± 0.14) %		1649
$D_{s0}(2317)^- K^+ \times B(D_{s0}(2317)^- \rightarrow D_s^- \pi^0)$	(4.2 ± 1.4) × 10 ⁻⁵		2097
$D_{s0}(2317)^- \pi^+ \times B(D_{s0}(2317)^- \rightarrow D_s^- \pi^0)$	< 2.5 × 10 ⁻⁵	CL=90%	2128
$D_{sJ}(2457)^- K^+ \times B(D_{sJ}(2457)^- \rightarrow D_s^- \pi^0)$	< 9.4 × 10 ⁻⁶	CL=90%	-
$D_{sJ}(2457)^- \pi^+ \times B(D_{sJ}(2457)^- \rightarrow D_s^- \pi^0)$	< 4.0 × 10 ⁻⁶	CL=90%	-
$D_s^- D_s^+$	< 3.6 × 10 ⁻⁵	CL=90%	1759
$D_s^{*-} D_s^+$	< 1.3 × 10 ⁻⁴	CL=90%	1674
$D_s^{*-} D_s^{*+}$	< 2.4 × 10 ⁻⁴	CL=90%	1583
$D_{s0}(2317)^+ D^- \times B(D_{s0}(2317)^+ \rightarrow D_s^+ \pi^0)$	(9.7 \pm $\frac{4.0}{3.3}$) × 10 ⁻⁴	S=1.5	1602
$D_{s0}(2317)^+ D^- \times B(D_{s0}(2317)^+ \rightarrow D_s^{*+} \gamma)$	< 9.5 × 10 ⁻⁴	CL=90%	-
$D_{s0}(2317)^+ D^*(2010)^- \times B(D_{s0}(2317)^+ \rightarrow D_s^+ \pi^0)$	(1.5 ± 0.6) × 10 ⁻³		1509
$D_{sJ}(2457)^+ D^-$	(3.5 ± 1.1) × 10 ⁻³		-

$D_{sJ}(2457)^+ D^- \times$ $B(D_{sJ}(2457)^+ \rightarrow D_s^+ \gamma)$	$(6.5 \begin{smallmatrix} + \\ - \end{smallmatrix} \begin{smallmatrix} 1.7 \\ 1.4 \end{smallmatrix}) \times 10^{-4}$		—
$D_{sJ}(2457)^+ D^- \times$ $B(D_{sJ}(2457)^+ \rightarrow D_s^{*+} \gamma)$	$< 6.0 \quad \times 10^{-4}$	CL=90%	—
$D_{sJ}(2457)^+ D^- \times$ $B(D_{sJ}(2457)^+ \rightarrow D_s^+ \pi^+ \pi^-)$	$< 2.0 \quad \times 10^{-4}$	CL=90%	—
$D_{sJ}(2457)^+ D^- \times$ $B(D_{sJ}(2457)^+ \rightarrow D_s^+ \pi^0)$	$< 3.6 \quad \times 10^{-4}$	CL=90%	—
$D^*(2010)^- D_{sJ}(2457)^+$	$(9.3 \pm 2.2) \times 10^{-3}$		—
$D_{sJ}(2457)^+ D^*(2010) \times$ $B(D_{sJ}(2457)^+ \rightarrow D_s^+ \gamma)$	$(2.3 \begin{smallmatrix} + \\ - \end{smallmatrix} \begin{smallmatrix} 0.9 \\ 0.7 \end{smallmatrix}) \times 10^{-3}$		—
$D^- D_{s1}(2536)^+ \times$ $B(D_{s1}(2536)^+ \rightarrow D^{*0} K^+)$	$(1.7 \pm 0.6) \times 10^{-4}$		1444
$D^*(2010)^- D_{s1}(2536)^+ \times$ $B(D_{s1}(2536)^+ \rightarrow D^{*0} K^+)$	$(3.3 \pm 1.1) \times 10^{-4}$		1336
$D^- D_{s1}(2536)^+ \times$ $B(D_{s1}(2536)^+ \rightarrow D^{*+} K^0)$	$(2.6 \pm 1.1) \times 10^{-4}$		1444
$D^{*-} D_{s1}(2536)^+ \times$ $B(D_{s1}(2536)^+ \rightarrow D^{*+} K^0)$	$(5.0 \pm 1.7) \times 10^{-4}$		1336
$D^- D_{sJ}(2573)^+ \times$ $B(D_{sJ}(2573)^+ \rightarrow D^0 K^+)$	$< 1 \quad \times 10^{-4}$	CL=90%	1414
$D^*(2010)^- D_{sJ}(2573)^+ \times$ $B(D_{sJ}(2573)^+ \rightarrow D^0 K^+)$	$< 2 \quad \times 10^{-4}$	CL=90%	1303
$D_s^+ \pi^-$	$(2.4 \pm 0.4) \times 10^{-5}$		2270
$D_s^{*+} \pi^-$	$(2.1 \pm 0.4) \times 10^{-5}$	S=1.4	2215
$D_s^+ \rho^-$	$< 2.4 \quad \times 10^{-5}$	CL=90%	2197
$D_s^{*+} \rho^-$	$(4.1 \pm 1.3) \times 10^{-5}$		2138
$D_s^+ a_0^-$	$< 1.9 \quad \times 10^{-5}$	CL=90%	—
$D_s^{*+} a_0^-$	$< 3.6 \quad \times 10^{-5}$	CL=90%	—
$D_s^+ a_1(1260)^-$	$< 2.1 \quad \times 10^{-3}$	CL=90%	2080
$D_s^{*+} a_1(1260)^-$	$< 1.7 \quad \times 10^{-3}$	CL=90%	2015
$D_s^+ a_2^-$	$< 1.9 \quad \times 10^{-4}$	CL=90%	—
$D_s^{*+} a_2^-$	$< 2.0 \quad \times 10^{-4}$	CL=90%	—
$D_s^- K^+$	$(3.0 \pm 0.4) \times 10^{-5}$		2242
$D_s^{*-} K^+$	$(2.19 \pm 0.30) \times 10^{-5}$		2185
$D_s^- K^*(892)^+$	$(3.5 \pm 1.0) \times 10^{-5}$		2172
$D_s^{*-} K^*(892)^+$	$(3.2 \begin{smallmatrix} + \\ - \end{smallmatrix} \begin{smallmatrix} 1.5 \\ 1.3 \end{smallmatrix}) \times 10^{-5}$		2112
$D_s^- \pi^+ K^0$	$(1.10 \pm 0.33) \times 10^{-4}$		2222
$D_s^{*-} \pi^+ K^0$	$< 1.10 \quad \times 10^{-4}$	CL=90%	2164
$D_s^- \pi^+ K^*(892)^0$	$< 3.0 \quad \times 10^{-3}$	CL=90%	2138
$D_s^{*-} \pi^+ K^*(892)^0$	$< 1.6 \quad \times 10^{-3}$	CL=90%	2076
$\overline{D}^0 K^0$	$(5.2 \pm 0.7) \times 10^{-5}$		2280
$\overline{D}^0 K^+ \pi^-$	$(8.8 \pm 1.7) \times 10^{-5}$		2261
$\overline{D}^0 K^*(892)^0$	$(4.2 \pm 0.6) \times 10^{-5}$		2213
$D_2^*(2460)^- K^+ \times$ $B(D_2^*(2460)^- \rightarrow \overline{D}^0 \pi^-)$	$(1.8 \pm 0.5) \times 10^{-5}$		2031
$\overline{D}^0 K^+ \pi^-$ non-resonant	$< 3.7 \quad \times 10^{-5}$	CL=90%	—
$\overline{D}^0 \pi^0$	$(2.61 \pm 0.24) \times 10^{-4}$		2308
$\overline{D}^0 \rho^0$	$(3.2 \pm 0.5) \times 10^{-4}$		2237
$\overline{D}^0 f_2$	$(1.2 \pm 0.4) \times 10^{-4}$		—

$\overline{D}^0 \eta$	(2.02 ± 0.35) × 10 ⁻⁴	S=1.6	2274
$\overline{D}^0 \eta'$	(1.25 ± 0.23) × 10 ⁻⁴	S=1.1	2198
$\overline{D}^0 \omega$	(2.59 ± 0.30) × 10 ⁻⁴		2235
$D^0 \phi$	< 1.16 × 10 ⁻⁵	CL=90%	2182
$D^0 K^+ \pi^-$	(6 ± 4) × 10 ⁻⁶		2261
$D^0 K^*(892)^0$	< 1.1 × 10 ⁻⁵	CL=90%	2213
$\overline{D}^{*0} \gamma$	< 2.5 × 10 ⁻⁵	CL=90%	2258
$\overline{D}^*(2007)^0 \pi^0$	(1.7 ± 0.4) × 10 ⁻⁴	S=1.5	2256
$\overline{D}^*(2007)^0 \rho^0$	< 5.1 × 10 ⁻⁴	CL=90%	2182
$\overline{D}^*(2007)^0 \eta$	(2.0 ± 0.5) × 10 ⁻⁴		2220
$\overline{D}^*(2007)^0 \eta'$	(1.23 ± 0.35) × 10 ⁻⁴		2141
$\overline{D}^*(2007)^0 \pi^+ \pi^-$	(6.2 ± 2.2) × 10 ⁻⁴		2248
$\overline{D}^*(2007)^0 K^0$	(3.6 ± 1.2) × 10 ⁻⁵		2227
$\overline{D}^*(2007)^0 K^*(892)^0$	< 6.9 × 10 ⁻⁵	CL=90%	2157
$D^*(2007)^0 K^*(892)^0$	< 4.0 × 10 ⁻⁵	CL=90%	2157
$D^*(2007)^0 \pi^+ \pi^+ \pi^- \pi^-$	(2.7 ± 0.5) × 10 ⁻³		2219
$D^*(2010)^+ D^*(2010)^-$	(8.2 ± 0.9) × 10 ⁻⁴		1711
$\overline{D}^*(2007)^0 \omega$	(3.3 ± 0.7) × 10 ⁻⁴		2180
$D^*(2010)^+ D^-$	(6.1 ± 1.5) × 10 ⁻⁴	S=1.6	1790
$D^*(2007)^0 \overline{D}^*(2007)^0$	< 9 × 10 ⁻⁵	CL=90%	1715
$D^- D^0 K^+$	(1.7 ± 0.4) × 10 ⁻³		1574
$D^- D^*(2007)^0 K^+$	(4.6 ± 1.0) × 10 ⁻³		1478
$D^*(2010)^- D^0 K^+$	(3.1 ± 0.6 / - 0.5) × 10 ⁻³		1479
$D^*(2010)^- D^*(2007)^0 K^+$	(1.18 ± 0.20) %		1366
$D^- D^+ K^0$	< 1.7 × 10 ⁻³	CL=90%	1568
$D^*(2010)^- D^+ K^0 + D^- D^*(2010)^+ K^0$	(6.5 ± 1.6) × 10 ⁻³		1473
$D^*(2010)^- D^*(2010)^+ K^0$	(7.8 ± 1.1) × 10 ⁻³		1360
$D^{*-} D_{s1}(2536)^+ \times B(D_{s1}(2536)^+ \rightarrow D^{*+} K^0)$	(8.0 ± 2.4) × 10 ⁻⁴		1336
$\overline{D}^0 D^0 K^0$	< 1.4 × 10 ⁻³	CL=90%	1574
$\overline{D}^0 D^*(2007)^0 K^0 + \overline{D}^*(2007)^0 D^0 K^0$	< 3.7 × 10 ⁻³	CL=90%	1478
$\overline{D}^*(2007)^0 D^*(2007)^0 K^0$	< 6.6 × 10 ⁻³	CL=90%	1365
$(\overline{D} + \overline{D}^*)(D + D^*) K$	(4.3 ± 0.7) %		-

Charmonium modes

$\eta_c K^0$	(8.9 ± 1.6) × 10 ⁻⁴		1753
$\eta_c K^*(892)^0$	(6.1 ± 1.0) × 10 ⁻⁴		1648
$\eta_c(2S) K^{*0}$	< 3.9 × 10 ⁻⁴	CL=90%	1159
$J/\psi(1S) K^0$	(8.71 ± 0.32) × 10 ⁻⁴		1683
$J/\psi(1S) K^+ \pi^-$	(1.2 ± 0.6) × 10 ⁻³		1652
$J/\psi(1S) K^*(892)^0$	(1.33 ± 0.06) × 10 ⁻³		1571
$J/\psi(1S) \eta K_S^0$	(8 ± 4) × 10 ⁻⁵		1508
$J/\psi(1S) \eta' K_S^0$	< 2.5 × 10 ⁻⁵	CL=90%	1271
$J/\psi(1S) \phi K^0$	(9.4 ± 2.6) × 10 ⁻⁵		1224
$J/\psi(1S) \omega K^0$ nonresonant	(3.1 ± 0.7) × 10 ⁻⁴		1386
$J/\psi(1S) K(1270)^0$	(1.3 ± 0.5) × 10 ⁻³		1390
$J/\psi(1S) \pi^0$	(1.76 ± 0.16) × 10 ⁻⁵	S=1.1	1728
$J/\psi(1S) \eta$	(9.5 ± 1.9) × 10 ⁻⁶		1672
$J/\psi(1S) \pi^+ \pi^-$	(4.6 ± 0.9) × 10 ⁻⁵		1716
$J/\psi(1S) \pi^+ \pi^-$ nonresonant	< 1.2 × 10 ⁻⁵	CL=90%	1716
$J/\psi(1S) f_2$	< 4.6 × 10 ⁻⁶	CL=90%	-
$J/\psi(1S) \rho^0$	(2.7 ± 0.4) × 10 ⁻⁵		1612
$J/\psi(1S) \omega$	< 2.7 × 10 ⁻⁴	CL=90%	1609

$J/\psi(1S)\phi$	< 9.4	$\times 10^{-7}$	CL=90%	1520
$J/\psi(1S)\eta'(958)$	< 6.3	$\times 10^{-5}$	CL=90%	1546
$J/\psi(1S)K^0\pi^+\pi^-$	(1.0 \pm 0.4)	$\times 10^{-3}$		1611
$J/\psi(1S)K^0\rho^0$	(5.4 \pm 3.0)	$\times 10^{-4}$		1390
$J/\psi(1S)K^*(892)^+\pi^-$	(8 \pm 4)	$\times 10^{-4}$		1514
$J/\psi(1S)K^*(892)^0\pi^+\pi^-$	(6.6 \pm 2.2)	$\times 10^{-4}$		1447
$X(3872)^-K^+$	< 5	$\times 10^{-4}$	CL=90%	-
$X(3872)^-K^+ \times B(X(3872)^- \rightarrow [sss])$	< 5.4	$\times 10^{-6}$	CL=90%	-
$J/\psi(1S)\pi^-\pi^0$				
$X(3872)K^0 \times B(X \rightarrow J/\psi\pi^+\pi^-)$	< 6.0	$\times 10^{-6}$	CL=90%	1140
$X(3872)K^0 \times B(X \rightarrow J/\psi\gamma)$	< 4.9	$\times 10^{-6}$	CL=90%	1140
$X(3872)K^*(892)^0 \times B(X \rightarrow J/\psi\gamma)$	< 2.8	$\times 10^{-6}$	CL=90%	940
$X(3872)K^0 \times B(X \rightarrow \psi(2S)\gamma)$	< 1.9	$\times 10^{-5}$	CL=90%	1140
$X(3872)K^*(892)^0 \times B(X \rightarrow \psi(2S)\gamma)$	< 4.4	$\times 10^{-6}$	CL=90%	940
$X(3872)K^0 \times B(X \rightarrow D^0\bar{D}^0\pi^0)$	(1.7 \pm 0.8)	$\times 10^{-4}$		1140
$X(3872)K^0 \times B(X \rightarrow \bar{D}^{*0}D^0)$	(1.2 \pm 0.4)	$\times 10^{-4}$		1140
$X(4430)^\pm K^\mp \times B(X^\pm \rightarrow \psi(2S)\pi^\pm)$	(3.2 $\begin{smallmatrix} + \\ - \end{smallmatrix}$ 6.0 / 1.8)	$\times 10^{-5}$		621
$X(4430)^\pm K^\mp \times B(X^\pm \rightarrow J/\psi\pi^\pm)$	< 4	$\times 10^{-6}$	CL=95%	621
$J/\psi(1S)\rho\bar{\rho}$	< 8.3	$\times 10^{-7}$	CL=90%	862
$J/\psi(1S)\gamma$	< 1.6	$\times 10^{-6}$	CL=90%	1731
$J/\psi(1S)\bar{D}^0$	< 1.3	$\times 10^{-5}$	CL=90%	877
$\psi(2S)K^0$	(6.2 \pm 0.5)	$\times 10^{-4}$		1283
$\psi(3770)K^0 \times B(\psi \rightarrow \bar{D}^0 D^0)$	< 1.23	$\times 10^{-4}$	CL=90%	1217
$\psi(3770)K^0 \times B(\psi \rightarrow D^- D^+)$	< 1.88	$\times 10^{-4}$	CL=90%	1217
$\psi(2S)K^+\pi^-$	(5.7 \pm 0.4)	$\times 10^{-4}$		1238
$\psi(2S)K^*(892)^0$	(6.1 \pm 0.5)	$\times 10^{-4}$	S=1.1	1116
$\chi_{c0}(1P)K^0$	(1.4 $\begin{smallmatrix} + \\ - \end{smallmatrix}$ 0.6 / 0.5)	$\times 10^{-4}$		1477
$\chi_{c0}K^*(892)^0$	(1.7 \pm 0.4)	$\times 10^{-4}$		1341
$\chi_{c2}K^0$	< 2.6	$\times 10^{-5}$	CL=90%	1378
$\chi_{c2}K^*(892)^0$	(6.6 \pm 1.9)	$\times 10^{-5}$		1228
$\chi_{c1}(1P)\pi^0$	(1.12 \pm 0.28)	$\times 10^{-5}$		1468
$\chi_{c1}(1P)K^0$	(3.90 \pm 0.33)	$\times 10^{-4}$		1411
$\chi_{c1}(1P)K^-\pi^+$	(3.8 \pm 0.4)	$\times 10^{-4}$		1371
$\chi_{c1}(1P)K^*(892)^0$	(2.22 $\begin{smallmatrix} + \\ - \end{smallmatrix}$ 0.40 / 0.31)	$\times 10^{-4}$	S=1.6	1265
$X(4051)^+K^- \times B(X^+ \rightarrow \chi_{c1}\pi^+)$	(3.0 $\begin{smallmatrix} + \\ - \end{smallmatrix}$ 4.0 / 1.8)	$\times 10^{-5}$		-
$X(4248)^+K^- \times B(X^+ \rightarrow \chi_{c1}\pi^+)$	(4.0 $\begin{smallmatrix} + \\ - \end{smallmatrix}$ 20.0 / 1.0)	$\times 10^{-5}$		-

K or K* modes

$K^+\pi^-$	(1.94 \pm 0.06)	$\times 10^{-5}$		2615
$K^0\pi^0$	(9.5 \pm 0.8)	$\times 10^{-6}$	S=1.3	2615
$\eta'K^0$	(6.6 \pm 0.4)	$\times 10^{-5}$	S=1.4	2528
$\eta'K^*(892)^0$	(3.8 \pm 1.2)	$\times 10^{-6}$		2472
ηK^0	(1.1 \pm 0.4)	$\times 10^{-6}$		2587
$\eta K^*(892)^0$	(1.59 \pm 0.10)	$\times 10^{-5}$		2534
$\eta K_0^*(1430)^0$	(1.10 \pm 0.22)	$\times 10^{-5}$		2414
$\eta K_2^*(1430)^0$	(9.6 \pm 2.1)	$\times 10^{-6}$		2414

ωK^0	(5.0 ± 0.6) × 10 ⁻⁶		2557
$a_0(980)^0 K^0 \times B(a_0(980)^0 \rightarrow \eta \pi^0)$	< 7.8 × 10 ⁻⁶	CL=90%	-
$b_1^0 K^0 \times B(b_1^0 \rightarrow \omega \pi^0)$	< 7.8 × 10 ⁻⁶	CL=90%	-
$a_0(980)^\pm K^\mp \times B(a_0(980)^\pm \rightarrow \eta \pi^\pm)$	< 1.9 × 10 ⁻⁶	CL=90%	-
$b_1^- K^+ \times B(b_1^- \rightarrow \omega \pi^-)$	(7.4 ± 1.4) × 10 ⁻⁶		-
$b_1^0 K^{*0} \times B(b_1^0 \rightarrow \omega \pi^0)$	< 8.0 × 10 ⁻⁶	CL=90%	-
$b_1^- K^{*+} \times B(b_1^- \rightarrow \omega \pi^-)$	< 5.0 × 10 ⁻⁶	CL=90%	-
$a_0(1450)^\pm K^\mp \times B(a_0(1450)^\pm \rightarrow \eta \pi^\pm)$	< 3.1 × 10 ⁻⁶	CL=90%	-
$K_S^0 X^0$ (Familon)	< 5.3 × 10 ⁻⁵	CL=90%	-
$\omega K^*(892)^0$	(2.0 ± 0.5) × 10 ⁻⁶		2503
$\omega (K\pi)_0^{*0}$	(1.84 ± 0.25) × 10 ⁻⁵		-
$\omega K_0^*(1430)^0$	(1.60 ± 0.34) × 10 ⁻⁵		2380
$\omega K_2^*(1430)^0$	(1.01 ± 0.23) × 10 ⁻⁵		2380
$\omega K^+ \pi^-$ nonresonant	(5.1 ± 1.0) × 10 ⁻⁶		2542
$K^+ \pi^- \pi^0$	(3.59 ⁺ ₋ 0.28 _{0.24}) × 10 ⁻⁵		2609
$K^+ \rho^-$	(8.4 ⁺ ₋ 1.6 _{2.2}) × 10 ⁻⁶	S=1.6	2559
$K^+ \rho(1450)^-$	< 2.1 × 10 ⁻⁶	CL=90%	-
$K^+ \rho(1700)^-$	< 1.1 × 10 ⁻⁶	CL=90%	-
$(K^+ \pi^- \pi^0)$ non-resonant	(4.4 ± 1.0) × 10 ⁻⁶		-
$(K\pi)_0^{*+} \pi^- \times B((K\pi)_0^{*+} \rightarrow K^+ \pi^0)$	(9.4 ± 2.5) × 10 ⁻⁶		-
$(K\pi)_0^{*0} \pi^0 \times B((K\pi)_0^{*0} \rightarrow K^+ \pi^-)$	(8.7 ± 2.9) × 10 ⁻⁶		-
$K_2^*(1430)^0 \pi^0$	< 4.0 × 10 ⁻⁶	CL=90%	2445
$K^*(1680)^0 \pi^0$	< 7.5 × 10 ⁻⁶	CL=90%	2358
$K_x^{*0} \pi^0$	[vuv] (6.1 ± 1.6) × 10 ⁻⁶		-
$K^0 \pi^+ \pi^-$ charmless	(4.96 ± 0.20) × 10 ⁻⁵		2609
$K^0 \pi^+ \pi^-$ non-resonant	(1.47 ⁺ ₋ 0.40 _{0.26}) × 10 ⁻⁵	S=2.1	-
$K^0 \rho^0$	(4.7 ± 0.6) × 10 ⁻⁶		2558
$K^*(892)^+ \pi^-$	(9.4 ⁺ ₋ 1.3 _{1.2}) × 10 ⁻⁶	S=1.5	2562
$K_0^*(1430)^+ \pi^-$	(3.3 ± 0.7) × 10 ⁻⁵	S=2.0	-
$K_x^{*+} \pi^-$	[vuv] (5.1 ± 1.6) × 10 ⁻⁶		-
$K^*(1410)^+ \pi^- \times B(K^*(1410)^+ \rightarrow K^0 \pi^+)$	< 3.8 × 10 ⁻⁶	CL=90%	-
$f_0(980) K^0 \times B(f_0(980) \rightarrow \pi^+ \pi^-)$	(7.0 ± 0.9) × 10 ⁻⁶		2524
$f_2(1270) K^0$	(2.7 ⁺ ₋ 1.3 _{1.2}) × 10 ⁻⁶		2459
$f_x(1300) K^0 \times B(f_x \rightarrow \pi^+ \pi^-)$	(1.8 ± 0.7) × 10 ⁻⁶		-
$K^*(892)^0 \pi^0$	(3.6 ± 0.8) × 10 ⁻⁶		2563
$K_2^*(1430)^+ \pi^-$	< 6 × 10 ⁻⁶	CL=90%	2445
$K^*(1680)^+ \pi^-$	< 1.0 × 10 ⁻⁵	CL=90%	2358
$K^+ \pi^- \pi^+ \pi^-$	[www] < 2.3 × 10 ⁻⁴	CL=90%	2600
$\rho^0 K^+ \pi^-$	(2.8 ± 0.7) × 10 ⁻⁶		2543
$f_0(980) K^+ \pi^-$	(1.4 ⁺ ₋ 0.5 _{0.6}) × 10 ⁻⁶		2508
$K^+ \pi^- \pi^+ \pi^-$ nonresonant	< 2.1 × 10 ⁻⁶	CL=90%	2600
$K^*(892)^0 \pi^+ \pi^-$	(5.4 ± 0.5) × 10 ⁻⁵		2557

$K^*(892)^0 \rho^0$	$(3.4 \pm_{-1.3}^{+1.7}) \times 10^{-6}$	S=1.8	2504
$K^*(892)^0 f_0(980)$	$< 2.2 \times 10^{-6}$	CL=90%	2468
$K_1(1270)^+ \pi^-$	$< 3.0 \times 10^{-5}$	CL=90%	2484
$K_1(1400)^+ \pi^-$	$< 2.7 \times 10^{-5}$	CL=90%	2451
$a_1(1260)^- K^+$	[www] $(1.6 \pm 0.4) \times 10^{-5}$		2471
$K^*(892)^+ \rho^-$	$< 1.20 \times 10^{-5}$	CL=90%	2504
$K_1(1400)^0 \rho^0$	$< 3.0 \times 10^{-3}$	CL=90%	2388
$K^+ K^-$	$< 4.1 \times 10^{-7}$	CL=90%	2593
$K^0 \bar{K}^0$	$(9.6 \pm_{-1.8}^{+2.0}) \times 10^{-7}$		2592
$\frac{K^0 K^- \pi^+}{\bar{K}^{*0} K^0 + K^{*0} \bar{K}^0}$	$< 1.8 \times 10^{-5}$	CL=90%	2578
$K^+ K^- \pi^0$	$< 1.9 \times 10^{-6}$		-
$K^+ K^- \pi^0$	$< 1.9 \times 10^{-5}$	CL=90%	2579
$K_S^0 K_S^0 \pi^0$	$< 9 \times 10^{-7}$	CL=90%	2578
$K_S^0 K_S^0 \eta$	$< 1.0 \times 10^{-6}$	CL=90%	2515
$K_S^0 K_S^0 \eta'$	$< 2.0 \times 10^{-6}$	CL=90%	2452
$K^0 K^+ K^-$	$(2.47 \pm 0.23) \times 10^{-5}$		2522
$K^0 \phi$	$(8.6 \pm_{-1.1}^{+1.3}) \times 10^{-6}$		2516
$K_S^0 K_S^0 K_S^0$	$(6.2 \pm_{-1.1}^{+1.2}) \times 10^{-6}$	S=1.3	2521
$K_S^0 K_S^0 K_L^0$	$< 1.6 \times 10^{-5}$	CL=90%	2521
$K^*(892)^0 K^+ K^-$	$(2.75 \pm 0.26) \times 10^{-5}$		2466
$K^*(892)^0 \phi$	$(9.8 \pm 0.6) \times 10^{-6}$		2460
$K^*(892)^0 K^- \pi^+$	$(4.6 \pm 1.4) \times 10^{-6}$		2524
$K^*(892)^0 \bar{K}^* (892)^0$	$(1.28 \pm_{-0.32}^{+0.40}) \times 10^{-6}$		2485
$K^*(892)^0 K^+ \pi^-$	$< 2.2 \times 10^{-6}$	CL=90%	2524
$K^*(892)^0 K^* (892)^0$	$< 4.1 \times 10^{-7}$	CL=90%	2485
$K^*(892)^+ K^* (892)^-$	$< 2.0 \times 10^{-6}$	CL=90%	2485
$K_1(1400)^0 \phi$	$< 5.0 \times 10^{-3}$	CL=90%	2339
$\phi(K\pi)_0^{*0}$	$(4.3 \pm 0.7) \times 10^{-6}$		-
$\phi(K\pi)_0^{*0} (1.60 < m_{K\pi} < 2.15)$	[xxx] $< 1.7 \times 10^{-6}$	CL=90%	-
$K_0^*(1430)^0 \phi$	$(3.9 \pm 0.8) \times 10^{-6}$		2333
$K^*(1680)^0 \phi$	$< 3.5 \times 10^{-6}$	CL=90%	2238
$K^*(1780)^0 \phi$	$< 2.7 \times 10^{-6}$	CL=90%	-
$K^*(2045)^0 \phi$	$< 1.53 \times 10^{-5}$	CL=90%	-
$K_2^*(1430)^0 \rho^0$	$< 1.1 \times 10^{-3}$	CL=90%	2381
$K_2^*(1430)^0 \phi$	$(7.5 \pm 1.0) \times 10^{-6}$		2333
$K^0 \phi \phi$	$(4.1 \pm_{-1.5}^{+1.7}) \times 10^{-6}$		2305
$\eta' \eta' K^0$	$< 3.1 \times 10^{-5}$	CL=90%	2337
$\eta K^0 \gamma$	$(7.6 \pm 1.8) \times 10^{-6}$		2587
$\eta' K^0 \gamma$	$< 6.6 \times 10^{-6}$	CL=90%	2528
$K^0 \phi \gamma$	$< 2.7 \times 10^{-6}$	CL=90%	2516
$K^+ \pi^- \gamma$	$(4.6 \pm 1.4) \times 10^{-6}$		2615
$K^*(892)^0 \gamma$	$(4.33 \pm 0.15) \times 10^{-5}$		2564
$K^*(1410) \gamma$	$< 1.3 \times 10^{-4}$	CL=90%	2450
$K^+ \pi^- \gamma$ nonresonant	$< 2.6 \times 10^{-6}$	CL=90%	2615
$K^0 \pi^+ \pi^- \gamma$	$(1.95 \pm 0.22) \times 10^{-5}$		2609
$K^+ \pi^- \pi^0 \gamma$	$(4.1 \pm 0.4) \times 10^{-5}$		2609
$K_1(1270)^0 \gamma$	$< 5.8 \times 10^{-5}$	CL=90%	2486
$K_1(1400)^0 \gamma$	$< 1.5 \times 10^{-5}$	CL=90%	2453
$K_2^*(1430)^0 \gamma$	$(1.24 \pm 0.24) \times 10^{-5}$		2447

$K^*(1680)^0 \gamma$	< 2.0	$\times 10^{-3}$	CL=90%	2361
$K_3^*(1780)^0 \gamma$	< 8.3	$\times 10^{-5}$	CL=90%	2341
$K_4^*(2045)^0 \gamma$	< 4.3	$\times 10^{-3}$	CL=90%	2244
Light unflavored meson modes				
$\rho^0 \gamma$	(8.6 \pm 1.5)	$\times 10^{-7}$		2583
$\omega \gamma$	(4.4 \pm 1.8)	$\times 10^{-7}$		2582
$\phi \gamma$	< 8.5	$\times 10^{-7}$	CL=90%	2541
$\pi^+ \pi^-$	(5.13 \pm 0.24)	$\times 10^{-6}$		2636
$\pi^0 \pi^0$	(1.62 \pm 0.31)	$\times 10^{-6}$	S=1.3	2636
$\eta \pi^0$	< 1.5	$\times 10^{-6}$	CL=90%	2610
$\eta \eta$	< 1.0	$\times 10^{-6}$	CL=90%	2582
$\eta' \pi^0$	(1.2 \pm 0.6)	$\times 10^{-6}$	S=1.7	2551
$\eta' \eta'$	< 1.7	$\times 10^{-6}$	CL=90%	2460
$\eta' \eta$	< 1.2	$\times 10^{-6}$	CL=90%	2522
$\eta' \rho^0$	< 1.3	$\times 10^{-6}$	CL=90%	2492
$\eta' f_0(980) \times B(f_0(980) \rightarrow \pi^+ \pi^-)$	< 1.5	$\times 10^{-6}$	CL=90%	2455
$\eta \rho^0$	< 1.5	$\times 10^{-6}$	CL=90%	2553
$\eta f_0(980) \times B(f_0(980) \rightarrow \pi^+ \pi^-)$	< 4	$\times 10^{-7}$	CL=90%	2518
$\omega \eta$	(9.4 \pm 4.0)	$\times 10^{-7}$		2552
$\omega \eta'$	(1.0 \pm 0.5)	$\times 10^{-6}$		2491
$\omega \rho^0$	< 1.6	$\times 10^{-6}$	CL=90%	2522
$\omega f_0(980) \times B(f_0(980) \rightarrow \pi^+ \pi^-)$	< 1.5	$\times 10^{-6}$	CL=90%	2487
$\omega \omega$	< 4.0	$\times 10^{-6}$	CL=90%	2521
$\phi \pi^0$	< 2.8	$\times 10^{-7}$	CL=90%	2539
$\phi \eta$	< 5	$\times 10^{-7}$	CL=90%	2511
$\phi \eta'$	< 5	$\times 10^{-7}$	CL=90%	2447
$\phi \rho^0$	< 3.3	$\times 10^{-7}$	CL=90%	2480
$\phi f_0(980) \times B(f_0 \rightarrow \pi^+ \pi^-)$	< 3.8	$\times 10^{-7}$	CL=90%	2443
$\phi \omega$	< 1.2	$\times 10^{-6}$	CL=90%	2479
$\phi \phi$	< 2	$\times 10^{-7}$	CL=90%	2435
$a_0(980)^\pm \pi^\mp \times B(a_0(980)^\pm \rightarrow \eta \pi^\pm)$	< 3.1	$\times 10^{-6}$	CL=90%	—
$a_0(1450)^\pm \pi^\mp \times B(a_0(1450)^\pm \rightarrow \eta \pi^\pm)$	< 2.3	$\times 10^{-6}$	CL=90%	—
$\pi^+ \pi^- \pi^0$	< 7.2	$\times 10^{-4}$	CL=90%	2631
$\rho^0 \pi^0$	(2.0 \pm 0.5)	$\times 10^{-6}$		2581
$\rho^\mp \pi^\pm$	[ee] (2.30 \pm 0.23)	$\times 10^{-5}$		2581
$\pi^+ \pi^- \pi^+ \pi^-$	< 1.93	$\times 10^{-5}$	CL=90%	2621
$\rho^0 \pi^+ \pi^-$	< 8.8	$\times 10^{-6}$	CL=90%	2575
$\rho^0 \rho^0$	(7.3 \pm 2.8)	$\times 10^{-7}$		2523
$f_0(980) \pi^+ \pi^-$	< 3.8	$\times 10^{-6}$	CL=90%	2541
$\rho^0 f_0(980) \times B(f_0(980) \rightarrow \pi^+ \pi^-)$	< 3	$\times 10^{-7}$	CL=90%	2488
$f_0(980) f_0(980) \times B^2(f_0(980) \rightarrow \pi^+ \pi^-)$	< 1	$\times 10^{-7}$	CL=90%	2451
$f_0(980) f_0(980) \times B(f_0 \rightarrow \pi^+ \pi^-) \times B(f_0 \rightarrow K^+ K^-)$	< 2.3	$\times 10^{-7}$	CL=90%	2451
$a_1(1260)^\mp \pi^\pm$	[ee] (3.3 \pm 0.5)	$\times 10^{-5}$		2494
$a_2(1320)^\mp \pi^\pm$	[ee] < 3.0	$\times 10^{-4}$	CL=90%	2473
$\pi^+ \pi^- \pi^0 \pi^0$	< 3.1	$\times 10^{-3}$	CL=90%	2622
$\rho^+ \rho^-$	(2.42 \pm 0.31)	$\times 10^{-5}$		2523
$a_1(1260)^0 \pi^0$	< 1.1	$\times 10^{-3}$	CL=90%	2495

$\omega\pi^0$	< 5	$\times 10^{-7}$	CL=90%	2580
$\pi^+\pi^+\pi^-\pi^-\pi^0$	< 9.0	$\times 10^{-3}$	CL=90%	2609
$a_1(1260)^+\rho^-$	< 6.1	$\times 10^{-5}$	CL=90%	2433
$a_1(1260)^0\rho^0$	< 2.4	$\times 10^{-3}$	CL=90%	2433
$b_1^\mp\pi^\pm \times B(b_1^\mp \rightarrow \omega\pi^\mp)$	(1.09 ± 0.15)	$\times 10^{-5}$		—
$b_1^0\pi^0 \times B(b_1^0 \rightarrow \omega\pi^0)$	< 1.9	$\times 10^{-6}$	CL=90%	—
$b_1^-\rho^+ \times B(b_1^- \rightarrow \omega\pi^-)$	< 1.4	$\times 10^{-6}$	CL=90%	—
$b_1^0\rho^0 \times B(b_1^0 \rightarrow \omega\pi^0)$	< 3.4	$\times 10^{-6}$	CL=90%	—
$\pi^+\pi^+\pi^+\pi^-\pi^-\pi^0$	< 3.0	$\times 10^{-3}$	CL=90%	2592
$a_1(1260)^+ a_1(1260)^- \times B^2(a_1^+ \rightarrow 2\pi^+\pi^-)$	(1.18 ± 0.31)	$\times 10^{-5}$		2336
$\pi^+\pi^+\pi^+\pi^-\pi^-\pi^0$	< 1.1	%	CL=90%	2572

Baryon modes

$p\bar{p}$	< 1.1	$\times 10^{-7}$	CL=90%	2467
$p\bar{p}\pi^+\pi^-$	< 2.5	$\times 10^{-4}$	CL=90%	2406
$p\bar{p}K^0$	(2.66 ± 0.32)	$\times 10^{-6}$		2347
$\Theta(1540)^+\bar{p} \times B(\Theta(1540)^+ \rightarrow [yyy]$	< 5	$\times 10^{-8}$	CL=90%	2318
$\rho K_S^0)$				
$f_J(2220)K^0 \times B(f_J(2220) \rightarrow \rho\bar{p})$	< 4.5	$\times 10^{-7}$	CL=90%	2135
$p\bar{p}K^*(892)^0$	(1.24 \pm $\frac{0.28}{0.25}$)	$\times 10^{-6}$		2215
$f_J(2220)K_0^* \times B(f_J(2220) \rightarrow \rho\bar{p})$	< 1.5	$\times 10^{-7}$	CL=90%	—
$p\bar{\Lambda}\pi^-$	(3.14 ± 0.29)	$\times 10^{-6}$		2401
$p\bar{\Sigma}(1385)^-$	< 2.6	$\times 10^{-7}$	CL=90%	2363
$\Delta^0\bar{\Lambda}$	< 9.3	$\times 10^{-7}$	CL=90%	2364
$p\bar{\Lambda}K^-$	< 8.2	$\times 10^{-7}$	CL=90%	2308
$p\bar{\Sigma}^0\pi^-$	< 3.8	$\times 10^{-6}$	CL=90%	2383
$\bar{\Lambda}\Lambda$	< 3.2	$\times 10^{-7}$	CL=90%	2392
$\bar{\Lambda}\Lambda K^0$	(4.8 \pm $\frac{1.0}{0.9}$)	$\times 10^{-6}$		2250
$\bar{\Lambda}\Lambda K^{*0}$	(2.5 \pm $\frac{0.9}{0.8}$)	$\times 10^{-6}$		2098
$\bar{\Lambda}\Lambda D^0$	(1.1 \pm $\frac{0.6}{0.5}$)	$\times 10^{-5}$		1661
$\Delta^0\bar{\Delta}^0$	< 1.5	$\times 10^{-3}$	CL=90%	2335
$\Delta^{++}\bar{\Delta}^{--}$	< 1.1	$\times 10^{-4}$	CL=90%	2335
$\bar{D}^0 p\bar{p}$	(1.14 ± 0.09)	$\times 10^{-4}$		1862
$D_S^- \bar{\Lambda}\rho$	(2.8 ± 0.9)	$\times 10^{-5}$		1710
$\bar{D}^*(2007)^0 p\bar{p}$	(1.03 ± 0.13)	$\times 10^{-4}$		1788
$D^*(2010)^- p\bar{n}$	(1.5 ± 0.4)	$\times 10^{-3}$		1785
$D^- p\bar{p}\pi^+$	(3.38 ± 0.32)	$\times 10^{-4}$		1786
$D^*(2010)^- p\bar{p}\pi^+$	(5.0 ± 0.5)	$\times 10^{-4}$		1707
$\Theta_c \bar{p}\pi^+ \times B(\Theta_c \rightarrow D^- p)$	< 9	$\times 10^{-6}$	CL=90%	—
$\Theta_c \bar{p}\pi^+ \times B(\Theta_c \rightarrow D^{*-} p)$	< 1.4	$\times 10^{-5}$	CL=90%	—
$\bar{\Sigma}_c^{--} \Delta^{++}$	< 1.0	$\times 10^{-3}$	CL=90%	1839
$\bar{\Lambda}_c^- p\pi^+\pi^-$	(1.3 ± 0.4)	$\times 10^{-3}$		1934
$\bar{\Lambda}_c^- \rho$	(2.0 ± 0.4)	$\times 10^{-5}$		2021
$\bar{\Lambda}_c^- p\pi^0$	< 5.9	$\times 10^{-4}$	CL=90%	1982
$\bar{\Lambda}_c^- p\pi^+\pi^-\pi^0$	< 5.07	$\times 10^{-3}$	CL=90%	1882
$\bar{\Lambda}_c^- p\pi^+\pi^-\pi^+\pi^-$	< 2.74	$\times 10^{-3}$	CL=90%	1821
$\bar{\Lambda}_c^- p\pi^+\pi^-$	(1.12 ± 0.32)	$\times 10^{-3}$		1934
$\bar{\Lambda}_c^- p\pi^+\pi^-$ (nonresonant)	(6.4 ± 1.9)	$\times 10^{-4}$		1934

$\bar{\Sigma}_c(2520)^{--} p \pi^+$	(1.2 ± 0.4) × 10 ⁻⁴		1860
$\bar{\Sigma}_c(2520)^0 p \pi^-$	< 3.8 × 10 ⁻⁵	CL=90%	1860
$\bar{\Sigma}_c(2455)^0 p \pi^-$	(1.5 ± 0.5) × 10 ⁻⁴		1895
$\bar{\Sigma}_c(2455)^0 N^0 \times B(N^0 \rightarrow p \pi^-)$	(8.0 ± 2.9) × 10 ⁻⁵		—
$\bar{\Sigma}_c(2455)^{--} p \pi^+$	(2.2 ± 0.7) × 10 ⁻⁴		1895
$\Lambda_c^- p K^+ \pi^-$	(4.3 ± 1.4) × 10 ⁻⁵		—
$\bar{\Sigma}_c(2455)^{--} p K^+ \times B(\bar{\Sigma}_c^{--} \rightarrow \bar{\Lambda}_c^- \pi^-)$	(1.1 ± 0.4) × 10 ⁻⁵		1754
$\Lambda_c^- p K^*(892)^0$	< 2.42 × 10 ⁻⁵	CL=90%	—
$\bar{\Lambda}_c^- \Lambda_c^+$	< 6.2 × 10 ⁻⁵	CL=90%	1319
$\bar{\Lambda}_c(2593)^- / \bar{\Lambda}_c(2625)^- p$	< 1.1 × 10 ⁻⁴	CL=90%	—
$\bar{\Xi}_c^- \Lambda_c^+ \times B(\bar{\Xi}_c^- \rightarrow \bar{\Xi}^+ \pi^- \pi^-)$	(2.2 ± 2.3) × 10 ⁻⁵	S=1.9	1147
$\Lambda_c^+ \Lambda_c^- K^0$	(5.4 ± 3.2) × 10 ⁻⁴		—

**Lepton Family number (LF) violating modes, or
ΔB = 1 weak neutral current (BI) modes**

$\gamma\gamma$	B1	< 6.2 × 10 ⁻⁷	CL=90%	2640
$e^+ e^-$	B1	< 8.3 × 10 ⁻⁸	CL=90%	2640
$e^+ e^- \gamma$	B1	< 1.2 × 10 ⁻⁷	CL=90%	2640
$\mu^+ \mu^-$	B1	< 1.5 × 10 ⁻⁸	CL=90%	2638
$\mu^+ \mu^- \gamma$	B1	< 1.6 × 10 ⁻⁷	CL=90%	2638
$\tau^+ \tau^-$	B1	< 4.1 × 10 ⁻³	CL=90%	1952
$\pi^0 \ell^+ \ell^-$	B1	< 1.2 × 10 ⁻⁷	CL=90%	2638
$\pi^0 e^+ e^-$	B1	< 1.4 × 10 ⁻⁷	CL=90%	2638
$\pi^0 \mu^+ \mu^-$	B1	< 1.8 × 10 ⁻⁷	CL=90%	2634
$\pi^0 \nu \bar{\nu}$	B1	< 2.2 × 10 ⁻⁴	CL=90%	2638
$K^0 \ell^+ \ell^-$	B1 [nnn]	(3.1 $\begin{smallmatrix} + \\ - \end{smallmatrix}$ $\begin{smallmatrix} 0.8 \\ 0.7 \end{smallmatrix}$) × 10 ⁻⁷		2616
$K^0 e^+ e^-$	B1	(1.6 $\begin{smallmatrix} + \\ - \end{smallmatrix}$ $\begin{smallmatrix} 1.0 \\ 0.8 \end{smallmatrix}$) × 10 ⁻⁷		2616
$K^0 \mu^+ \mu^-$	B1	(4.5 $\begin{smallmatrix} + \\ - \end{smallmatrix}$ $\begin{smallmatrix} 1.2 \\ 1.0 \end{smallmatrix}$) × 10 ⁻⁷		2612
$K^0 \nu \bar{\nu}$	B1	< 1.6 × 10 ⁻⁴	CL=90%	2616
$\rho^0 \nu \bar{\nu}$	B1	< 4.4 × 10 ⁻⁴	CL=90%	2583
$K^*(892)^0 \ell^+ \ell^-$	B1 [nnn]	(9.9 $\begin{smallmatrix} + \\ - \end{smallmatrix}$ $\begin{smallmatrix} 1.2 \\ 1.1 \end{smallmatrix}$) × 10 ⁻⁷		2564
$K^*(892)^0 e^+ e^-$	B1	(1.03 $\begin{smallmatrix} + \\ - \end{smallmatrix}$ $\begin{smallmatrix} 0.19 \\ 0.17 \end{smallmatrix}$) × 10 ⁻⁶		2564
$K^*(892)^0 \mu^+ \mu^-$	B1	(1.05 $\begin{smallmatrix} + \\ - \end{smallmatrix}$ $\begin{smallmatrix} 0.16 \\ 0.13 \end{smallmatrix}$) × 10 ⁻⁶		2560
$K^*(892)^0 \nu \bar{\nu}$	B1	< 1.2 × 10 ⁻⁴	CL=90%	2564
$\phi \nu \bar{\nu}$	B1	< 5.8 × 10 ⁻⁵	CL=90%	2541
$e^\pm \mu^\mp$	LF [ee]	< 6.4 × 10 ⁻⁸	CL=90%	2639
$\pi^0 e^\pm \mu^\mp$	LF	< 1.4 × 10 ⁻⁷	CL=90%	2637
$K^0 e^\pm \mu^\mp$	LF	< 2.7 × 10 ⁻⁷	CL=90%	2615
$K^*(892)^0 e^+ \mu^-$	LF	< 5.3 × 10 ⁻⁷	CL=90%	2563
$K^*(892)^0 e^- \mu^+$	LF	< 3.4 × 10 ⁻⁷	CL=90%	2563
$K^*(892)^0 e^\pm \mu^\mp$	LF	< 5.8 × 10 ⁻⁷	CL=90%	2563
$e^\pm \tau^\mp$	LF [ee]	< 2.8 × 10 ⁻⁵	CL=90%	2341
$\mu^\pm \tau^\mp$	LF [ee]	< 2.2 × 10 ⁻⁵	CL=90%	2339
invisible	B1	< 2.2 × 10 ⁻⁴	CL=90%	—
$\nu \bar{\nu} \gamma$	B1	< 4.7 × 10 ⁻⁵	CL=90%	2640

B^\pm/B^0 ADMIXTURE

CP violation

$$A_{CP}(B \rightarrow K^*(892)\gamma) = -0.003 \pm 0.017$$

$$A_{CP}(B \rightarrow s\gamma) = -0.014 \pm 0.028$$

$$A_{CP}(b \rightarrow (s+d)\gamma) = -0.11 \pm 0.12$$

$$A_{CP}(b \rightarrow X_s \ell^+ \ell^-) = -0.22 \pm 0.26$$

$$A_{CP}(B \rightarrow K^* \ell^+ \ell^-) = -0.07 \pm 0.08$$

$$A_{CP}(B \rightarrow K^* e^+ e^-) = -0.18 \pm 0.15$$

$$A_{CP}(B \rightarrow K^* \mu^+ \mu^-) = -0.03 \pm 0.13$$

The branching fraction measurements are for an admixture of B mesons at the $\Upsilon(4S)$. The values quoted assume that $B(\Upsilon(4S) \rightarrow B\bar{B}) = 100\%$.

For inclusive branching fractions, e.g., $B \rightarrow D^\pm$ anything, the treatment of multiple D 's in the final state must be defined. One possibility would be to count the number of events with one-or-more D 's and divide by the total number of B 's. Another possibility would be to count the total number of D 's and divide by the total number of B 's, which is the definition of average multiplicity. The two definitions are identical if only one D is allowed in the final state. Event though the "one-or-more" definition seems sensible, for practical reasons inclusive branching fractions are almost always measured using the multiplicity definition. For heavy final state particles, authors call their results inclusive branching fractions while for light particles some authors call their results multiplicities. In the B sections, we list all results as inclusive branching fractions, adopting a multiplicity definition. This means that inclusive branching fractions can exceed 100% and that inclusive partial widths can exceed total widths, just as inclusive cross sections can exceed total cross section.

\bar{B} modes are charge conjugates of the modes below. Reactions indicate the weak decay vertex and do not include mixing.

B DECAY MODES	Fraction (Γ_i/Γ)	Scale factor/ Confidence level	p (MeV/c)
Semileptonic and leptonic modes			
$B \rightarrow e^+ \nu_e$ anything	[zzz] (10.74 ± 0.16) %		—
$B \rightarrow \bar{p} e^+ \nu_e$ anything	< 5.9 × 10 ⁻⁴	CL=90%	—
$B \rightarrow \mu^+ \nu_\mu$ anything	[zzz] (10.74 ± 0.16) %		—
$B \rightarrow \ell^+ \nu_\ell$ anything	[nnn,zzz] (10.74 ± 0.16) %		—
$B \rightarrow D^- \ell^+ \nu_\ell$ anything	[nnn] (2.8 ± 0.9) %		—
$B \rightarrow \bar{D}^0 \ell^+ \nu_\ell$ anything	[nnn] (7.2 ± 1.4) %		—
$B \rightarrow \bar{D} \ell \nu_\ell$	(2.40 ± 0.12) %		2310
$B \rightarrow D \tau^+ \nu_\tau$	(8.6 ± 2.7) × 10 ⁻³		1911
$B \rightarrow D^{*-} \ell^+ \nu_\ell$ anything	[aaa] (6.7 ± 1.3) × 10 ⁻³		—
$B \rightarrow D^* \tau^+ \nu_\tau$	(1.62 ± 0.33) %		1837
$B \rightarrow \bar{D}^{*+} \ell^+ \nu_\ell$	[nnn,bbbb] (2.7 ± 0.7) %		—
$B \rightarrow \bar{D}_1(2420) \ell^+ \nu_\ell$ anything	(3.8 ± 1.3) × 10 ⁻³	S=2.4	—
$B \rightarrow D \pi \ell^+ \nu_\ell$ anything + $D^* \pi \ell^+ \nu_\ell$ anything	(2.6 ± 0.5) %	S=1.5	—
$B \rightarrow D \pi \ell^+ \nu_\ell$ anything	(1.5 ± 0.6) %		—
$B \rightarrow D^* \pi \ell^+ \nu_\ell$ anything	(1.9 ± 0.4) %		—
$B \rightarrow \bar{D}_2^*(2460) \ell^+ \nu_\ell$ anything	(4.4 ± 1.6) × 10 ⁻³		—
$B \rightarrow D^{*-} \pi^+ \ell^+ \nu_\ell$ anything	(1.00 ± 0.34) %		—
$B \rightarrow D_5^- \ell^+ \nu_\ell$ anything	[nnn] < 7 × 10 ⁻³	CL=90%	—

$B \rightarrow D_s^- \ell^+ \nu_\ell K^+$ anything	$[nnn] < 5$	$\times 10^{-3}$	CL=90%	-
$B \rightarrow D_s^- \ell^+ \nu_\ell K^0$ anything	$[nnn] < 7$	$\times 10^{-3}$	CL=90%	-
$B \rightarrow \ell^+ \nu_\ell$ charm	$(10.58 \pm 0.15) \%$			-
$B \rightarrow X_u \ell^+ \nu_\ell$	$(2.33 \pm 0.22) \times 10^{-3}$			-
$B \rightarrow \pi \ell \nu_\ell$	$(1.35 \pm 0.10) \times 10^{-4}$			2638
$B \rightarrow K^+ \ell^+ \nu_\ell$ anything	$[nnn] (6.2 \pm 0.5) \%$			-
$B \rightarrow K^- \ell^+ \nu_\ell$ anything	$[nnn] (10 \pm 4) \times 10^{-3}$			-
$B \rightarrow K^0 / \bar{K}^0 \ell^+ \nu_\ell$ anything	$[nnn] (4.5 \pm 0.5) \%$			-
D, D*, or D_s modes				
$B \rightarrow D^\pm$ anything	$(23.1 \pm 1.5) \%$			-
$B \rightarrow D^0 / \bar{D}^0$ anything	$(62.5 \pm 2.9) \%$		S=1.3	-
$B \rightarrow D^*(2010)^\pm$ anything	$(22.5 \pm 1.5) \%$			-
$B \rightarrow D^*(2007)^0$ anything	$(26.0 \pm 2.7) \%$			-
$B \rightarrow D_s^\pm$ anything	$[ee] (8.3 \pm 0.8) \%$			-
$B \rightarrow D_s^{*\pm}$ anything	$(6.3 \pm 1.0) \%$			-
$B \rightarrow D_s^{*\pm} \bar{D}^*$	$(3.4 \pm 0.6) \%$			-
$B \rightarrow D^*(*) \bar{D}^*(*) K^0 + D^*(*) \bar{D}^*(*) K^\pm$	$[ee,cccc] (7.1 \begin{smallmatrix} + 2.7 \\ - 1.7 \end{smallmatrix}) \%$			-
$b \rightarrow c \bar{c} s$	$(22 \pm 4) \%$			-
$B \rightarrow D_s^*(*) \bar{D}^*(*)$	$[ee,cccc] (3.9 \pm 0.4) \%$			-
$B \rightarrow D^* D^*(2010)^\pm$	$[ee] < 5.9$	$\times 10^{-3}$	CL=90%	1711
$B \rightarrow D D^*(2010)^\pm + D^* D^\pm$	$[ee] < 5.5$	$\times 10^{-3}$	CL=90%	-
$B \rightarrow D D^\pm$	$[ee] < 3.1$	$\times 10^{-3}$	CL=90%	1866
$B \rightarrow D_s^*(*)^\pm \bar{D}^*(*) X (n\pi^\pm)$	$[ee,cccc] (9 \begin{smallmatrix} + 5 \\ - 4 \end{smallmatrix}) \%$			-
$B \rightarrow D^*(2010)\gamma$	< 1.1	$\times 10^{-3}$	CL=90%	2257
$B \rightarrow D_s^+ \pi^-, D_s^{*+} \pi^-, D_s^+ \rho^-, D_s^{*+} \rho^-, D_s^+ \pi^0, D_s^{*+} \pi^0, D_s^+ \eta, D_s^{*+} \eta, D_s^+ \rho^0, D_s^{*+} \rho^0, D_s^+ \omega, D_s^{*+} \omega$	$[ee] < 4$	$\times 10^{-4}$	CL=90%	-
$B \rightarrow D_{s1}(2536)^+$ anything	< 9.5	$\times 10^{-3}$	CL=90%	-
Charmonium modes				
$B \rightarrow J/\psi(1S)$ anything	$(1.094 \pm 0.032) \%$		S=1.1	-
$B \rightarrow J/\psi(1S)$ (direct) anything	$(7.8 \pm 0.4) \times 10^{-3}$		S=1.1	-
$B \rightarrow \psi(2S)$ anything	$(3.07 \pm 0.21) \times 10^{-3}$			-
$B \rightarrow \chi_{c1}(1P)$ anything	$(3.86 \pm 0.27) \times 10^{-3}$			-
$B \rightarrow \chi_{c1}(1P)$ (direct) anything	$(3.22 \pm 0.25) \times 10^{-3}$			-
$B \rightarrow \chi_{c2}(1P)$ anything	$(1.3 \pm 0.4) \times 10^{-3}$		S=1.9	-
$B \rightarrow \chi_{c2}(1P)$ (direct) anything	$(1.65 \pm 0.31) \times 10^{-3}$			-
$B \rightarrow \eta_c(1S)$ anything	< 9	$\times 10^{-3}$	CL=90%	-
$B \rightarrow KX(3872) \times B(X \rightarrow D^0 \bar{D}^0 \pi^0)$	$(1.2 \pm 0.4) \times 10^{-4}$			1141

$B \rightarrow K X(3872) \times B(X \rightarrow D^{*0} D^0)$	$(8.0 \pm 2.2) \times 10^{-5}$		1141
$B \rightarrow K X(3940) \times B(X \rightarrow D^{*0} D^0)$	$< 6.7 \times 10^{-5}$	CL=90%	1084
$B \rightarrow K X(3945) \times B(X \rightarrow \omega J/\psi)$	$[dddd] (7.1 \pm 3.4) \times 10^{-5}$		1106

K or K* modes

$B \rightarrow K^\pm$ anything	[ee] $(78.9 \pm 2.5) \%$		-
$B \rightarrow K^+$ anything	$(66 \pm 5) \%$		-
$B \rightarrow K^-$ anything	$(13 \pm 4) \%$		-
$B \rightarrow K^0 / \bar{K}^0$ anything	[ee] $(64 \pm 4) \%$		-
$B \rightarrow K^*(892)^\pm$ anything	$(18 \pm 6) \%$		-
$B \rightarrow K^*(892)^0 / \bar{K}^*(892)^0$ anything	[ee] $(14.6 \pm 2.6) \%$		-
$B \rightarrow K^*(892)\gamma$	$(4.2 \pm 0.6) \times 10^{-5}$		2564
$B \rightarrow \eta K \gamma$	$(8.5 \begin{smallmatrix} +1.8 \\ -1.6 \end{smallmatrix}) \times 10^{-6}$		2588
$B \rightarrow K_1(1400)\gamma$	$< 1.27 \times 10^{-4}$	CL=90%	2453
$B \rightarrow K_2^*(1430)\gamma$	$(1.7 \begin{smallmatrix} +0.6 \\ -0.5 \end{smallmatrix}) \times 10^{-5}$		2447
$B \rightarrow K_2(1770)\gamma$	$< 1.2 \times 10^{-3}$	CL=90%	2342
$B \rightarrow K_3^*(1780)\gamma$	$< 3.7 \times 10^{-5}$	CL=90%	2341
$B \rightarrow K_4^*(2045)\gamma$	$< 1.0 \times 10^{-3}$	CL=90%	2244
$B \rightarrow K \eta'(958)$	$(8.3 \pm 1.1) \times 10^{-5}$		2528
$B \rightarrow K^*(892)\eta'(958)$	$(4.1 \pm 1.1) \times 10^{-6}$		2472
$B \rightarrow K \eta$	$< 5.2 \times 10^{-6}$	CL=90%	2588
$B \rightarrow K^*(892)\eta$	$(1.8 \pm 0.5) \times 10^{-5}$		2534
$B \rightarrow K \phi \phi$	$(2.3 \pm 0.9) \times 10^{-6}$		2306
$B \rightarrow \bar{b} \rightarrow \bar{s} \gamma$	$(3.60 \pm 0.23) \times 10^{-4}$		-
$B \rightarrow \bar{b} \rightarrow \bar{d} \gamma$	$(1.2 \pm 0.6) \times 10^{-5}$		-
$B \rightarrow \bar{b} \rightarrow \bar{s} \text{gluon}$	$< 6.8 \%$	CL=90%	-
$B \rightarrow \eta$ anything	$< 4.4 \times 10^{-4}$	CL=90%	-
$B \rightarrow \eta'$ anything	$(4.2 \pm 0.9) \times 10^{-4}$		-

Light unflavored meson modes

$B \rightarrow \rho \gamma$	$(1.39 \pm 0.25) \times 10^{-6}$	S=1.2	2583
$B \rightarrow \rho/\omega \gamma$	$(1.30 \pm 0.23) \times 10^{-6}$	S=1.2	-
$B \rightarrow \pi^\pm$ anything	[ee,eeee] $(358 \pm 7) \%$		-
$B \rightarrow \pi^0$ anything	$(235 \pm 11) \%$		-
$B \rightarrow \eta$ anything	$(17.6 \pm 1.6) \%$		-
$B \rightarrow \rho^0$ anything	$(21 \pm 5) \%$		-
$B \rightarrow \omega$ anything	$< 81 \%$	CL=90%	-
$B \rightarrow \phi$ anything	$(3.43 \pm 0.12) \%$		-
$B \rightarrow \phi K^*(892)$	$< 2.2 \times 10^{-5}$	CL=90%	2460

Baryon modes

$B \rightarrow \Lambda_c^+ / \bar{\Lambda}_c^-$ anything	$(4.5 \pm 1.2) \%$		-
$B \rightarrow \bar{\Lambda}_c^- e^+$ anything	$< 2.3 \times 10^{-3}$	CL=90%	-
$B \rightarrow \bar{\Lambda}_c^- p$ anything	$(2.6 \pm 0.8) \%$		-
$B \rightarrow \bar{\Lambda}_c^- p e^+ \nu_e$	$< 1.0 \times 10^{-3}$	CL=90%	2021
$B \rightarrow \bar{\Sigma}_c^{--}$ anything	$(4.2 \pm 2.4) \times 10^{-3}$		-
$B \rightarrow \bar{\Sigma}_c^-$ anything	$< 9.6 \times 10^{-3}$	CL=90%	-
$B \rightarrow \bar{\Sigma}_c^0$ anything	$(4.6 \pm 2.4) \times 10^{-3}$		-
$B \rightarrow \bar{\Sigma}_c^0 N (N = p \text{ or } n)$	$< 1.5 \times 10^{-3}$	CL=90%	1938

$B \rightarrow \Xi_c^0$ anything	(1.93 ± 0.30) × 10 ⁻⁴	S=1.1	-
× $B(\Xi_c^0 \rightarrow \Xi^- \pi^+)$			
$B \rightarrow \Xi_c^+$ anything	(4.5 ± 1.3 / 1.2) × 10 ⁻⁴		-
× $B(\Xi_c^+ \rightarrow \Xi^- \pi^+ \pi^+)$			
$B \rightarrow p/\bar{p}$ anything	[ee] (8.0 ± 0.4) %		-
$B \rightarrow p/\bar{p}$ (direct) anything	[ee] (5.5 ± 0.5) %		-
$B \rightarrow \Lambda/\bar{\Lambda}$ anything	[ee] (4.0 ± 0.5) %		-
$B \rightarrow \Xi^-/\Xi^+$ anything	[ee] (2.7 ± 0.6) × 10 ⁻³		-
$B \rightarrow$ baryons anything	(6.8 ± 0.6) %		-
$B \rightarrow p\bar{p}$ anything	(2.47 ± 0.23) %		-
$B \rightarrow \Lambda\bar{\Lambda}/\bar{\Lambda}p$ anything	[ee] (2.5 ± 0.4) %		-
$B \rightarrow \Lambda\bar{\Lambda}$ anything	< 5 × 10 ⁻³	CL=90%	-

Lepton Family number (LF) violating modes or ΔB = 1 weak neutral current (BI) modes

$B \rightarrow s e^+ e^-$	B1	(4.7 ± 1.3) × 10 ⁻⁶		
$B \rightarrow s \mu^+ \mu^-$	B1	(4.3 ± 1.2) × 10 ⁻⁶		
$B \rightarrow s \ell^+ \ell^-$	B1	[nnn] (4.5 ± 1.0) × 10 ⁻⁶		
$B \rightarrow \pi \ell^+ \ell^-$		< 6.2 × 10 ⁻⁸	CL=90%	2638
$B \rightarrow K e^+ e^-$	B1	(4.4 ± 0.6) × 10 ⁻⁷		2617
$B \rightarrow K^*(892) e^+ e^-$	B1	(1.19 ± 0.20) × 10 ⁻⁶	S=1.2	2564
$B \rightarrow K \mu^+ \mu^-$	B1	(4.8 ± 0.6) × 10 ⁻⁷		2612
$B \rightarrow K^*(892) \mu^+ \mu^-$	B1	(1.15 ± 0.15) × 10 ⁻⁶		2560
$B \rightarrow K \ell^+ \ell^-$	B1	(4.5 ± 0.4) × 10 ⁻⁷		2617
$B \rightarrow K^*(892) \ell^+ \ell^-$	B1	(1.08 ± 0.11) × 10 ⁻⁶		2564
$B \rightarrow K^* \nu \bar{\nu}$		< 8 × 10 ⁻⁵	CL=90%	-
$B \rightarrow s e^\pm \mu^\mp$	LF [ee]	< 2.2 × 10 ⁻⁵	CL=90%	-
$B \rightarrow \pi e^\pm \mu^\mp$	LF	< 9.2 × 10 ⁻⁸	CL=90%	2637
$B \rightarrow \rho e^\pm \mu^\mp$	LF	< 3.2 × 10 ⁻⁶	CL=90%	2582
$B \rightarrow K e^\pm \mu^\mp$	LF	< 3.8 × 10 ⁻⁸	CL=90%	2616
$B \rightarrow K^*(892) e^\pm \mu^\mp$	LF	< 5.1 × 10 ⁻⁷	CL=90%	2563

$B^\pm/B^0/B_s^0/b$ -baryon ADMIXTURE

These measurements are for an admixture of bottom particles at high energy (LEP, Tevatron, $S\bar{p}\bar{p}S$).

Mean life $\tau = (1.568 \pm 0.009) \times 10^{-12}$ s

Mean life $\tau = (1.72 \pm 0.10) \times 10^{-12}$ s Charged b -hadron admixture

Mean life $\tau = (1.58 \pm 0.14) \times 10^{-12}$ s Neutral b -hadron admixture

$\tau_{\text{charged } b\text{-hadron}}/\tau_{\text{neutral } b\text{-hadron}} = 1.09 \pm 0.13$

$|\Delta\tau_b|/\tau_{b,\bar{b}} = -0.001 \pm 0.014$

The branching fraction measurements are for an admixture of B mesons and baryons at energies above the $\Upsilon(4S)$. Only the highest energy results (LEP, Tevatron, $S\bar{p}\bar{p}S$) are used in the branching fraction averages. In the following, we assume that the production fractions are the same at the LEP and at the Tevatron.

For inclusive branching fractions, e.g., $B \rightarrow D^\pm$ anything, the values usually are multiplicities, not branching fractions. They can be greater than one.

The modes below are listed for a \bar{b} initial state. b modes are their charge conjugates. Reactions indicate the weak decay vertex and do not include mixing.

\bar{b} DECAY MODES	Fraction (Γ_i/Γ)	Scale factor/ Confidence level	p (MeV/c)
-----------------------	--------------------------------	-----------------------------------	----------------

PRODUCTION FRACTIONS

The production fractions for weakly decaying b -hadrons at high energy have been calculated from the best values of mean lives, mixing parameters, and branching fractions in this edition by the Heavy Flavor Averaging Group (HFAG) as described in the note “ B^0 - \bar{B}^0 Mixing” in the B^0 Particle Listings. The production fractions in b -hadronic Z decay or $p\bar{p}$ collisions at the Tevatron are also listed at the end of the section. Values assume

$$\begin{aligned} B(\bar{b} \rightarrow B^+) &= B(\bar{b} \rightarrow B^0) \\ B(\bar{b} \rightarrow B^+) + B(\bar{b} \rightarrow B^0) + B(\bar{b} \rightarrow B_s^0) + B(b \rightarrow b\text{-baryon}) &= 100\%. \end{aligned}$$

The correlation coefficients between production fractions are also reported:

$$\begin{aligned} \text{cor}(B_s^0, b\text{-baryon}) &= -0.041 \\ \text{cor}(B_s^0, B^\pm=B^0) &= -0.483 \\ \text{cor}(b\text{-baryon}, B^\pm=B^0) &= -0.855. \end{aligned}$$

The notation for production fractions varies in the literature (f_d , d_{B^0} , $f(b \rightarrow \bar{B}^0)$, $\text{Br}(b \rightarrow \bar{B}^0)$). We use our own branching fraction notation here, $B(\bar{b} \rightarrow B^0)$.

B^+	(40.1 \pm 1.3) %	—
B^0	(40.1 \pm 1.3) %	—
B_s^0	(11.3 \pm 1.3) %	—
b -baryon	(8.5 \pm 2.2) %	—
B_C	—	—

DECAY MODES

Semileptonic and leptonic modes

ν anything	(23.1 \pm 1.5) %	—
$\ell^+ \nu_\ell$ anything	[nnn] (10.69 \pm 0.22) %	—
$e^+ \nu_e$ anything	(10.86 \pm 0.35) %	—
$\mu^+ \nu_\mu$ anything	(10.95 $^{+0.29}_{-0.25}$) %	—
$D^- \ell^+ \nu_\ell$ anything	[nnn] (2.2 \pm 0.4) %	S=1.8 —
$D^- \pi^+ \ell^+ \nu_\ell$ anything	(4.9 \pm 1.9) $\times 10^{-3}$	—
$D^- \pi^- \ell^+ \nu_\ell$ anything	(2.6 \pm 1.6) $\times 10^{-3}$	—
$\bar{D}^0 \ell^+ \nu_\ell$ anything	[nnn] (6.84 \pm 0.35) %	—
$\bar{D}^0 \pi^- \ell^+ \nu_\ell$ anything	(1.07 \pm 0.27) %	—
$\bar{D}^0 \pi^+ \ell^+ \nu_\ell$ anything	(2.3 \pm 1.6) $\times 10^{-3}$	—
$D^{*-} \ell^+ \nu_\ell$ anything	[nnn] (2.75 \pm 0.19) %	—
$D^{*-} \pi^- \ell^+ \nu_\ell$ anything	(6 \pm 7) $\times 10^{-4}$	—
$D^{*-} \pi^+ \ell^+ \nu_\ell$ anything	(4.8 \pm 1.0) $\times 10^{-3}$	—
$\bar{D}_j^0 \ell^+ \nu_\ell$ anything $\times B(\bar{D}_j^0 [nnn, ffff])$	(2.6 \pm 0.9) $\times 10^{-3}$	—
$D^{*+} \pi^-$		
$D_j^- \ell^+ \nu_\ell$ anything $\times [nnn, ffff]$	(7.0 \pm 2.3) $\times 10^{-3}$	—
$B(D_j^- \rightarrow D^0 \pi^-)$		
$\bar{D}_2^*(2460)^0 \ell^+ \nu_\ell$ anything $\times B(\bar{D}_2^*(2460)^0 \rightarrow D^{*-} \pi^+)$	< 1.4 $\times 10^{-3}$	CL=90% —
$D_2^*(2460)^- \ell^+ \nu_\ell$ anything $\times B(D_2^*(2460)^- \rightarrow D^0 \pi^-)$	(4.2 $^{+1.5}_{-1.8}$) $\times 10^{-3}$	—
$\bar{D}_2^*(2460)^0 \ell^+ \nu_\ell$ anything $\times B(\bar{D}_2^*(2460)^0 \rightarrow D^- \pi^+)$	(1.6 \pm 0.8) $\times 10^{-3}$	—
charmless $\ell \bar{\nu}_\ell$	[nnn] (1.7 \pm 0.5) $\times 10^{-3}$	—

$\tau^+ \nu_\tau$ anything	(2.41 ± 0.23) %	—
$D^{*-} \tau \nu_\tau$ anything	(9 ± 4) × 10 ⁻³	—
$\bar{c} \rightarrow \ell^- \bar{\nu}_\ell$ anything	[<i>nnn</i>] (8.02 ± 0.19) %	—
$c \rightarrow \ell^+ \nu$ anything	(1.6 ± 0.4) %	—
Charmed meson and baryon modes		
\bar{D}^0 anything	(59.6 ± 2.9) %	—
$D^0 D_S^\pm$ anything	[<i>ee</i>] (9.1 ± 4.0 / 2.8) %	—
$D^\mp D_S^\pm$ anything	[<i>ee</i>] (4.0 ± 2.3 / 1.8) %	—
$\bar{D}^0 D^0$ anything	[<i>ee</i>] (5.1 ± 2.0 / 1.8) %	—
$D^0 D^\pm$ anything	[<i>ee</i>] (2.7 ± 1.8 / 1.6) %	—
$D^\pm D^\mp$ anything	[<i>ee</i>] < 9 × 10 ⁻³ CL=90%	—
D^- anything	(22.7 ± 1.8) %	—
$D^*(2010)^+$ anything	(17.3 ± 2.0) %	—
$D_1(2420)^0$ anything	(5.0 ± 1.5) %	—
$D^*(2010)^\mp D_S^\pm$ anything	[<i>ee</i>] (3.3 ± 1.6 / 1.3) %	—
$D^0 D^*(2010)^\pm$ anything	[<i>ee</i>] (3.0 ± 1.1 / 0.9) %	—
$D^*(2010)^\pm D^\mp$ anything	[<i>ee</i>] (2.5 ± 1.2 / 1.0) %	—
$D^*(2010)^\pm D^*(2010)^\mp$ anything	[<i>ee</i>] (1.2 ± 0.4) %	—
$\bar{D} D$ anything	(10 ± 11 / -10) %	—
$D_2^*(2460)^0$ anything	(4.7 ± 2.7) %	—
D_S^- anything	(14.7 ± 2.1) %	—
D_S^+ anything	(10.1 ± 3.1) %	—
Λ_c^+ anything	(9.7 ± 2.9) %	—
\bar{c} / c anything	[<i>eeee</i>] (116.2 ± 3.2) %	—
Charmonium modes		
$J/\psi(1S)$ anything	(1.16 ± 0.10) %	—
$\psi(2S)$ anything	(4.8 ± 2.4) × 10 ⁻³	—
$\chi_{c1}(1P)$ anything	(1.4 ± 0.4) %	—
K or K* modes		
$\bar{s} \gamma$	(3.1 ± 1.1) × 10 ⁻⁴	—
$\bar{s} \bar{\nu} \nu$	< 6.4 × 10 ⁻⁴ CL=90%	—
K^\pm anything	(74 ± 6) %	—
K_S^0 anything	(29.0 ± 2.9) %	—
Pion modes		
π^\pm anything	(397 ± 21) %	—
π^0 anything	[<i>eeee</i>] (278 ± 60) %	—
ϕ anything	(2.82 ± 0.23) %	—
Baryon modes		
p / \bar{p} anything	(13.1 ± 1.1) %	—
Other modes		
charged anything	[<i>eeee</i>] (497 ± 7) %	—
hadron ⁺ hadron ⁻	(1.7 ± 1.0 / 0.7) × 10 ⁻⁵	—
charmless	(7 ± 21) × 10 ⁻³	—

Baryon modes

$\Lambda/\bar{\Lambda}$ anything	(5.9 ± 0.6) %	—
b -baryon anything	(10.2 ± 2.8) %	—

 $\Delta B = 1$ weak neutral current (B_1) modes

$\mu^+ \mu^-$ anything	B_1	< 3.2	$\times 10^{-4}$	CL=90%	—
------------------------	-------	-------	------------------	--------	---

 B^*

$$I(J^P) = \frac{1}{2}(1^-)$$

I, J, P need confirmation. Quantum numbers shown are quark-model predictions.

$$\text{Mass } m_{B^*} = 5325.1 \pm 0.5 \text{ MeV}$$

$$m_{B^*} - m_B = 45.78 \pm 0.35 \text{ MeV}$$

 B^* DECAY MODESFraction (Γ_i/Γ) ρ (MeV/c)

$B\gamma$	dominant	45
-----------	----------	----

 $B_1(5721)^0$

$$I(J^P) = \frac{1}{2}(1^+)$$

I, J, P need confirmation.

$$B_1(5721)^0 \text{ MASS} = 5723.4 \pm 2.0 \text{ MeV} \quad (S = 1.1)$$

$$m_{B_1^0} - m_{B^+} = 444.3 \pm 2.0 \text{ MeV} \quad (S = 1.1)$$

 $B_1(5721)^0$ DECAY MODESFraction (Γ_i/Γ) ρ (MeV/c)

$B^{*+} \pi^-$	dominant	—
----------------	----------	---

 $B_2^*(5747)^0$

$$I(J^P) = \frac{1}{2}(2^+)$$

I, J, P need confirmation.

$$B_2^*(5747)^0 \text{ MASS} = 5743 \pm 5 \text{ MeV} \quad (S = 2.8)$$

$$\text{Full width } \Gamma = 23_{-11}^{+5} \text{ MeV}$$

$$m_{B_2^{*0}} - m_{B_1^0} = 19 \pm 6 \text{ MeV} \quad (S = 3.0)$$

 $B_2^*(5747)^0$ DECAY MODESFraction (Γ_i/Γ) ρ (MeV/c)

$B^+ \pi^-$	dominant	424
$B^{*+} \pi^-$	dominant	—

BOTTOM, STRANGE MESONS

($B = \pm 1, S = \mp 1$)

$$B_S^0 = s\bar{b}, \bar{B}_S^0 = \bar{s}b, \quad \text{similarly for } B_S^{*\prime}\text{'s}$$

 B_S^0

$$I(J^P) = 0(0^-)$$

I, J, P need confirmation. Quantum numbers shown are quark-model predictions.

$$\text{Mass } m_{B_S^0} = 5366.3 \pm 0.6 \text{ MeV} \quad (S = 1.1)$$

$$\text{Mean life } \tau = (1.472_{-0.026}^{+0.024}) \times 10^{-12} \text{ s}$$

$$c\tau = 441 \mu\text{m}$$

$$\begin{aligned} \Delta\Gamma_{B_S^0} &= \Gamma_{B_S^0 L} - \Gamma_{B_S^0 H} = (0.062_{-0.037}^{+0.034}) \times 10^{12} \text{ s}^{-1} \\ &= 18.6_{-11.1}^{+10.2} \mu\text{m} \end{aligned}$$

B_S^0 - \bar{B}_S^0 mixing parameters

$$\begin{aligned} \Delta m_{B_S^0} &= m_{B_S^0 H} - m_{B_S^0 L} = (17.77 \pm 0.12) \times 10^{12} \hbar \text{ s}^{-1} \\ &= (117.0 \pm 0.8) \times 10^{-10} \text{ MeV} \end{aligned}$$

$$x_S = \Delta m_{B_S^0} / \Gamma_{B_S^0} = 26.2 \pm 0.5$$

$$\chi_S = 0.49927 \pm 0.00003$$

CP violation parameters in B_S^0

$$\text{Re}(\epsilon_{B_S^0}) / (1 + |\epsilon_{B_S^0}|^2) = (-0.9 \pm 2.6) \times 10^{-3}$$

$$\text{CP Violation phase } \beta_S = 0.47_{-0.21}^{+0.13} \text{ or } 1.09_{-0.13}^{+0.21}$$

These branching fractions all scale with $B(\bar{b} \rightarrow B_S^0)$, the LEP B_S^0 production fraction. The first four were evaluated using $B(\bar{b} \rightarrow B_S^0) = (10.7 \pm 1.2)\%$ and the rest assume $B(\bar{b} \rightarrow B_S^0) = 12\%$.

The branching fraction $B(B_S^0 \rightarrow D_S^- \ell^+ \nu_\ell \text{ anything})$ is not a pure measurement since the measured product branching fraction $B(\bar{b} \rightarrow B_S^0) \times B(B_S^0 \rightarrow D_S^- \ell^+ \nu_\ell \text{ anything})$ was used to determine $B(\bar{b} \rightarrow B_S^0)$, as described in the note on " B^0 - \bar{B}^0 Mixing"

For inclusive branching fractions, e.g., $B \rightarrow D^\pm \text{ anything}$, the values usually are multiplicities, not branching fractions. They can be greater than one.

B_S^0 DECAY MODES	Fraction (Γ_i/Γ)	Confidence level	P (MeV/c)
$D_S^- \text{ anything}$	(93 \pm 25) %		—
$D_S^- \ell^+ \nu_\ell \text{ anything}$	[gggg] (7.9 \pm 2.4) %		—
$D_{S1}(2536)^- \mu^+ \nu_\mu X \times$ $B(D_{S1}^- \rightarrow D^{*-} K_S^0)$	(2.4 \pm 0.7) $\times 10^{-3}$		—
$D_S^- \pi^+$	(3.2 \pm 0.5) $\times 10^{-3}$		2320
$D_S^- \pi^+ \pi^+ \pi^-$	(8.4 \pm 3.3) $\times 10^{-3}$		2301
$D_S^\mp K^\pm$	(3.0 \pm 0.7) $\times 10^{-4}$		2292
$D_S^+ D_S^-$	(1.04 \pm 0.35) %		1823
$D_S^{*+} D_S^-$	< 12.1 %	90%	1742
$D_S^{*+} D_S^{*-}$	< 25.7 %	90%	1655

$D_s^{(*)} + D_s^{(*)-}$		$(4.0 \pm 1.5) \%$		—
$J/\psi(1S)\phi$		$(1.3 \pm 0.4) \times 10^{-3}$		1587
$J/\psi(1S)\pi^0$		$< 1.2 \times 10^{-3}$	90%	1786
$J/\psi(1S)\eta$		$< 3.8 \times 10^{-3}$	90%	1733
$\psi(2S)\phi$		$(6.8 \pm 2.7) \times 10^{-4}$		1119
$\pi^+ \pi^-$		$< 1.2 \times 10^{-6}$	90%	2680
$\pi^0 \pi^0$		$< 2.1 \times 10^{-4}$	90%	2680
$\eta \pi^0$		$< 1.0 \times 10^{-3}$	90%	2653
$\eta \eta$		$< 1.5 \times 10^{-3}$	90%	2627
$\rho^0 \rho^0$		$< 3.20 \times 10^{-4}$	90%	2569
$\phi \rho^0$		$< 6.17 \times 10^{-4}$	90%	2526
$\phi \phi$		$(1.4 \pm 0.8) \times 10^{-5}$		2482
$\pi^+ K^-$		$(4.9 \pm 1.0) \times 10^{-6}$		2659
$K^+ K^-$		$(3.3 \pm 0.9) \times 10^{-5}$		2637
$\bar{K}^*(892)^0 \rho^0$		$< 7.67 \times 10^{-4}$	90%	2550
$\bar{K}^*(892)^0 K^*(892)^0$		$< 1.681 \times 10^{-3}$	90%	2531
$\phi K^*(892)^0$		$< 1.013 \times 10^{-3}$	90%	2507
$\rho \bar{\rho}$		$< 5.9 \times 10^{-5}$	90%	2514
$\gamma \gamma$	B1	$< 8.7 \times 10^{-6}$	90%	2683
$\phi \gamma$		$(5.7 \pm_{-1.9}^{2.2}) \times 10^{-5}$		2586

**Lepton Family number (LF) violating modes or
 $\Delta B = 1$ weak neutral current (B1) modes**

$\mu^+ \mu^-$	B1	$< 4.7 \times 10^{-8}$	90%	2681
$e^+ e^-$	B1	$< 2.8 \times 10^{-7}$	90%	2683
$e^\pm \mu^\mp$	LF [ee]	$< 2.0 \times 10^{-7}$	90%	2682
$\phi(1020)\mu^+ \mu^-$	B1	$< 3.2 \times 10^{-6}$	90%	2582
$\phi \nu \bar{\nu}$	B1	$< 5.4 \times 10^{-3}$	90%	2586

B_s^*

$$I(J^P) = 0(1^-)$$

I, J, P need confirmation. Quantum numbers shown are quark-model predictions.

$$\text{Mass } m = 5415.4 \pm 1.4 \text{ MeV} \quad (S = 2.5)$$

$$m_{B_s^*} - m_{B_s} = 49.0 \pm 1.5 \text{ MeV} \quad (S = 2.0)$$

B_s^* DECAY MODES

	Fraction (Γ_i/Γ)	p (MeV/c)
$B_s \gamma$	dominant	—

$B_{s1}(5830)^0$

$$I(J^P) = \frac{1}{2}(1^+)$$

I, J, P need confirmation.

$$\text{Mass } m = 5829.4 \pm 0.7 \text{ MeV}$$

$$m_{B_{s1}^0} - m_{B^{*+}} = 504.41 \pm 0.25 \text{ MeV}$$

$B_{s1}(5830)^0$ DECAY MODES

	Fraction (Γ_i/Γ)	p (MeV/c)
$B^{*+} K^-$	dominant	—

$B_{s2}^*(5840)^0$

$$I(J^P) = \frac{1}{2}(2^+)$$

 I, J, P need confirmation.

Mass $m = 5839.7 \pm 0.6$ MeV

$$m_{B_{s2}^{*0}} - m_{B_{s1}^0} = 10.5 \pm 0.6$$
 MeV

 $B_{s2}^*(5840)^0$ DECAY MODESFraction (Γ_i/Γ) ρ (MeV/c) $B^+ K^-$

dominant

252

BOTTOM, CHARMED MESONS
($B = C = \pm 1$)

$$B_c^+ = c\bar{b}, B_c^- = \bar{c}b, \text{ similarly for } B_c^{*'}\text{'s}$$

 B_c^\pm

$$I(J^P) = 0(0^-)$$

 I, J, P need confirmation.

Quantum numbers shown are quark-model predictions.

Mass $m = 6.277 \pm 0.006$ GeV ($S = 1.6$)

Mean life $\tau = (0.453 \pm 0.041) \times 10^{-12}$ s

 B_c^- modes are charge conjugates of the modes below. **B_c^\pm DECAY MODES $\times B(\bar{b} \rightarrow B_c)$** Fraction (Γ_i/Γ)

Confidence level

 ρ
(MeV/c)The following quantities are not pure branching ratios; rather the fraction $\Gamma_i/\Gamma \times B(\bar{b} \rightarrow B_c)$.

$J/\psi(1S) \ell^+ \nu_\ell$ anything	$(5.2^{+2.4}_{-2.1}) \times 10^{-5}$	—	—
$J/\psi(1S) \pi^+$	$< 8.2 \times 10^{-5}$	90%	2372
$J/\psi(1S) \pi^+ \pi^+ \pi^-$	$< 5.7 \times 10^{-4}$	90%	2352
$J/\psi(1S) a_1(1260)$	$< 1.2 \times 10^{-3}$	90%	2171
$D^*(2010)^+ \bar{D}^0$	$< 6.2 \times 10^{-3}$	90%	2468

c \bar{c} MESONS

 $\eta_c(1S)$

$$J^{PC} = 0^+(0^-+)$$

$$\text{Mass } m = 2980.3 \pm 1.2 \text{ MeV} \quad (S = 1.6)$$

$$\text{Full width } \Gamma = 28.6 \pm 2.2 \text{ MeV} \quad (S = 2.0)$$

$\eta_c(1S)$ DECAY MODES	Fraction (Γ_i/Γ)	Confidence level	ρ (MeV/c)
--	--------------------------------	------------------	-------------------

Decays involving hadronic resonances

$\eta'(958)\pi\pi$	(4.1 \pm 1.7) %		1321
$\rho\rho$	(2.0 \pm 0.7) %		1272
$K^*(892)^0 K^- \pi^+ + \text{c.c.}$	(2.0 \pm 0.7) %		1276
$K^*(892)\bar{K}^*(892)$	(9.2 \pm 3.4) $\times 10^{-3}$		1194
$K^{*0}\bar{K}^{*0}\pi^+\pi^-$	(1.1 \pm 0.5) %		1071
$\phi K^+ K^-$	(2.9 \pm 1.4) $\times 10^{-3}$		1102
$\phi\phi$	(2.7 \pm 0.9) $\times 10^{-3}$		1087
$\phi 2(\pi^+\pi^-)$	< 3.5 $\times 10^{-3}$	90%	1249
$a_0(980)\pi$	< 2 %	90%	1325
$a_2(1320)\pi$	< 2 %	90%	1194
$K^*(892)\bar{K} + \text{c.c.}$	< 1.28 %	90%	1308
$f_2(1270)\eta$	< 1.1 %	90%	1143
$\omega\omega$	< 3.1 $\times 10^{-3}$	90%	1268
$\omega\phi$	< 1.7 $\times 10^{-3}$	90%	1183
$f_2(1270)f_2(1270)$	(7.6 $^{+3.0}_{-3.4}$) $\times 10^{-3}$		771
$f_2(1270)f_2'(1525)$	(2.7 \pm 1.5) %		509

Decays into stable hadrons

$K\bar{K}\pi$	(7.0 \pm 1.2) %		1379
$\eta\pi\pi$	(4.9 \pm 1.8) %		1427
$\pi^+\pi^-K^+K^-$	(1.5 \pm 0.6) %		1343
$K^+K^-2(\pi^+\pi^-)$	(7.1 \pm 2.9) $\times 10^{-3}$		1252
$2(K^+K^-)$	(1.6 \pm 0.7) $\times 10^{-3}$		1053
$2(\pi^+\pi^-)$	(1.20 \pm 0.30) %		1457
$3(\pi^+\pi^-)$	(1.5 \pm 0.5) %		1405
$\rho\bar{\rho}$	(1.3 \pm 0.4) $\times 10^{-3}$		1158
$\Lambda\bar{\Lambda}$	(1.04 \pm 0.31) $\times 10^{-3}$		988
$K\bar{K}\eta$	< 3.1 %	90%	1263
$\pi^+\pi^-\rho\bar{\rho}$	< 1.2 %	90%	1024

Radiative decays

$\gamma\gamma$	(6.3 \pm 2.9) $\times 10^{-5}$		1490
----------------	-----------------------------------	--	------

Charge conjugation (C), Parity (P), Lepton family number (LF) violating modes

$\pi^+\pi^-$	P, CP < 6 $\times 10^{-4}$	90%	1484
$\pi^0\pi^0$	P, CP < 4 $\times 10^{-4}$	90%	1484
K^+K^-	P, CP < 6 $\times 10^{-4}$	90%	1406
$K_S^0 K_S^0$	P, CP < 3.1 $\times 10^{-4}$	90%	1405

J/ψ(1S)

$$J^G(J^{PC}) = 0^-(1^{--})$$

Mass $m = 3096.916 \pm 0.011$ MeVFull width $\Gamma = 92.9 \pm 2.8$ keV ($S = 1.1$) $\Gamma_{ee} = 5.55 \pm 0.14 \pm 0.02$ keV

J/ψ(1S) DECAY MODES	Fraction (Γ_i/Γ)	Scale factor/ Confidence level	p (MeV/c)
hadrons	(87.7 ± 0.5) %		—
virtual $\gamma \rightarrow$ hadrons	(13.50 ± 0.30) %		—
$g g g$	(64.1 ± 1.0) %		—
$\gamma g g$	(8.8 ± 0.5) %		—
$e^+ e^-$	(5.94 ± 0.06) %		1548
$\mu^+ \mu^-$	(5.93 ± 0.06) %		1545
Decays involving hadronic resonances			
$\rho\pi$	(1.69 ± 0.15) %	S=2.4	1448
$\rho^0\pi^0$	(5.6 ± 0.7) × 10 ⁻³		1448
$a_2(1320)\rho$	(1.09 ± 0.22) %		1123
$\omega\pi^+\pi^+\pi^-\pi^-$	(8.5 ± 3.4) × 10 ⁻³		1392
$\omega\pi^+\pi^-\pi^0$	(4.0 ± 0.7) × 10 ⁻³		1418
$\omega\pi^+\pi^-$	(8.6 ± 0.7) × 10 ⁻³	S=1.1	1435
$\omega f_2(1270)$	(4.3 ± 0.6) × 10 ⁻³		1142
$K^*(892)^0\bar{K}_2^*(1430)^0 + \text{c.c.}$	(6.0 ± 0.6) × 10 ⁻³		1012
$K^*(892)^0\bar{K}_2^*(1770)^0 + \text{c.c.} \rightarrow$ $K^*(892)^0 K^-\pi^+ + \text{c.c.}$	(6.9 ± 0.9) × 10 ⁻⁴		—
$\omega K^*(892)\bar{K} + \text{c.c.}$	(6.1 ± 0.9) × 10 ⁻³		1097
$K^+\bar{K}^*(892)^- + \text{c.c.}$	(5.12 ± 0.30) × 10 ⁻³		1373
$K^+\bar{K}^*(892)^- + \text{c.c.} \rightarrow$ $K^+ K^-\pi^0$	(1.97 ± 0.20) × 10 ⁻³		—
$K^+\bar{K}^*(892)^- + \text{c.c.} \rightarrow$ $K^0 K^\pm\pi^\mp$	(3.0 ± 0.4) × 10 ⁻³		—
$K^0\bar{K}^*(892)^0 + \text{c.c.}$	(4.39 ± 0.31) × 10 ⁻³		1373
$K^0\bar{K}^*(892)^0 + \text{c.c.} \rightarrow$ $K^0 K^\pm\pi^\mp$	(3.2 ± 0.4) × 10 ⁻³		—
$K_1(1400)^\pm K^\mp$	(3.8 ± 1.4) × 10 ⁻³		1170
$\bar{K}^*(892)^0 K^+\pi^- + \text{c.c.}$	seen		1343
$\omega\pi^0\pi^0$	(3.4 ± 0.8) × 10 ⁻³		1436
$b_1(1235)^\pm\pi^\mp$	[ee] (3.0 ± 0.5) × 10 ⁻³		1300
$\omega K^\pm K_S^0\pi^\mp$	[ee] (3.4 ± 0.5) × 10 ⁻³		1210
$b_1(1235)^0\pi^0$	(2.3 ± 0.6) × 10 ⁻³		1300
$\eta K^\pm K_S^0\pi^\mp$	[ee] (2.2 ± 0.4) × 10 ⁻³		1278
$\phi K^*(892)\bar{K} + \text{c.c.}$	(2.18 ± 0.23) × 10 ⁻³		969
$\omega K\bar{K}$	(1.6 ± 0.5) × 10 ⁻⁴		1268
$\omega f_0(1710) \rightarrow \omega K\bar{K}$	(4.8 ± 1.1) × 10 ⁻⁴		878
$\phi 2(\pi^+\pi^-)$	(1.66 ± 0.23) × 10 ⁻³		1318
$\Delta(1232)^{++}\bar{p}\pi^-$	(1.6 ± 0.5) × 10 ⁻³		1030
$\omega\eta$	(1.74 ± 0.20) × 10 ⁻³	S=1.6	1394
$\phi K\bar{K}$	(1.83 ± 0.24) × 10 ⁻³	S=1.5	1179
$\phi f_0(1710) \rightarrow \phi K\bar{K}$	(3.6 ± 0.6) × 10 ⁻⁴		875
$\Delta(1232)^{++}\bar{\Delta}(1232)^{--}$	(1.10 ± 0.29) × 10 ⁻³		938
$\Sigma(1385)^-\bar{\Sigma}(1385)^+ (\text{or c.c.})$	[ee] (1.03 ± 0.13) × 10 ⁻³		697
$\phi f_2'(1525)$	(8 ± 4) × 10 ⁻⁴	S=2.7	871
$\phi\pi^+\pi^-$	(8.7 ± 0.8) × 10 ⁻⁴		1365
$\phi\pi^0\pi^0$	(5.6 ± 1.6) × 10 ⁻⁴		1366
$\phi K^\pm K_S^0\pi^\mp$	[ee] (7.2 ± 0.8) × 10 ⁻⁴		1114

$\omega f_1(1420)$		$(6.8 \pm 2.4) \times 10^{-4}$		1062
$\phi\eta$		$(7.5 \pm 0.8) \times 10^{-4}$	S=1.5	1320
$\Xi^0\Xi^0$		$(1.20 \pm 0.24) \times 10^{-3}$		818
$\Xi(1530)^-\Xi^+$		$(5.9 \pm 1.5) \times 10^{-4}$		600
$\rho K^-\bar{\Sigma}(1385)^0$		$(5.1 \pm 3.2) \times 10^{-4}$		646
$\omega\pi^0$		$(4.5 \pm 0.5) \times 10^{-4}$	S=1.4	1446
$\phi\eta'(958)$		$(4.0 \pm 0.7) \times 10^{-4}$	S=2.1	1192
$\phi f_0(980)$		$(3.2 \pm 0.9) \times 10^{-4}$	S=1.9	1182
$\phi f_0(980) \rightarrow \phi\pi^+\pi^-$		$(2.2 \pm 0.4) \times 10^{-4}$		—
$\phi f_0(980) \rightarrow \phi\pi^0\pi^0$		$(1.7 \pm 0.7) \times 10^{-4}$		—
$\Xi(1530)^0\Xi^0$		$(3.2 \pm 1.4) \times 10^{-4}$		608
$\Sigma(1385)^-\bar{\Sigma}^+(or\ c.c.)$	[ee]	$(3.1 \pm 0.5) \times 10^{-4}$		855
$\phi f_1(1285)$		$(2.6 \pm 0.5) \times 10^{-4}$	S=1.1	1032
$\eta\pi^+\pi^-$		$(4.0 \pm 1.7) \times 10^{-4}$		1487
$\rho\eta$		$(1.93 \pm 0.23) \times 10^{-4}$		1396
$\omega\eta'(958)$		$(1.82 \pm 0.21) \times 10^{-4}$		1279
$\omega f_0(980)$		$(1.4 \pm 0.5) \times 10^{-4}$		1271
$\rho\eta'(958)$		$(1.05 \pm 0.18) \times 10^{-4}$		1281
$a_2(1320)^\pm\pi^\mp$	[ee]	$< 4.3 \times 10^{-3}$	CL=90%	1263
$K\bar{K}_2^*(1430)+c.c.$		$< 4.0 \times 10^{-3}$	CL=90%	1159
$K_1(1270)^\pm K^\mp$		$< 3.0 \times 10^{-3}$	CL=90%	1231
$K_2^*(1430)^0\bar{K}_2^*(1430)^0$		$< 2.9 \times 10^{-3}$	CL=90%	604
$K^*(892)^0\bar{K}^*(892)^0$		$(2.3 \pm 0.7) \times 10^{-4}$		1266
$\phi f_2(1270)$		$(7.2 \pm 1.3) \times 10^{-4}$		1036
$\phi\eta(1405) \rightarrow \phi\eta\pi\pi$		$< 2.5 \times 10^{-4}$	CL=90%	946
$\omega f_2'(1525)$		$< 2.2 \times 10^{-4}$	CL=90%	1003
$\Sigma(1385)^0\bar{\Lambda}$		$< 2 \times 10^{-4}$	CL=90%	912
$\Delta(1232)^+\bar{p}$		$< 1 \times 10^{-4}$	CL=90%	1100
$\Theta(1540)\bar{\Theta}(1540) \rightarrow K_S^0\rho K^-\bar{n}+c.c.$		$< 1.1 \times 10^{-5}$	CL=90%	—
$\Theta(1540)K^-\bar{n} \rightarrow K_S^0\rho K^-\bar{n}$		$< 2.1 \times 10^{-5}$	CL=90%	—
$\Theta(1540)K_S^0\bar{p} \rightarrow K_S^0\bar{p}K^+n$		$< 1.6 \times 10^{-5}$	CL=90%	—
$\bar{\Theta}(1540)K^+n \rightarrow K_S^0\bar{p}K^+n$		$< 5.6 \times 10^{-5}$	CL=90%	—
$\bar{\Theta}(1540)K_S^0p \rightarrow K_S^0\rho K^-\bar{n}$		$< 1.1 \times 10^{-5}$	CL=90%	—
$\Sigma^0\bar{\Lambda}$		$< 9 \times 10^{-5}$	CL=90%	1032
$\phi\pi^0$		$< 6.4 \times 10^{-6}$	CL=90%	1377

Decays into stable hadrons

$2(\pi^+\pi^-)\pi^0$		$(5.5 \pm 0.4) \%$		1496
$3(\pi^+\pi^-)\pi^0$		$(2.9 \pm 0.6) \%$		1433
$\pi^+\pi^-\pi^0$		$(2.07 \pm 0.12) \%$	S=1.6	1533
$\pi^+\pi^-\pi^0 K^+K^-$		$(1.94 \pm 0.15) \%$		1368
$4(\pi^+\pi^-)\pi^0$		$(9.0 \pm 3.0) \times 10^{-3}$		1345
$\pi^+\pi^-K^+K^-$		$(6.6 \pm 0.5) \times 10^{-3}$		1407
$\pi^+\pi^-K^+K^-\eta$		$(1.84 \pm 0.28) \times 10^{-3}$		1221
$\pi^0\pi^0 K^+K^-$		$(2.45 \pm 0.31) \times 10^{-3}$		1410
$\eta\phi f_0(980) \rightarrow \eta\phi\pi^+\pi^-$		$(3.2 \pm 1.0) \times 10^{-4}$		—
$K\bar{K}\pi$		$(6.1 \pm 1.0) \times 10^{-3}$		1442
$2(\pi^+\pi^-)$		$(3.55 \pm 0.23) \times 10^{-3}$		1517
$3(\pi^+\pi^-)$		$(4.3 \pm 0.4) \times 10^{-3}$		1466
$2(\pi^+\pi^-\pi^0)$		$(1.61 \pm 0.21) \%$		1468
$2(\pi^+\pi^-\eta)$		$(2.29 \pm 0.24) \times 10^{-3}$		1446
$3(\pi^+\pi^-\eta)$		$(7.2 \pm 1.5) \times 10^{-4}$		1379
$\rho\bar{p}$		$(2.17 \pm 0.07) \times 10^{-3}$		1232
$\rho\bar{p}\pi^0$		$(1.19 \pm 0.08) \times 10^{-3}$	S=1.1	1176

$p\bar{p}\pi^+\pi^-$		(6.0 ± 0.5) × 10 ⁻³	S=1.3	1107
$p\bar{p}\pi^+\pi^-\pi^0$	[hhhh]	(2.3 ± 0.9) × 10 ⁻³	S=1.9	1033
$p\bar{p}\eta$		(2.00 ± 0.12) × 10 ⁻³		948
$p\bar{p}\rho$		< 3.1 × 10 ⁻⁴	CL=90%	774
$p\bar{p}\omega$		(1.10 ± 0.15) × 10 ⁻³	S=1.3	768
$p\bar{p}\eta'(958)$		(2.1 ± 0.4) × 10 ⁻⁴		596
$p\bar{p}\phi$		(4.5 ± 1.5) × 10 ⁻⁵		527
$n\bar{n}$		(2.2 ± 0.4) × 10 ⁻³		1231
$n\bar{n}\pi^+\pi^-$		(4 ± 4) × 10 ⁻³		1106
$\Sigma^+\bar{\Sigma}^-$		(1.50 ± 0.24) × 10 ⁻³		992
$\Sigma^0\bar{\Sigma}^0$		(1.29 ± 0.09) × 10 ⁻³		988
$2(\pi^+\pi^-)K^+K^-$		(5.0 ± 0.5) × 10 ⁻³		1320
$p\bar{n}\pi^-$		(2.12 ± 0.09) × 10 ⁻³		1174
$nN(1440)$	seen			978
$nN(1520)$	seen			924
$nN(1535)$	seen			914
$\Xi^-\bar{\Xi}^+$		(8.5 ± 1.6) × 10 ⁻⁴	S=1.5	807
$\Lambda\bar{\Lambda}$		(1.61 ± 0.15) × 10 ⁻³	S=1.9	1074
$\Lambda\bar{\Sigma}^-\pi^+$ (or c.c.)	[ee]	(8.3 ± 0.7) × 10 ⁻⁴	S=1.2	950
$pK^-\bar{\Lambda}$		(8.9 ± 1.6) × 10 ⁻⁴		876
$2(K^+K^-)$		(7.6 ± 0.9) × 10 ⁻⁴		1131
$pK^-\bar{\Sigma}^0$		(2.9 ± 0.8) × 10 ⁻⁴		819
K^+K^-		(2.37 ± 0.31) × 10 ⁻⁴		1468
$K_S^0K_L^0$		(1.46 ± 0.26) × 10 ⁻⁴	S=2.7	1466
$\Lambda\bar{\Lambda}\eta$		(2.6 ± 0.7) × 10 ⁻⁴		672
$\Lambda\bar{\Lambda}\pi^0$		< 6.4 × 10 ⁻⁵	CL=90%	998
$\bar{\Lambda}nK_S^0$ + c.c.		(6.5 ± 1.1) × 10 ⁻⁴		872
$\pi^+\pi^-$		(1.47 ± 0.23) × 10 ⁻⁴		1542
$\Lambda\bar{\Sigma}^+$ + c.c.		< 1.5 × 10 ⁻⁴	CL=90%	1034
$K_S^0K_S^0$		< 1 × 10 ⁻⁶	CL=95%	1466

Radiative decays

3γ		(1.2 ± 0.4) × 10 ⁻⁵		1548
4γ		< 9 × 10 ⁻⁶	CL=90%	1548
5γ		< 1.5 × 10 ⁻⁵	CL=90%	1548
$\gamma\eta_c(1S)$		(1.7 ± 0.4) %	S=1.6	114
$\gamma\eta_c(1S) \rightarrow 3\gamma$		(1.2 ^{+2.7} _{-1.1}) × 10 ⁻⁶		-
$\gamma\pi^+\pi^-2\pi^0$		(8.3 ± 3.1) × 10 ⁻³		1518
$\gamma\eta\pi\pi$		(6.1 ± 1.0) × 10 ⁻³		1487
$\gamma\eta_2(1870) \rightarrow \gamma\eta\pi^+\pi^-$		(6.2 ± 2.4) × 10 ⁻⁴		-
$\gamma\eta(1405/1475) \rightarrow \gamma K\bar{K}\pi$	[n]	(2.8 ± 0.6) × 10 ⁻³	S=1.6	1223
$\gamma\eta(1405/1475) \rightarrow \gamma\gamma\rho^0$		(7.8 ± 2.0) × 10 ⁻⁵	S=1.8	1223
$\gamma\eta(1405/1475) \rightarrow \gamma\eta\pi^+\pi^-$		(3.0 ± 0.5) × 10 ⁻⁴		-
$\gamma\eta(1405/1475) \rightarrow \gamma\gamma\phi$		< 8.2 × 10 ⁻⁵	CL=95%	-
$\gamma\rho\rho$		(4.5 ± 0.8) × 10 ⁻³		1340
$\gamma\rho\omega$		< 5.4 × 10 ⁻⁴	CL=90%	1338
$\gamma\rho\phi$		< 8.8 × 10 ⁻⁵	CL=90%	1258
$\gamma\eta'(958)$		(5.28 ± 0.15) × 10 ⁻³		1400
$\gamma 2\pi^+2\pi^-$		(2.8 ± 0.5) × 10 ⁻³	S=1.9	1517
$\gamma f_2(1270)f_2(1270)$		(9.5 ± 1.7) × 10 ⁻⁴		879
$\gamma f_2(1270)f_2(1270)$ (non resonant)		(8.2 ± 1.9) × 10 ⁻⁴		-
$\gamma K^+K^-\pi^+\pi^-$		(2.1 ± 0.6) × 10 ⁻³		1407
$\gamma f_4(2050)$		(2.7 ± 0.7) × 10 ⁻³		891
$\gamma\omega\omega$		(1.61 ± 0.33) × 10 ⁻³		1336

$\gamma\eta(1405/1475) \rightarrow \gamma\rho^0\rho^0$	$(1.7 \pm 0.4) \times 10^{-3}$	S=1.3	1223
$\gamma f_2(1270)$	$(1.43 \pm 0.11) \times 10^{-3}$		1286
$\gamma f_0(1710) \rightarrow \gamma K\bar{K}$	$(8.5 \pm_{-0.9}^{+1.2}) \times 10^{-4}$	S=1.2	1075
$\gamma f_0(1710) \rightarrow \gamma\pi\pi$	$(4.0 \pm 1.0) \times 10^{-4}$		—
$\gamma f_0(1710) \rightarrow \gamma\omega\omega$	$(3.1 \pm 1.0) \times 10^{-4}$		—
$\gamma\eta$	$(1.104 \pm 0.034) \times 10^{-3}$		1500
$\gamma f_1(1420) \rightarrow \gamma K\bar{K}\pi$	$(7.9 \pm 1.3) \times 10^{-4}$		1220
$\gamma f_1(1285)$	$(6.1 \pm 0.8) \times 10^{-4}$		1283
$\gamma f_1(1510) \rightarrow \gamma\eta\pi^+\pi^-$	$(4.5 \pm 1.2) \times 10^{-4}$		—
$\gamma f_2'(1525)$	$(4.5 \pm_{-0.4}^{+0.7}) \times 10^{-4}$		1173
$\gamma f_2(1640) \rightarrow \gamma\omega\omega$	$(2.8 \pm 1.8) \times 10^{-4}$		—
$\gamma f_2(1910) \rightarrow \gamma\omega\omega$	$(2.0 \pm 1.4) \times 10^{-4}$		—
$\gamma f_2(1950) \rightarrow \gamma K^*(892)\bar{K}^*(892)$	$(7.0 \pm 2.2) \times 10^{-4}$		—
$\gamma K^*(892)\bar{K}^*(892)$	$(4.0 \pm 1.3) \times 10^{-3}$		1266
$\gamma\phi\phi$	$(4.0 \pm 1.2) \times 10^{-4}$	S=2.1	1166
$\gamma\rho\bar{\rho}$	$(3.8 \pm 1.0) \times 10^{-4}$		1232
$\gamma\eta(2225)$	$(3.3 \pm 0.5) \times 10^{-4}$		749
$\gamma\eta(1760) \rightarrow \gamma\rho^0\rho^0$	$(1.3 \pm 0.9) \times 10^{-4}$		1048
$\gamma\eta(1760) \rightarrow \gamma\omega\omega$	$(1.98 \pm 0.33) \times 10^{-3}$		—
$\gamma X(1835)$	$(2.2 \pm 0.6) \times 10^{-4}$		1006
$\gamma(K\bar{K}\pi) [J^{PC} = 0^{-+}]$	$(7 \pm 4) \times 10^{-4}$	S=2.1	1442
$\gamma\pi^0$	$(3.49 \pm_{-0.30}^{+0.33}) \times 10^{-5}$		1546
$\gamma\rho\bar{\rho}\pi^+\pi^-$	$< 7.9 \times 10^{-4}$	CL=90%	1107
$\gamma\Lambda\bar{\Lambda}$	$< 1.3 \times 10^{-4}$	CL=90%	1074
$\gamma f_J(2220)$	$> 2.50 \times 10^{-3}$	CL=99.9%	745
$\gamma f_J(2220) \rightarrow \gamma\pi\pi$	$(8 \pm 4) \times 10^{-5}$		—
$\gamma f_J(2220) \rightarrow \gamma K\bar{K}$	$(8.1 \pm 3.0) \times 10^{-5}$		—
$\gamma f_J(2220) \rightarrow \gamma\rho\bar{\rho}$	$(1.5 \pm 0.8) \times 10^{-5}$		—
$\gamma f_0(1500)$	$> (5.7 \pm 0.8) \times 10^{-4}$		1183
γe^+e^-	$(8.8 \pm 1.4) \times 10^{-3}$		1548

Weak decays

$D^- e^+ \nu_e + c.c.$	$< 1.2 \times 10^{-5}$	CL=90%	984
$\bar{D}^0 e^+ e^- + c.c.$	$< 1.1 \times 10^{-5}$	CL=90%	987
$D_s^- e^+ \nu_e + c.c.$	$< 3.6 \times 10^{-5}$	CL=90%	923
$D^- \pi^+ + c.c.$	$< 7.5 \times 10^{-5}$	CL=90%	977
$\bar{D}^0 \bar{K}^0 + c.c.$	$< 1.7 \times 10^{-4}$	CL=90%	898
$D_s^- \pi^+ + c.c.$	$< 1.3 \times 10^{-4}$	CL=90%	915

**Charge conjugation (C), Parity (P),
Lepton Family number (LF) violating modes**

$\gamma\gamma$	C	$< 5 \times 10^{-6}$	CL=90%	1548
$e^\pm \mu^\mp$	LF	$< 1.1 \times 10^{-6}$	CL=90%	1547
$e^\pm \tau^\mp$	LF	$< 8.3 \times 10^{-6}$	CL=90%	1039
$\mu^\pm \tau^\mp$	LF	$< 2.0 \times 10^{-6}$	CL=90%	1035

Other decays

invisible	$< 7 \times 10^{-4}$	CL=90%	—
-----------	----------------------	--------	---

$\chi_{c0}(1P)$

$$J^PC = 0^+(0^{++})$$

$$\text{Mass } m = 3414.75 \pm 0.31 \text{ MeV}$$

$$\text{Full width } \Gamma = 10.3 \pm 0.6 \text{ MeV}$$

$\chi_{c0}(1P)$ DECAY MODES	Fraction (Γ_i/Γ)	Scale factor/ Confidence level	p (MeV/c)
Hadronic decays			
$2(\pi^+\pi^-)$	$(2.27 \pm 0.19) \%$		1679
$\rho^0\pi^+\pi^-$	$(8.9 \pm 2.8) \times 10^{-3}$		1607
$f_0(980)f_0(980)$	$(6.8 \pm 2.2) \times 10^{-4}$		1398
$\pi^+\pi^-\pi^0\pi^0$	$(3.4 \pm 0.4) \%$		1680
$\rho^+\pi^-\pi^0 + \text{c.c.}$	$(2.9 \pm 0.4) \%$		1607
$\pi^+\pi^-K^+K^-$	$(1.80 \pm 0.15) \%$		1580
$K_0^*(1430)^0\bar{K}_0^*(1430)^0 \rightarrow$ $\pi^+\pi^-K^+K^-$	$(1.00^{+0.40}_{-0.29}) \times 10^{-3}$		—
$K_0^*(1430)^0\bar{K}_2^*(1430)^0 + \text{c.c.} \rightarrow$ $\pi^+\pi^-K^+K^-$	$(8.1^{+2.0}_{-2.5}) \times 10^{-4}$		—
$K_1(1270)^+K^- + \text{c.c.} \rightarrow$ $\pi^+\pi^-K^+K^-$	$(6.4 \pm 1.9) \times 10^{-3}$		—
$K_1(1400)^+K^- + \text{c.c.} \rightarrow$ $\pi^+\pi^-K^+K^-$	$< 2.7 \times 10^{-3}$	CL=90%	—
$f_0(980)f_0(980)$	$(1.7^{+1.1}_{-0.9}) \times 10^{-4}$		1398
$f_0(980)f_0(2200)$	$(8.1^{+2.1}_{-2.6}) \times 10^{-4}$		595
$f_0(1370)f_0(1370)$	$< 2.8 \times 10^{-4}$	CL=90%	1019
$f_0(1370)f_0(1500)$	$< 1.7 \times 10^{-4}$	CL=90%	920
$f_0(1370)f_0(1710)$	$(6.8^{+4.0}_{-2.4}) \times 10^{-4}$		723
$f_0(1500)f_0(1370)$	$< 1.3 \times 10^{-4}$	CL=90%	920
$f_0(1500)f_0(1500)$	$< 5 \times 10^{-5}$	CL=90%	805
$f_0(1500)f_0(1710)$	$< 7 \times 10^{-5}$	CL=90%	559
$K^+K^-\pi^0\pi^0$	$(5.7 \pm 0.9) \times 10^{-3}$		1582
$K^+\pi^-K^0\pi^0 + \text{c.c.}$	$(2.53 \pm 0.34) \%$		1581
$\rho^+K^-K^0 + \text{c.c.}$	$(1.23 \pm 0.22) \%$		1458
$K^*(892)^-K^+\pi^0 \rightarrow$ $K^+\pi^-K^0\pi^0 + \text{c.c.}$	$(4.7 \pm 1.2) \times 10^{-3}$		—
$K_S^0K_S^0\pi^+\pi^-$	$(5.8 \pm 1.1) \times 10^{-3}$		1579
$K^+K^-\eta\pi^0$	$(3.1 \pm 0.7) \times 10^{-3}$		1468
$3(\pi^+\pi^-)$	$(1.20 \pm 0.18) \%$		1633
$K^+\bar{K}^*(892)^0\pi^- + \text{c.c.}$	$(7.3 \pm 1.6) \times 10^{-3}$		1523
$K^*(892)^0\bar{K}^*(892)^0$	$(1.7 \pm 0.6) \times 10^{-3}$		1456
$\pi\pi$	$(8.4 \pm 0.4) \times 10^{-3}$		1702
$\pi^0\eta$	$< 1.8 \times 10^{-4}$		1661
$\pi^0\eta'$	$< 1.1 \times 10^{-3}$		1570
$\eta\eta$	$(2.68 \pm 0.28) \times 10^{-3}$		1617
$\eta\eta'$	$< 2.4 \times 10^{-4}$	CL=90%	1521
$\eta'\eta'$	$(2.03 \pm 0.22) \times 10^{-3}$		1413
$\omega\omega$	$(2.2 \pm 0.7) \times 10^{-3}$		1517
K^+K^-	$(6.10 \pm 0.35) \times 10^{-3}$		1634
$K_S^0K_S^0$	$(3.16 \pm 0.18) \times 10^{-3}$		1633
$\pi^+\pi^-\eta$	$< 2.0 \times 10^{-4}$	CL=90%	1651
$\pi^+\pi^-\eta'$	$< 4 \times 10^{-4}$	CL=90%	1560
$\bar{K}^0K^+\pi^- + \text{c.c.}$	$< 1.0 \times 10^{-4}$	CL=90%	1610
$K^+K^-\pi^0$	$< 6 \times 10^{-5}$	CL=90%	1611

$K^+ K^- \eta$	$< 2.3 \times 10^{-4}$	CL=90%	1512
$K^+ K^- K_S^0 K_S^0$	$(1.4 \pm 0.5) \times 10^{-3}$		1331
$K^+ K^- K^+ K^-$	$(2.81 \pm 0.30) \times 10^{-3}$		1333
$K^+ K^- \phi$	$(9.9 \pm 2.5) \times 10^{-4}$		1381
$\phi \phi$	$(9.2 \pm 1.9) \times 10^{-4}$		1370
$\rho \bar{\rho}$	$(2.28 \pm 0.13) \times 10^{-4}$		1426
$\rho \bar{\rho} \pi^0$	$(5.7 \pm 1.2) \times 10^{-4}$		1379
$\rho \bar{\rho} \eta$	$(3.7 \pm 1.1) \times 10^{-4}$		1187
$\pi^+ \pi^- \rho \bar{\rho}$	$(2.1 \pm 0.7) \times 10^{-3}$	S=1.4	1320
$\pi^0 \pi^0 \rho \bar{\rho}$	$(1.05 \pm 0.28) \times 10^{-3}$		1324
$K_S^0 K_S^0 \rho \bar{\rho}$	$< 8.8 \times 10^{-4}$	CL=90%	884
$\rho \bar{\rho} \pi^-$	$(1.14 \pm 0.31) \times 10^{-3}$		1376
$\Lambda \bar{\Lambda}$	$(3.3 \pm 0.4) \times 10^{-4}$		1292
$\Lambda \bar{\Lambda} \pi^+ \pi^-$	$< 4.0 \times 10^{-3}$	CL=90%	1153
$K^+ \bar{p} \Lambda + \text{c.c.}$	$(1.03 \pm 0.20) \times 10^{-3}$		1132
$\Sigma^0 \bar{\Sigma}^0$	$(4.2 \pm 0.7) \times 10^{-4}$		1222
$\Sigma^+ \bar{\Sigma}^-$	$(3.1 \pm 0.7) \times 10^{-4}$		1225
$\Xi^0 \bar{\Xi}^0$	$(3.2 \pm 0.8) \times 10^{-4}$		1089
$\Xi^- \bar{\Xi}^+$	$(4.9 \pm 0.7) \times 10^{-4}$		1081

Radiative decays

$\gamma J/\psi(1S)$	$(1.16 \pm 0.08) \%$		303
$\gamma \rho^0$	$< 9 \times 10^{-6}$	CL=90%	1619
$\gamma \omega$	$< 8 \times 10^{-6}$	CL=90%	1618
$\gamma \phi$	$< 6 \times 10^{-6}$	CL=90%	1555
$\gamma \gamma$	$(2.22 \pm 0.17) \times 10^{-4}$		1707

$\chi_{c1}(1P)$

$$J^{PC} = 0^+(1^+ +)$$

Mass $m = 3510.66 \pm 0.07$ MeV (S = 1.5)

Full width $\Gamma = 0.86 \pm 0.05$ MeV

$\chi_{c1}(1P)$ DECAY MODES	Fraction (Γ_i/Γ)	Scale factor/ Confidence level	ρ (MeV/c)
-----------------------------	--------------------------------	-----------------------------------	-------------------

Hadronic decays

$3(\pi^+ \pi^-)$	$(5.8 \pm 1.4) \times 10^{-3}$	S=1.2	1683
$2(\pi^+ \pi^-)$	$(7.6 \pm 2.6) \times 10^{-3}$		1728
$\pi^+ \pi^- \pi^0 \pi^0$	$(1.26 \pm 0.17) \%$		1729
$\rho^+ \pi^- \pi^0 + \text{c.c.}$	$(1.53 \pm 0.26) \%$		1658
$\rho^0 \pi^+ \pi^-$	$(3.9 \pm 3.5) \times 10^{-3}$		1657
$\pi^+ \pi^- K^+ K^-$	$(4.5 \pm 1.0) \times 10^{-3}$		1632
$K^+ K^- \pi^0 \pi^0$	$(1.18 \pm 0.29) \times 10^{-3}$		1634
$K^+ \pi^- K^0 \pi^0 + \text{c.c.}$	$(9.0 \pm 1.5) \times 10^{-3}$		1632
$\rho^+ K^- K^0 + \text{c.c.}$	$(5.3 \pm 1.3) \times 10^{-3}$		1514
$K^*(892)^0 K^0 \pi^0 \rightarrow$	$(2.5 \pm 0.7) \times 10^{-3}$		-
$K^+ \pi^- K^0 \pi^0 + \text{c.c.}$			
$K^+ K^- \eta \pi^0$	$(1.2 \pm 0.4) \times 10^{-3}$		1523
$\pi^+ \pi^- K_S^0 K_S^0$	$(7.2 \pm 3.1) \times 10^{-4}$		1630
$K^+ K^- \eta$	$(3.3 \pm 1.0) \times 10^{-4}$		1566
$K^0 K^+ \pi^- + \text{c.c.}$	$(7.3 \pm 0.6) \times 10^{-3}$		1661
$K^*(892)^0 \bar{K}^0 + \text{c.c.}$	$(1.0 \pm 0.4) \times 10^{-3}$		1602
$K^*(892)^+ K^- + \text{c.c.}$	$(1.5 \pm 0.7) \times 10^{-3}$		1602
$K_J^*(1430)^0 \bar{K}^0 + \text{c.c.} \rightarrow$	$< 8 \times 10^{-4}$	CL=90%	-
$K_S^0 K^+ \pi^- + \text{c.c.}$			

$K_J^*(1430)^+ K^- + \text{c.c.} \rightarrow$	< 2.3	$\times 10^{-3}$	CL=90%	-
$K_S^0 K^+ \pi^- + \text{c.c.}$				
$K^+ K^- \pi^0$	(1.91 ± 0.26)	$\times 10^{-3}$		1662
$\eta \pi^+ \pi^-$	(5.0 ± 0.5)	$\times 10^{-3}$		1701
$a_0(980)^+ \pi^- + \text{c.c.} \rightarrow \eta \pi^+ \pi^-$	(1.9 ± 0.7)	$\times 10^{-3}$		-
$f_2(1270) \eta$	(2.8 ± 0.8)	$\times 10^{-3}$		1468
$\pi^+ \pi^- \eta'$	(2.4 ± 0.5)	$\times 10^{-3}$		1612
$K^+ \bar{K}^*(892)^0 \pi^- + \text{c.c.}$	(3.2 ± 2.1)	$\times 10^{-3}$		1577
$K^*(892)^0 \bar{K}^*(892)^0$	(1.5 ± 0.4)	$\times 10^{-3}$		1512
$K^+ K^- K_S^0 K_S^0$	< 5	$\times 10^{-4}$	CL=90%	1390
$K^+ K^- K^+ K^-$	(5.6 ± 1.2)	$\times 10^{-4}$		1393
$K^+ K^- \phi$	(4.3 ± 1.6)	$\times 10^{-4}$		1440
$\rho \bar{\rho}$	(7.3 ± 0.4)	$\times 10^{-5}$		1484
$\rho \bar{\rho} \pi^0$	(1.2 ± 0.5)	$\times 10^{-4}$		1438
$\rho \bar{\rho} \eta$	< 1.6	$\times 10^{-4}$	CL=90%	1254
$\pi^+ \pi^- \rho \bar{\rho}$	(5.0 ± 1.9)	$\times 10^{-4}$		1381
$K_S^0 K_S^0 \rho \bar{\rho}$	< 4.5	$\times 10^{-4}$	CL=90%	968
$\Lambda \bar{\Lambda}$	(1.18 ± 0.19)	$\times 10^{-4}$		1355
$\Lambda \bar{\Lambda} \pi^+ \pi^-$	< 1.5	$\times 10^{-3}$	CL=90%	1223
$K^+ \bar{p} \Lambda$	(3.2 ± 1.0)	$\times 10^{-4}$		1203
$\Sigma^0 \bar{\Sigma}^0$	< 4	$\times 10^{-5}$	CL=90%	1288
$\Sigma^+ \bar{\Sigma}^-$	< 6	$\times 10^{-5}$	CL=90%	1291
$\Xi^0 \bar{\Xi}^0$	< 6	$\times 10^{-5}$	CL=90%	1163
$\Xi^- \bar{\Xi}^+$	(8.4 ± 2.3)	$\times 10^{-5}$		1155
$\pi^+ \pi^- + K^+ K^-$	< 2.1	$\times 10^{-3}$		-
$K_S^0 K_S^0$	< 6	$\times 10^{-5}$	CL=90%	1683

Radiative decays

$\gamma J/\psi(1S)$	(34.4 ± 1.5)	%		389
$\gamma \rho^0$	(2.29 ± 0.27)	$\times 10^{-4}$		1670
$\gamma \omega$	(7.8 ± 1.8)	$\times 10^{-5}$		1668
$\gamma \phi$	< 2.4	$\times 10^{-5}$	CL=90%	1607

 $h_c(1P)$

$$JG(J^{PC}) = ?^?(1^{+-})$$

Mass $m = 3525.42 \pm 0.29$ MeV (S = 1.7)Full width $\Gamma < 1$ MeV

$h_c(1P)$ DECAY MODES	Fraction (Γ_i/Γ)	p (MeV/c)
$J/\psi(1S) \pi \pi$	not seen	312
$\eta_c \gamma$	seen	503
$\pi^+ \pi^- \pi^0$	not seen	1749
$2\pi^+ 2\pi^- \pi^0$	seen	1716
$3\pi^+ 3\pi^- \pi^0$	not seen	1661

 $\chi_{c2}(1P)$

$$JG(J^{PC}) = 0^+(2^{++})$$

Mass $m = 3556.20 \pm 0.09$ MeVFull width $\Gamma = 1.97 \pm 0.11$ MeV

$\chi_{c2}(1P)$ DECAY MODES	Fraction (Γ_i/Γ)	Confidence level	p (MeV/c)
---	--------------------------------	------------------	-------------

Hadronic decays

$2(\pi^+\pi^-)$	$(1.11 \pm 0.11) \%$	1751
$\pi^+\pi^-\pi^0\pi^0$	$(2.00 \pm 0.26) \%$	1752
$\rho^+\pi^-\pi^0 + \text{c.c.}$	$(2.4 \pm 0.4) \%$	1682
$K^+K^-\pi^0\pi^0$	$(2.2 \pm 0.4) \times 10^{-3}$	1658
$K^+\pi^-K^0\pi^0 + \text{c.c.}$	$(1.50 \pm 0.22) \%$	1657
$\rho^+K^-K^0 + \text{c.c.}$	$(4.5 \pm 1.4) \times 10^{-3}$	1540
$K^*(892)^0K^+\pi^- \rightarrow$ $K^+\pi^-K^0\pi^0 + \text{c.c.}$	$(3.2 \pm 0.9) \times 10^{-3}$	—
$K^*(892)^0K^0\pi^0 \rightarrow$ $K^+\pi^-K^0\pi^0 + \text{c.c.}$	$(4.2 \pm 0.9) \times 10^{-3}$	—
$K^*(892)^-K^+\pi^0 \rightarrow$ $K^+\pi^-K^0\pi^0 + \text{c.c.}$	$(4.1 \pm 0.9) \times 10^{-3}$	—
$K^*(892)^+K^0\pi^- \rightarrow$ $K^+\pi^-K^0\pi^0 + \text{c.c.}$	$(3.2 \pm 0.9) \times 10^{-3}$	—
$K^+K^-\eta\pi^0$	$(1.4 \pm 0.5) \times 10^{-3}$	1549
$\pi^+\pi^-K^+K^-$	$(9.2 \pm 1.1) \times 10^{-3}$	1656
$K^+\bar{K}^*(892)^0\pi^-\pi^0 + \text{c.c.}$	$(2.3 \pm 1.2) \times 10^{-3}$	1602
$K^*(892)^0\bar{K}^*(892)^0$	$(2.5 \pm 0.5) \times 10^{-3}$	1538
$3(\pi^+\pi^-)$	$(8.6 \pm 1.8) \times 10^{-3}$	1707
$\phi\phi$	$(1.48 \pm 0.28) \times 10^{-3}$	1457
$\omega\omega$	$(1.9 \pm 0.6) \times 10^{-3}$	1597
$\pi\pi$	$(2.39 \pm 0.14) \times 10^{-3}$	1773
$\rho^0\pi^+\pi^-$	$(4.0 \pm 1.7) \times 10^{-3}$	1681
$\pi^+\pi^-\eta$	$(5.2 \pm 1.4) \times 10^{-4}$	1724
$\pi^+\pi^-\eta'$	$(5.4 \pm 2.0) \times 10^{-4}$	1636
$\eta\eta$	$(5.4 \pm 0.8) \times 10^{-4}$	1692
K^+K^-	$(1.09 \pm 0.08) \times 10^{-3}$	1708
$K_S^0K_S^0$	$(5.8 \pm 0.5) \times 10^{-4}$	1707
$\bar{K}^0K^+\pi^- + \text{c.c.}$	$(1.32 \pm 0.20) \times 10^{-3}$	1685
$K^+K^-\pi^0$	$(3.3 \pm 0.8) \times 10^{-4}$	1686
$K^+K^-\eta$	$< 3.5 \times 10^{-4}$	90% 1592
$\eta\eta'$	$< 6 \times 10^{-5}$	90% 1600
$\eta'\eta'$	$< 1.1 \times 10^{-4}$	90% 1498
$\pi^+\pi^-K_S^0K_S^0$	$(2.4 \pm 0.6) \times 10^{-3}$	1655
$K^+K^-K_S^0K_S^0$	$< 4 \times 10^{-4}$	90% 1418
$K^+K^-K^+K^-$	$(1.78 \pm 0.22) \times 10^{-3}$	1421
$K^+K^-\phi$	$(1.55 \pm 0.32) \times 10^{-3}$	1468
$K_S^0K_S^0\rho\bar{\rho}$	$< 7.9 \times 10^{-4}$	90% 1007
$\rho\bar{\rho}$	$(7.2 \pm 0.4) \times 10^{-5}$	1510
$\rho\bar{\rho}\pi^0$	$(4.7 \pm 1.0) \times 10^{-4}$	1465
$\rho\bar{\rho}\eta$	$(2.0 \pm 0.8) \times 10^{-4}$	1285
$\pi^+\pi^-\rho\bar{\rho}$	$(1.32 \pm 0.34) \times 10^{-3}$	1410
$\pi^0\pi^0\rho\bar{\rho}$	$(8.5 \pm 2.6) \times 10^{-4}$	1414
$\rho\bar{\rho}\pi^-\pi^+$	$(1.1 \pm 0.4) \times 10^{-3}$	1463
$\Lambda\bar{\Lambda}$	$(1.86 \pm 0.27) \times 10^{-4}$	1385
$\Lambda\bar{\Lambda}\pi^+\pi^-$	$< 3.5 \times 10^{-3}$	90% 1255
$K^+\bar{\rho}\Lambda + \text{c.c.}$	$(9.1 \pm 1.8) \times 10^{-4}$	1236
$\Sigma^0\bar{\Sigma}^0$	$< 8 \times 10^{-5}$	90% 1319
$\Sigma^+\bar{\Sigma}^-$	$< 7 \times 10^{-5}$	90% 1322
$\Xi^0\bar{\Xi}^0$	$< 1.1 \times 10^{-4}$	90% 1197
$\Xi^-\bar{\Xi}^+$	$(1.55 \pm 0.35) \times 10^{-4}$	1189
$J/\psi(1S)\pi^+\pi^-\pi^0$	$< 1.5 \%$	90% 185

Radiative decays

$\gamma J/\psi(1S)$	$(19.5 \pm 0.8) \%$		430
$\gamma \rho^0$	$< 5 \times 10^{-5}$	90%	1694
$\gamma \omega$	$< 6 \times 10^{-6}$	90%	1692
$\gamma \phi$	$< 1.2 \times 10^{-5}$	90%	1632
$\gamma \gamma$	$(2.56 \pm 0.16) \times 10^{-4}$		1778

 $\eta_c(2S)$

$$JG(J^{PC}) = 0^+(0^-+)$$

Quantum numbers are quark model predictions.

$$\text{Mass } m = 3637 \pm 4 \text{ MeV} \quad (S = 1.7)$$

$$\text{Full width } \Gamma = 14 \pm 7 \text{ MeV}$$

$\eta_c(2S)$ DECAY MODES	Fraction (Γ_i/Γ)	Confidence level	p (MeV/c)
hadrons	not seen		—
$K \bar{K} \pi$	$(1.9 \pm 1.2) \%$		1729
$2\pi^+ 2\pi^-$	not seen		1792
$3\pi^+ 3\pi^-$	not seen		1749
$K^+ K^- \pi^+ \pi^-$	not seen		1700
$K^+ K^- \pi^+ \pi^- \pi^0$	not seen		1667
$K^+ K^- 2\pi^+ 2\pi^-$	not seen		1627
$K_S^0 K^- 2\pi^+ \pi^- + \text{c.c.}$	not seen		1666
$2K^+ 2K^-$	not seen		1470
$p \bar{p}$	not seen		1558
$\gamma \gamma$	$< 5 \times 10^{-4}$	90%	1819
$\pi^+ \pi^- \eta$	not seen		1766
$\pi^+ \pi^- \eta'$	not seen		1680
$K^+ K^- \eta$	not seen		1637
$\pi^+ \pi^- \eta_c(1S)$	not seen		541

 $\psi(2S)$

$$JG(J^{PC}) = 0^-(1^{--})$$

$$\text{Mass } m = 3686.09 \pm 0.04 \text{ MeV} \quad (S = 1.6)$$

$$\text{Full width } \Gamma = 304 \pm 9 \text{ keV}$$

$$\Gamma_{ee} = 2.35 \pm 0.04 \text{ keV}$$

$\psi(2S)$ DECAY MODES	Fraction (Γ_i/Γ)	Scale factor/ Confidence level	p (MeV/c)
hadrons	$(97.85 \pm 0.13) \%$		—
virtual $\gamma \rightarrow$ hadrons	$(1.73 \pm 0.14) \%$	S=1.5	—
$g g g$	$(10.6 \pm 1.6) \%$		—
$\gamma g g$	$(1.02 \pm 0.29) \%$		—
light hadrons	$(15.4 \pm 1.5) \%$		—
$e^+ e^-$	$(7.72 \pm 0.17) \times 10^{-3}$		1843
$\mu^+ \mu^-$	$(7.7 \pm 0.8) \times 10^{-3}$		1840
$\tau^+ \tau^-$	$(3.0 \pm 0.4) \times 10^{-3}$		490

Decays into $J/\psi(1S)$ and anything

$J/\psi(1S)$ anything	$(59.5 \pm 0.8) \%$		—
$J/\psi(1S)$ neutrals	$(24.5 \pm 0.4) \%$		—
$J/\psi(1S) \pi^+ \pi^-$	$(33.6 \pm 0.4) \%$		477
$J/\psi(1S) \pi^0 \pi^0$	$(17.73 \pm 0.34) \%$		481
$J/\psi(1S) \eta$	$(3.28 \pm 0.07) \%$		199
$J/\psi(1S) \pi^0$	$(1.30 \pm 0.10) \times 10^{-3}$	S=1.4	528

Hadronic decays

$\pi^0 h_c(1P)$	seen		85
$3(\pi^+ \pi^-) \pi^0$	$(3.5 \pm 1.6) \times 10^{-3}$		1746
$2(\pi^+ \pi^-) \pi^0$	$(2.9 \pm 1.0) \times 10^{-3}$	S=4.6	1799
$\rho \varrho_2(1320)$	$(2.6 \pm 0.9) \times 10^{-4}$		1500
$\rho \bar{\rho}$	$(2.76 \pm 0.12) \times 10^{-4}$		1586
$\Delta^{++} \bar{\Delta}^{--}$	$(1.28 \pm 0.35) \times 10^{-4}$		1371
$\Lambda \bar{\Lambda} \pi^0$	$< 1.2 \times 10^{-4}$	CL=90%	1412
$\Lambda \bar{\Lambda} \eta$	$< 4.9 \times 10^{-5}$	CL=90%	1197
$\Lambda \bar{\rho} K^+$	$(1.00 \pm 0.14) \times 10^{-4}$		1327
$\Lambda \bar{\rho} K^+ \pi^+ \pi^-$	$(1.8 \pm 0.4) \times 10^{-4}$		1167
$\Lambda \bar{\Lambda} \pi^+ \pi^-$	$(2.8 \pm 0.6) \times 10^{-4}$		1346
$\Lambda \bar{\Lambda}$	$(2.8 \pm 0.5) \times 10^{-4}$	S=2.6	1467
$\Sigma^+ \bar{\Sigma}^-$	$(2.6 \pm 0.8) \times 10^{-4}$		1408
$\Sigma^0 \bar{\Sigma}^0$	$(2.2 \pm 0.4) \times 10^{-4}$	S=1.5	1405
$\Sigma(1385)^+ \bar{\Sigma}(1385)^-$	$(1.1 \pm 0.4) \times 10^{-4}$		1218
$\Xi^- \bar{\Xi}^+$	$(1.8 \pm 0.6) \times 10^{-4}$	S=2.8	1284
$\Xi^0 \bar{\Xi}^0$	$(2.8 \pm 0.9) \times 10^{-4}$		1291
$\Xi(1530)^0 \bar{\Xi}(1530)^0$	$< 8.1 \times 10^{-5}$	CL=90%	1025
$\Omega^- \bar{\Omega}^+$	$< 7.3 \times 10^{-5}$	CL=90%	774
$\pi^0 \rho \bar{\rho}$	$(1.33 \pm 0.17) \times 10^{-4}$		1543
$\eta \rho \bar{\rho}$	$(6.0 \pm 1.2) \times 10^{-5}$		1373
$\omega \rho \bar{\rho}$	$(6.9 \pm 2.1) \times 10^{-5}$		1247
$\phi \rho \bar{\rho}$	$< 2.4 \times 10^{-5}$	CL=90%	1109
$\pi^+ \pi^- \rho \bar{\rho}$	$(6.0 \pm 0.4) \times 10^{-4}$		1491
$\rho \bar{\eta} \pi^-$ or c.c.	$(2.48 \pm 0.17) \times 10^{-4}$		—
$\rho \bar{\eta} \pi^- \pi^0$	$(3.2 \pm 0.7) \times 10^{-4}$		1492
$2(\pi^+ \pi^- \pi^0)$	$(4.8 \pm 1.5) \times 10^{-3}$		1776
$\eta \pi^+ \pi^-$	$< 1.6 \times 10^{-4}$	CL=90%	1791
$\eta \pi^+ \pi^- \pi^0$	$(9.5 \pm 1.7) \times 10^{-4}$		1778
$2(\pi^+ \pi^-) \eta$	$(1.2 \pm 0.6) \times 10^{-3}$		1758
$\eta' \pi^+ \pi^- \pi^0$	$(4.5 \pm 2.1) \times 10^{-4}$		1692
$\omega \pi^+ \pi^-$	$(7.3 \pm 1.2) \times 10^{-4}$	S=2.1	1748
$b_1^\pm \pi^\mp$	$(4.0 \pm 0.6) \times 10^{-4}$	S=1.1	1635
$b_1^0 \pi^0$	$(2.4 \pm 0.6) \times 10^{-4}$		—
$\omega f_2(1270)$	$(2.2 \pm 0.4) \times 10^{-4}$		1515
$\pi^+ \pi^- K^+ K^-$	$(7.5 \pm 0.9) \times 10^{-4}$	S=1.9	1726
$\rho^0 K^+ K^-$	$(2.2 \pm 0.4) \times 10^{-4}$		1616
$K^*(892)^0 \bar{K}_2^*(1430)^0$	$(1.9 \pm 0.5) \times 10^{-4}$		1418
$K^+ K^- \pi^+ \pi^- \eta$	$(1.3 \pm 0.7) \times 10^{-3}$		1574
$K^+ K^- 2(\pi^+ \pi^-) \pi^0$	$(1.00 \pm 0.31) \times 10^{-3}$		1611
$K^+ K^- 2(\pi^+ \pi^-)$	$(1.9 \pm 0.9) \times 10^{-3}$		1654
$K_1(1270)^\pm K^\mp$	$(1.00 \pm 0.28) \times 10^{-3}$		1581
$K_S^0 K_S^0 \pi^+ \pi^-$	$(2.2 \pm 0.4) \times 10^{-4}$		1724
$\rho^0 \rho \bar{\rho}$	$(5.0 \pm 2.2) \times 10^{-5}$		1251
$K^+ \bar{K}^*(892)^0 \pi^- + c.c.$	$(6.7 \pm 2.5) \times 10^{-4}$		1674
$2(\pi^+ \pi^-)$	$(2.4 \pm 0.6) \times 10^{-4}$	S=2.2	1817
$\rho^0 \pi^+ \pi^-$	$(2.2 \pm 0.6) \times 10^{-4}$	S=1.4	1750
$K^+ K^- \pi^+ \pi^- \pi^0$	$(1.26 \pm 0.09) \times 10^{-3}$		1694
$\omega f_0(1710) \rightarrow \omega K^+ K^-$	$(5.9 \pm 2.2) \times 10^{-5}$		—
$K^*(892)^0 K^- \pi^+ \pi^0 + c.c.$	$(8.6 \pm 2.2) \times 10^{-4}$		—
$K^*(892)^+ K^- \pi^+ \pi^- + c.c.$	$(9.6 \pm 2.8) \times 10^{-4}$		—
$K^*(892)^+ K^- \rho^0 + c.c.$	$(7.3 \pm 2.6) \times 10^{-4}$		—
$K^*(892)^0 K^- \rho^+ + c.c.$	$(6.1 \pm 1.8) \times 10^{-4}$		—
$\eta K^+ K^-$	$< 1.3 \times 10^{-4}$	CL=90%	1664

$\omega K^+ K^-$	$(1.85 \pm 0.25) \times 10^{-4}$	S=1.1	1614
$3(\pi^+ \pi^-)$	$(3.5 \pm 2.0) \times 10^{-4}$	S=2.8	1774
$\rho \bar{\rho} \pi^+ \pi^- \pi^0$	$(7.3 \pm 0.7) \times 10^{-4}$		1435
$K^+ K^-$	$(6.3 \pm 0.7) \times 10^{-5}$		1776
$K_S^0 K_L^0$	$(5.4 \pm 0.5) \times 10^{-5}$		1775
$\pi^+ \pi^- \pi^0$	$(1.68 \pm 0.26) \times 10^{-4}$	S=1.4	1830
$\rho(2150) \pi \rightarrow \pi^+ \pi^- \pi^0$	$(1.9 \pm_{-0.4}^{+1.2}) \times 10^{-4}$		—
$\rho(770) \pi \rightarrow \pi^+ \pi^- \pi^0$	$(3.2 \pm 1.2) \times 10^{-5}$	S=1.8	—
$\pi^+ \pi^-$	$(8 \pm 5) \times 10^{-5}$		1838
$K_1(1400)^\pm K^\mp$	$< 3.1 \times 10^{-4}$	CL=90%	1532
$K^+ K^- \pi^0$	$< 2.96 \times 10^{-5}$	CL=90%	1754
$K^+ \bar{K}^*(892)^- + \text{c.c.}$	$(1.7 \pm_{-0.7}^{+0.8}) \times 10^{-5}$		1698
$K^*(892)^0 \bar{K}^0 + \text{c.c.}$	$(1.09 \pm 0.20) \times 10^{-4}$		1697
$\phi \pi^+ \pi^-$	$(1.17 \pm 0.29) \times 10^{-4}$	S=1.7	1690
$\phi f_0(980) \rightarrow \pi^+ \pi^-$	$(6.8 \pm 2.4) \times 10^{-5}$	S=1.1	—
$2(K^+ K^-)$	$(6.0 \pm 1.4) \times 10^{-5}$		1499
$\phi K^+ K^-$	$(7.0 \pm 1.6) \times 10^{-5}$		1546
$2(K^+ K^-) \pi^0$	$(1.10 \pm 0.28) \times 10^{-4}$		1440
$\phi \eta$	$(2.8 \pm_{-0.8}^{+1.0}) \times 10^{-5}$		1654
$\phi \eta'$	$(3.1 \pm 1.6) \times 10^{-5}$		1555
$\omega \eta'$	$(3.2 \pm_{-2.1}^{+2.5}) \times 10^{-5}$		1623
$\omega \pi^0$	$(2.1 \pm 0.6) \times 10^{-5}$		1757
$\rho \eta'$	$(1.9 \pm_{-1.2}^{+1.7}) \times 10^{-5}$		1625
$\rho \eta$	$(2.2 \pm 0.6) \times 10^{-5}$	S=1.1	1717
$\omega \eta$	$< 1.1 \times 10^{-5}$	CL=90%	1715
$\phi \pi^0$	$< 4 \times 10^{-6}$	CL=90%	1699
$\eta_c \pi^+ \pi^- \pi^0$	$< 1.0 \times 10^{-3}$	CL=90%	—
$\rho \bar{\rho} K^+ K^-$	$(2.7 \pm 0.7) \times 10^{-5}$		1118
$\bar{\Lambda} n K_S^0 + \text{c.c.}$	$(8.1 \pm 1.8) \times 10^{-5}$		1324
$\phi f_2'(1525)$	$(4.4 \pm 1.6) \times 10^{-5}$		1321
$\Theta(1540) \bar{\Theta}(1540) \rightarrow K_S^0 \rho K^- \bar{n} + \text{c.c.}$	$< 8.8 \times 10^{-6}$	CL=90%	—
$\Theta(1540) K^- \bar{n} \rightarrow K_S^0 \rho K^- \bar{n}$	$< 1.0 \times 10^{-5}$	CL=90%	—
$\Theta(1540) K_S^0 \bar{p} \rightarrow K_S^0 \bar{p} K^+ n$	$< 7.0 \times 10^{-6}$	CL=90%	—
$\bar{\Theta}(1540) K^+ n \rightarrow K_S^0 \bar{p} K^+ n$	$< 2.6 \times 10^{-5}$	CL=90%	—
$\bar{\Theta}(1540) K_S^0 \rho \rightarrow K_S^0 \rho K^- \bar{n}$	$< 6.0 \times 10^{-6}$	CL=90%	—
$K_S^0 K_S^0$	$< 4.6 \times 10^{-6}$		1775

Radiative decays

$\gamma \chi_{c0}(1P)$	$(9.62 \pm 0.31) \%$		261
$\gamma \chi_{c1}(1P)$	$(9.2 \pm 0.4) \%$		171
$\gamma \chi_{c2}(1P)$	$(8.74 \pm 0.35) \%$		128
$\pi^0 h_c \rightarrow \gamma \eta_c(1S) \pi^0$	$(4.2 \pm 0.5) \times 10^{-4}$		—
$\gamma \eta_c(1S)$	$(3.4 \pm 0.5) \times 10^{-3}$	S=1.3	638
$\gamma \eta_c(2S)$	$< 8 \times 10^{-4}$	CL=90%	48
$\gamma \pi^0$	$< 5 \times 10^{-6}$	CL=90%	1841
$\gamma \eta'(958)$	$(1.21 \pm 0.08) \times 10^{-4}$		1719
$\gamma f_2(1270)$	$(2.1 \pm 0.4) \times 10^{-4}$		1622
$\gamma f_0(1710) \rightarrow \gamma \pi \pi$	$(3.0 \pm 1.3) \times 10^{-5}$		—
$\gamma f_0(1710) \rightarrow \gamma K \bar{K}$	$(6.0 \pm 1.6) \times 10^{-5}$		—
$\gamma \gamma$	$< 1.4 \times 10^{-4}$	CL=90%	1843
$\gamma \eta$	$< 2 \times 10^{-6}$	CL=90%	1802

$\gamma\eta\pi^+\pi^-$	$(8.7 \pm 2.1) \times 10^{-4}$		1791
$\gamma\eta(1405) \rightarrow \gamma K\bar{K}\pi$	$< 9 \times 10^{-5}$	CL=90%	1569
$\gamma\eta(1405) \rightarrow \eta\pi^+\pi^-$	$(3.6 \pm 2.5) \times 10^{-5}$		—
$\gamma\eta(1475) \rightarrow K\bar{K}\pi$	$< 1.4 \times 10^{-4}$	CL=90%	—
$\gamma\eta(1475) \rightarrow \eta\pi^+\pi^-$	$< 8.8 \times 10^{-5}$	CL=90%	—
$\gamma 2(\pi^+\pi^-)$	$(4.0 \pm 0.6) \times 10^{-4}$		1817
$\gamma K^{*0}K^+\pi^- + \text{c.c.}$	$(3.7 \pm 0.9) \times 10^{-4}$		1674
$\gamma K^{*0}\bar{K}^{*0}$	$(2.4 \pm 0.7) \times 10^{-4}$		1613
$\gamma K_S^0 K^+\pi^- + \text{c.c.}$	$(2.6 \pm 0.5) \times 10^{-4}$		1753
$\gamma K^+ K^-\pi^+\pi^-$	$(1.9 \pm 0.5) \times 10^{-4}$		1726
$\gamma\rho\bar{\rho}$	$(2.9 \pm 0.6) \times 10^{-5}$		1586
$\gamma\pi^+\pi^-\rho\bar{\rho}$	$(2.8 \pm 1.4) \times 10^{-5}$		1491
$\gamma 2(\pi^+\pi^-)K^+K^-$	$< 2.2 \times 10^{-4}$	CL=90%	1654
$\gamma 3(\pi^+\pi^-)$	$< 1.7 \times 10^{-4}$	CL=90%	1774
$\gamma K^+ K^- K^+ K^-$	$< 4 \times 10^{-5}$	CL=90%	1499

 $\psi(3770)$

$$J^G(J^{PC}) = 0^-(1^{--})$$

Mass $m = 3772.92 \pm 0.35$ MeV ($S = 1.1$)

Full width $\Gamma = 27.3 \pm 1.0$ MeV

$\Gamma_{ee} = 0.265 \pm 0.018$ keV ($S = 1.3$)

In addition to the dominant decay mode to $D\bar{D}$, $\psi(3770)$ was found to decay into the final states containing the J/ψ (BAI 05, ADAM 06). ADAMS 06 and HUANG 06A searched for various decay modes with light hadrons and found a statistically significant signal for the decay to $\phi\eta$ only (ADAMS 06).

$\psi(3770)$ DECAY MODES	Fraction (Γ_i/Γ)	Scale factor/ Confidence level	ρ (MeV/c)
$D\bar{D}$	$(93 \pm 8) \%$	$S=2.0$	285
$D^0\bar{D}^0$	$(52 \pm 5) \%$	$S=2.0$	285
D^+D^-	$(41 \pm 4) \%$	$S=2.0$	252
$J/\psi\pi^+\pi^-$	$(1.93 \pm 0.28) \times 10^{-3}$		560
$J/\psi\pi^0\pi^0$	$(8.0 \pm 3.0) \times 10^{-4}$		564
$J/\psi\eta$	$(9 \pm 4) \times 10^{-4}$		359
$J/\psi\pi^0$	$< 2.8 \times 10^{-4}$	CL=90%	603
$\gamma\chi_{c0}$	$(7.3 \pm 0.9) \times 10^{-3}$		341
$\gamma\chi_{c1}$	$(2.9 \pm 0.6) \times 10^{-3}$		253
$\gamma\chi_{c2}$	$< 9 \times 10^{-4}$	CL=90%	210
e^+e^-	$(9.7 \pm 0.7) \times 10^{-6}$	$S=1.2$	1886
$K_S^0 K_L^0$	$< 1.2 \times 10^{-5}$	CL=90%	1820
$2(\pi^+\pi^-)$	$< 1.12 \times 10^{-3}$	CL=90%	1861
$2(\pi^+\pi^-)\pi^0$	$< 1.06 \times 10^{-3}$	CL=90%	1843
$2(\pi^+\pi^-\pi^0)$	$< 5.85 \%$	CL=90%	1821
$\omega\pi^+\pi^-$	$< 6.0 \times 10^{-4}$	CL=90%	1794
$3(\pi^+\pi^-)$	$< 9.1 \times 10^{-3}$		1819
$3(\pi^+\pi^-\pi^0)$	$< 1.37 \%$		1792
$3(\pi^+\pi^-)2\pi^0$	$< 11.74 \%$	CL=90%	1759
$\eta\pi^+\pi^-$	$< 1.24 \times 10^{-3}$	CL=90%	1836
$\pi^+\pi^-2\pi^0$	$< 8.9 \times 10^{-3}$	CL=90%	1862
$\rho^0\pi^+\pi^-$	$< 6.9 \times 10^{-3}$	CL=90%	1796
$\eta 3\pi$	$< 1.34 \times 10^{-3}$	CL=90%	1824
$\eta 2(\pi^+\pi^-)$	$< 2.43 \%$		1804
$\eta' 3\pi$	$< 2.44 \times 10^{-3}$	CL=90%	1740
$K^+K^-\pi^+\pi^-$	$< 9.0 \times 10^{-4}$	CL=90%	1772

$\phi\pi^+\pi^-$	< 4.1	$\times 10^{-4}$	CL=90%	1737
$K^+K^-2\pi^0$	< 4.2	$\times 10^{-3}$	CL=90%	1774
$\phi\pi^0$	not seen			1746
$\phi\eta$	$(3.1 \pm 0.7) \times 10^{-4}$			1703
$4(\pi^+\pi^-)$	< 1.67	%	CL=90%	1757
$4(\pi^+\pi^-)\pi^0$	< 3.06	%	CL=90%	1720
$\phi f_0(980)$	< 4.5	$\times 10^{-4}$	CL=90%	1600
$K^+K^-\pi^+\pi^-\pi^0$	< 2.36	$\times 10^{-3}$	CL=90%	1741
$K^+K^-\rho^0\pi^0$	< 8	$\times 10^{-4}$	CL=90%	1624
$K^+K^-\rho^+\pi^-$	< 1.46	%	CL=90%	1622
ωK^+K^-	< 3.4	$\times 10^{-4}$	CL=90%	1664
$\phi\pi^+\pi^-\pi^0$	< 3.8	$\times 10^{-3}$	CL=90%	1722
$K^{*0}K^-\pi^+\pi^0 + \text{c.c.}$	< 1.62	%	CL=90%	1693
$K^{*+}K^-\pi^+\pi^-\pi^0 + \text{c.c.}$	< 3.23	%	CL=90%	1692
$K^+K^-\pi^+\pi^-2\pi^0$	< 2.67	%	CL=90%	1705
$K^+K^-2(\pi^+\pi^-)$	< 1.03	%	CL=90%	1702
$K^+K^-2(\pi^+\pi^-)\pi^0$	< 3.60	%	CL=90%	1660
ηK^+K^-	< 4.1	$\times 10^{-4}$	CL=90%	1711
$\rho^0 K^+K^-$	< 5.0	$\times 10^{-3}$	CL=90%	1665
$2(K^+K^-)$	< 6.0	$\times 10^{-4}$	CL=90%	1551
ϕK^+K^-	< 7.5	$\times 10^{-4}$	CL=90%	1597
$2(K^+K^-)\pi^0$	< 2.9	$\times 10^{-4}$	CL=90%	1493
$2(K^+K^-)\pi^+\pi^-$	< 3.2	$\times 10^{-3}$	CL=90%	1425
$K_S^0 K^-\pi^+$	< 3.2	$\times 10^{-3}$	CL=90%	1799
$K_S^0 K^-\pi^+\pi^0$	< 1.33	%	CL=90%	1773
$K_S^0 K^-\rho^+$	< 6.6	$\times 10^{-3}$	CL=90%	1664
$K_S^0 K^-2\pi^+\pi^-$	< 8.7	$\times 10^{-3}$	CL=90%	1739
$K_S^0 K^-\pi^+\rho^0$	< 1.6	%	CL=90%	1621
$K_S^0 K^-\pi^+\eta$	< 1.3	%	CL=90%	1669
$K_S^0 K^-2\pi^+\pi^-\pi^0$	< 4.18	%	CL=90%	1703
$K_S^0 K^-2\pi^+\pi^-\eta$	< 4.8	%	CL=90%	1570
$K_S^0 K^-\pi^+2(\pi^+\pi^-)$	< 1.22	%	CL=90%	1658
$K_S^0 K^-\pi^+2\pi^0$	< 2.65	%	CL=90%	1741
$K_S^0 K^-K^+K^-\pi^+$	< 4.9	$\times 10^{-3}$	CL=90%	1490
$K_S^0 K^-K^+K^-\pi^+\pi^0$	< 3.0	%	CL=90%	1427
$K_S^0 K^-K^+K^-\pi^+\eta$	< 2.2	%	CL=90%	1214
$K^{*0}K^-\pi^+ + \text{c.c.}$	< 9.7	$\times 10^{-3}$	CL=90%	1721
$\rho\bar{p}\pi^0$	< 1.2	$\times 10^{-3}$		1595
$\rho\bar{p}\pi^+\pi^-$	< 5.8	$\times 10^{-4}$	CL=90%	1544
$\Lambda\bar{\Lambda}$	< 1.2	$\times 10^{-4}$	CL=90%	1521
$\rho\bar{p}\pi^+\pi^-\pi^0$	< 1.85	$\times 10^{-3}$	CL=90%	1490
$\omega\rho\bar{p}$	< 2.9	$\times 10^{-4}$	CL=90%	1309
$\Lambda\bar{\Lambda}\pi^0$	< 1.2	$\times 10^{-3}$	CL=90%	1468
$\rho\bar{p}2(\pi^+\pi^-)$	< 2.6	$\times 10^{-3}$	CL=90%	1425
$\eta\rho\bar{p}$	< 5.4	$\times 10^{-4}$	CL=90%	1430
$\rho^0\rho\bar{p}$	< 1.7	$\times 10^{-3}$	CL=90%	1313
$\rho\bar{p}K^+K^-$	< 3.2	$\times 10^{-4}$	CL=90%	1185
$\phi\rho\bar{p}$	< 1.3	$\times 10^{-4}$	CL=90%	1178
$\Lambda\bar{\Lambda}\pi^+\pi^-$	< 2.5	$\times 10^{-4}$	CL=90%	1404
$\Lambda\bar{\Lambda}K^+$	< 2.8	$\times 10^{-4}$	CL=90%	1387
$\Lambda\bar{\Lambda}K^+\pi^+\pi^-$	< 6.3	$\times 10^{-4}$	CL=90%	1234
$\pi^+\pi^-\pi^0$	not seen			1874
$\rho\pi$	not seen			1804
$\omega\pi^0$	not seen			1803

$\rho\eta$	not seen	1763
$\omega\eta$	not seen	1762
$\rho\eta'$	not seen	1674
$\omega\eta'$	not seen	1672
$\phi\eta'$	not seen	1606
$K^{*0}\bar{K}^0$	not seen	1744
$K^{*+}K^-$	not seen	1745
$b_1\pi$	not seen	1683

Radiative decays

$\gamma\pi^0$	< 2	$\times 10^{-4}$	CL=90%	1884
$\gamma\eta$	< 1.5	$\times 10^{-4}$	CL=90%	1847
$\gamma\eta'$	< 1.8	$\times 10^{-4}$	CL=90%	1765

X(3872)

$$I^G(J^{PC}) = 0^?(?^{?+})$$

Quantum numbers not established.

Mass $m = 3871.56 \pm 0.22$ MeV $m_{X(3872)} - m_{J/\psi} = 775 \pm 4$ MeV $m_{X(3872)} - m_{\psi(2S)}$ Full width $\Gamma < 2.3$ MeV, CL = 90%

X(3872) DECAY MODES	Fraction (Γ_i/Γ)	ρ (MeV/c)
$\pi^+\pi^-J/\psi(1S)$	>2.6%	650
$D^0\bar{D}^0\pi^0$	$>3.2 \times 10^{-3}$	116
$\bar{D}^{*0}D^0$	$>5 \times 10^{-3}$	†
$\gamma J/\psi$	$>9 \times 10^{-3}$	697
$\gamma\psi(2S)$	>3.0%	181

 $\psi(4040)$ [iiii]

$$I^G(J^{PC}) = 0^-(1^{--})$$

Mass $m = 4039 \pm 1$ MeVFull width $\Gamma = 80 \pm 10$ MeV $\Gamma_{ee} = 0.86 \pm 0.07$ keV

$\psi(4040)$ DECAY MODES	Fraction (Γ_i/Γ)	Confidence level	ρ (MeV/c)
e^+e^-	$(1.07 \pm 0.16) \times 10^{-5}$		2019
$D\bar{D}$	seen		775
$D^0\bar{D}^0$	seen		775
D^+D^-	seen		764
$D^*\bar{D} + \text{c.c.}$	seen		569
$D^*(2007)^0\bar{D}^0 + \text{c.c.}$	seen		575
$D^*(2010)^+D^- + \text{c.c.}$	seen		561
$D^*\bar{D}^*$	not seen		193
$D^*(2007)^0\bar{D}^*(2007)^0$	not seen		225
$D^*(2010)^+D^*(2010)^-$	not seen		193
$J/\psi\pi^+\pi^-$	< 4	$\times 10^{-3}$	90% 794
$J/\psi\pi^0\pi^0$	< 2	$\times 10^{-3}$	90% 797
$J/\psi\eta$	< 7	$\times 10^{-3}$	90% 675
$J/\psi\pi^0$	< 2	$\times 10^{-3}$	90% 823
$J/\psi\pi^+\pi^-\pi^0$	< 2	$\times 10^{-3}$	90% 746

$\chi_{c1} \gamma$	< 1.1	%	90%	494
$\chi_{c2} \gamma$	< 1.7	%	90%	454
$\chi_{c1} \pi^+ \pi^- \pi^0$	< 1.1	%	90%	306
$\chi_{c2} \pi^+ \pi^- \pi^0$	< 3.2	%	90%	233
$\phi \pi^+ \pi^-$	< 3	$\times 10^{-3}$	90%	1880

 $\psi(4160)$ [iiii]

$$J^G(J^{PC}) = 0^-(1^{--})$$

Mass $m = 4153 \pm 3$ MeV

Full width $\Gamma = 103 \pm 8$ MeV

$\Gamma_{ee} = 0.83 \pm 0.07$ keV

$\psi(4160)$ DECAY MODES	Fraction (Γ_i/Γ)	Confidence level	ρ (MeV/c)
$e^+ e^-$	$(8.1 \pm 0.9) \times 10^{-6}$		2076
$D \bar{D}$	not seen		913
$D^0 \bar{D}^0$	not seen		913
$D^+ D^-$	not seen		904
$D^* \bar{D} + \text{c.c.}$	not seen		746
$D^*(2007)^0 \bar{D}^0 + \text{c.c.}$	not seen		751
$D^*(2010)^+ D^- + \text{c.c.}$	not seen		740
$D^* \bar{D}^*$	seen		520
$D^*(2007)^0 \bar{D}^*(2007)^0$	seen		533
$D^*(2010)^+ D^*(2010)^-$	seen		520
$J/\psi \pi^+ \pi^-$	< 3 $\times 10^{-3}$	90%	888
$J/\psi \pi^0 \pi^0$	< 3 $\times 10^{-3}$	90%	891
$J/\psi K^+ K^-$	< 2 $\times 10^{-3}$	90%	324
$J/\psi \eta$	< 8 $\times 10^{-3}$	90%	786
$J/\psi \pi^0$	< 1 $\times 10^{-3}$	90%	914
$J/\psi \eta'$	< 5 $\times 10^{-3}$	90%	385
$J/\psi \pi^+ \pi^- \pi^0$	< 1 $\times 10^{-3}$	90%	847
$\psi(2S) \pi^+ \pi^-$	< 4 $\times 10^{-3}$	90%	353
$\chi_{c1} \gamma$	< 7 $\times 10^{-3}$	90%	593
$\chi_{c2} \gamma$	< 1.3 %	90%	554
$\chi_{c1} \pi^+ \pi^- \pi^0$	< 2 $\times 10^{-3}$	90%	452
$\chi_{c2} \pi^+ \pi^- \pi^0$	< 8 $\times 10^{-3}$	90%	398
$\phi \pi^+ \pi^-$	< 2 $\times 10^{-3}$	90%	1941

 $X(4260)$

$$J^G(J^{PC}) = ?(1^{--})$$

Mass $m = 4263_{-9}^{+8}$ MeV ($S = 1.1$)

Full width $\Gamma = 95 \pm 14$ MeV

$X(4260)$ DECAY MODES	Fraction (Γ_i/Γ)	ρ (MeV/c)
$J/\psi \pi^+ \pi^-$	seen	976
$J/\psi \pi^0 \pi^0$	[jjjj] seen	978
$J/\psi K^+ K^-$	[jjjj] seen	530
$J/\psi \eta$	[jjjj] not seen	886
$J/\psi \pi^0$	[jjjj] not seen	999
$J/\psi \eta'$	[jjjj] not seen	569
$J/\psi \pi^+ \pi^- \pi^0$	[jjjj] not seen	939
$J/\psi \eta \eta$	[jjjj] not seen	339
$\psi(2S) \pi^+ \pi^-$	[jjjj] not seen	470
$\psi(2S) \eta$	[jjjj] not seen	167

$\chi_{c0}\omega$	$[jjj]$ not seen	292
$\chi_{c1}\gamma$	$[jjj]$ not seen	686
$\chi_{c2}\gamma$	$[jjj]$ not seen	648
$\chi_{c1}\pi^+\pi^-\pi^0$	$[jjj]$ not seen	571
$\chi_{c2}\pi^+\pi^-\pi^0$	$[jjj]$ not seen	524
$\phi\pi^+\pi^-$	$[jjj]$ not seen	1999
$\phi f_0(980) \rightarrow \phi\pi^+\pi^-$	not seen	—
$D\bar{D}$	not seen	1032
$D^0 D^{*-}\pi^+$	not seen	716
$D^* \bar{D}$	not seen	887
$D^* \bar{D}^*$	not seen	708
$D^* \bar{D}\pi$	not seen	723
$D^* \bar{D}^* \pi$	not seen	474
$D_s^+ D_s^-$	not seen	817
$D_s^{*+} D_s^-$	not seen	615
$D_s^{*+} D_s^{*-}$	not seen	284
$p\bar{p}$	not seen	1914
$K_S^0 K^\pm \pi^\mp$	not seen	2054
$K^+ K^- \pi^0$	not seen	2055

$\psi(4415)$ $[jjjj]$

$$I^G(J^{PC}) = 0^-(1^{--})$$

Mass $m = 4421 \pm 4$ MeV

Full width $\Gamma = 62 \pm 20$ MeV

$\Gamma_{ee} = 0.58 \pm 0.07$ keV

$\psi(4415)$ DECAY MODES	Fraction (Γ_i/Γ)	Confidence level	ρ (MeV/c)
hadrons	dominant		—
$D\bar{D}$	not seen		1187
$D^0 \bar{D}^0$	not seen		1187
$D^+ D^-$	not seen		1179
$D^* \bar{D} + \text{c.c.}$	not seen		1063
$D^*(2007)^0 \bar{D}^0 + \text{c.c.}$	not seen		1067
$D^*(2010)^+ D^- + \text{c.c.}$	not seen		1059
$D^* \bar{D}^*$	not seen		919
$D^*(2007)^0 \bar{D}^*(2007)^0 + \text{c.c.}$	not seen		927
$D^*(2010)^+ D^*(2010)^- + \text{c.c.}$	not seen		919
$(D^0 D^- \pi^+)_{\text{non-res}}$	< 2.3 %	90%	—
$D\bar{D}_2^*(2460) \rightarrow D^0 D^- \pi^+$	(10 ± 4) %		—
$D^0 D^{*-}\pi^+$	< 11 %	90%	926
$e^+ e^-$	$(9.4 \pm 3.2) \times 10^{-6}$		2210

$b\bar{b}$ MESONS

 $\Upsilon(1S)$

$$J^G(J^{PC}) = 0^-(1^{--})$$

 Mass $m = 9460.30 \pm 0.26$ MeV ($S = 3.3$)

 Full width $\Gamma = 54.02 \pm 1.25$ keV

 $\Gamma_{ee} = 1.340 \pm 0.018$ keV

$\Upsilon(1S)$ DECAY MODES	Fraction (Γ_i/Γ)	Confidence level	P (MeV/c)
$\tau^+ \tau^-$	(2.60±0.10) %		4384
$e^+ e^-$	(2.48±0.07) %		4730
$\mu^+ \mu^-$	(2.48±0.05) %		4729
Hadronic decays			
$g g g$	(81.7 ± 0.7) %		—
$\gamma g g$	(2.21±0.22) %		—
$\eta'(958)$ anything	(2.94±0.24) %		—
$J/\psi(1S)$ anything	(6.5 ± 0.7) × 10 ⁻⁴		4223
χ_{c0} anything	< 5 × 10 ⁻³	90%	—
χ_{c1} anything	(2.3 ± 0.7) × 10 ⁻⁴		—
χ_{c2} anything	(3.4 ± 1.0) × 10 ⁻⁴		—
$\psi(2S)$ anything	(2.7 ± 0.9) × 10 ⁻⁴		—
$\rho\pi$	< 2 × 10 ⁻⁴	90%	4697
$\pi^+ \pi^-$	< 5 × 10 ⁻⁴	90%	4728
$K^+ K^-$	< 5 × 10 ⁻⁴	90%	4704
$p\bar{p}$	< 5 × 10 ⁻⁴	90%	4636
$\pi^0 \pi^+ \pi^-$	< 1.84 × 10 ⁻⁵	90%	4725
$D^*(2010)^\pm$ anything	(2.52±0.20) %		—
\bar{d} anything	(2.86±0.28) × 10 ⁻⁵		—
Radiative decays			
$\gamma \pi^+ \pi^-$	(6.3 ± 1.8) × 10 ⁻⁵		4728
$\gamma \pi^0 \pi^0$	(1.7 ± 0.7) × 10 ⁻⁵		4728
$\gamma \pi^0 \eta$	< 2.4 × 10 ⁻⁶	90%	4713
$\gamma K^+ K^-$	[kkkk] (1.14±0.13) × 10 ⁻⁵		4704
$\gamma p\bar{p}$	[llll] < 6 × 10 ⁻⁶	90%	4636
$\gamma 2h^+ 2h^-$	(7.0 ± 1.5) × 10 ⁻⁴		4720
$\gamma 3h^+ 3h^-$	(5.4 ± 2.0) × 10 ⁻⁴		4703
$\gamma 4h^+ 4h^-$	(7.4 ± 3.5) × 10 ⁻⁴		4679
$\gamma \pi^+ \pi^- K^+ K^-$	(2.9 ± 0.9) × 10 ⁻⁴		4686
$\gamma 2\pi^+ 2\pi^-$	(2.5 ± 0.9) × 10 ⁻⁴		4720
$\gamma 3\pi^+ 3\pi^-$	(2.5 ± 1.2) × 10 ⁻⁴		4703
$\gamma 2\pi^+ 2\pi^- K^+ K^-$	(2.4 ± 1.2) × 10 ⁻⁴		4658
$\gamma \pi^+ \pi^- p\bar{p}$	(1.5 ± 0.6) × 10 ⁻⁴		4604
$\gamma 2\pi^+ 2\pi^- p\bar{p}$	(4 ± 6) × 10 ⁻⁵		4563
$\gamma 2K^+ 2K^-$	(2.0 ± 2.0) × 10 ⁻⁵		4601
$\gamma \eta'(958)$	< 1.9 × 10 ⁻⁶	90%	4682
$\gamma \eta$	< 1.0 × 10 ⁻⁶	90%	4714
$\gamma f_0(980)$	< 3 × 10 ⁻⁵	90%	4679
$\gamma f_2'(1525)$	(3.7 ^{+1.2} _{-1.1}) × 10 ⁻⁵		4607
$\gamma f_2(1270)$	(1.01±0.09) × 10 ⁻⁴		4644
$\gamma \eta(1405)$	< 8.2 × 10 ⁻⁵	90%	4625

$\gamma f_0(1500)$	< 1.5	$\times 10^{-5}$	90%	4610
$\gamma f_0(1710)$	< 2.6	$\times 10^{-4}$	90%	4574
$\gamma f_0(1710) \rightarrow \gamma K^+ K^-$	< 7	$\times 10^{-6}$	90%	—
$\gamma f_0(1710) \rightarrow \gamma \pi^0 \pi^0$	< 1.4	$\times 10^{-6}$	90%	—
$\gamma f_0(1710) \rightarrow \gamma \eta \eta$	< 1.8	$\times 10^{-6}$	90%	—
$\gamma f_4(2050)$	< 5.3	$\times 10^{-5}$	90%	4515
$\gamma f_0(2200) \rightarrow \gamma K^+ K^-$	< 2	$\times 10^{-4}$	90%	4475
$\gamma f_J(2220) \rightarrow \gamma K^+ K^-$	< 8	$\times 10^{-7}$	90%	4469
$\gamma f_J(2220) \rightarrow \gamma \pi^+ \pi^-$	< 6	$\times 10^{-7}$	90%	—
$\gamma f_J(2220) \rightarrow \gamma \rho \bar{\rho}$	< 1.1	$\times 10^{-6}$	90%	—
$\gamma \eta(2225) \rightarrow \gamma \phi \phi$	< 3	$\times 10^{-3}$	90%	4469
γX	[mmmm] < 3	$\times 10^{-5}$	90%	—
$\gamma X \bar{X}$	[nnnn] < 1	$\times 10^{-3}$	90%	—
$\gamma X \rightarrow \gamma + \geq 4$ prongs	[oooo] < 1.78	$\times 10^{-4}$	95%	—
$\gamma a_1^0 \rightarrow \gamma \mu^+ \mu^-$	[pppp] < 9	$\times 10^{-6}$	90%	—
$\gamma a_1^0 \rightarrow \gamma \tau^+ \tau^-$	[kkkk] < 5.0	$\times 10^{-5}$	90%	—

Lepton Flavor (LF) violating or Invisible decays

$\mu^\pm \tau^\mp$	LF	< 6.0	$\times 10^{-6}$	95%	4563
invisible		< 3.0	$\times 10^{-4}$	90%	—

$\chi_{b0}(1P)$ [qqqq]

$J^G(J^{PC}) = 0^+(0^{++})$
J needs confirmation.

Mass $m = 9859.44 \pm 0.42 \pm 0.31$ MeV

$\chi_{b0}(1P)$ DECAY MODES	Fraction (Γ_i/Γ)	Confidence level	ρ (MeV/c)
$\gamma \Upsilon(1S)$	< 6 %	90%	391
$D^0 X$	< 10.4 %	90%	—
$\pi^+ \pi^- K^+ K^- \pi^0$	< 1.6 $\times 10^{-4}$	90%	4875
$2\pi^+ \pi^- K^- K_S^0$	< 5 $\times 10^{-5}$	90%	4875
$2\pi^+ \pi^- K^- K_S^0 2\pi^0$	< 5 $\times 10^{-4}$	90%	4846
$2\pi^+ 2\pi^- 2\pi^0$	< 2.1 $\times 10^{-4}$	90%	4905
$2\pi^+ 2\pi^- K^+ K^-$	(1.1 \pm 0.6) $\times 10^{-4}$		4861
$2\pi^+ 2\pi^- K^+ K^- \pi^0$	< 2.7 $\times 10^{-4}$	90%	4846
$2\pi^+ 2\pi^- K^+ K^- 2\pi^0$	< 5 $\times 10^{-4}$	90%	4828
$3\pi^+ 2\pi^- K^- K_S^0 \pi^0$	< 1.6 $\times 10^{-4}$	90%	4827
$3\pi^+ 3\pi^-$	< 8 $\times 10^{-5}$	90%	4904
$3\pi^+ 3\pi^- 2\pi^0$	< 6 $\times 10^{-4}$	90%	4881
$3\pi^+ 3\pi^- K^+ K^-$	(2.4 \pm 1.2) $\times 10^{-4}$		4827
$3\pi^+ 3\pi^- K^+ K^- \pi^0$	< 1.0 $\times 10^{-3}$	90%	4808
$4\pi^+ 4\pi^-$	< 8 $\times 10^{-5}$	90%	4880
$4\pi^+ 4\pi^- 2\pi^0$	< 2.1 $\times 10^{-3}$	90%	4850

$\chi_{b1}(1P)$ [qqqq]

$J^G(J^{PC}) = 0^+(1^{++})$
J needs confirmation.

Mass $m = 9892.78 \pm 0.26 \pm 0.31$ MeV

$\chi_{b1}(1P)$ DECAY MODES	Fraction (Γ_i/Γ)	Confidence level	ρ (MeV/c)
$\gamma \Upsilon(1S)$	(35 \pm 8) %		423
$D^0 X$	(12.6 \pm 2.2) %		—
$\pi^+ \pi^- K^+ K^- \pi^0$	(2.0 \pm 0.6) $\times 10^{-4}$		4892
$2\pi^+ \pi^- K^- K_S^0$	(1.3 \pm 0.5) $\times 10^{-4}$		4892

$2\pi^+\pi^-K^-K_S^02\pi^0$	$< 6 \times 10^{-4}$	90%	4863
$2\pi^+2\pi^-2\pi^0$	$(8.0 \pm 2.5) \times 10^{-4}$		4921
$2\pi^+2\pi^-K^+K^-$	$(1.5 \pm 0.5) \times 10^{-4}$		4878
$2\pi^+2\pi^-K^+K^-\pi^0$	$(3.5 \pm 1.2) \times 10^{-4}$		4863
$2\pi^+2\pi^-K^+K^-2\pi^0$	$(8.6 \pm 3.2) \times 10^{-4}$		4845
$3\pi^+2\pi^-K^-K_S^0\pi^0$	$(9.3 \pm 3.3) \times 10^{-4}$		4844
$3\pi^+3\pi^-$	$(1.9 \pm 0.6) \times 10^{-4}$		4921
$3\pi^+3\pi^-2\pi^0$	$(1.7 \pm 0.5) \times 10^{-3}$		4898
$3\pi^+3\pi^-K^+K^-$	$(2.6 \pm 0.8) \times 10^{-4}$		4844
$3\pi^+3\pi^-K^+K^-\pi^0$	$(7.5 \pm 2.6) \times 10^{-4}$		4825
$4\pi^+4\pi^-$	$(2.6 \pm 0.9) \times 10^{-4}$		4897
$4\pi^+4\pi^-2\pi^0$	$(1.4 \pm 0.6) \times 10^{-3}$		4867

$\chi_{b2}(1P)$ [qqqq]

$$J^G(J^{PC}) = 0^+(2^{++})$$

J needs confirmation.

$$\text{Mass } m = 9912.21 \pm 0.26 \pm 0.31 \text{ MeV}$$

$\chi_{b2}(1P)$ DECAY MODES	Fraction (Γ_i/Γ)	Confidence level	p (MeV/c)
$\gamma \Upsilon(1S)$	$(22 \pm 4) \%$		442
$D^0 X$	$< 7.9 \%$	90%	-
$\pi^+\pi^-K^+K^-\pi^0$	$(8 \pm 5) \times 10^{-5}$		4902
$2\pi^+\pi^-K^-K_S^0$	$< 1.0 \times 10^{-4}$	90%	4901
$2\pi^+\pi^-K^-K_S^02\pi^0$	$(5.3 \pm 2.4) \times 10^{-4}$		4873
$2\pi^+2\pi^-2\pi^0$	$(3.5 \pm 1.4) \times 10^{-4}$		4931
$2\pi^+2\pi^-K^+K^-$	$(1.1 \pm 0.4) \times 10^{-4}$		4888
$2\pi^+2\pi^-K^+K^-\pi^0$	$(2.1 \pm 0.9) \times 10^{-4}$		4872
$2\pi^+2\pi^-K^+K^-2\pi^0$	$(3.9 \pm 1.8) \times 10^{-4}$		4855
$3\pi^+2\pi^-K^-K_S^0\pi^0$	$< 5 \times 10^{-4}$	90%	4854
$3\pi^+3\pi^-$	$(7.0 \pm 3.1) \times 10^{-5}$		4931
$3\pi^+3\pi^-2\pi^0$	$(1.0 \pm 0.4) \times 10^{-3}$		4908
$3\pi^+3\pi^-K^+K^-$	$< 8 \times 10^{-5}$	90%	4854
$3\pi^+3\pi^-K^+K^-\pi^0$	$(3.6 \pm 1.5) \times 10^{-4}$		4835
$4\pi^+4\pi^-$	$(8 \pm 4) \times 10^{-5}$		4907
$4\pi^+4\pi^-2\pi^0$	$(1.8 \pm 0.7) \times 10^{-3}$		4877

$\Upsilon(2S)$

$$J^G(J^{PC}) = 0^-(1^{--})$$

$$\text{Mass } m = 10.02326 \pm 0.00031 \text{ GeV}$$

$$\text{Full width } \Gamma = 31.98 \pm 2.63 \text{ keV}$$

$$\Gamma_{ee} = 0.612 \pm 0.011 \text{ keV}$$

$\Upsilon(2S)$ DECAY MODES	Fraction (Γ_i/Γ)	Scale factor/ Confidence level	p (MeV/c)
$\Upsilon(1S)\pi^+\pi^-$	$(18.1 \pm 0.4) \%$		475
$\Upsilon(1S)\pi^0\pi^0$	$(8.6 \pm 0.4) \%$		480
$\tau^+\tau^-$	$(2.00 \pm 0.21) \%$		4686
$\mu^+\mu^-$	$(1.93 \pm 0.17) \%$	S=2.2	5011
e^+e^-	$(1.91 \pm 0.16) \%$		5012
$\Upsilon(1S)\pi^0$	$< 1.8 \times 10^{-4}$	CL=90%	531
$\Upsilon(1S)\eta$	$(2.1 \pm_{-0.7}^{0.8}) \times 10^{-4}$		126

$J/\psi(1S)$ anything	$< 6 \times 10^{-3}$	CL=90%	4533
\bar{d} anything	$(3.4 \pm 0.6) \times 10^{-5}$		—
hadrons	$(94 \pm 11) \%$		—
ggg	$(58.8 \pm 1.2) \%$		—
γgg	$(1.87 \pm 0.28) \%$		—

Radiative decays

$\gamma \chi_{b1}(1P)$	$(6.9 \pm 0.4) \%$		130
$\gamma \chi_{b2}(1P)$	$(7.15 \pm 0.35) \%$		110
$\gamma \chi_{b0}(1P)$	$(3.8 \pm 0.4) \%$		162
$\gamma f_0(1710)$	$< 5.9 \times 10^{-4}$	CL=90%	4864
$\gamma f_2'(1525)$	$< 5.3 \times 10^{-4}$	CL=90%	4896
$\gamma f_2(1270)$	$< 2.41 \times 10^{-4}$	CL=90%	4931
$\gamma \eta_b(1S)$	$(3.9 \pm 1.5) \times 10^{-4}$		612
$\gamma X \rightarrow \gamma + \geq 4$ prongs	$[rrrr] < 1.95 \times 10^{-4}$	CL=95%	—

Lepton Flavor (LF) violating decays

$\mu^\pm \tau^\mp$	LF $< 1.44 \times 10^{-5}$	CL=95%	4854
--------------------	----------------------------	--------	------

$\chi_{b0}(2P)$ [qqqq]

$I^G(J^{PC}) = 0^+(0^{++})$
J needs confirmation.

Mass $m = 10.2325 \pm 0.0004 \pm 0.0005$ GeV

$\chi_{b0}(2P)$ DECAY MODES	Fraction (Γ_i/Γ)	Confidence level	ρ (MeV/c)
$\gamma \Upsilon(2S)$	$(4.6 \pm 2.1) \%$		207
$\gamma \Upsilon(1S)$	$(9 \pm 6) \times 10^{-3}$		743
$D^0 X$	$< 8.2 \%$	90%	—
$\pi^+ \pi^- K^+ K^- \pi^0$	$< 3.4 \times 10^{-5}$	90%	5064
$2\pi^+ \pi^- K^- K_S^0$	$< 5 \times 10^{-5}$	90%	5063
$2\pi^+ \pi^- K^- K_S^0 2\pi^0$	$< 2.2 \times 10^{-4}$	90%	5036
$2\pi^+ 2\pi^- 2\pi^0$	$< 2.4 \times 10^{-4}$	90%	5092
$2\pi^+ 2\pi^- K^+ K^-$	$< 1.5 \times 10^{-4}$	90%	5050
$2\pi^+ 2\pi^- K^+ K^- \pi^0$	$< 2.2 \times 10^{-4}$	90%	5035
$2\pi^+ 2\pi^- K^+ K^- 2\pi^0$	$< 1.1 \times 10^{-3}$	90%	5019
$3\pi^+ 2\pi^- K^- K_S^0 \pi^0$	$< 7 \times 10^{-4}$	90%	5018
$3\pi^+ 3\pi^-$	$< 7 \times 10^{-5}$	90%	5091
$3\pi^+ 3\pi^- 2\pi^0$	$< 1.2 \times 10^{-3}$	90%	5070
$3\pi^+ 3\pi^- K^+ K^-$	$< 1.5 \times 10^{-4}$	90%	5017
$3\pi^+ 3\pi^- K^+ K^- \pi^0$	$< 7 \times 10^{-4}$	90%	4999
$4\pi^+ 4\pi^-$	$< 1.7 \times 10^{-4}$	90%	5069
$4\pi^+ 4\pi^- 2\pi^0$	$< 6 \times 10^{-4}$	90%	5039

$\chi_{b1}(2P)$ [qqqq]

$I^G(J^{PC}) = 0^+(1^{++})$
J needs confirmation.

Mass $m = 10.25546 \pm 0.00022 \pm 0.00050$ GeV

$m_{\chi_{b1}(2P)} - m_{\chi_{b0}(2P)} = 23.5 \pm 1.0$ MeV

$\chi_{b1}(2P)$ DECAY MODES	Fraction (Γ_i/Γ)	Scale factor	ρ (MeV/c)
$\omega \Upsilon(1S)$	$(1.63^{+0.40}_{-0.34}) \%$		135
$\gamma \Upsilon(2S)$	$(21 \pm 4) \%$	1.5	230
$\gamma \Upsilon(1S)$	$(8.5 \pm 1.3) \%$	1.3	764
$\pi\pi\chi_{b1}(1P)$	$(8.6 \pm 3.1) \times 10^{-3}$		238

$D^0 X$	(8.8 ± 1.7) %	—
$\pi^+ \pi^- K^+ K^- \pi^0$	(3.1 ± 1.0) × 10 ⁻⁴	5075
$2\pi^+ \pi^- K^- K_S^0$	(1.1 ± 0.5) × 10 ⁻⁴	5075
$2\pi^+ \pi^- K^- K_S^0 2\pi^0$	(7.7 ± 3.2) × 10 ⁻⁴	5047
$2\pi^+ 2\pi^- 2\pi^0$	(5.9 ± 2.0) × 10 ⁻⁴	5104
$2\pi^+ 2\pi^- K^+ K^-$	(10 ± 4) × 10 ⁻⁵	5062
$2\pi^+ 2\pi^- K^+ K^- \pi^0$	(5.5 ± 1.8) × 10 ⁻⁴	5047
$2\pi^+ 2\pi^- K^+ K^- 2\pi^0$	(10 ± 4) × 10 ⁻⁴	5030
$3\pi^+ 2\pi^- K^- K_S^0 \pi^0$	(6.7 ± 2.6) × 10 ⁻⁴	5029
$3\pi^+ 3\pi^-$	(1.2 ± 0.4) × 10 ⁻⁴	5103
$3\pi^+ 3\pi^- 2\pi^0$	(1.2 ± 0.4) × 10 ⁻³	5081
$3\pi^+ 3\pi^- K^+ K^-$	(2.0 ± 0.8) × 10 ⁻⁴	5029
$3\pi^+ 3\pi^- K^+ K^- \pi^0$	(6.1 ± 2.2) × 10 ⁻⁴	5011
$4\pi^+ 4\pi^-$	(1.7 ± 0.6) × 10 ⁻⁴	5080
$4\pi^+ 4\pi^- 2\pi^0$	(1.9 ± 0.7) × 10 ⁻³	5051

$\chi_{b2}(2P)$ [qqqq]

$$J^G(J^{PC}) = 0^+(2^{++})$$

J needs confirmation.

$$\text{Mass } m = 10.26865 \pm 0.00022 \pm 0.00050 \text{ GeV}$$

$$m_{\chi_{b2}(2P)} - m_{\chi_{b1}(2P)} = 13.5 \pm 0.6 \text{ MeV}$$

$\chi_{b2}(2P)$ DECAY MODES	Fraction (Γ_i/Γ)	Confidence level	ρ (MeV/c)
$\omega \Upsilon(1S)$	(1.10 ^{+0.34} _{-0.30}) %		194
$\gamma \Upsilon(2S)$	(16.2 ± 2.4) %		242
$\gamma \Upsilon(1S)$	(7.1 ± 1.0) %		777
$\pi\pi \chi_{b2}(1P)$	(6.0 ± 2.1) × 10 ⁻³		229
$D^0 X$	< 2.4 %	90%	—
$\pi^+ \pi^- K^+ K^- \pi^0$	< 1.1 × 10 ⁻⁴	90%	5082
$2\pi^+ \pi^- K^- K_S^0$	< 9 × 10 ⁻⁵	90%	5082
$2\pi^+ \pi^- K^- K_S^0 2\pi^0$	< 7 × 10 ⁻⁴	90%	5054
$2\pi^+ 2\pi^- 2\pi^0$	(3.9 ± 1.6) × 10 ⁻⁴		5110
$2\pi^+ 2\pi^- K^+ K^-$	(9 ± 4) × 10 ⁻⁵		5068
$2\pi^+ 2\pi^- K^+ K^- \pi^0$	(2.4 ± 1.1) × 10 ⁻⁴		5054
$2\pi^+ 2\pi^- K^+ K^- 2\pi^0$	(4.7 ± 2.3) × 10 ⁻⁴		5037
$3\pi^+ 2\pi^- K^- K_S^0 \pi^0$	< 4 × 10 ⁻⁴	90%	5036
$3\pi^+ 3\pi^-$	(9 ± 4) × 10 ⁻⁵		5110
$3\pi^+ 3\pi^- 2\pi^0$	(1.2 ± 0.4) × 10 ⁻³		5088
$3\pi^+ 3\pi^- K^+ K^-$	(1.4 ± 0.7) × 10 ⁻⁴		5036
$3\pi^+ 3\pi^- K^+ K^- \pi^0$	(4.2 ± 1.7) × 10 ⁻⁴		5017
$4\pi^+ 4\pi^-$	(9 ± 5) × 10 ⁻⁵		5087
$4\pi^+ 4\pi^- 2\pi^0$	(1.3 ± 0.5) × 10 ⁻³		5058

$\Upsilon(3S)$

$$J^G(J^{PC}) = 0^-(1^{--})$$

$$\text{Mass } m = 10.3552 \pm 0.0005 \text{ GeV}$$

$$\text{Full width } \Gamma = 20.32 \pm 1.85 \text{ keV}$$

$$\Gamma_{ee} = 0.443 \pm 0.008 \text{ keV}$$

$\Upsilon(3S)$ DECAY MODES	Fraction (Γ_i/Γ)	Scale factor/ Confidence level	ρ (MeV/c)
$\Upsilon(2S)$ anything	(10.6 ± 0.8) %		296
$\Upsilon(2S) \pi^+ \pi^-$	(2.45 ± 0.23) %	S=1.1	177

$\Upsilon(2S)\pi^0\pi^0$	(1.85±0.14) %		190
$\Upsilon(2S)\gamma\gamma$	(5.0 ± 0.7) %		327
$\Upsilon(2S)\pi^0$	< 5.1 × 10 ⁻⁴	CL=90%	298
$\Upsilon(1S)\pi^+\pi^-$	(4.40±0.10) %		813
$\Upsilon(1S)\pi^0\pi^0$	(2.20±0.13) %		816
$\Upsilon(1S)\eta$	< 1.8 × 10 ⁻⁴	CL=90%	677
$\Upsilon(1S)\pi^0$	< 7 × 10 ⁻⁵	CL=90%	846
$\tau^+\tau^-$	(2.29±0.30) %		4863
$\mu^+\mu^-$	(2.18±0.21) %	S=2.1	5177
e^+e^-	seen		5178
ggg	(35.7 ± 2.6) %		—
γgg	(9.7 ± 1.8) × 10 ⁻³		—

Radiative decays

$\gamma\chi_{b2}(2P)$	(13.1 ± 1.6) %	S=3.4	86
$\gamma\chi_{b1}(2P)$	(12.6 ± 1.2) %	S=2.4	99
$\gamma\chi_{b0}(2P)$	(5.9 ± 0.6) %	S=1.4	122
$\gamma\chi_{b2}(1P)$	< 1.9 %	CL=90%	434
$\gamma\chi_{b1}(1P)$	< 1.7 × 10 ⁻³	CL=90%	452
$\gamma\chi_{b0}(1P)$	(3.0 ± 1.1) × 10 ⁻³		484
$\gamma\eta_b(2S)$	< 6.2 × 10 ⁻⁴	CL=90%	—
$\gamma\eta_b(1S)$	(5.1 ± 0.7) × 10 ⁻⁴		919
$\gamma X \rightarrow \gamma + \geq 4$ prongs	[ssss] < 2.2 × 10 ⁻⁴	CL=95%	—
$\gamma a_1^0 \rightarrow \gamma\tau^+\tau^-$	[tttt] < 1.6 × 10 ⁻⁴	CL=90%	—

Lepton Flavor (LF) violating decays

$\mu^\pm\tau^\mp$	LF < 2.03 × 10 ⁻⁵	CL=95%	5025
-------------------	------------------------------	--------	------

$\Upsilon(4S)$
or **$\Upsilon(10580)$**

$$J^PC = 0^-(1^--)$$

Mass $m = 10.5794 \pm 0.0012$ GeV

Full width $\Gamma = 20.5 \pm 2.5$ MeV

$\Gamma_{ee} = 0.272 \pm 0.029$ keV (S = 1.5)

$\Upsilon(4S)$ DECAY MODES	Fraction (Γ_i/Γ)	Confidence level	ρ (MeV/c)
$B\bar{B}$	> 96 %	95%	328
B^+B^-	(51.6 ± 0.6) %		334
D_S^+ anything + c.c.	(17.8 ± 2.6) %		—
$B^0\bar{B}^0$	(48.4 ± 0.6) %		328
$J/\psi K_S^0 (J/\psi, \eta_c) K_S^0$	< 4 × 10 ⁻⁷	90%	—
non- $B\bar{B}$	< 4 %	95%	—
e^+e^-	(1.57±0.08) × 10 ⁻⁵		5290
$\rho^+\rho^-$	< 5.7 × 10 ⁻⁶	90%	5233
$J/\psi(1S)$ anything	< 1.9 × 10 ⁻⁴	95%	—
D^{*+} anything + c.c.	< 7.4 %	90%	5099
ϕ anything	(7.1 ± 0.6) %		5240
$\phi\eta$	< 1.8 × 10 ⁻⁶	90%	5226
$\phi\eta'$	< 4.3 × 10 ⁻⁶	90%	5196
$\rho\eta$	< 1.3 × 10 ⁻⁶	90%	5247
$\rho\eta'$	< 2.5 × 10 ⁻⁶	90%	5217
$\Upsilon(1S)$ anything	< 4 × 10 ⁻³	90%	1053
$\Upsilon(1S)\pi^+\pi^-$	(8.1 ± 0.6) × 10 ⁻⁵		1026

$\Upsilon(1S)\eta$	$(1.96 \pm 0.11) \times 10^{-4}$	924
$\Upsilon(2S)\pi^+\pi^-$	$(8.6 \pm 1.3) \times 10^{-5}$	468
\bar{d} anything	$< 1.3 \times 10^{-5}$	90% -

 $\Upsilon(10860)$

$$J^{PC} = 0^-(1^{--})$$

Mass $m = 10.865 \pm 0.008$ GeV ($S = 1.1$)Full width $\Gamma = 110 \pm 13$ MeV $\Gamma_{ee} = 0.31 \pm 0.07$ keV ($S = 1.3$)

$\Upsilon(10860)$ DECAY MODES	Fraction (Γ_i/Γ)	Confidence level	ρ (MeV/c)
e^+e^-	$(2.8 \pm 0.7) \times 10^{-6}$		5432
$B\bar{B}X$	$(59 \pm 14)\%$		-
$B\bar{B}$	$< 13.8\%$	90%	1280
$B\bar{B}^* + \text{c.c.}$	$(14 \pm 6)\%$		-
$B^*\bar{B}^*$	$(44 \pm 11)\%$		-
$B\bar{B}^{(*)}\pi$	$< 19.7\%$	90%	-
$B\bar{B}\pi\pi$	$< 8.9\%$	90%	442
$B_s^{(*)}\bar{B}_s^{(*)}$	$(19.3 \pm 2.9)\%$		-
$B_s\bar{B}_s$	$(5 \pm 5) \times 10^{-3}$		-
$B_s\bar{B}_s^* + \text{c.c.}$	$(1.4 \pm 0.6)\%$		-
$B_s^*\bar{B}_s^*$	$(17.4 \pm 2.7)\%$		-
$\Upsilon(1S)\pi^+\pi^-$	$(5.3 \pm 0.6) \times 10^{-3}$		1288
$\Upsilon(2S)\pi^+\pi^-$	$(7.8 \pm 1.3) \times 10^{-3}$		763
$\Upsilon(3S)\pi^+\pi^-$	$(4.8 \pm_{-1.7}^{1.9}) \times 10^{-3}$		416
$\Upsilon(1S)K^+K^-$	$(6.1 \pm 1.8) \times 10^{-4}$		933

Inclusive Decays.

These decay modes are submodes of one or more of the decay modes above.

ϕ anything	$(13.8 \pm_{-1.7}^{2.4})\%$	-
D^0 anything + c.c.	$(108 \pm 8)\%$	-
D_s anything + c.c.	$(46 \pm 6)\%$	-
J/ψ anything	$(2.06 \pm 0.21)\%$	-

 $\Upsilon(11020)$

$$J^{PC} = 0^-(1^{--})$$

Mass $m = 11.019 \pm 0.008$ GeVFull width $\Gamma = 79 \pm 16$ MeV $\Gamma_{ee} = 0.130 \pm 0.030$ keV

$\Upsilon(11020)$ DECAY MODES	Fraction (Γ_i/Γ)	ρ (MeV/c)
e^+e^-	$(1.6 \pm 0.5) \times 10^{-6}$	5510

NOTES

In this Summary Table:

When a quantity has “(S = ...)” to its right, the error on the quantity has been enlarged by the “scale factor” S, defined as $S = \sqrt{\chi^2/(N-1)}$, where N is the number of measurements used in calculating the quantity. We do this when $S > 1$, which often indicates that the measurements are inconsistent. When $S > 1.25$, we also show in the Particle Listings an ideogram of the measurements. For more about S, see the Introduction.

A decay momentum p is given for each decay mode. For a 2-body decay, p is the momentum of each decay product in the rest frame of the decaying particle. For a 3-or-more-body decay, p is the largest momentum any of the products can have in this frame.

- [a] See the “Note on $\pi^\pm \rightarrow \ell^\pm \nu \gamma$ and $K^\pm \rightarrow \ell^\pm \nu \gamma$ Form Factors” in the π^\pm Particle Listings in the Full *Review of Particle Physics* for definitions and details.
- [b] Measurements of $\Gamma(e^+ \nu_e)/\Gamma(\mu^+ \nu_\mu)$ always include decays with γ 's, and measurements of $\Gamma(e^+ \nu_e \gamma)$ and $\Gamma(\mu^+ \nu_\mu \gamma)$ never include low-energy γ 's. Therefore, since no clean separation is possible, we consider the modes with γ 's to be subreactions of the modes without them, and let $[\Gamma(e^+ \nu_e) + \Gamma(\mu^+ \nu_\mu)]/\Gamma_{\text{total}} = 100\%$.
- [c] See the π^\pm Particle Listings in the Full *Review of Particle Physics* for the energy limits used in this measurement; low-energy γ 's are not included.
- [d] Derived from an analysis of neutrino-oscillation experiments.
- [e] Astrophysical and cosmological arguments give limits of order 10^{-13} ; see the π^0 Particle Listings in the Full *Review of Particle Physics*.
- [f] C parity forbids this to occur as a single-photon process.
- [g] See the “Note on scalar mesons” in the $f_0(1370)$ Particle Listings in the Full *Review of Particle Physics*. The interpretation of this entry as a particle is controversial.
- [h] See the “Note on $\rho(770)$ ” in the $\rho(770)$ Particle Listings in the Full *Review of Particle Physics*.
- [i] The $\omega\rho$ interference is then due to $\omega\rho$ mixing only, and is expected to be small. If $e\mu$ universality holds, $\Gamma(\rho^0 \rightarrow \mu^+ \mu^-) = \Gamma(\rho^0 \rightarrow e^+ e^-) \times 0.99785$.
- [j] See the “Note on scalar mesons” in the $f_0(1370)$ Particle Listings in the Full *Review of Particle Physics*.
- [k] See the “Note on $a_1(1260)$ ” in the $a_1(1260)$ Particle Listings in PDG 06, *Journal of Physics*, G **33** 1 (2006).
- [l] This is only an educated guess; the error given is larger than the error on the average of the published values. See the Particle Listings in the Full *Review of Particle Physics* for details.
- [m] See the “Note on non- $q\bar{q}$ mesons” in the Particle Listings in PDG 06, *Journal of Physics*, G **33** 1 (2006).
- [n] See the “Note on the $\eta(1405)$ ” in the $\eta(1405)$ Particle Listings in the Full *Review of Particle Physics*.
- [o] See the “Note on the $f_1(1420)$ ” in the $\eta(1405)$ Particle Listings in the Full *Review of Particle Physics*.
- [p] See also the $\omega(1650)$ Particle Listings.
- [q] See the “Note on the $\rho(1450)$ and the $\rho(1700)$ ” in the $\rho(1700)$ Particle Listings in the Full *Review of Particle Physics*.
- [r] See also the $\omega(1420)$ Particle Listings.

- [s] See the “Note on $f_0(1710)$ ” in the $f_0(1710)$ Particle Listings in 2004 edition of *Review of Particle Physics*.
- [t] See the note in the K^\pm Particle Listings in the Full *Review of Particle Physics*.
- [u] The definition of the slope parameter g of the $K \rightarrow 3\pi$ Dalitz plot is as follows (see also “Note on Dalitz Plot Parameters for $K \rightarrow 3\pi$ Decays” in the K^\pm Particle Listings in the Full *Review of Particle Physics*):

$$|M|^2 = 1 + g(s_3 - s_0)/m_{\pi^+}^2 + \dots$$

- [v] For more details and definitions of parameters see Particle Listings in the Full *Review of Particle Physics*.
- [w] See the K^\pm Particle Listings in the Full *Review of Particle Physics* for the energy limits used in this measurement.
- [x] Most of this radiative mode, the low-momentum γ part, is also included in the parent mode listed without γ 's.
- [y] Structure-dependent part.
- [z] Direct-emission branching fraction.
- [aa] Violates angular-momentum conservation.
- [bb] Derived from measured values of ϕ_{+-} , ϕ_{00} , $|\eta|$, $|m_{K_L^0} - m_{K_S^0}|$, and $\tau_{K_S^0}$, as described in the introduction to “Tests of Conservation Laws.”
- [cc] The CP -violation parameters are defined as follows (see also “Note on CP Violation in $K_S \rightarrow 3\pi$ ” and “Note on CP Violation in K_L^0 Decay” in the Particle Listings in the Full *Review of Particle Physics*):

$$\eta_{+-} = |\eta_{+-}|e^{i\phi_{+-}} = \frac{A(K_L^0 \rightarrow \pi^+\pi^-)}{A(K_S^0 \rightarrow \pi^+\pi^-)} = \epsilon + \epsilon'$$

$$\eta_{00} = |\eta_{00}|e^{i\phi_{00}} = \frac{A(K_L^0 \rightarrow \pi^0\pi^0)}{A(K_S^0 \rightarrow \pi^0\pi^0)} = \epsilon - 2\epsilon'$$

$$\delta = \frac{\Gamma(K_L^0 \rightarrow \pi^-\ell^+\nu) - \Gamma(K_L^0 \rightarrow \pi^+\ell^-\nu)}{\Gamma(K_L^0 \rightarrow \pi^-\ell^+\nu) + \Gamma(K_L^0 \rightarrow \pi^+\ell^-\nu)},$$

$$\text{Im}(\eta_{+-0})^2 = \frac{\Gamma(K_S^0 \rightarrow \pi^+\pi^-\pi^0)^{CP \text{ viol.}}}{\Gamma(K_L^0 \rightarrow \pi^+\pi^-\pi^0)},$$

$$\text{Im}(\eta_{000})^2 = \frac{\Gamma(K_S^0 \rightarrow \pi^0\pi^0\pi^0)}{\Gamma(K_L^0 \rightarrow \pi^0\pi^0\pi^0)}.$$

where for the last two relations CPT is assumed valid, i.e., $\text{Re}(\eta_{+-0}) \simeq 0$ and $\text{Re}(\eta_{000}) \simeq 0$.

- [dd] See the K_S^0 Particle Listings in the Full *Review of Particle Physics* for the energy limits used in this measurement.
- [ee] The value is for the sum of the charge states or particle/antiparticle states indicated.
- [ff] $\text{Re}(\epsilon'/\epsilon) = \epsilon'/\epsilon$ to a very good approximation provided the phases satisfy CPT invariance.
- [gg] This mode includes gammas from inner bremsstrahlung but not the direct emission mode $K_L^0 \rightarrow \pi^+\pi^-\gamma$ (DE).
- [hh] See the K_L^0 Particle Listings in the Full *Review of Particle Physics* for the energy limits used in this measurement.
- [ii] Allowed by higher-order electroweak interactions.

- [jj] Violates CP in leading order. Test of direct CP violation since the indirect CP -violating and CP -conserving contributions are expected to be suppressed.
- [kk] See the “Note on $f_0(1370)$ ” in the $f_0(1370)$ Particle Listings in the Full *Review of Particle Physics* and in the 1994 edition.
- [ll] See the note in the $L(1770)$ Particle Listings in *Reviews of Modern Physics* **56** S1 (1984), p. S200. See also the “Note on $K_2(1770)$ and the $K_2(1820)$ ” in the $K_2(1770)$ Particle Listings in the Full *Review of Particle Physics*.
- [mm] See the “Note on $K_2(1770)$ and the $K_2(1820)$ ” in the $K_2(1770)$ Particle Listings in the Full *Review of Particle Physics*.
- [nn] This result applies to $Z^0 \rightarrow c\bar{c}$ decays only. Here ℓ^+ is an average (not a sum) of e^+ and μ^+ decays.
- [oo] The branching fraction for this mode may differ from the sum of the submodes that contribute to it, due to interference effects. See the relevant papers in the Particle Listings in the Full *Review of Particle Physics*.
- [pp] These subfractions of the $K^- 2\pi^+$ mode are uncertain: see the Particle Listings.
- [qq] Submodes of the $D^+ \rightarrow K^- 2\pi^+ \pi^0$ and $K_S^0 2\pi^+ \pi^-$ modes were studied by ANJOS 92C and COFFMAN 92B, but with at most 142 events for the first mode and 229 for the second – not enough for precise results. With nothing new for 18 years, we refer to our 2008 edition, *Physics Letters* **B667** 1 (2008), for those results.
- [rr] The unseen decay modes of the resonances are included.
- [ss] This is *not* a test for the $\Delta C=1$ weak neutral current, but leads to the $\pi^+ \ell^+ \ell^-$ final state.
- [tt] This mode is not a useful test for a $\Delta C=1$ weak neutral current because both quarks must change flavor in this decay.
- [uu] This value is obtained by subtracting the branching fractions for 2-, 4- and 6-prongs from unity.
- [vv] This is the sum of our $K^- 2\pi^+ \pi^-$, $K^- 2\pi^+ \pi^- \pi^0$, $\bar{K}^0 2\pi^+ 2\pi^-$, $K^+ 2K^- \pi^+$, $2\pi^+ 2\pi^-$, $2\pi^+ 2\pi^- \pi^0$, $K^+ K^- \pi^+ \pi^-$, and $K^+ K^- \pi^+ \pi^- \pi^0$, branching fractions.
- [ww] This is the sum of our $K^- 3\pi^+ 2\pi^-$ and $3\pi^+ 3\pi^-$ branching fractions.
- [xx] The branching fractions for the $K^- e^+ \nu_e$, $K^*(892)^- e^+ \nu_e$, $\pi^- e^+ \nu_e$, and $\rho^- e^+ \nu_e$ modes add up to 6.20 ± 0.17 %.
- [yy] This is a doubly Cabibbo-suppressed mode.
- [zz] The two experiments measuring this fraction are in serious disagreement. See the Particle Listings in the Full *Review of Particle Physics*.
- [aaa] Submodes of the $D^0 \rightarrow K_S^0 \pi^+ \pi^- \pi^0$ mode with a K^* and/or ρ were studied by COFFMAN 92B, but with only 140 events. With nothing new for 18 years, we refer to our 2008 edition, *Physics Letters* **B667** 1 (2008), for those results.
- [bbb] This branching fraction includes all the decay modes of the resonance in the final state.
- [ccc] The experiments on the division of this charge mode amongst its submodes disagree, and the submode branching fractions here add up to considerably more than the charged-mode fraction.
- [ddd] However, these upper limits are in serious disagreement with values obtained in another experiment.
- [eee] This limit is for either D^0 or \bar{D}^0 to ρe^- .

- [fff] This limit is for either D^0 or \bar{D}^0 to $\bar{p}e^+$.
- [ggg] See the Particle Listings for the (complicated) definition of this quantity.
- [hhh] This is the purely e^+ semileptonic branching fraction: the e^+ fraction from τ^+ decays has been subtracted off. The sum of our (non- τ) e^+ exclusive fractions — an $e^+\nu_e$ with an η , η' , ϕ , K^0 , K^{*0} , or $f_0(980)$ — is $6.90 \pm 0.4\%$
- [iii] This fraction includes η from η' decays.
- [jij] Two times (to include μ decays) the $\eta' e^+\nu_e$ branching fraction, plus the $\eta'\pi^+$, $\eta'\rho^+$, and $\eta'K^+$ fractions, is $(18.4 \pm 2.3)\%$, which considerably exceeds the inclusive η' fraction of $(11.7 \pm 1.8)\%$. Our best guess is that the $\eta'\rho^+$ fraction, $(12.5 \pm 2.2)\%$, is too large.
- [kkk] This branching fraction includes all the decay modes of the final-state resonance.
- [lll] We decouple the $D_s^+ \rightarrow \phi\pi^+$ branching fraction obtained from mass projections (and used to get some of the other branching fractions) from the $D_s^+ \rightarrow \phi\pi^+$, $\phi \rightarrow K^+K^-$ branching fraction obtained from the Dalitz-plot analysis of $D_s^+ \rightarrow K^+K^-\pi^+$. That is, the ratio of these two branching fractions is not exactly the $\phi \rightarrow K^+K^-$ branching fraction 0.491.
- [mmm] This comes from a model-independent and a K -matrix parametrization of the $\pi^+\pi^-$ S -wave and is a sum over several f_0 mesons.
- [nnn] An ℓ indicates an e or a μ mode, not a sum over these modes.
- [ooo] An $CP(\pm 1)$ indicates the $CP=+1$ and $CP=-1$ eigenstates of the D^0 - \bar{D}^0 system.
- [ppp] D denotes D^0 or \bar{D}^0 .
- [qqq] D_{CP+}^{*0} decays into $D^0\pi^0$ with the D^0 reconstructed in CP -even eigenstates K^+K^- and $\pi^+\pi^-$.
- [rrr] \bar{D}^{**} represents an excited state with mass $2.2 < M < 2.8$ GeV/ c^2 .
- [sss] $X(3872)^+$ is a hypothetical charged partner of the $X(3872)$.
- [ttt] $\Theta(1710)^{++}$ is a possible narrow pentaquark state and $G(2220)$ is a possible glueball resonance.
- [uuu] $(\bar{A}_c^- p)_s$ denotes a low-mass enhancement near 3.35 GeV/ c^2 .
- [vvv] Stands for the possible candidates of $K^*(1410)$, $K_0^*(1430)$ and $K_2^*(1430)$.
- [www] B^0 and B_s^0 contributions not separated. Limit is on weighted average of the two decay rates.
- [xxx] This decay refers to the coherent sum of resonant and nonresonant $J^P = 0^+ K\pi$ components with $1.60 < m_{K\pi} < 2.15$ GeV/ c^2 .
- [yyy] $\Theta(1540)^+$ denotes a possible narrow pentaquark state.
- [zzz] These values are model dependent.
- [aaaa] Here “anything” means at least one particle observed.
- [bbbb] D^{**} stands for the sum of the $D(1^1P_1)$, $D(1^3P_0)$, $D(1^3P_1)$, $D(1^3P_2)$, $D(2^1S_0)$, and $D(2^1S_1)$ resonances.
- [cccc] $D^{(*)}\bar{D}^{(*)}$ stands for the sum of $D^*\bar{D}^*$, $D^*\bar{D}$, $D\bar{D}^*$, and $D\bar{D}$.
- [dddd] $X(3945)$ denotes a near-threshold enhancement in the $\omega J/\psi$ mass spectrum.
- [eeee] Inclusive branching fractions have a multiplicity definition and can be greater than 100%.

[ffff] D_j represents an unresolved mixture of pseudoscalar and tensor D^{**} (P -wave) states.

[gggg] Not a pure measurement. See note at head of B_s^0 Decay Modes.

[hhhh] Includes $\rho\bar{\rho}\pi^+\pi^-\gamma$ and excludes $\rho\bar{\rho}\eta$, $\rho\bar{\rho}\omega$, $\rho\bar{\rho}\eta'$.

[iiii] J^{PC} known by production in e^+e^- via single photon annihilation. I^G is not known; interpretation of this state as a single resonance is unclear because of the expectation of substantial threshold effects in this energy region.

[jjjj] See COAN 06 for details.

[kkkk] $2m_\tau < M(\tau^+\tau^-) < 7500$ MeV.

[llll] $2 < m_{K^+K^-} < 3$ GeV.

[mmmm] X = pseudoscalar with $m < 7.2$ GeV

[nnnn] $X\bar{X}$ = vectors with $m < 3.1$ GeV

[oooo] 1.5 GeV $< m_X < 5.0$ GeV

[pppp] $201 < M(\mu^+\mu^-) < 3565$ MeV.

[qqqq] Spectroscopic labeling for these states is theoretical, pending experimental information.

[rrrr] 1.5 GeV $< m_X < 5.0$ GeV

[ssss] 1.5 GeV $< m_X < 5.0$ GeV

[tttt] For $m_{\tau^+\tau^-}$ in the ranges 4.03–9.52 and 9.61–10.10 GeV.

N BARYONS

($S = 0, I = 1/2$)

$$p, N^+ = uud; \quad n, N^0 = udd$$

p

$$I(J^P) = \frac{1}{2}(\frac{1}{2}^+)$$

Mass $m = 1.00727646677 \pm 0.00000000010$ u

Mass $m = 938.272013 \pm 0.000023$ MeV [a]

$$|m_p - m_{\bar{p}}|/m_p < 2 \times 10^{-9}, \text{ CL} = 90\% \text{ [b]}$$

$$|\frac{q_{\bar{p}}}{m_{\bar{p}}}|/(\frac{q_p}{m_p}) = 0.99999999991 \pm 0.00000000009$$

$$|q_p + q_{\bar{p}}|/e < 2 \times 10^{-9}, \text{ CL} = 90\% \text{ [b]}$$

$$|q_p + q_e|/e < 1.0 \times 10^{-21} \text{ [c]}$$

Magnetic moment $\mu = 2.792847356 \pm 0.000000023 \mu_N$

$$(\mu_p + \mu_{\bar{p}}) / \mu_p = (-0.1 \pm 2.1) \times 10^{-3}$$

Electric dipole moment $d < 0.54 \times 10^{-23}$ e cm

Electric polarizability $\alpha = (12.0 \pm 0.6) \times 10^{-4}$ fm³

Magnetic polarizability $\beta = (1.9 \pm 0.5) \times 10^{-4}$ fm³

Charge radius = 0.877 ± 0.007 fm

Mean life $\tau > 2.1 \times 10^{29}$ years, CL = 90% [d] ($p \rightarrow$ invisible mode)

Mean life $\tau > 10^{31}$ to 10^{33} years [d] (mode dependent)

See the "Note on Nucleon Decay" in our 1994 edition (Phys. Rev. **D50**, 1173) for a short review.

The "partial mean life" limits tabulated here are the limits on τ/B_i , where τ is the total mean life and B_i is the branching fraction for the mode in question. For N decays, p and n indicate proton and neutron partial lifetimes.

p DECAY MODES	Partial mean life (10^{30} years)	Confidence level	p (MeV/c)
Antilepton + meson			
$N \rightarrow e^+ \pi$	$> 158 (n), > 1600 (p)$	90%	459
$N \rightarrow \mu^+ \pi$	$> 100 (n), > 473 (p)$	90%	453
$N \rightarrow \nu \pi$	$> 112 (n), > 25 (p)$	90%	459
$p \rightarrow e^+ \eta$	> 313	90%	309
$p \rightarrow \mu^+ \eta$	> 126	90%	297
$n \rightarrow \nu \eta$	> 158	90%	310
$N \rightarrow e^+ \rho$	$> 217 (n), > 75 (p)$	90%	149
$N \rightarrow \mu^+ \rho$	$> 228 (n), > 110 (p)$	90%	113
$N \rightarrow \nu \rho$	$> 19 (n), > 162 (p)$	90%	149
$p \rightarrow e^+ \omega$	> 107	90%	143
$p \rightarrow \mu^+ \omega$	> 117	90%	105
$n \rightarrow \nu \omega$	> 108	90%	144
$N \rightarrow e^+ K$	$> 17 (n), > 150 (p)$	90%	339
$p \rightarrow e^+ K_S^0$	> 120	90%	337
$p \rightarrow e^+ K_L^0$	> 51	90%	337
$N \rightarrow \mu^+ K$	$> 26 (n), > 120 (p)$	90%	329
$p \rightarrow \mu^+ K_S^0$	> 150	90%	326
$p \rightarrow \mu^+ K_L^0$	> 83	90%	326
$N \rightarrow \nu K$	$> 86 (n), > 670 (p)$	90%	339

$n \rightarrow \nu K_S^0$	> 51	90%	338
$p \rightarrow e^+ K^*(892)^0$	> 84	90%	45
$N \rightarrow \nu K^*(892)$	> 78 (n), > 51 (p)	90%	45

Antilepton + mesons

$p \rightarrow e^+ \pi^+ \pi^-$	> 82	90%	448
$p \rightarrow e^+ \pi^0 \pi^0$	> 147	90%	449
$n \rightarrow e^+ \pi^- \pi^0$	> 52	90%	449
$p \rightarrow \mu^+ \pi^+ \pi^-$	> 133	90%	425
$p \rightarrow \mu^+ \pi^0 \pi^0$	> 101	90%	427
$n \rightarrow \mu^+ \pi^- \pi^0$	> 74	90%	427
$n \rightarrow e^+ K^0 \pi^-$	> 18	90%	319

Lepton + meson

$n \rightarrow e^- \pi^+$	> 65	90%	459
$n \rightarrow \mu^- \pi^+$	> 49	90%	453
$n \rightarrow e^- \rho^+$	> 62	90%	150
$n \rightarrow \mu^- \rho^+$	> 7	90%	114
$n \rightarrow e^- K^+$	> 32	90%	340
$n \rightarrow \mu^- K^+$	> 57	90%	330

Lepton + mesons

$p \rightarrow e^- \pi^+ \pi^+$	> 30	90%	448
$n \rightarrow e^- \pi^+ \pi^0$	> 29	90%	449
$p \rightarrow \mu^- \pi^+ \pi^+$	> 17	90%	425
$n \rightarrow \mu^- \pi^+ \pi^0$	> 34	90%	427
$p \rightarrow e^- \pi^+ K^+$	> 75	90%	320
$p \rightarrow \mu^- \pi^+ K^+$	> 245	90%	279

Antilepton + photon(s)

$p \rightarrow e^+ \gamma$	> 670	90%	469
$p \rightarrow \mu^+ \gamma$	> 478	90%	463
$n \rightarrow \nu \gamma$	> 28	90%	470
$p \rightarrow e^+ \gamma \gamma$	> 100	90%	469
$n \rightarrow \nu \gamma \gamma$	> 219	90%	470

Three (or more) leptons

$p \rightarrow e^+ e^+ e^-$	> 793	90%	469
$p \rightarrow e^+ \mu^+ \mu^-$	> 359	90%	457
$p \rightarrow e^+ \nu \nu$	> 17	90%	469
$n \rightarrow e^+ e^- \nu$	> 257	90%	470
$n \rightarrow \mu^+ e^- \nu$	> 83	90%	464
$n \rightarrow \mu^+ \mu^- \nu$	> 79	90%	458
$p \rightarrow \mu^+ e^+ e^-$	> 529	90%	463
$p \rightarrow \mu^+ \mu^+ \mu^-$	> 675	90%	439
$p \rightarrow \mu^+ \nu \nu$	> 21	90%	463
$p \rightarrow e^- \mu^+ \mu^+$	> 6	90%	457
$n \rightarrow 3\nu$	> 0.0005	90%	470

Inclusive modes

$N \rightarrow e^+$ anything	> 0.6 (n , p)	90%	—
$N \rightarrow \mu^+$ anything	> 12 (n , p)	90%	—
$N \rightarrow e^+ \pi^0$ anything	> 0.6 (n , p)	90%	—

$\Delta B = 2$ dinucleon modes

The following are lifetime limits per iron nucleus.

$pp \rightarrow \pi^+ \pi^+$	> 0.7	90%	—
$pn \rightarrow \pi^+ \pi^0$	> 2	90%	—
$nn \rightarrow \pi^+ \pi^-$	> 0.7	90%	—
$nn \rightarrow \pi^0 \pi^0$	> 3.4	90%	—
$pp \rightarrow e^+ e^+$	> 5.8	90%	—
$pp \rightarrow e^+ \mu^+$	> 3.6	90%	—
$pp \rightarrow \mu^+ \mu^+$	> 1.7	90%	—
$pn \rightarrow e^+ \bar{\nu}$	> 2.8	90%	—
$pn \rightarrow \mu^+ \bar{\nu}$	> 1.6	90%	—
$nn \rightarrow \nu_e \bar{\nu}_e$	> 0.000049	90%	—
$pn \rightarrow$ invisible	$> 2.1 \times 10^{-5}$	90%	—
$pp \rightarrow$ invisible	> 0.00005	90%	—

 \bar{p} DECAY MODES

Mode	Partial mean life (years)	Confidence level	p (MeV/c)
$\bar{p} \rightarrow e^- \gamma$	$> 7 \times 10^5$	90%	469
$\bar{p} \rightarrow \mu^- \gamma$	$> 5 \times 10^4$	90%	463
$\bar{p} \rightarrow e^- \pi^0$	$> 4 \times 10^5$	90%	459
$\bar{p} \rightarrow \mu^- \pi^0$	$> 5 \times 10^4$	90%	453
$\bar{p} \rightarrow e^- \eta$	$> 2 \times 10^4$	90%	309
$\bar{p} \rightarrow \mu^- \eta$	$> 8 \times 10^3$	90%	297
$\bar{p} \rightarrow e^- K_S^0$	> 900	90%	337
$\bar{p} \rightarrow \mu^- K_S^0$	$> 4 \times 10^3$	90%	326
$\bar{p} \rightarrow e^- K_L^0$	$> 9 \times 10^3$	90%	337
$\bar{p} \rightarrow \mu^- K_L^0$	$> 7 \times 10^3$	90%	326
$\bar{p} \rightarrow e^- \gamma \gamma$	$> 2 \times 10^4$	90%	469
$\bar{p} \rightarrow \mu^- \gamma \gamma$	$> 2 \times 10^4$	90%	463
$\bar{p} \rightarrow e^- \omega$	> 200	90%	143

 n

$$I(J^P) = \frac{1}{2}(\frac{1}{2}^+)$$

Mass $m = 1.0086649160 \pm 0.0000000004$ uMass $m = 939.565346 \pm 0.000023$ MeV [a]

$$(m_n - m_{\bar{n}}) / m_n = (9 \pm 6) \times 10^{-5}$$

 $m_n - m_p = 1.2933321 \pm 0.0000004$ MeV

$$= 0.00138844920(46)$$
 u

Mean life $\tau = 885.7 \pm 0.8$ s

$$c\tau = 2.655 \times 10^8$$
 km

Magnetic moment $\mu = -1.9130427 \pm 0.0000005 \mu_N$ Electric dipole moment $d < 0.29 \times 10^{-25}$ e cm, CL = 90%Mean-square charge radius $\langle r_n^2 \rangle = -0.1161 \pm 0.0022$

$$\text{fm}^2 \quad (S = 1.3)$$

Electric polarizability $\alpha = (11.6 \pm 1.5) \times 10^{-4}$ fm³Magnetic polarizability $\beta = (3.7 \pm 2.0) \times 10^{-4}$ fm³Charge $q = (-0.4 \pm 1.1) \times 10^{-21}$ eMean $n\bar{n}$ -oscillation time $> 8.6 \times 10^7$ s, CL = 90% (free n)Mean $n\bar{n}$ -oscillation time $> 1.3 \times 10^8$ s, CL = 90% [e] (bound n)Mean nn' -oscillation time > 414 s, CL = 90% [f]

$p e^- \nu_e$ decay parameters [g]

$$\lambda \equiv g_A / g_V = -1.2694 \pm 0.0028 \quad (S = 2.0)$$

$$A = -0.1173 \pm 0.0013 \quad (S = 2.3)$$

$$B = 0.9807 \pm 0.0030$$

$$C = -0.2377 \pm 0.0026$$

$$a = -0.103 \pm 0.004$$

$$\phi_{AV} = (180.06 \pm 0.07)^\circ \text{ [h]}$$

$$D = (-4 \pm 6) \times 10^{-4} \text{ [i]}$$

$$R = 0.008 \pm 0.016 \text{ [j]}$$

n DECAY MODES	Fraction (Γ_i/Γ)	Confidence level	ρ (MeV/c)
$p e^- \bar{\nu}_e$	100	%	1
$p e^- \bar{\nu}_e \gamma$	[j] (3.13±0.35) × 10 ⁻³		1
Charge conservation (Q) violating mode			
$p \nu_e \bar{\nu}_e$	Q < 8	× 10 ⁻²⁷	68% 1

$N(1440) P_{11}$

$$I(J^P) = \frac{1}{2}(\frac{1}{2}^+)$$

Breit-Wigner mass = 1420 to 1470 (\approx 1440) MeV
 Breit-Wigner full width = 200 to 450 (\approx 300) MeV
 Re(pole position) = 1350 to 1380 (\approx 1365) MeV
 -2Im(pole position) = 160 to 220 (\approx 190) MeV

The following branching fractions are our estimates, not fits or averages.

$N(1440)$ DECAY MODES	Fraction (Γ_i/Γ)	ρ (MeV/c)
$N \pi$	0.55 to 0.75	398
$N \pi \pi$	30-40 %	347
$\Delta \pi$	20-30 %	147
$N \rho$	<8 %	†
$N(\pi\pi)_{S\text{-wave}}^{I=0}$	5-10 %	-
$p \gamma$	0.035-0.048 %	414
$p \gamma$, helicity=1/2	0.035-0.048 %	414
$n \gamma$	0.009-0.032 %	413
$n \gamma$, helicity=1/2	0.009-0.032 %	413

$N(1520) D_{13}$

$$I(J^P) = \frac{1}{2}(\frac{3}{2}^-)$$

Breit-Wigner mass = 1515 to 1525 (\approx 1520) MeV
 Breit-Wigner full width = 100 to 125 (\approx 115) MeV
 Re(pole position) = 1505 to 1515 (\approx 1510) MeV
 -2Im(pole position) = 105 to 120 (\approx 110) MeV

The following branching fractions are our estimates, not fits or averages.

$N(1520)$ DECAY MODES	Fraction (Γ_i/Γ)	ρ (MeV/c)
$N \pi$	0.55 to 0.65	457
$N \eta$	(2.3 ± 0.4) × 10 ⁻³	154
$N \pi \pi$	40-50 %	414
$\Delta \pi$	15-25 %	230
$N \rho$	15-25 %	†

$N(\pi\pi)_{S\text{-wave}}^{I=0}$	<8 %	—
$p\gamma$	0.46–0.56 %	470
$p\gamma$, helicity=1/2	0.001–0.034 %	470
$p\gamma$, helicity=3/2	0.44–0.53 %	470
$n\gamma$	0.30–0.53 %	470
$n\gamma$, helicity=1/2	0.04–0.10 %	470
$n\gamma$, helicity=3/2	0.25–0.45 %	470

 $N(1535) S_{11}$

$$I(J^P) = \frac{1}{2}(\frac{1}{2}^-)$$

Breit-Wigner mass = 1525 to 1545 (≈ 1535) MeV

Breit-Wigner full width = 125 to 175 (≈ 150) MeV

Re(pole position) = 1490 to 1530 (≈ 1510) MeV

$-2\text{Im}(\text{pole position}) = 90$ to 250 (≈ 170) MeV

The following branching fractions are our estimates, not fits or averages.

$N(1535)$ DECAY MODES	Fraction (Γ_i/Γ)	p (MeV/c)
$N\pi$	35–55 %	468
$N\eta$	45–60 %	186
$N\pi\pi$	1–10 %	426
$\Delta\pi$	<1 %	244
$N\rho$	<4 %	†
$N(\pi\pi)_{S\text{-wave}}^{I=0}$	<3 %	—
$N(1440)\pi$	<7 %	†
$p\gamma$	0.15–0.35 %	481
$p\gamma$, helicity=1/2	0.15–0.35 %	481
$n\gamma$	0.004–0.29 %	480
$n\gamma$, helicity=1/2	0.004–0.29 %	480

**$N(1650) S_{11}$, $N(1675) D_{15}$, $N(1680) F_{15}$, $N(1700) D_{13}$, $N(1710) P_{11}$,
 $N(1720) P_{13}$, $N(2190) G_{17}$, $N(2220) H_{19}$, $N(2250) G_{19}$, $N(2600) h_{1,11}$**

The N resonances listed above are omitted from this Booklet but not from the Summary Table in the full *Review*.

Δ BARYONS ($S = 0, I = 3/2$)

$$\Delta^{++} = uuu, \quad \Delta^+ = uud, \quad \Delta^0 = udd, \quad \Delta^- = ddd$$

$\Delta(1232) P_{33}$

$$I(J^P) = \frac{3}{2}(\frac{3}{2}^+)$$

Breit-Wigner mass (mixed charges) = 1231 to 1233 (\approx 1232) MeV
 Breit-Wigner full width (mixed charges) = 116 to 120 (\approx 118) MeV
 Re(pole position) = 1209 to 1211 (\approx 1210) MeV
 $-2\text{Im}(\text{pole position}) = 98$ to 102 (\approx 100) MeV

The following branching fractions are our estimates, not fits or averages.

$\Delta(1232)$ DECAY MODES	Fraction (Γ_i/Γ)	ρ (MeV/c)
$N\pi$	100 %	229
$N\gamma$	0.52–0.60 %	259
$N\gamma$, helicity=1/2	0.11–0.13 %	259
$N\gamma$, helicity=3/2	0.41–0.47 %	259

$\Delta(1600) P_{33}$

$$I(J^P) = \frac{3}{2}(\frac{3}{2}^+)$$

Breit-Wigner mass = 1550 to 1700 (\approx 1600) MeV
 Breit-Wigner full width = 250 to 450 (\approx 350) MeV
 Re(pole position) = 1500 to 1700 (\approx 1600) MeV
 $-2\text{Im}(\text{pole position}) = 200$ to 400 (\approx 300) MeV

The following branching fractions are our estimates, not fits or averages.

$\Delta(1600)$ DECAY MODES	Fraction (Γ_i/Γ)	ρ (MeV/c)
$N\pi$	10–25 %	513
$N\pi\pi$	75–90 %	477
$\Delta\pi$	40–70 %	303
$N\rho$	<25 %	†
$N(1440)\pi$	10–35 %	82
$N\gamma$	0.001–0.02 %	525
$N\gamma$, helicity=1/2	0.0–0.02 %	525
$N\gamma$, helicity=3/2	0.001–0.005 %	525

$\Delta(1620) S_{31}$

$$I(J^P) = \frac{3}{2}(\frac{1}{2}^-)$$

Breit-Wigner mass = 1600 to 1660 (\approx 1630) MeV
 Breit-Wigner full width = 135 to 150 (\approx 145) MeV
 Re(pole position) = 1590 to 1610 (\approx 1600) MeV
 $-2\text{Im}(\text{pole position}) = 115$ to 120 (\approx 118) MeV

The following branching fractions are our estimates, not fits or averages.

$\Delta(1620)$ DECAY MODES	Fraction (Γ_i/Γ)	ρ (MeV/c)
$N\pi$	20–30 %	534
$N\pi\pi$	70–80 %	499

$\Delta\pi$	30–60 %	328
$N\rho$	7–25 %	†
$N\gamma$	0.004–0.044 %	545
$N\gamma$, helicity=1/2	0.004–0.044 %	545

**$\Delta(1700) D_{33}$, $\Delta(1905) F_{35}$, $\Delta(1910) P_{31}$,
 $\Delta(1920) P_{33}$, $\Delta(1930) D_{35}$, $\Delta(1950) F_{37}$, $\Delta(2420) H_{3,11}$**

The Δ resonances listed above are omitted from this Booklet but not from the Summary Table in the full *Review*.

Λ BARYONS

$(S = -1, I = 0)$

$$\Lambda^0 = uds$$

Λ

$$I(J^P) = 0(\frac{1}{2}^+)$$

Mass $m = 1115.683 \pm 0.006$ MeV

$$(m_\Lambda - m_{\bar{\Lambda}}) / m_\Lambda = (-0.1 \pm 1.1) \times 10^{-5} \quad (S = 1.6)$$

$$\text{Mean life } \tau = (2.631 \pm 0.020) \times 10^{-10} \text{ s} \quad (S = 1.6)$$

$$(\tau_\Lambda - \tau_{\bar{\Lambda}}) / \tau_\Lambda = -0.001 \pm 0.009$$

$$c\tau = 7.89 \text{ cm}$$

Magnetic moment $\mu = -0.613 \pm 0.004 \mu_N$

Electric dipole moment $d < 1.5 \times 10^{-16} \text{ e cm}$, CL = 95%

Decay parameters

$$\rho\pi^- \quad \alpha_- = 0.642 \pm 0.013$$

$$\bar{\rho}\pi^+ \quad \alpha_+ = -0.71 \pm 0.08$$

$$\rho\pi^- \quad \phi_- = (-6.5 \pm 3.5)^\circ$$

$$" \quad \gamma_- = 0.76 [k]$$

$$" \quad \Delta_- = (8 \pm 4)^\circ [k]$$

$$n\pi^0 \quad \alpha_0 = 0.65 \pm 0.04$$

$$\rho e^- \bar{\nu}_e \quad g_A/g_V = -0.718 \pm 0.015 [g]$$

Λ DECAY MODES	Fraction (Γ_i/Γ)	ρ (MeV/c)
$\rho\pi^-$	(63.9 \pm 0.5) %	101
$n\pi^0$	(35.8 \pm 0.5) %	104
$n\gamma$	(1.75 \pm 0.15) $\times 10^{-3}$	162
$\rho\pi^- \gamma$	[/] (8.4 \pm 1.4) $\times 10^{-4}$	101
$\rho e^- \bar{\nu}_e$	(8.32 \pm 0.14) $\times 10^{-4}$	163
$\rho\mu^- \bar{\nu}_\mu$	(1.57 \pm 0.35) $\times 10^{-4}$	131

$\Lambda(1405) S_{01}$

$I(J^P) = 0(\frac{1}{2}^-)$

Mass $m = 1406 \pm 4$ MeV
 Full width $\Gamma = 50 \pm 2$ MeV
 Below $\bar{K}N$ threshold

$\Lambda(1405)$ DECAY MODES	Fraction (Γ_i/Γ)	ρ (MeV/c)
$\Sigma \pi$	100 %	157

$\Lambda(1520) D_{03}$

$I(J^P) = 0(\frac{3}{2}^-)$

Mass $m = 1519.5 \pm 1.0$ MeV [m]
 Full width $\Gamma = 15.6 \pm 1.0$ MeV [m]

$\Lambda(1520)$ DECAY MODES	Fraction (Γ_i/Γ)	ρ (MeV/c)
$N\bar{K}$	$45 \pm 1\%$	243
$\Sigma \pi$	$42 \pm 1\%$	268
$\Lambda\pi\pi$	$10 \pm 1\%$	259
$\Sigma \pi\pi$	$0.9 \pm 0.1\%$	169
$\Lambda\gamma$	$0.85 \pm 0.15\%$	350

**$\Lambda(1600) P_{01}$, $\Lambda(1670) S_{01}$, $\Lambda(1690) D_{03}$, $\Lambda(1800) S_{01}$, $\Lambda(1810) P_{01}$, $\Lambda(1820) F_{05}$,
 $\Lambda(1830) D_{05}$, $\Lambda(1890) P_{03}$, $\Lambda(2100) G_{07}$, $\Lambda(2110) F_{05}$, $\Lambda(2350) H_{09}$**

The Λ resonances listed above are omitted from this Booklet but not from the Summary Table in the full *Review*.

Σ BARYONS

$(S = -1, I = 1)$

$\Sigma^+ = uus, \Sigma^0 = uds, \Sigma^- = dds$

Σ^+

$I(J^P) = 1(\frac{1}{2}^+)$

Mass $m = 1189.37 \pm 0.07$ MeV ($S = 2.2$)
 Mean life $\tau = (0.8018 \pm 0.0026) \times 10^{-10}$ s
 $c\tau = 2.404$ cm
 $(\tau_{\Sigma^+} - \tau_{\Sigma^-}) / \tau_{\Sigma^+} = (-0.6 \pm 1.2) \times 10^{-3}$
 Magnetic moment $\mu = 2.458 \pm 0.010 \mu_N$ ($S = 2.1$)
 $(\mu_{\Sigma^+} + \mu_{\Sigma^-}) / \mu_{\Sigma^+} = 0.014 \pm 0.015$
 $\Gamma(\Sigma^+ \rightarrow n\ell^+\nu) / \Gamma(\Sigma^- \rightarrow n\ell^-\bar{\nu}) < 0.043$

Decay parameters

$p\pi^0$	$\alpha_0 = -0.980^{+0.017}_{-0.015}$
"	$\phi_0 = (36 \pm 34)^\circ$
"	$\gamma_0 = 0.16 [k]$
"	$\Delta_0 = (187 \pm 6)^\circ [k]$
$n\pi^+$	$\alpha_+ = 0.068 \pm 0.013$
"	$\phi_+ = (167 \pm 20)^\circ (S = 1.1)$
"	$\gamma_+ = -0.97 [k]$
"	$\Delta_+ = (-73^{+133}_{-10})^\circ [k]$
$p\gamma$	$\alpha_\gamma = -0.76 \pm 0.08$

Σ^+ DECAY MODES	Fraction (Γ_i/Γ)	Confidence level	ρ (MeV/c)
$p\pi^0$	$(51.57 \pm 0.30) \%$		189
$n\pi^+$	$(48.31 \pm 0.30) \%$		185
$p\gamma$	$(1.23 \pm 0.05) \times 10^{-3}$		225
$n\pi^+\gamma$	[I] $(4.5 \pm 0.5) \times 10^{-4}$		185
$\Lambda e^+ \nu_e$	$(2.0 \pm 0.5) \times 10^{-5}$		71

$\Delta S = \Delta Q$ (SQ) violating modes or
 $\Delta S = 1$ weak neutral current (S1) modes

$ne^+ \nu_e$	SQ	< 5	$\times 10^{-6}$	90%	224
$n\mu^+ \nu_\mu$	SQ	< 3.0	$\times 10^{-5}$	90%	202
$pe^+ e^-$	S1	< 7	$\times 10^{-6}$		225
$p\mu^+ \mu^-$	S1	(9^{+9}_{-8})	$\times 10^{-8}$		121

Σ^0

$$I(J^P) = 1(\frac{1}{2}^+)$$

Mass $m = 1192.642 \pm 0.024$ MeV
 $m_{\Sigma^-} - m_{\Sigma^0} = 4.807 \pm 0.035$ MeV ($S = 1.1$)
 $m_{\Sigma^0} - m_\Lambda = 76.959 \pm 0.023$ MeV
Mean life $\tau = (7.4 \pm 0.7) \times 10^{-20}$ s
 $c\tau = 2.22 \times 10^{-11}$ m
Transition magnetic moment $|\mu_{\Sigma\Lambda}| = 1.61 \pm 0.08 \mu_N$

Σ^0 DECAY MODES	Fraction (Γ_i/Γ)	Confidence level	ρ (MeV/c)
$\Lambda\gamma$	100 %		74
$\Lambda\gamma\gamma$	$< 3 \%$	90%	74
$\Lambda e^+ e^-$	[n] 5×10^{-3}		74

Σ^-

$$I(J^P) = 1(\frac{1}{2}^+)$$

Mass $m = 1197.449 \pm 0.030$ MeV ($S = 1.2$)
 $m_{\Sigma^-} - m_{\Sigma^+} = 8.08 \pm 0.08$ MeV ($S = 1.9$)
 $m_{\Sigma^-} - m_\Lambda = 81.766 \pm 0.030$ MeV ($S = 1.2$)
Mean life $\tau = (1.479 \pm 0.011) \times 10^{-10}$ s ($S = 1.3$)
 $c\tau = 4.434$ cm
Magnetic moment $\mu = -1.160 \pm 0.025 \mu_N$ ($S = 1.7$)
 Σ^- charge radius = 0.78 ± 0.10 fm

Decay parameters

$n\pi^-$	$\alpha_- = -0.068 \pm 0.008$
"	$\phi_- = (10 \pm 15)^\circ$
"	$\gamma_- = 0.98$ [k]
"	$\Delta_- = (249 \pm_{-120}^{12})^\circ$ [k]
$ne^- \bar{\nu}_e$	$g_A/g_V = 0.340 \pm 0.017$ [g]
"	$f_2(0)/f_1(0) = 0.97 \pm 0.14$
"	$D = 0.11 \pm 0.10$
$\Lambda e^- \bar{\nu}_e$	$g_V/g_A = 0.01 \pm 0.10$ [g] (S = 1.5)
"	$g_{WM}/g_A = 2.4 \pm 1.7$ [g]

Σ^- DECAY MODES	Fraction (Γ_i/Γ)	p (MeV/c)
$n\pi^-$	(99.848 ± 0.005) %	193
$n\pi^- \gamma$	[l] (4.6 ± 0.6) × 10 ⁻⁴	193
$ne^- \bar{\nu}_e$	(1.017 ± 0.034) × 10 ⁻³	230
$n\mu^- \bar{\nu}_\mu$	(4.5 ± 0.4) × 10 ⁻⁴	210
$\Lambda e^- \bar{\nu}_e$	(5.73 ± 0.27) × 10 ⁻⁵	79

 $\Sigma(1385) P_{13}$

$$I(J^P) = 1(\frac{3}{2}^+)$$

$\Sigma(1385)^+$ mass $m = 1382.8 \pm 0.4$ MeV (S = 2.0)
$\Sigma(1385)^0$ mass $m = 1383.7 \pm 1.0$ MeV (S = 1.4)
$\Sigma(1385)^-$ mass $m = 1387.2 \pm 0.5$ MeV (S = 2.2)
$\Sigma(1385)^+$ full width $\Gamma = 35.8 \pm 0.8$ MeV
$\Sigma(1385)^0$ full width $\Gamma = 36 \pm 5$ MeV
$\Sigma(1385)^-$ full width $\Gamma = 39.4 \pm 2.1$ MeV (S = 1.7)
Below $\bar{K}N$ threshold

$\Sigma(1385)$ DECAY MODES	Fraction (Γ_i/Γ)	Confidence level	p (MeV/c)
$\Lambda\pi$	(87.0 ± 1.5) %		208
$\Sigma\pi$	(11.7 ± 1.5) %		129
$\Lambda\gamma$	(1.3 ± 0.4) %		241
$\Sigma^- \gamma$	< 2.4 × 10 ⁻⁴	90%	173

 $\Sigma(1660) P_{11}$

$$I(J^P) = 1(\frac{1}{2}^+)$$

Mass $m = 1630$ to 1690 (≈ 1660) MeV
Full width $\Gamma = 40$ to 200 (≈ 100) MeV

$\Sigma(1660)$ DECAY MODES	Fraction (Γ_i/Γ)	p (MeV/c)
$N\bar{K}$	10–30 %	405
$\Lambda\pi$	seen	440
$\Sigma\pi$	seen	387

 **$\Sigma(1670) D_{13}$, $\Sigma(1750) S_{11}$, $\Sigma(1775) D_{15}$, $\Sigma(1915) F_{15}$,
 $\Sigma(1940) D_{13}$, $\Sigma(2030) F_{17}$, $\Sigma(2250)$**

The Σ resonances listed above are omitted from this Booklet but not from the Summary Table in the full Review.

Ξ BARYONS

($S = -2, I = 1/2$)

$$\Xi^0 = u s s, \quad \Xi^- = d s s$$

Ξ^0

$$I(J^P) = \frac{1}{2}(\frac{1}{2}^+)$$

P is not yet measured; + is the quark model prediction.

$$\text{Mass } m = 1314.86 \pm 0.20 \text{ MeV}$$

$$m_{\Xi^-} - m_{\Xi^0} = 6.85 \pm 0.21 \text{ MeV}$$

$$\text{Mean life } \tau = (2.90 \pm 0.09) \times 10^{-10} \text{ s}$$

$$c\tau = 8.71 \text{ cm}$$

$$\text{Magnetic moment } \mu = -1.250 \pm 0.014 \mu_N$$

Decay parameters

$$\Lambda\pi^0 \quad \alpha = -0.411 \pm 0.022 \quad (S = 2.1)$$

$$" \quad \phi = (21 \pm 12)^\circ$$

$$" \quad \gamma = 0.85 [k]$$

$$" \quad \Delta = (218^{+12}_{-19})^\circ [k]$$

$$\Lambda\gamma \quad \alpha = -0.73 \pm 0.17$$

$$\Lambda e^+ e^- \quad \alpha = -0.8 \pm 0.2$$

$$\Sigma^0 \gamma \quad \alpha = -0.63 \pm 0.09$$

$$\Sigma^+ e^- \bar{\nu}_e \quad g_1(0)/f_1(0) = 1.21 \pm 0.05$$

$$\Sigma^+ e^- \bar{\nu}_e \quad f_2(0)/f_1(0) = 2.0 \pm 1.3$$

Ξ^0 DECAY MODES	Fraction (Γ_i/Γ)	Confidence level	P (MeV/c)
$\Lambda\pi^0$	(99.525 ± 0.012) %		135
$\Lambda\gamma$	(1.17 ± 0.07) × 10 ⁻³		184
$\Lambda e^+ e^-$	(7.6 ± 0.6) × 10 ⁻⁶		184
$\Sigma^0 \gamma$	(3.33 ± 0.10) × 10 ⁻³		117
$\Sigma^+ e^- \bar{\nu}_e$	(2.53 ± 0.08) × 10 ⁻⁴		120
$\Sigma^+ \mu^- \bar{\nu}_\mu$	(4.6 $^{+1.8}_{-1.4}$) × 10 ⁻⁶		64

$\Delta S = \Delta Q$ (SQ) violating modes or $\Delta S = 2$ forbidden (S2) modes

$\Sigma^- e^+ \nu_e$	SQ	< 9	× 10 ⁻⁴	90%	112
$\Sigma^- \mu^+ \nu_\mu$	SQ	< 9	× 10 ⁻⁴	90%	49
$p\pi^-$	S2	< 8	× 10 ⁻⁶	90%	299
$p e^- \bar{\nu}_e$	S2	< 1.3	× 10 ⁻³		323
$p \mu^- \bar{\nu}_\mu$	S2	< 1.3	× 10 ⁻³		309

Ξ^-

$$I(J^P) = \frac{1}{2}(\frac{1}{2}^+)$$

P is not yet measured; + is the quark model prediction.

$$\text{Mass } m = 1321.71 \pm 0.07 \text{ MeV}$$

$$(m_{\Xi^-} - m_{\Xi^+}) / m_{\Xi^-} = (-3 \pm 9) \times 10^{-5}$$

$$\text{Mean life } \tau = (1.639 \pm 0.015) \times 10^{-10} \text{ s}$$

$$c\tau = 4.91 \text{ cm}$$

$$(\tau_{\Xi^-} - \tau_{\Xi^+}) / \tau_{\Xi^-} = -0.01 \pm 0.07$$

$$\text{Magnetic moment } \mu = -0.6507 \pm 0.0025 \mu_N$$

$$(\mu_{\Xi^-} + \mu_{\Xi^+}) / |\mu_{\Xi^-}| = +0.01 \pm 0.05$$

Decay parameters

$$\Lambda\pi^- \quad \alpha = -0.458 \pm 0.012 \quad (S = 1.8)$$

$$[\alpha(\Xi^-)\alpha_-(\Lambda) - \alpha(\Xi^+)\alpha_+(\bar{\Lambda})] / [\text{sum}] = (0 \pm 7) \times 10^{-4}$$

$$\text{"} \quad \phi = (-2.1 \pm 0.8)^\circ$$

$$\text{"} \quad \gamma = 0.89 [k]$$

$$\text{"} \quad \Delta = (175.9 \pm 1.5)^\circ [k]$$

$$\Lambda e^- \bar{\nu}_e \quad g_A/g_V = -0.25 \pm 0.05 [g]$$

Ξ^- DECAY MODES	Fraction (Γ_i/Γ)	Confidence level	ρ (MeV/c)
$\Lambda\pi^-$	$(99.887 \pm 0.035) \%$		140
$\Sigma^- \gamma$	$(1.27 \pm 0.23) \times 10^{-4}$		118
$\Lambda e^- \bar{\nu}_e$	$(5.63 \pm 0.31) \times 10^{-4}$		190
$\Lambda\mu^- \bar{\nu}_\mu$	$(3.5 \pm 2.2) \times 10^{-4}$		163
$\Sigma^0 e^- \bar{\nu}_e$	$(8.7 \pm 1.7) \times 10^{-5}$		123
$\Sigma^0 \mu^- \bar{\nu}_\mu$	$< 8 \times 10^{-4}$	90%	70
$\Xi^0 e^- \bar{\nu}_e$	$< 2.3 \times 10^{-3}$	90%	7

 $\Delta S = 2$ forbidden (S2) modes

$n\pi^-$	S2	$< 1.9 \times 10^{-5}$	90%	304
$ne^- \bar{\nu}_e$	S2	$< 3.2 \times 10^{-3}$	90%	327
$n\mu^- \bar{\nu}_\mu$	S2	$< 1.5 \%$	90%	314
$\rho\pi^- \pi^-$	S2	$< 4 \times 10^{-4}$	90%	223
$\rho\pi^- e^- \bar{\nu}_e$	S2	$< 4 \times 10^{-4}$	90%	305
$\rho\pi^- \mu^- \bar{\nu}_\mu$	S2	$< 4 \times 10^{-4}$	90%	251
$\rho\mu^- \mu^-$	L	$< 4 \times 10^{-8}$	90%	272

 $\Xi(1530) P_{13}$

$$I(J^P) = \frac{1}{2}(\frac{3}{2}^+)$$

$$\Xi(1530)^0 \text{ mass } m = 1531.80 \pm 0.32 \text{ MeV} \quad (S = 1.3)$$

$$\Xi(1530)^- \text{ mass } m = 1535.0 \pm 0.6 \text{ MeV}$$

$$\Xi(1530)^0 \text{ full width } \Gamma = 9.1 \pm 0.5 \text{ MeV}$$

$$\Xi(1530)^- \text{ full width } \Gamma = 9.9^{+1.7}_{-1.9} \text{ MeV}$$

$\Xi(1530)$ DECAY MODES	Fraction (Γ_i/Γ)	Confidence level	ρ (MeV/c)
$\Xi\pi$	100 %		158
$\Xi\gamma$	$< 4 \%$	90%	202

 $\Xi(1690), \Xi(1820) D_{13}, \Xi(1950), \Xi(2030)$

The Ξ resonances listed above are omitted from this Booklet but not from the Summary Table in the full Review.

Ω BARYONS

(S = -3, I = 0)

$$\Omega^- = sss$$

Ω⁻

$$I(J^P) = 0(\frac{3}{2}^+)$$

$J^P = \frac{3}{2}^+$ is the quark-model prediction; and $J = 3/2$ is fairly well established.

$$\text{Mass } m = 1672.45 \pm 0.29 \text{ MeV}$$

$$(m_{\Omega^-} - m_{\bar{\Omega}^+}) / m_{\Omega^-} = (-1 \pm 8) \times 10^{-5}$$

$$\text{Mean life } \tau = (0.821 \pm 0.011) \times 10^{-10} \text{ s}$$

$$c\tau = 2.461 \text{ cm}$$

$$(\tau_{\Omega^-} - \tau_{\bar{\Omega}^+}) / \tau_{\Omega^-} = 0.00 \pm 0.05$$

$$\text{Magnetic moment } \mu = -2.02 \pm 0.05 \mu_N$$

Decay parameters

$$\Lambda K^- \quad \alpha = 0.0180 \pm 0.0024$$

$$\Lambda K^-, \bar{\Lambda} K^+ \quad (\alpha + \bar{\alpha}) / (\alpha - \bar{\alpha}) = -0.02 \pm 0.13$$

$$\Xi^0 \pi^- \quad \alpha = 0.09 \pm 0.14$$

$$\Xi^- \pi^0 \quad \alpha = 0.05 \pm 0.21$$

Ω ⁻ DECAY MODES	Fraction (Γ _i /Γ)	Confidence level	^p (MeV/c)
ΛK ⁻	(67.8 ± 0.7) %		211
Ξ ⁰ π ⁻	(23.6 ± 0.7) %		294
Ξ ⁻ π ⁰	(8.6 ± 0.4) %		289
Ξ ⁻ π ⁺ π ⁻	(4.3 ^{+3.4} _{-1.3}) × 10 ⁻⁴		189
Ξ(1530) ⁰ π ⁻	(6.4 ^{+5.0} _{-2.0}) × 10 ⁻⁴		17
Ξ ⁰ e ⁻ $\bar{\nu}_e$	(5.6 ± 2.8) × 10 ⁻³		319
Ξ ⁻ γ	< 4.6 × 10 ⁻⁴	90%	314
ΔS = 2 forbidden (S2) modes			
Λπ ⁻	S2 < 2.9 × 10 ⁻⁶	90%	449

Ω(2250)⁻

$$I(J^P) = 0(?^?)$$

$$\text{Mass } m = 2252 \pm 9 \text{ MeV}$$

$$\text{Full width } \Gamma = 55 \pm 18 \text{ MeV}$$

Ω(2250) ⁻ DECAY MODES	Fraction (Γ _i /Γ)	^p (MeV/c)
Ξ ⁻ π ⁺ K ⁻	seen	532
Ξ(1530) ⁰ K ⁻	seen	437

CHARMED BARYONS (C = +1)

$$\Lambda_c^+ = udc, \quad \Sigma_c^{++} = uuc, \quad \Sigma_c^+ = udc, \quad \Sigma_c^0 = ddc,$$

$$\Xi_c^+ = usc, \quad \Xi_c^0 = dsc, \quad \Omega_c^0 = ssc$$

Λ_c^+

$$I(J^P) = 0(\frac{1}{2}^+)$$

J is not well measured; $\frac{1}{2}$ is the quark-model prediction.

Mass $m = 2286.46 \pm 0.14$ MeV

Mean life $\tau = (200 \pm 6) \times 10^{-15}$ s ($S = 1.6$)

$c\tau = 59.9$ μ m

Decay asymmetry parameters

$$\Lambda\pi^+ \quad \alpha = -0.91 \pm 0.15$$

$$\Sigma^+\pi^0 \quad \alpha = -0.45 \pm 0.32$$

$$\Lambda\ell^+\nu_\ell \quad \alpha = -0.86 \pm 0.04$$

$$(\alpha + \bar{\alpha})/(\alpha - \bar{\alpha}) \text{ in } \Lambda_c^+ \rightarrow \Lambda\pi^+, \bar{\Lambda}_c^- \rightarrow \bar{\Lambda}\pi^- = -0.07 \pm 0.31$$

$$(\alpha + \bar{\alpha})/(\alpha - \bar{\alpha}) \text{ in } \Lambda_c^+ \rightarrow \Lambda e^+\nu_e, \bar{\Lambda}_c^- \rightarrow \bar{\Lambda}e^-\bar{\nu}_e = 0.00 \pm 0.04$$

Nearly all branching fractions of the Λ_c^+ are measured relative to the $\rho K^-\pi^+$ mode, but there are no model-independent measurements of this branching fraction. We explain how we arrive at our value of $B(\Lambda_c^+ \rightarrow \rho K^-\pi^+)$ in a Note at the beginning of the branching-ratio measurements in the Listings. When this branching fraction is eventually well determined, all the other branching fractions will slide up or down proportionally as the true value differs from the value we use here.

Λ_c^+ DECAY MODES	Fraction (Γ_i/Γ)	Scale factor/ Confidence level	ρ (MeV/c)
---------------------------	--------------------------------	-----------------------------------	-------------------

Hadronic modes with a ρ : $S = -1$ final states

$\rho\bar{K}^0$	(2.3 \pm 0.6) %		873
$\rho K^-\pi^+$	[0] (5.0 \pm 1.3) %		823
$\rho\bar{K}^*(892)^0$	[ρ] (1.6 \pm 0.5) %		685
$\Delta(1232)^{++}K^-$	(8.6 \pm 3.0) $\times 10^{-3}$		710
$\Lambda(1520)\pi^+$	[ρ] (1.8 \pm 0.6) %		627
$\rho K^-\pi^+$ nonresonant	(2.8 \pm 0.8) %		823
$\rho\bar{K}^0\pi^0$	(3.3 \pm 1.0) %		823
$\rho\bar{K}^0\eta$	(1.2 \pm 0.4) %		568
$\rho\bar{K}^0\pi^+\pi^-$	(2.6 \pm 0.7) %		754
$\rho K^-\pi^+\pi^0$	(3.4 \pm 1.0) %		759
$\rho K^*(892)^-\pi^+$	[ρ] (1.1 \pm 0.5) %		580
$\rho(K^-\pi^+)_{\text{nonresonant}}\pi^0$	(3.6 \pm 1.2) %		759
$\Delta(1232)K^*(892)$	seen		419
$\rho K^-\pi^+\pi^+\pi^-$	(1.1 \pm 0.8) $\times 10^{-3}$		671
$\rho K^-\pi^+\pi^0\pi^0$	(8 \pm 4) $\times 10^{-3}$		678

Hadronic modes with a ρ : $S = 0$ final states

$\rho\pi^+\pi^-$	(3.5 \pm 2.0) $\times 10^{-3}$		927
$\rho f_0(980)$	[ρ] (2.8 \pm 1.9) $\times 10^{-3}$		622
$\rho\pi^+\pi^+\pi^-\pi^-$	(1.8 \pm 1.2) $\times 10^{-3}$		852
ρK^+K^-	(7.7 \pm 3.5) $\times 10^{-4}$		616
$\rho\phi$	[ρ] (8.2 \pm 2.7) $\times 10^{-4}$		590
ρK^+K^- non- ϕ	(3.5 \pm 1.7) $\times 10^{-4}$		616

Hadronic modes with a hyperon: $S = -1$ final states

$\Lambda\pi^+$	(1.07 ± 0.28) %		864
$\Lambda\pi^+\pi^0$	(3.6 ± 1.3) %		844
$\Lambda\rho^+$	< 5 %	CL=95%	635
$\Lambda\pi^+\pi^+\pi^-$	(2.6 ± 0.7) %		807
$\Sigma(1385)^+\pi^+\pi^-, \Sigma^{*+} \rightarrow$	(7 ± 4) × 10 ⁻³		688
$\Lambda\pi^+$			
$\Sigma(1385)^-\pi^+\pi^+, \Sigma^{*-} \rightarrow$	(5.5 ± 1.7) × 10 ⁻³		688
$\Lambda\pi^-$			
$\Lambda\pi^+\rho^0$	(1.1 ± 0.5) %		523
$\Sigma(1385)^+\rho^0, \Sigma^{*+} \rightarrow \Lambda\pi^+$	(3.7 ± 3.1) × 10 ⁻³		363
$\Lambda\pi^+\pi^+\pi^-$ nonresonant	< 8 × 10 ⁻³	CL=90%	807
$\Lambda\pi^+\pi^+\pi^-\pi^0$ total	(1.8 ± 0.8) %		757
$\Lambda\pi^+\eta$	[ρ] (1.8 ± 0.6) %		691
$\Sigma(1385)^+\eta$	[ρ] (8.5 ± 3.3) × 10 ⁻³		570
$\Lambda\pi^+\omega$	[ρ] (1.2 ± 0.5) %		517
$\Lambda\pi^+\pi^+\pi^-\pi^0$, no η or ω	< 7 × 10 ⁻³	CL=90%	757
$\Lambda K^+\bar{K}^0$	(4.7 ± 1.5) × 10 ⁻³	S=1.2	443
$\Xi(1690)^0 K^+, \Xi^{*0} \rightarrow \Lambda\bar{K}^0$	(1.3 ± 0.5) × 10 ⁻³		286
$\Sigma^0\pi^+$	(1.05 ± 0.28) %		825
$\Sigma^+\pi^0$	(1.00 ± 0.34) %		827
$\Sigma^+\eta$	(5.5 ± 2.3) × 10 ⁻³		713
$\Sigma^+\pi^+\pi^-$	(3.6 ± 1.0) %		804
$\Sigma^+\rho^0$	< 1.4 %	CL=95%	575
$\Sigma^-\pi^+\pi^+$	(1.7 ± 0.5) %		799
$\Sigma^0\pi^+\pi^0$	(1.8 ± 0.8) %		803
$\Sigma^0\pi^+\pi^+\pi^-$	(8.3 ± 3.1) × 10 ⁻³		763
$\Sigma^+\pi^+\pi^-\pi^0$	—		767
$\Sigma^+\omega$	[ρ] (2.7 ± 1.0) %		569
$\Sigma^+K^+K^-$	(2.8 ± 0.8) × 10 ⁻³		349
$\Sigma^+\phi$	[ρ] (3.1 ± 0.9) × 10 ⁻³		295
$\Xi(1690)^0 K^+, \Xi^{*0} \rightarrow \Sigma^+K^-$	(8.1 ± 3.0) × 10 ⁻⁴		286
$\Sigma^+K^+K^-$ nonresonant	< 6 × 10 ⁻⁴	CL=90%	349
$\Xi^0 K^+$	(3.9 ± 1.4) × 10 ⁻³		653
$\Xi^- K^+\pi^+$	(5.1 ± 1.4) × 10 ⁻³		565
$\Xi(1530)^0 K^+$	[ρ] (2.6 ± 1.0) × 10 ⁻³		473

Hadronic modes with a hyperon: $S = 0$ final states

ΛK^+	(5.0 ± 1.6) × 10 ⁻⁴		781
$\Lambda K^+\pi^+\pi^-$	< 4 × 10 ⁻⁴	CL=90%	637
$\Sigma^0 K^+$	(4.2 ± 1.3) × 10 ⁻⁴		735
$\Sigma^0 K^+\pi^+\pi^-$	< 2.1 × 10 ⁻⁴	CL=90%	574
$\Sigma^+ K^+\pi^-$	(1.7 ± 0.7) × 10 ⁻³		670
$\Sigma^+ K^*(892)^0$	[ρ] (2.8 ± 1.1) × 10 ⁻³		470
$\Sigma^- K^+\pi^+$	< 1.0 × 10 ⁻³	CL=90%	664

Doubly Cabibbo-suppressed modes

$p K^+\pi^-$	< 2.3 × 10 ⁻⁴	CL=90%	823
--------------	--------------------------	--------	-----

Semileptonic modes

$\Lambda\ell^+\nu_\ell$	[q] (2.0 ± 0.6) %		871
$\Lambda e^+\nu_e$	(2.1 ± 0.6) %		871
$\Lambda\mu^+\nu_\mu$	(2.0 ± 0.7) %		867

Inclusive modes			
e^+ anything		(4.5 ± 1.7) %	—
$p e^+$ anything		(1.8 ± 0.9) %	—
p anything		(50 ± 16) %	—
p anything (no Λ)		(12 ± 19) %	—
n anything		(50 ± 16) %	—
n anything (no Λ)		(29 ± 17) %	—
Λ anything		(35 ± 11) %	S=1.4 —
Σ^\pm anything	[r]	(10 ± 5) %	—
3prongs		(24 ± 8) %	—

**$\Delta C = 1$ weak neutral current ($C1$) modes, or
Lepton number (L) violating modes**

$p\mu^+\mu^-$	$C1$	< 3.4	$\times 10^{-4}$	CL=90%	937
$\Sigma^-\mu^+\mu^+$	L	< 7.0	$\times 10^{-4}$	CL=90%	812

$\Lambda_c(2595)^+$

$$I(J^P) = 0(\frac{1}{2}^-)$$

The spin-parity follows from the fact that $\Sigma_c(2455)\pi$ decays, with little available phase space, are dominant. This assumes that $J^P = 1/2^+$ for the $\Sigma_c(2455)$.

$$\text{Mass } m = 2595.4 \pm 0.6 \text{ MeV} \quad (S = 1.1)$$

$$m - m_{\Lambda_c^+} = 308.9 \pm 0.6 \text{ MeV} \quad (S = 1.1)$$

$$\text{Full width } \Gamma = 3.6_{-1.3}^{+2.0} \text{ MeV}$$

$\Lambda_c^+ \pi \pi$ and its submode $\Sigma_c(2455)\pi$ — the latter just barely — are the only strong decays allowed to an excited Λ_c^+ having this mass; and the submode seems to dominate.

$\Lambda_c(2595)^+$ DECAY MODES	Fraction (Γ_i/Γ)	p (MeV/c)
$\Lambda_c^+ \pi^+ \pi^-$	[s] $\approx 67\%$	124
$\Sigma_c(2455)^{++} \pi^-$	$24 \pm 7\%$	28
$\Sigma_c(2455)^0 \pi^+$	$24 \pm 7\%$	28
$\Lambda_c^+ \pi^+ \pi^-$ 3-body	$18 \pm 10\%$	124
$\Lambda_c^+ \pi^0$	[t] not seen	261
$\Lambda_c^+ \gamma$	not seen	291

$\Lambda_c(2625)^+$

$$I(J^P) = 0(\frac{3}{2}^-)$$

J^P has not been measured; $\frac{3}{2}^-$ is the quark-model prediction.

$$\text{Mass } m = 2628.1 \pm 0.6 \text{ MeV} \quad (S = 1.5)$$

$$m - m_{\Lambda_c^+} = 341.7 \pm 0.6 \text{ MeV} \quad (S = 1.6)$$

$$\text{Full width } \Gamma < 1.9 \text{ MeV, CL} = 90\%$$

$\Lambda_c^+ \pi \pi$ and its submode $\Sigma(2455)\pi$ are the only strong decays allowed to an excited Λ_c^+ having this mass.

$\Lambda_c(2625)^+$ DECAY MODES	Fraction (Γ_i/Γ)	Confidence level	p (MeV/c)
$\Lambda_c^+ \pi^+ \pi^-$	[s] $\approx 67\%$		184
$\Sigma_c(2455)^{++} \pi^-$	<5	90%	102

$\Sigma_c(2455)^0 \pi^+$	<5	90%	102
$\Lambda_c^+ \pi^+ \pi^-$ 3-body	large		184
$\Lambda_c^+ \pi^0$	[t] not seen		293
$\Lambda_c^+ \gamma$	not seen		319

$\Lambda_c(2880)^+$

$I(J^P) = 0(\frac{5}{2}^+)$

There is some good evidence that indeed $J^P = 5/2^+$

Mass $m = 2881.53 \pm 0.35$ MeV

$m - m_{\Lambda_c^+} = 595.1 \pm 0.4$ MeV

Full width $\Gamma = 5.8 \pm 1.1$ MeV

$\Lambda_c(2880)^+$ DECAY MODES	Fraction (Γ_i/Γ)	ρ (MeV/c)
$\Lambda_c^+ \pi^+ \pi^-$	seen	471
$\Sigma_c(2455)^{0,++} \pi^\pm$	seen	376
$\Sigma_c(2520)^{0,++} \pi^\pm$	seen	317
ρD^0	seen	316

$\Lambda_c(2940)^+$

$I(J^P) = 0(?^?)$

Mass $m = 2939.3^{+1.4}_{-1.5}$ MeV

Full width $\Gamma = 17^{+8}_{-6}$ MeV

$\Lambda_c(2940)^+$ DECAY MODES	Fraction (Γ_i/Γ)	ρ (MeV/c)
ρD^0	seen	420
$\Sigma_c(2455)^{0,++} \pi^\pm$	seen	-

$\Sigma_c(2455)$

$I(J^P) = 1(\frac{1}{2}^+)$

J^P has not been measured; $\frac{1}{2}^+$ is the quark-model prediction.

$\Sigma_c(2455)^{++}$ mass $m = 2454.02 \pm 0.18$ MeV

$\Sigma_c(2455)^+$ mass $m = 2452.9 \pm 0.4$ MeV

$\Sigma_c(2455)^0$ mass $m = 2453.76 \pm 0.18$ MeV

$m_{\Sigma_c^{++}} - m_{\Lambda_c^+} = 167.56 \pm 0.11$ MeV

$m_{\Sigma_c^+} - m_{\Lambda_c^+} = 166.4 \pm 0.4$ MeV

$m_{\Sigma_c^0} - m_{\Lambda_c^+} = 167.30 \pm 0.11$ MeV

$m_{\Sigma_c^{++}} - m_{\Sigma_c^0} = 0.27 \pm 0.11$ MeV (S = 1.1)

$m_{\Sigma_c^+} - m_{\Sigma_c^0} = -0.9 \pm 0.4$ MeV

$\Sigma_c(2455)^{++}$ full width $\Gamma = 2.23 \pm 0.30$ MeV

$\Sigma_c(2455)^+$ full width $\Gamma < 4.6$ MeV, CL = 90%

$\Sigma_c(2455)^0$ full width $\Gamma = 2.2 \pm 0.4$ MeV (S = 1.4)

$\Lambda_c^+ \pi$ is the only strong decay allowed to a Σ_c having this mass.

$\Sigma_c(2455)$ DECAY MODES	Fraction (Γ_i/Γ)	ρ (MeV/c)
$\Lambda_c^+ \pi$	$\approx 100\%$	94

$\Sigma_c(2520)$

$$I(J^P) = 1(\frac{3}{2}^+)$$

J^P has not been measured; $\frac{3}{2}^+$ is the quark-model prediction.

- $\Sigma_c(2520)^{++}$ mass $m = 2518.4 \pm 0.6$ MeV (S = 1.4)
- $\Sigma_c(2520)^+$ mass $m = 2517.5 \pm 2.3$ MeV
- $\Sigma_c(2520)^0$ mass $m = 2518.0 \pm 0.5$ MeV
- $m_{\Sigma_c(2520)^{++}} - m_{\Lambda_c^+} = 231.9 \pm 0.6$ MeV (S = 1.5)
- $m_{\Sigma_c(2520)^+} - m_{\Lambda_c^+} = 231.0 \pm 2.3$ MeV
- $m_{\Sigma_c(2520)^0} - m_{\Lambda_c^+} = 231.6 \pm 0.5$ MeV (S = 1.1)
- $m_{\Sigma_c(2520)^{++}} - m_{\Sigma_c(2520)^0} = 0.3 \pm 0.6$ MeV (S = 1.2)
- $\Sigma_c(2520)^{++}$ full width $\Gamma = 14.9 \pm 1.9$ MeV
- $\Sigma_c(2520)^+$ full width $\Gamma < 17$ MeV, CL = 90%
- $\Sigma_c(2520)^0$ full width $\Gamma = 16.1 \pm 2.1$ MeV

$\Lambda_c^+ \pi$ is the only strong decay allowed to a Σ_c having this mass.

$\Sigma_c(2520)$ DECAY MODES	Fraction (Γ_i/Γ)	p (MeV/c)
$\Lambda_c^+ \pi$	≈ 100 %	180

$\Sigma_c(2800)$

$$I(J^P) = 1(?^?)$$

- $\Sigma_c(2800)^{++}$ mass $m = 2801^{+4}_{-6}$ MeV
- $\Sigma_c(2800)^+$ mass $m = 2792^{+14}_{-5}$ MeV
- $\Sigma_c(2800)^0$ mass $m = 2802^{+4}_{-7}$ MeV
- $m_{\Sigma_c(2800)^{++}} - m_{\Lambda_c^+} = 514^{+4}_{-6}$ MeV
- $m_{\Sigma_c(2800)^+} - m_{\Lambda_c^+} = 505^{+14}_{-5}$ MeV
- $m_{\Sigma_c(2800)^0} - m_{\Lambda_c^+} = 515^{+4}_{-7}$ MeV
- $\Sigma_c(2800)^{++}$ full width $\Gamma = 75^{+22}_{-17}$ MeV
- $\Sigma_c(2800)^+$ full width $\Gamma = 62^{+60}_{-40}$ MeV
- $\Sigma_c(2800)^0$ full width $\Gamma = 61^{+28}_{-18}$ MeV

$\Sigma_c(2800)$ DECAY MODES	Fraction (Γ_i/Γ)	p (MeV/c)
$\Lambda_c^+ \pi$	seen	443

Ξ_c^+

$$I(J^P) = \frac{1}{2}(\frac{1}{2}^+)$$

J^P has not been measured; $\frac{1}{2}^+$ is the quark-model prediction.

- Mass $m = 2467.8^{+0.4}_{-0.6}$ MeV
- Mean life $\tau = (442 \pm 26) \times 10^{-15}$ s (S = 1.3)
- $c\tau = 132$ μ m

Ξ_c^+ DECAY MODES	Fraction (Γ_i/Γ)	Confidence level	p (MeV/c)
-----------------------	--------------------------------	------------------	-------------

No absolute branching fractions have been measured.
The following are branching *ratios* relative to $\Xi^- 2\pi^+$.

Cabibbo-favored ($S = -2$) decays

$\rho 2K_S^0$	[<i>u</i>]	0.087 ± 0.022		767
$\Lambda \bar{K}^0 \pi^+$		—		852
$\Sigma(1385)^+ \bar{K}^0$	[ρ, u]	1.0 ± 0.5		746
$\Lambda K^- 2\pi^+$	[<i>u</i>]	0.323 ± 0.033		787
$\Lambda \bar{K}^*(892)^0 \pi^+$	[ρ, u]	< 0.2	90%	608
$\Sigma(1385)^+ K^- \pi^+$	[ρ, u]	< 0.3	90%	678
$\Sigma^+ K^- \pi^+$	[<i>u</i>]	0.94 ± 0.11		810
$\Sigma^+ \bar{K}^*(892)^0$	[ρ, u]	0.81 ± 0.15		658
$\Sigma^0 K^- 2\pi^+$	[<i>u</i>]	0.29 ± 0.16		735
$\Xi^0 \pi^+$	[<i>u</i>]	0.55 ± 0.16		877
$\Xi^- 2\pi^+$	[<i>u</i>]	DEFINED AS 1		851
$\Xi(1530)^0 \pi^+$	[ρ, u]	< 0.1	90%	750
$\Xi^0 \pi^+ \pi^0$	[<i>u</i>]	2.34 ± 0.68		856
$\Xi^0 \pi^- 2\pi^+$	[<i>u</i>]	1.74 ± 0.50		818
$\Xi^0 e^+ \nu_e$	[<i>u</i>]	$2.3 \begin{smallmatrix} +0.7 \\ -0.9 \end{smallmatrix}$		884
$\Omega^- K^+ \pi^+$	[<i>u</i>]	0.07 ± 0.04		399

Cabibbo-suppressed decays

$\rho K^- \pi^+$	[<i>u</i>]	0.21 ± 0.03		944
$\rho \bar{K}^*(892)^0$	[ρ, u]	0.12 ± 0.02		828
$\Sigma^+ \pi^+ \pi^-$	[<i>u</i>]	0.48 ± 0.20		922
$\Sigma^- 2\pi^+$	[<i>u</i>]	0.18 ± 0.09		918
$\Sigma^+ K^+ K^-$	[<i>u</i>]	0.15 ± 0.07		579
$\Sigma^+ \phi$	[ρ, u]	< 0.11	90%	549
$\Xi(1690)^0 K^+, \Xi(1690)^0 \rightarrow \Sigma^+ K^-$	[<i>u</i>]	< 0.05	90%	501

Ξ_c^0

$$I(J^P) = \frac{1}{2}(\frac{1}{2}^+)$$

J^P has not been measured; $\frac{1}{2}^+$ is the quark-model prediction.

$$\text{Mass } m = 2470.88_{-0.80}^{+0.34} \text{ MeV} \quad (S = 1.1)$$

$$m_{\Xi_c^0} - m_{\Xi_c^+} = 3.1_{-0.5}^{+0.4} \text{ MeV}$$

$$\text{Mean life } \tau = (112_{-10}^{+13}) \times 10^{-15} \text{ s}$$

$$c\tau = 33.6 \text{ } \mu\text{m}$$

Decay asymmetry parameters

$$\Xi^- \pi^+ \quad \alpha = -0.6 \pm 0.4$$

No absolute branching fractions have been measured. Several measurements of ratios of fractions may be found in the Listings that follow.

Ξ_c^0 DECAY MODES	Fraction (Γ_i/Γ)	ρ (MeV/c)
$\rho K^- K^- \pi^+$	seen	676
$\rho K^- \bar{K}^*(892)^0$	seen	413
$\rho K^- K^- \pi^+$ no $\bar{K}^*(892)^0$	seen	676
ΛK_S^0	seen	906
$\Lambda \bar{K}^0 \pi^+ \pi^-$	seen	787

$\Lambda K^- \pi^+ \pi^+ \pi^-$	seen	703
$\Xi^- \pi^+$	seen	875
$\Xi^- \pi^+ \pi^+ \pi^-$	seen	816
$\Omega^- K^+$	seen	522
$\Xi^- e^+ \nu_e$	seen	882
$\Xi^- \ell^+$ anything	seen	—

$\Xi_c^{'+}$

$$I(J^P) = \frac{1}{2}(\frac{1}{2}^+)$$

J^P has not been measured; $\frac{1}{2}^+$ is the quark-model prediction.

$$\text{Mass } m = 2575.6 \pm 3.1 \text{ MeV}$$

$$m_{\Xi_c^{'+}} - m_{\Xi_c^+} = 107.8 \pm 3.0 \text{ MeV}$$

The $\Xi_c^{'+} - \Xi_c^+$ mass difference is too small for any strong decay to occur.

$\Xi_c^{'+}$ DECAY MODES	Fraction (Γ_i/Γ)	ρ (MeV/c)
$\Xi_c^+ \gamma$	seen	106

$\Xi_c^{'0}$

$$I(J^P) = \frac{1}{2}(\frac{1}{2}^+)$$

J^P has not been measured; $\frac{1}{2}^+$ is the quark-model prediction.

$$\text{Mass } m = 2577.9 \pm 2.9 \text{ MeV}$$

$$m_{\Xi_c^{'0}} - m_{\Xi_c^0} = 107.0 \pm 2.9 \text{ MeV}$$

The $\Xi_c^{'0} - \Xi_c^0$ mass difference is too small for any strong decay to occur.

$\Xi_c^{'0}$ DECAY MODES	Fraction (Γ_i/Γ)	ρ (MeV/c)
$\Xi_c^0 \gamma$	seen	105

$\Xi_c(2645)$

$$I(J^P) = \frac{1}{2}(\frac{3}{2}^+)$$

J^P has not been measured; $\frac{3}{2}^+$ is the quark-model prediction.

$$\Xi_c(2645)^+ \text{ mass } m = 2645.9_{-0.6}^{+0.5} \text{ MeV} \quad (S = 1.1)$$

$$\Xi_c(2645)^0 \text{ mass } m = 2645.9 \pm 0.5 \text{ MeV}$$

$$m_{\Xi_c(2645)^+} - m_{\Xi_c^0} = 175.0_{-0.6}^{+0.8} \text{ MeV} \quad (S = 1.2)$$

$$m_{\Xi_c(2645)^0} - m_{\Xi_c^+} = 178.1 \pm 0.6 \text{ MeV}$$

$$m_{\Xi_c(2645)^+} - m_{\Xi_c(2645)^0} = 0.0 \pm 0.5 \text{ MeV}$$

$$\Xi_c(2645)^+ \text{ full width } \Gamma < 3.1 \text{ MeV, CL} = 90\%$$

$$\Xi_c(2645)^0 \text{ full width } \Gamma < 5.5 \text{ MeV, CL} = 90\%$$

$\Xi_c \pi$ is the only strong decay allowed to a Ξ_c resonance having this mass.

$\Xi_c(2645)$ DECAY MODES	Fraction (Γ_i/Γ)	ρ (MeV/c)
$\Xi_c^0 \pi^+$	seen	102
$\Xi_c^+ \pi^-$	seen	107

$\Xi_c(2790)$

$$I(J^P) = \frac{1}{2}(\frac{1}{2}^-)$$

 J^P has not been measured; $\frac{1}{2}^-$ is the quark-model prediction.

$$\Xi_c(2790)^+ \text{ mass} = 2789.1 \pm 3.2 \text{ MeV}$$

$$\Xi_c(2790)^0 \text{ mass} = 2791.8 \pm 3.3 \text{ MeV}$$

$$m_{\Xi_c(2790)^+} - m_{\Xi_c^0} = 318.2 \pm 3.2 \text{ MeV}$$

$$m_{\Xi_c(2790)^0} - m_{\Xi_c^+} = 324.0 \pm 3.3 \text{ MeV}$$

$$\Xi_c(2790)^+ \text{ width} < 15 \text{ MeV, CL} = 90\%$$

$$\Xi_c(2790)^0 \text{ width} < 12 \text{ MeV, CL} = 90\%$$

 $\Xi_c(2790)$ DECAY MODESFraction (Γ_i/Γ) ρ (MeV/c) $\Xi_c' \pi$

seen

159

 $\Xi_c(2815)$

$$I(J^P) = \frac{1}{2}(\frac{3}{2}^-)$$

 J^P has not been measured; $\frac{3}{2}^-$ is the quark-model prediction.

$$\Xi_c(2815)^+ \text{ mass } m = 2816.6 \pm 0.9 \text{ MeV}$$

$$\Xi_c(2815)^0 \text{ mass } m = 2819.6 \pm 1.2 \text{ MeV}$$

$$m_{\Xi_c(2815)^+} - m_{\Xi_c^+} = 348.8 \pm 0.9 \text{ MeV}$$

$$m_{\Xi_c(2815)^0} - m_{\Xi_c^0} = 348.7 \pm 1.2 \text{ MeV}$$

$$m_{\Xi_c(2815)^+} - m_{\Xi_c(2815)^0} = -3.1 \pm 1.3 \text{ MeV}$$

$$\Xi_c(2815)^+ \text{ full width } \Gamma < 3.5 \text{ MeV, CL} = 90\%$$

$$\Xi_c(2815)^0 \text{ full width } \Gamma < 6.5 \text{ MeV, CL} = 90\%$$

The $\Xi_c \pi \pi$ modes are consistent with being entirely via $\Xi_c(2645) \pi$. **$\Xi_c(2815)$ DECAY MODES**Fraction (Γ_i/Γ) ρ (MeV/c) $\Xi_c^+ \pi^+ \pi^-$

seen

196

 $\Xi_c^0 \pi^+ \pi^-$

seen

191

 $\Xi_c(2980)$

$$I(J^P) = \frac{1}{2}(?)^?$$

$$\Xi_c(2980)^+ \text{ } m = 2971.4 \pm 3.3 \text{ MeV} \quad (S = 2.1)$$

$$\Xi_c(2980)^0 \text{ } m = 2968.0 \pm 2.6 \text{ MeV} \quad (S = 1.2)$$

$$\Xi_c(2980)^+ \text{ width } \Gamma = 26 \pm 7 \text{ MeV} \quad (S = 1.5)$$

$$\Xi_c(2980)^0 \text{ width } \Gamma = 20 \pm 7 \text{ MeV} \quad (S = 1.3)$$

 $\Xi_c(2980)$ DECAY MODESFraction (Γ_i/Γ) ρ (MeV/c) $\Lambda_c^+ \bar{K} \pi$

seen

231

 $\Sigma_c(2455) \bar{K}$

seen

134

 $\Lambda_c^+ \bar{K}$

not seen

414

 $\Xi_c 2\pi$

seen

-

 $\Xi_c(2645) \pi$

seen

277

$\Xi_c(3080)$

$I(J^P) = \frac{1}{2}(??)$

- $\Xi_c(3080)^+ m = 3077.0 \pm 0.4 \text{ MeV}$
- $\Xi_c(3080)^0 m = 3079.9 \pm 1.4 \text{ MeV} \quad (S = 1.3)$
- $\Xi_c(3080)^+ \text{ width } \Gamma = 5.8 \pm 1.0 \text{ MeV}$
- $\Xi_c(3080)^0 \text{ width } \Gamma = 5.6 \pm 2.2 \text{ MeV}$

$\Xi_c(3080)$ DECAY MODES	Fraction (Γ_i/Γ)	ρ (MeV/c)
$\Lambda_c^+ \bar{K} \pi$	seen	415
$\Sigma_c(2455) \bar{K}$	seen	342
$\Sigma_c(2455) \bar{K} + \Sigma_c(2520) \bar{K}$	seen	—
$\Lambda_c^+ \bar{K}$	not seen	536
$\Lambda_c^+ \bar{K} \pi^+ \pi^-$	not seen	143

Ω_c^0

$I(J^P) = 0(\frac{1}{2}^+)$

J^P has not been measured; $\frac{1}{2}^+$ is the quark-model prediction.

- Mass $m = 2695.2 \pm 1.7 \text{ MeV} \quad (S = 1.3)$
- Mean life $\tau = (69 \pm 12) \times 10^{-15} \text{ s}$
- $c\tau = 21 \text{ } \mu\text{m}$

No absolute branching fractions have been measured.

Ω_c^0 DECAY MODES	Fraction (Γ_i/Γ)	ρ (MeV/c)
$\Sigma^+ K^- K^- \pi^+$	seen	689
$\Xi^0 K^- \pi^+$	seen	901
$\Xi^- K^- \pi^+ \pi^+$	seen	830
$\Omega^- e^+ \nu_e$	seen	829
$\Omega^- \pi^+$	seen	821
$\Omega^- \pi^+ \pi^0$	seen	797
$\Omega^- \pi^- \pi^+ \pi^+$	seen	753

$\Omega_c(2770)^0$

$I(J^P) = 0(\frac{3}{2}^+)$

J^P has not been measured; $\frac{3}{2}^+$ is the quark-model prediction.

- Mass $m = 2765.9 \pm 2.0 \text{ MeV} \quad (S = 1.2)$
- $m_{\Omega_c(2770)^0} - m_{\Omega_c^0} = 70.7^{+0.8}_{-0.9} \text{ MeV}$

The $\Omega_c(2770)^0 - \Omega_c^0$ mass difference is too small for any strong decay to occur.

$\Omega_c(2770)^0$ DECAY MODES	Fraction (Γ_i/Γ)	ρ (MeV/c)
$\Omega_c^0 \gamma$	presumably 100%	70

BOTTOM BARYONS

($B = -1$)

$$\Lambda_b^0 = udb, \Xi_b^0 = usb, \Xi_b^- = dsb, \Omega_b^- = ssb$$

Λ_b^0

$$I(J^P) = 0(\frac{1}{2}^+)$$

$I(J^P)$ not yet measured; $0(\frac{1}{2}^+)$ is the quark model prediction.

$$\text{Mass } m = 5620.2 \pm 1.6 \text{ MeV}$$

$$m_{\Lambda_b} - m_{B^0} = 339.2 \pm 1.4 \text{ MeV}$$

$$\text{Mean life } \tau = (1.391_{-0.037}^{+0.038}) \times 10^{-12} \text{ s}$$

$$c\tau = 417 \mu\text{m}$$

The branching fractions $B(b\text{-baryon} \rightarrow \Lambda_c \ell^- \bar{\nu}_\ell \text{ anything})$ and $B(\Lambda_b^0 \rightarrow \Lambda_c^+ \ell^- \bar{\nu}_\ell \text{ anything})$ are not pure measurements because the underlying measured products of these with $B(b \rightarrow b\text{-baryon})$ were used to determine $B(b \rightarrow b\text{-baryon})$, as described in the note "Production and Decay of b -Flavored Hadrons."

For inclusive branching fractions, e.g., $\Lambda_b \rightarrow \bar{\Lambda}_c \text{ anything}$, the values usually are multiplicities, not branching fractions. They can be greater than one.

Λ_b^0 DECAY MODES	Fraction (Γ_i/Γ)	Confidence level	ρ (MeV/c)
$J/\psi(1S)\Lambda \times B(b \rightarrow \Lambda_b^0)$	$(4.7 \pm 2.3) \times 10^{-5}$		1741
$\Lambda_c^+ \pi^-$	$(8.8 \pm 3.2) \times 10^{-3}$		2343
$\Lambda_c^+ a_1(1260)^-$	seen		2153
$\Lambda_c^+ \ell^- \bar{\nu}_\ell \text{ anything}$	[v] $(10.7 \pm 3.2) \%$		—
$\Lambda_c^+ \ell^- \bar{\nu}_\ell$	$(5.0_{-1.4}^{+1.9}) \%$		2345
$\Lambda_c^+ \pi^+ \pi^- \ell^- \bar{\nu}_\ell$	$(5.6 \pm 3.1) \%$		2335
$\Lambda_c(2595)^+ \ell^- \bar{\nu}_\ell$	$(6.3_{-3.1}^{+4.0}) \times 10^{-3}$		2211
$\Lambda_c(2625)^+ \ell^- \bar{\nu}_\ell$	$(1.1_{-0.4}^{+0.6}) \%$		2196
$p h^-$	[w] $< 2.3 \times 10^{-5}$	90%	2730
$p \pi^-$	$(3.8 \pm 1.3) \times 10^{-6}$		2730
$p K^-$	$(6.0 \pm 1.9) \times 10^{-6}$		2709
$\Lambda \gamma$	$< 1.3 \times 10^{-3}$	90%	2699

Σ_b

$$I(J^P) = 1(\frac{1}{2}^+)$$

I, J, P need confirmation.

$$\text{Mass } m(\Sigma_b^+) = 5807.8 \pm 2.7 \text{ MeV}$$

$$\text{Mass } m(\Sigma_b^-) = 5815.2 \pm 2.0 \text{ MeV}$$

Σ_b DECAY MODES	Fraction (Γ_i/Γ)	ρ (MeV/c)
$\Lambda_b^0 \pi$	dominant	128

Σ_b^*

$I(J^P) = 1(\frac{3}{2}^+)$
 I, J, P need confirmation.

Mass $m(\Sigma_b^{*+}) = 5829.0 \pm 3.4$ MeV
 Mass $m(\Sigma_b^{*-}) = 5836.4 \pm 2.8$ MeV
 $m_{\Sigma_b^*} - m_{\Sigma_b} = 21.2 \pm 2.0$ MeV

Σ_b^* DECAY MODES	Fraction (Γ_i/Γ)	ρ (MeV/c)
$\Lambda_b^0 \pi$	dominant	156

Ξ_b^0, Ξ_b^-

$I(J^P) = \frac{1}{2}(\frac{1}{2}^+)$
 I, J, P need confirmation.

Mass $m = 5790.5 \pm 2.7$ MeV
 Mean life $\tau_{\Xi_b^-} = (1.56 \pm 0.26) \times 10^{-12}$ s
 Mean life $\tau_{\Xi_b^0} = (1.49_{-0.18}^{+0.19}) \times 10^{-12}$ s

Ξ_b DECAY MODES	Fraction (Γ_i/Γ)	Scale factor	ρ (MeV/c)
$\Xi_b^- \rightarrow \Xi^- \ell^- \bar{\nu}_\ell X \times B(\bar{b} \rightarrow \Xi_b^-)$	$(3.9 \pm 1.2) \times 10^{-4}$	1.4	-
$\Xi_b^- \rightarrow J/\psi \Xi^- \times B(b \rightarrow \Xi_b^-)$	$(8 \pm 4) \times 10^{-6}$		-

Ω_b^-

$I(J^P) = 0(\frac{1}{2}^+)$
 I, J, P need confirmation.

Mass $m = 6071 \pm 40$ MeV ($S = 6.2$)
 Mean life $\tau = (1.1_{-0.4}^{+0.5}) \times 10^{-12}$ s

Ω_b^- DECAY MODES	Fraction (Γ_i/Γ)	ρ (MeV/c)
$J/\psi \Omega^- \times B(b \rightarrow \Omega_b^-)$	$(2.4 \pm 1.2) \times 10^{-6}$	1826

b -baryon ADMIXTURE ($\Lambda_b, \Xi_b, \Sigma_b, \Omega_b$)

Mean life $\tau = (1.345 \pm 0.032) \times 10^{-12}$ s

These branching fractions are actually an average over weakly decaying b -baryons weighted by their production rates in Z decay (or high-energy $p\bar{p}$), branching ratios, and detection efficiencies. They scale with the LEP b -baryon production fraction $B(b \rightarrow b\text{-baryon})$ and are evaluated for our value $B(b \rightarrow b\text{-baryon}) = (9.2 \pm 1.8)\%$.

The branching fractions $B(b\text{-baryon} \rightarrow \Lambda \ell^- \bar{\nu}_\ell \text{anything})$ and $B(\Lambda_b^0 \rightarrow \Lambda_c^+ \ell^- \bar{\nu}_\ell \text{anything})$ are not pure measurements because the underlying measured products of these with $B(b \rightarrow b\text{-baryon})$ were used to determine $B(b \rightarrow b\text{-baryon})$, as described in the note "Production and Decay of b -Flavored Hadrons."

For inclusive branching fractions, e.g., $B \rightarrow D^\pm \text{anything}$, the values usually are multiplicities, not branching fractions. They can be greater than one.

b -baryon ADMIXTURE DECAY MODES ($\Lambda_b, \Xi_b, \Sigma_b, \Omega_b$)	Fraction (Γ_i/Γ)	ρ (MeV/c)
$p \mu^- \bar{\nu}$ anything	$(5.8_{-2.4}^{+2.6})\%$	-
$p \ell \bar{\nu}_\ell$ anything	$(5.6 \pm 1.7)\%$	-

p anything	(69 \pm 27) %	—
$\Lambda \ell^- \bar{\nu}_\ell$ anything	(3.7 \pm 1.0) %	—
$\Lambda / \bar{\Lambda}$ anything	(39 \pm 11) %	—
$\Xi^- \ell^- \bar{\nu}_\ell$ anything	(6.5 \pm 2.2) $\times 10^{-3}$	—

NOTES

This Summary Table only includes established baryons. The Particle Listings include evidence for other baryons. The masses, widths, and branching fractions for the resonances in this Table are Breit-Wigner parameters, but pole positions are also given for most of the N and Δ resonances.

For most of the resonances, the parameters come from various partial-wave analyses of more or less the same sets of data, and it is not appropriate to treat the results of the analyses as independent or to average them together. Furthermore, the systematic errors on the results are not well understood. Thus, we usually only give ranges for the parameters. We then also give a best guess for the mass (as part of the name of the resonance) and for the width. The *Note on N and Δ Resonances* and the *Note on Λ and Σ Resonances* in the Particle Listings review the partial-wave analyses.

When a quantity has “(S = . . .)” to its right, the error on the quantity has been enlarged by the “scale factor” S, defined as $S = \sqrt{\chi^2/(N-1)}$, where N is the number of measurements used in calculating the quantity. We do this when $S > 1$, which often indicates that the measurements are inconsistent. When $S > 1.25$, we also show in the Particle Listings an ideogram of the measurements. For more about S, see the Introduction.

A decay momentum p is given for each decay mode. For a 2-body decay, p is the momentum of each decay product in the rest frame of the decaying particle. For a 3-or-more-body decay, p is the largest momentum any of the products can have in this frame. For any resonance, the *nominal* mass is used in calculating p . A dagger (“†”) in this column indicates that the mode is forbidden when the nominal masses of resonances are used, but is in fact allowed due to the nonzero widths of the resonances.

- [a] The masses of the p and n are most precisely known in u (unified atomic mass units). The conversion factor to MeV, $1 \text{ u} = 931.494028(23) \text{ MeV}$, is less well known than are the masses in u.
- [b] The $|m_p - m_{\bar{p}}|/m_p$ and $|q_p + q_{\bar{p}}|/e$ are not independent, and both use the more precise measurement of $|q_{\bar{p}}/m_{\bar{p}}|/(q_p/m_p)$.
- [c] The limit is from neutrality-of-matter experiments; it assumes $q_n = q_p + q_e$. See also the charge of the neutron.
- [d] The first limit is for $p \rightarrow$ anything or “disappearance” modes of a bound proton. The second entry, a rough range of limits, assumes the dominant decay modes are among those investigated. For antiprotons the best limit, inferred from the observation of cosmic ray \bar{p} 's is $\tau_{\bar{p}} > 10^7 \text{ yr}$, the cosmic-ray storage time, but this limit depends on a number of assumptions. The best direct observation of stored antiprotons gives $\tau_{\bar{p}}/B(\bar{p} \rightarrow e^- \gamma) > 7 \times 10^5 \text{ yr}$.
- [e] There is some controversy about whether nuclear physics and model dependence complicate the analysis for bound neutrons (from which the best limit comes). The first limit here is from reactor experiments with free neutrons.
- [f] Lee and Yang in 1956 proposed the existence of a mirror world in an attempt to restore global parity symmetry—thus a search for oscillations between the two worlds. Oscillations between the worlds would be maximal when the magnetic fields B and B' were equal. The limit for any B' in the range 0 to 12.5 μT is $>12 \text{ s}$ (95% CL).

[g] The parameters g_A , g_V , and g_{WM} for semileptonic modes are defined by $\bar{B}_f[\gamma_\lambda(g_V + g_A\gamma_5) + i(g_{WM}/m_{B_i})\sigma_{\lambda\nu}q^\nu]B_i$, and ϕ_{AV} is defined by $g_A/g_V = |g_A/g_V|e^{i\phi_{AV}}$. See the “Note on Baryon Decay Parameters” in the neutron Particle Listings in the Full *Review of Particle Physics*.

[h] Time-reversal invariance requires this to be 0° or 180° .

[i] This coefficient is zero if time invariance is not violated.

[j] This limit is for γ energies between 15 and 340 keV.

[k] The decay parameters γ and Δ are calculated from α and ϕ using

$$\gamma = \sqrt{1-\alpha^2} \cos\phi, \quad \tan\Delta = -\frac{1}{\alpha} \sqrt{1-\alpha^2} \sin\phi.$$

See the “Note on Baryon Decay Parameters” in the neutron Particle Listings in the Full *Review of Particle Physics*.

[l] See Particle Listings in the Full *Review of Particle Physics* for the pion momentum range used in this measurement.

[m] The error given here is only an educated guess. It is larger than the error on the weighted average of the published values.

[n] A theoretical value using QED.

[o] See the note on “ Λ_c^+ Branching Fractions” in the Λ_c^+ Particle Listings in the Full *Review of Particle Physics*.

[p] This branching fraction includes all the decay modes of the final-state resonance.

[q] An ℓ indicates an e or a μ mode, not a sum over these modes.

[r] The value is for the sum of the charge states or particle/antiparticle states indicated.

[s] Assuming isospin conservation, so that the other third is $\Lambda_c^+ \pi^0 \pi^0$.

[t] A test that the isospin is indeed 0, so that the particle is indeed a Λ_c^+ .

[u] No absolute branching fractions have been measured. The value here is the branching *ratio* relative to $\Xi^- 2\pi^+$.

[v] Not a pure measurement. See note at head of Λ_b^0 Decay Modes.

[w] Here h^- means π^- or K^- .

SEARCHES FOR MONOPOLES, SUPERSYMMETRY, TECHNICOLOR, COMPOSITENESS, EXTRA DIMENSIONS, etc.

Magnetic Monopole Searches

Isolated supermassive monopole candidate events have not been confirmed. The most sensitive experiments obtain negative results.

Best cosmic-ray supermassive monopole flux limit:

$$< 1.0 \times 10^{-15} \text{ cm}^{-2}\text{sr}^{-1}\text{s}^{-1} \quad \text{for } 1.1 \times 10^{-4} < \beta < 0.1$$

Supersymmetric Particle Searches

Limits are based on the Minimal Supersymmetric Standard Model.

Assumptions include: 1) $\tilde{\chi}_1^0$ (or $\tilde{\gamma}$) is lightest supersymmetric particle; 2) R -parity is conserved; 3) With the exception of \tilde{t} and \tilde{b} , all scalar quarks are assumed to be degenerate in mass and $m_{\tilde{q}_R} = m_{\tilde{q}_L}$. 4) Limits for sleptons refer to the $\tilde{\ell}_R$ states. 5) Gaugino mass unification at the GUT scale.

See the Particle Listings in the Full *Review of Particle Physics* for a Note giving details of supersymmetry.

$\tilde{\chi}_i^0$ — neutralinos (mixtures of $\tilde{\gamma}$, \tilde{Z}^0 , and \tilde{H}_i^0)

Mass $m_{\tilde{\chi}_1^0} > 46 \text{ GeV}$, CL = 95%

[all $\tan\beta$, all m_0 , all $m_{\tilde{\chi}_2^0} - m_{\tilde{\chi}_1^0}$]

Mass $m_{\tilde{\chi}_2^0} > 62.4 \text{ GeV}$, CL = 95%

[$1 < \tan\beta < 40$, all m_0 , all $m_{\tilde{\chi}_2^0} - m_{\tilde{\chi}_1^0}$]

Mass $m_{\tilde{\chi}_3^0} > 99.9 \text{ GeV}$, CL = 95%

[$1 < \tan\beta < 40$, all m_0 , all $m_{\tilde{\chi}_2^0} - m_{\tilde{\chi}_1^0}$]

Mass $m_{\tilde{\chi}_4^0} > 116 \text{ GeV}$, CL = 95%

[$1 < \tan\beta < 40$, all m_0 , all $m_{\tilde{\chi}_2^0} - m_{\tilde{\chi}_1^0}$]

$\tilde{\chi}_i^\pm$ — charginos (mixtures of \tilde{W}^\pm and \tilde{H}_i^\pm)

Mass $m_{\tilde{\chi}_1^\pm} > 94 \text{ GeV}$, CL = 95%

[$\tan\beta < 40$, $m_{\tilde{\chi}_1^\pm} - m_{\tilde{\chi}_1^0} > 3 \text{ GeV}$, all m_0]

\tilde{e} — scalar electron (selectron)

Mass $m > 107 \text{ GeV}$, CL = 95% [all $m_{\tilde{e}_R} - m_{\tilde{\chi}_1^0}$]

$\tilde{\mu}$ — scalar muon (smuon)

Mass $m > 94 \text{ GeV}$, CL = 95%

[$1 \leq \tan\beta \leq 40$, $m_{\tilde{\mu}_R} - m_{\tilde{\chi}_1^0} > 10 \text{ GeV}$]

$\tilde{\tau}$ — scalar tau (stau)

Mass $m > 81.9$ GeV, CL = 95%

$$[m_{\tilde{\tau}_R} - m_{\tilde{\chi}_1^0} > 15 \text{ GeV, all } \theta_\tau]$$

\tilde{q} — scalar quark (squark)

These limits include the effects of cascade decays, evaluated assuming a fixed value of the parameters μ and $\tan\beta$. The limits are weakly sensitive to these parameters over much of parameter space. Limits assume GUT relations between gaugino masses and the gauge coupling.

Mass $m > 379$ GeV, CL = 95% [$\tan\beta=3, \mu < 0, A=0, \text{ any } m_{\tilde{g}}$]

\tilde{b} — scalar bottom (sbottom)

Mass $m > 89$ GeV, CL = 95% [$m_{\tilde{b}_1} - m_{\tilde{\chi}_1^0} > 8 \text{ GeV, all } \theta_b$]

\tilde{t} — scalar top (stop)

Mass $m > 95.7$ GeV, CL = 95%

$$[\tilde{t} \rightarrow c\tilde{\chi}_1^0, \text{ all } \theta_t, m_{\tilde{t}} - m_{\tilde{\chi}_1^0} > 10 \text{ GeV}]$$

\tilde{g} — gluino

The limits summarised here refer to the high-mass region ($m_{\tilde{g}} \gtrsim 5$ GeV), and include the effects of cascade decays, evaluated assuming a fixed value of the parameters μ and $\tan\beta$. The limits are weakly sensitive to these parameters over much of parameter space. Limits assume GUT relations between gaugino masses and the gauge coupling,

Mass $m > 308$ GeV, CL = 95% [any $m_{\tilde{q}}$]

Mass $m > 392$ GeV, CL = 95% [$m_{\tilde{q}} = m_{\tilde{g}}$]

Technicolor

Searches for a color-octet techni- ρ constrain its mass to be greater than 260 to 480 GeV, depending on allowed decay channels. Similar bounds exist on the color-octet techni- ω .

**Quark and Lepton Compositeness,
Searches for**
**Scale Limits Λ for Contact Interactions
(the lowest dimensional interactions with four fermions)**

If the Lagrangian has the form

$$\pm \frac{g^2}{2\Lambda^2} \bar{\psi}_L \gamma_\mu \psi_L \bar{\psi}_L \gamma^\mu \psi_L$$

(with $g^2/4\pi$ set equal to 1), then we define $\Lambda \equiv \Lambda_{LL}^\pm$. For the full definitions and for other forms, see the Note in the Listings on Searches for Quark and Lepton Compositeness in the full *Review* and the original literature.

$\Lambda_{LL}^+(eeee)$	> 8.3 TeV, CL = 95%
$\Lambda_{LL}^-(eeee)$	> 10.3 TeV, CL = 95%
$\Lambda_{LL}^+(ee\mu\mu)$	> 8.5 TeV, CL = 95%
$\Lambda_{LL}^-(ee\mu\mu)$	> 9.5 TeV, CL = 95%
$\Lambda_{LL}^+(ee\tau\tau)$	> 7.9 TeV, CL = 95%
$\Lambda_{LL}^-(ee\tau\tau)$	> 7.2 TeV, CL = 95%
$\Lambda_{LL}^+(\ell\ell\ell\ell)$	> 9.1 TeV, CL = 95%
$\Lambda_{LL}^-(\ell\ell\ell\ell)$	> 10.3 TeV, CL = 95%
$\Lambda_{LL}^+(eeuu)$	> 23.3 TeV, CL = 95%
$\Lambda_{LL}^-(eeuu)$	> 12.5 TeV, CL = 95%
$\Lambda_{LL}^+(eedd)$	> 11.1 TeV, CL = 95%
$\Lambda_{LL}^-(eedd)$	> 26.4 TeV, CL = 95%
$\Lambda_{LL}^+(eccc)$	> 9.4 TeV, CL = 95%
$\Lambda_{LL}^-(eccc)$	> 5.6 TeV, CL = 95%
$\Lambda_{LL}^+(eebb)$	> 9.4 TeV, CL = 95%
$\Lambda_{LL}^-(eebb)$	> 4.9 TeV, CL = 95%
$\Lambda_{LL}^+(\mu\mu qq)$	> 2.9 TeV, CL = 95%
$\Lambda_{LL}^-(\mu\mu qq)$	> 4.2 TeV, CL = 95%
$\Lambda(\ell\nu\ell\nu)$	> 3.10 TeV, CL = 90%
$\Lambda(e\nu qq)$	> 2.81 TeV, CL = 95%
$\Lambda_{LL}^+(qqqq)$	> 2.7 TeV, CL = 95%
$\Lambda_{LL}^-(qqqq)$	> 2.4 TeV, CL = 95%
$\Lambda_{LL}^+(\nu\nu qq)$	> 5.0 TeV, CL = 95%
$\Lambda_{LL}^-(\nu\nu qq)$	> 5.4 TeV, CL = 95%

Excited Leptons

The limits from $\ell^{*\pm} \ell^{*\mp}$ do not depend on λ (where λ is the $\ell \ell^*$ transition coupling). The λ -dependent limits assume chiral coupling.

$e^{*\pm}$ — excited electron

Mass $m > 103.2$ GeV, CL = 95% (from $e^* e^*$)

Mass $m > 272$ GeV, CL = 95% (from $e e^*$)

Mass $m > 310$ GeV, CL = 95% (if $\lambda_\gamma = 1$)

$\mu^{*\pm}$ — excited muon

Mass $m > 103.2$ GeV, CL = 95% (from $\mu^* \mu^*$)

Mass $m > 221$ GeV, CL = 95% (from $\mu \mu^*$)

$\tau^{*\pm}$ — excited tau

Mass $m > 103.2$ GeV, CL = 95% (from $\tau^* \tau^*$)

Mass $m > 185$ GeV, CL = 95% (from $\tau \tau^*$)

ν^* — excited neutrino

Mass $m > 102.6$ GeV, CL = 95% (from $\nu^* \nu^*$)

Mass $m > 213$ GeV, CL = 95% (from $\nu \nu^*$)

q^* — excited quark

Mass $m > 45.6$ GeV, CL = 95% (from $q^* q^*$)

Mass m (from $q^* X$)

Color Sextet and Octet Particles

Color Sextet Quarks (q_6)

Mass $m > 84$ GeV, CL = 95% (Stable q_6)

Color Octet Charged Leptons (ℓ_8)

Mass $m > 86$ GeV, CL = 95% (Stable ℓ_8)

Color Octet Neutrinos (ν_8)

Mass $m > 110$ GeV, CL = 90% ($\nu_8 \rightarrow \nu g$)

Extra Dimensions

Please refer to the Extra Dimensions section of the full *Review* for a discussion of the model-dependence of these bounds, and further constraints.

Constraints on the fundamental gravity scale

$M_H > 1.1$ TeV, CL = 95% (dim-8 operators; $p\bar{p} \rightarrow e^+ e^-, \gamma\gamma$)

$M_D > 1.1$ TeV, CL = 95% ($e^+ e^- \rightarrow G\gamma$; 2-flat dimensions)

$M_D > 3\text{--}1000$ TeV (astrophys. and cosmology; 2-flat dimensions; limits depend on technique and assumptions)

Constraints on the radius of the extra dimensions, for the case of two-flat dimensions of equal radii

$r < 90\text{--}660$ nm (astrophysics; limits depend on technique and assumptions)

$r < 0.22$ mm, CL = 95% (direct tests of Newton's law; cited in Extra Dimensions review)

TESTS OF CONSERVATION LAWS

Updated May 2010 by L. Wolfenstein (Carnegie-Mellon University), T.G. Trippe (LBNL), and C.-J. Lin (LBNL).

In keeping with the current interest in tests of conservation laws, we collect together a Table of experimental limits on all weak and electromagnetic decays, mass differences, and moments, and on a few reactions, whose observation would violate conservation laws. The Table is given only in the full *Review of Particle Physics*, not in the Particle Physics Booklet. For the benefit of Booklet readers, we include the best limits from the Table in the following text. Limits in this text are for CL=90% unless otherwise specified. The Table is in two parts: “Discrete Space-Time Symmetries,” *i.e.*, C , P , T , CP , and CPT ; and “Number Conservation Laws,” *i.e.*, lepton, baryon, hadronic flavor, and charge conservation. The references for these data can be found in the the Particle Listings in the *Review*. A discussion of these tests follows.

CPT INVARIANCE

General principles of relativistic field theory require invariance under the combined transformation CPT . The simplest tests of CPT invariance are the equality of the masses and lifetimes of a particle and its antiparticle. The best test comes from the limit on the mass difference between K^0 and \bar{K}^0 . Any such difference contributes to the CP -violating parameter ϵ . Assuming CPT invariance, ϕ_ϵ , the phase of ϵ should be very close to 44° . (See the review “ CP Violation in K_L decay” in this edition.) In contrast, if the entire source of CP violation in K^0 decays were a $K^0 - \bar{K}^0$ mass difference, ϕ_ϵ would be $44^\circ + 90^\circ$.

Assuming that there is no other source of CPT violation than this mass difference, it is possible to deduce that[1]

$$m_{\bar{K}^0} - m_{K^0} \approx \frac{2(m_{K_L^0} - m_{K_S^0}) |\eta| (\frac{2}{3}\phi_{+-} + \frac{1}{3}\phi_{00} - \phi_{SW})}{\sin \phi_{SW}},$$

where $\phi_{SW} = (43.51 \pm 0.05)^\circ$, the superweak angle. Using our best values of the CP -violation parameters, we get $|(m_{\bar{K}^0} - m_{K^0})/m_{K^0}| \leq 0.8 \times 10^{-18}$ at CL=90%. Limits can also be placed on specific CPT -violating decay amplitudes. Given the small value of $(1 - |\eta_{00}/\eta_{+-}|)$, the value of $\phi_{00} - \phi_{+-}$ provides a measure of CPT violation in $K_L^0 \rightarrow 2\pi$ decay. Results from CERN [1] and Fermilab [2] indicate no CPT -violating effect.

CP AND T INVARIANCE

Given *CPT* invariance, *CP* violation and *T* violation are equivalent. The original evidence for *CP* violation came from the measurement of $|\eta_{+-}| = |A(K_L^0 \rightarrow \pi^+\pi^-)/A(K_S^0 \rightarrow \pi^+\pi^-)| = (2.232 \pm 0.011) \times 10^{-3}$. This could be explained in terms of $K^0-\bar{K}^0$ mixing, which also leads to the asymmetry $[\Gamma(K_L^0 \rightarrow \pi^-e^+\nu) - \Gamma(K_L^0 \rightarrow \pi^+e^-\bar{\nu})]/[\text{sum}] = (0.334 \pm 0.007)\%$. Evidence for *CP* violation in the kaon decay amplitude comes from the measurement of $(1 - |\eta_{00}/\eta_{+-}|)/3 = \text{Re}(\epsilon'/\epsilon) = (1.65 \pm 0.26) \times 10^{-3}$. In the Standard Model much larger *CP*-violating effects are expected. The first of these, which is associated with $B-\bar{B}$ mixing, is the parameter $\sin(2\beta)$ now measured quite accurately to be 0.671 ± 0.023 . A number of other *CP*-violating observables are being measured in *B* decays; direct evidence for *CP* violation in the *B* decay amplitude comes from the asymmetry $[\Gamma(\bar{B}^0 \rightarrow K^-\pi^+) - \Gamma(B^0 \rightarrow K^+\pi^-)]/[\text{sum}] = -0.098 \pm 0.013$. Direct tests of *T* violation are much more difficult; a measurement by CPLEAR of the difference between the oscillation probabilities of K^0 to \bar{K}^0 and \bar{K}^0 to K^0 is related to *T* violation [3]. Other searches for *CP* or *T* violation involve effects that are expected to be unobservable in the Standard Model. The most sensitive are probably the searches for an electric dipole moment of the neutron, measured to be $< 2.9 \times 10^{-26}$ e cm, and the electron $(0.07 \pm 0.07) \times 10^{-26}$ e cm. A nonzero value requires both *P* and *T* violation.

CONSERVATION OF LEPTON NUMBERS

Present experimental evidence and the standard electroweak theory are consistent with the absolute conservation of three separate lepton numbers: electron number L_e , muon number L_μ , and tau number L_τ , except for the effect of neutrino mixing associated with neutrino masses. Searches for violations are of the following types:

a) $\Delta L = 2$ for one type of charged lepton. The best limit comes from the search for neutrinoless double beta decay (Z, A) $\rightarrow (Z + 2, A) + e^- + e^-$. The best laboratory limit is $t_{1/2} > 1.9 \times 10^{25}$ yr (CL=90%) for ^{76}Ge .

b) Conversion of one charged-lepton type to another. For purely leptonic processes, the best limits are on $\mu \rightarrow e\gamma$ and $\mu \rightarrow 3e$, measured as $\Gamma(\mu \rightarrow e\gamma)/\Gamma(\mu \rightarrow \text{all}) < 1.2 \times 10^{-11}$ and $\Gamma(\mu \rightarrow 3e)/\Gamma(\mu \rightarrow \text{all}) < 1.0 \times 10^{-12}$. For semileptonic processes, the best limit comes from the coherent conversion process in a muonic atom, $\mu^- + (Z, A) \rightarrow e^- + (Z, A)$, measured as $\Gamma(\mu^- \text{Ti} \rightarrow e^- \text{Ti})/\Gamma(\mu^- \text{Ti} \rightarrow \text{all}) < 4.3 \times 10^{-12}$. Of special interest

is the case in which the hadronic flavor also changes, as in $K_L \rightarrow e\mu$ and $K^+ \rightarrow \pi^+e^-\mu^+$, measured as $\Gamma(K_L \rightarrow e\mu)/\Gamma(K_L \rightarrow \text{all}) < 4.7 \times 10^{-12}$ and $\Gamma(K^+ \rightarrow \pi^+e^-\mu^+)/\Gamma(K^+ \rightarrow \text{all}) < 1.3 \times 10^{-11}$. Limits on the conversion of τ into e or μ are found in τ decay and are much less stringent than those for $\mu \rightarrow e$ conversion, *e.g.*, $\Gamma(\tau \rightarrow \mu\gamma)/\Gamma(\tau \rightarrow \text{all}) < 4.4 \times 10^{-8}$ and $\Gamma(\tau \rightarrow e\gamma)/\Gamma(\tau \rightarrow \text{all}) < 3.3 \times 10^{-8}$.

c) Conversion of one type of charged lepton into another type of charged antilepton. The case most studied is $\mu^- + (Z, A) \rightarrow e^+ + (Z - 2, A)$, the strongest limit being $\Gamma(\mu^- \text{Ti} \rightarrow e^+ \text{Ca})/\Gamma(\mu^- \text{Ti} \rightarrow \text{all}) < 3.6 \times 10^{-11}$.

d) Neutrino oscillations. It is expected even in the standard electroweak theory that the lepton numbers are not separately conserved, as a consequence of lepton mixing analogous to Cabibbo-Kobayashi-Maskawa quark mixing. However, if the only source of lepton-number violation is the mixing of low-mass neutrinos then processes such as $\mu \rightarrow e\gamma$ are expected to have extremely small unobservable probabilities. For small neutrino masses, the lepton-number violation would be observed first in neutrino oscillations, which have been the subject of extensive experimental searches. Strong evidence for neutrino mixing has come from atmospheric and solar neutrinos. The SNO experiment has detected the total flux of neutrinos from the sun measured via neutral current interactions and found it greater than the flux of ν_e . This confirms previous indications of a deficit of ν_e . Furthermore, evidence for such oscillations for reactor $\bar{\nu}$ has been found by the KAMLAND detector. A global analysis combining all solar neutrino data (SNO, Borexino, Super-Kamiokande, Chlorine, Gallium) and the KamLAND data yields $\Delta(m^2) = (7.59 \pm 0.20) \times 10^{-5} \text{ eV}^2$ [4].

Underground detectors observing neutrinos produced by cosmic rays in the atmosphere have found a factor of 2 deficiency of upward going ν_μ compared to downward. This provides compelling evidence for ν_μ disappearance, for which the most probable explanation is $\nu_\mu \rightarrow \nu_\tau$ oscillations with nearly maximal mixing. This mixing space can also be explored by accelerator-based long-baseline experiments. The most recent result from MINOS gives $\Delta(m^2) = (2.43 \pm 0.13) \times 10^{-3} \text{ eV}^2$ [5].

CONSERVATION OF HADRONIC FLAVORS

In strong and electromagnetic interactions, hadronic flavor is conserved, *i.e.* the conversion of a quark of one flavor (d, u, s, c, b, t) into a quark of another flavor is forbidden. In the

Standard Model, the weak interactions violate these conservation laws in a manner described by the Cabibbo-Kobayashi-Maskawa mixing (see the section “CKM Mixing Matrix”). The way in which these conservation laws are violated is tested as follows:

(a) $\Delta S = \Delta Q$ rule. In the strangeness-changing semileptonic decay of strange particles, the strangeness change equals the change in charge of the hadrons. Tests come from limits on decay rates such as $\Gamma(\Sigma^+ \rightarrow ne^+\nu)/\Gamma(\Sigma^+ \rightarrow \text{all}) < 5 \times 10^{-6}$, and from a detailed analysis of $K_L \rightarrow \pi e \nu$, which yields the parameter x , measured to be $(\text{Re } x, \text{Im } x) = (-0.002 \pm 0.006, 0.0012 \pm 0.0021)$. Corresponding rules are $\Delta C = \Delta Q$ and $\Delta B = \Delta Q$.

(b) Change of flavor by two units. In the Standard Model this occurs only in second-order weak interactions. The classic example is $\Delta S = 2$ via $K^0 - \bar{K}^0$ mixing, which is directly measured by $m(K_L) - m(K_S) = (0.5292 \pm 0.0009) \times 10^{10} \hbar s^{-1}$. The $\Delta B = 2$ transitions in the B^0 and B_s^0 systems via mixing are also well established. The measured mass differences between the eigenstates are $(m_{B_H^0} - m_{B_L^0}) = (0.507 \pm 0.005) \times 10^{12} \hbar s^{-1}$ and $(m_{B_{sH}^0} - m_{B_{sL}^0}) = (17.77 \pm 0.12) \times 10^{12} \hbar s^{-1}$. There is now strong evidence of $\Delta C = 2$ transition in the charm sector with the mass difference $m_{D_H^0} - m_{D_L^0} = (2.39_{-0.63}^{+0.59}) \times 10^{10} \hbar s^{-1}$. All results are consistent with the second-order calculations in the Standard Model.

(c) Flavor-changing neutral currents. In the Standard Model the neutral-current interactions do not change flavor. The low rate $\Gamma(K_L \rightarrow \mu^+\mu^-)/\Gamma(K_L \rightarrow \text{all}) = (6.84 \pm 0.11) \times 10^{-9}$ puts limits on such interactions; the nonzero value for this rate is attributed to a combination of the weak and electromagnetic interactions. The best test should come from $K^+ \rightarrow \pi^+\nu\bar{\nu}$, which occurs in the Standard Model only as a second-order weak process with a branching fraction of $(0.4 \text{ to } 1.2) \times 10^{-10}$. Combining results from BNL-E787 and BNL-E949 experiments yield $\Gamma(K^+ \rightarrow \pi^+\nu\bar{\nu})/\Gamma(K^+ \rightarrow \text{all}) = (1.7 \pm 1.1) \times 10^{-10}$ [6]. Limits for charm-changing or bottom-changing neutral currents are much less stringent: $\Gamma(D^0 \rightarrow \mu^+\mu^-)/\Gamma(D^0 \rightarrow \text{all}) < 1.3 \times 10^{-6}$ and $\Gamma(B^0 \rightarrow \mu^+\mu^-)/\Gamma(B^0 \rightarrow \text{all}) < 1.5 \times 10^{-8}$. One cannot isolate flavor-changing neutral current (FCNC) effects in non leptonic decays. For example, the FCNC transition $s \rightarrow d + (\bar{u} + u)$ is equivalent to the charged-current transition $s \rightarrow u + (\bar{u} + d)$. Tests for FCNC are therefore limited to hadron decays into lepton pairs. Such decays are expected only in second-order in the electroweak coupling in the Standard Model.

See the full *Review of Particle Physics* for references and Summary Tables.

9. QUANTUM CHROMODYNAMICS

Written October 2009 by G. Dissertori (ETH, Zurich) and G.P. Salam (LPTHE, Paris).

9.1. Basics

Quantum Chromodynamics (QCD), the gauge field theory that describes the strong interactions of colored quarks and gluons, is the SU(3) component of the SU(3)×SU(2)×U(1) Standard Model of Particle Physics.

The Lagrangian of QCD is given by

$$\mathcal{L} = \sum_q \bar{\psi}_{q,a} (i\gamma^\mu \partial_\mu \delta_{ab} - g_s \gamma^\mu t_{ab}^C \mathcal{A}_\mu^C - m_q \delta_{ab}) \psi_{q,b} - \frac{1}{4} F_{\mu\nu}^A F^{A\mu\nu}, \quad (9.1)$$

where repeated indices are summed over. The γ^μ are the Dirac γ -matrices. The $\psi_{q,a}$ are quark-field spinors for a quark of flavor q and mass m_q , with a color-index a that runs from $a = 1$ to $N_c = 3$, *i.e.* quarks come in three “colors.” Quarks are said to be in the fundamental representation of the SU(3) color group.

The \mathcal{A}_μ^C correspond to the gluon fields, with C running from 1 to $N_c^2 - 1 = 8$, *i.e.* there are eight kinds of gluon. Gluons are said to be in the adjoint representation of the SU(3) color group. The t_{ab}^C correspond to eight 3×3 matrices and are the generators of the SU(3) group. They encode the fact that a gluon’s interaction with a quark rotates the quark’s color in SU(3) space. The quantity g_s is the QCD coupling constant. Finally, the field tensor $F_{\mu\nu}^A$ is given by

$$F_{\mu\nu}^A = \partial_\mu \mathcal{A}_\nu^A - \partial_\nu \mathcal{A}_\mu^A - g_s f_{ABC} \mathcal{A}_\mu^B \mathcal{A}_\nu^C \quad [t^A, t^B] = i f_{ABC} t^C, \quad (9.2)$$

where the f_{ABC} are the structure constants of the SU(3) group.

Neither quarks nor gluons are observed as free particles. Hadrons are color-singlet (*i.e.* color-neutral) combinations of quarks, anti-quarks, and gluons.

Ab-initio predictive methods for QCD include lattice gauge theory and perturbative expansions in the coupling. The Feynman rules of QCD involve a quark-antiquark-gluon ($q\bar{q}g$) vertex, a 3-gluon vertex (both proportional to g_s), and a 4-gluon vertex (proportional to g_s^2).

Useful color-algebra relations include: $t_{ab}^A t_{bc}^A = C_F \delta_{ac}$, where $C_F \equiv (N_c^2 - 1)/(2N_c) = 4/3$ is the color-factor (“Casimir”) associated with gluon emission from a quark; $f^{ACD} f^{BCD} = C_A \delta_{AB}$ where $C_A \equiv N_c = 3$ is the color-factor associated with gluon emission from a gluon; $t_{ab}^A t_{ab}^B = T_R \delta_{AB}$, where $T_R = 1/2$ is the color-factor for a gluon to split to a $q\bar{q}$ pair.

The fundamental parameters of QCD are the coupling g_s (or $\alpha_s = \frac{g_s^2}{4\pi}$) and the quark masses m_q .

9.1.1. Running coupling: In the framework of perturbative QCD (pQCD), predictions for observables are expressed in terms of the renormalized coupling $\alpha_s(\mu_R^2)$, a function of an (unphysical) renormalization scale μ_R . When one takes μ_R close to the scale of the momentum transfer Q in a given process, then $\alpha_s(\mu_R^2 \simeq Q^2)$ is indicative of the effective strength of the strong interaction in that process.

The coupling satisfies the following renormalization group equation (RGE):

$$\mu_R^2 \frac{d\alpha_s}{d\mu_R^2} = \beta(\alpha_s) = -(b_0\alpha_s^2 + b_1\alpha_s^3 + b_2\alpha_s^4 + \dots) \quad (9.3)$$

where $b_0 = (11C_A - 4n_f T_R)/(12\pi) = (33 - 2n_f)/(12\pi)$ is the 1-loop beta-function coefficient, and the 2, 3 and 4-loop coefficients are $b_1 = (17C_A^2 - n_f T_R(10C_A + 6C_F))/(24\pi^2) = (153 - 19n_f)/(24\pi^2)$, $b_2 = (2857 - \frac{5033}{9}n_f + \frac{325}{27}n_f^2)/(128\pi^3)$, and $b_3 = ((\frac{149753}{6} + 3564\zeta_3) - (\frac{1078361}{162} + \frac{6508}{27}\zeta_3)n_f + (\frac{50065}{162} + \frac{6472}{81}\zeta_3)n_f^2 + \frac{1093}{729}n_f^3)/(4\pi)^4$ [9,10], the last two specifically in the $\overline{\text{MS}}$ scheme (here $\zeta_3 \simeq 1.2020569$). The minus sign in Eq. (9.3) is the origin of asymptotic freedom, *i.e.* the fact that the strong coupling becomes weak for processes involving large momentum transfers (“hard processes”), $\alpha_s \sim 0.1$ for momentum transfers in the 100 GeV–TeV range.

The β -function coefficients, the b_i , are given for the coupling of an *effective theory* in which n_f of the quark flavors are considered light ($m_q \ll \mu_R$), and in which the remaining heavier quark flavors decouple from the theory. One may relate the coupling for the theory with $n_f + 1$ light flavors to that with n_f flavors through an equation of the form

$$\alpha_s^{(n_f+1)}(\mu_R^2) = \alpha_s^{(n_f)}(\mu_R^2) \left(1 + \sum_{n=1}^{\infty} \sum_{\ell=0}^n c_{n\ell} [\alpha_s^{(n_f)}(\mu_R^2)]^n \ln^\ell \frac{\mu_R^2}{m_h^2} \right), \quad (9.4)$$

where m_h is the mass of the $(n_f + 1)^{\text{th}}$ flavor, and the first few $c_{n\ell}$ coefficients are $c_{11} = \frac{1}{6\pi}$, $c_{10} = 0$, $c_{22} = c_{11}^2$, $c_{21} = \frac{19}{24\pi^2}$, and $c_{20} = -\frac{11}{72\pi^2}$ when m_h is the $\overline{\text{MS}}$ mass at scale m_h ($c_{20} = \frac{7}{24\pi^2}$ when m_h is the pole mass — see the review on “Quark Masses”). Terms up to $c_{4\ell}$ are to be found in Refs. 11, 12. Numerically, when one chooses $\mu_R = m_h$, the matching is a small effect, owing to the zero value for the c_{10} coefficient.

Working in an energy range where the number of flavors is constant, a simple exact analytic solution exists for Eq. (9.3) only if one neglects all but the b_0 term, giving $\alpha_s(\mu_R^2) = (b_0 \ln(\mu_R^2/\Lambda^2))^{-1}$. Here Λ is a constant of integration, which corresponds to the scale where the perturbatively-defined coupling would diverge, *i.e.* it is the non-perturbative scale of QCD. A convenient approximate analytic solution to the RGE that includes also the b_1 , b_2 , and b_3 terms is given by (*e.g.* Ref. 13),

$$\alpha_s(\mu_R^2) \simeq \frac{1}{b_0 t} \left(1 - \frac{b_1}{b_0^2} \frac{\ln t}{t} + \frac{b_1^2(\ln^2 t - \ln t - 1) + b_0 b_2}{b_0^4 t^2} - \frac{b_1^3(\ln^3 t - \frac{5}{2}\ln^2 t - 2\ln t + \frac{1}{2}) + 3b_0 b_1 b_2 \ln t - \frac{1}{2}b_0^2 b_3}{b_0^6 t^3} \right), \quad t \equiv \ln \frac{\mu_R^2}{\Lambda^2}, \quad (9.5)$$

again parametrized in terms of a constant Λ . Note that Eq. (9.5) is one of several possible approximate 4-loop solutions for $\alpha_s(\mu_R^2)$, and that a value for Λ only defines $\alpha_s(\mu_R^2)$ once one knows which particular approximation is being used. An alternative to the use of formulas such as Eq. (9.5) is to solve the RGE exactly, numerically (including the discontinuities, Eq. (9.4), at flavor thresholds). In such cases the quantity Λ is not defined

at all. For these reasons, in determinations of the coupling, it has become standard practice to quote the value of α_s at a given scale (typically M_Z) rather than to quote a value for Λ .

The value of the coupling, as well as the exact forms of the b_2 , c_{10} (and higher order) coefficients, depend on the renormalization scheme in which the coupling is defined, *i.e.* the convention used to subtract infinities in the context of renormalization. The coefficients given above hold for a coupling defined in the modified minimal subtraction ($\overline{\text{MS}}$) scheme [14], by far the most widely used scheme.

9.3.4. Measurements of the strong coupling constant : For this review it was decided to quote a recent analysis by Bethke [172], which incorporates results with recently improved theoretical predictions and/or experimental precision. The central value is determined as the weighted average of the individual measurements. For the error an overall, a-priori unknown, correlation coefficient is introduced and determined by requiring that the total χ^2 of the combination equals the number of degrees of freedom. The world average quoted in Ref. 172 is

$$\alpha_s(M_Z^2) = 0.1184 \pm 0.0007 .$$

It is worth noting that a cross check performed in Ref. 172, consisting in excluding each of the single measurements from the combination, resulted in variations of the central value well below the quoted uncertainty, and in a maximal increase of the combined error up to 0.0012. Most notably, excluding the most precise determination from lattice QCD gives only a marginally different average value. Nevertheless, there remains an apparent and long-standing systematic difference between the results from structure functions and other determinations of similar accuracy. This is evidenced in Fig. 9.2 (left), where the various inputs to this combination, evolved to the Z mass scale, are shown. Fig. 9.2 (right) provides strongest evidence for the correct prediction by QCD of the scale dependence of the strong coupling.

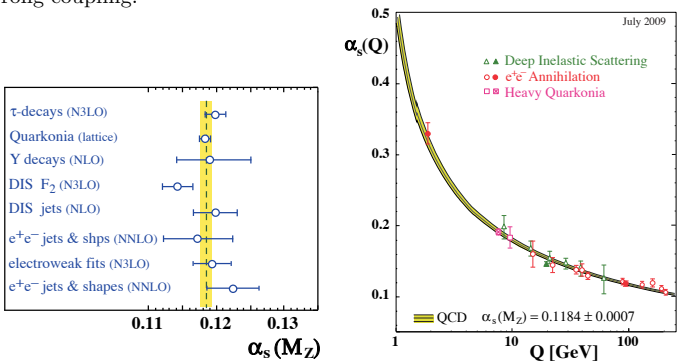


Figure 9.1: Left: Summary of measurements of $\alpha_s(M_Z^2)$, used as input for the world average value; Right: Summary of measurements of α_s as a function of the respective energy scale Q . Both plots are taken from Ref. 172.

10. ELECTROWEAK MODEL AND CONSTRAINTS ON NEW PHYSICS

Revised November 2009 by J. Erler (U. Mexico) and P. Langacker (Institute for Advanced Study).

10.1. Introduction

The standard electroweak model (SM) is based on the gauge group [1] $SU(2) \times U(1)$, with gauge bosons W_μ^i , $i = 1, 2, 3$, and B_μ for the $SU(2)$ and $U(1)$ factors, respectively, and the corresponding gauge coupling constants g and g' . The left-handed fermion fields of the i^{th} fermion family transform as doublets $\Psi_i = \begin{pmatrix} \nu_i \\ \ell_i^- \end{pmatrix}$ and $\begin{pmatrix} u_i \\ d_i \end{pmatrix}$ under $SU(2)$, where $d_i' \equiv \sum_j V_{ij} d_j$, and V is the Cabibbo-Kobayashi-Maskawa mixing matrix. (Constraints on V and tests of universality are discussed in Ref. 2 and in the Section on "The CKM Quark-Mixing Matrix". The extension of the formalism to allow an analogous leptonic mixing matrix is discussed in the Section on "Neutrino Mass, Mixing, and Flavor Change".) The right-handed fields are $SU(2)$ singlets. In the minimal model there are three fermion families and a single complex Higgs doublet $\phi \equiv \begin{pmatrix} \phi^+ \\ \phi^0 \end{pmatrix}$ which is introduced for mass generation.

After spontaneous symmetry breaking the Lagrangian for the fermion fields, ψ_i , is

$$\begin{aligned} \mathcal{L}_F = & \sum_i \bar{\psi}_i \left(i \not{\partial} - m_i - \frac{gm_i H}{2M_W} \right) \psi_i \\ & - \frac{g}{2\sqrt{2}} \sum_i \bar{\Psi}_i \gamma^\mu (1 - \gamma^5) (T^+ W_\mu^+ + T^- W_\mu^-) \Psi_i \\ & - e \sum_i q_i \bar{\psi}_i \gamma^\mu \psi_i A_\mu \\ & - \frac{g}{2 \cos \theta_W} \sum_i \bar{\psi}_i \gamma^\mu (g_V^i - g_A^i \gamma^5) \psi_i Z_\mu. \end{aligned} \quad (10.1)$$

$\theta_W \equiv \tan^{-1}(g'/g)$ is the weak angle; $e = g \sin \theta_W$ is the positron electric charge; and $A \equiv B \cos \theta_W + W^3 \sin \theta_W$ is the (massless) photon field. $W^\pm \equiv (W^1 \mp iW^2)/\sqrt{2}$ and $Z \equiv -B \sin \theta_W + W^3 \cos \theta_W$ are the massive charged and neutral weak boson fields, respectively. T^+ and T^- are the weak isospin raising and lowering operators. The vector and axial-vector couplings are

$$g_V^i \equiv t_{3L}(i) - 2q_i \sin^2 \theta_W, \quad (10.2a)$$

$$g_A^i \equiv t_{3L}(i), \quad (10.2b)$$

where $t_{3L}(i)$ is the weak isospin of fermion i ($+1/2$ for u_i and ν_i ; $-1/2$ for d_i and e_i) and q_i is the charge of ψ_i in units of e .

The second term in \mathcal{L}_F represents the charged-current weak interaction [3,4]. For example, the coupling of a W to an electron and a neutrino is

$$-\frac{e}{2\sqrt{2} \sin \theta_W} \left[W_\mu^- \bar{\nu} \gamma^\mu (1 - \gamma^5) \nu + W_\mu^+ \bar{\nu} \gamma^\mu (1 - \gamma^5) e \right]. \quad (10.3)$$

For momenta small compared to M_W , this term gives rise to the effective four-fermion interaction with the Fermi constant given (at tree level, *i.e.*, lowest order in perturbation theory) by $G_F/\sqrt{2} = g^2/8M_W^2$. CP violation is incorporated in the SM by a single observable phase in V_{ij} . The third term in \mathcal{L}_F describes electromagnetic interactions (QED), and the last is the weak neutral-current interaction.

In Eq. (10.1), m_i is the mass of the i^{th} fermion ψ_i . In the presence of right-handed neutrinos, Eq. (10.1) gives rise also to Dirac neutrino masses. The possibility of Majorana masses is discussed in the Section on “Neutrino Mass, Mixing, and Flavor Change”.

H is the physical neutral Higgs scalar which is the only remaining part of ϕ after spontaneous symmetry breaking. The Yukawa coupling of H to ψ_i , which is flavor diagonal in the minimal model, is $gm_i/2M_W$. In non-minimal models there are additional charged and neutral scalar Higgs particles [10].

10.2. Renormalization and radiative corrections

The SM has three parameters (not counting the Higgs boson mass, M_H , and the fermion masses and mixings). A particularly useful set contains the Z -boson mass, $M_Z = 91.1876 \pm 0.0021$ GeV, which has been determined from the Z lineshape scan at LEP 1; the fine structure constant, $\alpha = 1/137.035999084(51)$, which is currently best determined from the e^\pm anomalous magnetic moment; and the Fermi constant, $G_F = 1.166364(5) \times 10^{-5}$ GeV $^{-2}$, which is derived from the muon lifetime formula. See the full *Review* for more details.

With these inputs, $\sin^2\theta_W$ and the W boson mass, M_W , can be calculated when values for m_t and M_H are given; conversely (as is done at present), M_H can be constrained by $\sin^2\theta_W$ and M_W . The value of $\sin^2\theta_W$ is extracted from Z pole observables and neutral-current processes [11,60], and depends on the renormalization prescription. There are a number of popular schemes [61–68] leading to values which differ by small factors depending on m_t and M_H , including the $\overline{\text{MS}}$ definition \widehat{s}_Z^2 and the on-shell definition $s_W^2 \equiv 1 - M_W^2/M_Z^2$.

Experiments are at such level of precision that complete $\mathcal{O}(\alpha)$ radiative corrections must be applied. These are discussed in the full edition of this *Review*. A variety of related cross-section and asymmetry formulae are also discussed there.

10.3.1. W and Z decays :

The partial decay width for gauge bosons to decay into massless fermions $f_1\bar{f}_2$ (the numerical values include the small electroweak radiative corrections and final state mass effects) is

$$\Gamma(W^+ \rightarrow e^+\nu_e) = \frac{G_F M_W^3}{6\sqrt{2}\pi} \approx 226.31 \pm 0.07 \text{ MeV} , \quad (10.33a)$$

$$\Gamma(W^+ \rightarrow u_i\bar{d}_j) = \frac{CG_F M_W^3}{6\sqrt{2}\pi} |V_{ij}|^2 \approx 706.18 \pm 0.22 \text{ MeV} |V_{ij}|^2 (10.33b)$$

$$\Gamma(Z \rightarrow \psi_i\bar{\psi}_i) = \frac{CG_F M_Z^3}{6\sqrt{2}\pi} [g_V^{i2} + g_A^{i2}]$$

$$\approx \begin{cases} 167.21 \pm 0.02 \text{ MeV } (\nu\bar{\nu}), \\ 83.99 \pm 0.01 \text{ MeV } (e^+e^-), \\ 300.20 \pm 0.06 \text{ MeV } (u\bar{u}), \\ 382.98 \pm 0.06 \text{ MeV } (d\bar{d}), \\ 375.94 \mp 0.04 \text{ MeV } (b\bar{b}). \end{cases} \quad (10.33c)$$

For leptons $C = 1$, while for quarks

$$C = 3 \left[1 + \frac{\alpha_s(M_V)}{\pi} + 1.409 \frac{\alpha_s^2}{\pi^2} - 12.77 \frac{\alpha_s^3}{\pi^3} - 80.0 \frac{\alpha_s^4}{\pi^4} \right], \quad (10.34)$$

where the 3 is due to color and the factor in brackets represents the universal part of the QCD corrections [164] for massless quarks [165]. The $\mathcal{O}(\alpha_s^4)$ contribution in Eq. (10.34) is new [166]. The $Z \rightarrow f\bar{f}$ widths contain a number of additional corrections: universal (non-singlet) top quark mass contributions [167]; fermion mass effects and further QCD corrections proportional to $\hat{m}_q^2(M_Z^2)$ [168] which are different for vector and axial-vector partial widths; and singlet contributions starting from two-loop order which are large, strongly top quark mass dependent, family universal, and flavor non-universal [169]. The QED factor $1 + 3\alpha q_f^2/4\pi$, as well as two-loop order $\alpha\alpha_s$ and α^2 self-energy corrections [170] are also included. Working in the on-shell scheme, *i.e.*, expressing the widths in terms of $G_F M_{W,Z}^3$, incorporates the largest radiative corrections from the running QED coupling [61,171]. Electroweak corrections to the Z widths are then incorporated by replacing $g_{V,A}^2$ by the effective couplings $\bar{g}_{V,A}^2$ defined in Eq. (10.31) of the full *Review*. Hence, in the on-shell scheme the Z widths are proportional to $1 + \rho_t$, where $\rho_t = 3G_F m_t^2/8\sqrt{2}\pi^2$. The $\overline{\text{MS}}$ normalization accounts also for the leading electroweak corrections [66]. There is additional (negative) quadratic m_t dependence in the $Z \rightarrow b\bar{b}$ vertex corrections [172] which causes $\Gamma(b\bar{b})$ to decrease with m_t . The dominant effect is to multiply $\Gamma(b\bar{b})$ by the vertex correction $1 + \delta\rho_{b\bar{b}}$, where $\delta\rho_{b\bar{b}} \sim 10^{-2}(-\frac{1}{2}\frac{m_t^2}{M_Z^2} + \frac{1}{5})$. In practice, the corrections are included in $\bar{g}_{V,A}^b$, as discussed before.

For 3 fermion families the total widths are predicted to be

$$\Gamma_Z \approx 2.4957 \pm 0.0003 \text{ GeV}, \quad \Gamma_W \approx 2.0910 \pm 0.0007 \text{ GeV}. \quad (10.35)$$

We have assumed $\alpha_s(M_Z) = 0.1200$. An uncertainty in α_s of ± 0.0016 introduces an additional uncertainty of 0.05% in the hadronic widths, corresponding to ± 0.8 MeV in Γ_Z . These predictions are to be compared with the experimental results $\Gamma_Z = 2.4952 \pm 0.0023$ GeV [11] and $\Gamma_W = 2.085 \pm 0.042$ GeV [173] (see the Gauge & Higgs Boson Particle Listings for more details).

10.4. Precision flavor physics

In addition to cross-sections, asymmetries, parity violation, W and Z decays, there is a large number of experiments and observables testing the flavor structure of the SM. These are addressed elsewhere in this *Review*, and generally not included in this Section. However, we identify three precision observables with sensitivity to similar types of new physics as the other processes discussed here. The branching fraction of the flavor changing transition $b \rightarrow s\gamma$ is of comparatively low precision, but since

it is a loop-level process (in the SM) its sensitivity to new physics (and SM parameters, such as heavy quark masses) is enhanced. The τ -lepton lifetime and leptonic branching ratios are primarily sensitive to α_s and not affected significantly by many types of new physics. However, having an independent and reliable low energy measurement of α_s in a global analysis allows the comparison with the Z lineshape determination of α_s which shifts easily in the presence of new physics contributions. By far the most precise observable discussed here is the anomalous magnetic moment of the muon (the electron magnetic moment is measured to even greater precision, but its new physics sensitivity is suppressed by an additional factor of m_e^2/m_μ^2). Its combined experimental and theoretical uncertainty is comparable to typical new physics contributions. See the full *Review* for more details.

10.5. Experimental results

The values for m_t [6], M_W [160,207], neutrino scattering [98,114–116], the weak charges of the electron [125], cesium [132,133] and thallium [134], the $b \rightarrow s\gamma$ observable [174–175], the muon anomalous magnetic moment [189], and the τ lifetime are listed in Table 10.5. Likewise, the principal Z pole observables can be found in Table 10.6 where the LEP 1 averages of the ALEPH, DELPHI, L3, and OPAL results include common systematic errors and correlations [11]. The heavy flavor results of LEP 1 and SLD are based on common inputs and correlated, as well [11]. Note that the values of $\Gamma(\ell^+\ell^-)$, $\Gamma(\text{had})$, and $\Gamma(\text{inv})$ are not independent of Γ_Z , the R_ℓ , and σ_{had} and that the SM errors in those latter are largely dominated by the uncertainty in α_s . Also shown in both Tables are the SM predictions for the values of M_Z , M_H , $\alpha_s(M_Z)$, $\Delta\alpha_{\text{had}}^{(3)}$ and the heavy quark masses shown in Table 10.4 in the full *Review*. The predictions result from a global least-square (χ^2) fit to all data using the minimization package MINUIT [208] and the electroweak library GAPP [90]. In most cases, we treat all input errors (the uncertainties of the values) as Gaussian. The reason is not that we assume that theoretical and systematic errors are intrinsically bell-shaped (which they are not) but because in most cases the input errors are combinations of many different (including statistical) error sources, which should yield approximately Gaussian *combined* errors by the large number theorem. Thus, it suffices if either the statistical components dominate or there are many components of similar size. An exception is the theory dominated error on the τ lifetime, which we recalculate in each χ^2 -function call since it depends itself on α_s . Sizes and shapes of the output errors (the uncertainties of the predictions and the SM fit parameters) are fully determined by the fit, and 1σ errors are defined to correspond to $\Delta\chi^2 = \chi^2 - \chi_{\text{min}}^2 = 1$, and do not necessarily correspond to the 68.3% probability range or the 39.3% probability contour (for 2 parameters).

The agreement is generally very good. Despite the few discrepancies discussed in the following, the fit describes well the data with a $\chi^2/\text{d.o.f.} = 43.0/44$. Only the final result for $g_\mu - 2$ from BNL and $A_{FB}^{(0,b)}$ from LEP 1 are currently showing large (2.5σ and 2.7σ) deviations. In addition, A_{LR}^0 (SLD) from hadronic final states differs by 1.8σ . The SM prediction of σ_{had} (LEP 1) moved closer to the measurement value which is slightly higher. R_b , whose measured value deviated in the past by as much as 3.7σ from the SM prediction, is now in agreement, and a 2σ discrepancy in $Q_W(\text{Cs})$ has also been resolved. g_L^2 from NuTeV is

Table 10.3: Principal non- Z pole observables, compared with the SM best fit predictions. The first M_W value is from the Tevatron [207] and the second one from LEP 2 [160]. The values of M_W and m_t differ from those in the Particle Listings when they include recent preliminary results. g_L^2 , which has been adjusted as discussed in Sec. 10.3, and g_R^2 are from NuTeV [98] and have a very small (-1.7%) residual anti-correlation. e -DIS [123] and the older ν -DIS constraints from CDHS [92], CHARM [93], and CCFR [94] are included, as well, but not shown in the Table. The world averages for $g_{V,A}^{\nu e}$ are dominated by the CHARM II [116] results, $g_V^{\nu e} = -0.035 \pm 0.017$ and $g_A^{\nu e} = -0.503 \pm 0.017$. The errors are the total (experimental plus theoretical) uncertainties. The τ_τ value is the τ lifetime world average computed by combining the direct measurements with values derived from the leptonic branching ratios [5]; in this case, the theory uncertainty is included in the SM prediction. In all other SM predictions, the uncertainty is from M_Z , M_H , m_t , m_b , m_c , $\hat{\alpha}(M_Z)$, and α_s , and their correlations have been accounted for. The column denoted Pull gives the standard deviations for the principal fit with M_H free, while the column denoted Dev. (Deviation) is for $M_H = 117$ GeV fixed.

Quantity	Value	Standard Model	Pull	Dev.
m_t [GeV]	173.1 ± 1.3	173.2 ± 1.3	-0.1	-0.5
M_W [GeV]	80.420 ± 0.031	80.384 ± 0.014	1.2	1.5
	80.376 ± 0.033		-0.2	0.1
g_L^2	0.3027 ± 0.0018	0.30399 ± 0.00017	-0.7	-0.6
g_R^2	0.0308 ± 0.0011	0.03001 ± 0.00002	0.7	0.7
$g_V^{\nu e}$	-0.040 ± 0.015	-0.0398 ± 0.0003	0.0	0.0
$g_A^{\nu e}$	-0.507 ± 0.014	-0.5064 ± 0.0001	0.0	0.0
$Q_W(e)$	-0.0403 ± 0.0053	-0.0473 ± 0.0005	1.3	1.2
$Q_W(\text{Cs})$	-73.20 ± 0.35	-73.15 ± 0.02	-0.1	-0.1
$Q_W(\text{Tl})$	-116.4 ± 3.6	-116.76 ± 0.04	0.1	0.1
τ_τ [fs]	291.09 ± 0.48	290.02 ± 2.09	0.5	0.5
$\frac{\Gamma(b \rightarrow s\gamma)}{\Gamma(b \rightarrow Xev)}$	$(3.38^{+0.51}_{-0.44}) \times 10^{-3}$	$(3.11 \pm 0.07) \times 10^{-3}$	0.6	0.6
$\frac{1}{2}(g_\mu - 2 - \frac{\alpha}{\pi})$	$(4511.07 \pm 0.77) \times 10^{-9}$	$(4509.13 \pm 0.08) \times 10^{-9}$	2.5	2.5

currently in agreement with the SM but this statement is preliminary (see Sec. 10.3).

A_b can be extracted from $A_{FB}^{(0,b)}$ when $A_e = 0.1501 \pm 0.0016$ is taken from a fit to leptonic asymmetries (using lepton universality). The result, $A_b = 0.881 \pm 0.017$, is 3.2σ below the SM prediction[†] and also 1.6σ below $A_b = 0.923 \pm 0.020$ obtained from $A_{LR}^{FB}(b)$ at SLD. Thus, it appears that

[†] Alternatively, one can use $A_\ell = 0.1481 \pm 0.0027$, which is from LEP 1 alone and in excellent agreement with the SM, and obtain $A_b = 0.893 \pm 0.022$ which is 1.9σ low. This illustrates that some of the discrepancy is related to the one in A_{LR} .

Table 10.4: Principal Z pole observables and their SM predictions (cf. Table 10.3). The first $\bar{s}_\ell^2(A_{FB}^{(0,q)})$ is the effective angle extracted from the hadronic charge asymmetry while the second is the combined lepton asymmetry from CDF [157] and DØ [158]. The three values of A_e are (i) from A_{LR} for hadronic final states [152]; (ii) from A_{LR} for leptonic final states and from polarized Bhabba scattering [154]; and (iii) from the angular distribution of the τ polarization at LEP 1. The two A_τ values are from SLD and the total τ polarization, respectively.

Quantity	Value	Standard Model	Pull	Dev.
M_Z [GeV]	91.1876 ± 0.0021	91.1874 ± 0.0021	0.1	0.0
Γ_Z [GeV]	2.4952 ± 0.0023	2.4954 ± 0.0009	-0.1	0.1
$\Gamma(\text{had})$ [GeV]	1.7444 ± 0.0020	1.7418 ± 0.0009	—	—
$\Gamma(\text{inv})$ [MeV]	499.0 ± 1.5	501.69 ± 0.07	—	—
$\Gamma(\ell^+\ell^-)$ [MeV]	83.984 ± 0.086	84.005 ± 0.015	—	—
σ_{had} [nb]	41.541 ± 0.037	41.484 ± 0.008	1.5	1.5
R_e	20.804 ± 0.050	20.735 ± 0.010	1.4	1.4
R_μ	20.785 ± 0.033	20.735 ± 0.010	1.5	1.6
R_τ	20.764 ± 0.045	20.780 ± 0.010	-0.4	-0.3
R_b	0.21629 ± 0.00066	0.21578 ± 0.00005	0.8	0.8
R_c	0.1721 ± 0.0030	0.17224 ± 0.00003	0.0	0.0
$A_{FB}^{(0,e)}$	0.0145 ± 0.0025	0.01633 ± 0.00021	-0.7	-0.7
$A_{FB}^{(0,\mu)}$	0.0169 ± 0.0013		0.4	0.6
$A_{FB}^{(0,\tau)}$	0.0188 ± 0.0017		1.5	1.6
$A_{FB}^{(0,b)}$	0.0992 ± 0.0016	0.1034 ± 0.0007	-2.7	-2.3
$A_{FB}^{(0,c)}$	0.0707 ± 0.0035	0.0739 ± 0.0005	-0.9	-0.8
$A_{FB}^{(0,s)}$	0.0976 ± 0.0114	0.1035 ± 0.0007	-0.6	-0.4
$\bar{s}_\ell^2(A_{FB}^{(0,q)})$	0.2324 ± 0.0012	0.23146 ± 0.00012	0.8	0.7
	0.2316 ± 0.0018		0.1	0.0
A_e	0.15138 ± 0.00216	0.1475 ± 0.0010	1.8	2.2
	0.1544 ± 0.0060		1.1	1.3
	0.1498 ± 0.0049		0.5	0.6
A_μ	0.142 ± 0.015		-0.4	-0.3
A_τ	0.136 ± 0.015		-0.8	-0.7
	0.1439 ± 0.0043		-0.8	-0.7
A_b	0.923 ± 0.020	0.9348 ± 0.0001	-0.6	-0.6
A_c	0.670 ± 0.027	0.6680 ± 0.0004	0.1	0.1
A_s	0.895 ± 0.091	0.9357 ± 0.0001	-0.4	-0.4

at least some of the problem in $A_{FB}^{(0,b)}$ is experimental. Note, however, that the uncertainty in $A_{FB}^{(0,b)}$ is strongly statistics dominated. The combined value, $A_b = 0.899 \pm 0.013$ deviates by 2.8σ . It would be difficult to account for this 4.0% deviation by new physics that enters only at the level of radiative corrections since about a 20% correction to $\hat{\kappa}_b$ would be necessary to account for the central value of A_b [211]. If this deviation is due to new physics, it is most likely of tree-level type affecting preferentially the third generation. Examples include the decay of a scalar neutrino resonance [209], mixing of the b quark with heavy exotics [210], and

a heavy Z' with family-nonuniversal couplings [212,213]. It is difficult, however, to simultaneously account for R_b , which has been measured on the Z peak and off-peak [214] at LEP 1. An average of R_b measurements at LEP 2 at energies between 133 and 207 GeV is 2.1σ below the SM prediction, while $A_{FB}^{(b)}$ (LEP 2) is 1.6σ low [160].

The left-right asymmetry, $A_{LR}^0 = 0.15138 \pm 0.00216$ [152], based on all hadronic data from 1992–1998 differs 1.8σ from the SM expectation of 0.1475 ± 0.0010 . The combined value of $A_\ell = 0.1513 \pm 0.0021$ from SLD (using lepton-family universality and including correlations) is also 1.8σ above the SM prediction; but there is now experimental agreement between this SLD value and the LEP 1 value, $A_\ell = 0.1481 \pm 0.0027$, obtained from a fit to $A_{FB}^{(0,\ell)}$, $A_e(\mathcal{P}_\tau)$, and $A_\tau(\mathcal{P}_\tau)$, again assuming universality.

The observables in Table 10.3 and Table 10.4, as well as some other less precise observables, are used in the global fits described below. In all fits, the errors include full statistical, systematic, and theoretical uncertainties. The correlations on the LEP 1 lineshape and τ polarization, the LEP/SLD heavy flavor observables, the SLD lepton asymmetries, and the deep inelastic and ν - e scattering observables, are included. The theoretical correlations between $\Delta\alpha_{\text{had}}^{(5)}$ and $g_\mu - 2$, and between the charm and bottom quark masses, are also accounted for.

The data allow a simultaneous determination of M_Z , M_H , m_t , and the strong coupling $\alpha_s(M_Z)$. (\widehat{m}_c , \widehat{m}_b , and $\Delta\alpha_{\text{had}}^{(3)}$ are also allowed to float in the fits, subject to the theoretical constraints [5,17] described in Sec. 10.1–Sec. 10.2. These are correlated with α_s .) α_s is determined mainly from R_ℓ , Γ_Z , σ_{had} , and τ_τ and is only weakly correlated with the other variables. The global fit to all data, including the CDF/DØ average $m_t = 173.1 \pm 1.3$ GeV, yields the result in Table 10.4 (the $\overline{\text{MS}}$ top quark mass given there corresponds to $m_t = 173.2 \pm 1.3$ GeV). The weak mixing angle is determined to

$$\widehat{s}_Z^2 = 0.23116 \pm 0.00013, \quad s_W^2 = 0.22292 \pm 0.00028,$$

where the larger error in the on-shell scheme is due to the stronger sensitivity to m_t , while the corresponding effective angle is related by Eq. (10.32), *i.e.*, $\widehat{s}_\ell^2 = 0.23146 \pm 0.00012$.

The weak mixing angle can be determined from Z pole observables, M_W , and from a variety of neutral-current processes spanning a very wide Q^2 range. The results (for the older low energy neutral-current data see Refs. 58 and 59) shown in Table 10.7 of the full *Review* are in reasonable agreement with each other, indicating the quantitative success of the SM. The largest discrepancy is the value $\widehat{s}_Z^2 = 0.23193 \pm 0.00028$ from the forward-backward asymmetries into bottom and charm quarks, which is 2.7σ above the value 0.23116 ± 0.00013 from the global fit to all data. Similarly, $\widehat{s}_Z^2 = 0.23067 \pm 0.00029$ from the SLD asymmetries (in both cases when combined with M_Z) is 1.7σ low. The SLD result has the additional difficulty (within the SM) of implying very low and excluded [161] Higgs masses. This is also true for $\widehat{s}_Z^2 = 0.23100 \pm 0.00023$ from M_W and M_Z and — as a consequence — for the global fit. We have therefore included in Table 10.3 and Table 10.4 an additional column (denoted Deviation) indicating the deviations if $M_H = 117$ GeV is fixed.

The extracted Z pole value of $\alpha_s(M_Z)$ is based on a formula with negligible theoretical uncertainty if one assumes the exact validity of the SM. One should keep in mind, however, that this value,

Table 10.5: Values of \hat{s}_Z^2 , s_W^2 , α_s , and M_H [in GeV] for various (combinations of) observables. Unless indicated otherwise, the top quark mass, $m_t = 170.9 \pm 1.9$ GeV, is used as an additional constraint in the fits. The (†) symbol indicates a fixed parameter.

Data	\hat{s}_Z^2	s_W^2	$\alpha_s(M_Z)$	M_H
All data	0.23116(13)	0.22292(28)	0.1183(15)	90_{-22}^{+27}
All indirect (no m_t)	0.23118(14)	0.22283(34)	0.1183(16)	112_{-52}^{+110}
Z pole (no m_t)	0.23121(17)	0.22311(59)	0.1198(28)	90_{-44}^{+114}
LEP 1 (no m_t)	0.23152(21)	0.22376(67)	0.1213(30)	170_{-93}^{+234}
SLD + M_Z	0.23067(29)	0.22201(54)	0.1183 (†)	33_{-17}^{+27}
$A_{FB}^{(b,c)} + M_Z$	0.23193(28)	0.22484(76)	0.1183 (†)	389_{-158}^{+264}
$M_W + M_Z$	0.23100(23)	0.22262(48)	0.1183 (†)	67_{-28}^{+38}
M_Z	0.23128(6)	0.22321(17)	0.1183 (†)	117 (†)
Q_W (APV)	0.2314(14)	0.2233(14)	0.1183 (†)	117 (†)
$Q_W(e)$	0.2332(15)	0.2251(15)	0.1183 (†)	117 (†)
ν_μ -N DIS (isoscalar)	0.2335(18)	0.2254(18)	0.1183 (†)	117 (†)
Elastic $\nu_\mu(\bar{\nu}_\mu)$ -e	0.2311(77)	0.2230(77)	0.1183 (†)	117 (†)
e-D DIS (SLAC)	0.222(18)	0.213(19)	0.1183 (†)	117 (†)
Elastic $\nu_\mu(\bar{\nu}_\mu)$ -p	0.211(33)	0.203(33)	0.1183 (†)	117 (†)

$\alpha_s(M_Z) = 0.1198 \pm 0.0028$, is very sensitive to such types of new physics as non-universal vertex corrections. In contrast, the value derived from τ decays, $\alpha_s(M_Z) = 0.1174_{-0.0016}^{+0.0018}$, is theory dominated but less sensitive to new physics. The two values are in remarkable agreement with each other. They are also in agreement with other recent values, such as from jet-event shapes at LEP [215] (0.1202 ± 0.0050) the average from HERA [216] (0.1198 ± 0.0032), and the most recent unquenched lattice calculation [217] (0.1183 ± 0.0008). For more details and other determinations, see our Section 9 on “Quantum Chromodynamics” in this *Review*.

Using $\alpha(M_Z)$ and \hat{s}_Z^2 as inputs, one can predict $\alpha_s(M_Z)$ assuming grand unification. One predicts [218] $\alpha_s(M_Z) = 0.130 \pm 0.001 \pm 0.01$ for the simplest theories based on the minimal supersymmetric extension of the SM, where the first (second) uncertainty is from the inputs (thresholds). This is slightly larger, but consistent with the experimental $\alpha_s(M_Z) = 0.1183 \pm 0.0015$ from the Z lineshape and the τ lifetime, as well as with other determinations. Non-supersymmetric unified theories predict the low value $\alpha_s(M_Z) = 0.073 \pm 0.001 \pm 0.001$. See also the note on “Supersymmetry” in the Searches Particle Listings.

The data indicate a preference for a small Higgs mass. There is a strong correlation between the quadratic m_t and logarithmic M_H terms in $\hat{\rho}$ in all of the indirect data except for the $Z \rightarrow b\bar{b}$ vertex.

Therefore, observables (other than R_b) which favor m_t values higher than the Tevatron range favor lower values of M_H . M_W has additional M_H dependence through $\Delta\hat{r}_W$ which is not coupled to m_t^2 effects. The strongest individual pulls toward smaller M_H are from M_W and A_{LR}^0 , while $A_{FB}^{(0,b)}$ favors higher values. The difference in χ^2 for the global fit is $\Delta\chi^2 = \chi^2(M_H = 300 \text{ GeV}) - \chi_{\min}^2 \approx 25$. Hence, the data favor a small value of M_H , as in supersymmetric extensions of the SM. The central value of the global fit result, $M_H = 90_{-22}^{+27} \text{ GeV}$, is below the direct lower bound, $M_H \geq 114.4 \text{ GeV}$ (95% CL) [161].

The 90% central confidence range from all precision data is

$$55 \text{ GeV} \leq M_H \leq 135 \text{ GeV}. \quad (10.36)$$

Including the results of the direct searches at LEP 2 [161] and the Tevatron [219] as extra contributions to the likelihood function drives the 95% upper limit to $M_H \leq 147 \text{ GeV}$. As two further refinements, we account for (i) theoretical uncertainties from uncalculated higher order contributions by allowing the T parameter (see next subsection) subject to the constraint $T = 0 \pm 0.02$, (ii) the M_H dependence of the correlation matrix which gives slightly more weight to lower Higgs masses [220]. The resulting limits at 95 (90, 99)% CL are, respectively,

$$M_H \leq 149 \text{ (145, 194) GeV}. \quad (10.37)$$

10.7. Constraints on new physics

A number of authors [226–231] have considered the general effects on neutral-current and Z and W boson observables of various types of heavy (*i.e.*, $M_{\text{new}} \gg M_Z$) physics which contribute to the W and Z self-energies but which do not have any direct coupling to the ordinary fermions. In addition to non-degenerate multiplets, which break the vector part of weak $SU(2)$, these include heavy degenerate multiplets of chiral fermions which break the axial generators. These effects can be described, for example, by the so-called T and S parameters, respectively, where the latter is typically rather large in Technicolor theories.

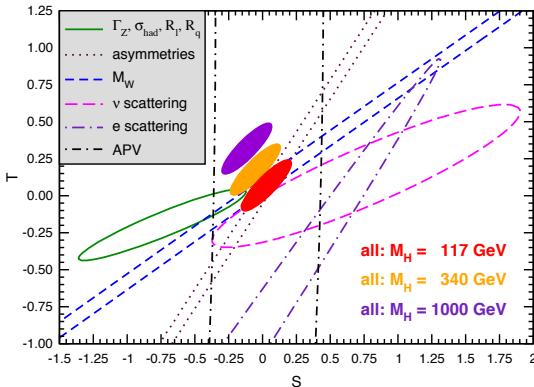


Figure 10.1: 1σ constraints (39.35%) on S and T from various inputs combined with M_Z . S and T represent the contributions of new physics only.

Further discussion and all references may be found in the full *Review*.

11. THE CKM QUARK-MIXING MATRIX

Revised February 2010 by A. Ceccucci (CERN), Z. Ligeti (LBNL), and Y. Sakai (KEK).

11.1. Introduction

The masses and mixings of quarks have a common origin in the Standard Model (SM). They arise from the Yukawa interactions of the quarks with the Higgs condensate. When the Higgs field acquires a vacuum expectation value, quark mass terms are generated. The physical states are obtained by diagonalizing the up and down quark mass matrices by four unitary matrices, $V_{L,R}^{u,d}$. As a result, the charged current W^\pm interactions couple to the physical up and down-type quarks with couplings given by

$$V_{\text{CKM}} \equiv V_L^u V_L^{d\dagger} = \begin{pmatrix} V_{ud} & V_{us} & V_{ub} \\ V_{cd} & V_{cs} & V_{cb} \\ V_{td} & V_{ts} & V_{tb} \end{pmatrix}. \quad (11.2)$$

This Cabibbo-Kobayashi-Maskawa (CKM) matrix [1,2] is a 3×3 unitary matrix. It can be parameterized by three mixing angles and a CP -violating phase,

$$V = \begin{pmatrix} c_{12}c_{13} & s_{12}c_{13} & s_{13}e^{-i\delta} \\ -s_{12}c_{23} - c_{12}s_{23}s_{13}e^{i\delta} & c_{12}c_{23} - s_{12}s_{23}s_{13}e^{i\delta} & s_{23}c_{13} \\ s_{12}s_{23} - c_{12}c_{23}s_{13}e^{i\delta} & -c_{12}s_{23} - s_{12}c_{23}s_{13}e^{i\delta} & c_{23}c_{13} \end{pmatrix}, \quad (11.3)$$

where $s_{ij} = \sin \theta_{ij}$, $c_{ij} = \cos \theta_{ij}$, and δ is the phase responsible for all CP -violating phenomena in flavor changing processes in the SM. The angles θ_{ij} can be chosen to lie in the first quadrant.

It is known experimentally that $s_{13} \ll s_{23} \ll s_{12} \ll 1$, and it is convenient to exhibit this hierarchy using the Wolfenstein parameterization. We define [4–6]

$$s_{12} = \lambda = \frac{|V_{us}|}{\sqrt{|V_{ud}|^2 + |V_{us}|^2}}, \quad s_{23} = A\lambda^2 = \lambda \left| \frac{V_{cb}}{V_{us}} \right|, \\ s_{13}e^{i\delta} = V_{ub}^* = A\lambda^3(\rho + i\eta) = \frac{A\lambda^3(\bar{\rho} + i\bar{\eta})\sqrt{1 - A^2\lambda^4}}{\sqrt{1 - \lambda^2}[1 - A^2\lambda^4(\bar{\rho} + i\bar{\eta})]}. \quad (11.4)$$

These ensure that $\bar{\rho} + i\bar{\eta} = -(V_{ud}V_{ub}^*)/(V_{cd}V_{cb}^*)$ is phase-convention independent and the CKM matrix written in terms of λ , A , $\bar{\rho}$ and $\bar{\eta}$ is unitary to all orders in λ . To $\mathcal{O}(\lambda^4)$,

$$V = \begin{pmatrix} 1 - \lambda^2/2 & \lambda & A\lambda^3(\rho - i\eta) \\ -\lambda & 1 - \lambda^2/2 & A\lambda^2 \\ A\lambda^3(1 - \rho - i\eta) & -A\lambda^2 & 1 \end{pmatrix} + \mathcal{O}(\lambda^4). \quad (11.5)$$

Unitarity implies $\sum_i V_{ij}V_{ik}^* = \delta_{jk}$ and $\sum_j V_{ij}V_{kj}^* = \delta_{ik}$. The six vanishing combinations can be represented as triangles in a complex plane. The most commonly used unitarity triangle arises from

$$V_{ud}V_{ub}^* + V_{cd}V_{cb}^* + V_{td}V_{tb}^* = 0, \quad (11.6)$$

by dividing each side by $V_{cd}V_{cb}^*$ (see Fig. 1). The vertices are exactly $(0, 0)$, $(1, 0)$ and, due to the definition in Eq. (11.4), $(\bar{\rho}, \bar{\eta})$. An important goal of flavor physics is to overconstrain the CKM elements, many of which can be displayed and compared in the $\bar{\rho}, \bar{\eta}$ plane.

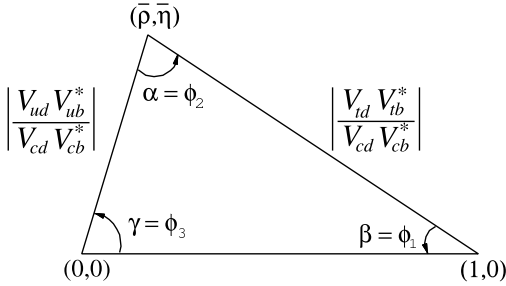


Figure 11.1: Sketch of the unitarity triangle.

11.2. Magnitudes of CKM elements

11.2.1. $|V_{ud}|$:

The most precise determination of $|V_{ud}|$ comes from the study of superallowed $0^+ \rightarrow 0^+$ nuclear beta decays, which are pure vector transitions. Taking the average of the nine most precise determinations [8] yields [9]

$$|V_{ud}| = 0.97425 \pm 0.00022. \quad (11.7)$$

11.2.2. $|V_{us}|$:

The magnitude of V_{us} is extracted from semileptonic kaon decays or leptonic kaon decays. Combining the data on $K_L^0 \rightarrow \pi e \nu$, $K_L^0 \rightarrow \pi \mu \nu$, $K^\pm \rightarrow \pi^0 e^\pm \nu$, $K^\pm \rightarrow \pi^0 \mu^\pm \nu$ and $K_S^0 \rightarrow \pi e \nu$ gives $|V_{us}| = 0.2246 \pm 0.0012$ with the unquenched lattice QCD calculation value, $f_+(0) = 0.9644 \pm 0.0049$ [12]. The KLOE measurement of the $K^+ \rightarrow \mu^+ \nu(\gamma)$ branching ratio [16] with the lattice QCD value, $f_K/f_\pi = 1.189 \pm 0.007$ [17] leads to $|V_{us}| = 0.2259 \pm 0.0014$. The average of these two determinations is quoted by Ref. [9] as

$$|V_{us}| = 0.2252 \pm 0.0009. \quad (11.8)$$

11.2.3. $|V_{cd}|$:

The most precise determination of $|V_{cd}|$ is based on neutrino and antineutrino interactions. The difference of the ratio of double-muon to single-muon production by neutrino and antineutrino beams is proportional to the charm cross section off valence d -quarks. Combining the results [26–29], we obtain

$$|V_{cd}| = 0.230 \pm 0.011. \quad (11.9)$$

11.2.4. $|V_{cs}|$:

The determination of $|V_{cs}|$ is possible from semileptonic D or leptonic D_s decays. Using the recent $D_s^+ \rightarrow \mu^+ \nu$ [37,38,40] and $D_s^+ \rightarrow \tau^+ \nu$ [38,41] data gives $|V_{cs}| = 1.030 \pm 0.038$ with $f_{D_s} = (242.8 \pm 3.2 \pm 5.3) \text{ MeV}$ [42]. The recent $D \rightarrow K \ell \nu$ measurements [24,25,43] combined with the lattice QCD calculation of the form factor [23] gives $|V_{cs}| = 0.98 \pm 0.01 \pm 0.10$. Averaging these two determinations, we obtain

$$|V_{cs}| = 1.023 \pm 0.036. \quad (11.10)$$

11.2.5. $|V_{cb}|$:

The determination of $|V_{cb}|$ from inclusive semileptonic B decays use the semileptonic rate measurement together with the leptonic energy and the hadronic invariant-mass spectra. Determinations from exclusive $B \rightarrow D^{(*)} \ell \bar{\nu}$ decays are based on the fact that in the $m_{b,c} \gg \Lambda_{\text{QCD}}$ limit all form factors are given by a single Isgur-Wise function [49], which is normalized at zero recoil. The V_{cb} and V_{ub} minireview [48] quotes the combination with a scaled error as

$$|V_{cb}| = (40.6 \pm 1.3) \times 10^{-3}. \quad (11.11)$$

11.2.6. $|V_{ub}|$:

The determination of $|V_{ub}|$ from inclusive $B \rightarrow X_u \ell \bar{\nu}$ decay suffers from large $B \rightarrow X_c \ell \bar{\nu}$ backgrounds. In most regions of phase space where the charm background is kinematically forbidden the rate is determined by nonperturbative shape functions. At leading order in Λ_{QCD}/m_b there is only one such function, which is related to the photon energy spectrum in $B \rightarrow X_s \gamma$ [50,51]. The large and pure $B\bar{B}$ samples at the B factories permit the selection of $B \rightarrow X_u \ell \bar{\nu}$ decays in events where the other B is fully reconstructed [56]. With this full-reconstruction tag method, one can measure the four-momenta of both the leptonic and hadronic systems, and access wider kinematic regions because of improved signal purity.

To extract $|V_{ub}|$ from exclusive channels, the form factors have to be known. Unquenched lattice QCD calculations of the $B \rightarrow \pi \ell \bar{\nu}$ form factor for $q^2 > 16 \text{ GeV}^2$ are available [57,58]. The theoretical uncertainties in the inclusive and exclusive determinations are different. The V_{cb} and V_{ub} minireview [48] quotes the combination

$$|V_{ub}| = (3.89 \pm 0.44) \times 10^{-3}. \quad (11.12)$$

11.2.7. $|V_{td}|$ and $|V_{ts}|$:

These CKM elements cannot be measured from tree-level top quark decays, so one has to use B - \bar{B} oscillations or loop-mediated rare K and B decays. The mass difference of the two neutral B meson mass eigenstates is well measured, $\Delta m_d = (0.507 \pm 0.005) \text{ ps}^{-1}$ [60]. For the B_s^0 system, CDF measured $\Delta m_s = (17.77 \pm 0.10 \pm 0.07) \text{ ps}^{-1}$ [61] with more than 5σ significance. Using unquenched lattice QCD calculations [63] and assuming $|V_{tb}| = 1$, we find

$$|V_{td}| = (8.4 \pm 0.6) \times 10^{-3}, \quad |V_{ts}| = (38.7 \pm 2.1) \times 10^{-3}. \quad (11.13)$$

Several uncertainties are reduced in the lattice QCD calculation of the ratio $\Delta m_d/\Delta m_s$, which gives a new and significantly improved constraint,

$$|V_{td}/V_{ts}| = 0.211 \pm 0.001 \pm 0.005. \quad (11.14)$$

11.2.8. $|V_{tb}|$:

The determination of $|V_{tb}|$ from top decays uses the ratio of branching fractions $\mathcal{B}(t \rightarrow Wb)/\mathcal{B}(t \rightarrow Wq) = |V_{tb}|^2/(\sum_q |V_{tq}|^2) = |V_{tb}|^2$, where $q = b, s, d$ [69,70]. The direct determination of $|V_{tb}|$ without assuming unitarity has become possible from the single top quark production cross section. The $(2.76_{-0.47}^{+0.58}) \text{ pb}$ [71] average cross section measured by DØ [72] and CDF [73] implies

$$|V_{tb}| = 0.88 \pm 0.07. \quad (11.15)$$

11.3. Phases of CKM elements

The angles of the unitarity triangle are

$$\begin{aligned}\beta = \phi_1 &= \arg\left(-\frac{V_{cd}V_{cb}^*}{V_{td}V_{tb}^*}\right), & \alpha = \phi_2 &= \arg\left(-\frac{V_{td}V_{tb}^*}{V_{ud}V_{ub}^*}\right), \\ \gamma = \phi_3 &= \arg\left(-\frac{V_{ud}V_{ub}^*}{V_{cd}V_{cb}^*}\right).\end{aligned}\quad (11.16)$$

Since CP violation involves phases of CKM elements, many measurements of CP -violating observables can be used to constrain these angles and the $\bar{\rho}, \bar{\eta}$ parameters.

11.3.1. ϵ and ϵ' :

The measurement of CP violation in $K^0-\bar{K}^0$ mixing, $|\epsilon| = (2.233 \pm 0.015) \times 10^{-3}$ [75], provides constraints in the $\bar{\rho}, \bar{\eta}$ plane bounded by hyperbolas approximately. The dominant uncertainties are due to the bag parameter and the parametric uncertainty proportional to $\sigma(A^4)$ [*i.e.*, $\sigma(|V_{cb}|^4)$].

The measurement of ϵ' provides a qualitative test of the CKM mechanism because its nonzero experimental average, $\text{Re}(\epsilon'/\epsilon) = (1.67 \pm 0.23) \times 10^{-3}$ [75], demonstrated the existence of direct CP violation, a prediction of the KM ansatz. While $\text{Re}(\epsilon'/\epsilon) \propto \text{Im}(V_{td}V_{ts}^*)$, this quantity cannot easily be used to extract CKM parameters, because of large hadronic uncertainties.

11.3.2. β / ϕ_1 :

The time-dependent CP asymmetry of neutral B decays to a final state f common to B^0 and \bar{B}^0 is given by [85,86]

$$A_f = \frac{\Gamma(\bar{B}^0(t) \rightarrow f) - \Gamma(B^0(t) \rightarrow f)}{\Gamma(\bar{B}^0(t) \rightarrow f) + \Gamma(B^0(t) \rightarrow f)} = S_f \sin(\Delta m t) - C_f \cos(\Delta m t), \quad (11.18)$$

where $S_f = 2\text{Im}\lambda_f/(1 + |\lambda_f|^2)$, $C_f = (1 - |\lambda_f|^2)/(1 + |\lambda_f|^2)$, and $\lambda_f = (q/p)(\bar{A}_f/A_f)$. Here q/p describes $B^0-\bar{B}^0$ mixing and, to a good approximation in the SM, $q/p = V_{tb}^*V_{td}/V_{tb}V_{td}^* = e^{-2i\beta + \mathcal{O}(\lambda^4)}$ in the usual phase convention. A_f (\bar{A}_f) is the amplitude of $B^0 \rightarrow f$ ($\bar{B}^0 \rightarrow f$) decay. If f is a CP eigenstate and amplitudes with one CKM phase dominate, then $|A_f| = |\bar{A}_f|$, $C_f = 0$ and $S_f = \sin(\arg \lambda_f) = \eta_f \sin 2\phi$, where η_f is the CP eigenvalue of f and 2ϕ is the phase difference between the $B^0 \rightarrow f$ and $B^0 \rightarrow \bar{B}^0 \rightarrow f$ decay paths.

The $b \rightarrow c\bar{c}s$ decays to CP eigenstates ($B^0 \rightarrow$ charmonium $K_{S,L}^0$) are the theoretically cleanest examples, measuring $S_f = -\eta_f \sin 2\beta$. The world average is [64]

$$\sin 2\beta = 0.673 \pm 0.023. \quad (11.20)$$

This measurement of β has a four-fold ambiguity. Of these, $\beta \rightarrow \pi/2 - \beta$ (but not $\beta \rightarrow \pi + \beta$) has been resolved by a time-dependent angular analysis of $B^0 \rightarrow J/\psi K^{*0}$ [90,91] and a time-dependent Dalitz plot analysis of $B^0 \rightarrow \bar{D}^0 h^0$ ($h^0 = \pi^0, \eta, \omega$) [92,93].

The $b \rightarrow s\bar{q}q$ penguin dominated decays have the same CKM phase as the $b \rightarrow c\bar{c}s$ tree dominated decays, up to corrections suppressed by λ^2 . Therefore, decays such as $B^0 \rightarrow \phi K^0$ and $\eta' K^0$ provide $\sin 2\beta$ measurements in the SM. If new physics contributes to the $b \rightarrow s$

loop diagrams and has a different weak phase, it would give rise to $S_f \neq -\eta_f \sin 2\beta$ and possibly $C_f \neq 0$. The results and their uncertainties are summarized in Fig. 12.3 and Table 12.1 of Ref. [86].

11.3.3. α / ϕ_2 :

Since α is the phase between $V_{tb}^*V_{td}$ and $V_{ub}^*V_{ud}$, only time-dependent CP asymmetries in $b \rightarrow u\bar{u}d$ dominated modes can directly measure it. In such decays the penguin contribution can be sizable. Then $S_{\pi^+\pi^-}$ no longer measures $\sin 2\alpha$, but α can still be extracted using the isospin relations among the $B^0 \rightarrow \pi^+\pi^-$, $B^0 \rightarrow \pi^0\pi^0$, and $B^+ \rightarrow \pi^+\pi^0$ amplitudes and their CP conjugates [94]. Because the isospin analysis gives 16 mirror solutions, and the sizable experimental error of $B^0 \rightarrow \pi^0\pi^0$, only a loose constraint is obtained at present.

The $B^0 \rightarrow \rho^+\rho^-$ decay can in general have a mixture of CP -even and CP -odd components. However, the longitudinal polarization fractions in $B^+ \rightarrow \rho^+\rho^0$ and $B^0 \rightarrow \rho^+\rho^-$ are measured to be close to unity [96], which implies that the final states are almost purely CP -even. Furthermore, $\mathcal{B}(B^0 \rightarrow \rho^0\rho^0) = (0.73_{-0.28}^{+0.27}) \times 10^{-6}$ implies that the effect of the penguin diagrams is small. The isospin analysis gives $\alpha = (89.9 \pm 5.4)^\circ$ [95] with a mirror solution at $3\pi/2 - \alpha$.

The final state in $B^0 \rightarrow \rho^+\pi^-$ decay is not a CP eigenstate, but mixing induced CP violations can still occur in the four decay amplitudes, $B^0, \bar{B}^0 \rightarrow \rho^\pm\pi^\mp$. Because of the more complicated isospin relations, the time-dependent Dalitz plot analysis of $B^0 \rightarrow \pi^+\pi^-\pi^0$ gives the best model independent extraction of α [99]. The Belle [100] and BABAR [101] measurements yield $\alpha = (120_{-7}^{+11})^\circ$ [95].

Combining these three decay modes [95], α is constrained as

$$\alpha = (89.0_{-4.2}^{+4.4})^\circ. \quad (11.23)$$

11.3.4. γ / ϕ_3 :

The angle γ does not depend on CKM elements involving the top quark, so it can be measured in tree level B decays. This is an important distinction from α and β , implying that the measurements of γ are unlikely to be affected by physics beyond the SM.

The interference of $B^- \rightarrow D^0K^-$ ($b \rightarrow c\bar{u}s$) and $B^- \rightarrow \bar{D}^0K^-$ ($b \rightarrow u\bar{c}s$) transitions can be studied in final states accessible in both D^0 and \bar{D}^0 decays [85]. It is possible to extract from the data the B and D decay amplitudes, the relative strong phases, and γ . Analyses in two-body D decays using the GLW [103,104] and ADS methods [105] have been made by the B factories [106], as well as in a Dalitz plot analysis of $D^0, \bar{D}^0 \rightarrow K_S\pi^+\pi^-$ [109,110]. Combining these analyses [95], γ is constrained as

$$\gamma = (73_{-25}^{+22})^\circ. \quad (11.25)$$

11.4. Global fit in the Standard Model

Using the independently measured CKM elements mentioned in the previous sections, the unitarity of the CKM matrix can be checked. We obtain $|V_{ud}|^2 + |V_{us}|^2 + |V_{ub}|^2 = 0.9999 \pm 0.0006$ (1st row), $|V_{cd}|^2 + |V_{cs}|^2 + |V_{cb}|^2 = 1.101 \pm 0.074$ (2nd row), $|V_{ud}|^2 + |V_{cd}|^2 + |V_{td}|^2 = 1.002 \pm 0.005$ (1st column), and $|V_{us}|^2 + |V_{cs}|^2 + |V_{ts}|^2 = 1.098 \pm 0.074$ (2nd column), respectively. For the second row, a more stringent check

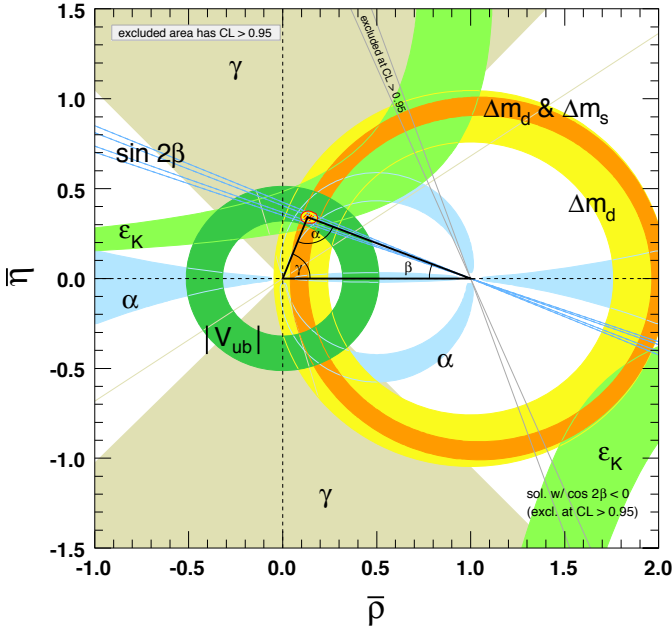


Figure 11.2: 95% CL constraints on the $\bar{\rho}, \bar{\eta}$ plane.

is obtained subtracting the sum of the first row from the measurement of $\sum_{u,c,d,s,b} |V_{ij}|^2$ from the W leptonic branching ratio [35], yielding $|V_{cd}|^2 + |V_{cs}|^2 + |V_{cb}|^2 = 1.002 \pm 0.027$. The sum of the three angles, $\alpha + \beta + \gamma = (183^{+22}_{-25})^\circ$, is also consistent with the SM expectation.

The CKM matrix elements can be most precisely determined by a global fit that uses all available measurements and imposes the SM constraints. There are several approaches to combining the experimental data [6,95,102,118], which provide similar results. The results for the Wolfenstein parameters are

$$\begin{aligned} \lambda &= 0.2253 \pm 0.0007, & A &= 0.808^{+0.022}_{-0.015}, \\ \bar{\rho} &= 0.132^{+0.022}_{-0.014}, & \bar{\eta} &= 0.341 \pm 0.013. \end{aligned} \quad (11.26)$$

The allowed ranges of the magnitudes of all nine CKM elements are

$$V_{\text{CKM}} = \begin{pmatrix} 0.97428 \pm 0.00015 & 0.2253 \pm 0.0007 & 0.00347^{+0.00016}_{-0.00012} \\ 0.2252 \pm 0.0007 & 0.97345^{+0.00015}_{-0.00016} & 0.0410^{+0.0011}_{-0.0007} \\ 0.00862^{+0.00026}_{-0.00020} & 0.0403^{+0.0011}_{-0.0007} & 0.999152^{+0.000030}_{-0.000045} \end{pmatrix}, \quad (11.27)$$

and the Jarlskog invariant is $J = (2.91^{+0.19}_{-0.11}) \times 10^{-5}$. Fig. 11.2 illustrates the constraints on the $\bar{\rho}, \bar{\eta}$ plane from various measurements and the global fit result. The shaded 95% CL regions all overlap consistently around the global fit region.

11.5. Implications beyond the SM

The effects in B , K , and D decays and mixings due to high-scale physics (W , Z , t , h in the SM, or new physics particles) can be parameterized by operators composed of SM fields, obeying the $SU(3) \times SU(2) \times U(1)$ gauge symmetry. The observable effects of non-SM interactions are encoded in the coefficients of these operators, and are suppressed by powers of the new physics scale. In the SM, these coefficients are determined by just the four CKM parameters, and the W , Z , and quark masses. For example, Δm_d , $\Gamma(B \rightarrow \rho\gamma)$, and $\Gamma(B \rightarrow X_d \ell^+ \ell^-)$ are all proportional to $|V_{td} V_{tb}^*|^2$ in the SM, however, they may receive unrelated new physics contributions. Similar to measurements of $\sin 2\beta$ in tree- and loop-dominated decays, overconstraining the magnitudes and phases of flavor-changing neutral current amplitudes give good sensitivity to new physics.

To illustrate the level of suppression required for non-SM contributions, consider a class of models in which the dominant effect of new physics is to modify the neutral meson mixing amplitudes [121] by $(z_{ij}/\Lambda^2)(\bar{q}_i \gamma^\mu P_L q_j)^2$. New physics with a generic weak phase may still contribute to meson mixings at a significant fraction of the SM [125,118]. The data imply that $\Lambda/|z_{ij}|^{1/2}$ has to exceed about 10^4 TeV for $K^0 - \bar{K}^0$ mixing, 10^3 TeV for $D^0 - \bar{D}^0$ mixing, 500 TeV for $B^0 - \bar{B}^0$ mixing, and 100 TeV for $B_s^0 - \bar{B}_s^0$ mixing [118,123]. Thus, if there is new physics at the TeV scale, $|z_{ij}| \ll 1$ is required. Even if $|z_{ij}|$ are suppressed by a loop factor and $|V_{ti}^* V_{tj}|^2$ (in the down quark sector), as in the SM, one expects percent-level effects, which may be observable in forthcoming experiments.

The CKM elements are fundamental parameters, so they should be measured as precisely as possible. The overconstraining measurements of CP asymmetries, mixing, semileptonic, and rare decays severely constrain the magnitudes and phases of possible new physics contributions to flavor-changing interactions. When new particles are seen at the LHC, it will be important to know the flavor parameters as precisely as possible to understand the underlying physics.

Further discussion and all references may be found in the full *Review of Particle Physics*. The numbering of references and equations used here corresponds to that version.

12. *CP VIOLATION IN MESON DECAYS*

Revised September 2009 by D. Kirkby (UC Irvine) and Y. Nir (Weizmann Institute).

The *CP* transformation combines charge conjugation *C* with parity *P*. Under *C*, particles and antiparticles are interchanged, by conjugating all internal quantum numbers, *e.g.*, $Q \rightarrow -Q$ for electromagnetic charge. Under *P*, the handedness of space is reversed, $\vec{x} \rightarrow -\vec{x}$. Thus, for example, a left-handed electron e_L^- is transformed under *CP* into a right-handed positron, e_R^+ .

We observe that most phenomena are *C*- and *P*-symmetric, and therefore, also *CP*-symmetric. In particular, these symmetries are respected by the gravitational, electromagnetic, and strong interactions. The weak interactions, on the other hand, violate *C* and *P* in the strongest possible way. For example, the charged *W* bosons couple to left-handed electrons, e_L^- , and to their *CP*-conjugate right-handed positrons, e_R^+ , but to neither their *C*-conjugate left-handed positrons, e_L^+ , nor their *P*-conjugate right-handed electrons, e_R^- . While weak interactions violate *C* and *P* separately, *CP* is still preserved in most weak interaction processes. The *CP* symmetry is, however, violated in certain rare processes, as discovered in neutral *K* decays in 1964 [1], and observed in recent years in *B* decays.

The present measurements of *CP* asymmetries provide some of the strongest constraints on the weak couplings of quarks. Future measurements of *CP* violation in *K*, *D*, *B*, and *B_s* meson decays will provide additional constraints on the flavor parameters of the Standard Model, and can probe new physics. In this review, we give the formalism and basic physics that are relevant to present and near future measurements of *CP* violation in meson decays.

12.1. Formalism

In this section, we present a general formalism for, and classification of, *CP* violation in the decay of a pseudoscalar meson *M* that might be a charged or neutral *K*, *D*, *B*, or *B_s* meson. Subsequent sections describe the *CP*-violating phenomenology, approximations, and alternative formalisms that are specific to each system.

12.1.1. Charged- and neutral-meson decays: We define decay amplitudes of *M* (which could be charged or neutral) and its *CP* conjugate \bar{M} to a multi-particle final state *f* and its *CP* conjugate \bar{f} as

$$\begin{aligned} A_f &= \langle f | \mathcal{H} | M \rangle \quad , \quad \bar{A}_f = \langle f | \mathcal{H} | \bar{M} \rangle \quad , \\ A_{\bar{f}} &= \langle \bar{f} | \mathcal{H} | M \rangle \quad , \quad \bar{A}_{\bar{f}} = \langle \bar{f} | \mathcal{H} | \bar{M} \rangle \quad , \end{aligned} \quad (12.13)$$

where \mathcal{H} is the Hamiltonian governing weak interactions.

12.1.2. Neutral-meson mixing: A state that is initially a superposition of M^0 and \bar{M}^0 , say

$$|\psi(0)\rangle = a(0)|M^0\rangle + b(0)|\bar{M}^0\rangle \quad , \quad (12.17)$$

will evolve in time acquiring components that describe all possible decay final states $\{f_1, f_2, \dots\}$, that is,

$$|\psi(t)\rangle = a(t)|M^0\rangle + b(t)|\bar{M}^0\rangle + c_1(t)|f_1\rangle + c_2(t)|f_2\rangle + \dots \quad (12.18)$$

If we are interested in computing only $a(t)$ and $b(t)$, we can use a simplified formalism. The simplified time evolution is determined by a 2×2 effective

Hamiltonian \mathbf{H} that is not Hermitian, since otherwise the mesons would only oscillate and not decay. Any complex matrix, such as \mathbf{H} , can be written in terms of Hermitian matrices \mathbf{M} and $\mathbf{\Gamma}$ as

$$\mathbf{H} = \mathbf{M} - \frac{i}{2} \mathbf{\Gamma}. \quad (12.19)$$

The eigenvectors of \mathbf{H} have well-defined masses and decay widths. To specify the components of the strong interaction eigenstates, M^0 and \overline{M}^0 , in the light (M_L) and heavy (M_H) mass eigenstates, we introduce two complex parameters, p and q :

$$\begin{aligned} |M_L\rangle &\propto p|M^0\rangle + q|\overline{M}^0\rangle \\ |M_H\rangle &\propto p|M^0\rangle - q|\overline{M}^0\rangle, \end{aligned} \quad (12.20)$$

with the normalization $|q|^2 + |p|^2 = 1$.

Solving the eigenvalue problem for \mathbf{H} yields

$$\left(\frac{q}{p}\right)^2 = \frac{\mathbf{M}_{12}^* - (i/2)\mathbf{\Gamma}_{12}^*}{\mathbf{M}_{12} - (i/2)\mathbf{\Gamma}_{12}}. \quad (12.22)$$

12.1.3. CP-violating observables : All CP-violating observables in M and \overline{M} decays to final states f and \overline{f} can be expressed in terms of phase-convention-independent combinations of A_f , \overline{A}_f , $A_{\overline{f}}$, and $\overline{A}_{\overline{f}}$, together with, for neutral-meson decays only, q/p . CP violation in charged-meson decays depends only on the combination $|\overline{A}_{\overline{f}}/A_f|$, while CP violation in neutral-meson decays is complicated by $M^0 \leftrightarrow \overline{M}^0$ oscillations, and depends, additionally, on $|q/p|$ and on $\lambda_f \equiv (q/p)(\overline{A}_f/A_f)$.

Defining $x \equiv \Delta m/\Gamma$ and $y \equiv \Delta\Gamma/(2\Gamma)$, one obtains the following time-dependent decay rates:

$$\begin{aligned} \frac{d\Gamma[M_{\text{phys}}^0(t) \rightarrow f]/dt}{e^{-\Gamma t}\mathcal{N}_f} &= \\ &\left(|A_f|^2 + |(q/p)\overline{A}_f|^2\right) \cosh(y\Gamma t) + \left(|A_f|^2 - |(q/p)\overline{A}_f|^2\right) \cos(x\Gamma t) \\ &+ 2\mathcal{R}e((q/p)A_f^*\overline{A}_f) \sinh(y\Gamma t) - 2\mathcal{I}m((q/p)A_f^*\overline{A}_f) \sin(x\Gamma t), \end{aligned} \quad (12.30)$$

$$\begin{aligned} \frac{d\Gamma[\overline{M}_{\text{phys}}^0(t) \rightarrow f]/dt}{e^{-\Gamma t}\mathcal{N}_f} &= \\ &\left(|(p/q)A_f|^2 + |\overline{A}_f|^2\right) \cosh(y\Gamma t) - \left(|(p/q)A_f|^2 - |\overline{A}_f|^2\right) \cos(x\Gamma t) \\ &+ 2\mathcal{R}e((p/q)A_f\overline{A}_f^*) \sinh(y\Gamma t) - 2\mathcal{I}m((p/q)A_f\overline{A}_f^*) \sin(x\Gamma t), \end{aligned} \quad (12.31)$$

where \mathcal{N}_f is a common, time-independent, normalization factor.

12.1.4. Classification of CP-violating effects : We distinguish three types of CP-violating effects in meson decays:

I. CP violation in decay is defined by

$$|\overline{A}_{\overline{f}}/A_f| \neq 1. \quad (12.34)$$

In charged meson decays, where mixing effects are absent, this is the only possible source of CP asymmetries:

$$A_{f\pm} \equiv \frac{\Gamma(M^- \rightarrow f^-) - \Gamma(M^+ \rightarrow f^+)}{\Gamma(M^- \rightarrow f^-) + \Gamma(M^+ \rightarrow f^+)} = \frac{|\overline{A}_{f-}/A_{f+}|^2 - 1}{|\overline{A}_{f-}/A_{f+}|^2 + 1}. \quad (12.35)$$

II. *CP* (and *T*) violation in mixing is defined by

$$|q/p| \neq 1. \quad (12.36)$$

In charged-current semileptonic neutral meson decays $M, \bar{M} \rightarrow \ell^\pm X$ (taking $|A_{\ell^+ X}| = |\bar{A}_{\ell^- X}|$ and $A_{\ell^- X} = \bar{A}_{\ell^+ X} = 0$, as is the case in the Standard Model, to lowest order in G_F , and in most of its reasonable extensions), this is the only source of *CP* violation, and can be measured via the asymmetry of “wrong-sign” decays induced by oscillations:

$$\begin{aligned} \mathcal{A}_{\text{SL}}(t) &\equiv \frac{d\Gamma/dt[\bar{M}_{\text{phys}}^0(t) \rightarrow \ell^+ X] - d\Gamma/dt[M_{\text{phys}}^0(t) \rightarrow \ell^- X]}{d\Gamma/dt[\bar{M}_{\text{phys}}^0(t) \rightarrow \ell^+ X] + d\Gamma/dt[M_{\text{phys}}^0(t) \rightarrow \ell^- X]} \\ &= \frac{1 - |q/p|^4}{1 + |q/p|^4}. \end{aligned} \quad (12.37)$$

Note that this asymmetry of time-dependent decay rates is actually time-independent.

III. *CP* violation in interference between a decay without mixing, $M^0 \rightarrow f$, and a decay with mixing, $M^0 \rightarrow \bar{M}^0 \rightarrow f$ (such an effect occurs only in decays to final states that are common to M^0 and \bar{M}^0 , including all *CP* eigenstates), is defined by

$$\text{Im}(\lambda_f) \neq 0, \quad (12.38)$$

with

$$\lambda_f \equiv \frac{q \bar{A}_f}{p A_f}. \quad (12.39)$$

This form of *CP* violation can be observed, for example, using the asymmetry of neutral meson decays into final *CP* eigenstates f_{CP}

$$\mathcal{A}_{f_{CP}}(t) \equiv \frac{d\Gamma/dt[\bar{M}_{\text{phys}}^0(t) \rightarrow f_{CP}] - d\Gamma/dt[M_{\text{phys}}^0(t) \rightarrow f_{CP}]}{d\Gamma/dt[\bar{M}_{\text{phys}}^0(t) \rightarrow f_{CP}] + d\Gamma/dt[M_{\text{phys}}^0(t) \rightarrow f_{CP}]}. \quad (12.40)$$

If $\Delta\Gamma = 0$ and $|q/p| = 1$, as expected to a good approximation for *B* mesons, but not for *K* mesons, then $\mathcal{A}_{f_{CP}}$ has a particularly simple form (see Eq. (12.74), below). If, in addition, the decay amplitudes fulfill $|\bar{A}_{f_{CP}}| = |A_{f_{CP}}|$, the interference between decays with and without mixing is the only source of the asymmetry and $\mathcal{A}_{f_{CP}}(t) = \text{Im}(\lambda_{f_{CP}}) \sin(x\Gamma t)$.

12.2. Theoretical Interpretation: The KM Mechanism

Of all the Standard Model quark parameters, only the Kobayashi-Maskawa (KM) phase is *CP*-violating. The Cabibbo-Kobayashi-Maskawa (CKM) mixing matrix for quarks is described in the preceding CKM review and in the full edition.

12.3. *K* Decays

The decay amplitudes actually measured in neutral *K* decays refer to the mass eigenstates K_L and K_S , rather than to the *K* and \bar{K} states referred to in Eq. (12.13). The final $\pi^+\pi^-$ and $\pi^0\pi^0$ states are *CP*-even. In the *CP* limit, $K_S(K_L)$ would be *CP*-even (odd), and therefore would (would not) decay to two pions. We define *CP*-violating amplitude ratios for two-pion final states,

$$\eta_{00} \equiv \frac{\langle \pi^0 \pi^0 | \mathcal{H} | K_L \rangle}{\langle \pi^0 \pi^0 | \mathcal{H} | K_S \rangle}, \quad \eta_{+-} \equiv \frac{\langle \pi^+ \pi^- | \mathcal{H} | K_L \rangle}{\langle \pi^+ \pi^- | \mathcal{H} | K_S \rangle}. \quad (12.50)$$

Another important observable is the asymmetry of time-integrated semileptonic decay rates:

$$\delta_L \equiv \frac{\Gamma(K_L \rightarrow \ell^+ \nu_\ell \pi^-) - \Gamma(K_L \rightarrow \ell^- \bar{\nu}_\ell \pi^+)}{\Gamma(K_L \rightarrow \ell^+ \nu_\ell \pi^-) + \Gamma(K_L \rightarrow \ell^- \bar{\nu}_\ell \pi^+)}. \quad (12.51)$$

CP violation has been observed as an appearance of K_L decays to two-pion final states [19],

$$|\eta_{00}| = (2.222 \pm 0.010) \times 10^{-3} \quad |\eta_{+-}| = (2.233 \pm 0.010) \times 10^{-3} \quad (12.52)$$

$$|\eta_{00}/\eta_{+-}| = 0.9950 \pm 0.0008, \quad (12.53)$$

where the phase ϕ_{ij} of the amplitude ratio η_{ij} has been determined:

$$\phi_{00} = (43.7 \pm 0.08)^\circ, \quad \phi_{+-} = (43.4 \pm 0.07)^\circ, \quad (12.54)$$

CP violation has also been observed in semileptonic K_L decays [19]

$$\delta_L = (3.32 \pm 0.06) \times 10^{-3}, \quad (12.56)$$

where δ_L is a weighted average of muon and electron measurements, as well as in K_L decays to $\pi^+ \pi^- \gamma$ and $\pi^+ \pi^- e^+ e^-$ [19]. CP violation in $K \rightarrow 3\pi$ decays has not yet been observed [19,29].

Historically, CP violation in neutral K decays has been described in terms of parameters ϵ and ϵ' . The observables η_{00} , η_{+-} , and δ_L are related to these parameters, and to those of Section 12.1, by

$$\eta_{00} = \frac{1 - \lambda_{\pi^0 \pi^0}}{1 + \lambda_{\pi^0 \pi^0}} = \epsilon - 2\epsilon', \quad \eta_{+-} = \frac{1 - \lambda_{\pi^+ \pi^-}}{1 + \lambda_{\pi^+ \pi^-}} = \epsilon + \epsilon',$$

$$\delta_L = \frac{1 - |q/p|^2}{1 + |q/p|^2} = \frac{2\mathcal{R}e(\epsilon)}{1 + |\epsilon|^2}. \quad (12.57)$$

12.4. D Decays

First evidence for $D^0 - \bar{D}^0$ mixing has been recently obtained [34–36]. Long-distance contributions make it difficult to calculate the Standard Model prediction for the $D^0 - \bar{D}^0$ mixing parameters. Therefore, the goal of the search for $D^0 - \bar{D}^0$ mixing is not to constrain the CKM parameters, but rather to probe new physics. Here CP violation plays an important role. Within the Standard Model, the CP -violating effects are predicted to be negligibly small, since the mixing and the relevant decays are described, to an excellent approximation, by physics of the first two generations. Observation of CP violation in $D^0 - \bar{D}^0$ mixing (at a level much higher than $\mathcal{O}(10^{-3})$) will constitute an unambiguous signal of new physics. At present, the most sensitive searches involve the $D \rightarrow K^+ K^-$ and $D \rightarrow K^\pm \pi^\mp$ modes.

12.5. B and B_s Decays

The upper bound on the CP asymmetry in semileptonic B decays [20] implies that CP violation in $B^0 - \bar{B}^0$ mixing is a small effect (we use $A_{\text{SL}}/2 \approx 1 - |q/p|$, see Eq. (12.37)):

$$A_{\text{SL}} = (-0.4 \pm 5.6) \times 10^{-3} \implies |q/p| = 1.0002 \pm 0.0028. \quad (12.70)$$

Thus, for the purpose of analyzing CP asymmetries in hadronic B decays, we can use

$$\lambda_f = e^{-i\phi_{M(B)}} (\bar{A}_f/A_f), \quad (12.72)$$

where $\phi_{M(B)}$ refers to the phase of \mathbf{M}_{12} appearing in Eq. (12.42) that is appropriate for $B^0 - \bar{B}^0$ oscillations. Within the Standard Model, the corresponding phase factor is given by

$$e^{-i\phi_{M(B)}} = (V_{tb}^* V_{td}) / (V_{ub} V_{ud}^*). \quad (12.73)$$

Some of the most interesting decays involve final states that are common to B^0 and \bar{B}^0 [40,41]. It is convenient to rewrite Eq. (12.40) for B decays as [42–44]

$$\begin{aligned} \mathcal{A}_f(t) &= S_f \sin(\Delta mt) - C_f \cos(\Delta mt), \\ S_f &\equiv \frac{2\mathcal{I}m(\lambda_f)}{1 + |\lambda_f|^2}, \quad C_f \equiv \frac{1 - |\lambda_f|^2}{1 + |\lambda_f|^2}, \end{aligned} \quad (12.74)$$

where we assume that $\Delta\Gamma = 0$ and $|q/p| = 1$. An alternative notation in use is $A_f \equiv -C_f$, but this A_f should not be confused with the A_f of Eq. (12.13).

A large class of interesting processes proceed via quark transitions of the form $\bar{b} \rightarrow \bar{q}q\bar{q}'$ with $q' = s$ or d . For $q = c$ or u , there are contributions from both tree (t) and penguin (p^{qu} , where $qu = u, c, t$ is the quark in the loop) diagrams (see Fig. 12.2) which carry different weak phases:

$$A_f = \left(V_{qb}^* V_{qq'} \right) t_f + \sum_{qu=u,c,t} \left(V_{qub}^* V_{quq'} \right) p_f^{qu}. \quad (12.75)$$

For $B \rightarrow J/\psi K_S$ and other $\bar{b} \rightarrow \bar{c}c\bar{s}$ processes, we can neglect the p^{qu} terms. Consequently, within the Standard Model, we have:

$$S_{\psi K_S} = \mathcal{I}m \left(-\frac{V_{tb}^* V_{td} V_{cb} V_{cd}^*}{V_{tb} V_{td}^* V_{cb}^* V_{cd}} \right), \quad C_{\psi K_S} = 0.$$

12.6. Summary and Outlook

CP violation has been experimentally established in neutral K and B meson decays:

1. All three types of CP violation have been observed in $K \rightarrow \pi\pi$ decays:

$$\mathcal{R}e(\epsilon') = \frac{1}{6} \left(\left| \frac{\bar{A}_{\pi^0\pi^0}}{A_{\pi^0\pi^0}} \right| - \left| \frac{\bar{A}_{\pi^+\pi^-}}{A_{\pi^+\pi^-}} \right| \right) = (2.5 \pm 0.4) \times 10^{-6} \text{ (I)}$$

$$\mathcal{R}e(\epsilon) = \frac{1}{2} \left(1 - \left| \frac{q}{p} \right| \right) = (1.66 \pm 0.02) \times 10^{-3} \quad \text{(II)}$$

$$\mathcal{I}m(\epsilon) = -\frac{1}{2} \mathcal{I}m(\lambda_{(\pi\pi)_{I=0}}) = (1.57 \pm 0.02) \times 10^{-3}. \quad \text{(III)}$$

(12.86)

2. Direct CP violation has been observed, first in $B^0 \rightarrow K^+\pi^-$ decays (and more recently also in $B \rightarrow \pi^+\pi^-$, $B^0 \rightarrow \eta K^{*0}$, and $B^+ \rightarrow \rho^0 K^+$ decays), and CP violation in interference of decays with and without mixing has been observed, first in $B \rightarrow J/\psi K_S$ decays and related modes (as well as other final CP eigenstates: $\eta' K_S$, $K^+ K^- K_S$, $J/\psi\pi^0$ and $\pi^+\pi^-$):

$$A_{K^+\pi^-} = \frac{|\bar{A}_{K^-\pi^+}/A_{K^+\pi^-}|^2 - 1}{|\bar{A}_{K^-\pi^+}/A_{K^+\pi^-}|^2 + 1} = -0.098 \pm 0.013 \quad \text{(I)}$$

$$S_{\psi K} = \mathcal{I}m(\lambda_{\psi K}) = 0.673 \pm 0.023. \quad \text{(III)}$$

(12.87)

Searches for additional CP asymmetries are ongoing in B , D , and K decays, and current limits are consistent with Standard Model expectations.

Further discussion and all references may be found in the full *Review of Particle Physics*.

13. NEUTRINO MASS, MIXING, AND OSCILLATIONS

Written May 2010 by K. Nakamura (IPMU, U. Tokyo and KEK) and S.T. Petcov (SISSA/INFN, Trieste and IPMU, U. Tokyo).

I. Massive neutrinos and neutrino mixing. It is a well-established experimental fact that the neutrinos and antineutrinos which take part in the standard charged current (CC) and neutral current (NC) weak interaction are of three varieties (types) or flavours: electron, ν_e and $\bar{\nu}_e$, muon, ν_μ and $\bar{\nu}_\mu$, and tauon, ν_τ and $\bar{\nu}_\tau$. The notion of neutrino type or flavour is dynamical: ν_e is the neutrino which is produced with e^+ , or produces an e^- , in CC weak interaction processes, *etc.* The flavour of a given neutrino is Lorentz invariant. Among the three different flavour neutrinos and antineutrinos, no two are identical.

The experiments with solar, atmospheric, reactor and accelerator neutrinos [4–16,20,21,22] have provided compelling evidences for the existence of neutrino oscillations [17,18], transitions in flight between the different flavour neutrinos ν_e , ν_μ , ν_τ (antineutrinos $\bar{\nu}_e$, $\bar{\nu}_\mu$, $\bar{\nu}_\tau$), caused by nonzero neutrino masses and neutrino mixing. The existence of oscillations implies that if a given flavour neutrino, say ν_μ , with energy E is produced in some weak interaction process, the probability that it will change into a different flavour neutrino, say ν_τ , after traveling a sufficiently large distance L , $P(\nu_\mu \rightarrow \nu_\tau; E, L)$, is different from zero. If the $\nu_\mu \rightarrow \nu_\tau$ oscillation or transition probability $P(\nu_\mu \rightarrow \nu_\tau; E, L) \neq 0$, the probability that ν_μ will not change into a neutrino of a different flavour, *i.e.*, the “ ν_μ survival probability”, $P(\nu_\mu \rightarrow \nu_\mu; E, L)$, will be smaller than one. One would observe a “disappearance” of muon neutrinos on the way from the ν_μ source to the detector if only ν_μ are detected and they take part in oscillations.

Oscillations of neutrinos are a consequence of the presence of neutrino mixing, or lepton mixing, in vacuum. In the formalism used to construct the Standard Model, this means that the LH flavour neutrino fields $\nu_{lL}(x)$, which enter into the expression for the lepton current in the CC weak interaction Lagrangian, are given by:

$$\nu_{lL}(x) = \sum_j U_{lj} \nu_{jL}(x), \quad l = e, \mu, \tau, \quad (13.1)$$

where $\nu_{jL}(x)$ is the LH component of the field of a neutrino ν_j possessing a mass m_j and U is a unitary matrix - the neutrino mixing matrix [1,17,18]. Eq. (13.1) implies that the individual lepton charges L_l , $l = e, \mu, \tau$, are not conserved.

All neutrino oscillation data, except for the LSND result [23], can be described assuming 3-neutrino mixing in vacuum. The number of massive neutrinos ν_j , n , can, in general, be bigger than 3 if, *e.g.*, there exist sterile neutrinos [1] and they mix with the flavour neutrinos. It follows from the current data that at least 3 of the neutrinos ν_j , say ν_1, ν_2, ν_3 , must be light, $m_{1,2,3} \lesssim 1$ eV, and must have different masses, $m_1 \neq m_2 \neq m_3$. At present there are no compelling experimental evidences for the existence of more than 3 light neutrinos.

Being electrically neutral, the massive neutrinos ν_j can be Dirac or Majorana particles [27,28]. The first possibility is realized when there exists a lepton charge L carried by ν_j (*e.g.*, $L = L_e + L_\mu + L_\tau$, $L(\nu_j) = 1$), which is conserved by the particle interactions. The neutrino ν_j has a distinctive antiparticle $\bar{\nu}_j$: $\bar{\nu}_j$ differs from ν_j by the value of L it carries

($L(\bar{\nu}_j) = -1$). The neutrinos ν_j can be Majorana particles if no lepton charge is conserved (see, *e.g.*, Ref. 29). A massive Majorana particle χ_j is identical with its antiparticle $\bar{\chi}_j$: $\chi_j \equiv \bar{\chi}_j$. On the basis of the existing neutrino data it is impossible to determine whether the massive neutrinos are Dirac or Majorana fermions.

In the case of n neutrino flavours and n massive neutrinos, the $n \times n$ unitary neutrino mixing matrix U can be parametrised by $n(n-1)/2$ Euler angles and $n(n+1)/2$ phases. If the massive neutrinos ν_j are Dirac particles, only $(n-1)(n-2)/2$ phases are physical and can be responsible for CP violation in the lepton sector. In this respect the neutrino mixing with Dirac massive neutrinos is similar to the quark mixing. For $n=3$ there is one CP violating phase in U , “the Dirac CP violating phase.” CP invariance holds if U is real, $U^* = U$.

If, however, the massive neutrinos are Majorana fermions, $\nu_j \equiv \chi_j$, the neutrino mixing matrix U contains $n(n-1)/2$ CP violation phases [30,31], *i.e.*, by $(n-1)$ phases more than in the Dirac neutrino case: in contrast to Dirac fields, the massive Majorana neutrino fields cannot “absorb” phases. In this case U can be cast in the form [30]

$$U = VP \tag{13.2}$$

where the matrix V contains the $(n-1)(n-2)/2$ Dirac CP violation phases, while P is a diagonal matrix with the additional $(n-1)$ Majorana CP violation phases $\alpha_{21}, \alpha_{31}, \dots, \alpha_{n1}$,

$$P = \text{diag} \left(1, e^{i\frac{\alpha_{21}}{2}}, e^{i\frac{\alpha_{31}}{2}}, \dots, e^{i\frac{\alpha_{n1}}{2}} \right). \tag{13.3}$$

The Majorana phases will conserve CP if [32] $\alpha_{j1} = \pi q_j$, $q_j = 0, 1, 2$, $j = 2, 3, \dots, n$. In this case $\exp[i(\alpha_{j1} - \alpha_{k1})] = \pm 1$ is the relative CP-parity of Majorana neutrinos χ_j and χ_k . The condition of CP invariance of the leptonic CC weak interaction reads [29]:

$$U_{lj}^* = U_{lj} \rho_j, \quad \rho_j = -i \eta_{CP}(\chi_j) = \pm 1, \tag{13.4}$$

where $\eta_{CP}(\chi_j)$ is the CP parity of the Majorana neutrino χ_j [32].

In the case of $n=3$ there are 3 CP violation phases - one Dirac and two Majorana. Even in the mixing involving only 2 massive Majorana neutrinos there is one physical CP violation Majorana phase.

II. Neutrino oscillations in vacuum. Neutrino oscillations are a quantum mechanical consequence of the existence of nonzero neutrino masses and neutrino (lepton) mixing, Eq. (13.1), and of the relatively small splitting between the neutrino masses.

Suppose the flavour neutrino ν_l is produced in a CC weak interaction process and is observed by a neutrino detector capable of detecting also neutrinos $\nu_{l'}$, $l' \neq l$. If lepton mixing, Eq. (13.1), takes place and the masses m_j of all neutrinos ν_j are sufficiently small, the state of the neutrino ν_l , $|\nu_l\rangle$, will be a coherent superposition of the states $|\nu_j\rangle$ of neutrinos ν_j :

$$|\nu_l\rangle = \sum_j U_{lj}^* |\nu_j; \tilde{p}_j\rangle, \quad l = e, \mu, \tau, \tag{13.5}$$

\tilde{p}_j being the 4-momentum of ν_j . For the state vector of the flavour antineutrino $\bar{\nu}_l$, produced in a weak interaction process, we get:

$$|\bar{\nu}_l\rangle = \sum_j U_{lj} |\bar{\nu}_j; \tilde{p}_j\rangle, \quad l = e, \mu, \tau. \tag{13.7}$$

Note the presence of U in Eq. (13.5) and U^* in Eq. (13.7).

We will consider the case of relativistic neutrinos ν_j , which corresponds to the conditions in both past and currently planned future neutrino oscillation experiments [36]. If the spectrum of neutrino masses is not degenerate, the states $|\nu_j; \tilde{p}_j\rangle$ in the r.h.s. of Eq. (13.5) will have different energies and different momenta, independently of the process in which they were produced: $\tilde{p}_j \neq \tilde{p}_k$, or $E_j \neq E_k$, $\mathbf{p}_j \neq \mathbf{p}_k$, $j \neq k$, where $E_j = \sqrt{p_j^2 + m_j^2}$, $p_j \equiv |\mathbf{p}_j|$. The deviations of E_j and p_j from the values for a massless neutrino E and $p = E$, are proportional to m_j^2/E_0 , E_0 being a characteristic energy of the process, and are extremely small.

Suppose that the neutrinos are observed via a CC weak interaction process and that in the detector's rest frame they are detected after time T after emission, after traveling a distance L . Then the amplitude of the probability that neutrino $\nu_{l'}$ will be observed if neutrino ν_l was produced by the neutrino source can be written as [33,35,37]:

$$A(\nu_l \rightarrow \nu_{l'}) = \sum_j U_{l'j} D_j U_{jl}^\dagger, \quad l, l' = e, \mu, \tau, \quad (13.8)$$

$$D_j \equiv D_j(\tilde{p}_j; L, T) = e^{-i\tilde{p}_j(x_f - x_0)} = e^{-i(E_j T - p_j L)}, \quad (13.9)$$

where D_j describes the propagation of ν_j between the source and the detector, U_{jl}^\dagger and $U_{l'j}$ are the amplitudes to find ν_j in the initial and in the final flavour neutrino state, respectively, x_0 and x_f are the space-time coordinates of the points of neutrino production and detection, $T = (t_f - t_0)$ and $L = \mathbf{k}(\mathbf{x}_f - \mathbf{x}_0)$, $\mathbf{p}_j = \mathbf{k}p_j$. What is relevant for the calculation of the probability $P(\nu_l \rightarrow \nu_{l'}) = |A(\nu_l \rightarrow \nu_{l'})|^2$ is the interference factor $D_j D_k^*$. The latter depends on the phase $\delta\varphi_{jk} = (E_j - E_k)T - (p_j - p_k)L$, which can be cast in the form:

$$\delta\varphi_{jk} = (E_j - E_k) \left[T - \frac{E_j + E_k}{p_j + p_k} L \right] + \frac{m_j^2 - m_k^2}{p_j + p_k} L. \quad (13.10)$$

The first term in the r.h.s. of Eq. (13.10) vanishes i) if [39] $T = (E_j + E_k)L/(p_j + p_k) = L/\bar{v}$, $\bar{v} = (E_j/(E_j + E_k))v_j + (E_k/(E_j + E_k))v_k$ being the "average" velocity of ν_j and ν_k , where $v_{j,k} = p_{j,k}/E_{j,k}$, or ii) if one assumes [40] that $E_j = E_k = E_0$. The relation $T = L/\bar{v}$ has not emerged so far from any dynamical (wave packet) calculations. If the states of ν_j and $\bar{\nu}_j$ in Eq. (13.5) - Eq. (13.7) have the same 3-momentum [37,41], $p_j = p_k = p$, the first term in the r.h.s. of Eq. (13.10) is negligible, being suppressed by the additional factor $(m_j^2 + m_k^2)/p^2$ since for relativistic neutrinos $L = T$ up to terms $\sim m_{j,k}^2/p^2$. One arrives at the same conclusion if $E_j \neq E_k$, $p_j \neq p_k$, $j \neq k$ [33].

Although the cases considered above are physically quite different, they lead to the same result for the phase difference $\delta\varphi_{jk}$:

$$\delta\varphi_{jk} \cong \frac{m_j^2 - m_k^2}{2p} L = 2\pi \frac{L}{L_{jk}^v} \text{sgn}(m_j^2 - m_k^2), \quad p = \frac{p_j + p_k}{2}, \quad (13.11)$$

where L_{jk}^v is the neutrino oscillation length associated with Δm_{jk}^2 ,

$$L_{jk}^v = 4\pi \frac{p}{|\Delta m_{jk}^2|} \cong 2.48 \text{ m} \frac{p[\text{MeV}]}{|\Delta m_{jk}^2|[\text{eV}^2]} \quad (13.12)$$

We can consider p to be the zero neutrino mass momentum, $p = E$. The phase difference $\delta\varphi_{jk}$, Eq. (13.11), is Lorentz-invariant.

Eq. (13.9) corresponds to a plane-wave description of the propagation of neutrinos ν_j . In the wave packet treatment of the problem, the interference

between the states of ν_j and ν_k is subject to a number of conditions, the localization condition and the condition of overlapping of the wave packets of ν_j and ν_k at the detection point being the most important (see, e.g., [33,35,37]).

For the $\nu_l \rightarrow \nu_{l'}$ and $\bar{\nu}_l \rightarrow \bar{\nu}_{l'}$ oscillation probabilities we get from Eq. (13.8), Eq. (13.9), and Eq. (13.11):

$$P(\nu_l \rightarrow \nu_{l'}) = \sum_j R_{jj}^{l'l} + 2 \sum_{j>k} |R_{jk}^{l'l}| \cos\left(\frac{\Delta m_{jk}^2}{2p} L - \phi_{jk}^{l'l}\right), \quad (13.13)$$

$$P(\bar{\nu}_l \rightarrow \bar{\nu}_{l'}) = \sum_j R_{jj}^{l'l} + 2 \sum_{j>k} |R_{jk}^{l'l}| \cos\left(\frac{\Delta m_{jk}^2}{2p} L + \phi_{jk}^{l'l}\right), \quad (13.14)$$

where $l, l' = e, \mu, \tau$, $R_{jk}^{l'l} = U_{lj} U_{lk}^* U_{lj}^* U_{lk}$ and $\phi_{jk}^{l'l} = \arg(R_{jk}^{l'l})$.

It follows from Eq. (13.8) - Eq. (13.10) that in order for neutrino oscillations to occur, at least two neutrinos ν_j should not be degenerate in mass and lepton mixing should take place, $U \neq \mathbf{1}$. The oscillations effects can be large if at least for one Δm_{jk}^2 we have $|\Delta m_{jk}^2 L|/(2p) = 2\pi L/L_{jk}^v \gtrsim 1$, i.e. the oscillation length L_{jk}^v is of the order of, or smaller, than source-detector distance L (otherwise the oscillations will not have time to develop before neutrinos reach the detector).

We see from Eq. (13.13) and Eq. (13.14) that $P(\nu_l \rightarrow \nu_{l'}) = P(\bar{\nu}_{l'} \rightarrow \bar{\nu}_l)$. This is a consequence of CPT invariance. The conditions of CP invariance read [30,42,43]: $P(\nu_l \rightarrow \nu_{l'}) = P(\bar{\nu}_l \rightarrow \bar{\nu}_{l'})$, $l, l' = e, \mu, \tau$. In the case of CPT invariance, which we will assume to hold, we get for the survival probabilities: $P(\nu_l \rightarrow \nu_l) = P(\bar{\nu}_l \rightarrow \bar{\nu}_l)$, $l, l' = e, \mu, \tau$. Thus, the study of the ‘‘disappearance’’ of ν_l and $\bar{\nu}_l$, caused by oscillations in vacuum, cannot be used to test the CP invariance in the lepton sector. It follows from Eq. (13.13) - Eq. (13.14) that we can have CP violation effects in neutrino oscillations only if U is not real. Eq. (13.2) and Eq. (13.13) - Eq. (13.14) imply that $P(\nu_l \rightarrow \nu_{l'})$ and $P(\bar{\nu}_l \rightarrow \bar{\nu}_{l'})$ do not depend on the Majorana phases in the neutrino mixing matrix U [30]. Thus, i) in the case of oscillations in vacuum, only the Dirac phase(s) in U can cause CP violating effects leading to $P(\nu_l \rightarrow \nu_{l'}) \neq P(\bar{\nu}_l \rightarrow \bar{\nu}_{l'})$, $l \neq l'$, and ii) the experiments investigating the $\nu_l \rightarrow \nu_{l'}$ and $\bar{\nu}_l \rightarrow \bar{\nu}_{l'}$ oscillations cannot provide information on the nature - Dirac or Majorana, of massive neutrinos [30,44].

As a measure of CP violation in neutrino oscillations we can consider the asymmetry: $A_{\text{CP}}^{(l'l)} = P(\nu_l \rightarrow \nu_{l'}) - P(\bar{\nu}_l \rightarrow \bar{\nu}_{l'}) = -A_{\text{CP}}^{(l'l)}$. In the case of 3-neutrino mixing one has [45]: $A_{\text{CP}}^{(\mu e)} = -A_{\text{CP}}^{(\tau e)} = A_{\text{CP}}^{(\tau \mu)}$,

$$A_{\text{CP}}^{(\mu e)} = 4 J_{\text{CP}} \left(\sin \frac{\Delta m_{32}^2}{2p} L + \sin \frac{\Delta m_{21}^2}{2p} L + \sin \frac{\Delta m_{13}^2}{2p} L \right), \quad (13.18)$$

where $J_{\text{CP}} = \text{Im}(U_{\mu 3} U_{e 3}^* U_{e 2} U_{\mu 2}^*)$ is analogous to the rephasing invariant associated with the CP violation in the quark mixing [46]. Thus, J_{CP} controls the magnitude of CP violation effects in neutrino oscillations in the case of 3-neutrino mixing. Even if $J_{\text{CP}} \neq 0$, we will have $A_{\text{CP}}^{(l'l)} = 0$ unless all three $\sin(\Delta m_{ij}^2/(2p))L \neq 0$ in Eq. (13.18).

Consider next neutrino oscillations in the case of one neutrino mass squared difference ‘‘dominance’’: suppose that $|\Delta m_{j1}^2| \ll |\Delta m_{n1}^2|$, $j = 2, \dots, (n-1)$, $|\Delta m_{n1}^2| L/(2p) \gtrsim 1$ and $|\Delta m_{j1}^2| L/(2p) \ll 1$, so that

$\exp[i(\Delta m_{j1}^2 L/(2p))] \cong 1$, $j = 2, \dots, (n-1)$. Under these conditions we obtain from Eq. (13.13) and Eq. (13.14), keeping only the oscillating terms involving Δm_{n1}^2 : $P(\nu_{l(l')} \rightarrow \nu_{l'(l)}) \cong P(\bar{\nu}_{l(l')} \rightarrow \bar{\nu}_{l'(l)})$,

$$P(\nu_{l(l')} \rightarrow \nu_{l'(l)}) \cong \delta_{ll'} - 4|U_{ln}|^2 \left[\delta_{ll'} - |U_{l'n}|^2 \right] \sin^2 \frac{\Delta m_{n1}^2 L}{4p}. \quad (13.20)$$

It follows from the neutrino oscillation data that in the case of 3-neutrino mixing, one of the two independent neutrino mass squared differences, say Δm_{21}^2 , is much smaller in absolute value than the second one, Δm_{31}^2 : $|\Delta m_{21}^2|/|\Delta m_{31}^2| \cong 0.032$, $|\Delta m_{31}^2| \cong 2.4 \times 10^{-3} \text{ eV}^2$. Eq. (13.20) with $n = 3$, describes with a relatively good precision the oscillations of i) reactor $\bar{\nu}_e$ ($l, l' = e$) on a distance $L \sim 1 \text{ km}$, corresponding to the CHOOZ and the Double Chooz, Daya Bay and RENO experiments, and of ii) the accelerator ν_μ ($l, l' = \mu$), seen in the K2K and MINOS experiments. The $\nu_\mu \rightarrow \nu_\tau$ oscillations, which the OPERA experiment is aiming to detect, can be described in the case of 3-neutrino mixing by Eq. (13.20) with $n = 3$ and $l = \mu, l' = \tau$.

In certain cases the dimensions of the neutrino source, ΔL , and/or the energy resolution of the detector, ΔE , have to be included in the analysis of the neutrino oscillation data. If [29] $2\pi\Delta L/L_{jk}^v \gg 1$, and/or $2\pi(L/L_{jk}^v)(\Delta E/E) \gg 1$, the interference terms in $P(\nu_l \rightarrow \nu_{l'})$ and $P(\bar{\nu}_{l'} \rightarrow \bar{\nu}_l)$ will be strongly suppressed and the neutrino flavour conversion will be determined by the average probabilities: $\bar{P}(\nu_l \rightarrow \nu_{l'}) = \bar{P}(\bar{\nu}_{l'} \rightarrow \bar{\nu}_l) \cong \sum_j |U_{l'j}|^2 |U_{lj}|^2$. Suppose next that in the case of 3-neutrino mixing, $|\Delta m_{21}^2|L/(2p) \sim 1$, while $|\Delta m_{31(32)}^2|L/(2p) \gg 1$, and the oscillations due to $\Delta m_{31(32)}^2$ are strongly suppressed (averaged out) due to integration over the region of neutrino production, *etc.* In this case we get for the ν_e and $\bar{\nu}_e$ survival probabilities: $P(\nu_e \rightarrow \nu_e) = P(\bar{\nu}_e \rightarrow \bar{\nu}_e) \equiv P_{ee}$,

$$P_{ee} \cong |U_{e3}|^4 + \left(1 - |U_{e3}|^2\right)^2 \left[1 - \sin^2 2\theta_{12} \sin^2 \frac{\Delta m_{21}^2 L}{4p}\right] \quad (13.26)$$

with θ_{12} determined by $\cos^2 \theta_{12} = |U_{e1}|^2/(1 - |U_{e3}|^2)$, $\sin^2 \theta_{12} = |U_{e2}|^2/(1 - |U_{e3}|^2)$. Eq. (13.26) describes the effects of reactor $\bar{\nu}_e$ oscillations observed by the KamLAND experiment ($L \sim 180 \text{ km}$).

The data of ν -oscillations experiments is often analyzed assuming 2-neutrino mixing: $|\nu_l\rangle = |\nu_1\rangle \cos \theta + |\nu_2\rangle \sin \theta$, $|\nu_x\rangle = -|\nu_1\rangle \sin \theta + |\nu_2\rangle \cos \theta$, where θ is the neutrino mixing angle in vacuum and ν_x is another flavour neutrino or sterile (anti-) neutrino, $x = l' \neq l$ or $\nu_x \equiv \bar{\nu}_s$. In this case we have [41]: $\Delta m^2 = m_2^2 - m_1^2 > 0$,

$$P^{2\nu}(\nu_l \rightarrow \nu_l) = 1 - \sin^2 2\theta \sin^2 \pi \frac{L}{L^v}, \quad L^v = 4\pi p/\Delta m^2, \quad (13.30)$$

$P^{2\nu}(\nu_l \rightarrow \nu_x) = 1 - P^{2\nu}(\nu_l \rightarrow \nu_l)$. Eq. (13.30) with $l = \mu, x = \tau$ was used, *e.g.*, in the atmospheric neutrino data analysis [13], in which the first compelling evidence for neutrino oscillations was obtained.

III. Matter effects in neutrino oscillations. When neutrinos propagate in matter (*e.g.*, in the Earth, Sun or a supernova), their coherent forward-scattering from the particles present in matter can change drastically the pattern of neutrino oscillations [25,26,52]. Thus, the probabilities of neutrino transitions in matter can differ significantly from the corresponding vacuum oscillation probabilities.

In the case of, *e.g.*, solar ν_e transitions in the Sun and 3-neutrino mixing, the oscillations due to Δm_{31}^2 are strongly suppressed by the

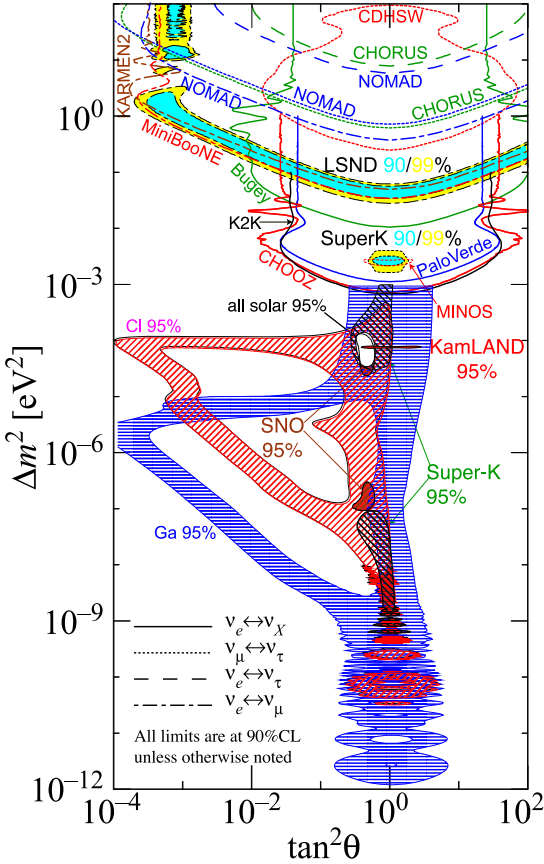


Figure 13.10: The regions of squared-mass splitting and mixing angle favored or excluded by various experiments. The figure was contributed by H. Murayama (University of California, Berkeley, and IPMU, University of Tokyo).

averaging over the region of neutrino production in the Sun. The ν_e undergo transitions into $(\nu_\mu + \nu_\tau)/\sqrt{2}$. As a consequence of the effects of the solar matter, the solar ν_e transitions observed by the Super-Kamiokande and SNO experiments exhibit a characteristic dependence on $\sin^2 \theta_{12}$: $P_{\odot}^{3\nu}(\nu_e \rightarrow \nu_e) \cong |U_{e3}|^4 + (1 - |U_{e3}|^2)^2 \sin^2 \theta_{12}$. The data show that $P_{\odot}^{3\nu} \cong 0.3$, which is a strong evidence for solar matter effects in the transitions [85] since in the case of transitions in vacuum $P_{\odot}^{3\nu} \cong |U_{e3}|^4 + (1 - |U_{e3}|^2)^2 (1 - 0.5 \sin^2 2\theta_{12}) \gtrsim 0.48$, where we used the experimental limits $|U_{e3}|^2 < 0.056$ and $\sin^2 2\theta_{12} \lesssim 0.93$.

IV. The evidence for flavour neutrino oscillations. The evidence for flavour neutrino oscillations/transitions is compelling. We discuss the relevant data in the full edition. The regions of the oscillation parameter space favored or excluded by various neutrino oscillation experiments are shown in Fig. 13.10.

V. Three neutrino mixing. All compelling data on neutrino oscillations can be described assuming 3-flavour neutrino mixing in vacuum. In this case U can be parametrised as

$$U = \begin{bmatrix} c_{12}c_{13} & s_{12}c_{13} & s_{13}e^{-i\delta} \\ -s_{12}c_{23} - c_{12}s_{23}s_{13}e^{i\delta} & c_{12}c_{23} - s_{12}s_{23}s_{13}e^{i\delta} & s_{23}c_{13} \\ s_{12}s_{23} - c_{12}c_{23}s_{13}e^{i\delta} & -c_{12}s_{23} - s_{12}c_{23}s_{13}e^{i\delta} & c_{23}c_{13} \end{bmatrix} \times \text{diag}(1, e^{i\frac{\alpha_{21}}{2}}, e^{i\frac{\alpha_{31}}{2}}). \quad (13.77)$$

where $c_{ij} = \cos \theta_{ij}$, $s_{ij} = \sin \theta_{ij}$, the angles $\theta_{ij} = [0, \pi/2]$, $\delta = [0, 2\pi]$ is the Dirac CP violation phase and α_{21} , α_{31} are the two Majorana phases. The existing neutrino oscillation data allow us to determine the parameters which drive the solar ν_e and the dominant atmospheric $\nu_\mu \rightarrow \nu_\tau$ oscillations, $\Delta m_{21}^2 > 0$, $\sin^2 \theta_{12}$, and $|\Delta m_{31}^2|$, $\sin^2 2\theta_{23}$, with a relatively good precision, and to obtain rather stringent limit on the angle θ_{13} : $\Delta m_{21}^2 \cong 7.65 \times 10^{-5} \text{ eV}^2$, $\sin^2 \theta_{12} \cong 0.304$, $|\Delta m_{31}^2| \cong 2.40 \times 10^{-3} \text{ eV}^2$, $\sin^2 2\theta_{23} \cong 1$, $\sin^2 \theta_{13} < 0.056$ (at 3σ). These results imply that $\Delta m_{21}^2 \ll |\Delta m_{31}^2|$ and that $\theta_{23} \cong \pi/4$, $\theta_{12} \cong \pi/5.4$ and $\theta_{13} < \pi/13$. Thus, the pattern of neutrino mixing is drastically different from the pattern of quark mixing.

The existing neutrino oscillation data do not allow to determine the sign of $\Delta m_{31(32)}^2$. Correspondingly, two types of neutrino mass spectrum are possible: *i) with normal ordering*: $m_1 < m_2 < m_3$, $\Delta m_{31}^2 > 0$, $\Delta m_{21}^2 > 0$, $m_{2(3)} = (m_1^2 + \Delta m_{21(31)}^2)^{\frac{1}{2}}$; *ii) with inverted ordering (IO)*: $m_3 < m_1 < m_2$, $\Delta m_{32(31)}^2 < 0$, $\Delta m_{21}^2 > 0$, $m_2 = (m_3^2 + \Delta m_{23}^2)^{\frac{1}{2}}$, $m_1 = (m_3^2 + \Delta m_{23}^2 - \Delta m_{21}^2)^{\frac{1}{2}}$. Depending on the values of the lightest neutrino mass [113], $\min(m_j)$, the neutrino mass spectrum can also be: *a) normal hierarchical (NH)*: $m_1 \ll m_2 < m_3$; or *b) inverted hierarchical (IH)*: $m_3 \ll m_1 < m_2$; or *c) quasi-degenerate (QD)*: $m_1 \cong m_2 \cong m_3 \equiv m_0$, $m_j^2 \gg |\Delta m_{21,31}^2|$, $m_0 \gtrsim 0.10 \text{ eV}$. All three types of spectrum are compatible with the existing data.

At present no experimental information on the CP violation phases in the mixing matrix U is available. The J_{CP} factor (see Eq. (13.18)) in the ‘‘standard’’ parametrisation (Eq. (13.77)) of U has the form: $J_{CP} = (1/8) \cos \theta_{13} \sin 2\theta_{12} \sin 2\theta_{23} \sin 2\theta_{13} \sin \delta$. Thus, the size of CP violation effects in neutrino oscillations depends on the currently unknown values of the ‘‘small’’ angle θ_{13} and the Dirac phase δ .

The Majorana nature of massive neutrinos ν_j manifests itself in the existence of $|\Delta L| = 2$ processes: $\mu^- + (A, Z) \rightarrow \mu^+ + (A, Z - 2)$, etc. The latter can be triggered by the exchange of the neutrino ν_j if it is identical with its antiparticle. The only feasible experiments having the potential of establishing that the massive neutrinos are Majorana particles are at present the experiments searching for $(\beta\beta)_{0\nu}$ -decay: $(A, Z) \rightarrow (A, Z + 2) + e^- + e^-$ (see e.g., Ref. 124). One may expect that the dominant contribution in the $(\beta\beta)_{0\nu}$ -decay amplitude is due to the exchange of the light Majorana neutrinos ν_j . In this case the $(\beta\beta)_{0\nu}$ -decay rate is proportional to $|\langle m \rangle|^2$, where $\langle m \rangle$ is the ‘‘ $(\beta\beta)_{0\nu}$ -decay effective Majorana mass’’, $|\langle m \rangle| = |\sum_j U_{ej}^2 m_j|$.

Determining the type of neutrino mass spectrum, the status of the CP symmetry in the lepton sector and the nature of massive neutrinos are among the major goals of the future studies in neutrino physics.

14. QUARK MODEL

Revised September 2009 by C. Amsler (University of Zürich), T. DeGrand (University of Colorado, Boulder), and B. Krusche (University of Basel).

14.1. Quantum numbers of the quarks

Quarks are strongly interacting fermions with spin 1/2 and, by convention, positive parity. Antiquarks have negative parity. Quarks have the additive baryon number 1/3, antiquarks -1/3. Table 14.1 gives the other additive quantum numbers (flavors) for the three generations of quarks. They are related to the charge Q (in units of the elementary charge e) through the generalized Gell-Mann-Nishijima formula

$$Q = I_z + \frac{B + S + C + B + T}{2}, \quad (14.1)$$

where B is the baryon number. The convention is that the *flavor* of a quark (I_z , S , C , B , or T) has the same sign as its *charge* Q . With this convention, any flavor carried by a charged meson has the same sign as its charge, *e.g.*, the strangeness of the K^+ is +1, the bottomness of the B^+ is +1, and the charm and strangeness of the D_s^- are each -1. Antiquarks have the opposite flavor signs.

14.2. Mesons

Mesons have baryon number $B = 0$. In the quark model, they are $q\bar{q}'$ bound states of quarks q and antiquarks \bar{q}' (the flavors of q and q' may be different). If the orbital angular momentum of the $q\bar{q}'$ state is ℓ , then the parity P is $(-1)^{\ell+1}$. The meson spin J is given by the usual relation $|\ell - s| \leq J \leq |\ell + s|$, where s is 0 (antiparallel quark spins) or 1 (parallel quark spins). The charge conjugation, or C -parity $C = (-1)^{\ell+s}$, is defined only for the $q\bar{q}$ states made of quarks and their own antiquarks. The C -parity can be generalized to the G -parity $G = (-1)^{I+\ell+s}$ for mesons made of quarks and their own antiquarks (isospin $I_z = 0$), and for the charged $u\bar{d}$ and $d\bar{u}$ states (isospin $I = 1$).

The mesons are classified in J^{PC} multiplets. The $\ell = 0$ states are the pseudoscalars (0^{-+}) and the vectors (1^{-}). The orbital excitations $\ell = 1$ are the scalars (0^{++}), the axial vectors (1^{++}) and (1^{+-}), and the tensors (2^{++}). Assignments for many of the known mesons are given in Tables 14.2 and 14.3. Radial excitations are denoted by the principal quantum number n . The very short lifetime of the t quark makes it likely that bound-state hadrons containing t quarks and/or antiquarks do not exist.

States in the natural spin-parity series $P = (-1)^J$ must, according to the above, have $s = 1$ and hence, $CP = +1$. Thus, mesons with natural spin-parity and $CP = -1$ (0^{+-} , 1^{-+} , 2^{+-} , 3^{-+} , *etc.*) are forbidden in the $q\bar{q}'$ model. The $J^{PC} = 0^{--}$ state is forbidden as well. Mesons with such *exotic* quantum numbers may exist, but would lie outside the $q\bar{q}'$ model (see section below on exotic mesons).

Following SU(3), the nine possible $q\bar{q}'$ combinations containing the light u , d , and s quarks are grouped into an octet and a singlet of light quark mesons:

$$\mathbf{3} \otimes \bar{\mathbf{3}} = \mathbf{8} \oplus \mathbf{1}. \quad (14.2)$$

A fourth quark such as charm c can be included by extending SU(3) to SU(4). However, SU(4) is badly broken owing to the much heavier c

quark. Nevertheless, in an SU(4) classification, the sixteen mesons are grouped into a 15-plet and a singlet:

$$4 \otimes \bar{4} = 15 \oplus 1. \quad (14.3)$$

The *weight diagrams* for the ground-state pseudoscalar (0^{-+}) and vector (1^{--}) mesons are depicted in Fig. 14.1. The light quark mesons are members of nonets building the middle plane in Fig. 14.1(a) and (b).

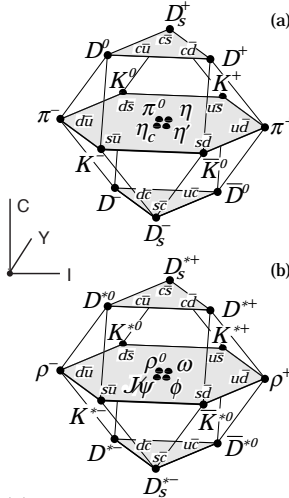


Figure 14.1: SU(4) weight diagram showing the 16-plets for the pseudoscalar (a) and vector mesons (b) made of the u , d , s , and c quarks as a function of isospin I , charm C , and hypercharge $Y = S + B - \frac{C}{3}$. The nonets of light mesons occupy the central planes to which the $c\bar{c}$ states have been added.

Isoscalar states with the same J^{PC} will mix, but mixing between the two light quark isoscalar mesons, and the much heavier charmonium or bottomonium states, are generally assumed to be negligible.

14.3. Baryons: qqq states

Baryons are fermions with baryon number $B = 1$, *i.e.*, in the most general case, they are composed of three quarks plus any number of quark - antiquark pairs. Although recently some experimental evidence for ($qqqq\bar{q}$) pentaquark states has been claimed (see review on Possible Exotic Baryon Resonance), so far all established baryons are 3-quark (qqq) configurations. The color part of their state functions is an SU(3) singlet, a completely antisymmetric state of the three colors. Since the quarks are fermions, the state function must be antisymmetric under interchange of any two equal-mass quarks (up and down quarks in the limit of isospin symmetry). Thus it can be written as

$$|qqq\rangle_A = |\text{color}\rangle_A \times |\text{space, spin, flavor}\rangle_S, \quad (14.21)$$

where the subscripts S and A indicate symmetry or antisymmetry under interchange of any two equal-mass quarks. Note the contrast with the state function for the three nucleons in ${}^3\text{H}$ or ${}^3\text{He}$:

$$|NNN\rangle_A = |\text{space, spin, isospin}\rangle_A. \quad (14.22)$$

This difference has major implications for internal structure, magnetic moments, *etc.*

The “ordinary” baryons are made up of u , d , and s quarks. The three flavors imply an approximate flavor $SU(3)$, which requires that baryons made of these quarks belong to the multiplets on the right side of

$$\mathbf{3} \otimes \mathbf{3} \otimes \mathbf{3} = \mathbf{10}_S \oplus \mathbf{8}_M \oplus \mathbf{8}_M \oplus \mathbf{1}_A \quad (14.23)$$

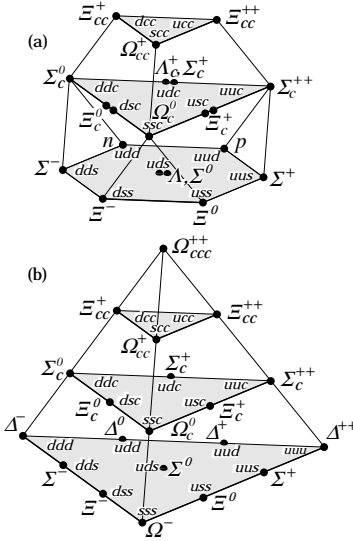


Figure 14.2: $SU(4)$ multiplets of baryons made of u , d , s , and c quarks. (a) The 20-plet with an $SU(3)$ octet. (b) The 20-plet with an $SU(3)$ decuplet.

Here the subscripts indicate symmetric, mixed-symmetry, or anti-symmetric states under interchange of any two quarks. The $\mathbf{1}$ is a uds state (Λ_1), and the octet contains a similar state (Λ_8). If these have the same spin and parity, they can mix. The mechanism is the same as for the mesons (see above). In the ground state multiplet, the $SU(3)$ flavor singlet Λ_1 is forbidden by Fermi statistics. Section 37, on “ $SU(3)$ Isoscalar Factors and Representation Matrices,” shows how relative decay rates in, say, $\mathbf{10} \rightarrow \mathbf{8} \otimes \mathbf{8}$ decays may be calculated. The addition of the c quark to the light quarks extends the flavor symmetry to $SU(4)$. However, due to the large mass of the c quark, this symmetry is much more strongly broken than the $SU(3)$ of the three light quarks. Figures 14.2(a) and 14.2(b) show the $SU(4)$ baryon multiplets that have as their bottom levels an $SU(3)$ octet, such as the octet that includes the nucleon, or an $SU(3)$ decuplet, such as the decuplet that includes the $\Delta(1232)$. All particles in a given $SU(4)$ multiplet have the same spin and parity. The charmed baryons are discussed in more detail in the “Note on Charmed Baryons” in the Particle Listings. The addition of a b quark extends the flavor symmetry to $SU(5)$; the existence of baryons with t -quarks is very unlikely due to the short lifetime of the top.

For further details, see the full *Review of Particle Physics*.

16. STRUCTURE FUNCTIONS

Updated September 2007 by B. Foster (University of Oxford), A.D. Martin (University of Durham), and M.G. Vincter (Carleton University).

16.1. Deep inelastic scattering

High-energy lepton-nucleon scattering (deep inelastic scattering) plays a key role in determining the partonic structure of the proton. The process $\ell N \rightarrow \ell' X$ is illustrated in Fig. 16.1. The filled circle in this figure represents the internal structure of the proton which can be expressed in terms of structure functions.

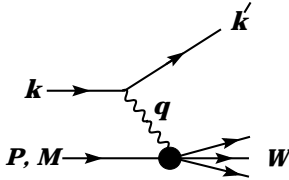


Figure 16.1: Kinematic quantities for the description of deep inelastic scattering. The quantities k and k' are the four-momenta of the incoming and outgoing leptons, P is the four-momentum of a nucleon with mass M , and W is the mass of the recoiling system X . The exchanged particle is a γ , W^\pm , or Z ; it transfers four-momentum $q = k - k'$ to the nucleon.

Invariant quantities:

$\nu = \frac{q \cdot P}{M} = E - E'$ is the lepton's energy loss in the nucleon rest frame (in earlier literature sometimes $\nu = q \cdot P$). Here, E and E' are the initial and final lepton energies in the nucleon rest frame.

$Q^2 = -q^2 = 2(E E' - \vec{k} \cdot \vec{k}') - m_\ell^2 - m_{\ell'}^2$ where $m_\ell(m_{\ell'})$ is the initial (final) lepton mass. If $E E' \sin^2(\theta/2) \gg m_\ell^2, m_{\ell'}^2$, then $\approx 4E E' \sin^2(\theta/2)$, where θ is the lepton's scattering angle with respect to the lepton beam direction.

$x = \frac{Q^2}{2M\nu}$ where, in the parton model, x is the fraction of the nucleon's momentum carried by the struck quark.

$y = \frac{q \cdot P}{k \cdot P} = \frac{\nu}{E}$ is the fraction of the lepton's energy lost in the nucleon rest frame.

$W^2 = (P + q)^2 = M^2 + 2M\nu - Q^2$ is the mass squared of the system X recoiling against the scattered lepton.

$s = (k + P)^2 = \frac{Q^2}{xy} + M^2 + m_\ell^2$ is the center-of-mass energy squared of the lepton-nucleon system.

The process in Fig. 16.1 is called deep ($Q^2 \gg M^2$) inelastic ($W^2 \gg M^2$) scattering (DIS). In what follows, the masses of the initial and scattered leptons, m_ℓ and $m_{\ell'}$, are neglected.

16.1.1. DIS cross sections :

$$\frac{d^2\sigma}{dx dy} = x(s - M^2) \frac{d^2\sigma}{dx dQ^2} = \frac{2\pi M\nu}{E'} \frac{d^2\sigma}{d\Omega_{\text{Nrest}} dE'} . \quad (16.1)$$

In lowest-order perturbation theory, the cross section for the scattering of polarized leptons on polarized nucleons can be expressed in terms of the products of leptonic and hadronic tensors associated with the coupling of the exchanged bosons at the upper and lower vertices in Fig. 16.1 (see Refs. 1-4)

$$\frac{d^2\sigma}{dx dy} = \frac{2\pi y \alpha^2}{Q^4} \sum_j \eta_j L_j^{\mu\nu} W_{\mu\nu}^j . \quad (16.2)$$

For neutral-current processes, the summation is over $j = \gamma, Z$ and γZ representing photon and Z exchange and the interference between them, whereas for charged-current interactions there is only W exchange, $j = W$. (For transverse nucleon polarization, there is a dependence on the azimuthal angle of the scattered lepton.) $L_{\mu\nu}$ is the lepton tensor associated with the coupling of the exchange boson to the leptons. For incoming leptons of charge $e = \pm 1$ and helicity $\lambda = \pm 1$,

$$\begin{aligned} L_{\mu\nu}^\gamma &= 2 \left(k_\mu k'_\nu + k'_\mu k_\nu - k \cdot k' g_{\mu\nu} - i\lambda \varepsilon_{\mu\nu\alpha\beta} k^\alpha k'^\beta \right), \\ L_{\mu\nu}^{\gamma Z} &= (g_V^e + e\lambda g_A^e) L_{\mu\nu}^\gamma, \quad L_{\mu\nu}^Z = (g_V^e + e\lambda g_A^e)^2 L_{\mu\nu}^\gamma, \\ L_{\mu\nu}^W &= (1 + e\lambda)^2 L_{\mu\nu}^\gamma, \end{aligned} \quad (16.3)$$

where $g_V^e = -\frac{1}{2} + 2\sin^2\theta_W$, $g_A^e = -\frac{1}{2}$. Although here the helicity formalism is adopted, an alternative approach is to express the tensors in Eq. (16.3) in terms of the polarization of the lepton.

The factors η_j in Eq. (16.2) denote the ratios of the corresponding propagators and couplings to the photon propagator and coupling squared

$$\begin{aligned} \eta_\gamma &= 1 \quad ; \quad \eta_{\gamma Z} = \left(\frac{G_F M_Z^2}{2\sqrt{2}\pi\alpha} \right) \left(\frac{Q^2}{Q^2 + M_Z^2} \right); \\ \eta_Z &= \eta_{\gamma Z}^2 \quad ; \quad \eta_W = \frac{1}{2} \left(\frac{G_F M_W^2}{4\pi\alpha} \frac{Q^2}{Q^2 + M_W^2} \right)^2 . \end{aligned} \quad (16.4)$$

The hadronic tensor, which describes the interaction of the appropriate electroweak currents with the target nucleon, is given by

$$W_{\mu\nu} = \frac{1}{4\pi} \int d^4z e^{iq \cdot z} \langle P, S \left[\left[J_\mu^\dagger(z), J_\nu(0) \right] \right] P, S \rangle, \quad (16.5)$$

where S denotes the nucleon-spin 4-vector, with $S^2 = -M^2$ and $S \cdot P = 0$.

16.2. Structure functions of the proton

The structure functions are defined in terms of the hadronic tensor (see Refs. 1-3)

$$\begin{aligned} W_{\mu\nu} &= \left(-g_{\mu\nu} + \frac{q_\mu q_\nu}{q^2} \right) F_1(x, Q^2) + \frac{\hat{P}_\mu \hat{P}_\nu}{P \cdot q} F_2(x, Q^2) \\ &- i\varepsilon_{\mu\nu\alpha\beta} \frac{q^\alpha P^\beta}{2P \cdot q} F_3(x, Q^2) \\ &+ i\varepsilon_{\mu\nu\alpha\beta} \frac{q^\alpha}{P \cdot q} \left[S^\beta g_1(x, Q^2) + \left(S^\beta - \frac{S \cdot q}{P \cdot q} P^\beta \right) g_2(x, Q^2) \right] \end{aligned}$$

$$\begin{aligned}
 & + \frac{1}{P \cdot q} \left[\frac{1}{2} (\hat{P}_\mu \hat{S}_\nu + \hat{S}_\mu \hat{P}_\nu) - \frac{S \cdot q}{P \cdot q} \hat{P}_\mu \hat{P}_\nu \right] g_3(x, Q^2) \\
 & + \frac{S \cdot q}{P \cdot q} \left[\frac{\hat{P}_\mu \hat{P}_\nu}{P \cdot q} g_4(x, Q^2) + \left(-g_{\mu\nu} + \frac{q_\mu q_\nu}{q^2} \right) g_5(x, Q^2) \right] \quad (16.6)
 \end{aligned}$$

where

$$\hat{P}_\mu = P_\mu - \frac{P \cdot q}{q^2} q_\mu, \quad \hat{S}_\mu = S_\mu - \frac{S \cdot q}{q^2} q_\mu. \quad (16.7)$$

The cross sections for neutral- and charged-current deep inelastic scattering on unpolarized nucleons can be written in terms of the structure functions in the generic form

$$\begin{aligned}
 \frac{d^2\sigma^i}{dx dy} &= \frac{4\pi\alpha^2}{xyQ^2} \eta^i \left\{ \left(1 - y - \frac{x^2 y^2 M^2}{Q^2} \right) F_2^i \right. \\
 & \left. + y^2 x F_1^i \mp \left(y - \frac{y^2}{2} \right) x F_3^i \right\}, \quad (16.8)
 \end{aligned}$$

where $i = \text{NC, CC}$ corresponds to neutral-current ($eN \rightarrow eX$) or charged-current ($eN \rightarrow \nu X$ or $\nu N \rightarrow eX$) processes, respectively. For incoming neutrinos, $L_{\mu\nu}^W$ of Eq. (16.3) is still true, but with e, λ corresponding to the outgoing charged lepton. In the last term of Eq. (16.8), the $-$ sign is taken for an incoming e^+ or $\bar{\nu}$ and the $+$ sign for an incoming e^- or ν . The factor $\eta^{\text{NC}} = 1$ for unpolarized e^\pm beams, whereas

$$\eta^{\text{CC}} = (1 \pm \lambda)^2 \eta_W \quad (16.9)$$

with \pm for ℓ^\pm ; and where λ is the helicity of the incoming lepton and η_W is defined in Eq. (16.4); for incoming neutrinos $\eta^{\text{CC}} = 4\eta_W$. The CC structure functions, which derive exclusively from W exchange, are

$$F_1^{\text{CC}} = F_1^W, \quad F_2^{\text{CC}} = F_2^W, \quad xF_3^{\text{CC}} = xF_3^W. \quad (16.10)$$

The NC structure functions $F_2^\gamma, F_2^{\gamma Z}, F_2^Z$ are, for $e^\pm N \rightarrow e^\pm X$, given by Ref. [5],

$$F_2^{\text{NC}} = F_2^\gamma - (g_V^\pm \pm \lambda g_A^e) \eta_{\gamma Z} F_2^{\gamma Z} + (g_V^{\pm 2} + g_A^{\pm 2} \pm 2\lambda g_V^e g_A^e) \eta_Z F_2^Z \quad (16.11)$$

and similarly for F_1^{NC} , whereas

$$xF_3^{\text{NC}} = -(g_A^\pm \pm \lambda g_V^e) \eta_{\gamma Z} xF_3^{\gamma Z} + [2g_V^e g_A^e \pm \lambda(g_V^{\pm 2} + g_A^{\pm 2})] \eta_Z xF_3^Z. \quad (16.12)$$

The polarized cross-section difference

$$\Delta\sigma = \sigma(\lambda_n = -1, \lambda_\ell) - \sigma(\lambda_n = 1, \lambda_\ell), \quad (16.13)$$

where λ_ℓ, λ_n are the helicities (± 1) of the incoming lepton and nucleon, respectively, may be expressed in terms of the five structure functions $g_{1, \dots, 5}(x, Q^2)$ of Eq. (16.6). Thus,

$$\begin{aligned}
 \frac{d^2\Delta\sigma^i}{dx dy} &= \frac{8\pi\alpha^2}{xyQ^2} \eta^i \left\{ -\lambda_\ell y \left(2 - y - 2x^2 y^2 \frac{M^2}{Q^2} \right) x g_1^i + \lambda_\ell 4x^3 y^2 \frac{M^2}{Q^2} g_2^i \right. \\
 & + 2x^2 y \frac{M^2}{Q^2} \left(1 - y - x^2 y^2 \frac{M^2}{Q^2} \right) g_3^i \\
 & \left. - \left(1 + 2x^2 y \frac{M^2}{Q^2} \right) \left[\left(1 - y - x^2 y^2 \frac{M^2}{Q^2} \right) g_4^i + xy^2 g_5^i \right] \right\} \quad (16.14)
 \end{aligned}$$

with $i = \text{NC}$ or CC as before. In the $M^2/Q^2 \rightarrow 0$ limit, Eq. (16.8) and Eq. (16.14) may be written in the form

$$\begin{aligned} \frac{d^2\sigma^i}{dxdy} &= \frac{2\pi\alpha^2}{xyQ^2} \eta^i \left[Y_+ F_2^i \mp Y_- x F_3^i - y^2 F_L^i \right], \\ \frac{d^2\Delta\sigma^i}{dxdy} &= \frac{4\pi\alpha^2}{xyQ^2} \eta^i \left[-Y_+ g_4^i \mp Y_- 2xg_1^i + y^2 g_L^i \right], \end{aligned} \quad (16.16)$$

with $i = \text{NC}$ or CC , where $Y_{\pm} = 1 \pm (1-y)^2$ and

$$F_L^i = F_2^i - 2xF_1^i, \quad g_L^i = g_4^i - 2xg_5^i. \quad (16.17)$$

In the naive quark-parton model, the analogy with the Callan-Gross relations [6] $F_L^i = 0$, are the Dicus relations [7] $g_L^i = 0$. Therefore, there are only two independent polarized structure functions: g_1 (parity conserving) and g_5 (parity violating), in analogy with the unpolarized structure functions F_1 and F_3 .

16.2.1. Structure functions in the quark-parton model :

In the quark-parton model [8,9], contributions to the structure functions F^i and g^i can be expressed in terms of the quark distribution functions $q(x, Q^2)$ of the proton, where $q = u, \bar{u}, d, \bar{d}$ etc. The quantity $q(x, Q^2)dx$ is the number of quarks (or antiquarks) of designated flavor that carry a momentum fraction between x and $x + dx$ of the proton's momentum in a frame in which the proton momentum is large.

For the neutral-current processes $ep \rightarrow eX$,

$$\begin{aligned} [F_2^\gamma, F_2^{\gamma Z}, F_2^Z] &= x \sum_q \left[e_q^2, 2e_q g_V^q, g_V^{q^2} + g_A^{q^2} \right] (q + \bar{q}), \\ [F_3^\gamma, F_3^{\gamma Z}, F_3^Z] &= \sum_q \left[0, 2e_q g_A^q, 2g_V^q g_A^q \right] (q - \bar{q}), \\ [g_1^\gamma, g_1^{\gamma Z}, g_1^Z] &= \frac{1}{2} \sum_q \left[e_q^2, 2e_q g_V^q, g_V^{q^2} + g_A^{q^2} \right] (\Delta q + \Delta \bar{q}), \\ [g_5^\gamma, g_5^{\gamma Z}, g_5^Z] &= \sum_q \left[0, e_q g_A^q, g_V^q g_A^q \right] (\Delta q - \Delta \bar{q}), \end{aligned} \quad (16.18)$$

where $g_V^q = \pm \frac{1}{2} - 2e_q \sin^2 \theta_W$ and $g_A^q = \pm \frac{1}{2}$, with \pm according to whether q is a u - or d -type quark respectively. The quantity Δq is the difference $q \uparrow - q \downarrow$ of the distributions with the quark spin parallel and antiparallel to the proton spin.

For the charged-current processes $e^-p \rightarrow \nu X$ and $\bar{\nu}p \rightarrow e^+X$, the structure functions are:

$$\begin{aligned} F_2^{W^-} &= 2x(u + \bar{d} + \bar{s} + c \dots), \quad F_3^{W^-} = 2(u - \bar{d} - \bar{s} + c \dots), \\ g_1^{W^-} &= (\Delta u + \Delta \bar{d} + \Delta \bar{s} + \Delta c \dots), \quad g_5^{W^-} = (-\Delta u + \Delta \bar{d} + \Delta \bar{s} - \Delta c \dots), \end{aligned} \quad (16.19)$$

where only the active flavors are to be kept and where CKM mixing has been neglected. For $e^+p \rightarrow \bar{\nu}X$ and $\nu p \rightarrow e^-X$, the structure functions F^{W^+}, g^{W^+} are obtained by the flavor interchanges $d \leftrightarrow u, s \leftrightarrow c$ in the expressions for F^{W^-}, g^{W^-} . The structure functions for scattering on a neutron are obtained from those of the proton by the interchange $u \leftrightarrow d$. For both the neutral- and charged-current processes, the quark-parton model predicts $2xF_1^i = F_2^i$ and $g_4^i = 2xg_5^i$.

Further discussion may be found in the full *Review of Particle Physics*.

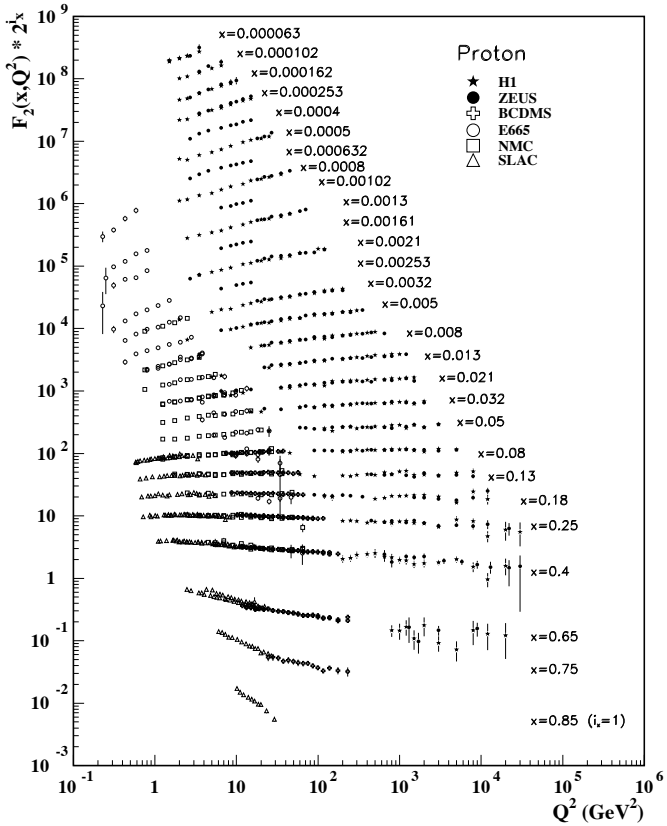


Figure 16.7: The proton structure function F_2^p measured in electromagnetic scattering of positrons on protons (collider experiments ZEUS and H1), in the kinematic domain of the HERA data, for $x > 0.00006$ (cf. Fig. 16.10 for data at smaller x and Q^2), and for electrons (SLAC) and muons (BCDMS, E665, NMC) on a fixed target. Statistical and systematic errors added in quadrature are shown. The data are plotted as a function of Q^2 in bins of fixed x . Some points have been slightly offset in Q^2 for clarity. The ZEUS binning in x is used in this plot; all other data are rebinned to the x values of the ZEUS data. For the purpose of plotting, F_2^p has been multiplied by 2^{i_x} , where i_x is the number of the x bin, ranging from $i_x = 1$ ($x = 0.85$) to $i_x = 28$ ($x = 0.000063$).

19. BIG-BANG COSMOLOGY

Revised September 2009 by K.A. Olive (University of Minnesota) and J.A. Peacock (University of Edinburgh).

19.1. Introduction to Standard Big-Bang Model

The observed expansion of the Universe [1,2,3] is a natural (almost inevitable) result of any homogeneous and isotropic cosmological model based on general relativity. In order to account for the possibility that the abundances of the elements had a cosmological origin, Alpher and Herman proposed that the early Universe which was once very hot and dense (enough so as to allow for the nucleosynthetic processing of hydrogen), and has expanded and cooled to its present state [4,5]. In 1948, Alpher and Herman predicted that a direct consequence of this model is the presence of a relic background radiation with a temperature of order a few K [6,7]. It was the observation of the 3 K background radiation that singled out the Big-Bang model as the prime candidate to describe our Universe. Subsequent work on Big-Bang nucleosynthesis further confirmed the necessity of our hot and dense past. These relativistic cosmological models face severe problems with their initial conditions, to which the best modern solution is inflationary cosmology.

19.1.1. The Robertson-Walker Universe :

The observed homogeneity and isotropy enable us to describe the overall geometry and evolution of the Universe in terms of two cosmological parameters accounting for the spatial curvature and the overall expansion (or contraction) of the Universe. These two quantities appear in the most general expression for a space-time metric which has a (3D) maximally symmetric subspace of a 4D space-time, known as the Robertson-Walker metric:

$$ds^2 = dt^2 - R^2(t) \left[\frac{dr^2}{1 - kr^2} + r^2 (d\theta^2 + \sin^2 \theta d\phi^2) \right]. \quad (19.1)$$

Note that we adopt $c = 1$ throughout. By rescaling the radial coordinate, we can choose the curvature constant k to take only the discrete values $+1$, -1 , or 0 corresponding to closed, open, or spatially flat geometries.

19.1.2. The redshift :

The cosmological redshift is a direct consequence of the Hubble expansion, determined by $R(t)$. A local observer detecting light from a distant emitter sees a redshift in frequency. We can define the redshift as

$$z \equiv \frac{\nu_1 - \nu_2}{\nu_2} \simeq \frac{v_{12}}{c}, \quad (19.3)$$

where ν_1 is the frequency of the emitted light, ν_2 is the observed frequency and v_{12} is the relative velocity between the emitter and the observer. While the definition, $z = (\nu_1 - \nu_2)/\nu_2$ is valid on all distance scales, relating the redshift to the relative velocity in this simple way is only true on small scales (*i.e.*, less than cosmological scales) such that the expansion velocity is non-relativistic. For light signals, we can use the metric given by Eq. (19.1) and $ds^2 = 0$ to write

$$1 + z = \frac{\nu_1}{\nu_2} = \frac{R_2}{R_1}. \quad (19.5)$$

This result does not depend on the non-relativistic approximation.

19.1.3. The Friedmann-Lemaître equations of motion :

The cosmological equations of motion are derived from Einstein's equations

$$\mathcal{R}_{\mu\nu} - \frac{1}{2}g_{\mu\nu}\mathcal{R} = 8\pi G_N T_{\mu\nu} + \Lambda g_{\mu\nu}. \quad (19.6)$$

Gliner [17] and Zeldovich [18] have pioneered the modern view, in which the Λ term is taken to the rhs and interpreted as an effective energy-momentum tensor $T_{\mu\nu}$ for the vacuum of $\Lambda g_{\mu\nu}/8\pi G_N$. It is common to assume that the matter content of the Universe is a perfect fluid, for which

$$T_{\mu\nu} = -p g_{\mu\nu} + (p + \rho) u_\mu u_\nu, \quad (19.7)$$

where $g_{\mu\nu}$ is the space-time metric described by Eq. (19.1), p is the isotropic pressure, ρ is the energy density and $u = (1, 0, 0, 0)$ is the velocity vector for the isotropic fluid in co-moving coordinates. With the perfect fluid source, Einstein's equations lead to the Friedmann-Lemaître equations

$$H^2 \equiv \left(\frac{\dot{R}}{R} \right)^2 = \frac{8\pi G_N \rho}{3} - \frac{k}{R^2} + \frac{\Lambda}{3}, \quad (19.8)$$

and

$$\frac{\ddot{R}}{R} = \frac{\Lambda}{3} - \frac{4\pi G_N}{3} (\rho + 3p), \quad (19.9)$$

where $H(t)$ is the Hubble parameter and Λ is the cosmological constant. The first of these is sometimes called the Friedmann equation. Energy conservation via $T^{\mu\nu}_{;\mu} = 0$, leads to a third useful equation

$$\dot{\rho} = -3H(\rho + p). \quad (19.10)$$

Eq. (19.10) can also be simply derived as a consequence of the first law of thermodynamics. For $\Lambda = 0$, it is clear that the Universe must be expanding or contracting.

19.1.4. Definition of cosmological parameters :

The Friedmann equation can be used to define a critical density such that $k = 0$ when $\Lambda = 0$,

$$\begin{aligned} \rho_c &\equiv \frac{3H^2}{8\pi G_N} = 1.88 \times 10^{-26} h^2 \text{ kg m}^{-3} \\ &= 1.05 \times 10^{-5} h^2 \text{ GeV cm}^{-3}, \end{aligned} \quad (19.11)$$

where the scaled Hubble parameter, h , is defined by

$$\begin{aligned} H &\equiv 100 h \text{ km s}^{-1} \text{ Mpc}^{-1} \\ \Rightarrow H^{-1} &= 9.78 h^{-1} \text{ Gyr} \\ &= 2998 h^{-1} \text{ Mpc}. \end{aligned} \quad (19.12)$$

The cosmological density parameter Ω_{tot} is defined as the energy density relative to the critical density,

$$\Omega_{\text{tot}} = \rho/\rho_c. \quad (19.13)$$

Note that one can now rewrite the Friedmann equation as

$$k/R^2 = H^2(\Omega_{\text{tot}} - 1). \quad (19.14)$$

From Eq. (19.14), one can see that when $\Omega_{\text{tot}} > 1$, $k = +1$ and the Universe is closed, when $\Omega_{\text{tot}} < 1$, $k = -1$ and the Universe is open, and when $\Omega_{\text{tot}} = 1$, $k = 0$, and the Universe is spatially flat.

It is often necessary to distinguish different contributions to the density. It is therefore convenient to define present-day density parameters for pressureless matter (Ω_m) and relativistic particles (Ω_r), plus the quantity $\Omega_\Lambda = \Lambda/3H^2$. In more general models, we may wish to drop the assumption that the vacuum energy density is constant, and we therefore denote the present-day density parameter of the vacuum by Ω_v . The Friedmann equation then becomes

$$k/R_0^2 = H_0^2(\Omega_m + \Omega_r + \Omega_v - 1), \quad (19.15)$$

where the subscript 0 indicates present-day values. Thus, it is the sum of the densities in matter, relativistic particles, and vacuum that determines the overall sign of the curvature. Note that the quantity $-k/R_0^2 H_0^2$ is sometimes (unfortunately) referred to as Ω_k .

19.1.5. Standard Model solutions :

During inflation and again today the expansion rate for the Universe is accelerating, and domination by a cosmological constant or some other form of dark energy should be considered.

Let us first assume a general equation of state parameter for a single component, $w = p/\rho$ which is constant. In this case, Eq. (19.10) can be written as $\dot{\rho} = -3(1+w)\rho\dot{R}/R$ and is easily integrated to yield

$$\rho \propto R^{-3(1+w)} . \tag{19.16}$$

Note that at early times when R is small, k/R^2 in the Friedmann equation can be neglected so long as $w > -1/3$. Curvature domination occurs at rather late times (if a cosmological constant term does not dominate sooner). For $w \neq -1$,

$$R(t) \propto t^{2/[3(1+w)]} . \tag{19.17}$$

19.1.5.2. A Radiation-dominated Universe:

In the early hot and dense Universe, it is appropriate to assume an equation of state corresponding to a gas of radiation (or relativistic particles) for which $w = 1/3$. In this case, Eq. (19.16) becomes $\rho \propto R^{-4}$. Similarly, one can substitute $w = 1/3$ into Eq. (19.17) to obtain

$$R(t) \propto t^{1/2} ; \quad H = 1/2t . \tag{19.18}$$

19.1.5.3. A Matter-dominated Universe:

Non-relativistic matter eventually dominates the energy density over radiation. A pressureless gas ($w = 0$) leads to the expected dependence $\rho \propto R^{-3}$, and, if $k = 0$, we get

$$R(t) \propto t^{2/3} ; \quad H = 2/3t . \tag{19.19}$$

If there is a dominant source of vacuum energy, acting as a cosmological constant with equation of state $w = -1$. This leads to an exponential expansion of the Universe

$$R(t) \propto e^{\sqrt{\Lambda/3}t} . \tag{19.20}$$

The equation of state of the vacuum need not be the $w = -1$ of Λ , and may not even be constant [19,20,21]. There is now much interest in the more general possibility of a dynamically evolving vacuum energy, for which the name ‘dark energy’ has become commonly used. A variety of techniques exist whereby the vacuum density as a function of time may be measured, usually expressed as the value of w as a function of epoch [22,23]. The best current measurement for the equation of state (assumed constant) is $w = -1.006^{+0.067}_{-0.068}$ [24]. Unless stated otherwise, we will assume that the vacuum energy is a cosmological constant with $w = -1$ exactly.

The presence of vacuum energy can dramatically alter the fate of the Universe. For example, if $\Lambda < 0$, the Universe will eventually recollapse independent of the sign of k . For large values of $\Lambda > 0$ (larger than the Einstein static value needed to halt any cosmological expansion or contraction), even a closed Universe will expand forever. One way to quantify this is the deceleration parameter, q_0 , defined as

$$q_0 = - \left. \frac{R\ddot{R}}{\dot{R}^2} \right|_0 = \frac{1}{2}\Omega_m + \Omega_r + \frac{(1+3w)}{2}\Omega_v . \tag{19.21}$$

This equation shows us that $w < -1/3$ for the vacuum may lead to an accelerating expansion. Current data indicate that vacuum energy is indeed the largest contributor to the cosmological density budget, with $\Omega_v = 0.74 \pm 0.03$ and $\Omega_m = 0.26 \pm 0.03$ if $k = 0$ is assumed (5-year mean WMAP) [24].

19.2. Introduction to Observational Cosmology

19.2.1. Fluxes, luminosities, and distances :

The key quantities for observational cosmology can be deduced quite directly from the metric.

(1) The *proper* transverse size of an object seen by us to subtend an angle $d\psi$ is its comoving size $d\psi r$ times the scale factor at the time of emission:

$$d\ell = d\psi R_0 r / (1 + z) . \tag{19.22}$$

(2) The apparent flux density of an object is deduced by allowing its photons to flow through a sphere of current radius $R_0 r$; but photon energies and arrival rates are redshifted, and the bandwidth $d\nu$ is reduced. These relations lead to the following common definitions:

$$\begin{aligned} \text{angular-diameter distance: } D_A &= (1 + z)^{-1} R_0 r \\ \text{luminosity distance: } D_L &= (1 + z) R_0 r . \end{aligned} \tag{19.24}$$

These distance-redshift relations are expressed in terms of observables by using the equation of a null radial geodesic plus the Friedmann equation:

$$\begin{aligned} \frac{R_0}{R(t)} dt = \frac{1}{H(z)} dz = \frac{1}{H_0} \left[(1 - \Omega_m - \Omega_v - \Omega_r)(1 + z)^2 \right. \\ \left. + \Omega_v(1 + z)^{3+3w} + \Omega_m(1 + z)^3 + \Omega_r(1 + z)^4 \right]^{-1/2} dz . \end{aligned} \tag{19.25}$$

The main scale for the distance here is the Hubble length, $1/H_0$.

In combination with Cepheid data from the HST and a direct geometrical distance to the maser galaxy NGC4258, SNe results extend the distance ladder to the point where deviations from uniform expansion are negligible, leading to the best existing direct value for H_0 : $74.2 \pm 3.6 \text{ km s}^{-1} \text{ Mpc}^{-1}$ [25]. Better still, the analysis of high- z SNe has allowed the first meaningful test of cosmological geometry to be carried out.

19.2.3. Age of the Universe :

The dynamical result for the age of the Universe may be written as

$$H_0 t_0 = \int_0^\infty \frac{dz}{(1 + z) [(1 + z)^2 (1 + \Omega_m z) - z(2 + z)\Omega_v]^{1/2}} , \tag{19.28}$$

where we have neglected Ω_r and chosen $w = -1$. Over the range of interest ($0.1 \lesssim \Omega_m \lesssim 1$, $|\Omega_v| \lesssim 1$), this exact answer may be approximated to a few % accuracy by

$$H_0 t_0 \simeq \frac{2}{3} (0.7\Omega_m + 0.3 - 0.3\Omega_v)^{-0.3} . \tag{19.29}$$

For the special case that $\Omega_m + \Omega_v = 1$, the integral in Eq. (19.28) can be expressed analytically as

$$H_0 t_0 = \frac{2}{3\sqrt{\Omega_v}} \ln \frac{1 + \sqrt{\Omega_v}}{\sqrt{1 - \Omega_v}} \quad (\Omega_m < 1) . \tag{19.30}$$

The present consensus favors ages for the oldest clusters of about 12 Gyr [36,37].

These methods are all consistent with the age deduced from studies of structure formation, using the microwave background and large-scale structure: $t_0 = 13.69 \pm 0.13$ Gyr [24], where the extra accuracy comes at the price of assuming the Cold Dark Matter model to be true.

19.3. The Hot Thermal Universe

19.3.1. Thermodynamics of the early Universe :

Through much of the radiation-dominated period, thermal equilibrium is established by the rapid rate of particle interactions relative to the expansion rate of the Universe. In equilibrium, it is straightforward to compute the thermodynamic quantities, ρ , p , and the entropy density, s .

In the Standard Model, a chemical potential is often associated with baryon number, and since the net baryon density relative to the photon density is known to be very small (of order 10^{-10}), we can neglect any such chemical potential when computing total thermodynamic quantities.

For photons, we have (in units where $\hbar = k_B = 1$)

$$\rho_\gamma = \frac{\pi^2}{15} T^4 ; \quad p_\gamma = \frac{1}{3} \rho_\gamma ; \quad s_\gamma = \frac{4\rho_\gamma}{3T} ; \quad n_\gamma = \frac{2\zeta(3)}{\pi^2} T^3 . \quad (19.39)$$

Eq. (19.10) can be converted into an equation for entropy conservation,

$$d(sR^3)/dt = 0 . \quad (19.40)$$

For radiation, this corresponds to the relationship between expansion and cooling, $T \propto R^{-1}$ in an adiabatically expanding universe. Note also that both s and n_γ scale as T^3 .

19.3.2. Radiation content of the Early Universe :

At the very high temperatures associated with the early Universe, massive particles are pair produced, and are part of the thermal bath. If for a given particle species i we have $T \gg m_i$, then we can neglect the mass and the thermodynamic quantities are easily computed. In general, we can approximate the energy density (at high temperatures) by including only those particles with $m_i \ll T$. In this case, we have

$$\rho = \left(\sum_B g_B + \frac{7}{8} \sum_F g_F \right) \frac{\pi^2}{30} T^4 \equiv \frac{\pi^2}{30} N(T) T^4 , \quad (19.41)$$

where $g_{B(F)}$ is the number of degrees of freedom of each boson (fermion) and the sum runs over all boson and fermion states with $m \ll T$.

Eq. (19.41) defines the effective number of degrees of freedom, $N(T)$, by taking into account new particle degrees of freedom as the temperature is raised.

The value of $N(T)$ at any given temperature depends on the particle physics model. In the standard $SU(3) \times SU(2) \times U(1)$ model, we can specify $N(T)$ up to temperatures of $O(100)$ GeV. The change in N (ignoring mass effects) can be seen in the table below. At higher temperatures, $N(T)$ will be model-dependent.

In the radiation-dominated epoch, Eq. (19.10) can be integrated (neglecting the T -dependence of N) giving us a relationship between the age of the Universe and its temperature

$$t = \left(\frac{90}{32\pi^3 G_N N(T)} \right)^{1/2} T^{-2} . \quad (19.42)$$

Put into a more convenient form

$$t T_{\text{MeV}}^2 = 2.4 [N(T)]^{-1/2} , \quad (19.43)$$

where t is measured in seconds and T_{MeV} in units of MeV.

Temperature	New Particles	$4N(T)$
$T < m_e$	γ 's + ν 's	29
$m_e < T < m_\mu$	e^\pm	43
$m_\mu < T < m_\pi$	μ^\pm	57
$m_\pi < T < T_c^\dagger$	π 's	69
$T_c < T < m_{\text{strange}}$	π 's + u, \bar{u}, d, \bar{d} + gluons	205
$m_s < T < m_{\text{charm}}$	s, \bar{s}	247
$m_c < T < m_\tau$	c, \bar{c}	289
$m_\tau < T < m_{\text{bottom}}$	τ^\pm	303
$m_b < T < m_{W,Z}$	b, \bar{b}	345
$m_{W,Z} < T < m_{\text{Higgs}}$	W^\pm, Z	381
$m_H < T < m_{\text{top}}$	H^0	385
$m_t < T$	t, \bar{t}	427

$^\dagger T_c$ corresponds to the confinement-deconfinement transition between quarks and hadrons.

19.3.7. Nucleosynthesis :

An essential element of the standard cosmological model is Big-Bang nucleosynthesis (BBN), the theory which predicts the abundances of the light element isotopes D, ^3He , ^4He , and ^7Li . Nucleosynthesis takes place at a temperature scale of order 1 MeV. The nuclear processes lead primarily to ^4He , with a primordial mass fraction of about 25%. Lesser amounts of the other light elements are produced: about 10^{-5} of D and ^3He and about 10^{-10} of ^7Li by number relative to H. The abundances of the light elements depend almost solely on one key parameter, the baryon-to-photon ratio, η . The nucleosynthesis predictions can be compared with observational determinations of the abundances of the light elements. Consistency between theory and observations leads to a conservative range of

$$5.1 \times 10^{-10} < \eta < 6.5 \times 10^{-10} . \quad (19.54)$$

η is related to the fraction of Ω contained in baryons, Ω_b

$$\Omega_b = 3.66 \times 10^7 \eta h^{-2} , \quad (19.55)$$

or $10^{10} \eta = 274 \Omega_b h^2$.

19.4. The Universe at late times

We are beginning to inventory the composition of the Universe:

$$\text{total: } \Omega = 1.005 \pm 0.006 \text{ (from CMB anisotropy)}$$

$$\text{matter: } \Omega_m = 0.26 \pm 0.03$$

$$\text{baryons: } \Omega_b = 0.044 \pm 0.004$$

$$\text{CDM: } \Omega_{\text{CDM}} = \Omega_m - \Omega_b$$

$$\text{neutrinos: } 0.001 \lesssim \Omega_\nu \lesssim 0.05$$

$$\text{dark energy: } \Omega_v = 0.74 \pm 0.03$$

$$\text{photons: } \Omega_\gamma = 4.6 \times 10^{-5}$$

Further discussion and all references may be found in the full *Review of Particle Physics*. The numbering of references and equations used here corresponds to that version.

21. THE COSMOLOGICAL PARAMETERS

Updated September 2009, by O. Lahav (University College London) and A.R. Liddle (University of Sussex).

21.1. Parametrizing the Universe

The term ‘cosmological parameters’ is forever increasing in its scope, and nowadays includes the parametrization of some functions, as well as simple numbers describing properties of the Universe. The original usage referred to the parameters describing the global dynamics of the Universe, such as its expansion rate and curvature. Also now of great interest is how the matter budget of the Universe is built up from its constituents: baryons, photons, neutrinos, dark matter, and dark energy. We need to describe the nature of perturbations in the Universe, through global statistical descriptors such as the matter and radiation power spectra. There may also be parameters describing the physical state of the Universe, such as the ionization fraction as a function of time during the era since recombination. Typical comparisons of cosmological models with observational data now feature between five and ten parameters.

21.1.1. *The global description of the Universe* : The complete present state of the homogeneous Universe can be described by giving the current values of all the density parameters and of the Hubble parameter h . These also allow us to track the history of the Universe back in time, at least until an epoch where interactions allow interchanges between the densities of the different species, which is believed to have last happened at neutrino decoupling, shortly before Big Bang Nucleosynthesis (BBN). To probe further back into the Universe’s history requires assumptions about particle interactions, and perhaps about the nature of physical laws themselves.

21.1.2. *The standard cosmological model* : The basic set of cosmological parameters is therefore as shown in Table 21.1. The spatial curvature does not appear in the list, because it can be determined from the other parameters using Eq. 21.1. The total present matter density $\Omega_m = \Omega_{\text{cdm}} + \Omega_b$ is usually used in place of the dark matter density.

As described in Sec. 21.3, models based on these eleven parameters are able to give a good fit to the complete set of high-quality data available at present, and indeed some simplification is possible. Observations are consistent with spatial flatness, and indeed the inflation models so far described automatically generate negligible spatial curvature, so we can set $k = 0$; the density parameters then must sum to unity, and so one can be eliminated. The neutrino energy density is often not taken as an independent parameter. Provided the neutrino sector has the standard interactions, the neutrino energy density, while relativistic, can be related to the photon density using thermal physics arguments, and it is currently difficult to see the effect of the neutrino mass, although observations of large-scale structure have already placed interesting upper limits. This reduces the standard parameter set to nine. In addition, there is no observational evidence for the existence of tensor perturbations (though the upper limits are quite weak), and so r could be set to zero. Presently n is in a somewhat controversial position regarding whether it needs to be varied in a fit, or can be set to the Harrison–Zel’dovich value $n = 1$. Parameter estimation [2] suggests $n = 1$ is ruled out at some significance,

Table 21.1: The basic set of cosmological parameters. We give values (with some additional rounding) as obtained using a fit of a Λ CDM cosmology with a power-law initial spectrum to WMAP5 data alone [2]. Tensors are assumed zero except in quoting a limit on them. The exact values and uncertainties depend on both the precise data-sets used and the choice of parameters allowed to vary (see Table 21.2 for the former). Limits on Ω_Λ and h weaken if the Universe is not assumed flat. The density perturbation amplitude is specified by the derived parameter σ_8 . Uncertainties are one-sigma/68% confidence unless otherwise stated.

Parameter	Symbol	Value
Hubble parameter	h	0.72 ± 0.03
Total matter density	Ω_m	$\Omega_m h^2 = 0.133 \pm 0.006$
Baryon density	Ω_b	$\Omega_b h^2 = 0.0227 \pm 0.0006$
Cosmological constant	Ω_Λ	$\Omega_\Lambda = 0.74 \pm 0.03$
Radiation density	Ω_r	$\Omega_r h^2 = 2.47 \times 10^{-5}$
Neutrino density	Ω_ν	See Sec. 21.1.2
Density perturb. amplitude at $k=2\text{Kpc}$	Δ_R^2	$(2.41 \pm 0.11) \times 10^{-9}$
Density perturb. spectral index	n	$n = 0.963^{+0.014}_{-0.015}$
Tensor to scalar ratio	r	$r < 0.43$ (95% conf.)
Ionization optical depth	τ	$\tau = 0.087 \pm 0.017$
Bias parameter	b	See Sec. 21.3.4

but Bayesian model selection techniques [9] suggest the data is not conclusive. With n set to one, this leaves seven parameters, which is the smallest set that can usefully be compared to the present cosmological data set. This model (usually with n kept as a parameter) is referred to by various names, including Λ CDM, the concordance cosmology, and the standard cosmological model.

21.2. Extensions to the standard model

21.2.1. More general perturbations: The standard cosmology assumes adiabatic, Gaussian perturbations. Adiabaticity means that all types of material in the Universe share a common perturbation, so that if the space-time is foliated by constant-density hypersurfaces, then all fluids and fields are homogeneous on those slices, with the perturbations completely described by the variation of the spatial curvature of the slices. Gaussianity means that the initial perturbations obey Gaussian statistics, with the amplitudes of waves of different wavenumbers being randomly drawn from a Gaussian distribution of width given by the power spectrum. Note that gravitational instability generates non-Gaussianity; in this context, Gaussianity refers to a property of the initial perturbations, before they evolve significantly.

The simplest inflation models, based on one dynamical field, predict adiabatic fluctuations and a level of non-Gaussianity which is too small to be detected by any experiment so far conceived. For present data, the primordial spectra are usually assumed to be power laws.

21.2.1.2. Isocurvature perturbations: An isocurvature perturbation is one which leaves the total density unperturbed, while perturbing the relative amounts of different materials. If the Universe contains N fluids, there is one growing adiabatic mode and $N - 1$ growing isocurvature modes (for reviews see Ref. 12 and Ref. 13). These can be excited, for example, in inflationary models where there are two or more fields which acquire dynamically-important perturbations. If one field decays to form normal matter, while the second survives to become the dark matter, this will generate a cold dark matter isocurvature perturbation.

In general, there are also correlations between the different modes, and so the full set of perturbations is described by a matrix giving the spectra and their correlations. Constraining such a general construct is challenging, though constraints on individual modes are beginning to become meaningful, with no evidence that any other than the adiabatic mode must be non-zero.

21.2.2. Dark energy: While the standard cosmological model given above features a cosmological constant, in order to explain observations indicating that the Universe is presently accelerating, further possibilities exist under the general heading ‘dark energy’.[†] A particularly attractive possibility (usually called quintessence, though that word is used with various different meanings in the literature) is that a scalar field is responsible, with the mechanism mimicking that of early Universe inflation [15]. As described by Olive and Peacock, a fairly model-independent description of dark energy can be given just using the equation of state parameter w , with $w = -1$ corresponding to a cosmological constant. In general, the function w could itself vary with redshift, though practical experiments devised so far would be sensitive primarily to some average value weighted over recent epochs. For high-precision predictions of CMB anisotropies, it is better to use a scalar-field description in order to have a self-consistent evolution of the ‘sound speed’ associated with the dark energy perturbations.

Present observations are consistent with a cosmological constant, but often w is kept as a free parameter to be added to the set described in the previous section. Most, but not all, researchers assume the weak energy condition $w \geq -1$. In the future, it may be necessary to use a more sophisticated parametrization of the dark energy.

21.3. Probes

21.3.1. Direct measures of the Hubble constant: One of the most reliable results on the Hubble constant comes from the Hubble Space Telescope Key Project [18]. This study used the empirical period–luminosity relations for Cepheid variable stars to obtain distances to 31 galaxies, and calibrated a number of secondary distance indicators (Type Ia Supernovae, Tully–Fisher relation, surface brightness fluctuations, and Type II Supernovae) measured over distances of 400 to 600 Mpc. They estimated $H_0 = 72 \pm 3$ (statistical) ± 7 (systematic) $\text{km s}^{-1} \text{Mpc}^{-1}$. A

[†] Unfortunately this is rather a misnomer, as it is the negative pressure of this material, rather than its energy, that is responsible for giving the acceleration. Furthermore, while generally in physics matter and energy are interchangeable terms, dark matter and dark energy are quite distinct concepts.

recent study [19] of 240 Cepheids observed with an improved camera onboard the Hubble Space Telescope has yielded an even more accurate figure, $H_0 = 74 \pm 4 \text{ km s}^{-1} \text{ Mpc}^{-1}$ (including both statistical and systematic errors). The major sources of uncertainty in these results are due to the heavy element abundance of the Cepheids and the distance to the fiducial nearby galaxy (called the Large Magellanic Cloud) relative to which all Cepheid distances are measured.

21.3.4.3. Limits on neutrino mass from galaxy surveys and other probes:

Large-scale structure data can put an upper limit on the ratio Ω_ν/Ω_m due to the neutrino ‘free streaming’ effect [37,38]. For example, by comparing the 2dF galaxy power spectrum with a four-component model (baryons, cold dark matter, a cosmological constant, and massive neutrinos), it is estimated that $\Omega_\nu/\Omega_m < 0.13$ (95% confidence limit), giving $\Omega_\nu < 0.04$ if a concordance prior of $\Omega_m = 0.3$ is imposed. The latter corresponds to an upper limit of about 2 eV on the total neutrino mass, assuming a prior of $h \approx 0.7$ [39]. Potential systematic effects include biasing of the galaxy distribution and non-linearities of the power spectrum. A similar upper limit of 2 eV has been derived from CMB anisotropies alone [40–42]. The above analyses assume that the primordial power spectrum is adiabatic, scale-invariant and Gaussian. Additional cosmological data sets have improved the results [43,44]. An upper limit on the total neutrino mass of 0.17 eV was reported by combining a large number of cosmological probes [45].

21.4. Bringing observations together

Although it contains two ingredients—dark matter and dark energy—which have not yet been verified by laboratory experiments, the Λ CDM model is almost universally accepted by cosmologists as the best description of the present data. The basic ingredients are given by the parameters listed in Sec. 21.1.1, with approximate values of some of the key parameters being $\Omega_b \approx 0.04$, $\Omega_{\text{cdm}} \approx 0.21$, $\Omega_\Lambda \approx 0.74$, and a Hubble constant $h \approx 0.72$. The spatial geometry is very close to flat (and usually assumed to be precisely flat), and the initial perturbations Gaussian, adiabatic, and nearly scale-invariant.

The baryon density Ω_b is now measured with quite high accuracy from the CMB and large-scale structure, and is consistent with the determination from BBN; Fields and Sarkar in this volume quote the range $0.019 \leq \Omega_b h^2 \leq 0.024$ (95% confidence).

While Ω_Λ is measured to be non-zero with very high confidence, there is no evidence of evolution of the dark energy density. The WMAP team find the limit $w < -0.86$ at 95% confidence from a compilation of data including SNe Ia, with the cosmological constant case $w = -1$ giving an excellent fit to the data.

One parameter which is very robust is the age of the Universe, as there is a useful coincidence that for a flat Universe the position of the first peak is strongly correlated with the age. The WMAP5 result is 13.69 ± 0.13 Gyr (assuming flatness). This is in good agreement with the ages of the oldest globular clusters [61] and radioactive dating [62].

For further details and all references, see the full *Review of Particle Physics*. See also “Astrophysical Constants,” table 2.1 in this Booklet.

22. DARK MATTER

Revised September 2009 by M. Drees (Bonn University) and G. Gerbier (Saclay, CEA).

22.1. Theory

22.1.1. Evidence for Dark Matter : The existence of Dark (*i.e.*, non-luminous and non-absorbing) Matter (DM) is by now well established. An important example is the measurement of galactic rotation curves. The rotational velocity v of an object on a stable Keplerian orbit with radius r around a galaxy scales like $v(r) \propto \sqrt{M(r)/r}$, where $M(r)$ is the mass inside the orbit. If r lies outside the visible part of the galaxy and mass tracks light, one would expect $v(r) \propto 1/\sqrt{r}$. Instead, in most galaxies one finds that v becomes approximately constant out to the largest values of r where the rotation curve can be measured. This implies the existence of a *dark halo*, with mass density $\rho(r) \propto 1/r^2$, *i.e.*, $M(r) \propto r$, and a lower bound on the DM mass density, $\Omega_{\text{DM}} \gtrsim 0.1$.

The observation of clusters of galaxies tends to give somewhat larger values, $\Omega_{\text{DM}} \simeq 0.2$. These observations include measurements of the peculiar velocities of galaxies in the cluster, which are a measure of their potential energy if the cluster is virialized; measurements of the *X-ray* temperature of hot gas in the cluster, which again correlates with the gravitational potential felt by the gas; and—most directly—studies of (weak) gravitational lensing of background galaxies on the cluster.

The currently most accurate, if somewhat indirect, determination of Ω_{DM} comes from global fits of cosmological parameters to a variety of observations; see the Section on Cosmological Parameters for details. For example, using measurements of the anisotropy of the cosmic microwave background (CMB) and of the spatial distribution of galaxies, Ref. 3 finds a density of cold, non-baryonic matter

$$\Omega_{\text{nbm}} h^2 = 0.110 \pm 0.006 , \quad (22.1)$$

where h is the Hubble constant in units of 100 km/(s-Mpc). Some part of the baryonic matter density [3],

$$\Omega_{\text{b}} h^2 = 0.0227 \pm 0.0006 , \quad (22.2)$$

may well contribute to (baryonic) DM, *e.g.*, MACHOs [4] or cold molecular gas clouds [5].

The most recent estimate of the DM density in the “neighborhood” of our solar system is 0.3 GeV cm^{-3} .

22.1.2. Candidates for Dark Matter : Candidates for non-baryonic DM in Eq. (22.1) must satisfy several conditions: they must be stable on cosmological time scales (otherwise they would have decayed by now), they must interact very weakly with electromagnetic radiation (otherwise they wouldn’t qualify as *dark* matter), and they must have the right relic density. Candidates include primordial black holes, axions, and weakly interacting massive particles (WIMPs).

The existence of axions [9] was first postulated to solve the strong *CP* problem of QCD; they also occur naturally in superstring theories. They are pseudo Nambu-Goldstone bosons associated with the (mostly) spontaneous breaking of a new global “Peccei-Quinn” (PQ) U(1) symmetry at scale f_a ; see the Section on Axions in this *Review* for further details. Although very light, axions would constitute cold DM, since they were

produced non-thermally. At temperatures well above the QCD phase transition, the axion is massless, and the axion field can take any value, parameterized by the “misalignment angle” θ_i . At $T \lesssim 1$ GeV, the axion develops a mass m_a due to instanton effects. Unless the axion field happens to find itself at the minimum of its potential ($\theta_i = 0$), it will begin to oscillate once m_a becomes comparable to the Hubble parameter H . These coherent oscillations transform the energy originally stored in the axion field into physical axion quanta. The contribution of this mechanism to the present axion relic density is [9]

$$\Omega_a h^2 = \kappa_a \left(f_a / 10^{12} \text{ GeV} \right)^{1.175} \theta_i^2, \quad (22.5)$$

where the numerical factor κ_a lies roughly between 0.5 and a few. If $\theta_i \sim \mathcal{O}(1)$, Eq. (22.5) will saturate Eq. (22.1) for $f_a \sim 10^{11}$ GeV, comfortably above laboratory and astrophysical constraints [9]; this would correspond to an axion mass around 0.1 meV. However, if the post-inflationary reheat temperature $T_R > f_a$, cosmic strings will form during the PQ phase transition at $T \simeq f_a$. Their decay will give an additional contribution to Ω_a , which is often bigger than that in Eq. (22.5) [10], leading to a smaller preferred value of f_a , *i.e.*, larger m_a . On the other hand, values of f_a near the Planck scale become possible if θ_i is for some reason very small.

Weakly interacting massive particles (WIMPs) χ are particles with mass roughly between 10 GeV and a few TeV, and with cross sections of approximately weak strength. Their present relic density can be calculated reliably if the WIMPs were in thermal and chemical equilibrium with the hot “soup” of Standard Model (SM) particles after inflation. Their present relic density is then approximately given by (ignoring logarithmic corrections) [11]

$$\Omega_\chi h^2 \simeq \text{const.} \cdot \frac{T_0^3}{M_{\text{Pl}}^3 \langle \sigma_A v \rangle} \simeq \frac{0.1 \text{ pb} \cdot c}{\langle \sigma_A v \rangle}. \quad (22.6)$$

Here T_0 is the current CMB temperature, M_{Pl} is the Planck mass, c is the speed of light, σ_A is the total annihilation cross section of a pair of WIMPs into SM particles, v is the relative velocity between the two WIMPs in their cms system, and $\langle \dots \rangle$ denotes thermal averaging. Freeze out happens at temperature $T_F \simeq m_\chi/20$ almost independently of the properties of the WIMP. Notice that the 0.1 pb in Eq. (22.6) contains factors of T_0 and M_{Pl} ; it is, therefore, quite intriguing that it “happens” to come out near the typical size of weak interaction cross sections.

The currently best motivated WIMP candidate is, therefore, the lightest superparticle (LSP) in supersymmetric models [12] with exact R-parity (which guarantees the stability of the LSP). Detailed calculations [15] show that the lightest neutralino will have the desired thermal relic density Eq. (22.1) in at least four distinct regions of parameter space. χ could be (mostly) a bino or photino (the superpartner of the $U(1)_Y$ gauge boson and photon, respectively), if both χ and some sleptons have mass below ~ 150 GeV, or if m_χ is close to the mass of some sfermion (so that its relic density is reduced through co-annihilation with this sfermion), or if $2m_\chi$ is close to the mass of the CP -odd Higgs boson present in supersymmetric models. Finally, Eq. (22.1) can also be satisfied if χ has a large higgsino or wino component.

22.2. Experimental detection of Dark Matter

22.2.2. Axion searches : Axions can be detected by looking for $a \rightarrow \gamma$ conversion in a strong magnetic field [26]. Such a conversion proceeds through the loop-induced $a\gamma\gamma$ coupling, whose strength $g_{a\gamma\gamma}$ is an important parameter of axion models. There currently are two experiments searching for axionic DM. They both employ high quality cavities. The cavity “Q factor” enhances the conversion rate on resonance, *i.e.*, for $m_a c^2 = \hbar\omega_{\text{res}}$. One then needs to scan the resonance frequency in order to cover a significant range in m_a or, equivalently, f_a .

22.2.3. Basics of direct WIMP search : The WIMP mean velocity inside our galaxy relative to its center is expected to be similar to that of stars, *i.e.*, a few hundred kilometers per second at the location of our solar system. For these velocities, WIMPs interact with ordinary matter through elastic scattering on nuclei. With expected WIMP masses in the range 10 GeV to 10 TeV, typical nuclear recoil energies are of order of 1 to 100 keV.

Expected interaction rates depend on the product of the local WIMP flux and the interaction cross section. The first term is fixed by the local density of dark matter, taken as $0.3 \text{ GeV}/\text{cm}^3$ (see above), the mean WIMP velocity, typically 220 km/s, and the mass of the WIMP. The expected interaction rate then mainly depends on two unknowns, the mass and cross section of the WIMP (with some uncertainty [6] due to the halo model). This is why the experimental observable, which is basically the scattering rate as a function of energy, is usually expressed as a contour in the WIMP mass–cross section plane.

The cross section depends on the nature of the couplings. For non-relativistic WIMPs, one in general has to distinguish spin-independent and spin-dependent couplings. The former can involve scalar and vector WIMP and nucleon currents (vector currents are absent for Majorana WIMPs, *e.g.*, the neutralino), while the latter involve axial vector currents (and obviously only exist if χ carries spin). Due to coherence effects, the spin-independent cross section scales approximately as the square of the mass of the nucleus, so higher mass nuclei, from Ge to Xe, are preferred for this search. For spin-dependent coupling, the cross section depends on the nuclear spin factor; used target nuclei include ^{19}F , ^{23}Na , ^{73}Ge , ^{127}I , ^{129}Xe , ^{131}Xe , and ^{133}Cs .

Cross sections calculated in MSSM models induce rates of at most $1 \text{ evt day}^{-1} \text{ kg}^{-1}$ of detector, much lower than the usual radioactive backgrounds. This indicates the need for underground laboratories to protect against cosmic ray induced backgrounds, and for the selection of extremely radio-pure materials.

The typical shape of exclusion contours can be anticipated from this discussion: at low WIMP mass, the sensitivity drops because of the detector energy threshold, whereas at high masses, the sensitivity also decreases because, for a fixed mass density, the WIMP flux decreases $\propto 1/m_\chi$. The sensitivity is best for WIMP masses near the mass of the recoiling nucleus.

Further discussion and all references may be found in the full *Review*. The numbering of references and equations used here corresponds to that version.

23. COSMIC MICROWAVE BACKGROUND

Revised August 2009 by D. Scott (University of British Columbia) and G.F. Smoot (UCB/LBNL).

23.2. Description of CMB Anisotropies

Observations show that the CMB contains anisotropies at the 10^{-5} level, over a wide range of angular scales. These anisotropies are usually expressed by using a spherical harmonic expansion of the CMB sky:

$$T(\theta, \phi) = \sum_{\ell m} a_{\ell m} Y_{\ell m}(\theta, \phi).$$

The vast majority of the cosmological information is contained in the temperature 2-point function, *i.e.*, the variance as a function only of angular separation, since we notice no preferred direction. Equivalently, the power per unit $\ln \ell$ is $\ell \sum_m |a_{\ell m}|^2 / 4\pi$.

23.2.1. The Monopole :

The CMB has a mean temperature of $T_\gamma = 2.725 \pm 0.001$ K (1σ) [7], which can be considered as the monopole component of CMB maps, a_{00} . Since all mapping experiments involve difference measurements, they are insensitive to this average level. Monopole measurements can only be made with absolute temperature devices, such as the FIRAS instrument on the *COBE* satellite [7]. Such measurements of the spectrum are consistent with a blackbody distribution over more than three decades in frequency (with some recent evidence for deviation at low frequencies [8]). A blackbody of the measured temperature corresponds to $n_\gamma = (2\zeta(3)/\pi^2) T_\gamma^3 \simeq 411$ cm $^{-3}$ and $\rho_\gamma = (\pi^2/15) T_\gamma^4 \simeq 4.64 \times 10^{-34}$ g cm $^{-3} \simeq 0.260$ eV cm $^{-3}$.

23.2.2. The Dipole :

The largest anisotropy is in the $\ell = 1$ (dipole) first spherical harmonic, with amplitude 3.355 ± 0.008 mK [6]. The dipole is interpreted to be the result of the Doppler shift caused by the solar system motion relative to the nearly isotropic blackbody field, as confirmed by measurements of the radial velocities of local galaxies [9].

The dipole is a frame-dependent quantity, and one can thus determine the ‘absolute rest frame’ as that in which the CMB dipole would be zero.

23.2.3. Higher-Order Multipoles :

The variations in the CMB temperature maps at higher multipoles ($\ell \geq 2$) are interpreted as being mostly the result of perturbations in the density of the early Universe, manifesting themselves at the epoch of the last scattering of the CMB photons. In the hot Big Bang picture, the expansion of the Universe cools the plasma so that by a redshift $z \simeq 1100$ (with little dependence on the details of the model), the hydrogen and helium nuclei can bind electrons into neutral atoms, a process usually referred to as recombination [12]. Before this epoch, the CMB photons are tightly coupled to the baryons, while afterwards they can freely stream towards us.

Theoretical models generally predict that the $a_{\ell m}$ modes are Gaussian random fields to high precision, *e.g.*, standard slow-roll inflation’s non-Gaussian contribution is expected to be one or two orders of magnitude below current observational limits [13]. Although non-Gaussianity of various forms is possible in early Universe models, tests show that Gaussianity is an extremely good simplifying approximation [14], with

only some relatively weak indications of non-Gaussianity or statistical anisotropy at large scales. Such signatures found in existing WMAP data are generally considered to be subtle foreground or instrumental artefacts [15,16].

A statistically isotropic sky means that all ms are equivalent, *i.e.*, there is no preferred axis. Together with the assumption of Gaussian statistics, the variance of the temperature field (or equivalently the power spectrum in ℓ) then fully characterizes the anisotropies. The power summed over all ms at each ℓ is $(2\ell + 1)C_\ell/(4\pi)$, where $C_\ell \equiv \langle |a_{\ell m}|^2 \rangle$. Thus averages of $a_{\ell m}$ s over m can be used as estimators of the C_ℓ s to constrain their expectation values, which are the quantities predicted by a theoretical model. For an idealized full-sky observation, the variance of each measured C_ℓ (*i.e.*, the variance of the variance) is $[2/(2\ell + 1)]C_\ell^2$. This sampling uncertainty (known as ‘cosmic variance’) comes about because each C_ℓ is χ^2 distributed with $(2\ell + 1)$ degrees of freedom for our observable volume of the Universe. For fractional sky coverage, f_{sky} , this variance is increased by $1/f_{\text{sky}}$ and the modes become partially correlated.

It is important to understand that theories predict the expectation value of the power spectrum, whereas our sky is a single realization. Hence the cosmic variance is an unavoidable source of uncertainty when constraining models; it dominates the scatter at lower ℓ s, while the effects of instrumental noise and resolution dominate at higher ℓ s [17].

23.2.4. Angular Resolution and Binning :

There is no one-to-one conversion between multipole ℓ and the angle subtended by a particular spatial scale projected onto the sky. However, a single spherical harmonic $Y_{\ell m}$ corresponds to angular variations of $\theta \sim \pi/\ell$. CMB maps contain anisotropy information from the size of the map (or in practice some fraction of that size) down to the beam-size of the instrument, σ . One can think of the effect of a Gaussian beam as rolling off the power spectrum with the function $e^{-\ell(\ell+1)\sigma^2}$.

23.5. Current Anisotropy Data

There has been a steady improvement in the quality of CMB data that has led to the development of the present-day cosmological model. Probably the most robust constraints currently available come from the combination of the WMAP five year data [34] with smaller scale results from the ACBAR [35] and QUAD [36] experiments (together with constraints from other cosmological data-sets). We plot power spectrum estimates from these experiments, as well as BOOMERANG [38] and CBI [39] in Fig. 23.2. Other recent experiments also give powerful constraints, which are quite consistent with what we describe below.

23.6. CMB Polarization

Since Thomson scattering of an anisotropic radiation field also generates linear polarization, the CMB is predicted to be polarized at the roughly 5% level of the temperature anisotropies [42]. Polarization is a spin-2 field on the sky, and the algebra of the modes in ℓ -space is strongly analogous to spin-orbit coupling in quantum mechanics [43]. The linear polarization pattern can be decomposed in a number of ways, with two quantities required for each pixel in a map, often given as the Q and U Stokes parameters. However, the most intuitive and physical decomposition is a geometrical one, splitting the polarization pattern into a part that comes from a divergence (often referred to as the ‘E-mode’) and a part with a curl (called the ‘B-mode’) [44]. More explicitly, the modes are defined

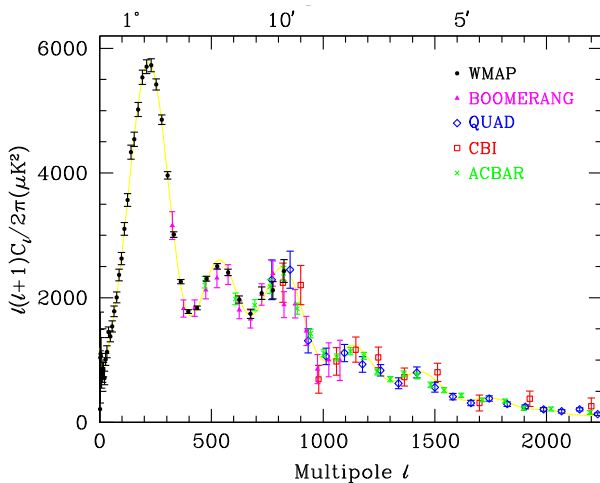


Figure 23.2: Band-power estimates from the WMAP, BOOMERANG, QUAD, CBI, and ACBAR experiments.

in terms of second derivatives of the polarization amplitude, with the Hessian for the E-modes having principle axes in the same sense as the polarization, while the B-mode pattern can be thought of simply as a 45° rotation of the E-mode pattern. Globally one sees that the E-modes have $(-1)^\ell$ parity (like the spherical harmonics), while the B-modes have $(-1)^{\ell+1}$ parity.

Since inflationary scalar perturbations give only E-modes, while tensors generate roughly equal amounts of E- and B-modes, then the determination of a non-zero B-mode signal is a way to measure the gravitational wave contribution (and thus potentially derive the energy scale of inflation), even if it is rather weak. However, one must first eliminate the foreground contributions and other systematic effects down to very low levels.

23.8. Constraints on Cosmologies

The 5-year WMAP data alone, together with constraints from Hubble constant determination [18], supernovae [64] and baryon acoustic oscillations [29], within the context of a 6 parameter family of models (which fixes $\Omega_{\text{tot}} = 1$ and $r = 0$), yield the following results [14]: $A = (2.44 \pm 0.10) \times 10^{-9}$, $n = 0.960 \pm 0.013$, $h = 0.705 \pm 0.013$, $\Omega_b h^2 = 0.0227 \pm 0.0006$, $\Omega_m h^2 = 0.136 \pm 0.004$ and $\tau = 0.084 \pm 0.016$. Note that for h , the CMB data alone provide only a very weak constraint, unless spatial flatness or some other cosmological data are used. For $\Omega_b h^2$, the precise value depends sensitively on how much freedom is allowed in the shape of the primordial power spectrum.

For Ω_{tot} , perhaps the best WMAP constraint is 1.006 ± 0.006 , from the combination with supernova and baryon acoustic oscillation constraints (and setting $w = -1$). The 95% confidence upper limit on r is 0.43 using WMAP alone, tightening to $r < 0.22$ with the addition of other data [14]. This limit depends on how the slope n is restricted and whether $dn/d \ln k \neq 0$ is allowed.

Further discussion and all references may be found in the full *Review*.

24. COSMIC RAYS

Written August 2008 by D.E. Groom (LBNL).

At ~ 10 GeV/nucleon the primary cosmic rays are mostly protons (79%) and alpha particles (15% of the cosmic ray nucleons). The abundance ratios of heavier nuclei follow the solar abundance ratios. The exception is the Li-Be-B group, which is overabundant by a large factor relative to solar abundance, probably due to the spallation of heavier nuclei in the interstellar medium. The intensity from a few GeV to beyond 100 TeV is proportional to $E^{-2.7}$. The spectrum is evidently truncated at a few times 10^{19} eV by inelastic collisions with the CMB (GZK mechanism).

The primary cosmic rays initiate hadronic cascades in the atmosphere, whose thickness is $11.5 \lambda_I$ or $28 X_0$. Most of the energy is converted to gamma rays via $\pi^0 \rightarrow \gamma\gamma$ and deposited by ionization in EM showers; few hadrons reach the ground. For charged pions, $\pi^\pm \rightarrow \mu^\pm + \nu$ competes with further nuclear interaction. The muon energy spectrum at the surface is almost flat below 1 GeV, gradually steepens to reflect the primary spectrum in the 10–100 GeV range, and steepens further at higher energies because pions with $E_\pi \gtrsim 100$ GeV tend to interact before they decay. Above ~ 10 TeV, and below ~ 100 TeV, when prompt muon production becomes important, the energy spectrum of atmospheric muons is one power steeper than the primary spectrum.

The average muon flux at the surface goes as $\cos^2\theta$, characteristic of ~ 3 GeV muons. The rate in a thin horizontal detector is roughly $1 \text{ cm}^{-2}\text{min}^{-1}$; it is half this in a vertical detector.

The vertical muon flux for $E > 1$ GeV goes through a broad maximum at an atmospheric depth $h \approx 170 \text{ g cm}^{-2}$, but for $h \gtrsim 300 \text{ g cm}^{-2}$ it can be fairly well represented by $I/I_{\text{surface}} = \exp[(h - 1033 \text{ g cm}^{-2}) / (630 \text{ g cm}^{-2})]$. Calculators to convert h to altitude in a "standard atmosphere" can be found on the web. At the summit of Mauna Kea ($4205 \text{ m} = 600 \text{ g cm}^{-2}$) the vertical flux is about twice that at sea level.

The vertical $p + n$ flux at sea level is about 2% of the muon flux, but scales with depth as $\exp(-h/\lambda_I)$. The pion flux is 50 times smaller. The e^+/e^- flux for $E > 1$ GeV averages about 0.004 of the muon flux, but these EM shower remnants are much more abundant at lower energies.

The energy loss rate for muons is usually written as $a(E) + b(E)E$, where $a(E)$ (ionization) and $b(E)$ (radiative loss rate/ E) are slowly-varying functions of E . Ionization and radiative loss rates are equal at the muon critical energy $E_{\mu c}$, which is typically several hundred GeV. If $a(E_{\mu c})$ and $b(E_{\mu c})$ are assumed constant, then the range is given by $\ln(1 + E/E_{\mu c})$. (Straggling is extremely important, but it is also neglected here.) Furthermore, since the differential muon flux at very high energies is proportional to $E^{-\alpha}$ (one power steeper than the primary spectrum), the total vertical flux at depth X is proportional to $(e^{bX} - 1)^{-\alpha+1}$. This function, with $b = 4.0 \times 10^{-6} \text{ cm}^2\text{g}^{-1}$ and $\alpha = 3.6$, normalized to $0.013 \text{ m}^{-2}\text{s}^{-1}\text{sr}^{-1}$ at $X = 1 \text{ km.w.e.}$ (km water equivalent), gives a reasonable fit to the depth-intensity data shown in Fig. 24.5 of the full *Review*. The flux at depths $\gtrsim 10\text{--}20 \text{ km.w.e.}$, entirely due to neutrino interactions, is about $2 \times 10^{-9} \text{ m}^{-2}\text{s}^{-1}\text{sr}^{-1}$.

For details and references, see the full *Review*.

25. ACCELERATOR PHYSICS OF COLLIDERS

Revised August 2005 by K. Desler and D. A. Edwards (DESY).

25.2. Luminosity

The event rate R in a collider is proportional to the interaction cross section σ_{int} and the factor of proportionality is called the *luminosity*:

$$R = \mathcal{L}\sigma_{\text{int}} . \quad (25.1)$$

If two bunches containing n_1 and n_2 particles collide with frequency f , the luminosity is

$$\mathcal{L} = f \frac{n_1 n_2}{4\pi\sigma_x\sigma_y} \quad (25.2)$$

where σ_x and σ_y characterize the Gaussian transverse beam profiles in the horizontal (bend) and vertical directions and to simplify the expression it is assumed that the bunches are identical in transverse profile, that the profiles are independent of position along the bunch, and the particle distributions are not altered during collision. Whatever the distribution at the source, by the time the beam reaches high energy, the normal form is a good approximation thanks to the central limit theorem of probability and the diminished importance of space charge effects.

The beam size can be expressed in terms of two quantities, one termed the *transverse emittance*, ϵ , and the other, the *amplitude function*, β . The transverse emittance is a beam quality concept reflecting the process of bunch preparation, extending all the way back to the source for hadrons and, in the case of electrons, mostly dependent on synchrotron radiation. The amplitude function is a beam optics quantity and is determined by the accelerator magnet configuration. When expressed in terms of σ and β the transverse emittance becomes

$$\epsilon = \pi\sigma^2/\beta . \quad (25.3)$$

Of particular significance is the value of the amplitude function at the interaction point, β^* . Clearly one wants β^* to be as small as possible; how small depends on the capability of the hardware to make a near-focus at the interaction point.

Eq. (25.2) can now be recast in terms of emittances and amplitude functions as

$$\mathcal{L} = f \frac{n_1 n_2}{4\sqrt{\epsilon_x \beta_x^* \epsilon_y \beta_y^*}} . \quad (25.4)$$

Thus, to achieve high luminosity, all one has to do is make high population bunches of low emittance to collide at high frequency at locations where the beam optics provides as low values of the amplitude functions as possible.

Further discussion and references may be found in the full *Review of Particle Physics*.

26. HIGH-ENERGY COLLIDER PARAMETERS: e^+e^- Colliders (I)

Updated in early 2010 with numbers received from representatives of the colliders (contact J. Beringer, LBNL). For existing (future) colliders the latest achieved (design) values are given. quantities are, where appropriate, r.m.s.; H and V indicate horizontal and vertical directions; s.c. stands for superconducting. Parameters for the defunct SPEAR, DORIS, PETRA, PEP, SLC, TRISTAN, and VEPP-2M colliders may be found in our 1996 edition (Phys. Rev. **D54**, 1 July 1996, Part I).

	VEPP-2000 (Novosibirsk)	VEPP-4M (Novosibirsk)	CESR-C (Cornell)	BEP-C-II (China)	DAΦNE (Frascati)
Physics start date	2008	1994	2002	2008	1999
Physics end date	—	—	2008	—	2013
Maximum beam energy (GeV)	1.0	6	6	1.89 (2.3 max)	0.700
Luminosity ($10^{30} \text{ cm}^{-2}\text{s}^{-1}$)	100	20	76 at 2.08 GeV/beam	330	450 (1000 achievable)
Time between collisions (μs)	0.04	0.6	0.014 to 0.22	0.008	0.0027
Energy spread (units 10^{-3})	0.64	1	0.82 at 2.08 GeV/beam	0.52	0.40
Bunch length (cm)	4	5	1.2	1.3	low current: 1 high current: 2
Beam radius (10^{-6} m)	125 (round)	H : 1000 V : 30	H : 340 V : 6.5	H : 380 V : 5.7	H : 800 V : 4.8
Free space at interaction point (m)	± 1	± 2	$\pm 2.2 (\pm 0.3$ to PM quads)	± 0.63	± 0.40
β^* , amplitude function at interaction point (m)	H : 0.06 – 0.11 V : 0.06 – 0.10	H : 0.75 V : 0.05	H : 0.94 V : 0.012	H : 1.0 V : 0.015	H : 0.25 V : 0.009
Interaction regions	2	1	1	1	1

HIGH-ENERGY COLLIDER PARAMETERS: e^+e^- Colliders (II)

Updated in early 2010 (contact J. Beringer, LBNL). For existing (future) colliders the latest achieved (design) values are given. Quantities are, where appropriate, r.m.s.; H and V indicate horizontal and vertical directions; s.c. stands for superconducting.

	KEKB (KEK)	PEP-II (SLAC)	SuperB (Italy)	SuperKEKB (KEK)	ILC (TBD)
Physics start date	1999	1999	TBD	2014?	TBD
Physics end date	—	2008	—	—	—
Maximum beam energy (GeV)	$e^- : 8.33$ (8.0 nominal) $e^+ : 3.64$ (3.5 nominal)	$e^- : 7-12$ (9.0 nominal) $e^+ : 2.5-4$ (3.1 nominal) (nominal $E_{\text{cm}} = 10.5$ GeV)	$e^- : 4.2$ $e^+ : 6.7$	$e^- : 7$ $e^+ : 4$	250 (upgrade-able to 500)
Luminosity ($10^{30} \text{ cm}^{-2} \text{ s}^{-1}$)	21083	12069 (design: 3000)	1.0×10^6	8×10^5	2×10^4
Time between collisions (μs)	0.00590 or 0.00786	0.0042	0.0042	0.004	0.3^\ddagger
Energy spread (units 10^{-3})	0.7	$e^-/e^+ : 0.61/0.77$	$e^-/e^+ : 0.73/0.64$	$e^-/e^+ : 0.58/0.84$	1
Bunch length (cm)	0.65	$e^-/e^+ : 1.1/1.0$	0.5	$e^-/e^+ : 0.5/0.6$	0.03
Beam radius (μm)	$H : 124$ (e^-), 117 (e^+) $V : 0.94$	$H : 157$ $V : 4.7$	$H : 8$ $V : 0.04$	$e^- : 11(H), 0.062(V)$ $e^+ : 10(H), 0.048(V)$	$H : 0.639$ $V : 0.0057$
Free space at interaction point (m)	$+0.75/-0.58$ ($+300/-500$) mrad cone	± 0.2 , ± 300 mrad cone	± 0.35	$e^- : +1.20/-1.28, e^+ : +0.78/-0.73$ ($+300/-500$) mrad cone)	± 3.5
β^* , amplitude function at interaction point (m)	$e^- : 1.2$ (0.27^*)(H), 0.0059 (V) $e^+ : 1.2$ (0.23^*)(H), 0.0059 (V)	$e^- : 0.50$ (H), 0.012 (V) $e^+ : 0.50$ (H), 0.012 (V)	$e^- : 0.032(H), 0.00021(V)$ $e^+ : 0.026(H), 0.00025(V)$	$e^- : 0.025(H), 3 \times 10^{-4}(V)$ $e^+ : 0.032(H), 2.7 \times 10^{-4}(V)$	$H : 0.02$ $V : 0.0004$
Interaction regions	1	1	1	1	1

‡ Time between bunch trains: 200ms.

* With dynamic beam-beam effect.

HIGH-ENERGY COLLIDER PARAMETERS: *ep*, $\bar{p}p$, *pp*, and Heavy Ion Colliders

Updated in early 2010 (contact J. Beringer, LBNL). For existing (future) colliders the latest achieved (design) values are given. Quantities are, where appropriate, r.m.s.; *H* and *V* indicate horizontal and vertical directions; s.c. stands for superconducting; pk and ave denote peak and average values.

	HERA (DESY)	TEVATRON (Fermilab)	RHIC (Brookhaven)				LHC† (CERN)	
	1992 2007	1987	2001	2000	2004	2002	2009	2010
Physics start date								
Physics end date								
Particles collided	<i>ep</i>	$p\bar{p}$	<i>pp</i> (pol.)	Au Au	Cu Cu	d Au	<i>pp</i>	Pb Pb
Maximum beam energy (TeV)	<i>e</i> : 0.030 <i>p</i> : 0.92	0.980	0.25 34% pol	0.1 TeV/n	0.1 TeV/n	0.1 TeV/n	7.0 (3.5)	2.76 TeV/n (1.38 TeV/n)
Luminosity ($10^{30} \text{ cm}^{-2} \text{ s}^{-1}$)	75	402	85 (pk) 55 (ave)	0.0040 (pk) 0.0020 (ave)	0.020 (pk) 0.0008 (ave)	0.27 (pk) 0.14 (ave)	1.0×10^4 (170)	1.0×10^{-3} (1.3×10^{-5})
Time between collisions (ns)	96	396	107	107	321	107	24.95 (49.90)	99.8 (1347)
Bunch length (cm)	<i>e</i> : 0.83 <i>p</i> : 8.5	<i>p</i> : 50 \bar{p} : 45	55	30	30	30	7.55 (5.87)	7.94 (5.83)
Beam radius (10^{-6} m)	<i>e</i> : 280(<i>H</i>), 50(<i>V</i>) <i>p</i> : 265(<i>H</i>), 50(<i>V</i>)	<i>p</i> : 28 \bar{p} : 16	90	135	145	145	16.6 (45)	15.9 (45)
Free space at interaction point (m)	±2	±6.5			16		38	38
β^* ; ampl. function at interaction point (m)	<i>e</i> : 0.6(<i>H</i>), 0.26(<i>V</i>) <i>p</i> : 2.45(<i>H</i>), 0.18(<i>V</i>)	0.28	0.7	0.75	0.9	0.85	0.55 (2.0)	0.5 (2.0)
Circumference (km)	6.336	6.28	3.834				26.659	
Interaction regions	2 colliding beams 1 fixed target (<i>e</i> beam)	2 high \mathcal{L}	6 total, 2 high \mathcal{L}				2 high \mathcal{L} +2	1 dedicated +2

† Numbers in parentheses refer to goals for operation in 2010.

27. PASSAGE OF PARTICLES THROUGH MATTER

Revised January 2010 by H. Bichsel (University of Washington), D.E. Groom (LBNL), and S.R. Klein (LBNL).

27.1. Notation

Table 27.1: Summary of variables used in this section. The kinematic variables β and γ have their usual meanings.

Symbol	Definition	Units or Value
α	Fine structure constant $(e^2/4\pi\epsilon_0\hbar c)$	1/137.035 999 11(46)
M	Incident particle mass	MeV/ c^2
E	Incident part. energy $\gamma M c^2$	MeV
T	Kinetic energy	MeV
$m_e c^2$	Electron mass $\times c^2$	0.510 998 918(44) MeV
r_e	Classical electron radius $e^2/4\pi\epsilon_0 m_e c^2$	2.817 940 325(28) fm
N_A	Avogadro's number	$6.022 1415(10) \times 10^{23} \text{ mol}^{-1}$
ze	Charge of incident particle	
Z	Atomic number of absorber	
A	Atomic mass of absorber	g mol^{-1}
K/A	$4\pi N_A r_e^2 m_e c^2 / A$	$0.307 075 \text{ MeV g}^{-1} \text{ cm}^2$ for $A = 1 \text{ g mol}^{-1}$
I	Mean excitation energy	eV (<i>Nota bene!</i>)
$\delta(\beta\gamma)$	Density effect correction to ionization energy loss	
$\hbar\omega_p$	Plasma energy $(\sqrt{4\pi N_e r_e^3} m_e c^2 / \alpha)$	$\sqrt{\rho \langle Z/A \rangle} \times 28.816 \text{ eV}$ (ρ in g cm^{-3})
N_e	Electron density	(units of r_e) $^{-3}$
w_j	Weight fraction of the j th element in a compound or mixture	
n_j	\times number of j th kind of atoms in a compound or mixture	
—	$4\alpha r_e^2 N_A / A$	$(716.408 \text{ g cm}^{-2})^{-1}$ for $A = 1 \text{ g mol}^{-1}$
X_0	Radiation length	g cm^{-2}
E_c	Critical energy for electrons	MeV
$E_{\mu c}$	Critical energy for muons	GeV
E_s	Scale energy $\sqrt{4\pi/\alpha} m_e c^2$	21.2052 MeV
R_M	Molière radius	g cm^{-2}

27.2. Electronic energy loss by heavy particles [1–32]

27.2.1. Moments and cross sections :

The electronic interactions of fast charged particles with speed $v = \beta c$ occur in *single collisions with energy losses* E [1], leading to ionization, atomic, or collective excitation. Most frequently the energy losses are small (for 90% of all collisions the energy losses are less than 100 eV). In thin absorbers few collisions will take place and the total energy loss will show a large variance [1]; also see Sec. 27.2.7 below. For particles with

27.2.2. Stopping power at intermediate energies : The mean rate of energy loss by moderately relativistic charged heavy particles, $M_1/\delta x$, is well-described by the “Bethe” equation,

$$-\left\langle \frac{dE}{dx} \right\rangle = Kz^2 \frac{Z}{A} \frac{1}{\beta^2} \left[\frac{1}{2} \ln \frac{2m_e c^2 \beta^2 \gamma^2 T_{\max}}{I^2} - \beta^2 - \frac{\delta(\beta\gamma)}{2} \right]. \quad (27.3)$$

It describes the mean loss rate in the region $0.1 \lesssim \beta\gamma \lesssim 1000$ for intermediate- Z materials with an accuracy of a few %. At the lower limit the projectile velocity becomes comparable to atomic electron “velocities” (Sec. 27.2.3), and at the upper limit radiative effects begin to be important (Sec. 27.6). Both limits are Z dependent. Here T_{\max} is the maximum kinetic energy which can be imparted to a free electron in a single collision, and the other variables are defined in Table 27.1. A minor dependence on M at the highest energies is introduced through T_{\max} , but for all practical purposes $\langle dE/dx \rangle$ in a given material is a function of β alone. With the symbol definitions and values given in Table 27.1, the units are MeV g⁻¹cm².

Few concepts in high-energy physics are as misused as $\langle dE/dx \rangle$. The main problem is that the mean is weighted by very rare events with large single-collision energy deposits. Even with samples of hundreds of events a dependable value for the mean energy loss cannot be obtained. Far better and more easily measured is the most probable energy loss, discussed in Sec. 27.2.7. It is considerably below the mean given by the Bethe equation.

In a TPC (Sec. 28.6.5), the mean of 50%–70% of the samples with the smallest signals is often used as an estimator.

Although it must be used with cautions and caveats, $\langle dE/dx \rangle$ as described in Eq. (27.3) still forms the basis of much of our understanding of energy loss by charged particles. Extensive tables are available[5,4, pdg.lbl.gov/AtomicNuclearProperties/].

The function as computed for muons on copper is shown as the “Bethe” region of Fig. 27.1. Mean energy loss behavior below this region is discussed in Sec. 27.2.3, and the radiative effects at high energy are discussed in Sec. 27.6. Only in the Bethe region is it a function of β alone; the mass dependence is more complicated elsewhere. The stopping power in several other materials is shown in Fig. 27.2. Except in hydrogen, particles with the same velocity have similar rates of energy loss in different materials, although there is a slow decrease in the rate of energy loss with increasing Z . The qualitative behavior difference at high energies between a gas (He in the figure) and the other materials shown in the figure is due to the density-effect correction, $\delta(\beta\gamma)$, discussed in Sec. 27.2.4. The stopping power functions are characterized by broad minima whose position drops from $\beta\gamma = 3.5$ to 3.0 as Z goes from 7 to 100. The values of minimum ionization go roughly as $0.235 - 0.28 \ln(Z)$, in MeV g⁻¹cm⁻², for $Z > 6$.

Eq. (27.3) may be integrated to find the total (or partial) “continuous slowing-down approximation” (CSDA) range R for a particle which loses energy only through ionization and atomic excitation. Since dE/dx in the “Bethe region” depends only on β , R/M is a function of E/M or pc/M . In practice, range is a useful concept only for low-energy hadrons ($R \lesssim \lambda_I$, where λ_I is the nuclear interaction length), and for muons below a few hundred GeV (above which radiative effects dominate). R/M as a function of $\beta\gamma = p/Mc$ is shown for a variety of materials in Fig. 27.4.

The mass scaling of dE/dx and range is valid for the electronic losses described by the Bethe equation, but not for radiative losses, relevant only for muons and pions.

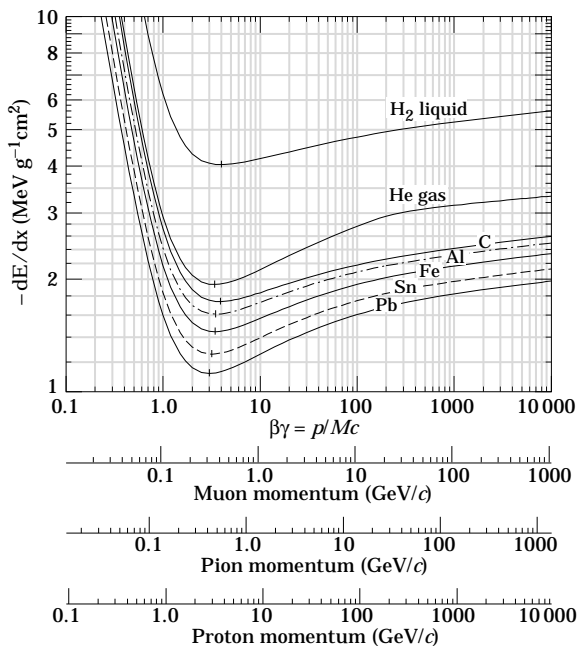


Figure 27.2: Mean energy loss rate in liquid (bubble chamber) hydrogen, gaseous helium, carbon, aluminum, iron, tin, and lead. Radiative effects, relevant for muons and pions, are not included. These become significant for muons in iron for $\beta\gamma \gtrsim 1000$, and at lower momenta in higher- Z absorbers. See Fig. 27.21.

For a particle with mass M and momentum $M\beta\gamma c$, T_{\max} is given by

$$T_{\max} = \frac{2m_e c^2 \beta^2 \gamma^2}{1 + 2\gamma m_e/M + (m_e/M)^2}. \quad (27.4)$$

In older references [2,7] the “low-energy” approximation $T_{\max} = 2m_e c^2 \beta^2 \gamma^2$, valid for $2\gamma m_e/M \ll 1$, is often implicit. For hadrons with $E \simeq 100$ GeV, it is limited by structure effects.

Estimates of the mean excitation energy I based on experimental stopping-power measurements for protons, deuterons, and alpha particles are given in ICRU 37 [10]; see also [pdg.lbl.gov.AtomicNuclearProperties](http://pdg.lbl.gov/AtomicNuclearProperties).

27.2.4. Density effect: As the particle energy increases, its electric field flattens and extends, so that the distant-collision contribution to Eq. (27.3) increases as $\ln \beta\gamma$. However, real media become polarized, limiting the field extension and effectively truncating this part of the logarithmic rise [2–7,18–20]. At very high energies,

$$\delta/2 \rightarrow \ln(\hbar\omega_p/I) + \ln \beta\gamma - 1/2, \quad (27.5)$$

where $\delta(\beta\gamma)/2$ is the density effect correction introduced in Eq. (27.3) and $\hbar\omega_p$ is the plasma energy defined in Table 27.1. A comparison with Eq. (27.3) shows that $|dE/dx|$ then grows as $\ln \beta\gamma$ rather than $\ln \beta^2 \gamma^2$, and that the mean excitation energy I is replaced by the plasma energy

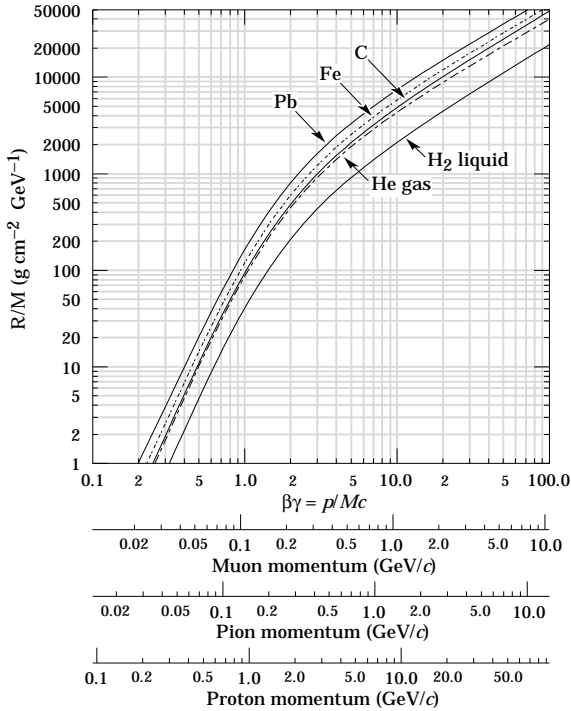


Figure 27.4: Range of heavy charged particles in liquid (bubble chamber) hydrogen, helium gas, carbon, iron, and lead. For example: For a K^+ whose momentum is $700 \text{ MeV}/c$, $\beta\gamma = 1.42$. For lead we read $R/M \approx 396$, and so the range is 195 g cm^{-2} .

$\hbar\omega_p$. Since the plasma frequency scales as the square root of the electron density, the correction is much larger for a liquid or solid than for a gas, as is illustrated by the examples in Fig. 27.2.

The remaining relativistic rise comes from the $\beta^2\gamma^2$ growth of T_{\max} , which in turn is due to (rare) large energy transfers to a few electrons. When these events are excluded, the energy deposit in an absorbing layer approaches a constant value, the Fermi plateau (see Sec. 27.2.6 below). At extreme energies (*e.g.*, $> 332 \text{ GeV}$ for muons in iron, and at a considerably higher energy for protons in iron), radiative effects are more important than ionization losses. These are especially relevant for high-energy muons, as discussed in Sec. 27.6.

27.2.5. Energetic knock-on electrons (δ rays): The distribution of secondary electrons with kinetic energies $T \gg I$ is [2]

$$\frac{d^2N}{dTdx} = \frac{1}{2} K z^2 \frac{Z}{A} \frac{1}{\beta^2} \frac{F(T)}{T^2} \quad (27.7)$$

for $I \ll T \leq T_{\max}$, where T_{\max} is given by Eq. (27.4). Here β is the velocity of the primary particle. The factor F is spin-dependent, but is about unity for $T \ll T_{\max}$. For spin-0 particles $F(T) = (1 - \beta^2 T/T_{\max})$; forms for spins $1/2$ and 1 are also given by Rossi [2]. For incident electrons, the indistinguishability of projectile and target means that the

range of T extends only to half the kinetic energy of the incident particle. Additional formulae are given in Ref. 22. Equation (27.7) is inaccurate for T close to I . The cosine of the production angle is essentially unity in practical cases.

δ rays of even modest energy are rare. For $\beta \approx 1$ particle, for example, on average only one collision with $T_e > 1$ keV will occur along a path length of 90 cm of Ar gas [1].

27.2.6. Restricted energy loss rates for relativistic ionizing particles: Further insight can be obtained by examining the mean energy deposit by an ionizing particle when energy transfers are restricted to $T \leq T_{\text{cut}} \leq T_{\text{max}}$. The restricted energy loss rate is

$$-\frac{dE}{dx} \Big|_{T < T_{\text{cut}}} = Kz^2 \frac{Z}{A} \frac{1}{\beta^2} \left[\frac{1}{2} \ln \frac{2m_e c^2 \beta^2 \gamma^2 T_{\text{cut}}}{I^2} - \frac{\beta^2}{2} \left(1 + \frac{T_{\text{cut}}}{T_{\text{max}}} \right) - \frac{\delta}{2} \right]. \quad (27.9)$$

This form approaches the normal Bethe function (Eq. (27.3)) as $T_{\text{cut}} \rightarrow T_{\text{max}}$. It can be verified that the difference between Eq. (27.3) and Eq. (27.9) is equal to $\int_{T_{\text{cut}}}^{T_{\text{max}}} T(d^2N/dTdx)dT$, where $d^2N/dTdx$ is given by Eq. (27.7).

Since T_{cut} replaces T_{max} in the argument of the logarithmic term of Eq. (27.3), the $\beta\gamma$ term producing the relativistic rise in the close-collision part of dE/dx is replaced by a constant, and $|dE/dx|_{T < T_{\text{cut}}}$ approaches the constant ‘‘Fermi plateau.’’ (The density effect correction δ eliminates the explicit $\beta\gamma$ dependence produced by the distant-collision contribution.) This behavior is illustrated in Fig. 27.6, where restricted loss rates for two examples of T_{cut} are shown in comparison with the full Bethe dE/dx and the Landau-Vavilov most probable energy loss (to be discussed in Sec. 27.2.7 below).

27.2.7. Fluctuations in energy loss: For detectors of moderate thickness x (e.g. scintillators or LAr cells),* the energy loss probability distribution $f(\Delta; \beta\gamma, x)$ is adequately described by the highly-skewed Landau (or Landau-Vavilov) distribution [24,25]. The most probable energy loss is [26]

$$\Delta_p = \xi \left[\ln \frac{2mc^2 \beta^2 \gamma^2}{I} + \ln \frac{\xi}{I} + j - \beta^2 - \delta(\beta\gamma) \right], \quad (27.10)$$

where $\xi = (K/2) \langle Z/A \rangle (x/\beta^2)$ MeV for a detector with a thickness x in g cm⁻², and $j = 0.200$ [26]. † While dE/dx is independent of thickness, Δ_p/x scales as $a \ln x + b$. The density correction $\delta(\beta\gamma)$ was not included in Landau’s or Vavilov’s work, but it was later included by Bichsel [26]. The high-energy behavior of $\delta(\beta\gamma)$ (Eq. (27.5)), is such that

$$\Delta_p \xrightarrow{\beta\gamma \gtrsim 100} \xi \left[\ln \frac{2mc^2 \xi}{(\hbar\omega_p)^2} + j \right]. \quad (27.11)$$

Thus the Landau-Vavilov most probable energy loss, like the restricted energy loss, reaches a Fermi plateau. The Bethe dE/dx and Landau-Vavilov-Bichsel Δ_p/x in silicon are shown as a function of muon energy in Fig. 27.6. The case $x/\rho = 1600 \mu\text{m}$ was chosen since it has about

* $G \lesssim 0.05\text{--}0.1$, where G is given by Rossi [Ref. 2, Eq. 2.7.10]. It is Vavilov’s κ [25].

† Rossi [2], Talman [27], and others give somewhat different values for j . The most probable loss is not sensitive to its value.

the same stopping power as does 3 mm of plastic scintillator. Folding in experimental resolution displaces the peak of the distribution, usually toward a higher value.

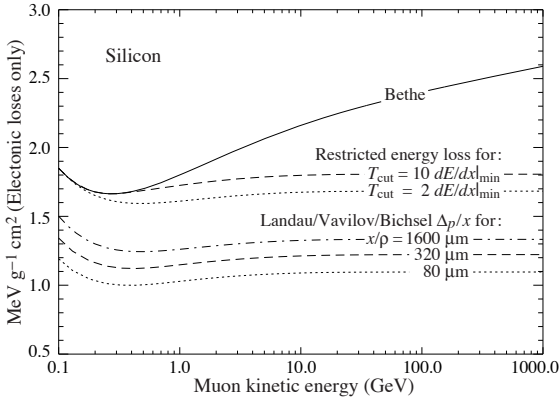


Figure 27.6: Bethe dE/dx , two examples of restricted energy loss, and the Landau most probable energy per unit thickness in silicon. The change of $\Delta p/x$ with thickness x illustrates its $a \ln x + b$ dependence. Minimum ionization ($dE/dx|_{\min}$) is $1.664 \text{ MeV g}^{-1} \text{ cm}^2$. Radiative losses are excluded. The incident particles are muons.

The mean of the energy-loss given by the Bethe equation, Eq. (27.3), is ill-defined experimentally and is not useful for describing energy loss by single particles. (It finds its application in dosimetry, where only bulk deposit is of relevance.) It rises as $\ln \beta\gamma$ because T_{\max} increases as $\beta^2\gamma^2$. The large single-collision energy transfers that increasingly extend the long tail are rare, making the mean of an experimental distribution consisting of a few hundred events subject to large fluctuations and sensitive to cuts as well as to background. The most probable energy loss should be used.

For very thick absorbers the distribution is less skewed but never approaches a Gaussian. In the case of Si illustrated in Fig. 27.6, the most probable energy loss per unit thickness for $x \approx 35 \text{ g cm}^{-2}$ is very close to the restricted energy loss with $T_{\text{cut}} = 2 dE/dx|_{\min}$.

The Landau distribution fails to describe energy loss in thin absorbers such as gas TPC cells [1] and Si detectors [26], as shown clearly in Fig. 1 of Ref. 1 for an argon-filled TPC cell. Also see Talman [27]. While $\Delta p/x$ may be calculated adequately with Eq. (27.10), the distributions are significantly wider than the Landau width $w = 4\xi$ [Ref. 26, Fig. 15]. Examples for thin silicon detectors are shown in Fig. 27.7.

27.2.8. Energy loss in mixtures and compounds: A mixture or compound can be thought of as made up of thin layers of pure elements in the right proportion (Bragg additivity). In this case,

$$\frac{dE}{dx} = \sum w_j \left. \frac{dE}{dx} \right|_j, \quad (27.12)$$

where $dE/dx|_j$ is the mean rate of energy loss (in MeV g cm^{-2}) in the j th element. Eq. (27.3) can be inserted into Eq. (27.12) to find expressions for $\langle Z/A \rangle$, $\langle I \rangle$, and $\langle \delta \rangle$; for example, $\langle Z/A \rangle = \sum w_j Z_j/A_j = \sum n_j Z_j / \sum n_j A_j$. However, $\langle I \rangle$ as defined this way is

an underestimate, because in a compound electrons are more tightly bound than in the free elements, and $\langle\delta\rangle$ as calculated this way has little relevance, because it is the electron density that matters. If possible, one uses the tables given in Refs. 20 and 28, or the recipes given in Ref. 21 (repeated in Ref. 5), which include effective excitation energies and interpolation coefficients for calculating the density effect correction.

27.3. Multiple scattering through small angles

A charged particle traversing a medium is deflected by many small-angle scatters. Most of this deflection is due to Coulomb scattering from nuclei, and hence the effect is called multiple Coulomb scattering. (However, for hadronic projectiles, the strong interactions also contribute to multiple scattering.) The Coulomb scattering distribution is well represented by the theory of Molière [33]. It is roughly Gaussian for small deflection angles, but at larger angles (greater than a few θ_0 , defined below) it behaves like Rutherford scattering, with larger tails than does a Gaussian distribution.

If we define

$$\theta_0 = \theta_{\text{plane}}^{\text{rms}} = \frac{1}{\sqrt{2}} \theta_{\text{space}}^{\text{rms}}. \quad (27.13)$$

then it is usually sufficient to use a Gaussian approximation for the central 98% of the projected angular distribution, with a width given by [34,35]

$$\theta_0 = \frac{13.6 \text{ MeV}}{\beta c p} z \sqrt{x/X_0} \left[1 + 0.038 \ln(x/X_0) \right]. \quad (27.14)$$

Here p , βc , and z are the momentum, velocity, and charge number of the incident particle, and x/X_0 is the thickness of the scattering medium in radiation lengths (defined below). This value of θ_0 is from a fit to Molière distribution [33] for singly charged particles with $\beta = 1$ for all Z , and is accurate to 11% or better for $10^{-3} < x/X_0 < 100$.

27.4. Photon and electron interactions in matter

27.4.1. Radiation length: High-energy electrons predominantly lose energy in matter by bremsstrahlung, and high-energy photons by e^+e^- pair production. The characteristic amount of matter traversed for these related interactions is called the radiation length X_0 , usually measured in g cm^{-2} . It is both (a) the mean distance over which a high-energy electron loses all but $1/e$ of its energy by bremsstrahlung, and (b) $\frac{7}{9}$ of the mean free path for pair production by a high-energy photon [37]. It is also the appropriate scale length for describing high-energy electromagnetic cascades. X_0 has been calculated and tabulated by Y.S. Tsai [38]:

$$\frac{1}{X_0} = 4\alpha r_e^2 \frac{N_A}{A} \left\{ Z^2 [L_{\text{rad}} - f(Z)] + Z L'_{\text{rad}} \right\}. \quad (27.22)$$

For $A = 1 \text{ g mol}^{-1}$, $4\alpha r_e^2 N_A/A = (716.408 \text{ g cm}^{-2})^{-1}$. L_{rad} and L'_{rad} are given in Table 27.2. The function $f(Z)$ is an infinite sum, but for elements up to uranium can be represented to 4-place accuracy by

$$f(Z) = a^2 [(1+a^2)^{-1} + 0.20206 - 0.0369 a^2 + 0.0083 a^4 - 0.002 a^6], \quad (27.23)$$

where $a = \alpha Z$ [39].

27.4.2. Energy loss by electrons: At low energies electrons and positrons primarily lose energy by ionization, although other processes (Møller scattering, Bhabha scattering, e^+ annihilation) contribute, as shown in Fig. 27.10. While ionization loss rates rise logarithmically with energy, bremsstrahlung losses rise nearly linearly (fractional loss is nearly independent of energy), and dominates above a few tens of MeV in most materials.

Table 27.2: Tsai's L_{rad} and L'_{rad} , for use in calculating the radiation length in an element using Eq. (27.22).

Element	Z	L_{rad}	L'_{rad}
H	1	5.31	6.144
He	2	4.79	5.621
Li	3	4.74	5.805
Be	4	4.71	5.924
Others	> 4	$\ln(184.15 Z^{-1/3})$	$\ln(1194 Z^{-2/3})$

Ionization loss by electrons and positrons differs from loss by heavy particles because of the kinematics, spin, and the identity of the incident electron with the electrons which it ionizes. Complete discussions and tables can be found in Refs. 9, 10, and 28.

At very high energies and except at the high-energy tip of the bremsstrahlung spectrum, the cross section can be approximated in the “complete screening case” as [38]

$$d\sigma/dk = (1/k)4\alpha r_e^2 \left\{ \left(\frac{4}{3} - \frac{4}{3}y + y^2 \right) [Z^2(L_{\text{rad}} - f(Z)) + Z L'_{\text{rad}}] + \frac{1}{9}(1-y)(Z^2 + Z) \right\}, \quad (27.26)$$

where $y = k/E$ is the fraction of the electron's energy transferred to the radiated photon. At small y (the “infrared limit”) the term on the second line ranges from 1.7% (low Z) to 2.5% (high Z) of the total. If it is ignored and the first line simplified with the definition of X_0 given in Eq. (27.22), we have

$$\frac{d\sigma}{dk} = \frac{A}{X_0 N_A k} \left(\frac{4}{3} - \frac{4}{3}y + y^2 \right). \quad (27.27)$$

This formula is accurate except in near $y = 1$, where screening may become incomplete, and near $y = 0$, where the infrared divergence is removed by the interference of bremsstrahlung amplitudes from nearby scattering centers (the LPM effect) [41,42] and dielectric suppression [43,44]. These and other suppression effects in bulk media are discussed in Sec. 27.4.5.

Except at these extremes, and still in the complete-screening approximation, the number of photons with energies between k_{min} and k_{max} emitted by an electron travelling a distance $d \ll X_0$ is

$$N_\gamma = \frac{d}{X_0} \left[\frac{4}{3} \ln \left(\frac{k_{\text{max}}}{k_{\text{min}}} \right) - \frac{4(k_{\text{max}} - k_{\text{min}})}{3E} + \frac{k_{\text{max}}^2 - k_{\text{min}}^2}{2E^2} \right]. \quad (27.28)$$

27.4.3. Critical energy: An electron loses energy by bremsstrahlung at a rate nearly proportional to its energy, while the ionization loss rate varies only logarithmically with the electron energy. The *critical energy* E_c is sometimes defined as the energy at which the two loss rates are equal [46]. Among alternate definitions is that of Rossi [2], who defines the critical energy as the energy at which the ionization loss per radiation length is equal to the electron energy. Equivalently, it is the same as the first definition with the approximation $|dE/dx|_{\text{brems}} \approx E/X_0$. This form has been found to describe transverse electromagnetic shower development more accurately (see below).

The accuracy of approximate forms for E_c has been limited by the failure to distinguish between gases and solid or liquids, where there is a substantial difference in ionization at the relevant energy because of

the density effect. Separate fits to $E_c(Z)$, using the Rossi definition, have been made with functions of the form $a/(Z+b)^\alpha$, but α was found to be essentially unity. For $Z > 6$ we obtain

$$E_c \approx \frac{610 \text{ MeV}}{Z + 1.24} \quad (\text{solids and liquids}), \quad \approx \frac{710 \text{ MeV}}{Z + 0.92} \quad (\text{gases}).$$

Since E_c also depends on A , I , and other factors, such forms are at best approximate.

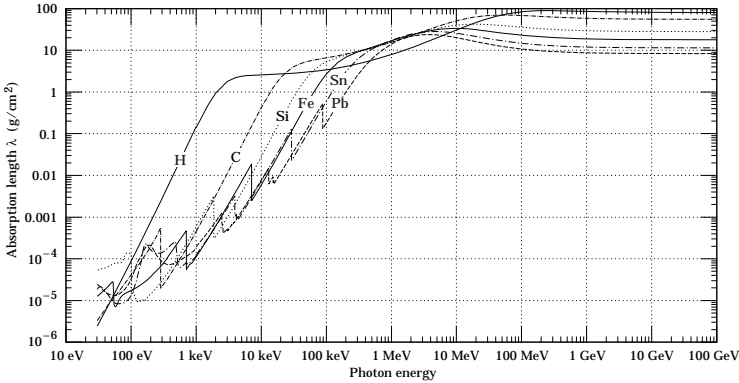


Fig. 27.16: The photon mass attenuation length (or mean free path) $\lambda = 1/(\mu/\rho)$ for various elemental absorbers as a function of photon energy. The mass attenuation coefficient is μ/ρ , where ρ is the density. The intensity I remaining after traversal of thickness t (in mass/unit area) is given by $I = I_0 \exp(-t/\lambda)$. The accuracy is a few percent. For a chemical compound or mixture, $1/\lambda_{\text{eff}} \approx \sum_{\text{elements}} w_Z/\lambda_Z$, where w_Z is the proportion by weight of the element with atomic number Z . The processes responsible for attenuation are given in Fig. 27.10. Since coherent processes are included, not all these processes result in energy deposition.

27.4.4. Energy loss by photons : Contributions to the photon cross section in a light element (carbon) and a heavy element (lead) are shown in Fig. 27.14. At low energies it is seen that the photoelectric effect dominates, although Compton scattering, Rayleigh scattering, and photonuclear absorption also contribute. The photoelectric cross section is characterized by discontinuities (absorption edges) as thresholds for photoionization of various atomic levels are reached. Photon attenuation lengths for a variety of elements are shown in Fig. 27.15, and data for $30 \text{ eV} < k < 100 \text{ GeV}$ for all elements is available from the web pages given in the caption. Here k is the photon energy.

The increasing domination of pair production as the energy increases is shown in Fig. 27.17 of the full *Review*. Using approximations similar to those used to obtain Eq. (27.27), Tsai's formula for the differential cross section [38] reduces to

$$\frac{d\sigma}{dx} = \frac{A}{X_0 N_A} \left[1 - \frac{4}{3}x(1-x) \right] \quad (27.29)$$

in the complete-screening limit valid at high energies. Here $x = E/k$ is the fractional energy transfer to the pair-produced electron (or positron), and

k is the incident photon energy. The cross section is very closely related to that for bremsstrahlung, since the Feynman diagrams are variants of one another. The cross section is of necessity symmetric between x and $1 - x$, as can be seen by the solid curve in See the review by Motz, Olsen, & Koch for a more detailed treatment [51].

Eq. (27.29) may be integrated to find the high-energy limit for the total e^+e^- pair-production cross section:

$$\sigma = \frac{7}{9}(A/X_0N_A) . \quad (27.30)$$

Equation Eq. (27.30) is accurate to within a few percent down to energies as low as 1 GeV, particularly for high- Z materials.

27.4.5. Bremsstrahlung and pair production at very high energies : At ultrahigh energies, Eqns. 27.26–27.30 will fail because of quantum mechanical interference between amplitudes from different scattering centers. Since the longitudinal momentum transfer to a given center is small ($\propto k/E(E - k)$, in the case of bremsstrahlung), the interaction is spread over a comparatively long distance called the formation length ($\propto E(E - k)/k$) via the uncertainty principle. In alternate language, the formation length is the distance over which the highly relativistic electron and the photon “split apart.” The interference is usually destructive. Calculations of the “Landau-Pomeranchuk-Migdal” (LPM) effect may be made semi-classically based on the average multiple scattering, or more rigorously using a quantum transport approach [41,42].

In amorphous media, bremsstrahlung is suppressed if the photon energy k is less than $E^2/(E + E_{LPM})$ [42], where*

$$E_{LPM} = \frac{(m_e c^2)^2 \alpha X_0}{4\pi \hbar c \rho} = (7.7 \text{ TeV/cm}) \times \frac{X_0}{\rho} . \quad (27.31)$$

Since physical distances are involved, X_0/ρ , in cm, appears. The energy-weighted bremsstrahlung spectrum for lead, $k d\sigma_{LPM}/dk$, is shown in Fig. 27.11 of the full *Review*. With appropriate scaling by X_0/ρ , other materials behave similarly.

For photons, pair production is reduced for $E(k - E) > k E_{LPM}$. The pair-production cross sections for different photon energies are shown in Fig. 27.15 of the full *Review*.

If $k \ll E$, several additional mechanisms can also produce suppression. When the formation length is long, even weak factors can perturb the interaction. For example, the emitted photon can coherently forward scatter off of the electrons in the media. Because of this, for $k < \omega_p E/m_e \sim 10^{-4}$, bremsstrahlung is suppressed by a factor $(k m_e / \omega_p E)^2$ [44]. Magnetic fields can also suppress bremsstrahlung. In crystalline media, the situation is more complicated, with coherent enhancement or suppression possible [42].

27.5. Electromagnetic cascades

When a high-energy electron or photon is incident on a thick absorber, it initiates an electromagnetic cascade as pair production and bremsstrahlung generate more electrons and photons with lower energy. The longitudinal development is governed by the high-energy part of the cascade, and therefore scales as the radiation length in the material. Electron energies eventually fall below the critical energy, and then dissipate their energy by ionization and excitation rather than by the generation of more shower

* This definition differs from that of Ref. 52 by a factor of two. E_{LPM} scales as the 4th power of the mass of the incident particle, so that $E_{LPM} = (1.4 \times 10^{10} \text{ TeV/cm}) \times X_0/\rho$ for a muon.

particles. In describing shower behavior, it is therefore convenient to introduce the scale variables $t = x/X_0$ and $y = E/E_c$, so that distance is measured in units of radiation length and energy in units of critical energy.

The mean longitudinal profile of the energy deposition in an electromagnetic cascade is reasonably well described by a gamma distribution [58]:

$$\frac{dE}{dt} = E_0 b \frac{(bt)^{a-1} e^{-bt}}{\Gamma(a)} \quad (27.33)$$

The maximum t_{\max} occurs at $(a-1)/b$. We have made fits to shower profiles in elements ranging from carbon to uranium, at energies from 1 GeV to 100 GeV. The energy deposition profiles are well described by Eq. (27.33) with

$$t_{\max} = (a-1)/b = 1.0 \times (\ln y + C_j), \quad j = e, \gamma, \quad (27.34)$$

where $C_e = -0.5$ for electron-induced cascades and $C_\gamma = +0.5$ for photon-induced cascades. To use Eq. (27.33), one finds $(a-1)/b$ from Eq. (27.34), then finds a either by assuming $b \approx 0.5$ or by finding a more accurate value from Fig. 27.19. The results are very similar for the electron number profiles, but there is some dependence on the atomic number of the medium. A similar form for the electron number maximum was obtained by Rossi in the context of his ‘‘Approximation B,’’ [2] but with $C_e = -1.0$ and $C_\gamma = -0.5$; we regard this as superseded by the EGS4 result.

The ‘‘shower length’’ $X_s = X_0/b$ is less conveniently parameterized, since b depends upon both Z and incident energy, as shown in Fig. 27.19. As a corollary of this Z dependence, the number of electrons crossing a plane near shower maximum is underestimated using Rossi’s approximation for carbon and seriously overestimated for uranium. Essentially the same b values are obtained for incident electrons and photons. For many purposes it is sufficient to take $b \approx 0.5$.

The gamma function distribution is very flat near the origin, while the EGS4 cascade (or a real cascade) increases more rapidly. As a result Eq. (27.33) fails badly for about the first two radiation lengths, which are excluded from fits. Because fluctuations are important, Eq. (27.33) should be used only in applications where average behavior is adequate.

The transverse development of electromagnetic showers in different materials scales fairly accurately with the *Molière radius* R_M , given by [60,61]

$$R_M = X_0 E_s/E_c, \quad (27.35)$$

where $E_s \approx 21$ MeV (Table 27.1), and the Rossi definition of E_c is used.

Measurements of the lateral distribution in electromagnetic cascades are shown in Refs. 60 and 61. On the average, only 10% of the energy lies outside the cylinder with radius R_M . About 99% is contained inside of $3.5R_M$, but at this radius and beyond composition effects become important and the scaling with R_M fails. The distributions are characterized by a narrow core, and broaden as the shower develops. They are often represented as the sum of two Gaussians, and Grindhammer [59] describes them with the function

$$f(r) = \frac{2r R^2}{(r^2 + R^2)^2}, \quad (27.37)$$

where R is a phenomenological function of x/X_0 and $\ln E$.

At high enough energies, the LPM effect (Sec. 27.4.5) reduces the cross sections for bremsstrahlung and pair production, and hence can cause significant elongation of electromagnetic cascades [42].

27.6. Muon energy loss at high energy

At sufficiently high energies, radiative processes become more important than ionization for all charged particles. For muons and pions in materials such as iron, this “critical energy” occurs at several hundred GeV. (There is no simple scaling with particle mass, but for protons the “critical energy” is much, much higher.) Radiative effects dominate the energy loss of energetic muons found in cosmic rays or produced at the newest accelerators. These processes are characterized by small cross sections, hard spectra, large energy fluctuations, and the associated generation of electromagnetic and (in the case of photonuclear interactions) hadronic showers [62–70]. At these energies the treatment of energy loss as a uniform and continuous process is for many purposes inadequate.

It is convenient to write the average rate of muon energy loss as [71]

$$-dE/dx = a(E) + b(E)E. \quad (27.38)$$

Here $a(E)$ is the ionization energy loss given by Eq. (27.3), and $b(E)$ is the sum of e^+e^- pair production, bremsstrahlung, and photonuclear contributions. To the approximation that these slowly-varying functions are constant, the mean range x_0 of a muon with initial energy E_0 is given by

$$x_0 \approx (1/b) \ln(1 + E_0/E_{\mu c}), \quad (27.39)$$

where $E_{\mu c} = a/b$.

The “muon critical energy” $E_{\mu c}$ can be defined more exactly as the energy at which radiative and ionization losses are equal, and can be found by solving $E_{\mu c} = a(E_{\mu c})/b(E_{\mu c})$. This definition corresponds to the solid-line intersection in Fig. 27.12 of the full *Review*, and is different from the Rossi definition we used for electrons. It serves the same function: below $E_{\mu c}$ ionization losses dominate, and above $E_{\mu c}$ radiative effects dominate. The dependence of $E_{\mu c}$ on atomic number Z is shown in Fig. 27.22 in the full *Review*.

The radiative cross sections are expressed as functions of the fractional energy loss ν . The bremsstrahlung cross section goes roughly as $1/\nu$ over most of the range, while for the pair production case the distribution goes as ν^{-3} to ν^{-2} [72]. “Hard” losses are therefore more probable in bremsstrahlung, and in fact energy losses due to pair production may very nearly be treated as continuous. The simulated [70] momentum distribution of an incident 1 TeV/ c muon beam after it crosses 3 m of iron is shown in Fig. 27.23 of the full *Review*. The hard bremsstrahlung photons and hadronic debris from photonuclear interactions induce cascades which can obscure muon tracks in detector planes and reduce tracking efficiency [74].

27.7. Cherenkov and transition radiation [75,76,32]

A charged particle radiates if its velocity is greater than the local phase velocity of light (Cherenkov radiation) or if it crosses suddenly from one medium to another with different optical properties (transition radiation). Neither process is important for energy loss, but both are used in high-energy physics detectors.

Cherenkov radiation. The cosine of the angle θ_c of Cherenkov radiation, relative to the particle’s direction, for a particle with velocity βc in a medium with index of refraction n , is $1/n\beta$, or

$$\tan \theta_c = \sqrt{\beta^2 n^2 - 1} \approx \sqrt{2(1 - 1/n\beta)} \quad (27.40)$$

for small θ_c , e.g., in gases. The threshold velocity β_t is $1/n$, and $\gamma_t = 1/(1 - \beta_t^2)^{1/2}$. Therefore, $\beta_t \gamma_t = 1/(2\delta + \delta^2)^{1/2}$, where $\delta = n - 1$. Values of δ for various commonly used gases are given as a function of

pressure and wavelength in Ref. 77. For values at atmospheric pressure, see Table 6.1. Data for other commonly used materials are given in Ref. 78.

Practical Cherenkov radiator materials are dispersive. Let ω be the photon's frequency, and let $k = 2\pi/\lambda$ be its wavenumber. The photons propagate at the group velocity $v_g = d\omega/dk = c/[n(\omega) + \omega(dn/d\omega)]$. In a non-dispersive medium, this simplifies to $v_g = c/n$.

In his classical paper, Tamm [79] showed that for dispersive media the radiation is concentrated in a thin conical shell whose vertex is at the moving charge, and whose opening half-angle η is given by

$$\cot \eta = \left[\frac{d}{d\omega} (\omega \tan \theta_c) \right]_{\omega_0} = \left[\tan \theta_c + \beta^2 \omega n(\omega) \frac{dn}{d\omega} \cot \theta_c \right]_{\omega_0}, \quad (27.41)$$

where ω_0 is the central value of the small frequency range under consideration. (See Fig. 27.24.) This cone has a opening half-angle η , and, unless the medium is non-dispersive ($dn/d\omega = 0$), $\theta_c + \eta \neq 90^\circ$. The Cherenkov wavefront 'sideslips' along with the particle [80]. This effect may have timing implications for ring imaging Cherenkov counters [81], but it is probably unimportant for most applications.

The number of photons produced per unit path length of a particle with charge ze and per unit energy interval of the photons is

$$\begin{aligned} \frac{d^2N}{dE dx} &= \frac{\alpha z^2}{\hbar c} \sin^2 \theta_c = \frac{\alpha^2 z^2}{r_e m_e c^2} \left(1 - \frac{1}{\beta^2 n^2(E)} \right) \\ &\approx 370 \sin^2 \theta_c(E) \text{ eV}^{-1} \text{ cm}^{-1} \quad (z = 1), \end{aligned} \quad (27.42)$$

or, equivalently,

$$\frac{d^2N}{dx d\lambda} = \frac{2\pi\alpha z^2}{\lambda^2} \left(1 - \frac{1}{\beta^2 n^2(\lambda)} \right). \quad (27.43)$$

The index of refraction n is a function of photon energy $E = \hbar\omega$. For practical use, Eq. (27.42) must be multiplied by the photodetector response function and integrated over the region for which $\beta n(\omega) > 1$.

When two particles are within $\lesssim 1$ wavelength, the electromagnetic fields from the particles may add coherently, affecting the Cherenkov radiation. The radiation from an e^+e^- pair at close separation is suppressed compared to two independent leptons [82].

Coherent Cherenkov radiation from electromagnetic showers (containing a net excess of e^- over e^+) has been used to study cosmic ray air showers [84] and to search for ν_e induced showers.

Transition radiation. The energy I radiated when a particle with charge ze crosses the boundary between vacuum and a medium with plasma frequency ω_p is $\alpha z^2 \gamma \hbar \omega_p / 3$, where

$$\hbar \omega_p = \sqrt{4\pi N_e r_e^3 m_e c^2 / \alpha} = \sqrt{\rho \text{ (in g/cm}^3\text{)} \langle Z/A \rangle \times 28.81 \text{ eV}}. \quad (27.45)$$

For styrene and similar materials, $\hbar \omega_p \approx 20$ eV; for air it is 0.7 eV.

The number spectrum $dN_\gamma/d(\hbar\omega)$ diverges logarithmically at low energies and decreases rapidly for $\hbar\omega/\gamma\hbar\omega_p > 1$. About half the energy is emitted in the range $0.1 \leq \hbar\omega/\gamma\hbar\omega_p \leq 1$. Inevitable absorption in a practical detector removes the divergence. For a particle with $\gamma = 10^3$, the radiated photons are in the soft x-ray range 2 to 40 keV. The γ dependence of the emitted energy thus comes from the hardening of the spectrum rather than from an increased quantum yield.

The number of photons with energy $\hbar\omega > \hbar\omega_0$ is given by the answer

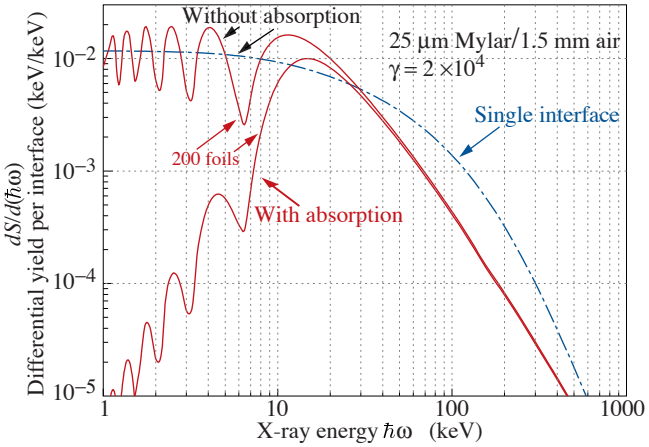


Figure 27.25: X-ray photon energy spectra for a radiator consisting of 200 25 μm thick foils of Mylar with 1.5 mm spacing in air (solid lines) and for a single surface (dashed line). Curves are shown with and without absorption. Adapted from Ref. 85.

to problem 13.15 in Ref. 32,

$$N_\gamma(\hbar\omega > \hbar\omega_0) = \frac{\alpha z^2}{\pi} \left[\left(\ln \frac{\gamma \hbar\omega_p}{\hbar\omega_0} - 1 \right)^2 + \frac{\pi^2}{12} \right], \quad (27.46)$$

within corrections of order $(\hbar\omega_0/\gamma\hbar\omega_p)^2$. The number of photons above a fixed energy $\hbar\omega_0 \ll \gamma\hbar\omega_p$ thus grows as $(\ln \gamma)^2$, but the number above a fixed fraction of $\gamma\hbar\omega_p$ (as in the example above) is constant. For example, for $\hbar\omega > \gamma\hbar\omega_p/10$, $N_\gamma = 2.519 \alpha z^2/\pi = 0.59\% \times z^2$.

The particle stays “in phase” with the x ray over a distance called the formation length, $d(\omega)$. Most of the radiation is produced in a distance $d(\omega) = (2c/\omega)(1/\gamma^2 + \theta^2 + \omega_p^2/\omega^2)^{-1}$. Here θ is the x-ray emission angle, characteristically $1/\gamma$. For $\theta = 1/\gamma$ the formation length has a maximum at $d(\gamma\omega_p/\sqrt{2}) = \gamma c/\sqrt{2}\omega_p$. In practical situations it is tens of μm .

Since the useful x-ray yield from a single interface is low, in practical detectors it is enhanced by using a stack of N foil radiators—foils L thick, where L is typically several formation lengths—separated by gas-filled gaps. The amplitudes at successive interfaces interfere to cause oscillations about the single-interface spectrum. At increasing frequencies above the position of the last interference maximum ($L/d(\omega) = \pi/2$), the formation zones, which have opposite phase, overlap more and more and the spectrum saturates, $dI/d\omega$ approaching zero as $L/d(\omega) \rightarrow 0$. This is illustrated in Fig. 27.25 for a realistic detector configuration.

For regular spacing of the layers fairly complicated analytic solutions for the intensity have been obtained [85]. (See also Ref. 86 and references therein.) Although one might expect the intensity of coherent radiation from the stack of foils to be proportional to N^2 , the angular dependence of the formation length conspires to make the intensity $\propto N$.

Further discussion and all references may be found in the full *Review of Particle Physics*. The equation and reference numbering corresponds to that version.

28. PARTICLE DETECTORS AT ACCELERATORS

This is an abridgment of the discussion given in the full *Review of Particle Physics* (the “full *Review*”); the equation and reference numbering corresponds to that version. The quoted numbers are usually based on typical devices, and should be regarded only as rough approximations for new designs. A more detailed discussion of detectors can be found in Refs. 1 and 56.

28.1. Summary of detector spatial resolution, temporal resolution, and deadtime

In this section we give various parameters for common detector components. The quoted numbers are usually based on typical devices, and should be regarded only as rough approximations for new designs. More detailed discussions of detectors and their underlying physics can be found in books by Ferbel [1], Kleinknecht [2], Knoll [3], Green [4], Leroy & Rancoita [5], and Grupen [6]. In Table 28.1 are given typical resolutions and deadtimes of common detectors.

Table 28.1: Typical resolutions and deadtimes of common detectors. Revised September 2009.

Detector Type	Accuracy (rms)	Resolution Time	Dead Time
Bubble chamber	10–150 μm	1 ms	50 ms ^a
Streamer chamber	300 μm	2 μs	100 ms
Proportional chamber	50–100 μm^a	2 ns	200 ns
Drift chamber	50–100 μm	2 ns ^d	100 ns
Scintillator	—	100 ps/ n^a	10 ns
Emulsion	1 μm	—	—
Liquid argon drift [7]	$\sim 175\text{--}450 \mu\text{m}$	$\sim 200 \text{ ns}$	$\sim 2 \mu\text{s}$
Micro-pattern gas detectors [8]	30–40 μm	< 10 ns	20 ns
Resistive plate chamber [9]	$\lesssim 10 \mu\text{m}$	1–2 ns	—
Silicon strip	pitch/(3 to 7) ^a	a	a
Silicon pixel	2 μm^a	a	a

^a See full *Review* for qualifications and assumptions.

28.2. Photon detectors

Updated September 2009 by D. Chakraborty (Northern Illinois U) and T. Sumiyoshi (Tokyo Metro U).

Most detectors in high-energy, nuclear, and astrophysics rely on the detection of photons in or near the visible range, $100 \text{ nm} \lesssim \lambda \lesssim 1000 \text{ nm}$, or $E \approx a \text{ few eV}$. This range covers scintillation and Cherenkov radiation as well as the light detected in many astronomical observations.

Generally, photodetection involves generating a detectable electrical signal proportional to the (usually very small) number of incident photons.

28.2.1. Vacuum photodetectors: Vacuum photodetectors can be broadly subdivided into three types: photomultiplier tubes, microchannel plates, and hybrid photodetectors.

28.2.1.1. Photomultiplier tubes: A versatile class of photon detectors, vacuum photomultiplier tubes (PMT) has been employed by a vast majority of all particle physics experiments to date [11]. Both “transmission-” and “reflection-type” PMT’s are widely used. In the former, the photocathode material is deposited on the inside of a transparent window

through which the photons enter, while in the latter, the photocathode material rests on a separate surface that the incident photons strike. The cathode material has a low work function, chosen for the wavelength band of interest. When a photon hits the cathode and liberates an electron (the photoelectric effect), the latter is accelerated and guided by electric fields to impinge on a secondary-emission electrode, or dynode, which then emits a few (~ 5) secondary electrons. The multiplication process is repeated typically 10 times in series to generate a sufficient number of electrons, which are collected at the anode for delivery to the external circuit. The total gain of a PMT depends on the applied high voltage V as $G = AV^{kn}$, where $k \approx 0.7-0.8$ (depending on the dynode material), n is the number of dynodes in the chain, and A a constant (which also depends on n). Typically, G is in the range of 10^5-10^6 .

28.2.2. Gaseous photon detectors : In gaseous photomultipliers (GPM) a photoelectron in a suitable gas mixture initiates an avalanche in a high-field region, producing a large number of secondary impact-ionization electrons. In principle the charge multiplication and collection processes are identical to those employed in gaseous tracking detectors such as multiwire proportional chambers, micromesh gaseous detectors (Micromegas), or gas electron multipliers (GEM). These are discussed in Sec. 28.6.4.

28.2.3. Solid-state photon detectors : In a phase of rapid development, solid-state photodetectors are competing with vacuum- or gas-based devices for many existing applications and making way for a multitude of new ones. Compared to traditional vacuum- and gaseous photodetectors, solid-state devices are more compact, lightweight, rugged, tolerant to magnetic fields, and often cheaper. They also allow fine pixelization, are easy to integrate into large systems, and can operate at low electric potentials, while matching or exceeding most performance criteria. They are particularly well suited for detection of γ - and X-rays. Except for applications where coverage of very large areas or dynamic range is required, solid-state detectors are proving to be the better choice.

Silicon photodiodes (PD) are widely used in high-energy physics as particle detectors and in a great number of applications (including solar cells!) as light detectors. The structure is discussed in some detail in Sec. 28.7.

Very large arrays containing $O(10^7)$ of $O(10 \mu\text{m}^2)$ -sized photodiodes pixelizing a plane are widely used to photograph all sorts of things from everyday subjects at visible wavelengths to crystal structures with X-rays and astronomical objects from infrared to UV. To limit the number of readout channels, these are made into charge-coupled devices (CCD), where pixel-to-pixel signal transfer takes place over thousands of synchronous cycles with sequential output through shift registers [16]. Thus, high spatial resolution is achieved at the expense of speed and timing precision. Custom-made CCD's have virtually replaced photographic plates and other imagers for astronomy and in spacecraft.

In avalanche photodiodes (APD), an exponential cascade of impact ionizations initiated by the initial photogenerated $e-h$ pair under a large reverse-bias voltage leads to an avalanche breakdown [17]. As a result, detectable electrical response can be obtained from low-intensity optical signals down to single photons.

28.3. Organic scintillators

Revised September 2007 by K.F. Johnson (FSU).

Organic scintillators are broadly classed into three types, crystalline, liquid, and plastic, all of which utilize the ionization produced by charged particles to generate optical photons, usually in the blue to green wavelength regions [21]. Plastic scintillators are by far the most widely used. Crystalline organic scintillators are practically unused in high-energy physics.

Densities range from 1.03 to 1.20 g cm⁻³. Typical photon yields are about 1 photon per 100 eV of energy deposit [22]. A one-cm-thick scintillator traversed by a minimum-ionizing particle will therefore yield $\approx 2 \times 10^4$ photons. The resulting photoelectron signal will depend on the collection and transport efficiency of the optical package and the quantum efficiency of the photodetector.

Decay times are in the ns range; rise times are much faster. Ease of fabrication into desired shapes and low cost has made plastic scintillators a common detector component. Recently, plastic scintillators in the form of scintillating fibers have found widespread use in tracking and calorimetry [25].

28.3.3. Scintillating and wavelength-shifting fibers :

The clad optical fiber is an incarnation of scintillator and wavelength shifter (WLS) which is particularly useful [33]. Since the initial demonstration of the scintillating fiber (SCIFI) calorimeter [34], SCIFI techniques have become mainstream [35].

SCIFI calorimeters are fast, dense, radiation hard, and can have leadglass-like resolution. SCIFI trackers can handle high rates and are radiation tolerant, but the low photon yield at the end of a long fiber (see below) forces the use of sensitive photodetectors. WLS scintillator readout of a calorimeter allows a very high level of hermeticity since the solid angle blocked by the fiber on its way to the photodetector is very small.

28.4. Inorganic scintillators:

Revised September 2009 by R.-Y. Zhu (California Institute of Technology) and C.L. Woody (BNL).

Inorganic crystals form a class of scintillating materials with much higher densities than organic plastic scintillators (typically $\sim 4\text{--}8$ g/cm³) with a variety of different properties for use as scintillation detectors. Due to their high density and high effective atomic number, they can be used in applications where high stopping power or a high conversion efficiency for electrons or photons is required. These include total absorption electromagnetic calorimeters (see Sec. 28.9.1), which consist of a totally active absorber (as opposed to a sampling calorimeter), as well as serving as gamma ray detectors over a wide range of energies. Many of these crystals also have very high light output, and can therefore provide excellent energy resolution down to very low energies (\sim few hundred keV).

28.5. Cherenkov detectors

Revised September 2009 by B.N. Ratcliff (SLAC).

Although devices using Cherenkov radiation are often thought of as only particle identification (PID) detectors, in practice they are used over a broader range of applications including; (1) fast particle counters; (2) hadronic PID; and (3) tracking detectors performing complete event reconstruction. Cherenkov counters contain two main elements; (1) a radiator through which the charged particle passes, and (2) a photodetector. As Cherenkov radiation is a weak source of photons, light collection and detection must be as efficient as possible. The refractive index n and the particle's path length through the radiator L appear in the Cherenkov relations allowing the tuning of these quantities for particular applications.

Cherenkov detectors utilize one or more of the properties of Cherenkov radiation discussed in the Passages of Particles through Matter section (Sec. 27 of this *Review*): the prompt emission of a light pulse; the existence of a velocity threshold for radiation; and the dependence of the Cherenkov cone half-angle θ_c and the number of emitted photons on the velocity of the particle and the refractive index of the medium.

28.6. Gaseous detectors

28.6.1. Energy loss and charge transport in gases : Revised March 2010 by F. Sauli (CERN) and M. Titov (CEA Saclay).

Gas-filled detectors localize the ionization produced by charged particles, generally after charge multiplication. The statistics of ionization processes having asymmetries in the ionization trails, affect the coordinate determination deduced from the measurement of drift time, or of the center of gravity of the collected charge. For thin gas layers, the width of the energy loss distribution can be larger than its average, requiring multiple sample or truncated mean analysis to achieve good particle identification. The energy loss of charged particles and photons in matter is discussed in Sec. 27. Table 28.5 provides values of relevant parameters in some commonly used gases at NTP (normal temperature, 20° C, and pressure, 1 atm) for unit-charge minimum-ionizing particles (MIPs) [57–63].

Table 28.5: Properties of noble and molecular gases at normal temperature and pressure (NTP: 20° C, one atm). E_X , E_I : first excitation, ionization energy; W_I : average energy per ion pair; $dE/dx|_{\min}$, N_P , N_T : differential energy loss, primary and total number of electron-ion pairs per cm, for unit charge minimum ionizing particles.

Gas	Density, mg cm ⁻³	E_x eV	E_I eV	W_I eV	$dE/dx _{\min}$ keV cm ⁻¹	N_P cm ⁻¹	N_T cm ⁻¹
He	0.179	19.8	24.6	41.3	0.32	3.5	8
Ne	0.839	16.7	21.6	37	1.45	13	40
Ar	1.66	11.6	15.7	26	2.53	25	97
Xe	5.495	8.4	12.1	22	6.87	41	312
CH ₄	0.667	8.8	12.6	30	1.61	28	54
C ₂ H ₆	1.26	8.2	11.5	26	2.91	48	112
iC ₄ H ₁₀	2.49	6.5	10.6	26	5.67	90	220
CO ₂	1.84	7.0	13.8	34	3.35	35	100
CF ₄	3.78	10.0	16.0	54	6.38	63	120

When an ionizing particle passes through the gas, it creates electron-ion pairs, but often the ejected electrons have sufficient energy to further ionize the medium. As shown in Table 28.5, the total number of electron-ion pairs (N_T) is usually a few times larger than the number of primaries (N_P).

The probability for a released electron to have an energy E or larger follows an approximate $1/E^2$ dependence (Rutherford law), taking into account the electronic structure of the medium. The number of electron-ion pairs per primary ionization, or cluster size, has an exponentially decreasing probability; for argon, there is about 1% probability for primary clusters to contain ten or more electron-ion pairs [59].

Once released in the gas, and under the influence of an applied electric field, electrons and ions drift in opposite directions and diffuse towards the electrodes. The drift velocity and diffusion of electrons depend very strongly on the nature of the gas. Large drift velocities are achieved by adding polyatomic gases (usually CH_4 , CO_2 , or CF_4) having large inelastic cross sections at moderate energies, which results in “cooling” electrons into the energy range of the Ramsauer-Townsend minimum (at ~ 0.5 eV) of the elastic cross-section of argon. In a simple approximation, gas kinetic theory provides the drift velocity v as a function of the mean collision time τ and the electric field E : $v = eE\tau/m_e$ (Townsend’s expression). In the presence of an external magnetic field, the Lorentz force acting on electrons between collisions deflects the drifting electrons and modifies the drift properties.

If the electric field is increased sufficiently, electrons gain enough energy between collisions to ionize molecules. Above a gas-dependent threshold, the mean free path for ionization, λ_i , decreases exponentially with the field; its inverse, $\alpha = 1/\lambda_i$, is the first Townsend coefficient. In wire chambers, most of the increase of avalanche particle density occurs very close to the anode wires, and a simple electrostatic consideration shows that the largest fraction of the detected signal is due to the motion of positive ions receding from the wires. The electron component, although very fast, contributes very little to the signal. This determines the characteristic shape of the detected signals in the proportional mode: a fast rise followed by a gradual increase.

28.6.2. Multi-Wire Proportional and Drift Chambers : Revised March 2010 by Fabio Sauli (CERN) and Maxim Titov (CEA Saclay).

Multiwire proportional chambers (MWPCs) [65,66], introduced in the late ’60’s, detect, localize and measure energy deposit by charged particles over large areas. A mesh of parallel anode wires at a suitable potential, inserted between two cathodes, acts almost as a set of independent proportional counters. Electrons released in the gas volume drift towards the anodes and produce avalanches in the increasing field.

Detection of charge on the wires over a predefined threshold provides the transverse coordinate to the wire with an accuracy comparable to that of the wire spacing. The coordinate along each wire can be obtained by measuring the ratio of collected charge at the two ends of resistive wires. Making use of the charge profile induced on segmented cathodes, the so-called center-of gravity (COG) method, permits localization of tracks to sub-mm accuracy.

Drift chambers, developed in the early ’70’s, can be used to estimate the longitudinal position of a track by exploiting the arrival time of electrons at the anodes if the time of interaction is known [69]. The distance between anode wires is usually several cm, allowing coverage of large areas at reduced cost.

28.6.4. Micro-Pattern Gas Detectors : Revised March 2010 by Fabio Sauli (CERN) and Maxim Titov (CEA Saclay)

By using pitch size of a few hundred μm , an order of magnitude improvement in granularity over wire chambers, these detectors offer intrinsic high rate capability ($> 10^6$ Hz/mm²), excellent spatial resolution (~ 30 μm), multi-particle resolution (~ 500 μm), and single photo-electron time resolution in the ns range.

The Gas Electron Multiplier (GEM) detector consists of a thin-foil copper-insulator-copper sandwich chemically perforated to obtain a high density of holes in which avalanches occur [86]. The hole diameter is typically between 25 μm and 150 μm , while the corresponding distance between holes varies between 50 μm and 200 μm . The central insulator is usually (in the original design) the polymer Kapton, with a thickness of 50 μm . Application of a potential difference between the two sides of the GEM generates the electric fields. Each hole acts as an independent proportional counter. Electrons released by the primary ionization particle in the upper conversion region (above the GEM foil) drift into the holes, where charge multiplication occurs in the high electric field (50–70 kV/cm). Most of avalanche electrons are transferred into the gap below the GEM. Several GEM foils can be cascaded, allowing the multi-layer GEM detectors to operate at overall gas gain above 10^4 in the presence of highly ionizing particles, while strongly reducing the risk of discharges.

The micro-mesh gaseous structure (Micromegas) is a thin parallel-plate avalanche counter. It consists of a drift region and a narrow multiplication gap (25–150 μm) between a thin metal grid (micromesh) and the readout electrode (strips or pads of conductor printed on an insulator board). Electrons from the primary ionization drift through the holes of the mesh into the narrow multiplication gap, where they are amplified. The small amplification gap produces a narrow avalanche, giving rise to excellent spatial resolution: 12 μm accuracy, limited by the micro-mesh pitch, has been achieved for MIPs, as well as very good time resolution and energy resolution ($\sim 12\%$ FWHM with 6 keV x rays) [89].

The performance and robustness of GEM and Micromegas have encouraged their use in high-energy and nuclear physics, UV and visible photon detection, astroparticle and neutrino physics, neutron detection and medical physics.

28.6.5. Time-projection chambers : Written September 2007 by D. Karlen (U. of Victoria and TRIUMF, Canada)

The Time Projection Chamber (TPC) concept, invented by David Nygren in the late 1970's [74], is the basis for charged particle tracking in a large number of particle and nuclear physics experiments. A uniform electric field drifts tracks of electrons produced by charged particles traversing a medium, either gas or liquid, towards a surface segmented into 2D readout pads. The signal amplitudes and arrival times are recorded to provide full 3D measurements of the particle trajectories. The intrinsic 3D segmentation gives the TPC a distinct advantage over other large volume tracking detector designs which record information only in a 2D projection with less overall segmentation, particularly for pattern recognition in events with large numbers of particles.

Gaseous TPC's are often designed to operate within a strong magnetic field (typically parallel to the drift field) so that particle momenta can be estimated from the track curvature. For this application, precise spatial measurements in the plane transverse to the magnetic field are most important. Since the amount of ionization along the length of the track depends on the velocity of the particle, ionization and momentum

measurements can be combined to identify the types of particles observed in the TPC.

Gas amplification of 10^3 – 10^4 at the readout endplate is usually required in order to provide signals with sufficient amplitude for conventional electronics to sense the drifted ionization. Until recently, the gas amplification system used in TPC's have exclusively been planes of anode wires operated in proportional mode placed close to the readout pads. Performance has been recently improved by replacing these wire planes with micro-pattern gas detectors, namely GEM [86] and Micromegas [88] devices.

Diffusion degrades the position information of ionization that drifts a long distance. For a gaseous TPC, the effect can be alleviated by the choice of a gas with low intrinsic diffusion or by operating in a strong magnetic field parallel to the drift field with a gas which exhibits a significant reduction in transverse diffusion with magnetic field.

28.6.6. Transition radiation detectors (TRD's) : Written August 2007 by P. Nevski (BNL) and A. Romaniouk (Moscow Eng. & Phys. Inst.)

Transition radiation (TR) x rays are produced when a highly relativistic particle ($\gamma \gtrsim 10^3$) crosses a refractive index interface, as discussed in Sec. 27.7. The x rays, ranging from a few keV to a few dozen keV, are emitted at a characteristic angle $1/\gamma$ from the particle trajectory. Since the TR yield is about 1% per boundary crossing, radiation from multiple surface crossings is used in practical detectors. In the simplest concept, a detector module might consist of low- Z foils followed by a high- Z active layer made of proportional counters filled with a Xe-rich gas mixture. The atomic number considerations follow from the dominant photoelectric absorption cross section per atom going roughly as Z^n/E_x^3 , where n varies between 4 and 5 over the region of interest, and the x-ray energy is E_x . To minimize self-absorption, materials such as polypropylene, Mylar, carbon, and (rarely) lithium are used as radiators. The TR signal in the active regions is in most cases superimposed upon the particle's ionization losses. These drop a little faster than Z/A with increasing Z , providing another reason for active layers with high Z .

The TR intensity for a single boundary crossing always increases with γ , but for multiple boundary crossings interference leads to saturation near a Lorentz factor $\gamma_{\text{sat}} = 0.6 \omega_1 \sqrt{\ell_1 \ell_2} / c$ [101], where ω_1 is the radiator plasma frequency, ℓ_1 is its thickness, and ℓ_2 the spacing. In most of the detectors used in particle physics the radiator parameters are chosen to provide $\gamma_{\text{sat}} \approx 2000$. Those detectors normally work as threshold devices, ensuring the best electron/pion separation in the momentum range $1 \text{ GeV}/c \lesssim p \lesssim 150 \text{ GeV}/c$.

The discrimination between electrons and pions can be based on the charge deposition measured in each detection module, on the number of clusters—energy depositions observed above an optimal threshold (usually in the 5 to 7 keV region), or on more sophisticated methods analyzing the pulse shape as a function of time. The total energy measurement technique is more suitable for thick gas volumes, which absorb most of the TR radiation and where the ionization loss fluctuations are small. The cluster-counting method works better for detectors with thin gas layers, where the fluctuations of the ionization losses are big.

Recent TRDs for particle astrophysics are designed to directly measure the Lorentz factor of high-energy nuclei by using the quadratic dependence of the TR yield on nuclear charge; see Cherry and Müller papers in Ref. 103.

28.7. Semiconductor detectors

Updated September 2009 by H. Spieler (LBNL).

28.7.1. Materials Requirements : Semiconductor detectors are essentially solid state ionization chambers. Absorbed energy forms electron-hole pairs, *i.e.*, negative and positive charge carriers, which under an applied electric field move towards their respective collection electrodes, where they induce a signal current. The energy required to form an electron-hole pair is proportional to the bandgap. In tracking detectors the energy loss in the detector should be minimal, whereas for energy spectroscopy the stopping power should be maximized, so for gamma rays high- Z materials are desirable.

Measurements on silicon photodiodes [112] show that for photon energies below 4 eV one electron-hole ($e-h$) pair is formed per incident photon. The mean energy E_i required to produce an $e-h$ pair peaks at 4.4 eV for a photon energy around 6 eV. Above ~ 1.5 keV it assumes a constant value, 3.67 eV at room temperature. It is larger than the bandgap energy because momentum conservation requires excitation of lattice vibrations (phonons). For minimum-ionizing particles, the most probable charge deposition in a 300 μm thick silicon detector is about 3.5 fC (22000 electrons). Other typical ionization energies are 2.96 eV in Ge, 4.2 eV in GaAs, and 4.43 eV in CdTe.

Since both electronic and lattice excitations are involved, the variance in the number of charge carriers $N = E/E_i$ produced by an absorbed energy E is reduced by the Fano factor F (about 0.1 in Si and Ge). Thus, $\sigma_N = \sqrt{FN}$ and the energy resolution $\sigma_E/E = \sqrt{FE_i/E}$. However, the measured signal fluctuations are usually dominated by electronic noise or energy loss fluctuations in the detector.

A major effort is to find high- Z materials with a bandgap that is sufficiently high to allow room-temperature operation while still providing good energy resolution. Compound semiconductors, *e.g.*, CdZnTe, can allow this, but typically suffer from charge collection problems, characterized by the product $\mu\tau$ of mobility and carrier lifetime. In Si and Ge $\mu\tau > 1 \text{ cm}^2 \text{ V}^{-1}$ for both electrons and holes, whereas in compound semiconductors it is in the range 10^{-3} – 10^{-8} . Since for holes $\mu\tau$ is typically an order of magnitude smaller than for electrons, detector configurations where the electron contribution to the charge signal dominates—*e.g.*, strip or pixel structures—can provide better performance.

28.7.2. Detector Configurations : A $p-n$ junction operated at reverse bias forms a sensitive region depleted of mobile charge and sets up an electric field that sweeps charge liberated by radiation to the electrodes. Detectors typically use an asymmetric structure, *e.g.*, a highly doped p electrode and a lightly doped n region, so that the depletion region extends predominantly into the lightly doped volume.

In a planar device the thickness of the depleted region is

$$W = \sqrt{2\epsilon(V + V_{bi})/Ne} = \sqrt{2\rho\mu\epsilon(V + V_{bi})}, \quad (28.1)$$

where V = external bias voltage

V_{bi} = “built-in” voltage (≈ 0.5 V for resistivities typically used in Si detectors)

N = doping concentration

e = electronic charge

ϵ = dielectric constant = $11.9 \epsilon_0 \approx 1$ pF/cm in Si

ρ = resistivity (typically 1–10 k Ω cm in Si)

μ = charge carrier mobility

= 1350 $\text{cm}^2 \text{ V}^{-1} \text{ s}^{-1}$ for electrons in Si

In Si $\mu = 450 \text{ cm}^2 \text{ V}^{-1} \text{ s}^{-1}$ for holes in Si
 $W = 0.5 \left[\mu\text{m} / \sqrt{\Omega\text{-cm} \cdot \text{V}} \right] \times \sqrt{\rho(V + V_{bi})}$ for n -type Si, and

$W = 0.3 \left[\mu\text{m} / \sqrt{\Omega\text{-cm} \cdot \text{V}} \right] \times \sqrt{\rho(V + V_{bi})}$ for p -type Si.

Large volume ($\sim 10^2\text{--}10^3 \text{ cm}^3$) Ge detectors are commonly configured as coaxial detectors, *e.g.*, a cylindrical n -type crystal with 5–10 cm diameter and 10 cm length with an inner 5–10 mm diameter n^+ electrode and an outer p^+ layer forming the diode junction. Ge can be grown with very low impurity levels, $10^9\text{--}10^{10} \text{ cm}^{-3}$ (HPGe), so these large volumes can be depleted with several kV.

28.7.3. Signal Formation : The signal pulse shape depends on the instantaneous carrier velocity $v(x) = \mu E(x)$ and the electrode geometry, which determines the distribution of induced charge (*e.g.*, see Ref. 111, pp. 71–83). Charge collection time decreases with increasing bias voltage, and can be reduced further by operating the detector with “overbias,” *i.e.*, a bias voltage exceeding the value required to fully deplete the device. The collection time is limited by velocity saturation at high fields (in Si approaching 10^7 cm/s at $E > 10^4 \text{ V/cm}$); at an average field of 10^4 V/cm the collection time is about 15 ps/ μm for electrons and 30 ps/ μm for holes. In typical fully-depleted detectors 300 μm thick, electrons are collected within about 10 ns, and holes within about 25 ns.

Position resolution is limited by transverse diffusion during charge collection (typically 5 μm for 300 μm thickness) and by knock-on electrons. Resolutions of 2–4 μm (rms) have been obtained in beam tests. In magnetic fields, the Lorentz drift deflects the electron and hole trajectories and the detector must be tilted to reduce spatial spreading (see “Hall effect” in semiconductor textbooks).

Electrodes can be in the form of cm-scale pads, strips, or μm -scale pixels. Various readout structures have been developed for pixels, *e.g.*, CCDs, DEPFETs, monolithic pixel devices that integrate sensor and electronics (MAPS), and hybrid pixel devices that utilize separate sensors and readout ICs connected by two-dimensional arrays of solder bumps. For an overview and further discussion see Ref. 111.

28.7.4. Radiation Damage : Radiation damage occurs through two basic mechanisms:

1. Bulk damage due to displacement of atoms from their lattice sites. This leads to increased leakage current, carrier trapping, and build-up of space charge that changes the required operating voltage. Displacement damage depends on the nonionizing energy loss and the energy imparted to the recoil atoms, which can initiate a chain of subsequent displacements, *i.e.*, damage clusters. Hence, it is critical to consider both particle type and energy.
2. Surface damage due to charge build-up in surface layers, which leads to increased surface leakage currents. In strip detectors the inter-strip isolation is affected. The effects of charge build-up are strongly dependent on the device structure and on fabrication details. Since the damage is proportional to the absorbed energy (when ionization dominates), the dose can be specified in rad (or Gray) independent of particle type.

Strip and pixel detectors have remained functional at fluences beyond 10^{15} cm^{-2} for minimum ionizing protons. At this damage level, charge loss due to recombination and trapping becomes significant and the high signal-to-noise ratio obtainable with low-capacitance pixel structures

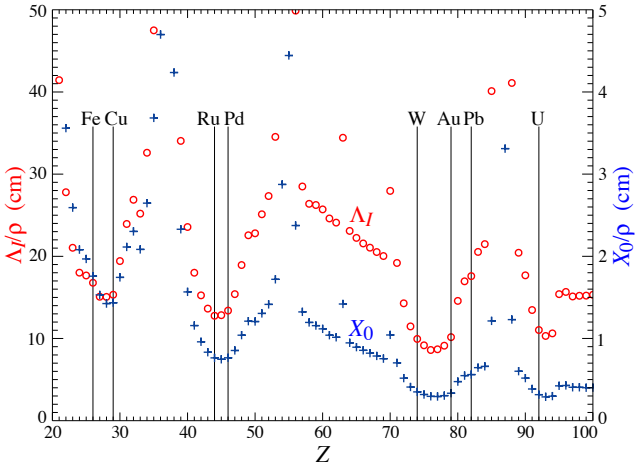


Figure 28.21: Nuclear interaction length λ_I/ρ (circles) and radiation length X_0/ρ (+'s) in cm for the chemical elements with $Z > 20$ and $\lambda_I < 50$ cm.

extends detector lifetime. The higher mobility of electrons makes them less sensitive to carrier lifetime than holes, so detector configurations that emphasize the electron contribution to the charge signal are advantageous, *e.g.*, n^+ strips or pixels on a p-substrate. The occupancy of the defect charge states is strongly temperature dependent; competing processes can increase or decrease the required operating voltage. It is critical to choose the operating temperature judiciously (-10 to 0°C in typical collider detectors) and limit warm-up periods during maintenance. For a more detailed summary see Ref. 117 and the web-sites of the ROSE and RD50 collaborations at <http://RD48.web.cern.ch/rd48> and <http://RD50.web.cern.ch/rd50>. Materials engineering, *e.g.*, introducing oxygen interstitials, can improve certain aspects and is under investigation. At high fluences diamond is an alternative, but operates as an insulator rather than a reverse-biased diode.

28.9. Calorimeters

A calorimeter is designed to measure the energy deposition and its direction for a contained electromagnetic (EM) or hadronic shower. The characteristic interaction distance for an electromagnetic interaction is the radiation length X_0 , which ranges from 13.8 g cm^{-2} in iron to 6.0 g cm^{-2} in uranium.* Similarly, the characteristic nuclear interaction length λ_I varies from 132.1 g cm^{-2} (Fe) to 209 g cm^{-2} (U).† In either case, a calorimeter must be many interaction lengths deep, where “many” is determined by physical size, cost, and other factors. EM calorimeters tend to be $15\text{--}30 X_0$ deep, while hadronic calorimeters are usually compromised at $5\text{--}8 \lambda_I$. In real experiments there is likely to be an EM calorimeter in front of the hadronic section, which in turn has less sampling density in the back, so the hadronic cascade occurs in a succession of different structures.

* $X_0 = 120\text{ g cm}^{-2} Z^{-2/3}$ to better than 5% for $Z > 23$.

† $\lambda_I = 37.8\text{ g cm}^{-2} A^{0.312}$ to within 0.8% for $Z > 15$.

See pdg.lbl.gov/AtomicNuclearProperties for actual values.

In all cases there is a premium on small λ_I/ρ and X_0/ρ (both with units of length). These quantities are shown for $Z > 20$ for the chemical elements in Fig. 28.21.

These considerations are for *sampling calorimeters* consisting of metallic absorber sandwiched or (threaded) with an active material which generates signal. The active medium may be a scintillator, an ionizing noble liquid, a gas chamber, a semiconductor, or a Cherenkov radiator.

There are also *homogeneous calorimeters*, in which the entire volume is sensitive, *i.e.*, contributes signal. Homogeneous calorimeters (so far usually electromagnetic) may be built with inorganic heavy (high density, high $\langle Z \rangle$) scintillating crystals, or non-scintillating Cherenkov radiators such as lead glass and lead fluoride. Scintillation light and/or ionization in noble liquids can be detected. Nuclear interaction lengths in inorganic crystals range from 17.8 cm (LuAlO₃) to 42.2 cm (NaI).

28.9.1. Electromagnetic calorimeters :

Revised October 2009 by R.-Y. Zhu (California Inst. of Technology).

The development of electromagnetic showers is discussed in the section on "Passage of Particles Through Matter" (Sec. 27 of this *Review*).

The energy resolution σ_E/E of a calorimeter can be parametrized as $a/\sqrt{E} \oplus b \oplus c/E$, where \oplus represents addition in quadrature and E is in GeV. The stochastic term a represents statistics-related fluctuations such as intrinsic shower fluctuations, photoelectron statistics, dead material at the front of the calorimeter, and sampling fluctuations. For a fixed number of radiation lengths, the stochastic term a for a sampling calorimeter is expected to be proportional to $\sqrt{t/f}$, where t is plate thickness and f is sampling fraction [123,124]. While a is at a few percent level for a homogeneous calorimeter, it is typically 10% for sampling calorimeters. The main contributions to the systematic, or constant, term b are detector non-uniformity and calibration uncertainty. In the case of the hadronic cascades discussed below, non-compensation also contributes to the constant term. One additional contribution to the constant term for calorimeters built for modern high-energy physics experiments, operated in a high-beam intensity environment, is radiation damage of the active medium. This can be minimized by developing radiation-hard active media [47] and by frequent *in situ* calibration and monitoring [46,124].

28.9.2. Hadronic calorimeters : [1-5,124]

Written April 2008 by D. E. Groom (LBNL).

Most large hadron calorimeters are sampling calorimeters which are parts of complicated 4π detectors at colliding beam facilities. Typically, the basic structure is plates of absorber (Fe, Pb, Cu, or occasionally U or W) alternating with plastic scintillators (plates, tiles, bars), liquid argon (LAr), or gaseous detectors. The ionization is measured directly, as in LAr calorimeters, or via scintillation light observed by photodetectors (usually PMT's). Waveshifting fibers are often used to solve difficult problems of geometry and light collection uniformity. Silicon sensors are being studied for ILC detectors; in this case $e-h$ pairs are collected.

In an inelastic hadronic collision a significant fraction f_{em} of the energy is removed from further hadronic interaction by the production of secondary π^0 's and η 's, whose decay photons generate high-energy electromagnetic (EM) cascades. Charged secondaries (π^\pm , p , ...) deposit energy via ionization and excitation, but also interact with nuclei, producing spallation protons and neutrons, evaporation neutrons, and recoiling nuclei in highly excited states. The charged collision products produce detectable ionization, as do the showering γ -rays from the prompt de-excitation of highly excited nuclei. The recoiling nuclei generate little

or no detectable signal. The neutrons lose kinetic energy in elastic collisions over hundreds of ns, gradually thermalize and are captured, with the production of more γ -rays—usually outside the acceptance gate of the electronics. Between endothermic spallation losses, nuclear recoils, and late neutron capture, a significant fraction of the hadronic energy (20%–35%, depending on the absorber and energy of the incident particle) is invisible.

For $h/e \neq 1$, when h and e are the hadronic and electromagnetic calorimeter responses, respectively, fluctuations in f_{em} significantly contribute to the resolution, in particular contributing a larger fraction of the variance at high energies. Since the f_{em} distribution has a tail on the high side, the calorimeter response is non-Gaussian with a high-energy tail if $h/e < 1$. *Noncompensation* ($h/e \neq 1$) thus seriously degrades resolution as well as producing a nonlinear response.

It is clearly desirable to *compensate* the response, *i.e.*, to design the calorimeter such that $h/e = 1$. This is possible only in a sampling calorimeter, where several variables can be chosen or tuned:

1. Decrease the EM sensitivity. The absorber usually has higher $\langle Z \rangle$ than does the sensor, the EM energy deposit rate, relative to minimum ionization, is greater than this ratio in the sensor.
2. Increase the hadronic sensitivity. The abundant neutrons have a large n - p scattering cross section, with the production of low-energy scattered protons in hydrogenous sampling materials such as butane-filled proportional counters or plastic scintillator. (When scattering off a nucleus with mass number A , a neutron can at most lose $4/(1+A)^2$ of its kinetic energy.)

Motivated very much by the work of Brau, Gabriel, Brückmann, and Wigmans [134], several groups built calorimeters which were very nearly compensating. The degree of compensation was sensitive to the acceptance gate width, and so could be somewhat tuned.

The average longitudinal distribution rises to a smooth peak, increasing slowly with energy but about one nuclear interaction length (λ_I) into the calorimeter. After several interaction lengths its fall is reasonably exponential. It has been found that a gamma distribution fairly well describes the longitudinal development of an EM shower, as discussed in Sec. 27.5.

The transverse energy deposit is characterized by a central core dominated by EM cascades, together with a wide “skirt” produced by wide-angle hadronic interactions [139].

Further discussion and all references may be found in the full *Review of Particle Physics*. The numbering of references and equations used here corresponds to that version.

29. PARTICLE DETECTORS FOR NON-ACCELERATOR PHYSICS

Written 2009 (see the various sections for authors).

29.1. Introduction

Non-accelerator experiments have become increasingly important in particle physics. These include classical cosmic ray experiments, neutrino oscillation measurements, and searches for double-beta decay, dark matter candidates, and magnetic monopoles. The experimental methods are sometimes those familiar at accelerators (plastic scintillators, drift chambers, TRD's, *etc.*) but there is also instrumentation either not found at accelerators or applied in a radically different way. Examples are atmospheric scintillation detectors (Fly's Eye), massive Cherenkov detectors (Super-Kamiokande, IceCube), ultracold solid state detectors (CDMS). And, except for the cosmic ray detectors, there is a demand for radiologically ultra-pure materials.

In this section, some more important detectors special to terrestrial non-accelerator experiments are discussed. Techniques used in both accelerator and non-accelerator experiments are described in Sec. 28, Particle Detectors at Accelerators, some of which have been modified to accommodate the non-accelerator nuances. Space-based detectors also use some unique methods, but these are beyond the present scope of *RPP*.

29.2. High-energy cosmic-ray hadron and gamma-ray detectors

29.2.1. Atmospheric fluorescence detectors :

Written September 2009 by L.R. Wiencke (Colorado School of Mines).

Cosmic-ray fluorescence detectors (FD) use the atmosphere as a giant calorimeter to measure isotropic scintillation light that traces the development profiles of extensive air showers (EAS). The EASs observed are produced by the interactions of high-energy ($E > 10^{17}$ eV) subatomic particles in the stratosphere and upper troposphere. The amount of scintillation light generated is proportional to energy deposited in the atmosphere and nearly independent of the primary species.

The scintillation light is emitted between 290 and 430 nm, when relativistic charged particles, primarily electrons and positrons, excite nitrogen molecules in air, resulting in transitions of the 1P and 2P systems.

An FD element (telescope) consists of a non-tracking spherical mirror ($3.5\text{--}13\text{ m}^2$ and less than astronomical quality), a close-packed "camera" of PMTs near the focal plane, and flash ADC readout system with a pulse and track-finding trigger scheme [7]. Simple reflector optics ($12^\circ \times 16^\circ$ degree field of view (FOV) on 256 PMTs) and Schmidt optics ($30^\circ \times 30^\circ$ on 440 PMTs), including a correcting element, have been used.

The EAS generates a track consistent with a light source moving at $v = c$ across the FOV. The number of photons (N_γ) as a function of atmospheric depth (X) can be expressed as [6]

$$\frac{dN_\gamma}{dX} = \frac{dE_{\text{dep}}^{\text{tot}}}{dX} \int Y(\lambda, P, T, u) \cdot \tau_{\text{atm}}(\lambda, X) \cdot \varepsilon_{\text{FD}}(\lambda) d\lambda \quad , \quad (29.1)$$

where $\tau_{atm}(\lambda, X)$ is atmospheric transmission, including wavelength (λ) dependence, and $\varepsilon_{FD}(\lambda)$ is FD efficiency. $\varepsilon_{FD}(\lambda)$ includes geometric factors and collection efficiency of the optics, quantum efficiency of the PMTs, and other throughput factors. The typical systematic uncertainties, Y (10–15%), τ_{atm} (10%) and ε_{FD} (photometric calibration 10%), currently dominate the total reconstructed EAS energy uncertainty. $\Delta E/E$ of 20–25% is possible, provided the geometric fit of the EAS axis is constrained by multi-eye stereo projection, or by timing from a collocated sparse array of surface detectors.

29.2.2. Atmospheric Cherenkov telescopes for high-energy γ -ray astronomy :

Written August 2009 by J. Holder (Bartol Research Inst., Univ. of Delaware).

Atmospheric Cherenkov detectors achieve effective collection areas of $\sim 10^5 \text{ m}^2$ by employing the Earth's atmosphere as an intrinsic part of the detection technique. A hadronic cosmic ray or high energy γ -ray incident on the Earth's atmosphere triggers a particle cascade, or air shower. Relativistic charged particles in the cascade produce Cherenkov radiation, which is emitted along the shower direction, resulting in a light pool on the ground with a radius of $\sim 130 \text{ m}$. Maximum emission occurs when the number of particles in the cascade is largest. The Cherenkov light at ground level peaks at a wavelength, $\lambda \approx 300\text{--}350 \text{ nm}$. The photon density is typically $\sim 100 \text{ photons/m}^2$ at 1 TeV, arriving in a brief flash of a few nanoseconds duration.

Modern atmospheric Cherenkov telescopes consist of large ($> 100 \text{ m}^2$) segmented mirrors on steerable altitude-azimuth mounts. A camera, made from an array of up to 1000 photomultiplier tubes (PMTs) covering a field-of-view of up to 5.0° in diameter, is placed at the mirror focus and used to record a Cherenkov image of each air shower. Images are recorded at a rate of a few hundred Hz, the vast majority of which are due to showers with hadronic cosmic-ray primaries. The shape and orientation of the Cherenkov images are used to discriminate γ -ray photon events from this cosmic-ray background, and to reconstruct the photon energy and arrival direction.

The total Cherenkov yield from the air shower is proportional to the energy of the primary particle. The energy resolution of this technique, also energy-dependent, is typically 15–20 at energies above a few hundred GeV. Energy spectra of γ -ray sources can be measured over a wide range; potentially from $\sim 50 \text{ GeV}$ to $\sim 100 \text{ TeV}$, depending upon the instrument characteristics, source strength, and exposure time.

29.3. Large neutrino detectors

29.3.1. Deep liquid detectors for rare processes :

Written September 2009 by K. Scholberg & C.W. Walter (Duke University)

Deep, large detectors for rare processes tend to be multi-purpose with physics reach that includes not only solar, reactor, supernova and atmospheric neutrinos, but also searches for baryon number violation, searches for exotic particles such as magnetic monopoles, and neutrino and cosmic ray astrophysics in different energy regimes. The detectors may also serve as targets for long-baseline neutrino beams for neutrino

oscillation physics studies. In general, detector design considerations can be divided into high- and low-energy regimes, for which background and event reconstruction issues differ. The high-energy regime, from about 100 MeV to a few hundred GeV, is relevant for proton decay searches, atmospheric neutrinos and high-energy astrophysical neutrinos. The low-energy regime (a few tens of MeV or less) is relevant for supernova, solar, reactor and geological neutrinos.

Large water Cherenkov and scintillator detectors (see Table 29.1) usually consist of a volume of transparent liquid viewed by photomultiplier tubes (PMTs). Because photosensors lining an inner surface represent a driving cost that scales as surface area, very large volumes can be used for comparatively reasonable cost. A common configuration is to have at least one concentric outer layer of liquid material separated from the inner part of the detector to serve as shielding against ambient background. If optically separated and instrumented with PMTs, an outer layer may also serve as an active veto against entering cosmic rays and other background

Because in most cases one is searching for rare events, large detectors are usually sited underground to reduce cosmic-ray related background (see Chapter 24). The minimum depth required varies according to the physics goals [22].

29.3.1.1. *Liquid scintillator detectors:*

Past and current large underground detectors based on hydrocarbon scintillators include LVD, MACRO, Baksan, Borexino, KamLAND and SNO+. Experiments at nuclear reactors include Chooz, Double Chooz, Daya Bay, and RENO. Organic liquid scintillators for large detectors are chosen for high light yield and attenuation length, good stability, compatibility with other detector materials, high flash point, low toxicity, appropriate density for mechanical stability, and low cost.

Scintillation detectors have an advantage over water Cherenkov detectors in the lack of Cherenkov threshold and the high light yield. However, scintillation light emission is nearly isotropic, and therefore directional capabilities are relatively weak.

29.3.1.2. *Water Cherenkov detectors:*

Very large-imaging water detectors reconstruct ten-meter-scale Cherenkov rings produced by charged particles (see Sec. 28.5.0). The first such large detectors were IMB and Kamiokande. The only currently existing instance of this class is Super-Kamiokande (Super-K).

Cherenkov detectors are excellent electromagnetic calorimeters, and the number of Cherenkov photons produced by an e/γ is nearly proportional to its kinetic energy. The number of collected photoelectrons depends on the scattering and attenuation in the water along with the photocathode coverage, quantum efficiency and the optical parameters of any external light collection systems or protective material surrounding them. Event-by-event corrections are made for geometry and attenuation.

High-energy (~ 100 MeV or more) neutrinos from the atmosphere or beams interact with nucleons; for the nucleons bound inside the ^{16}O nucleus, the nuclear effects both at the interaction, and as the particles leave the nucleus must be considered when reconstructing the interaction. Various event topologies can be distinguished by their timing and fit patterns, and by presence or absence of light in a veto.

Low-energy neutrino interactions of solar neutrinos in water are predominantly elastic scattering off atomic electrons; single electron events are then reconstructed. At solar neutrino energies, the visible energy resolution ($\sim 30\%/\sqrt{\xi E_{\text{vis}}(\text{MeV})}$) is about 20% worse than photoelectron counting statistics would imply. At these energies, radioactive backgrounds become a dominant issue.

The Sudbury Neutrino Observatory (SNO) detector [27] is the only instance of a large heavy water detector and deserves mention here. In addition to an outer 1.7 kton of light water, SNO contained 1 kton of D_2O , giving it unique sensitivity to neutrino neutral current ($\nu_x + d \rightarrow \nu_x + p + n$), and charged current ($\nu_e + d \rightarrow p + p + e^-$) deuteron breakup reactions.

29.3.2. Neutrino telescopes :

Written November 2009 by A. Karle (University of Wisconsin).

Neutrino telescopes are large water or ice Cherenkov detectors designed to do neutrino astronomy in the energy range 10^{11} – 10^{18} eV. The primary physics goal is the detection of high-energy extra-terrestrial neutrinos. Neutrinos offer a unique view of the high-energy Universe because they are not deflected by magnetic fields like charged cosmic rays, and can travel vast distances without being absorbed like high-energy photons.

Neutrino telescopes detect neutrinos via the process $\nu_l(\bar{\nu}_l) + N \rightarrow l^\pm + X$ of primarily upward-going or horizontal neutrinos interacting with a nucleon N of the matter comprising or surrounding the detector volume. A significant fraction of the neutrino energy E_ν will be carried away by the produced lepton. For the important case of a lepton being a muon, the angle $\Delta\psi$ between the parent neutrino and the muon is $\approx 0.7^\circ (E_\nu/\text{TeV})^{-0.7}$ [28].

The small cross sections combined with small expected fluxes of high-energy cosmic neutrinos necessitate very large, km-scale detection volumes. Neutrino telescopes make use of large natural transparent target media such as deep sea water or the deep glacial ice in Antarctica. The target volume is instrumented with large photomultipliers (PMTs). The goal is to maximize the number of detected Cherenkov photons produced by energetic charged particles, and thus to maximize the number of well reconstructed events while keeping the density of PMTs (and thus the cost of the experiment) low. The sensors are deployed at depths of one to several km to reduce backgrounds from the cosmic-ray-generated muon flux.

The IceCube Neutrino Observatory [37] is a km-scale detector which will be completed in 2011. IceCube will consist of 5160 optical sensors deployed on 86 strings covering a volume of 1 km^3 . A surface detector component, IceTop, forms an air shower array with 320 standard photomultipliers deployed in 160 IceTop tanks on the ice surface directly above the strings. The optical sensors are located at depths between 1450 m and 2450 m. The detector is constructed by drilling holes in the ice with a hot-water drill.

Figure 29.3 contains three different predictions for the flux of neutrinos associated with the still-enigmatic sources of the highest energy cosmic rays. Kilometer-scale neutrino detectors have the sensitivity to reveal generic cosmic-ray sources with an energy density in neutrinos comparable to their energy density in cosmic rays and in TeV γ rays.

No detection of astrophysical neutrinos has been made yet. Two limits from AMANDA to such E neutrino fluxes are shown: one is a diffuse muon neutrino flux limit [48], the other is a limit based on all flavor analysis of non-contained events in the PeV to EeV energy region [49]

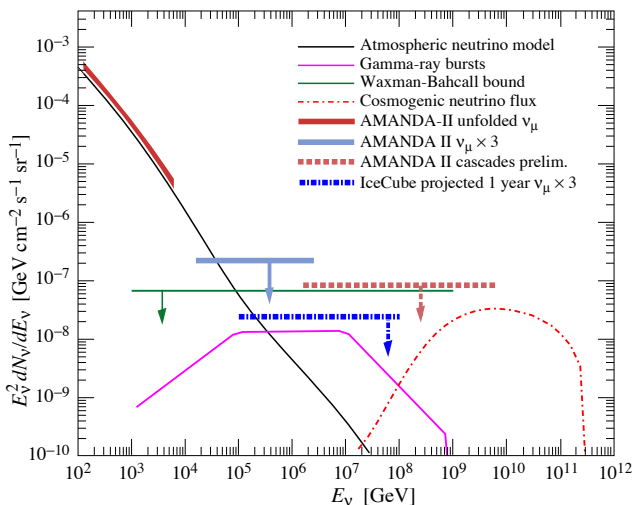


Figure 29.3: Measured atmospheric neutrino fluxes above 100 GeV are shown together with a few generic models for astrophysical neutrinos and some limits. See full-color version on color pages at end of book.

29.4. Large time-projection chambers for rare event detection

Written August 2009 by M. Heffner (LLNL).

TPCs in non-accelerator particle physics experiments are principally focused on rare event detection (*e.g.*, neutrino and dark matter experiments) and the physics of these experiments can place dramatically different constraints on the TPC design (only extensions of the traditional TPCs are discussed here). The drift gas or liquid is usually the target or matter under observation and due to very low signal rates a TPC with the largest possible active mass is desired. The large mass complicates particle tracking of short and sometimes very low-energy particles. Other special design issues include efficient light collection, background rejection, internal triggering, and optimal energy resolution.

The liquid-phase TPC can have a high density at low pressure that results in very good self-shielding and compact installation with lightweight containment. The down sides are the need for cryogenics, slower charge drift, tracks shorter than typical electron diffusion distances, lower-energy resolution (*e.g.*, xenon) and limited charge readout options. Slower charge drift requires long electron lifetimes, placing strict limits on the oxygen and other impurities with high electron affinity.

A high-pressure gas phase TPC has no cryogenics and density is easily optimized for the signal, but a large heavy-pressure vessel is required.

Although self shielding is reduced, it can in some cases approach that of the liquid phase; in xenon at 50 atm the density is about half that of water or about 1/6 of liquid xenon. A significant feature of high pressure xenon gas is the energy resolution.

Rare-event TPCs can be designed to detect scintillation light as well as charge to exploit the anti-correlation to improve energy resolution and/or signal to noise [63]. Electroluminescence can be used to proportionally amplify the drifted ionization, and it does not suffer the fluctuations of an avalanche or the small signals of direct collection. It works by setting up at the positive end of the drift volume parallel meshes or wire arrays with an electric field larger than the drift field, but less than the field needed for avalanche. In xenon, this is 3–6 kV cm⁻¹ bar⁻¹ for good energy resolution.

Differentiation of nuclear and electron recoils at low-energy deposition is important as a means of background rejection. The nuclear recoil deposits a higher density of ionization than an electron recoil and this results in a higher geminate recombination resulting in a higher output of primary scintillation and lower charge. The ratio of scintillation to charge can be used to distinguish the two. In the case of an electroluminescence readout, this is done simply with the ratio of primary light to secondary light.

29.5. Sub-Kelvin detectors

Written September 2009 by S. Golwala (Caltech).

Detectors operating below 1 K, also known as “low-temperature” or “cryogenic” detectors, use \lesssim meV quanta (phonons, superconducting quasiparticles) to provide better energy resolution than is typically available from conventional technologies. Such resolution can provide unique advantages to applications reliant on energy resolution, such as beta-decay experiments seeking to measure the ν_e mass or searches for neutrinoless double-beta decay. In addition, the sub-Kelvin mode is combined with conventional (eV quanta) ionization or scintillation measurements to provide discrimination of nuclear recoils from electron recoils, critical for searches for WIMP dark matter and for coherent neutrino-nucleus scattering.

29.5.1. Thermal Phonons :

The most basic kind of low-temperature detector employs a dielectric absorber coupled to a thermal bath via a weak link. A thermistor monitors the temperature of the absorber. The energy E deposited by a particle interaction causes a calorimetric temperature change by increasing the population of thermal phonons. The fundamental sensitivity is

$$\sigma_E^2 = \xi^2 kT [T C(T) + \beta E] , \quad (29.5)$$

where C is the heat capacity of the detector, T is the temperature of operation, k is Boltzmann’s constant, and ξ is a dimensionless factor of order unity that is precisely calculable from the nature of the thermal link and the non-thermodynamic noises (*e.g.*, Johnson and/or readout noise). The energy resolution typically acquires an additional energy dependence due to deviations from an ideal calorimetric model that cause position and/or energy dependence in the signal shape. The rise time of response is limited by the internal thermal conductivity of the absorber.

29.5.2. *Athermal Phonons and Superconducting Quasiparticles :*

The advantage of thermal phonons is also a disadvantage: energy resolution degrades as \sqrt{M} where M is the detector mass. This motivates the use of athermal phonons. There are three steps in the development of the phonon signal. The recoiling particle deposits energy along its track, with the majority going directly into phonons. The recoil and bandgap energy scales (keV and higher, and eV, respectively) are much larger than phonon energies (meV), so the full energy spectrum of phonons is populated, with phase space favoring the most energetic phonons.

Another mode is detection of superconducting quasiparticles in superconducting crystals. Energy absorption breaks superconducting Cooper pairs and yields quasiparticles, electron-like excitations that can diffuse through the material and that recombine after the quasiparticle lifetime.

29.5.3. *Ionization and Scintillation :*

While ionization and scintillation detectors usually operate at much higher temperatures, ionization and scintillation can be measured at low temperature and can be combined with a “sub-Kelvin” technique to discriminate nuclear recoils from background interactions producing electron recoils, which is critical for WIMP searches and coherent neutrino-nucleus scattering. With ionization, such techniques are based on Lindhard theory [55], which predicts substantially reduced ionization yield for nuclear recoils relative to electron recoils. For scintillation, application of Birks’ law Sec. 28.3.0) yields a similar prediction.

29.6. Low-radioactivity background techniques

Written August 2009 by A. Piepke (University of Alabama).

The physics reach of low-energy rare event searches *e.g.* for dark matter, neutrino oscillations, or double beta decay is often limited by background caused by radioactivity. Depending on the chosen detector design, the separation of the physics signal from this unwanted interference can be achieved on an event-by-event basis by active event tagging, utilizing some unique event feature, or by reducing the radiation background by appropriate shielding and material selection. In both cases, the background rate is proportional to the flux of background-creating radiation. Its reduction is thus essential for realizing the full physics potential of the experiment. In this context, “low energy” may be defined as the regime of natural, anthropogenic, or cosmogenic radioactivity, all at energies up to about 10 MeV. Following the classification of [64], sources of background may be categorized into the following classes:

1. environmental radioactivity,
2. radioimpurities in detector or shielding components,
3. radon and its progeny,
4. cosmic rays,
5. neutrons from natural fission, (α , n) reactions and from cosmic-ray muon spallation and capture.

Further discussion and all references may be found in the full *Review of Particle Physics*. The numbering of references and equations used here corresponds to that version.

30. RADIOACTIVITY AND RADIATION PROTECTION

Revised Sept. 2007 by S. Roesler (CERN) and J.C. Liu (SLAC).

30.1. Definitions

The International Commission on Radiation Units and Measurements (ICRU) recommends the use of SI units. Therefore we list SI units first, followed by cgs (or other common) units in parentheses, where they differ.

- **Activity** (unit: Becquerel):

1 Bq = 1 disintegration per second (= 27 pCi).

- **Absorbed dose** (unit: Gray): The absorbed dose is the energy imparted by ionizing radiation in a volume element of a specified material divided by the mass of this volume element.

1 Gy = 1 J/kg (= 10^4 erg/g = 100 rad)
 = 6.24×10^{12} MeV/kg deposited energy.

- **Kerma** (unit: Gray): Kerma is the sum of the initial kinetic energies of all charged particles liberated by indirectly ionizing particles in a volume element of the specified material divided by the mass of this volume element.

- **Exposure** (unit: C/kg of air [= 3880 Roentgen[†]]): The exposure is a measure of photon fluence at a certain point in space integrated over time, in terms of ion charge of either sign produced by secondary electrons in a small volume of air about the point. Implicit in the definition is the assumption that the small test volume is embedded in a sufficiently large uniformly irradiated volume that the number of secondary electrons entering the volume equals the number leaving (so-called charged particle equilibrium).

Table 30.1: Radiation weighting factors, w_R .

Radiation type	w_R
Photons	1
Electrons and muons	1
Neutrons, $E_n < 1$ MeV	$2.5 + 18.2 \times \exp[-(\ln E_n)^2/6]$
1 MeV $\leq E_n \leq 50$ MeV	$5.0 + 17.0 \times \exp[-(\ln(2E_n))^2/6]$
$E_n > 50$ MeV	$2.5 + 3.25 \times \exp[-(\ln(0.04E_n))^2/6]$
Protons and charged pions	2
Alpha particles, fission fragments, heavy ions	20

- **Equivalent dose** (unit: Sievert [= 100 rem (roentgen equivalent in man)]): The equivalent dose H_T in an organ or tissue T is equal to the sum of the absorbed doses $D_{T,R}$ in the organ or tissue caused by different radiation types R weighted with so-called radiation weighting factors w_R :

$$H_T = \sum_R w_R \times D_{T,R} . \quad (30.1)$$

[†] This unit is somewhat historical, but appears on some measuring instruments. One R is the amount of radiation required to liberate positive and negative charges of one electrostatic unit of charge in 1 cm³ of air at standard temperature and pressure (STP)

It expresses long-term risks (primarily cancer and leukemia) from low-level chronic exposure. The values for w_R recommended recently by ICRP [1] are given in Table 29.1. • **Effective dose** (unit: Sievert): The sum of the equivalent doses, weighted by the tissue weighting factors w_T ($\sum_T w_T = 1$) of several organs and tissues T of the body that are considered to be most sensitive [2], is called “effective dose” E :

$$E = \sum_T w_T \times H_T . \quad (30.2)$$

30.2. Radiation levels [3]

• **Natural annual background**, all sources: Most world areas, whole-body equivalent dose rate $\approx (0.4\text{--}4)$ mSv (40–400 mrem). Can range up to 50 mSv (5 rem) in certain areas. U.S. average ≈ 3.6 mSv, including ≈ 2 mSv (≈ 200 mrem) from inhaled natural radioactivity, mostly radon and radon daughters. (Average is for a typical house and varies by more than an order of magnitude. It can be more than two orders of magnitude higher in poorly ventilated mines. 0.1–0.2 mSv in open areas.)

• **Cosmic ray background** (sea level, mostly muons): $\sim 1 \text{ min}^{-1} \text{ cm}^{-2} \text{ sr}^{-1}$. For more accurate estimates and details, see the Cosmic Rays section (Sec. 24 of this *Review*).

• **Fluence** (per cm^2) to deposit one Gy, assuming uniform irradiation: \approx (**charged particles**) $6.24 \times 10^9 / (dE/dx)$, where dE/dx (MeV $\text{g}^{-1} \text{ cm}^2$), the energy loss per unit length, may be obtained from Figs. 27.2 and 27.4 in Sec. 27 of the *Review*, and pdg.lbl.gov/AtomicNuclearProperties.

$\approx 3.5 \times 10^9 \text{ cm}^{-2}$ minimum-ionizing singly-charged particles in carbon.
 \approx (**photons**) $6.24 \times 10^9 / [Ef/\ell]$, for photons of energy E (MeV), attenuation length ℓ (g cm^{-2}), and fraction $f \lesssim 1$ expressing the fraction of the photon’s energy deposited in a small volume of thickness $\ll \ell$ but large enough to contain the secondary electrons.

$\approx 2 \times 10^{11}$ photons cm^{-2} for 1 MeV photons on carbon ($f \approx 1/2$).

• **Recommended limits of effective dose to radiation workers (whole-body dose):***

EU/Switzerland: 20 mSv yr^{-1}

U.S.: 50 mSv yr^{-1} (5 rem yr^{-1})[†]

• **Lethal dose:** The whole-body dose from penetrating ionizing radiation resulting in 50% mortality in 30 days (assuming no medical treatment) is 2.5–4.5 Gy (250–450 rad), as measured internally on body longitudinal center line. Surface dose varies due to variable body attenuation and may be a strong function of energy.

• **Cancer induction by low LET radiation:** The cancer induction probability is about 5% per Sv on average for the entire population [2].

Footnotes:

* The ICRP recommendation [2] is 20 mSv yr^{-1} averaged over 5 years, with the dose in any one year ≤ 50 mSv.

† Many laboratories in the U.S. and elsewhere set lower limits.

31. COMMONLY USED RADIOACTIVE SOURCES

Table 31.1. Revised November 1993 by E. Browne (LBNL).

Nuclide	Half-life	Type of decay	Particle		Photon	
			Energy (MeV)	Emission prob.	Energy (MeV)	Emission prob.
$^{22}_{11}\text{Na}$	2.603 y	β^+ , EC	0.545	90%	0.511 1.275	Annih. 100%
$^{54}_{25}\text{Mn}$	0.855 y	EC			0.835	100% Cr K x rays 26%
$^{55}_{26}\text{Fe}$	2.73 y	EC			Mn K x rays: 0.00590 0.00649	24.4% 2.86%
$^{57}_{27}\text{Co}$	0.744 y	EC			0.014 0.122 0.136	9% 86% 11% Fe K x rays 58%
$^{60}_{27}\text{Co}$	5.271 y	β^-	0.316	100%	1.173 1.333	100% 100%
$^{68}_{32}\text{Ge}$	0.742 y	EC			Ga K x rays 44%	
$\rightarrow ^{68}_{31}\text{Ga}$		β^+ , EC	1.899	90%	0.511 1.077	Annih. 3%
$^{90}_{38}\text{Sr}$	28.5 y	β^-	0.546	100%		
$\rightarrow ^{90}_{39}\text{Y}$		β^-	2.283	100%		
$^{106}_{44}\text{Ru}$	1.020 y	β^-	0.039	100%		
$\rightarrow ^{106}_{45}\text{Rh}$		β^-	3.541	79%	0.512 0.622	21% 10%
$^{109}_{48}\text{Cd}$	1.267 y	EC	0.063 e^- 0.084 e^- 0.087 e^-	41% 45% 9%	0.088	3.6% Ag K x rays 100%
$^{113}_{50}\text{Sn}$	0.315 y	EC	0.364 e^- 0.388 e^-	29% 6%	0.392	65% In K x rays 97%
$^{137}_{55}\text{Cs}$	30.2 y	β^-	0.514 1.176	94% 6%	0.662	85%

$^{133}_{56}\text{Ba}$	10.54 y	EC	0.045 e^- 0.075 e^-	50% 6%	0.081 0.356	34% 62% Cs K x rays 121%
$^{207}_{83}\text{Bi}$	31.8 y	EC	0.481 e^- 0.975 e^- 1.047 e^-	2% 7% 2%	0.569 1.063 1.770	98% 75% 7% Pb K x rays 78%
$^{228}_{90}\text{Th}$	1.912 y	6α : $3\beta^-$:	5.341 to 8.785 0.334 to 2.246		0.239 0.583 2.614	44% 31% 36%
($\rightarrow^{224}_{88}\text{Ra} \rightarrow^{220}_{86}\text{Rn} \rightarrow^{216}_{84}\text{Po} \rightarrow^{212}_{82}\text{Pb} \rightarrow^{212}_{83}\text{Bi} \rightarrow^{212}_{84}\text{Po}$)						
$^{241}_{95}\text{Am}$	432.7 y	α	5.443 5.486	13% 85%	0.060	36% Np L x rays 38%
$^{241}_{95}\text{Am/Be}$	432.2 y	6×10^{-5} neutrons (4–8 MeV) and 4×10^{-5} γ 's (4.43 MeV) per Am decay				
$^{244}_{96}\text{Cm}$	18.11 y	α	5.763 5.805	24% 76%	Pu L x rays \sim 9%	
$^{252}_{98}\text{Cf}$	2.645 y	α (97%)	6.076 6.118	15% 82%		
		Fission (3.1%)	\approx 20 γ 's/fission; 80% < 1 MeV \approx 4 neutrons/fission; $\langle E_n \rangle = 2.14$ MeV			

“Emission probability” is the probability per decay of a given emission; because of cascades these may total more than 100%. Only principal emissions are listed. EC means electron capture, and e^- means monoenergetic internal conversion (Auger) electron. The intensity of 0.511 MeV e^+e^- annihilation photons depends upon the number of stopped positrons. Endpoint β^\pm energies are listed. In some cases when energies are closely spaced, the γ -ray values are approximate weighted averages. Radiation from short-lived daughter isotopes is included where relevant.

Half-lives, energies, and intensities are from E. Browne and R.B. Firestone, *Table of Radioactive Isotopes* (John Wiley & Sons, New York, 1986), recent *Nuclear Data Sheets*, and *X-ray and Gamma-ray Standards for Detector Calibration*, IAEA-TECDOC-619 (1991).

Neutron data are from *Neutron Sources for Basic Physics and Applications* (Pergamon Press, 1983).

32. PROBABILITY

Revised September 2009 by G. Cowan (RHUL).

The following is a much-shortened version of Sec. 31 of the full *Review*. Equation, section, and figure numbers follow the *Review*.

32.2. Random variables

- *Probability density function* (p.d.f.): x is a *random variable*.

Continuous: $f(x; \theta) dx =$ probability x is between x to $x + dx$, given parameter(s) θ ;

Discrete: $f(x; \theta) =$ probability of x given θ .

- *Cumulative distribution function*:

$$F(a) = \int_{-\infty}^a f(x) dx . \quad (32.6)$$

Here and below, if x is discrete-valued, the integral is replaced by a sum. The endpoint a is induced in the integral or sum.

- *Expectation values*: Given a function u :

$$E[u(x)] = \int_{-\infty}^{\infty} u(x) f(x) dx . \quad (32.7)$$

- *Moments*:

$$\text{nth moment of a random variable: } \alpha_n = E[x^n] , \quad (32.8a)$$

$$\text{nth central moment: } m_n = E[(x - \alpha_1)^n] . \quad (32.8b)$$

$$\text{Mean: } \mu \equiv \alpha_1 . \quad (32.9a)$$

$$\text{Variance: } \sigma^2 \equiv V[x] \equiv m_2 = \alpha_2 - \mu^2 . \quad (32.9b)$$

Coefficient of skewness: $\gamma_1 \equiv m_3/\sigma^3$.

Kurtosis: $\gamma_2 = m_4/\sigma^4 - 3$.

Median: $F(x_{\text{med}}) = 1/2$.

- *Marginal* p.d.f.: Let x, y be two random variables with joint p.d.f. $f(x, y)$.

$$f_1(x) = \int_{-\infty}^{\infty} f(x, y) dy ; \quad f_2(y) = \int_{-\infty}^{\infty} f(x, y) dx . \quad (32.10)$$

- *Conditional* p.d.f.:

$$f_4(x|y) = f(x, y)/f_2(y) ; \quad f_3(y|x) = f(x, y)/f_1(x) .$$

- *Bayes' theorem*:

$$f_4(x|y) = \frac{f_3(y|x)f_1(x)}{f_2(y)} = \frac{f_3(y|x)f_1(x)}{\int f_3(y|x')f_1(x') dx'} . \quad (32.11)$$

- *Correlation coefficient and covariance*:

$$\mu_x = \int_{-\infty}^{\infty} \int_{-\infty}^{\infty} x f(x, y) dx dy , \quad (32.12)$$

$$\rho_{xy} = E[(x - \mu_x)(y - \mu_y)] / \sigma_x \sigma_y \equiv \text{cov}[x, y] / \sigma_x \sigma_y ,$$

$$\sigma_x = \int_{-\infty}^{\infty} \int_{-\infty}^{\infty} (x - \mu_x)^2 f(x, y) dx dy . \text{ Note } \rho_{xy}^2 \leq 1 .$$

• *Independence:* x, y are independent if and only if $f(x, y) = f_1(x) \cdot f_2(y)$; then $\rho_{xy} = 0$, $E[u(x) v(y)] = E[u(x)] E[v(y)]$ and $V[x + y] = V[x] + V[y]$.

• *Change of variables:* From $\mathbf{x} = (x_1, \dots, x_n)$ to $\mathbf{y} = (y_1, \dots, y_n)$: $g(\mathbf{y}) = f(\mathbf{x}(\mathbf{y})) \cdot |J|$ where $|J|$ is the absolute value of the determinant of the Jacobian $J_{ij} = \partial x_i / \partial y_j$. For discrete variables, use $|J| = 1$.

32.3. Characteristic functions

Given a pdf $f(x)$ for a continuous random variable x , the characteristic function $\phi(u)$ is given by (31.6). Its derivatives are related to the algebraic moments of x by (31.7).

$$\phi(u) = E \left[e^{iux} \right] = \int_{-\infty}^{\infty} e^{iux} f(x) dx . \tag{32.17}$$

$$i^{-n} \left. \frac{d^n \phi}{du^n} \right|_{u=0} = \int_{-\infty}^{\infty} x^n f(x) dx = \alpha_n . \tag{32.18}$$

If the p.d.f.s $f_1(x)$ and $f_2(y)$ for independent random variables x and y have characteristic functions $\phi_1(u)$ and $\phi_2(u)$, then the characteristic function of the weighted sum $ax + by$ is $\phi_1(au)\phi_2(bu)$. The additional rules for several important distributions (e.g., that the sum of two Gaussian distributed variables also follows a Gaussian distribution) easily follow from this observation.

32.4. Some probability distributions

See Table 32.1.

32.4.2. Poisson distribution :

The Poisson distribution $f(n; \nu)$ gives the probability of finding exactly n events in a given interval of x (e.g., space or time) when the events occur independently of one another and of x at an average rate of ν per the given interval. The variance σ^2 equals ν . It is the limiting case $p \rightarrow 0$, $N \rightarrow \infty$, $Np = \nu$ of the binomial distribution. The Poisson distribution approaches the Gaussian distribution for large ν .

For example, a large number of radioactive nuclei of a given type will result in a certain number of decays in a fixed time interval. If this interval is small compared to the mean lifetime, then the probability for a given nucleus to decay is small, and thus the number of decays in the time interval is well modeled as a Poisson variable.

32.4.3. Normal or Gaussian distribution :

Its cumulative distribution, for mean 0 and variance 1, is usually tabulated as the *error function*

$$F(x; 0, 1) = \frac{1}{2} \left[1 + \operatorname{erf}(x/\sqrt{2}) \right] . \tag{32.24}$$

For mean μ and variance σ^2 , replace x by $(x - \mu)/\sigma$. The error function is accessible in libraries of computer routines such as CERNLIB.

$$P(x \text{ in range } \mu \pm \sigma) = 0.6827,$$

$$P(x \text{ in range } \mu \pm 0.6745\sigma) = 0.5,$$

$$E[|x - \mu|] = \sqrt{2/\pi}\sigma = 0.7979\sigma,$$

$$\text{half-width at half maximum} = \sqrt{2 \ln 2} \cdot \sigma = 1.177\sigma.$$

Table 32.1. Some common probability density functions, with corresponding characteristic functions and means and variances. In the Table, $\Gamma(k)$ is the gamma function, equal to $(k-1)!$ when k is an integer.

Distribution	Probability density function f (variable; parameters)	Characteristic function $\phi(u)$	Mean	Variance σ^2
Uniform	$f(x; a, b) = \begin{cases} 1/(b-a) & a \leq x \leq b \\ 0 & \text{otherwise} \end{cases}$	$\frac{e^{ibu} - e^{iau}}{(b-a)iu}$	$\frac{a+b}{2}$	$\frac{(b-a)^2}{12}$
Binomial	$f(r; N, p) = \frac{N!}{r!(N-r)!} p^r q^{N-r}$ $r = 0, 1, 2, \dots, N; \quad 0 \leq p \leq 1; \quad q = 1-p$	$(q + pe^{iu})^N$	Np	Npq
Poisson	$f(n; \nu) = \frac{\nu^n e^{-\nu}}{n!}; \quad n = 0, 1, 2, \dots; \quad \nu > 0$	$\exp[\nu(e^{iu} - 1)]$	ν	ν
Normal (Gaussian)	$f(x; \mu, \sigma^2) = \frac{1}{\sigma\sqrt{2\pi}} \exp(-(x-\mu)^2/2\sigma^2)$ $-\infty < x < \infty; \quad -\infty < \mu < \infty; \quad \sigma > 0$	$\exp(i\mu u - \frac{1}{2}\sigma^2 u^2)$	μ	σ^2
Multivariate Gaussian	$f(\mathbf{x}; \boldsymbol{\mu}, V) = \frac{1}{(2\pi)^{n/2} \sqrt{ V }} \times \exp[-\frac{1}{2}(\mathbf{x} - \boldsymbol{\mu})^T V^{-1}(\mathbf{x} - \boldsymbol{\mu})]$ $-\infty < x_j < \infty; \quad -\infty < \mu_j < \infty; \quad V > 0$	$\exp[i\boldsymbol{\mu} \cdot \mathbf{u} - \frac{1}{2}\mathbf{u}^T V \mathbf{u}]$	$\boldsymbol{\mu}$	V_{jk}
χ^2	$f(z; n) = \frac{z^{n/2-1} e^{-z/2}}{2^{n/2} \Gamma(n/2)}; \quad z \geq 0$	$(1-2iu)^{-n/2}$	n	$2n$
Student's t	$f(t; n) = \frac{1}{\sqrt{n\pi}} \frac{\Gamma[(n+1)/2]}{\Gamma(n/2)} \left(1 + \frac{t^2}{n}\right)^{-(n+1)/2}$ $-\infty < t < \infty; \quad n$ not required to be integer	—	0 for $n \geq 2$	$n/(n-2)$ for $n \geq 3$
Gamma	$f(x; \lambda, k) = \frac{x^{k-1} \lambda^k e^{-\lambda x}}{\Gamma(k)}$ $-\infty < t < \infty; \quad n$ not required to be integer	$(1-iu/\lambda)^{-k}$	k/λ	k/λ^2

For n Gaussian random variables \mathbf{x}_i , the joint p.d.f. is the multivariate Gaussian:

$$f(\mathbf{x}; \boldsymbol{\mu}, V) = \frac{1}{(2\pi)^{n/2} \sqrt{|V|}} \exp \left[-\frac{1}{2} (\mathbf{x} - \boldsymbol{\mu})^T V^{-1} (\mathbf{x} - \boldsymbol{\mu}) \right], \quad |V| > 0. \quad (32.27)$$

V is the $n \times n$ covariance matrix; $V_{ij} \equiv E[(x_i - \mu_i)(x_j - \mu_j)] \equiv \rho_{ij} \sigma_i \sigma_j$, and $V_{ii} = V[x_i]$; $|V|$ is the determinant of V . For $n = 2$, $f(\mathbf{x}; \boldsymbol{\mu}, V)$ is

$$f(x_1, x_2; \mu_1, \mu_2, \sigma_1, \sigma_2, \rho) = \frac{1}{2\pi\sigma_1\sigma_2\sqrt{1-\rho^2}} \times \exp \left\{ \frac{-1}{2(1-\rho^2)} \left[\frac{(x_1 - \mu_1)^2}{\sigma_1^2} - \frac{2\rho(x_1 - \mu_1)(x_2 - \mu_2)}{\sigma_1\sigma_2} + \frac{(x_2 - \mu_2)^2}{\sigma_2^2} \right] \right\}. \quad (32.28)$$

The marginal distribution of any x_i is a Gaussian with mean μ_i and variance V_{ii} . V is $n \times n$, symmetric, and positive definite. Therefore for any vector \mathbf{X} , the quadratic form $\mathbf{X}^T V^{-1} \mathbf{X} = C$, where C is any positive number, traces an n -dimensional ellipsoid as \mathbf{X} varies. If $X_i = x_i - \mu_i$, then C is a random variable obeying the χ^2 distribution with n degrees of freedom, discussed in the following section. The probability that \mathbf{X} corresponding to a set of Gaussian random variables x_i lies outside the ellipsoid characterized by a given value of C ($= \chi^2$) is given by $1 - F_{\chi^2}(C; n)$, where F_{χ^2} is the cumulative χ^2 distribution. This may be read from Fig. 33.1. For example, the “ s -standard-deviation ellipsoid” occurs at $C = s^2$. For the two-variable case ($n = 2$), the point \mathbf{X} lies outside the one-standard-deviation ellipsoid with 61% probability. The use of these ellipsoids as indicators of probable error is described in Sec. 33.3.2.4; the validity of those indicators assumes that $\boldsymbol{\mu}$ and V are correct.

32.4.4. χ^2 distribution :

If x_1, \dots, x_n are independent Gaussian random variables, the sum $z = \sum_{i=1}^n (x_i - \mu_i)^2 / \sigma_i^2$ follows the χ^2 p.d.f. with n degrees of freedom, which we denote by $\chi^2(n)$. More generally, for n correlated Gaussian variables as components of a vector \mathbf{X} with covariance matrix V , $z = \mathbf{X}^T V^{-1} \mathbf{X}$ follows $\chi^2(n)$ as in the previous section. For a set of z_i , each of which follows $\chi^2(n_i)$, $\sum z_i$ follows $\chi^2(\sum n_i)$. For large n , the χ^2 p.d.f. approaches a Gaussian with mean $\mu = n$ and variance $\sigma^2 = 2n$. The χ^2 p.d.f. is often used in evaluating the level of compatibility between observed data and a hypothesis for the p.d.f. that the data might follow. This is discussed further in Sec. 33.2.2 on tests of goodness-of-fit.

32.4.6. Gamma distribution :

For a process that generates events as a function of x (e.g., space or time) according to a Poisson distribution, the distance in x from an arbitrary starting point (which may be some particular event) to the k^{th} event follows a gamma distribution, $f(x; \lambda, k)$. The Poisson parameter μ is λ per unit x . The special case $k = 1$ (i.e., $f(x; \lambda, 1) = \lambda e^{-\lambda x}$) is called the exponential distribution. A sum of k' exponential random variables x_i is distributed as $f(\sum x_i; \lambda, k')$.

The parameter k is not required to be an integer. For $\lambda = 1/2$ and $k = n/2$, the gamma distribution reduces to the $\chi^2(n)$ distribution.

See the full Review for further discussion and all references.

33. STATISTICS

Revised September 2009 by G. Cowan (RHUL).

There are two main approaches to statistical inference, which we may call frequentist and Bayesian. In frequentist statistics, probability is interpreted as the frequency of the outcome of a repeatable experiment. The most important tools in this framework are parameter estimation, covered in Section 33.1, and statistical tests, discussed in Section 33.2. Frequentist confidence intervals, which are constructed so as to cover the true value of a parameter with a specified probability, are treated in Section 33.3.2. Note that in frequentist statistics one does not define a probability for a hypothesis or for a parameter.

In Bayesian statistics, the interpretation of probability is more general and includes *degree of belief* (called subjective probability). One can then speak of a probability density function (p.d.f.) for a parameter, which expresses one's state of knowledge about where its true value lies. Using Bayes' theorem Eq. (32.4), the prior degree of belief is updated by the data from the experiment. Bayesian methods for interval estimation are discussed in Sections 33.3.1 and 33.3.2.6

Following common usage in physics, the word "error" is often used in this chapter to mean "uncertainty." More specifically it can indicate the size of an interval as in "the standard error" or "error propagation," where the term refers to the standard deviation of an estimator.

33.1. Parameter estimation

Here we review the frequentist approach to *point estimation* of parameters. An estimator $\hat{\theta}$ (written with a hat) is a function of the data whose value, the *estimate*, is intended as a meaningful guess for the value of the parameter θ .

33.1.1. Estimators for mean, variance and median: Suppose we have a set of N independent measurements, x_i , assumed to be unbiased measurements of the same unknown quantity μ with a common, but unknown, variance σ^2 . Then

$$\hat{\mu} = \frac{1}{N} \sum_{i=1}^N x_i \quad (33.4)$$

$$\hat{\sigma}^2 = \frac{1}{N-1} \sum_{i=1}^N (x_i - \hat{\mu})^2 \quad (33.5)$$

are unbiased estimators of μ and σ^2 . The variance of $\hat{\mu}$ is σ^2/N and the variance of $\hat{\sigma}^2$ is

$$V[\hat{\sigma}^2] = \frac{1}{N} \left(m_4 - \frac{N-3}{N-1} \sigma^4 \right), \quad (33.6)$$

where m_4 is the 4th central moment of x . For Gaussian distributed x_i , this becomes $2\sigma^4/(N-1)$ for any $N \geq 2$, and for large N , the standard deviation of $\hat{\sigma}$ (the "error of the error") is $\sigma/\sqrt{2N}$. Again, if the x_i are Gaussian, $\hat{\mu}$ is an efficient estimator for μ , and the estimators $\hat{\mu}$ and $\hat{\sigma}^2$ are uncorrelated. Otherwise the arithmetic mean (33.4) is not necessarily the most efficient estimator.

If the x_i have different, known variances σ_i^2 , then the weighted average

$$\hat{\mu} = \frac{1}{w} \sum_{i=1}^N w_i x_i \quad (33.7)$$

is an unbiased estimator for μ with a smaller variance than an unweighted average; here $w_i = 1/\sigma_i^2$ and $w = \sum_i w_i$. The standard deviation of $\hat{\mu}$ is $1/\sqrt{w}$.

33.1.2. The method of maximum likelihood : Suppose we have a set of N measured quantities $\mathbf{x} = (x_1, \dots, x_N)$ described by a joint p.d.f. $f(\mathbf{x}; \boldsymbol{\theta})$, where $\boldsymbol{\theta} = (\theta_1, \dots, \theta_n)$ is set of n parameters whose values are unknown. The *likelihood function* is given by the p.d.f. evaluated with the data \mathbf{x} , but viewed as a function of the parameters, *i.e.*, $L(\boldsymbol{\theta}) = f(\mathbf{x}; \boldsymbol{\theta})$. If the measurements x_i are statistically independent and each follow the p.d.f. $f(x; \boldsymbol{\theta})$, then the joint p.d.f. for \mathbf{x} factorizes and the likelihood function is

$$L(\boldsymbol{\theta}) = \prod_{i=1}^N f(x_i; \boldsymbol{\theta}) . \tag{33.8}$$

The method of maximum likelihood takes the estimators $\hat{\boldsymbol{\theta}}$ to be those values of $\boldsymbol{\theta}$ that maximize $L(\boldsymbol{\theta})$.

Note that the likelihood function is *not* a p.d.f. for the parameters $\boldsymbol{\theta}$; in frequentist statistics this is not defined. In Bayesian statistics, one can obtain from the likelihood the posterior p.d.f. for $\boldsymbol{\theta}$, but this requires multiplying by a prior p.d.f. (see Sec. 33.3.1).

It is usually easier to work with $\ln L$, and since both are maximized for the same parameter values $\boldsymbol{\theta}$, the maximum likelihood (ML) estimators can be found by solving the *likelihood equations*,

$$\frac{\partial \ln L}{\partial \theta_i} = 0 , \quad i = 1, \dots, n . \tag{33.9}$$

In evaluating the likelihood function, it is important that any normalization factors in the p.d.f. that involve $\boldsymbol{\theta}$ be included.

The inverse V^{-1} of the covariance matrix $V_{ij} = \text{cov}[\hat{\theta}_i, \hat{\theta}_j]$ for a set of ML estimators can be estimated by using

$$(\hat{V}^{-1})_{ij} = - \left. \frac{\partial^2 \ln L}{\partial \theta_i \partial \theta_j} \right|_{\hat{\boldsymbol{\theta}}} . \tag{33.10}$$

For finite samples, however, Eq. (33.10) can result in an underestimate of the variances. In the large sample limit (or in a linear model with Gaussian errors), L has a Gaussian form and $\ln L$ is (hyper)parabolic. In this case, it can be seen that a numerically equivalent way of determining s -standard-deviation errors is from the contour given by the $\boldsymbol{\theta}'$ such that

$$\ln L(\boldsymbol{\theta}') = \ln L_{\max} - s^2/2 , \tag{33.11}$$

where $\ln L_{\max}$ is the value of $\ln L$ at the solution point (compare with Eq. (33.56)). The extreme limits of this contour on the θ_i axis give an approximate s -standard-deviation confidence interval for θ_i (see Section 33.3.2.4).

33.1.3. The method of least squares : The *method of least squares* (LS) coincides with the method of maximum likelihood in the following special case. Consider a set of N independent measurements y_i at known points x_i . The measurement y_i is assumed to be Gaussian distributed with mean $F(x_i; \boldsymbol{\theta})$ and known variance σ_i^2 . The goal is to construct estimators for the unknown parameters $\boldsymbol{\theta}$. The likelihood function contains the sum of squares

$$\chi^2(\boldsymbol{\theta}) = -2 \ln L(\boldsymbol{\theta}) + \text{constant} = \sum_{i=1}^N \frac{(y_i - F(x_i; \boldsymbol{\theta}))^2}{\sigma_i^2} . \tag{33.13}$$

The set of parameters $\boldsymbol{\theta}$ which maximize L is the same as those which minimize χ^2 .

The minimum of Equation (33.13) defines the least-squares estimators $\hat{\theta}$ for the more general case where the y_i are not Gaussian distributed as long as they are independent. If they are not independent but rather have a covariance matrix $V_{ij} = \text{cov}[y_i, y_j]$, then the LS estimators are determined by the minimum of

$$\chi^2(\theta) = (\mathbf{y} - \mathbf{F}(\theta))^T V^{-1} (\mathbf{y} - \mathbf{F}(\theta)), \quad (33.14)$$

where $\mathbf{y} = (y_1, \dots, y_N)$ is the vector of measurements, $\mathbf{F}(\theta)$ is the corresponding vector of predicted values (understood as a column vector in (33.14)), and the superscript T denotes transposed (*i.e.*, row) vector.

In many practical cases, one further restricts the problem to the situation where $F(x_i; \theta)$ is a linear function of the parameters, *i.e.*,

$$F(x_i; \theta) = \sum_{j=1}^m \theta_j h_j(x_i). \quad (33.15)$$

Here the $h_j(x)$ are m linearly independent functions, *e.g.*, $1, x, x^2, \dots, x^{m-1}$, or Legendre polynomials. We require $m < N$ and at least m of the x_i must be distinct.

Minimizing χ^2 in this case with m parameters reduces to solving a system of m linear equations. Defining $H_{ij} = h_j(x_i)$ and minimizing χ^2 by setting its derivatives with respect to the θ_i equal to zero gives the LS estimators,

$$\hat{\theta} = (H^T V^{-1} H)^{-1} H^T V^{-1} \mathbf{y} \equiv D \mathbf{y}. \quad (33.16)$$

The covariance matrix for the estimators $U_{ij} = \text{cov}[\hat{\theta}_i, \hat{\theta}_j]$ is given by

$$U = D V D^T = (H^T V^{-1} H)^{-1}. \quad (33.17)$$

Expanding $\chi^2(\theta)$ about $\hat{\theta}$, one finds that the contour in parameter space defined by

$$\chi^2(\theta) = \chi^2(\hat{\theta}) + 1 = \chi_{\min}^2 + 1 \quad (33.23)$$

has tangent planes located at approximately plus-or-minus-one standard deviation $\sigma_{\hat{\theta}}$ from the LS estimates $\hat{\theta}$.

As the minimum value of the χ^2 represents the level of agreement between the measurements and the fitted function, it can be used for assessing the goodness-of-fit; this is discussed further in Section 33.2.2.

33.1.5. Propagation of errors : Consider a set of n quantities $\theta = (\theta_1, \dots, \theta_n)$ and a set of m functions $\eta(\theta) = (\eta_1(\theta), \dots, \eta_m(\theta))$. Suppose we have estimated $\hat{\theta} = (\hat{\theta}_1, \dots, \hat{\theta}_n)$, using, say, maximum-likelihood or least-squares, and we also know or have estimated the covariance matrix $V_{ij} = \text{cov}[\hat{\theta}_i, \hat{\theta}_j]$. The goal of *error propagation* is to determine the covariance matrix for the functions, $U_{ij} = \text{cov}[\hat{\eta}_i, \hat{\eta}_j]$, where $\hat{\eta} = \eta(\hat{\theta})$. In particular, the diagonal elements $U_{ii} = V[\hat{\eta}_i]$ give the variances. The new covariance matrix can be found by expanding the functions $\eta(\theta)$ about the estimates $\hat{\theta}$ to first order in a Taylor series. Using this one finds

$$U_{ij} \approx \sum_{k,l} \left. \frac{\partial \eta_i}{\partial \theta_k} \frac{\partial \eta_j}{\partial \theta_l} \right|_{\hat{\theta}} V_{kl}. \quad (33.29)$$

This can be written in matrix notation as $U \approx A V A^T$ where the matrix of derivatives A is

$$A_{ij} = \left. \frac{\partial \eta_i}{\partial \theta_j} \right|_{\hat{\theta}}, \quad (33.30)$$

and A^T is its transpose. The approximation is exact if $\eta(\theta)$ is linear.

33.2. Statistical tests

33.2.1. Hypothesis tests : Consider an experiment whose outcome is characterized by a vector of data \mathbf{x} . A *hypothesis* is a statement about the distribution of \mathbf{x} . It could, for example, define completely the p.d.f. for the data (a simple hypothesis), or it could specify only the functional form of the p.d.f., with the values of one or more parameters left open (a composite hypothesis).

A *statistical test* is a rule that states for which values of \mathbf{x} a given hypothesis (often called the null hypothesis, H_0) should be rejected in favor of its alternative H_1 . This is done by defining a region of \mathbf{x} -space called the critical region; if the outcome of the experiment lands in this region, H_0 is rejected, otherwise it is accepted.

Rejecting H_0 if it is true is called an error of the first kind. The probability for this to occur is called the *size* or *significance level* of the test, α , which is chosen to be equal to some pre-specified value. It can also happen that H_0 is false and the true hypothesis is the alternative, H_1 . If H_0 is accepted in such a case, this is called an error of the second kind, which will have some probability β . The quantity $1 - \beta$ is called the *power* of the test relative to H_1 .

Often one tries to construct a test to maximize power for a given significance level, *i.e.*, to maximize the signal efficiency for a given significance level. The *Neyman-Pearson lemma* states that this is done by defining the acceptance region such that, for \mathbf{x} in that region, the ratio of p.d.f.s for the hypotheses H_1 (signal) and H_0 (background),

$$\lambda(\mathbf{x}) = \frac{f(\mathbf{x}|H_1)}{f(\mathbf{x}|H_0)}, \quad (33.31)$$

is greater than a given constant, the value of which is chosen to give the desired signal efficiency. Here H_0 and H_1 must be simple hypotheses, *i.e.*, they should not contain undetermined parameters. The lemma is equivalent to the statement that (33.31) represents the test statistic with which one may obtain the highest signal efficiency for a given purity for the selected sample. It can be difficult in practice, however, to determine $\lambda(\mathbf{x})$, since this requires knowledge of the joint p.d.f.s $f(\mathbf{x}|H_0)$ and $f(\mathbf{x}|H_1)$.

In the usual case where the likelihood ratio (33.31) cannot be used explicitly, there exist a variety of other multivariate classifiers that effectively separate different types of events. Methods often used in HEP include *neural networks* or *Fisher discriminants* (see [10]). Recently, further classification methods from machine-learning have been applied in HEP analyses; these include *probability density estimation (PDE)* techniques, *kernel-based PDE (KDE or Parzen window)*, *support vector machines*, and *decision trees*. Techniques such as “boosting” and “bagging” can be applied to combine a number of classifiers into a stronger one with greater stability with respect to fluctuations in the training data.

33.2.2. Significance tests : Often one wants to quantify the level of agreement between the data and a hypothesis without explicit reference to alternative hypotheses. This can be done by defining a statistic t , which is a function of the data whose value reflects in some way the level of agreement between the data and the hypothesis.

The hypothesis in question, say, H_0 , will determine the p.d.f. $g(t|H_0)$ for the statistic. The significance of a discrepancy between the data and what one expects under the assumption of H_0 is quantified by giving the p -value, defined as the probability to find t in the region of equal or lesser compatibility with H_0 than the level of compatibility observed with the

actual data. For example, if t is defined such that large values correspond to poor agreement with the hypothesis, then the p -value would be

$$p = \int_{t_{\text{obs}}}^{\infty} g(t|H_0) dt, \quad (33.32)$$

where t_{obs} is the value of the statistic obtained in the actual experiment. The p -value should not be confused with the size (significance level) of a test, or the confidence level of a confidence interval (Section 33.3), both of which are pre-specified constants.

The p -value is a function of the data, and is therefore itself a random variable. If the hypothesis used to compute the p -value is true, then for continuous data, p will be uniformly distributed between zero and one. Note that the p -value is not the probability for the hypothesis; in frequentist statistics, this is not defined. Rather, the p -value is the probability, under the assumption of a hypothesis H_0 , of obtaining data at least as incompatible with H_0 as the data actually observed.

When estimating parameters using the method of least squares, one obtains the minimum value of the quantity χ^2 (33.13). This statistic can be used to test the *goodness-of-fit*, *i.e.*, the test provides a measure of the significance of a discrepancy between the data and the hypothesized functional form used in the fit. It may also happen that no parameters are estimated from the data, but that one simply wants to compare a histogram, *e.g.*, a vector of Poisson distributed numbers $\mathbf{n} = (n_1, \dots, n_N)$, with a hypothesis for their expectation values $\nu_i = E[n_i]$. As the distribution is Poisson with variances $\sigma_i^2 = \nu_i$, the χ^2 (33.13) becomes *Pearson's χ^2 statistic*,

$$\chi^2 = \sum_{i=1}^N \frac{(n_i - \nu_i)^2}{\nu_i}. \quad (33.34)$$

If the hypothesis $\boldsymbol{\nu} = (\nu_1, \dots, \nu_N)$ is correct, and if the expected values ν_i in (33.34) are sufficiently large (in practice, this will be a good approximation if all $\nu_i > 5$), then the χ^2 statistic will follow the χ^2 p.d.f. with the number of degrees of freedom equal to the number of measurements N minus the number of fitted parameters. The minimized χ^2 from Eq. (33.13) also has this property if the measurements y_i are Gaussian.

Assuming the goodness-of-fit statistic follows a χ^2 p.d.f., the p -value for the hypothesis is then

$$p = \int_{\chi^2}^{\infty} f(z; n_d) dz, \quad (33.35)$$

where $f(z; n_d)$ is the χ^2 p.d.f. and n_d is the appropriate number of degrees of freedom. Values can be obtained from Fig. 33.1 or from the CERNLIB routine `PROB` or the ROOT function `TMath::Prob`.

Since the mean of the χ^2 distribution is equal to n_d , one expects in a "reasonable" experiment to obtain $\chi^2 \approx n_d$. Hence the quantity χ^2/n_d is sometimes reported. Since the p.d.f. of χ^2/n_d depends on n_d , however, one must report n_d as well if one wishes to determine the p -value. The p -values obtained for different values of χ^2/n_d are shown in Fig. 33.2.

33.2.3. Bayesian model selection : In Bayesian statistics, all of one's knowledge about a model is contained in its posterior probability, which one obtains using Bayes' theorem. Thus one could reject a hypothesis H if its posterior probability $P(H|\mathbf{x})$ is sufficiently small. The difficulty here is that $P(H|\mathbf{x})$ is proportional to the prior probability $P(H)$, and there

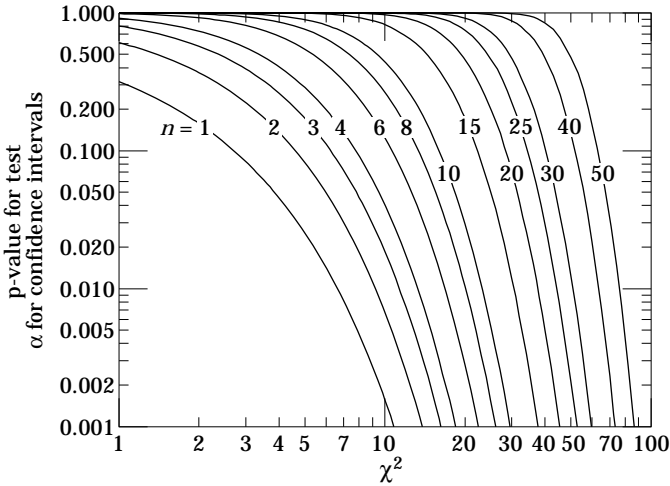


Figure 33.1: One minus the χ^2 cumulative distribution, $1 - F(\chi^2; n)$, for n degrees of freedom. This gives the p -value for the χ^2 goodness-of-fit test as well as one minus the coverage probability for confidence regions (see Sec. 33.3.2.4).

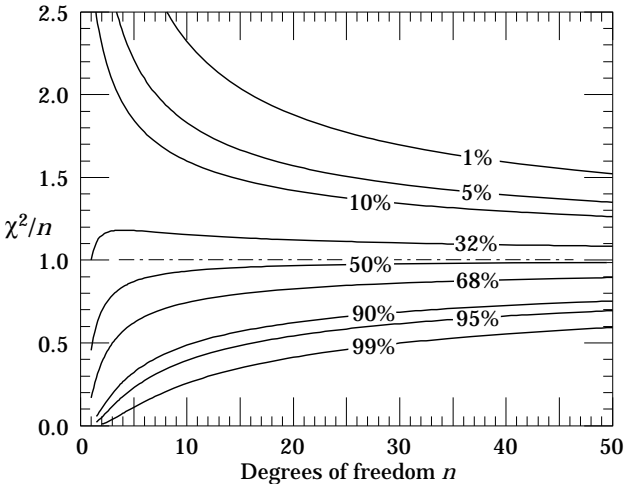


Figure 33.2: The ‘reduced’ χ^2 , equal to χ^2/n , for n degrees of freedom. The curves show as a function of n the χ^2/n that corresponds to a given p -value.

will not be a consensus about the prior probabilities for the existence of new phenomena. Nevertheless one can construct a quantity called the Bayes factor (described below), which can be used to quantify the degree to which the data prefer one hypothesis over another, and is independent of their prior probabilities.

Consider two models (hypotheses), H_i and H_j , described by vectors

of parameters θ_i and θ_j , respectively. Some of the components will be common to both models and others may be distinct. The full prior probability for each model can be written in the form

$$\pi(H_i, \theta_i) = P(H_i)\pi(\theta_i|H_i), \quad (33.36)$$

Here $P(H_i)$ is the overall prior probability for H_i , and $\pi(\theta_i|H_i)$ is the normalized p.d.f. of its parameters. For each model, the posterior probability is found using Bayes' theorem,

$$P(H_i|\mathbf{x}) = \frac{\int L(\mathbf{x}|\theta_i, H_i)P(H_i)\pi(\theta_i|H_i) d\theta_i}{P(\mathbf{x})}, \quad (33.37)$$

where the integration is carried out over the internal parameters θ_i of the model. The ratio of posterior probabilities for the models is therefore

$$\frac{P(H_i|\mathbf{x})}{P(H_j|\mathbf{x})} = \frac{\int L(\mathbf{x}|\theta_i, H_i)\pi(\theta_i|H_i) d\theta_i}{\int L(\mathbf{x}|\theta_j, H_j)\pi(\theta_j|H_j) d\theta_j} \frac{P(H_i)}{P(H_j)}. \quad (33.38)$$

The *Bayes factor* is defined as

$$B_{ij} = \frac{\int L(\mathbf{x}|\theta_i, H_i)\pi(\theta_i|H_i) d\theta_i}{\int L(\mathbf{x}|\theta_j, H_j)\pi(\theta_j|H_j) d\theta_j}. \quad (33.39)$$

This gives what the ratio of posterior probabilities for models i and j would be if the overall prior probabilities for the two models were equal. If the models have no nuisance parameters *i.e.*, no internal parameters described by priors, then the Bayes factor is simply the likelihood ratio. The Bayes factor therefore shows by how much the probability ratio of model i to model j changes in the light of the data, and thus can be viewed as a numerical measure of evidence supplied by the data in favour of one hypothesis over the other.

Although the Bayes factor is by construction independent of the overall prior probabilities $P(H_i)$ and $P(H_j)$, it does require priors for all internal parameters of a model, *i.e.*, one needs the functions $\pi(\theta_i|H_i)$ and $\pi(\theta_j|H_j)$. In a Bayesian analysis where one is only interested in the posterior p.d.f. of a parameter, it may be acceptable to take an unnormalizable function for the prior (an improper prior) as long as the product of likelihood and prior can be normalized. But improper priors are only defined up to an arbitrary multiplicative constant, which does not cancel in the ratio (33.39). Furthermore, although the range of a constant normalized prior is unimportant for parameter determination (provided it is wider than the likelihood), this is not so for the Bayes factor when such a prior is used for only one of the hypotheses. So to compute a Bayes factor, all internal parameters must be described by normalized priors that represent meaningful probabilities over the entire range where they are defined.

An exception to this rule may be considered when the identical parameter appears in the models for both numerator and denominator of the Bayes factor. In this case one can argue that the arbitrary constants would cancel. One must exercise some caution, however, as parameters with the same name and physical meaning may still play different roles in the two models. Both integrals in equation (33.39) are of the form

$$m = \int L(\mathbf{x}|\theta)\pi(\theta) d\theta, \quad (33.40)$$

which is called the *marginal likelihood* (or in some fields called the *evidence*). A review of Bayes factors including a discussion of computational issues is Ref. [26].

33.3. Intervals and limits

When the goal of an experiment is to determine a parameter θ , the result is usually expressed by quoting, in addition to the point estimate, some sort of interval which reflects the statistical precision of the

measurement. In the simplest case, this can be given by the parameter's estimated value $\hat{\theta}$ plus or minus an estimate of the standard deviation of $\hat{\theta}$, $\sigma_{\hat{\theta}}$. If, however, the p.d.f. of the estimator is not Gaussian or if there are physical boundaries on the possible values of the parameter, then one usually quotes instead an interval according to one of the procedures described below.

33.3.1. Bayesian intervals : As described in Sec. 33.1.4, a Bayesian posterior probability may be used to determine regions that will have a given probability of containing the true value of a parameter. In the single parameter case, for example, an interval (called a Bayesian or credible interval) $[\theta_{lo}, \theta_{up}]$ can be determined which contains a given fraction $1 - \alpha$ of the posterior probability, *i.e.*,

$$1 - \alpha = \int_{\theta_{lo}}^{\theta_{up}} p(\theta|\mathbf{x}) d\theta . \tag{33.41}$$

Sometimes an upper or lower limit is desired, *i.e.*, θ_{lo} can be set to zero or θ_{up} to infinity. In other cases, one might choose θ_{lo} and θ_{up} such that $p(\theta|\mathbf{x})$ is higher everywhere inside the interval than outside; these are called *highest posterior density* (HPD) intervals. Note that HPD intervals are not invariant under a nonlinear transformation of the parameter.

If a parameter is constrained to be non-negative, then the prior p.d.f. can simply be set to zero for negative values. An important example is the case of a Poisson variable n , which counts signal events with unknown mean s , as well as background with mean b , assumed known. For the signal mean s , one often uses the prior

$$\pi(s) = \begin{cases} 0 & s < 0 \\ 1 & s \geq 0 \end{cases} . \tag{33.42}$$

In the absence of a clear discovery, (*e.g.*, if $n = 0$ or if in any case n is compatible with the expected background), one usually wishes to place an upper limit on s (see, however, Sec. 33.3.2.6 on “flip-flopping” concerning frequentist coverage). Using the likelihood function for Poisson distributed n ,

$$L(n|s) = \frac{(s + b)^n}{n!} e^{-(s+b)} , \tag{33.43}$$

along with the prior (33.42) in (33.24) gives the posterior density for s . An upper limit s_{up} at confidence level (or here, rather, credibility level) $1 - \alpha$ can be obtained by requiring

$$1 - \alpha = \int_{-\infty}^{s_{up}} p(s|n) ds = \frac{\int_{-\infty}^{s_{up}} L(n|s) \pi(s) ds}{\int_{-\infty}^{\infty} L(n|s) \pi(s) ds} , \tag{33.44}$$

where the lower limit of integration is effectively zero because of the cut-off in $\pi(s)$. By relating the integrals in Eq. (33.44) to incomplete gamma functions, the equation reduces to

$$\alpha = e^{-s_{up}} \frac{\sum_{m=0}^n (s_{up} + b)^m / m!}{\sum_{m=0}^n b^m / m!} . \tag{33.45}$$

This must be solved numerically for the limit s_{up} . For the special case of $b = 0$, the sums can be related to the *quantile* $F_{\chi^2}^{-1}$ of the χ^2 distribution (inverse of the cumulative distribution) to give

$$s_{up} = \frac{1}{2} F_{\chi^2}^{-1}(1 - \alpha; n_d) , \tag{33.46}$$

where the number of degrees of freedom is $n_d = 2(n + 1)$. The quantile of the χ^2 distribution can be obtained using the CERNLIB routine `CHISIN`, or the ROOT function `TMath::ChisquareQuantile`. It so happens that for the case of $b = 0$, the upper limits from Eq. (33.46) coincide numerically

with the values of the frequentist upper limits discussed in Section 33.3.2.5. Values for $1 - \alpha = 0.9$ and 0.95 are given by the values ν_{up} in Table 33.3.

As in any Bayesian analysis, it is important to show how the result would change if one uses different prior probabilities. For example, one could consider the Jeffreys prior as described in Sec. 33.1.4. For this problem one finds the Jeffreys prior $\pi(s) \propto 1/\sqrt{s+b}$ for $s \geq 0$ and zero otherwise. As with the constant prior, one would not regard this as representing one's prior beliefs about s , both because it is improper and also as it depends on b . Rather it is used with Bayes' theorem to produce an interval whose frequentist properties can be studied.

33.3.2. Frequentist confidence intervals :

33.3.2.1. The Neyman construction for confidence intervals: Consider a p.d.f. $f(x; \theta)$ where x represents the outcome of the experiment and θ is the unknown parameter for which we want to construct a confidence interval. The variable x could (and often does) represent an estimator for θ . Using $f(x; \theta)$, we can find for a pre-specified probability $1 - \alpha$, and for every value of θ , a set of values $x_1(\theta, \alpha)$ and $x_2(\theta, \alpha)$ such that

$$P(x_1 < x < x_2; \theta) = 1 - \alpha = \int_{x_1}^{x_2} f(x; \theta) dx . \quad (33.47)$$

This is illustrated in Fig. 33.3: a horizontal line segment $[x_1(\theta, \alpha), x_2(\theta, \alpha)]$ is drawn for representative values of θ . The union of such intervals for all values of θ , designated in the figure as $D(\alpha)$, is known as the *confidence belt*. Typically the curves $x_1(\theta, \alpha)$ and $x_2(\theta, \alpha)$ are monotonic functions of θ , which we assume for this discussion.

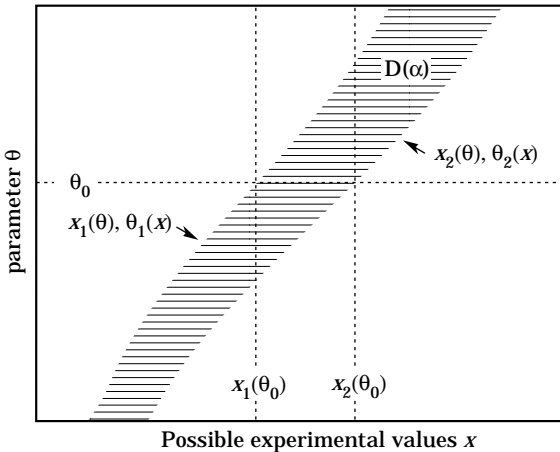


Figure 33.3: Construction of the confidence belt (see text).

Upon performing an experiment to measure x and obtaining a value x_0 , one draws a vertical line through x_0 . The confidence interval for θ is the set of all values of θ for which the corresponding line segment $[x_1(\theta, \alpha), x_2(\theta, \alpha)]$ is intercepted by this vertical line. Such confidence intervals are said to have a *confidence level* (CL) equal to $1 - \alpha$.

Now suppose that the true value of θ is θ_0 , indicated in the figure. We see from the figure that θ_0 lies between $\theta_1(x)$ and $\theta_2(x)$ if and only

if x lies between $x_1(\theta_0)$ and $x_2(\theta_0)$. The two events thus have the same probability, and since this is true for any value θ_0 , we can drop the subscript 0 and obtain

$$1 - \alpha = P(x_1(\theta) < x < x_2(\theta)) = P(\theta_2(x) < \theta < \theta_1(x)). \quad (33.48)$$

In this probability statement, $\theta_1(x)$ and $\theta_2(x)$, *i.e.*, the endpoints of the interval, are the random variables and θ is an unknown constant. If the experiment were to be repeated a large number of times, the interval $[\theta_1, \theta_2]$ would vary, covering the fixed value θ in a fraction $1 - \alpha$ of the experiments.

The condition of coverage in Eq. (33.47) does not determine x_1 and x_2 uniquely, and additional criteria are needed. The most common criterion is to choose *central intervals* such that the probabilities excluded below x_1 and above x_2 are each $\alpha/2$. In other cases, one may want to report only an upper or lower limit, in which case the probability excluded below x_1 or above x_2 can be set to zero. Another principle based on *likelihood ratio ordering* for determining which values of x should be included in the confidence belt is discussed in Sec. 33.3.2.2

When the observed random variable x is continuous, the coverage probability obtained with the Neyman construction is $1 - \alpha$, regardless of the true value of the parameter. If x is discrete, however, it is not possible to find segments $[x_1(\theta, \alpha), x_2(\theta, \alpha)]$ that satisfy Eq. (33.47) exactly for all values of θ . By convention, one constructs the confidence belt requiring the probability $P(x_1 < x < x_2)$ to be *greater than or equal to* $1 - \alpha$. This gives confidence intervals that include the true parameter with a probability greater than or equal to $1 - \alpha$.

33.3.2.4. Gaussian distributed measurements: An important example of constructing a confidence interval is when the data consists of a single random variable x that follows a Gaussian distribution; this is often the case when x represents an estimator for a parameter and one has a sufficiently large data sample. If there is more than one parameter being estimated, the multivariate Gaussian is used. For the univariate case with known σ ,

$$1 - \alpha = \frac{1}{\sqrt{2\pi}\sigma} \int_{\mu-\delta}^{\mu+\delta} e^{-(x-\mu)^2/2\sigma^2} dx = \operatorname{erf} \left(\frac{\delta}{\sqrt{2}\sigma} \right) \quad (33.53)$$

is the probability that the measured value x will fall within $\pm\delta$ of the true value μ . From the symmetry of the Gaussian with respect to x and μ , this is also the probability for the interval $x \pm \delta$ to include μ . Fig. 33.4 shows a $\delta = 1.64\sigma$ confidence interval unshaded. The choice $\delta = \sigma$ gives an interval called the *standard error* which has $1 - \alpha = 68.27\%$ if σ is known. Values of α for other frequently used choices of δ are given in Table 33.1.

Table 33.1: Area of the tails α outside $\pm\delta$ from the mean of a Gaussian distribution.

α	δ	α	δ
0.3173	1σ	0.2	1.28σ
4.55×10^{-2}	2σ	0.1	1.64σ
2.7×10^{-3}	3σ	0.05	1.96σ
6.3×10^{-5}	4σ	0.01	2.58σ
5.7×10^{-7}	5σ	0.001	3.29σ
2.0×10^{-9}	6σ	10^{-4}	3.89σ

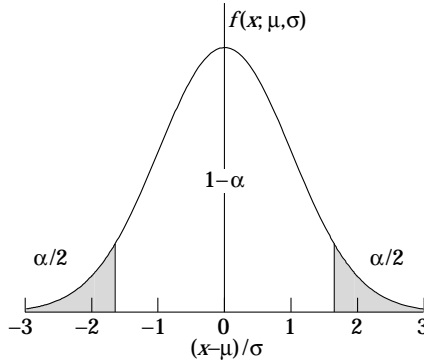


Figure 33.4: Illustration of a symmetric 90% confidence interval (unshaded) for a measurement of a single quantity with Gaussian errors. Integrated probabilities, defined by α , are as shown.

We can set a one-sided (upper or lower) limit by excluding above $x + \delta$ (or below $x - \delta$). The values of α for such limits are half the values in Table 33.1.

The relation (33.53) can be re-expressed using the cumulative distribution function for the χ^2 distribution as

$$\alpha = 1 - F(\chi^2; n), \quad (33.54)$$

for $\chi^2 = (\delta/\sigma)^2$ and $n = 1$ degree of freedom. This can be obtained from Fig. 33.1 on the $n = 1$ curve or by using the CERNLIB routine `PROB` or the ROOT function `TMath::Prob`.

For multivariate measurements of, say, n parameter estimates $\hat{\boldsymbol{\theta}} = (\hat{\theta}_1, \dots, \hat{\theta}_n)$, one requires the full covariance matrix $V_{ij} = \text{cov}[\hat{\theta}_i, \hat{\theta}_j]$, which can be estimated as described in Sections 33.1.2 and 33.1.3. Under fairly general conditions with the methods of maximum-likelihood or least-squares in the large sample limit, the estimators will be distributed according to a multivariate Gaussian centered about the true (unknown) values $\boldsymbol{\theta}$, and furthermore, the likelihood function itself takes on a Gaussian shape.

The standard error ellipse for the pair $(\hat{\theta}_i, \hat{\theta}_j)$ is shown in Fig. 33.5, corresponding to a contour $\chi^2 = \chi_{\min}^2 + 1$ or $\ln L = \ln L_{\max} - 1/2$. The ellipse is centered about the estimated values $\hat{\boldsymbol{\theta}}$, and the tangents to the ellipse give the standard deviations of the estimators, σ_i and σ_j . The angle of the major axis of the ellipse is given by

$$\tan 2\phi = \frac{2\rho_{ij}\sigma_i\sigma_j}{\sigma_j^2 - \sigma_i^2}, \quad (33.55)$$

where $\rho_{ij} = \text{cov}[\hat{\theta}_i, \hat{\theta}_j]/\sigma_i\sigma_j$ is the correlation coefficient.

The correlation coefficient can be visualized as the fraction of the distance σ_i from the ellipse's horizontal centerline at which the ellipse becomes tangent to vertical, *i.e.*, at the distance $\rho_{ij}\sigma_i$ below the centerline as shown. As ρ_{ij} goes to $+1$ or -1 , the ellipse thins to a diagonal line.

As in the single-variable case, because of the symmetry of the Gaussian function between $\boldsymbol{\theta}$ and $\hat{\boldsymbol{\theta}}$, one finds that contours of constant $\ln L$ or χ^2 cover the true values with a certain, fixed probability. That is, the

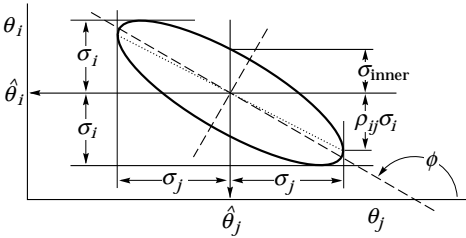


Figure 33.5: Standard error ellipse for the estimators $\hat{\theta}_i$ and $\hat{\theta}_j$. In this case the correlation is negative.

Table 33.2: $\Delta\chi^2$ or $2\Delta \ln L$ corresponding to a coverage probability $1 - \alpha$ in the large data sample limit, for joint estimation of m parameters.

$(1 - \alpha)$ (%)	$m = 1$	$m = 2$	$m = 3$
68.27	1.00	2.30	3.53
90.	2.71	4.61	6.25
95.	3.84	5.99	7.82
95.45	4.00	6.18	8.03
99.	6.63	9.21	11.34
99.73	9.00	11.83	14.16

confidence region is determined by

$$\ln L(\boldsymbol{\theta}) \geq \ln L_{\max} - \Delta \ln L, \tag{33.56}$$

or where a χ^2 has been defined for use with the method of least-squares,

$$\chi^2(\boldsymbol{\theta}) \leq \chi_{\min}^2 + \Delta\chi^2. \tag{33.57}$$

Values of $\Delta\chi^2$ or $2\Delta \ln L$ are given in Table 33.2 for several values of the coverage probability and number of fitted parameters.

For finite data samples, the probability for the regions determined by equations (33.56) or (33.57) to cover the true value of $\boldsymbol{\theta}$ will depend on $\boldsymbol{\theta}$, so these are not exact confidence regions according to our previous definition.

33.3.2.5. Poisson or binomial data: Another important class of measurements consists of counting a certain number of events, n . In this section, we will assume these are all events of the desired type, *i.e.*, there is no background. If n represents the number of events produced in a reaction with cross section σ , say, in a fixed integrated luminosity \mathcal{L} , then it follows a Poisson distribution with mean $\nu = \sigma\mathcal{L}$. If, on the other hand, one has selected a larger sample of N events and found n of them to have a particular property, then n follows a binomial distribution where the parameter p gives the probability for the event to possess the property in question. This is appropriate, *e.g.*, for estimates of branching ratios or selection efficiencies based on a given total number of events.

For the case of Poisson distributed n , the upper and lower limits on the mean value ν can be found from the Neyman procedure to be

$$\nu_{1\alpha} = \frac{1}{2}F_{\chi^2}^{-1}(\alpha_{1\alpha}; 2n), \tag{33.59a}$$

$$\nu_{\text{up}} = \frac{1}{2} F_{\chi^2}^{-1}(1 - \alpha_{\text{up}}; 2(n+1)), \quad (33.59b)$$

where the upper and lower limits are at confidence levels of $1 - \alpha_{\text{lo}}$ and $1 - \alpha_{\text{up}}$, respectively, and $F_{\chi^2}^{-1}$ is the *quantile* of the χ^2 distribution (inverse of the cumulative distribution). The quantiles $F_{\chi^2}^{-1}$ can be obtained from standard tables or from the CERNLIB routine CHISIN. For central confidence intervals at confidence level $1 - \alpha$, set $\alpha_{\text{lo}} = \alpha_{\text{up}} = \alpha/2$.

Table 33.3: Lower and upper (one-sided) limits for the mean ν of a Poisson variable given n observed events in the absence of background, for confidence levels of 90% and 95%.

n	$1 - \alpha = 90\%$		$1 - \alpha = 95\%$	
	ν_{lo}	ν_{up}	ν_{lo}	ν_{up}
0	–	2.30	–	3.00
1	0.105	3.89	0.051	4.74
2	0.532	5.32	0.355	6.30
3	1.10	6.68	0.818	7.75
4	1.74	7.99	1.37	9.15
5	2.43	9.27	1.97	10.51
6	3.15	10.53	2.61	11.84
7	3.89	11.77	3.29	13.15
8	4.66	12.99	3.98	14.43
9	5.43	14.21	4.70	15.71
10	6.22	15.41	5.43	16.96

It happens that the upper limit from Eq. (33.59a) coincides numerically with the Bayesian upper limit for a Poisson parameter, using a uniform prior p.d.f. for ν . Values for confidence levels of 90% and 95% are shown in Table 33.3. For the case of binomially distributed n successes out of N trials with probability of success p , the upper and lower limits on p are found to be

$$p_{\text{lo}} = \frac{n F_F^{-1}[\alpha_{\text{lo}}; 2n, 2(N-n+1)]}{N-n+1 + n F_F^{-1}[\alpha_{\text{lo}}; 2n, 2(N-n+1)]}, \quad (33.60a)$$

$$p_{\text{up}} = \frac{(n+1) F_F^{-1}[1 - \alpha_{\text{up}}; 2(n+1), 2(N-n)]}{(N-n) + (n+1) F_F^{-1}[1 - \alpha_{\text{up}}; 2(n+1), 2(N-n)]}. \quad (33.60b)$$

Here F_F^{-1} is the quantile of the F distribution (also called the Fisher–Snedecor distribution; see [4]).

33.3.2.6. Difficulties with intervals near a boundary:

A number of issues arise in the construction and interpretation of confidence intervals when the parameter can only take on values in a restricted range. Important examples are where the mean of a Gaussian variable is constrained on physical grounds to be non-negative and where the experiment finds a Poisson-distributed number of events, n , which includes both signal and background. Application of some standard recipes can lead to intervals that are partially or entirely in the unphysical region. Furthermore, if the decision whether to report a one- or two-sided interval

is based on the data, then the resulting intervals will not in general cover the parameter with the stated probability $1 - \alpha$.

Several problems with such intervals are overcome by using the unified approach of Feldman and Cousins [27]. Properties of these intervals are described further in the *Review*. Table 33.4 gives the unified confidence intervals $[\nu_1, \nu_2]$ for the mean of a Poisson variable given n observed events in the absence of background, for confidence levels of 90% and 95%. The values of $1 - \alpha$ given here refer to the coverage of the true parameter by the whole interval $[\nu_1, \nu_2]$. In Table 33.3 for the one-sided upper and lower limits, however, $1 - \alpha$ referred to the probability to have individually $\nu_{\text{up}} \geq \nu$ or $\nu_{\text{lo}} \leq \nu$.

Table 33.4: Unified confidence intervals $[\nu_1, \nu_2]$ for a the mean of a Poisson variable given n observed events in the absence of background, for confidence levels of 90% and 95%.

n	$1 - \alpha = 90\%$		$1 - \alpha = 95\%$	
	ν_1	ν_2	ν_1	ν_2
0	0.00	2.44	0.00	3.09
1	0.11	4.36	0.05	5.14
2	0.53	5.91	0.36	6.72
3	1.10	7.42	0.82	8.25
4	1.47	8.60	1.37	9.76
5	1.84	9.99	1.84	11.26
6	2.21	11.47	2.21	12.75
7	3.56	12.53	2.58	13.81
8	3.96	13.99	2.94	15.29
9	4.36	15.30	4.36	16.77
10	5.50	16.50	4.75	17.82

Another possibility is to construct a Bayesian interval as described in Section 33.3.1. The presence of the boundary can be incorporated simply by setting the prior density to zero in the unphysical region. Advantages and pitfalls of this approach are discussed further in the *Review*.

Another alternative is presented by the intervals found from the likelihood function or χ^2 using the prescription of Equations (33.56) or (33.57). As in the case of the Bayesian intervals, the coverage probability is not, in general, independent of the true parameter. Furthermore, these intervals can for some parameter values undercover.

In any case it is important to report sufficient information so that the result can be combined with other measurements. Often this means giving an unbiased estimator and its standard deviation, even if the estimated value is in the unphysical region. It is also useful to report the likelihood function or an appropriate summary of it. Although this by itself is not sufficient to construct a frequentist confidence interval, it can be used to find the Bayesian posterior probability density for any desired prior p.d.f.

Further discussion and all references may be found in the full *Review of Particle Physics*; the equation and reference numbering corresponds to that version.

40. KINEMATICS

Revised January 2000 by J.D. Jackson (LBNL) and June 2008 by D.R. Tovey (Sheffield).

Throughout this section units are used in which $\hbar = c = 1$. The following conversions are useful: $\hbar c = 197.3 \text{ MeV fm}$, $(\hbar c)^2 = 0.3894 \text{ (GeV)}^2 \text{ mb}$.

40.1. Lorentz transformations

The energy E and 3-momentum \mathbf{p} of a particle of mass m form a 4-vector $p = (E, \mathbf{p})$ whose square $p^2 \equiv E^2 - |\mathbf{p}|^2 = m^2$. The velocity of the particle is $\boldsymbol{\beta} = \mathbf{p}/E$. The energy and momentum (E^*, \mathbf{p}^*) viewed from a frame moving with velocity $\boldsymbol{\beta}_f$ are given by

$$\begin{pmatrix} E^* \\ p_{\parallel}^* \end{pmatrix} = \begin{pmatrix} \gamma_f & -\gamma_f \beta_f \\ -\gamma_f \beta_f & \gamma_f \end{pmatrix} \begin{pmatrix} E \\ p_{\parallel} \end{pmatrix}, \quad p_T^* = p_T, \quad (40.1)$$

where $\gamma_f = (1 - \beta_f^2)^{-1/2}$ and p_T (p_{\parallel}) are the components of \mathbf{p} perpendicular (parallel) to $\boldsymbol{\beta}_f$. Other 4-vectors, such as the space-time coordinates of events, of course transform in the same way. The scalar product of two 4-momenta $p_1 \cdot p_2 = E_1 E_2 - \mathbf{p}_1 \cdot \mathbf{p}_2$ is invariant (frame independent).

40.2. Center-of-mass energy and momentum

In the collision of two particles of masses m_1 and m_2 the total center-of-mass energy can be expressed in the Lorentz-invariant form

$$\begin{aligned} E_{\text{cm}} &= \left[(E_1 + E_2)^2 - (\mathbf{p}_1 + \mathbf{p}_2)^2 \right]^{1/2}, \\ &= \left[m_1^2 + m_2^2 + 2E_1 E_2 (1 - \beta_1 \beta_2 \cos \theta) \right]^{1/2}, \end{aligned} \quad (40.2)$$

where θ is the angle between the particles. In the frame where one particle (of mass m_2) is at rest (lab frame),

$$E_{\text{cm}} = (m_1^2 + m_2^2 + 2E_{1 \text{lab}} m_2)^{1/2}. \quad (40.3)$$

The velocity of the center-of-mass in the lab frame is

$$\boldsymbol{\beta}_{\text{cm}} = \mathbf{p}_{\text{lab}} / (E_{1 \text{lab}} + m_2), \quad (40.4)$$

where $\mathbf{p}_{\text{lab}} \equiv \mathbf{p}_{1 \text{lab}}$ and

$$\gamma_{\text{cm}} = (E_{1 \text{lab}} + m_2) / E_{\text{cm}}. \quad (40.5)$$

The c.m. momenta of particles 1 and 2 are of magnitude

$$p_{\text{cm}} = p_{\text{lab}} \frac{m_2}{E_{\text{cm}}}. \quad (40.6)$$

For example, if a 0.80 GeV/c kaon beam is incident on a proton target, the center of mass energy is 1.699 GeV and the center of mass momentum of either particle is 0.442 GeV/c. It is also useful to note that

$$E_{\text{cm}} dE_{\text{cm}} = m_2 dE_{1 \text{lab}} = m_2 \beta_{1 \text{lab}} dp_{\text{lab}}. \quad (40.7)$$

40.3. Lorentz-invariant amplitudes

The matrix elements for a scattering or decay process are written in terms of an invariant amplitude $-i\mathcal{M}$. As an example, the S -matrix for $2 \rightarrow 2$ scattering is related to \mathcal{M} by

$$\begin{aligned} \langle p'_1 p'_2 | S | p_1 p_2 \rangle &= I - i(2\pi)^4 \delta^4(p_1 + p_2 - p'_1 - p'_2) \\ &\times \frac{\mathcal{M}(p_1, p_2; p'_1, p'_2)}{(2E_1)^{1/2} (2E_2)^{1/2} (2E'_1)^{1/2} (2E'_2)^{1/2}}. \end{aligned} \quad (40.8)$$

The state normalization is such that

$$\langle p' | p \rangle = (2\pi)^3 \delta^3(\mathbf{p} - \mathbf{p}') . \quad (40.9)$$

40.4. Particle decays

The partial decay rate of a particle of mass M into n bodies in its rest frame is given in terms of the Lorentz-invariant matrix element \mathcal{M} by

$$d\Gamma = \frac{(2\pi)^4}{2M} |\mathcal{M}|^2 d\Phi_n(P; p_1, \dots, p_n), \quad (40.10)$$

where $d\Phi_n$ is an element of n -body phase space given by

$$d\Phi_n(P; p_1, \dots, p_n) = \delta^4(P - \sum_{i=1}^n p_i) \prod_{i=1}^n \frac{d^3 p_i}{(2\pi)^3 2E_i} . \quad (40.11)$$

This phase space can be generated recursively, viz.

$$\begin{aligned} d\Phi_n(P; p_1, \dots, p_n) &= d\Phi_j(q; p_1, \dots, p_j) \\ &\times d\Phi_{n-j+1}(P; q, p_{j+1}, \dots, p_n) (2\pi)^3 dq^2 , \end{aligned} \quad (40.12)$$

where $q^2 = (\sum_{i=1}^j E_i)^2 - |\sum_{i=1}^j \mathbf{p}_i|^2$. This form is particularly useful in the case where a particle decays into another particle that subsequently decays.

40.4.1. Survival probability: If a particle of mass M has mean proper lifetime τ ($= 1/\Gamma$) and has momentum (E, \mathbf{p}) , then the probability that it lives for a time t_0 or greater before decaying is given by

$$P(t_0) = e^{-t_0 \Gamma/\gamma} = e^{-Mt_0 \Gamma/E} , \quad (40.13)$$

and the probability that it travels a distance x_0 or greater is

$$P(x_0) = e^{-Mx_0 \Gamma/|\mathbf{p}|} . \quad (40.14)$$

40.4.2. Two-body decays:

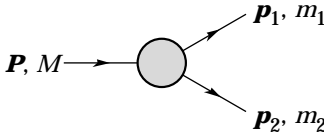


Figure 40.1: Definitions of variables for two-body decays.

In the rest frame of a particle of mass M , decaying into 2 particles labeled 1 and 2,

$$E_1 = \frac{M^2 - m_2^2 + m_1^2}{2M} , \quad (40.15)$$

$$\begin{aligned} |\mathbf{p}_1| &= |\mathbf{p}_2| \\ &= \frac{[(M^2 - (m_1 + m_2)^2)(M^2 - (m_1 - m_2)^2)]^{1/2}}{2M} , \end{aligned} \quad (40.16)$$

and

$$d\Gamma = \frac{1}{32\pi^2} |\mathcal{M}|^2 \frac{|\mathbf{p}_1|}{M^2} d\Omega , \quad (40.17)$$

where $d\Omega = d\phi_1 d(\cos\theta_1)$ is the solid angle of particle 1. The invariant mass M can be determined from the energies and momenta using Eq. (40.2) with $M = E_{\text{cm}}$.

40.4.3. Three-body decays :

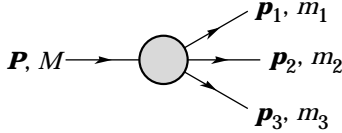


Figure 40.2: Definitions of variables for three-body decays.

Defining $p_{ij} = p_i + p_j$ and $m_{ij}^2 = p_{ij}^2$, then $m_{12}^2 + m_{23}^2 + m_{13}^2 = M^2 + m_1^2 + m_2^2 + m_3^2$ and $m_{12}^2 = (P - p_3)^2 = M^2 + m_3^2 - 2ME_3$, where E_3 is the energy of particle 3 in the rest frame of M . In that frame, the momenta of the three decay particles lie in a plane. The relative orientation of these three momenta is fixed if their energies are known. The momenta can therefore be specified in space by giving three Euler angles (α, β, γ) that specify the orientation of the final system relative to the initial particle [1]. Then

$$d\Gamma = \frac{1}{(2\pi)^5} \frac{1}{16M} |\mathcal{M}|^2 dE_1 dE_2 d\alpha d(\cos\beta) d\gamma. \quad (40.18)$$

Alternatively

$$d\Gamma = \frac{1}{(2\pi)^5} \frac{1}{16M^2} |\mathcal{M}|^2 |\mathbf{p}_1^*| |\mathbf{p}_3| dm_{12} d\Omega_1^* d\Omega_3, \quad (40.19)$$

where $(|\mathbf{p}_1^*|, \Omega_1^*)$ is the momentum of particle 1 in the rest frame of 1 and 2, and Ω_3 is the angle of particle 3 in the rest frame of the decaying particle. $|\mathbf{p}_1^*|$ and $|\mathbf{p}_3|$ are given by

$$|\mathbf{p}_1^*| = \frac{[(m_{12}^2 - (m_1 + m_2)^2)(m_{12}^2 - (m_1 - m_2)^2)]^{1/2}}{2m_{12}}, \quad (40.20a)$$

and

$$|\mathbf{p}_3| = \frac{[(M^2 - (m_{12} + m_3)^2)(M^2 - (m_{12} - m_3)^2)]^{1/2}}{2M}. \quad (40.20b)$$

[Compare with Eq. (40.16).]

If the decaying particle is a scalar or we average over its spin states, then integration over the angles in Eq. (40.18) gives

$$\begin{aligned} d\Gamma &= \frac{1}{(2\pi)^3} \frac{1}{8M} \overline{|\mathcal{M}|^2} dE_1 dE_2 \\ &= \frac{1}{(2\pi)^3} \frac{1}{32M^3} \overline{|\mathcal{M}|^2} dm_{12}^2 dm_{23}^2. \end{aligned} \quad (40.21)$$

This is the standard form for the Dalitz plot.

40.4.3.1. Dalitz plot: For a given value of m_{12}^2 , the range of m_{23}^2 is determined by its values when \mathbf{p}_2 is parallel or antiparallel to \mathbf{p}_3 :

$$(m_{23}^2)_{\max} = (E_2^* + E_3^*)^2 - \left(\sqrt{E_2^{*2} - m_2^2} - \sqrt{E_3^{*2} - m_3^2} \right)^2, \quad (40.22a)$$

$$(m_{23}^2)_{\min} = (E_2^* + E_3^*)^2 - \left(\sqrt{E_2^{*2} - m_2^2} + \sqrt{E_3^{*2} - m_3^2} \right)^2. \quad (40.22b)$$

Here $E_2^* = (m_{12}^2 - m_1^2 + m_2^2)/2m_{12}$ and $E_3^* = (M^2 - m_{12}^2 - m_3^2)/2m_{12}$ are the energies of particles 2 and 3 in the m_{12} rest frame. The scatter plot in m_{12}^2 and m_{23}^2 is called a Dalitz plot. If $|\mathcal{M}|^2$ is constant, the allowed region of the plot will be uniformly populated with events [see Eq. (40.21)]. A nonuniformity in the plot gives immediate information on $|\mathcal{M}|^2$. For example, in the case of $D \rightarrow K\pi\pi$, bands appear when $m_{(K\pi)} = m_{K^*(892)}$, reflecting the appearance of the decay chain $D \rightarrow K^*(892)\pi \rightarrow K\pi\pi$.

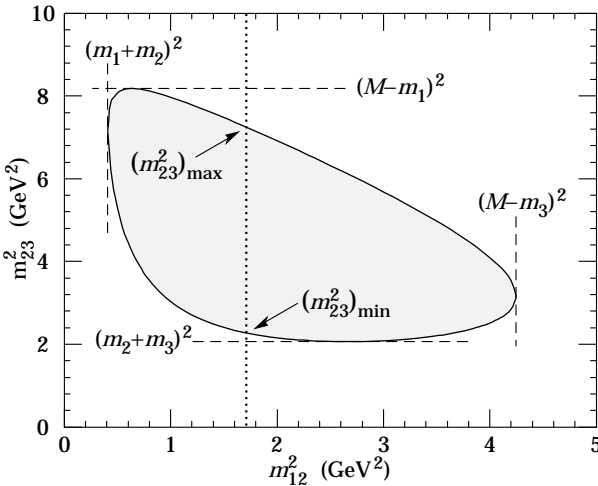


Figure 40.3: Dalitz plot for a three-body final state. In this example, the state is $\pi^+ \bar{K}^0 p$ at 3 GeV. Four-momentum conservation restricts events to the shaded region.

40.4.4. Kinematic limits :

40.4.4.1. Three-body decays: In a three-body decay (Fig. 40.2) the maximum of $|\mathbf{p}_3|$, [given by Eq. (40.20)], is achieved when $m_{12} = m_1 + m_2$, *i.e.*, particles 1 and 2 have the same vector velocity in the rest frame of the decaying particle. If, in addition, $m_3 > m_1, m_2$, then $|\mathbf{p}_3|_{\max} > |\mathbf{p}_1|_{\max}, |\mathbf{p}_2|_{\max}$. The distribution of m_{12} values possesses an end-point or maximum value at $m_{12} = M - m_3$. This can be used to constrain the mass difference of a parent particle and one invisible decay product.

40.4.5. Multibody decays : The above results may be generalized to final states containing any number of particles by combining some of the particles into “effective particles” and treating the final states as 2 or 3 “effective particle” states. Thus, if $p_{ijk\dots} = p_i + p_j + p_k + \dots$, then

$$m_{ijk\dots} = \sqrt{p_{ijk\dots}^2}, \quad (40.25)$$

and $m_{ijk\dots}$ may be used in place of *e.g.*, m_{12} in the relations in Sec. 40.4.3 or Sec. 40.4.4 above.

40.5. Cross sections

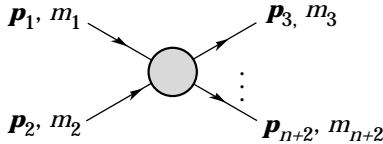


Figure 40.5: Definitions of variables for production of an n -body final state.

The differential cross section is given by

$$d\sigma = \frac{(2\pi)^4 |\mathcal{M}|^2}{4\sqrt{(p_1 \cdot p_2)^2 - m_1^2 m_2^2}} \times d\Phi_n(p_1 + p_2; p_3, \dots, p_{n+2}). \quad (40.26)$$

[See Eq. (40.11).] In the rest frame of $m_2(\text{lab})$,

$$\sqrt{(p_1 \cdot p_2)^2 - m_1^2 m_2^2} = m_2 p_{1\text{lab}}; \quad (40.27a)$$

while in the center-of-mass frame

$$\sqrt{(p_1 \cdot p_2)^2 - m_1^2 m_2^2} = p_{1\text{cm}} \sqrt{s}. \quad (40.27b)$$

40.5.1. Two-body reactions :

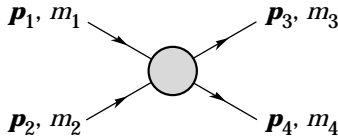


Figure 40.6: Definitions of variables for a two-body final state.

Two particles of momenta p_1 and p_2 and masses m_1 and m_2 scatter to particles of momenta p_3 and p_4 and masses m_3 and m_4 ; the Lorentz-invariant Mandelstam variables are defined by

$$s = (p_1 + p_2)^2 = (p_3 + p_4)^2 = m_1^2 + 2E_1 E_2 - 2\mathbf{p}_1 \cdot \mathbf{p}_2 + m_2^2, \quad (40.28)$$

$$t = (p_1 - p_3)^2 = (p_2 - p_4)^2 = m_1^2 - 2E_1 E_3 + 2\mathbf{p}_1 \cdot \mathbf{p}_3 + m_3^2, \quad (40.29)$$

$$\begin{aligned} u &= (p_1 - p_4)^2 = (p_2 - p_3)^2 \\ &= m_1^2 - 2E_1 E_4 + 2\mathbf{p}_1 \cdot \mathbf{p}_4 + m_4^2, \end{aligned} \quad (40.30)$$

and they satisfy

$$s + t + u = m_1^2 + m_2^2 + m_3^2 + m_4^2. \quad (40.31)$$

The two-body cross section may be written as

$$\frac{d\sigma}{dt} = \frac{1}{64\pi s} \frac{1}{|\mathbf{p}_{1\text{cm}}|^2} |\mathcal{M}|^2. \quad (40.32)$$

In the center-of-mass frame

$$\begin{aligned} t &= (E_{1\text{cm}} - E_{3\text{cm}})^2 - (p_{1\text{cm}} - p_{3\text{cm}})^2 - 4p_{1\text{cm}} p_{3\text{cm}} \sin^2(\theta_{\text{cm}}/2) \\ &= t_0 - 4p_{1\text{cm}} p_{3\text{cm}} \sin^2(\theta_{\text{cm}}/2), \end{aligned} \quad (40.33)$$

where θ_{cm} is the angle between particle 1 and 3. The limiting values t_0 ($\theta_{\text{cm}} = 0$) and t_1 ($\theta_{\text{cm}} = \pi$) for $2 \rightarrow 2$ scattering are

$$t_0(t_1) = \left[\frac{m_1^2 - m_3^2 - m_2^2 + m_4^2}{2\sqrt{s}} \right]^2 - (p_{1\text{cm}} \mp p_{3\text{cm}})^2. \quad (40.34)$$

In the literature the notation t_{\min} (t_{\max}) for t_0 (t_1) is sometimes used, which should be discouraged since $t_0 > t_1$. The center-of-mass energies and momenta of the incoming particles are

$$E_{1\text{cm}} = \frac{s + m_1^2 - m_2^2}{2\sqrt{s}}, \quad E_{2\text{cm}} = \frac{s + m_2^2 - m_1^2}{2\sqrt{s}}, \quad (40.35)$$

For $E_{3\text{cm}}$ and $E_{4\text{cm}}$, change m_1 to m_3 and m_2 to m_4 . Then

$$p_{i\text{cm}} = \sqrt{E_{i\text{cm}}^2 - m_i^2} \quad \text{and} \quad p_{1\text{cm}} = \frac{p_{1\text{lab}} m_2}{\sqrt{s}}. \quad (40.36)$$

Here the subscript lab refers to the frame where particle 2 is at rest. [For other relations see Eqs. (40.2)–(40.4).]

40.5.2. Inclusive reactions : Choose some direction (usually the beam direction) for the z -axis; then the energy and momentum of a particle can be written as

$$E = m_T \cosh y, \quad p_x, p_y, p_z = m_T \sinh y, \quad (40.37)$$

where m_T , conventionally called the ‘transverse mass’, is given by

$$m_T^2 = m^2 + p_x^2 + p_y^2. \quad (40.38)$$

and the rapidity y is defined by

$$\begin{aligned} y &= \frac{1}{2} \ln \left(\frac{E + p_z}{E - p_z} \right) \\ &= \ln \left(\frac{E + p_z}{m_T} \right) = \tanh^{-1} \left(\frac{p_z}{E} \right). \end{aligned} \quad (40.39)$$

Note that the definition of the transverse mass in Eq. (40.38) differs from that used by experimentalists at hadron colliders (see Sec. 40.6.1 below). Under a boost in the z -direction to a frame with velocity β , $y \rightarrow y - \tanh^{-1} \beta$. Hence the shape of the rapidity distribution dN/dy is invariant, as are differences in rapidity. The invariant cross section may

also be rewritten

$$E \frac{d^3\sigma}{d^3p} = \frac{d^3\sigma}{d\phi dy p_T dp_T} \implies \frac{d^2\sigma}{\pi dy d(p_T^2)}. \quad (40.40)$$

The second form is obtained using the identity $dy/dp_z = 1/E$, and the third form represents the average over ϕ .

Feynman's x variable is given by

$$x = \frac{p_z}{p_{z \max}} \approx \frac{E + p_z}{(E + p_z)_{\max}} \quad (p_T \ll |p_z|). \quad (40.41)$$

In the c.m. frame,

$$x \approx \frac{2p_{z \text{ cm}}}{\sqrt{s}} = \frac{2m_T \sinh y_{\text{cm}}}{\sqrt{s}} \quad (40.42)$$

and

$$= (y_{\text{cm}})_{\max} = \ln(\sqrt{s}/m). \quad (40.43)$$

The invariant mass M of the two-particle system described in Sec. 40.4.2 can be written in terms of these variables as

$$M^2 = m_1^2 + m_2^2 + 2[E_T(1)E_T(2) \cosh \Delta y - \mathbf{p}_T(1) \cdot \mathbf{p}_T(2)], \quad (40.44)$$

where

$$E_T(i) = \sqrt{|\mathbf{p}_T(i)|^2 + m_i^2}, \quad (40.45)$$

and $\mathbf{p}_T(i)$ denotes the transverse momentum vector of particle i .

For $p \gg m$, the rapidity [Eq. (40.39)] may be expanded to obtain

$$y = \frac{1}{2} \ln \frac{\cos^2(\theta/2) + m^2/4p^2 + \dots}{\sin^2(\theta/2) + m^2/4p^2 + \dots} \\ \approx -\ln \tan(\theta/2) \equiv \eta \quad (40.46)$$

where $\cos \theta = p_z/p$. The pseudorapidity η defined by the second line is approximately equal to the rapidity y for $p \gg m$ and $\theta \gg 1/\gamma$, and in any case can be measured when the mass and momentum of the particle are unknown. From the definition one can obtain the identities

$$\sinh \eta = \cot \theta, \quad \cosh \eta = 1/\sin \theta, \quad \tanh \eta = \cos \theta. \quad (40.47)$$

40.5.3. Partial waves: The amplitude in the center of mass for elastic scattering of spinless particles may be expanded in Legendre polynomials

$$f(k, \theta) = \frac{1}{k} \sum_{\ell} (2\ell + 1) a_{\ell} P_{\ell}(\cos \theta), \quad (40.48)$$

where k is the c.m. momentum, θ is the c.m. scattering angle, $a_{\ell} = (\eta_{\ell} e^{2i\delta_{\ell}} - 1)/2i$, $0 \leq \eta_{\ell} \leq 1$, and δ_{ℓ} is the phase shift of the ℓ^{th} partial wave. For purely elastic scattering, $\eta_{\ell} = 1$. The differential cross section is

$$\frac{d\sigma}{d\Omega} = |f(k, \theta)|^2. \quad (40.49)$$

The optical theorem states that

$$\sigma_{\text{tot}} = \frac{4\pi}{k} \text{Im} f(k, 0), \quad (40.50)$$

and the cross section in the ℓ^{th} partial wave is therefore bounded:

$$\sigma_{\ell} = \frac{4\pi}{k^2} (2\ell + 1) |a_{\ell}|^2 \leq \frac{4\pi(2\ell + 1)}{k^2}. \quad (40.51)$$

40.5.3.1. Resonances: The Breit-Wigner (nonrelativistic) form for an elastic amplitude a_ℓ with a resonance at c.m. energy E_R , elastic width Γ_{el} , and total width Γ_{tot} is

$$a_\ell = \frac{\Gamma_{\text{el}}/2}{E_R - E - i\Gamma_{\text{tot}}/2}, \quad (40.54)$$

where E is the c.m. energy.

The spin-averaged Breit-Wigner cross section for a spin- J resonance produced in the collision of particles of spin S_1 and S_2 is

$$\sigma_{BW}(E) = \frac{(2J+1)}{(2S_1+1)(2S_2+1)} \frac{\pi}{k^2} \frac{B_{\text{in}}B_{\text{out}}\Gamma_{\text{tot}}^2}{(E-E_R)^2 + \Gamma_{\text{tot}}^2/4}, \quad (40.55)$$

where k is the c.m. momentum, E is the c.m. energy, and B_{in} and B_{out} are the branching fractions of the resonance into the entrance and exit channels. The $2S+1$ factors are the multiplicities of the incident spin states, and are replaced by 2 for photons. This expression is valid only for an isolated state. If the width is not small, Γ_{tot} cannot be treated as a constant independent of E . There are many other forms for σ_{BW} , all of which are equivalent to the one given here in the narrow-width case. Some of these forms may be more appropriate if the resonance is broad.

The relativistic Breit-Wigner form corresponding to Eq. (40.54) is:

$$a_\ell = \frac{-m\Gamma_{\text{el}}}{s - m^2 + im\Gamma_{\text{tot}}}. \quad (40.56)$$

A better form incorporates the known kinematic dependences, replacing $m\Gamma_{\text{tot}}$ by $\sqrt{s}\Gamma_{\text{tot}}(s)$, where $\Gamma_{\text{tot}}(s)$ is the width the resonance particle would have if its mass were \sqrt{s} , and correspondingly $m\Gamma_{\text{el}}$ by $\sqrt{s}\Gamma_{\text{el}}(s)$ where $\Gamma_{\text{el}}(s)$ is the partial width in the incident channel for a mass \sqrt{s} :

$$a_\ell = \frac{-\sqrt{s}\Gamma_{\text{el}}(s)}{s - m^2 + i\sqrt{s}\Gamma_{\text{tot}}(s)}. \quad (40.57)$$

For the Z boson, all the decays are to particles whose masses are small enough to be ignored, so on dimensional grounds $\Gamma_{\text{tot}}(s) = \sqrt{s}\Gamma_0/m_Z$, where Γ_0 defines the width of the Z , and $\Gamma_{\text{el}}(s)/\Gamma_{\text{tot}}(s)$ is constant. A full treatment of the line shape requires consideration of dynamics, not just kinematics. For the Z this is done by calculating the radiative corrections in the Standard Model.

40.6. Transverse variables

At hadron colliders, a significant and unknown proportion of the energy of the incoming hadrons in each event escapes down the beam-pipe. Consequently if invisible particles are created in the final state, their net momentum can only be constrained in the plane transverse to the beam direction. Defining the z -axis as the beam direction, this net momentum is equal to the missing transverse energy vector

$$\mathbf{E}_T^{\text{miss}} = -\sum_i \mathbf{p}_T(i), \quad (40.58)$$

where the sum runs over the transverse momenta of all visible final state particles.

40.6.1. Single production with semi-invisible final state :

Consider a single heavy particle of mass M produced in association with visible particles which decays as in Fig. 40.1 to two particles, of which one (labeled particle 1) is invisible. The mass of the parent particle can be constrained with the quantity M_T defined by

$$M_T^2 \equiv [E_T(1) + E_T(2)]^2 - [\mathbf{p}_T(1) + \mathbf{p}_T(2)]^2 \\ = m_1^2 + m_2^2 + 2[E_T(1)E_T(2) - \mathbf{p}_T(1) \cdot \mathbf{p}_T(2)] , \quad (40.59)$$

where

$$\mathbf{p}_T(1) = \mathbf{E}_T^{\text{miss}} . \quad (40.60)$$

This quantity is called the ‘transverse mass’ by hadron collider experimentalists but it should be noted that it is quite different from that used in the description of inclusive reactions [Eq. (40.38)]. The distribution of event M_T values possesses an end-point at $M_T^{\text{max}} = M$. If $m_1 = m_2 = 0$ then

$$M_T^2 = 2|\mathbf{p}_T(1)||\mathbf{p}_T(2)|(1 - \cos \phi_{12}) , \quad (40.61)$$

where ϕ_{ij} is defined as the angle between particles i and j in the transverse plane.

40.6.2. Pair production with semi-invisible final states :

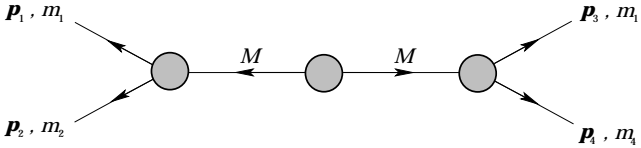


Figure 40.9: Definitions of variables for pair production of semi-invisible final states. Particles 1 and 3 are invisible while particles 2 and 4 are visible.

Consider two identical heavy particles of mass M produced such that their combined center-of-mass is at rest in the transverse plane (Fig. 40.9). Each particle decays to a final state consisting of an invisible particle of fixed mass m_1 together with an additional visible particle. M and m_1 can be constrained with the variables M_{T2} and M_{CT} which are defined in Refs. [4] and [5].

Further discussion and all references may be found in the full *Review of Particle Physics*. The numbering of references and equations used here corresponds to that version.

41. CROSS-SECTION FORMULAE FOR SPECIFIC PROCESSES

Revised October 2009 by H. Baer (Florida State University) and R.N. Cahn (LBNL).

PART I: STANDARD MODEL PROCESSES

Setting aside leptonproduction (for which, see Sec. 16 of this *Review*), the cross sections of primary interest are those with light incident particles, e^+e^- , $\gamma\gamma$, $q\bar{q}$, gq , gg , etc., where g and q represent gluons and light quarks. The produced particles include both light particles and heavy ones - t , W , Z , and the Higgs boson H . We provide the production cross sections calculated within the Standard Model for several such processes.

41.1. Resonance Formation

Resonant cross sections are generally described by the Breit-Wigner formula (Sec. 16 of this *Review*).

$$\sigma(E) = \frac{2J+1}{(2S_1+1)(2S_2+1)} \frac{4\pi}{k^2} \left[\frac{\Gamma^2/4}{(E-E_0)^2 + \Gamma^2/4} \right] B_{in}B_{out}, \quad (41.1)$$

where E is the c.m. energy, J is the spin of the resonance, and the number of polarization states of the two incident particles are $2S_1+1$ and $2S_2+1$. The c.m. momentum in the initial state is k , E_0 is the c.m. energy at the resonance, and Γ is the full width at half maximum height of the resonance. The branching fraction for the resonance into the initial-state channel is B_{in} and into the final-state channel is B_{out} . For a narrow resonance, the factor in square brackets may be replaced by $\pi\Gamma\delta(E-E_0)/2$.

41.2. Production of light particles

The production of point-like, spin-1/2 fermions in e^+e^- annihilation through a virtual photon, $e^+e^- \rightarrow \gamma^* \rightarrow f\bar{f}$, at c.m. energy squared s is

$$\frac{d\sigma}{d\Omega} = N_c \frac{\alpha^2}{4s} \beta [1 + \cos^2\theta + (1-\beta^2)\sin^2\theta] Q_f^2, \quad (41.2)$$

where β is v/c for the produced fermions in the c.m., θ is the c.m. scattering angle, and Q_f is the charge of the fermion. The factor N_c is 1 for charged leptons and 3 for quarks. In the ultrarelativistic limit, $\beta \rightarrow 1$,

$$\sigma = N_c Q_f^2 \frac{4\pi\alpha^2}{3s} = N_c Q_f^2 \frac{86.8 \text{ nb}}{s(\text{GeV}^2)}. \quad (41.3)$$

The cross section for the annihilation of a $q\bar{q}$ pair into a distinct pair $q'\bar{q}'$ through a gluon is completely analogous up to color factors, with the replacement $\alpha \rightarrow \alpha_s$. Treating all quarks as massless, averaging over the colors of the initial quarks and defining $t = -s \sin^2(\theta/2)$, $u = -s \cos^2(\theta/2)$, one finds

$$\frac{d\sigma}{d\Omega}(q\bar{q} \rightarrow q'\bar{q}') = \frac{\alpha_s^2}{9s} \frac{t^2 + u^2}{s^2}. \quad (41.4)$$

Crossing symmetry gives

$$\frac{d\sigma}{d\Omega}(qq' \rightarrow qq') = \frac{\alpha_s^2}{9s} \frac{s^2 + u^2}{t^2}. \quad (41.5)$$

If the quarks q and q' are identical, we have

$$\frac{d\sigma}{d\Omega}(q\bar{q} \rightarrow q\bar{q}) = \frac{\alpha_s^2}{9s} \left[\frac{t^2 + u^2}{s^2} + \frac{s^2 + u^2}{t^2} - \frac{2u^2}{3st} \right], \quad (41.6)$$

and by crossing

$$\frac{d\sigma}{d\Omega}(qq \rightarrow qq) = \frac{\alpha_s^2}{9s} \left[\frac{t^2 + s^2}{u^2} + \frac{s^2 + u^2}{t^2} - \frac{2s^2}{3ut} \right]. \quad (41.7)$$

Annihilation of e^+e^- into $\gamma\gamma$ has the cross section

$$\frac{d\sigma}{d\Omega}(e^+e^- \rightarrow \gamma\gamma) = \frac{\alpha^2}{2s} \frac{u^2 + t^2}{tu}. \quad (41.8)$$

The related QCD process also has a triple-gluon coupling. The cross section is

$$\frac{d\sigma}{d\Omega}(q\bar{q} \rightarrow gg) = \frac{8\alpha_s^2}{27s} (t^2 + u^2) \left(\frac{1}{tu} - \frac{9}{4s^2} \right). \quad (41.9)$$

The crossed reactions are

$$\frac{d\sigma}{d\Omega}(qq \rightarrow qq) = \frac{\alpha_s^2}{9s} (s^2 + u^2) \left(-\frac{1}{su} + \frac{9}{4t^2} \right), \quad (41.10)$$

$$\frac{d\sigma}{d\Omega}(gg \rightarrow q\bar{q}) = \frac{\alpha_s^2}{24s} (t^2 + u^2) \left(\frac{1}{tu} - \frac{9}{4s^2} \right), \quad (41.11)$$

$$\frac{d\sigma}{d\Omega}(gg \rightarrow gg) = \frac{9\alpha_s^2}{8s} \left(3 - \frac{ut}{s^2} - \frac{su}{t^2} - \frac{st}{u^2} \right). \quad (41.12)$$

Lepton-quark scattering is analogous (neglecting Z exchange)

$$\frac{d\sigma}{d\Omega}(eq \rightarrow eq) = \frac{\alpha^2}{2s} e_q^2 \frac{s^2 + u^2}{t^2}, \quad (41.13)$$

e_q is the quark charge. For ν -scattering with the four-Fermi interaction

$$\frac{d\sigma}{d\Omega}(\nu d \rightarrow \ell^- u) = \frac{G_F^2 s}{4\pi^2}, \quad (41.14)$$

where the Cabibbo angle suppression is ignored. Similarly

$$\frac{d\sigma}{d\Omega}(\nu \bar{u} \rightarrow \ell^+ \bar{d}) = \frac{G_F^2 s}{4\pi^2} \frac{(1 + \cos\theta)^2}{4}. \quad (41.15)$$

For deep inelastic scattering (presented in more detail in Section 16) we consider quarks of type i carrying a fraction $x = Q^2/(2M\nu)$ of the nucleon's energy, where $\nu = E - E'$ is the energy lost by the lepton in the nucleon rest frame. With $y = \nu/E$ we have the correspondences

$$1 + \cos\theta \rightarrow 2(1 - y), \quad d\Omega_{cm} \rightarrow 4\pi f_i(x) dx dy, \quad (41.16)$$

where the latter incorporates the quark distribution, $f_i(x)$. We find

$$\begin{aligned} \frac{d\sigma}{dx dy}(eN \rightarrow eX) &= \frac{4\pi\alpha^2 xs}{Q^4} \frac{1}{2} \left[1 + (1 - y)^2 \right] \\ &\times \left[\frac{4}{9}(u(x) + \bar{u}(x) + \dots) + \frac{1}{9}(d(x) + \bar{d}(x) + \dots) \right] \end{aligned} \quad (41.17)$$

where now $s = 2ME$ is the cm energy squared for the electron-nucleon collision and we have suppressed contributions from higher mass quarks.

Similarly,

$$\frac{d\sigma}{dx dy}(\nu N \rightarrow \ell^- X) = \frac{G_F^2 xs}{\pi} [(d(x) + \dots) + (1 - y)^2(\bar{u}(x) + \dots)], \quad (41.18)$$

$$\frac{d\sigma}{dx dy}(\bar{\nu} N \rightarrow \ell^+ X) = \frac{G_F^2 xs}{\pi} [(\bar{d}(x) + \dots) + (1 - y)^2(u(x) + \dots)]. \quad (41.19)$$

Quasi-elastic neutrino scattering ($\nu_\mu n \rightarrow \mu^- p$, $\bar{\nu}_\mu p \rightarrow \mu^+ n$) is directly related to the crossed reaction, neutron decay.

41.3. Hadroproduction of heavy quarks

For hadroproduction of heavy quarks $Q = c, b, t$, it is important to include mass effects in the formulae. For $q\bar{q} \rightarrow Q\bar{Q}$, one has

$$\frac{d\sigma}{d\Omega}(q\bar{q} \rightarrow Q\bar{Q}) = \frac{\alpha_s^2}{9s^3} \left[(m_Q^2 - t)^2 + (m_Q^2 - u)^2 + 2m_Q^2 s \right], \quad (41.20)$$

while for $gg \rightarrow Q\bar{Q}$ one has

$$\begin{aligned} \frac{d\sigma}{d\Omega}(gg \rightarrow Q\bar{Q}) &= \frac{\alpha_s^2}{32s} \left[\frac{6}{s^2} (m_Q^2 - t)(m_Q^2 - u) \right. \\ &\quad - \frac{m_Q^2(s - 4m_Q^2)}{3(m_Q^2 - t)(m_Q^2 - u)} + \frac{4(m_Q^2 - t)(m_Q^2 - u) - 2m_Q^2(m_Q^2 + t)}{3(m_Q^2 - t)^2} \\ &\quad \left. + \frac{4(m_Q^2 - t)(m_Q^2 - u) - 2m_Q^2(m_Q^2 + u)}{3(m_Q^2 - u)^2} \right. \\ &\quad \left. - \left[3 \frac{(m_Q^2 - t)(m_Q^2 - u) + m_Q^2(u - t)}{s(m_Q^2 - t)} - 3 \frac{(m_Q^2 - t)(m_Q^2 - u) + m_Q^2(t - u)}{s(m_Q^2 - u)} \right] \right]. \end{aligned} \quad (41.21)$$

41.4. Production of Weak Gauge Bosons

41.4.1. W and Z resonant production :

Resonant production of a single W or Z is governed by the partial widths

$$\Gamma(W \rightarrow \ell_i \bar{\nu}_i) = \frac{\sqrt{2}G_F m_W^3}{12\pi} \quad (41.22)$$

$$\Gamma(W \rightarrow q_i \bar{q}_j) = 3 \frac{\sqrt{2}G_F |V_{ij}|^2 m_W^3}{12\pi} \quad (41.23)$$

$$\begin{aligned} \Gamma(Z \rightarrow f\bar{f}) &= N_c \frac{\sqrt{2}G_F m_Z^3}{6\pi} \\ &\quad \times \left[(T_3 - Q_f \sin^2 \theta_W)^2 + (Q_f \sin \theta_W)^2 \right]. \end{aligned} \quad (41.24)$$

The weak mixing angle is θ_W . The CKM matrix elements are V_{ij} . N_c is 3 for $q\bar{q}$ and 1 for leptonic final states. These widths along with associated branching fractions may be applied to the resonance production formula of Sec. 41.1 to gain the total W or Z production cross section.

41.4.2. Production of pairs of weak gauge bosons :

The cross section for $f\bar{f} \rightarrow W^+W^-$ is given in term of the couplings of the left-handed and right-handed fermion f , $\ell = 2(T_3 - Qx_W)$, $r = -2Qx_W$, where T_3 is the third component of weak isospin for the left-handed f , Q is its electric charge (in units of the proton charge), and $x_W = \sin^2 \theta_W$:

$$\begin{aligned} \frac{d\sigma}{dt} &= \frac{2\pi\alpha^2}{N_c s^2} \left\{ \left[\left(Q + \frac{\ell + r}{4x_W} \frac{s}{s - m_Z^2} \right)^2 + \left(\frac{\ell - r}{4x_W} \frac{s}{s - m_Z^2} \right)^2 \right] A(s, t, u) \right. \\ &\quad + \frac{1}{2x_W} \left(Q + \frac{\ell}{2x_W} \frac{s}{s - m_Z^2} \right) (\Theta(-Q)I(s, t, u) - \Theta(Q)I(s, u, t)) \\ &\quad \left. + \frac{1}{8x_W^2} (\Theta(-Q)E(s, t, u) + \Theta(Q)E(s, u, t)) \right\}, \end{aligned} \quad (41.26)$$

where $\Theta(x)$ is 1 for $x > 0$ and 0 for $x < 0$, and where

$$\begin{aligned}
 A(s, t, u) &= \left(\frac{tu}{m_W^4} - 1 \right) \left(\frac{1}{4} - \frac{m_W^2}{s} + 3 \frac{m_W^4}{s^2} \right) + \frac{s}{m_W^2} - 4, \\
 I(s, t, u) &= \left(\frac{tu}{m_W^4} - 1 \right) \left(\frac{1}{4} - \frac{m_W^2}{2s} - \frac{m_W^4}{st} \right) + \frac{s}{m_W^2} - 2 + 2 \frac{m_W^2}{t}, \\
 E(s, t, u) &= \left(\frac{tu}{m_W^4} - 1 \right) \left(\frac{1}{4} + \frac{m_W^4}{t^2} \right) + \frac{s}{m_W^2}, \tag{41.27}
 \end{aligned}$$

and s, t, u are the usual Mandelstam variables with $s = (p_f + p_{\bar{f}})^2, t = (p_f - p_{W^-})^2, u = (p_f - p_{W^+})^2$. The factor N_c is 3 for quarks and 1 for leptons.

The analogous cross-section for $q_i \bar{q}_j \rightarrow W^\pm Z^0$ is

$$\begin{aligned}
 \frac{d\sigma}{dt} &= \frac{\pi\alpha^2 |V_{ij}|^2}{6s^2 x_W^2} \left\{ \left(\frac{1}{s - m_W^2} \right)^2 \left[\left(\frac{9 - 8x_W}{4} \right) (ut - m_W^2 m_Z^2) \right. \right. \\
 &\quad \left. \left. + (8x_W - 6) s (m_W^2 + m_Z^2) \right] \right. \\
 &\quad \left. + \left[\frac{ut - m_W^2 m_Z^2 - s(m_W^2 + m_Z^2)}{s - m_W^2} \right] \left[\frac{\ell_j}{t} - \frac{\ell_i}{u} \right] \right. \\
 &\quad \left. + \frac{ut - m_W^2 m_Z^2}{4(1 - x_W)} \left[\frac{\ell_j^2}{t^2} + \frac{\ell_i^2}{u^2} \right] + \frac{s(m_W^2 + m_Z^2)}{2(1 - x_W)} \frac{\ell_i \ell_j}{tu} \right\}, \tag{41.28}
 \end{aligned}$$

where ℓ_i and ℓ_j are the couplings of the left-handed q_i and q_j as defined above. The CKM matrix element between q_i and q_j is V_{ij} .

The cross section for $q_i \bar{q}_i \rightarrow Z^0 Z^0$ is

$$\frac{d\sigma}{dt} = \frac{\pi\alpha^2}{96} \frac{\ell_i^4 + r_i^4}{x_W^2 (1 - x_W^2)^2 s^2} \left[\frac{t}{u} + \frac{u}{t} + \frac{4m_Z^2 s}{tu} - m_Z^4 \left(\frac{1}{t^2} + \frac{1}{u^2} \right) \right]. \tag{41.29}$$

41.5. Production of Higgs Bosons

41.5.1. Resonant Production :

The Higgs boson of the Standard Model can be produced resonantly in the collisions of quarks, leptons, W or Z bosons, gluons, or photons. The production cross section is thus controlled by the partial width of the Higgs boson into the entrance channel and its total width. The partial widths are given by the relations

$$\Gamma(H \rightarrow f\bar{f}) = \frac{G_F m_f^2 m_H N_c}{4\pi\sqrt{2}} \left(1 - 4m_f^2/m_H^2 \right)^{3/2}, \tag{41.30}$$

$$\Gamma(H \rightarrow W^+W^-) = \frac{G_F m_H^3 \beta_W}{32\pi\sqrt{2}} \left(4 - 4a_W + 3a_W^2 \right), \tag{41.31}$$

$$\Gamma(H \rightarrow ZZ) = \frac{G_F m_H^3 \beta_Z}{64\pi\sqrt{2}} \left(4 - 4a_Z + 3a_Z^2 \right). \tag{41.32}$$

where N_c is 3 for quarks and 1 for leptons and where $a_W = 1 - \beta_W^2 = 4m_W^2/m_H^2$ and $a_Z = 1 - \beta_Z^2 = 4m_Z^2/m_H^2$. The decay to two gluons proceeds through quark loops, with the t quark dominating. Explicitly,

$$\Gamma(H \rightarrow gg) = \frac{\alpha_s^2 G_F m_H^3}{36\pi^3 \sqrt{2}} \left| \sum_q I(m_q^2/m_H^2) \right|^2, \quad (41.33)$$

where $I(z)$ is complex for $z < 1/4$. For $z < 2 \times 10^{-3}$, $|I(z)|$ is small so the light quarks contribute negligibly. For $m_H < 2m_t$, $z > 1/4$ and

$$I(z) = 3 \left[2z + 2z(1-4z) \left(\sin^{-1} \frac{1}{2\sqrt{z}} \right)^2 \right], \quad (41.34)$$

which has the limit $I(z) \rightarrow 1$ as $z \rightarrow \infty$.

41.5.2. Higgs Boson Production in W^* and Z^* decay :

The Standard Model Higgs boson can be produced in the decay of a virtual W or Z ("Higgstrahlung"): In particular, if k is the c.m. momentum of the Higgs boson,

$$\sigma(q_i \bar{q}_j \rightarrow WH) = \frac{\pi \alpha^2 |V_{ij}|^2}{36 \sin^4 \theta_W} \frac{2k}{\sqrt{s}} \frac{k^2 + 3m_W^2}{(s - m_W^2)^2} \quad (41.35)$$

$$\sigma(f \bar{f} \rightarrow ZH) = \frac{2\pi \alpha^2 (\ell_f^2 + r_f^2)}{48 N_c \sin^4 \theta_W \cos^4 \theta_W} \frac{2k}{\sqrt{s}} \frac{k^2 + 3m_Z^2}{(s - m_Z^2)^2}. \quad (41.36)$$

where ℓ and r are defined as above.

41.5.3. W and Z Fusion :

Just as high-energy electrons can be regarded as sources of virtual photon beams, at very high energies they are sources of virtual W and Z beams. For Higgs boson production, it is the longitudinal components of the W s and Z s that are important. The distribution of longitudinal W s carrying a fraction y of the electron's energy is

$$f(y) = \frac{g^2}{16\pi^2} \frac{1-y}{y}, \quad (41.37)$$

where $g = e/\sin \theta_W$. In the limit $s \gg m_H \gg m_W$, the rate $\Gamma(H \rightarrow W_L W_L) = (g^2/64\pi)(m_H^3/m_W^2)$ and in the equivalent W approximation

$$\begin{aligned} \sigma(e^+ e^- \rightarrow \bar{\nu}_e \nu_e H) &= \frac{1}{16m_W^2} \left(\frac{\alpha}{\sin^2 \theta_W} \right)^3 \\ &\times \left[\left(1 + \frac{m_H^2}{s} \right) \log \frac{s}{m_H^2} - 2 + 2 \frac{m_H^2}{s} \right]. \end{aligned} \quad (41.38)$$

There are significant corrections to this relation when m_H is not large compared to m_W . For $m_H = 150$ GeV, the estimate is too high by 51% for $\sqrt{s} = 1000$ GeV, 32% too high at $\sqrt{s} = 2000$ GeV, and 22% too high at $\sqrt{s} = 4000$ GeV. Fusion of ZZ to make a Higgs boson can be treated similarly. Identical formulae apply for Higgs production in the collisions of quarks whose charges permit the emission of a W^+ and a W^- , except that QCD corrections and CKM matrix elements are required. Even in the absence of QCD corrections, the fine-structure constant ought to be evaluated at the scale of the collision, say m_W . All quarks contribute to the ZZ fusion process.

Further discussion and all references may be found in the full *Review*; the equation and reference numbering corresponds to that version.

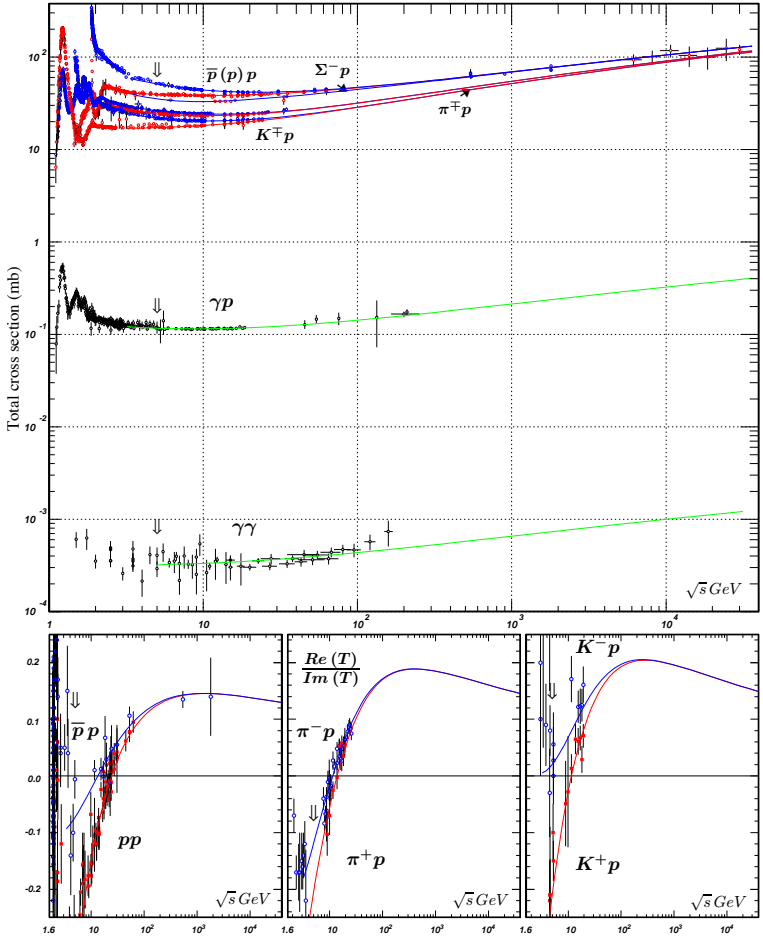


Figure 40.10: Summary of hadronic, γp , and $\gamma\gamma$ total cross sections, and ratio of the real to imaginary parts of the forward hadronic amplitudes. Corresponding computer-readable data files may be found at <http://pdg.lbl.gov/current/xsect/>. (Courtesy of the COMPAS group, IHEP, Protvino, August 2005)

6. ATOMIC AND NUCLEAR PROPERTIES OF MATERIALS

Table 6.1. Abridged from pdg.lbl.gov/AtomicNuclearProperties by D. E. Groom (2007). Quantities in parentheses are for NTP (20° C and 1 atm), and square brackets indicate quantities evaluated at STP. Boiling points are at 1 atm. Refractive indices n are evaluated at the sodium D line blend (589.2 nm); values ≥ 1 in brackets are for $(n - 1) \times 10^6$ (gases).

Material	Z	A	(Z/A)	Nucl.coll. length λ_T {g cm ⁻² }	Nucl.linter. length λ_I {g cm ⁻² }	Rad.len. X_0 {g cm ⁻² }	$dE/dx _{min}$ { MeV g ⁻¹ cm ⁻² }	Density {g cm ⁻³ }	Melting point (K)	Boiling point (K)	Refract. index (@ Na D)
H ₂	1	1.00794(7)	0.99212	42.8	52.0	63.04	(4.103)	0.071(0.084)	13.81	20.28	1.11[132.]
D ₂	1	2.01410177803(8)	0.49650	51.3	71.8	125.97	(2.053)	0.169(0.168)	18.7	23.65	1.11[138.]
He	2	4.002602(2)	0.49967	51.8	71.0	94.32	(1.937)	0.125(0.166)		4.220	1.02[35.0]
Li	3	6.941(2)	0.43221	52.2	71.3	82.78	1.639	0.534		1615.	
Be	4	9.012182(3)	0.44384	55.3	77.8	65.19	1.595	1.848		2744.	
C diamond	6	12.0107(8)	0.49955	59.2	85.8	42.70	1.725	3.520			2.42
C graphite	6	12.0107(8)	0.49955	59.2	85.8	42.70	1.742	2.210			
N ₂	7	14.0067(2)	0.49976	61.1	89.7	37.99	(1.825)	0.807(1.165)	63.15	77.29	1.20[298.]
O ₂	8	15.9994(3)	0.50002	61.3	90.2	34.24	(1.801)	1.141(1.332)	54.36	90.20	1.22[271.]
F ₂	9	18.9984032(5)	0.47372	65.0	97.4	32.93	(1.676)	1.507(1.580)	53.53	85.03	[195.]
Ne	10	20.1797(6)	0.49555	65.7	99.0	28.93	(1.724)	1.204(0.839)	24.56	27.07	1.09[67.1]
Al	13	26.9815386(8)	0.48181	69.7	107.2	24.01	1.615	2.699	933.5	2792.	
Si	14	28.0855(3)	0.49848	70.2	108.4	21.82	1.664	2.329	1687.	3538.	3.95
Cl ₂	17	35.453(2)	0.47951	73.8	115.7	19.28	(1.630)	1.574(2.980)	171.6	239.1	[773.]
Ar	18	39.948(1)	0.45059	75.7	119.7	19.55	(1.519)	1.396(1.662)	83.81	87.26	1.23[281.]
Tr	22	47.867(1)	0.45961	78.8	126.2	16.16	1.477	4.540	1941.	3560.	
Fe	26	55.845(2)	0.46557	81.7	132.1	13.84	1.451	7.874	1811.	3134.	
Cu	29	63.546(3)	0.45636	84.2	137.3	12.86	1.403	8.960	1358.	2835.	
Ge	32	72.64(1)	0.44053	86.9	143.0	12.25	1.370	5.323	1211.	3106.	
Su	50	118.710(7)	0.42119	98.2	166.7	8.82	1.263	7.310	505.1	2875.	
Xe	54	131.293(6)	0.41129	100.8	172.1	8.48	(1.255)	2.953(5.483)	161.4	165.1	1.39[701.]
W	74	183.84(1)	0.40252	110.4	191.9	6.76	1.145	19.300	3695.	5828.	
Pt	78	195.084(9)	0.39983	112.2	195.7	6.54	1.128	21.450	2042.	4098.	
Au	79	196.966569(4)	0.40108	112.5	196.3	6.46	1.134	19.320	1337.	3129.	
Pb	82	207.2(1)	0.39575	114.1	199.6	6.37	1.122	11.350	600.6	2022.	
U	92	[238.02891(3)]	0.38651	118.6	209.0	6.00	1.081	18.950	1408.	4404.	

Air (dry, 1 atm)	0.49919	61.3	90.1	36.62	(1.815)	(1.205)	78.80
Shielding concrete	0.50274	65.1	97.5	26.57	1.711	2.300	
Borosilicate glass (Pyrex)	0.49707	64.6	96.5	28.17	1.696	2.230	
Lead glass	0.42101	95.9	158.0	7.87	1.255	6.220	
Standard rock	0.50000	66.8	101.3	26.54	1.688	2.650	
Methane (CH ₄)	0.62334	54.0	73.8	46.47	(2.417)	(0.667)	111.7 [444.]
Ethane (C ₂ H ₆)	0.59861	55.0	75.9	45.66	(2.304)	(1.263)	184.5
Butane (C ₄ H ₁₀)	0.59497	55.5	77.1	45.23	(2.278)	(2.489)	134.9
Octane (C ₈ H ₁₈)	0.57778	55.8	77.8	45.00	2.123	0.703	214.4
Paraffin (CH ₃ (CH ₂) _n ≈23CH ₃)	0.57275	56.0	78.3	44.85	2.088	0.930	398.8
Nylon (type 6, 6/6)	0.54790	57.5	81.6	41.92	1.973	1.18	
Polycarbonate (Lexan)	0.52697	58.3	83.6	41.50	1.886	1.20	
Polyethylene ((CH ₂ CH ₂) _n)	0.57034	56.1	78.5	44.77	2.079	0.89	
Polyethylene terephthalate (Mylar)	0.52037	58.9	84.9	39.95	1.848	1.40	
Polymethylmethacrylate (acrylic)	0.53937	58.1	82.8	40.55	1.929	1.19	1.49
Polypropylene	0.55998	56.1	78.5	44.77	2.041	0.90	
Polystyrene ([C ₆ H ₅ CHCH ₂] _n)	0.53768	57.5	81.7	43.79	1.936	1.06	1.59
Polytetrafluoroethylene (Teflon)	0.47992	63.5	94.4	34.84	1.671	2.20	
Polyvinyltoluene	0.54141	57.3	81.3	43.90	1.956	1.03	1.58
Aluminum oxide (sapphire)	0.49038	65.5	98.4	27.94	1.647	3.970	3273.
Barium fluoride (BaF ₂)	0.42207	90.8	149.0	9.91	1.303	4.893	1.77
Carbon dioxide gas (CO ₂)	0.49989	60.7	88.9	36.20	1.819	(1.842)	1.47
Solid carbon dioxide (dry ice)	0.49989	60.7	88.9	36.20	1.787	1.563	[449.]
Cesium iodide (CsI)	0.41569	100.6	171.5	8.39	1.243	4.510	Sublimes at 194.7 K
Lithium fluoride (LiF)	0.46262	61.0	88.7	39.26	1.614	2.635	1121.
Lithium hydride (LiH)	0.50321	50.8	68.1	79.62	1.897	0.820	1.39
Lead tungstate (PbWO ₄)	0.41315	100.6	168.3	7.39	1.229	8.300	965.
Silicon dioxide (SiO ₂ , fused quartz)	0.49930	65.2	97.8	27.05	1.699	2.200	1403.
Sodium chloride (NaCl)	0.55509	71.2	110.1	21.91	1.847	2.170	1986.
Sodium iodide (NaI)	0.42697	93.1	154.6	9.49	1.305	3.667	1075.
Water (H ₂ O)	0.55509	58.5	83.3	36.08	1.992	1.000(0.756)	1738.
Silica aerogel	0.50093	65.0	97.3	27.25	1.740	0.200	1577.
							373.1
							(0.03 H ₂ O, 0.97 SiO ₂)

2010

JULY							AUGUST							SEPTEMBER						
S	M	T	W	T	F	S	S	M	T	W	T	F	S	S	M	T	W	T	F	S
1	2	3	4	5	6	7	1	2	3	4	5	6	7	1	2	3	4	5	6	7
8	9	10	11	12	13	14	8	9	10	11	12	13	14	8	9	10	11	12	13	14
15	16	17	18	19	20	21	15	16	17	18	19	20	21	15	16	17	18	19	20	21
22	23	24	25	26	27	28	22	23	24	25	26	27	28	22	23	24	25	26	27	28
29	30	31					29	30	31					26	27	28	29	30		
OCTOBER							NOVEMBER							DECEMBER						
S	M	T	W	T	F	S	S	M	T	W	T	F	S	S	M	T	W	T	F	S
1	2	3	4	5	6	7	1	2	3	4	5	6	7	1	2	3	4	5	6	7
8	9	10	11	12	13	14	8	9	10	11	12	13	14	8	9	10	11	12	13	14
15	16	17	18	19	20	21	15	16	17	18	19	20	21	15	16	17	18	19	20	21
22	23	24	25	26	27	28	22	23	24	25	26	27	28	22	23	24	25	26	27	28
29	30	31					29	30						26	27	28	29	30	31	
31																				

2011

JULY							AUGUST							SEPTEMBER						
S	M	T	W	T	F	S	S	M	T	W	T	F	S	S	M	T	W	T	F	S
1	2	3	4	5	6	7	1	2	3	4	5	6	7	1	2	3	4	5	6	7
8	9	10	11	12	13	14	8	9	10	11	12	13	14	8	9	10	11	12	13	14
15	16	17	18	19	20	21	15	16	17	18	19	20	21	15	16	17	18	19	20	21
22	23	24	25	26	27	28	22	23	24	25	26	27	28	22	23	24	25	26	27	28
29	30	31					29	30	31					25	26	27	28	29	30	
OCTOBER							NOVEMBER							DECEMBER						
S	M	T	W	T	F	S	S	M	T	W	T	F	S	S	M	T	W	T	F	S
1	2	3	4	5	6	7	1	2	3	4	5	6	7	1	2	3	4	5	6	7
8	9	10	11	12	13	14	8	9	10	11	12	13	14	8	9	10	11	12	13	14
15	16	17	18	19	20	21	15	16	17	18	19	20	21	15	16	17	18	19	20	21
22	23	24	25	26	27	28	22	23	24	25	26	27	28	22	23	24	25	26	27	28
29	30	31					29	30						25	26	27	28	29	30	31
31																				

2011

JANUARY							FEBRUARY							MARCH						
S	M	T	W	T	F	S	S	M	T	W	T	F	S	S	M	T	W	T	F	S
1	2	3	4	5	6	7	1	2	3	4	5	6	7	1	2	3	4	5	6	7
8	9	10	11	12	13	14	8	9	10	11	12	13	14	8	9	10	11	12	13	14
15	16	17	18	19	20	21	15	16	17	18	19	20	21	15	16	17	18	19	20	21
22	23	24	25	26	27	28	22	23	24	25	26	27	28	22	23	24	25	26	27	28
29	30	31					29	30						27	28	29	30	31		
APRIL							MAY							JUNE						
S	M	T	W	T	F	S	S	M	T	W	T	F	S	S	M	T	W	T	F	S
1	2	3	4	5	6	7	1	2	3	4	5	6	7	1	2	3	4	5	6	7
8	9	10	11	12	13	14	8	9	10	11	12	13	14	8	9	10	11	12	13	14
15	16	17	18	19	20	21	15	16	17	18	19	20	21	15	16	17	18	19	20	21
22	23	24	25	26	27	28	22	23	24	25	26	27	28	22	23	24	25	26	27	28
29	30	31					29	30	31					26	27	28	29	30	31	
31																				

2012

JANUARY							FEBRUARY							MARCH						
S	M	T	W	T	F	S	S	M	T	W	T	F	S	S	M	T	W	T	F	S
1	2	3	4	5	6	7	1	2	3	4	5	6	7	1	2	3	4	5	6	7
8	9	10	11	12	13	14	8	9	10	11	12	13	14	8	9	10	11	12	13	14
15	16	17	18	19	20	21	15	16	17	18	19	20	21	15	16	17	18	19	20	21
22	23	24	25	26	27	28	22	23	24	25	26	27	28	22	23	24	25	26	27	28
29	30	31					29	30						25	26	27	28	29	30	31
APRIL							MAY							JUNE						
S	M	T	W	T	F	S	S	M	T	W	T	F	S	S	M	T	W	T	F	S
1	2	3	4	5	6	7	1	2	3	4	5	6	7	1	2	3	4	5	6	7
8	9	10	11	12	13	14	8	9	10	11	12	13	14	8	9	10	11	12	13	14
15	16	17	18	19	20	21	15	16	17	18	19	20	21	15	16	17	18	19	20	21
22	23	24	25	26	27	28	22	23	24	25	26	27	28	22	23	24	25	26	27	28
29	30	31					29	30	31					24	25	26	27	28	29	30
31																				